National Aeronautics and Space Administration
Jet Propulsion Laboratory
California Institute of Technology
Goddard Space Flight Center

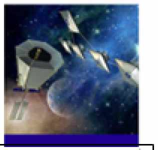

Lockheed Martin
Ball Aerospace & Technologies Corp.
Northrop Grumman Space Technology
TC Technology
nightsky systems

TPF Terrestrial Planet Finder

TPF Coronagraph Flight Baseline 1 Design Interim Status Report

Presentation Date: 11-12 July 2005
Report Date: 18 August 2005

Edited by Virginia Ford
contributors:

Alexander, J.	Engler, C.	Kissil, A.	Mouroulis, P.
Bikkannavar,	Fantano, L.	Krim, M.	Noecker, C.
Blaurock, C.	Feher, P.	Kwack, E.	Ohl, R.
Bruce, C.	Ford, V.	Levine, M.	Palacios, D.
Cafferty, T.	Green, J.	Lillie, C.	Peabody, S.
Chainyk, M.	Gutt, G.	Lisman, D.	Pitman, J.
Collins, D.	Ho, T.	Liu, A.	Renshall, J.
Content, D.	Howard, J.	Marchant, L.	Shaklan, S.
Dewell, L	Hunyadi, S.	Martin, N.	Shchiermeier, J.
Dumont, P.	Irish, S.	Martino, T.	Weng, I.

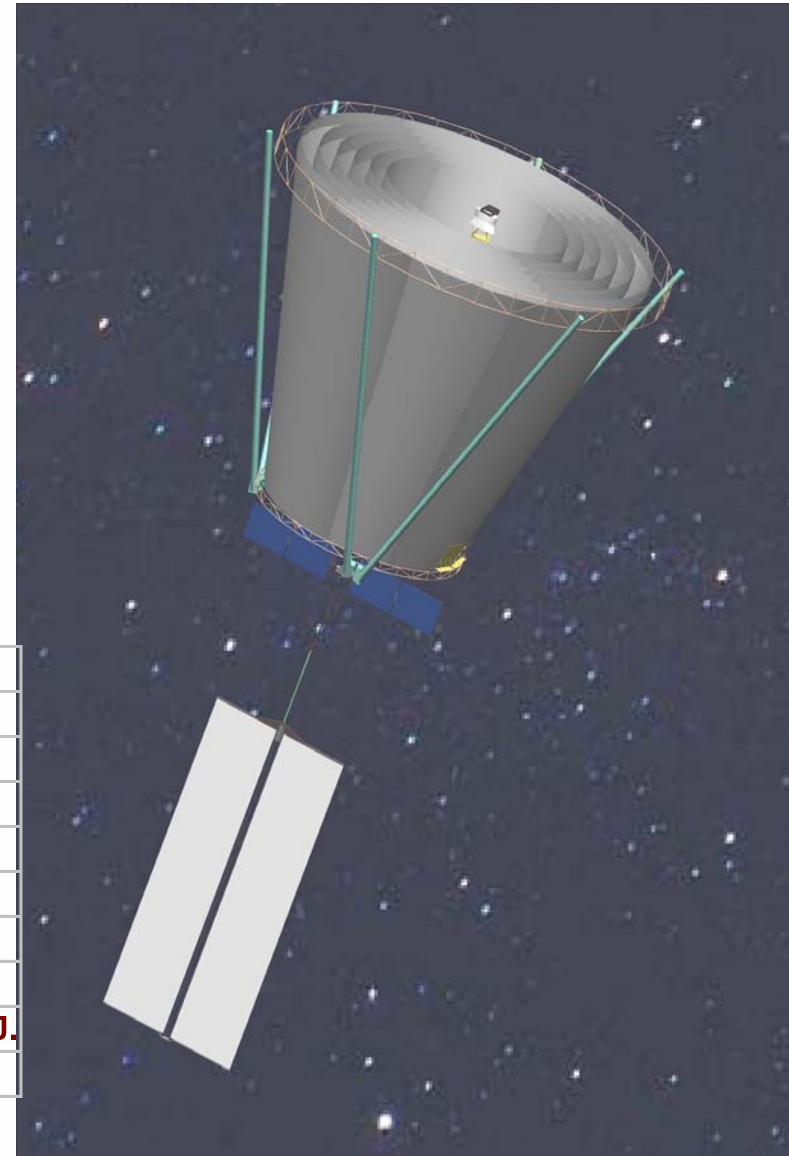

Prologue: TPF Coronagraph Design Team Presentation

Virginia Ford, TPF Coronagraph Systems Manager

Introduction:

Exciting things are occurring in astrophysics. Since the mid 1980s dust disks around distant stars have been observed to have swirls, lumps and clear features which are believed to indicate the presence of planets. During the past decade, Astronomers using ground-based telescopes have been detecting planets orbiting around nearby stars – the count is now above 163 detected planets external to our solar system.

With this in mind, NASA is funding a mission called Terrestrial Planet Finder (TPF) that intends to find and characterize terrestrial (or rocky) planets that might harbor life. This mission will look for Earth-like planets around nearby stars in the zone where liquid water could be present on the planet surface. In order to meet this criterion, the planets must be orbiting in the spherical region around a star called the habitable zone. The zone size is based on the temperature on the surface of the planet (where water will be liquid) and is related to the brightness of each star and the orbital radius range for each particular star where a planet would have the correct thermal characteristics.

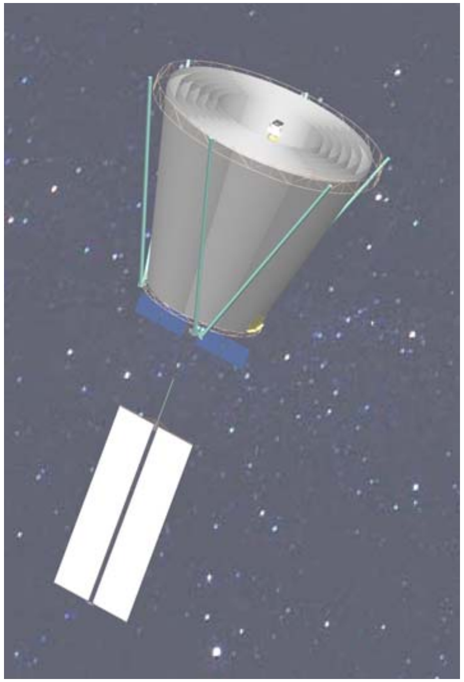

Figure 1. Terrestrial Planet Finder Coronagraph - Flight Baseline 1 Configuration (Ho)

When a planet is found in this zone, by studying the light from that planet, the presence of life can be detected from the spectrum of gases that are present in its atmosphere. The presence of life-indicating gases such as water, oxygen, ozone, carbon dioxide, nitrous oxide, methane, and chlorophyll in land plants can be detected in the spectrum of light reflecting off of a planet's atmosphere.

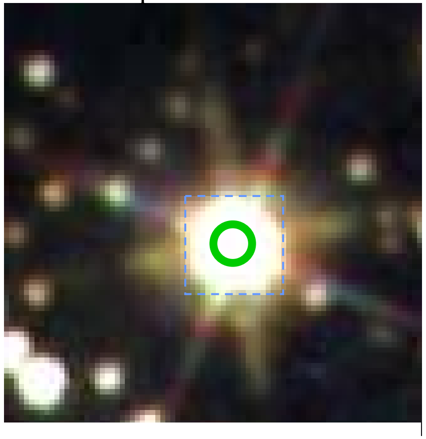

Figure 2. Star image from Hubble Space Telescope – green circle shows the habitable zone; dashed box shows the deep contrast region of TPF-C

In order to perform this mission, two instruments are being proposed: a visible coronagraph and an infrared interferometer. The coronagraph, called Terrestrial Planet Finder Coronagraph (TPF-C), shown in Figure 1, is currently scheduled for launch in 2016 and will be the focus of this report. The interferometer is currently scheduled to launch in the 2020 timeframe. Both instruments provide complementary data to establish the presence of life on any planets that may be found and studied.

Technology Challenges and Feasibility Demonstration:

The most challenging technology areas needing development for this project are related to optical wavefront accuracy. Extreme accuracy is needed in order to block out the parent starlight adequately so that the orbiting planet can be detected. In the visible wavelength range of TPF-C, the light from the planet is reflected from its parent star and is 10^{10} times fainter than the parent star. This intensity reduction factor of 10 billion times requires a deeper understanding of light propagation physics including the effect of optical components on polarization, diffraction, phase, amplitude and wavelength and the crosstalk between these parameters. Test beds, component fabrication, measurements and modeling developments form the core of the technology development efforts that are underway. Figure 2 shows a star imaged through the Hubble Space Telescope demonstrating the starlight scattered by the telescope. The solid green annulus is a representation of the habitable zone where TPF-C must look for planets. Figure 3 shows the type of image TPF-C will create with advanced technologies such as: a spatial frequency-specified primary mirror, deformable mirrors, advanced coronagraph components, and wave front sensing and control algorithms. The dark area is called the dark hole and is formed by the controlled deformable mirrors in the system correcting the wavefront to counteract errors caused by the telescope and coronagraph components.

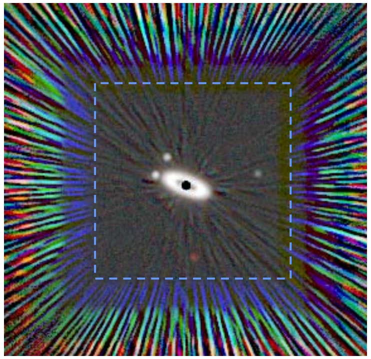

Figure 3. Simulation of TPF-C image of a star system similar to our solar system; dashed box designates the deep contrast area of TPF-C.

Currently, the most mature test bed is called the High Contrast Imaging Testbed (HCIT). It consists of a large isolated vacuum chamber containing an optical bench with a Lyot-style coronagraph and arrangements to test alternative components and coronagraphic systems, a fiber-optic star-simulating source, a deformable mirror, and a camera. To date, this test bed has created a half-dark hole (formed using only one DM to correct both phase and amplitude) reaching approximately 10^{-9} contrast between the light remaining in the dark half and the star-simulating source light. Figure 4 shows the layout of the HCIT. The HCIT team is working to meet Milestone 1: Demonstrate that the High Contrast Imaging Testbed (HCIT) is capable of achieving less than an average contrast of 1×10^{-9} throughout an area from $4\lambda/D$ inner working angle to $10\lambda/D$, at $\lambda=785$ nm, repeatably and stable for at least one hour. An average contrast of 8×10^{-10} has been attained repeatably and stably in the full area from $4\lambda/D$ to $10\lambda/D$; but in the area from $4\lambda/D$ to $5\lambda/D$, the test bed has only achieved a repeatable, stable contrast of 2×10^{-9}, so the team is working to drive that critical smaller area down.

Several areas of study support the HCIT by theorizing, modeling, fabricating, studying, and measuring characteristics of components in the HCIT. The goal is to measure and model accurately the optical propagation effects of these components, validate the models using HCIT performance, then use these validated measurements and models to explore the best methods of starlight suppression for TPF-C. There is a TPF-funded coordinated effort across the USA involving laboratories, NASA centers and universities that has led to increased understanding of electro-magnetic wave propagation in a coronagraph, and has given us a more accurate understanding of methods of suppressing diffracted and scattered starlight.

Following Milestone 1, two additional milestones need to be achieved before TPF-C is considered to have demonstrated technical readiness to proceed into the formal phases of a space flight project. Milestone 2 is to achieve the same contrast performance as Milestone 1, but using a wavelength bandwidth of 60 nm. Milestone 3 requires creating and validating a predictive model of the HCIT, using the same modeling technique to model a flight observatory and predicting a contrast performance of less than 10^{-10} over the habitable zone area (from $4\lambda/D$ to $10\lambda/D$) adequate to perform the TPF-C mission.

In order to achieve Milestone 3, a design team has been developing an observatory concept that explores the most challenging issues of this mission. The approach has been to engage in a series of design concept cycles, each leading to increased detail and further understanding of the technical challenges that will guide the next cycle closer towards a successful solution.

The first design cycle was called the Minimum Mission Design. It was an inexpensive, simplified, integrated modeling approach that enabled the team to study observatory environmental perturbations and their effect on the wave front and contrast. This study established a modeling process that successfully tied structural dynamics and thermal models to optical performance models. The study calculated contrast performance, related the performance to an operational scenario that predicted the ability to find planets and to explore star habitable zones completely. The Minimum Mission Design, modeling and analysis is fully documented in a report that was completed 22 April 2004 that can be found in the TPF library collection 2410. The cycle used simple beam models in non-critical areas, did not include a detailed starlight suppression system, but was successful in demonstrating that a feasible observatory design was thermally and dynamically stable enough to propagate star light adequately to a coronagraph system similar to the one represented in the HCIT. The wavefront delivered to the coronagraph would have small enough errors so that the deformable mirrors in the suppression system could correct them and develop an adequate contrast for finding terrestrial planets.

The design cycle following the Minimum Mission Design is called Flight Baseline 1 (FB1). In this cycle, observatory problems and weaknesses discovered during the Minimum Mission Design analysis were corrected. These included: smoothing the sunshade vanes from a set of flat panels into continuous conic shapes; and stiffening the base of the secondary tower using a panel rather than two linkage beams to provide more shear resistance. Also, more detail was added including: a detailed secondary mirror assembly; actual structural elements in the secondary tower; close-out panels in the back end of the sun shade; and spacecraft modifications to support the sunshade more realistically. Inside that thermal enclosure, much more detail was added. Behind the primary mirror, a set of heaters was added to provide the capability of controlling the temperature radiated onto the back of the primary mirror. Electronics were estimated and added in bays with heat pipes providing heat transfer to a passive radiator. Placeholder instruments were included (primarily as volumes) with the detectors co-located in a cold zone cooled by heat pipes connected to a dedicated cold radiator. Besides heat pipes and radiators, heaters were added behind the primary mirror, and within the thermal enclosure. For the FB1 analysis, constant power will be applied to the heaters to understand the system thermal sensitivity, and to gain understanding of the requirements for an active thermal control system. This work will be completed in September 2005.

For FB1, a complicated starlight suppression system was modeled that included many features that might possibly be desired – such as two complete separate polarization paths, focal planes for focal plane masks, pupil planes for pupil masks, filter wheels, multiple deformable mirrors, and Michelson interferometers where phase and amplitude would be adjusted for each wavefront. It was not intended that the instruments or the starlight suppression system be optimized. It was considered more important to provide an inclusive system to model that would capture many components and explore their effects and increase the level of understanding about how to best configure the starlight suppression system.

In parallel, the technology development teams have fabricated, measured and characterized properties of masks that have been included in the optical performance model. Wavelength effects have been tested in the HCIT with further increase in understanding of component effects on wavelength. A polarization-splitting Calcite crystal has been added to the HCIT to enable the study of polarization effects. Coatings have been modeled and measured. This increased knowledge has been added to the models that represent the FB1 telescope and starlight suppression system performance, resulting in a much better representation of how the system will actually perform.

Conclusions:

The FB1 analysis is scheduled to be completed in September 2005, and was not finished at the time of the FB1 Design Presentation or the publication of this report; but significant findings have already occurred.

1. Probably of most significance is that the all-inclusive starlight suppression system that was modeled will not produce deep enough contrast over broadband wavelengths. What is most important about this finding is that it points toward changes that can be made to solve this problem. Understanding has increased of the influence of how the two polarization states and phase and amplitude cross-talk affect the ability to attain contrast. How the components change these properties when the light beam hits or passes through them is being measured and applied to the models. How corrections for these effects are optimized for wavelength and the breadth of the wavelength ranges that can be corrected to within required levels is growing and will guide the design of a workable system. The next cycle will improve the starlight suppression system, but this area will probably require continued effort.

2. Another significant accomplishment is that the environmental perturbations during operation appear to be controlled adequately – both thermally and dynamically. The current sunshade isolates the telescope and payload adequately. Active dynamic control easily isolated the payload from reaction wheel vibrations. Passive dynamic control could be effective but with less margin and with more tuning necessary. Vibrations from mechanisms in the instruments and starlight suppression system haven't yet been included, but selective damping seems feasible and promising. The next cycle will include these. An important feature of this area is that the thermal and dynamic models have limitations that are becoming well understood. Nastran patches are used to correct known limitations. Better integrated modeling tools are being developed, but the team has learned how to produce believable results with commercially available tools. The newer modeling tools should increase to modeling speed and will help in the future.

3. The primary mirror assembly meets all operational requirements, but needs more consideration of fabrication, ground handling and testing accommodations. Launch loads were too severe around the mounting points. This complex assembly will need more development to address the full range of difficulties it will encounter. The next cycle will address this, but will probably require continuing development

4. The observatory mass was too high for adequate margin above the launch capability of the chosen launch vehicle. There are mass optimizations that can be done to reduce this as part of the final FB1 analysis. FB1 CAD models were not focused on mass optimizations and improvements can be readily projected and applied to the next cycle.

5. For the next cycle, the active thermal control system will be included in the stability calculations. FB1 purposely strove only to derive requirements on the active control system rather than include any features other than heater hardware with power applied. The goal was to use FB1 to understand how difficult and challenging the active control system will be before addressing how it should be implemented.

Finally, though all the analysis is not complete, FB1 has provided a lot of value. It will guide the next design cycle toward better performance and deeper detail. The team and community is gaining knowledge and preparation to develop an observatory system that will perform adequately and reach a closeout for Milestone 3 – perhaps not following an FB2 cycle, but hopefully after an FB3 design cycle.

The following presentation consists of a set of executive summary viewgraphs encompassing the topics of the presentation. This is followed by the full set of presentation viewgraphs. These are annotated, so should be viewed with the notes showing to understand the details of the material.

Table of Contents

TPF Library location: https://tpf-lib.jpl.nasa.gov/tpf-lib/dscgi/ds.py/View/Collection-3137

Executive Summary: Introduction

LOCKHEED MARTIN
Ball Aerospace & Technologies Corp.
NORTHROP GRUMMAN Space Technology
TC Technology
nightsky systems

- Attendees
  - Design Team is spread across the USA including members from JPL, Goddard, and Industry
  - Reviewing attendees consist of scientists and engineers from across the USA representing Universities, Industry, JPL, Goddard and NASA headquarters
- We have plans and detailed schedules that lead us (based on current budget)
  - Into Phase A in 2007
  - Based on projected Launch in 2016
- Four design concept cycles will take place prior to entering Phase A:
  - Minimum Mission Cycle
    - Completed April 22, 2004
  - Flight Baseline 1 Cycle
    - In work – being presented
  - Flight Baseline 2 Cycle
    - To be completed ~ January 2006
  - Flight Baseline 3 Cycle
    - To be completed ~ September 2006
- Presentation covers status of work in progress
  - Not a finished product
  - Are still open issues

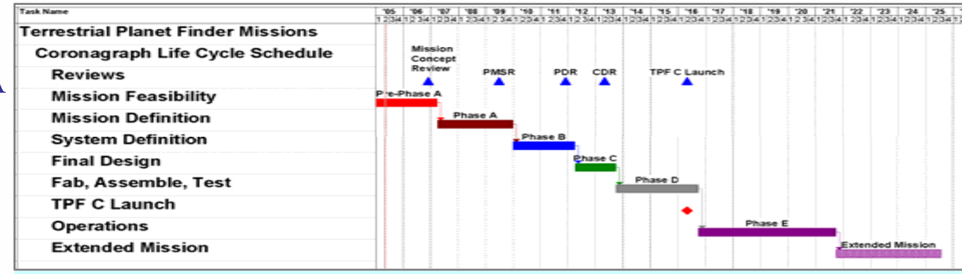

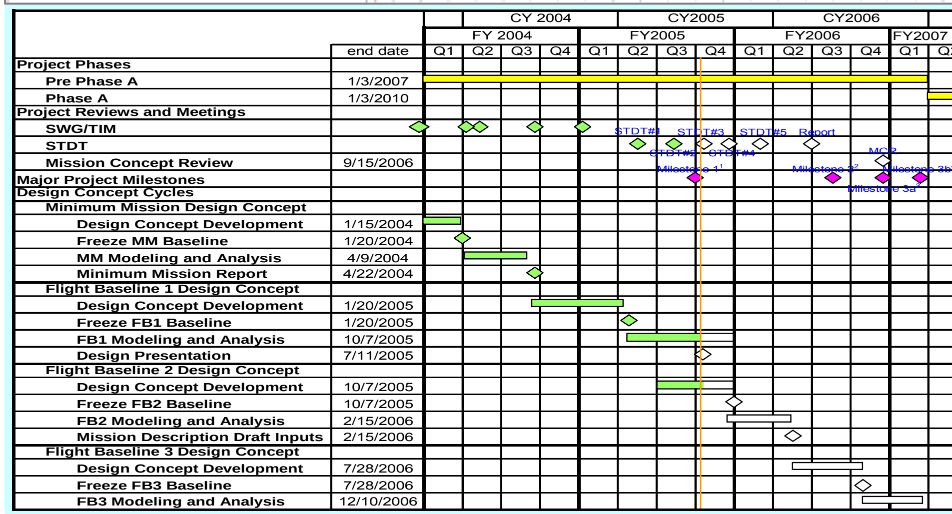

MINIMUM MISSION CONCEPT

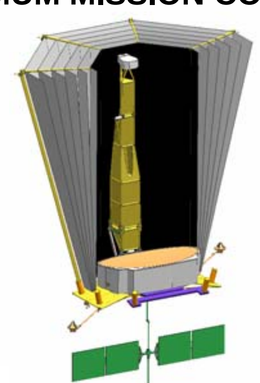

FLIGHT BASELINE 1 CONCEPT

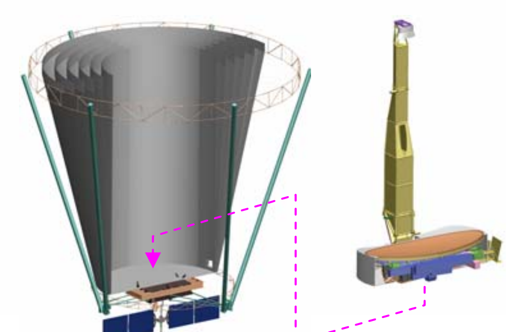

TPF Terrestrial Planet Finder

Executive Summary: Mission Description

Virginia Ford

Contributors: Doug Lisman, Peter Feher, Sarah Hunyadi, Architecture and Design Team

11-12 July 2005

- Choices have been made for the mission and spacecraft
  - form the basis for the observatory concept
- The selected orbit: Lissajous halo orbit around the L2 point
- The field of regard and target star observation scenario define the limits of the thermal environment of the observatory
- The resulting observatory concept schematic shows interfaces and relationships between components

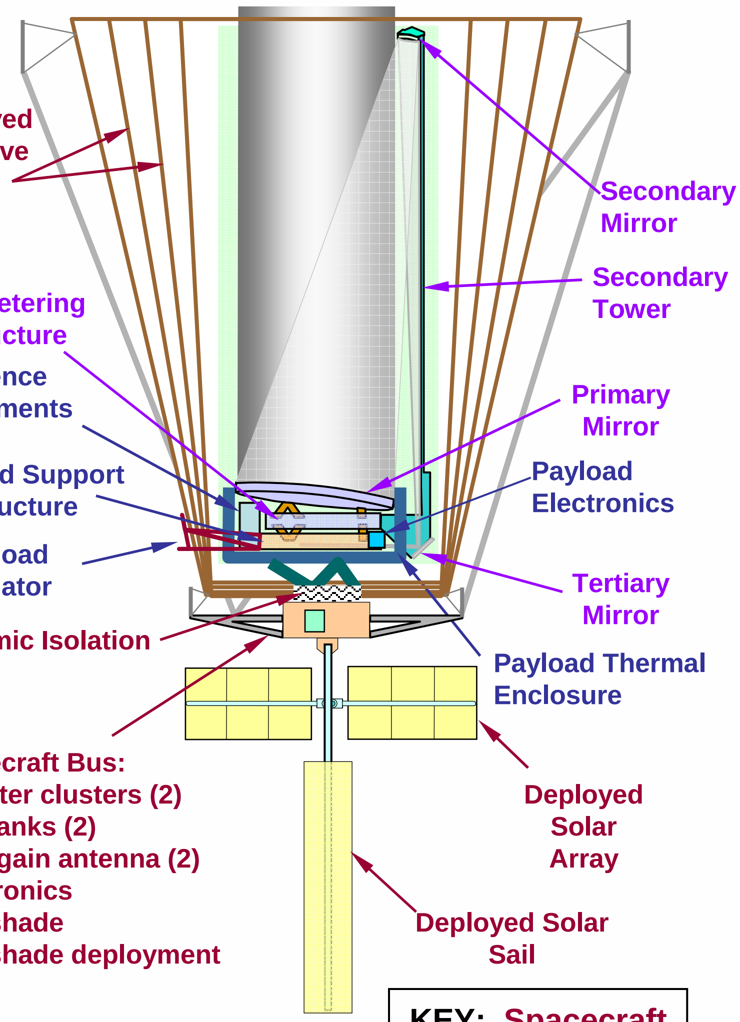

Executive Summary: DRM Completeness Studies

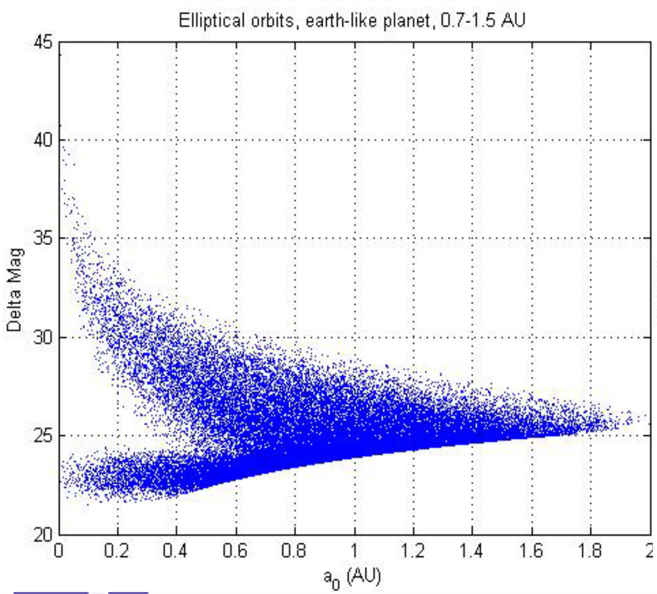

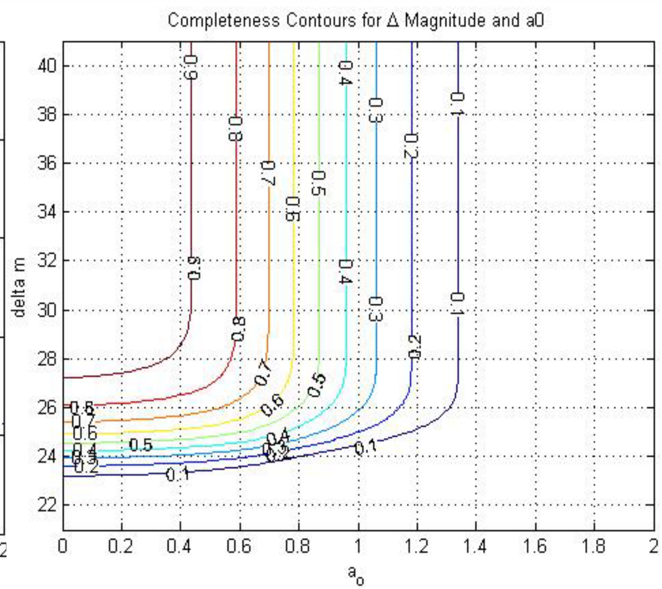

Completeness = probability of finding planet around star if one is there

- Elliptical planetary orbits expand range of habitable planets
- Probability distribution of planets gives completeness contours
- Completeness curves are optimized for highest planet count with auction optimization

Separate models: Equivalent Optimizations

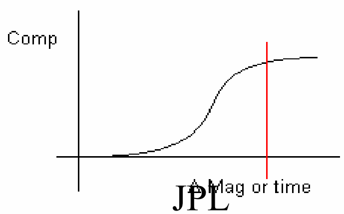

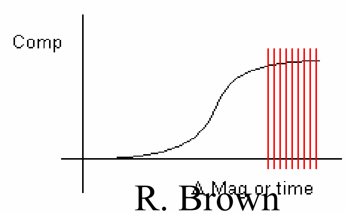

	JPL		R. Brown	
ΔMag	# Stars	# Planets	#Stars	#Planets
25	138	32.60	135.21	32.59
25.5	125	38.29	122.77	38.32
26	115	41.10	113	40.96
27	114	42.16	106	41.04

Optimized Results at ΔMag=25 and ΔMag=26

ΔMag=25

- Planets = 25.771 (JPL)
- Planets = 26.13 (Brown)
- Participating Stars = 146
- Limited improvement over Δmag=25 cutoff

ΔMag=26

- Planets = 39.038
- Participating Stars = 126
- Great improvement over both Δmag=25 cutoff and Δmag=26 cutoff

Executive Summary: Error Budget Status

Theoretical Contrast in Coronagraph dark hole

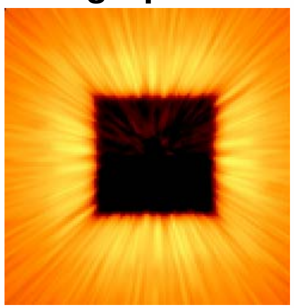

High Level TPF-Coronagraph Contrast Error Budget Requirements.

	Requirement	Comment
Static Contrast	6.00E-11	Coherent Terms
Contrast Stability	2.00E-11	Thermal + Jitter
Instrument Stray Light	1.50E-11	Incoherent light
Inner Working Angle	4 λ/D_{long}	57 mas at λ=550 nm, D_{long} = 8 m
Outer Working Angle	48 λ/D_{short}	1.5 arcsec at λ=550 nm, D_{short} = 3.5 m
Bandpass	500-800 nm	Separate observ. in three 100 nm bands.

Includes:

- Requirements:
  - Set limiting_delta_magnitude = 25
- Static Error Budget
  - Wave Front Sensing errors
  - Polarization effects
  - Mask errors and polarization effects
  - Contamination effects
  - Micrometeoroid effects
- Incoherent Light
  - Scattering model
- Dynamic Error Budget
  - Captures beam walk, rigid body motion, mirror surface aberration
  - Inputs from dynamic and thermal perturbation sources
- Will be improved and updated

Models used to calculate static and dynamic contrast

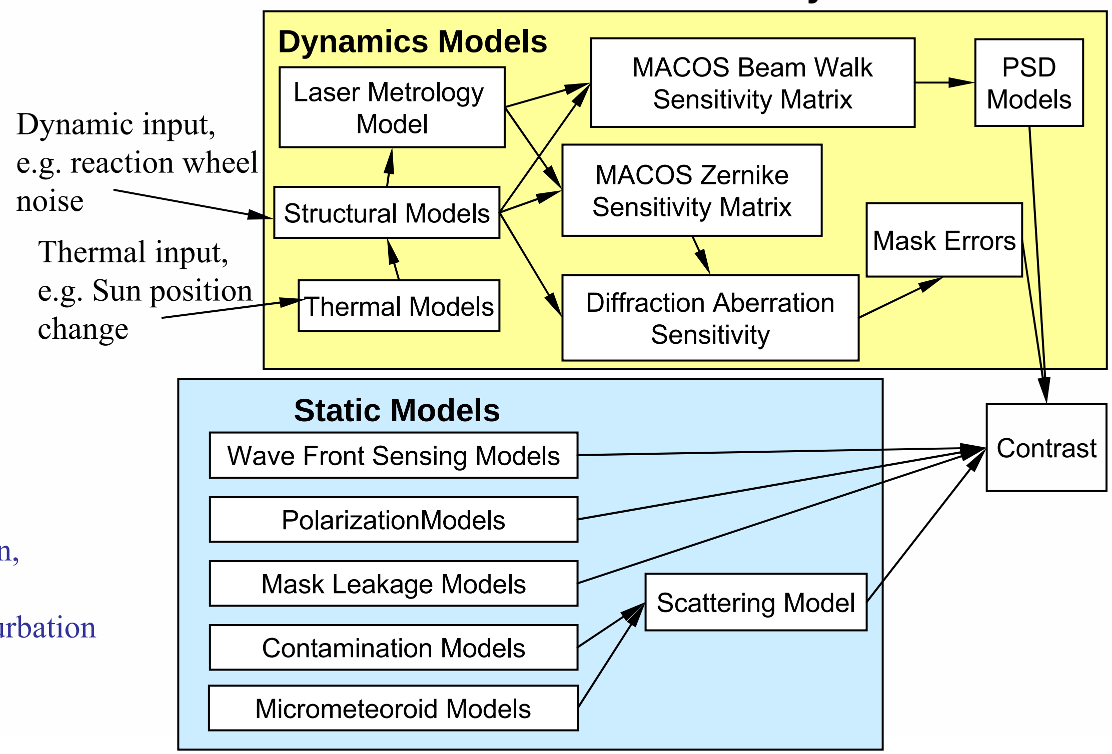

Executive Summary: Error Budget Engineering Allocations

Table 4: Rolled up Dynamic Contrast Contributors

Perturbation	Contributor	Nature	Contrast	Fraction
Structural Defomation	Beam Walk	Thermal	8.29E-13	16.12%
		Jitter	6.33E-13	12.31%
	Aberrations	Thermal	3.28E-14	0.64%
		Jitter	4.43E-17	0.00%
Bending of Optics	Aberrations	Thermal	8.60E-13	16.72%
		Jitter	8.60E-13	16.72%
Pointing	Beam Walk		1.29E-12	25.10%
	Image Motion		9.04E-14	1.76%
	Mask Error		5.46E-13	10.63%
SUM			5.14E-12	

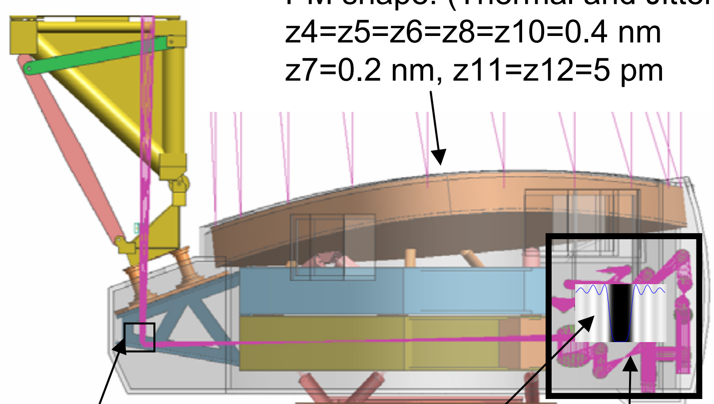

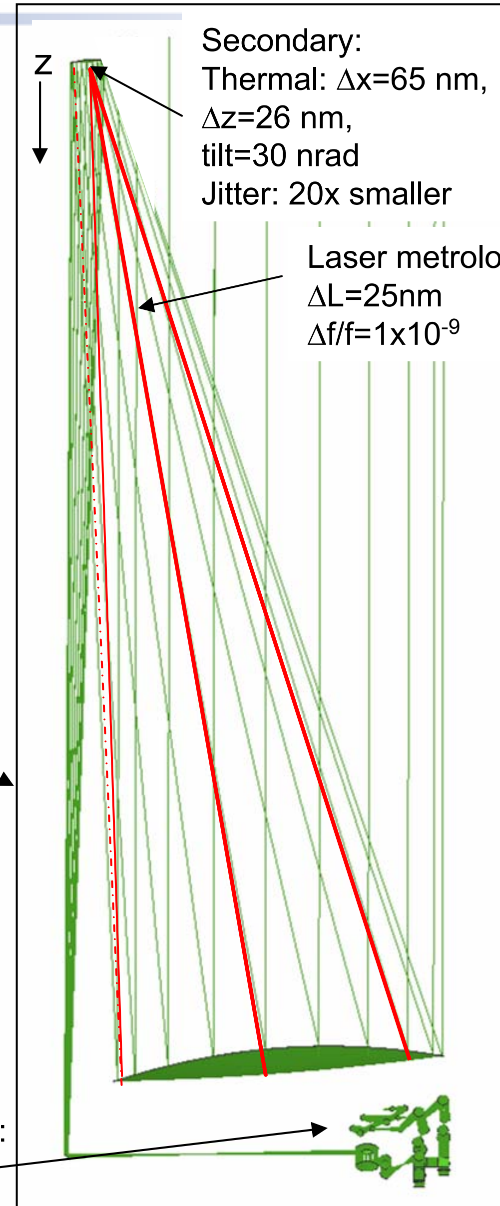

Executive Summary: Optical Design

TPF Terrestrial Planet Finder

Optical Schematic

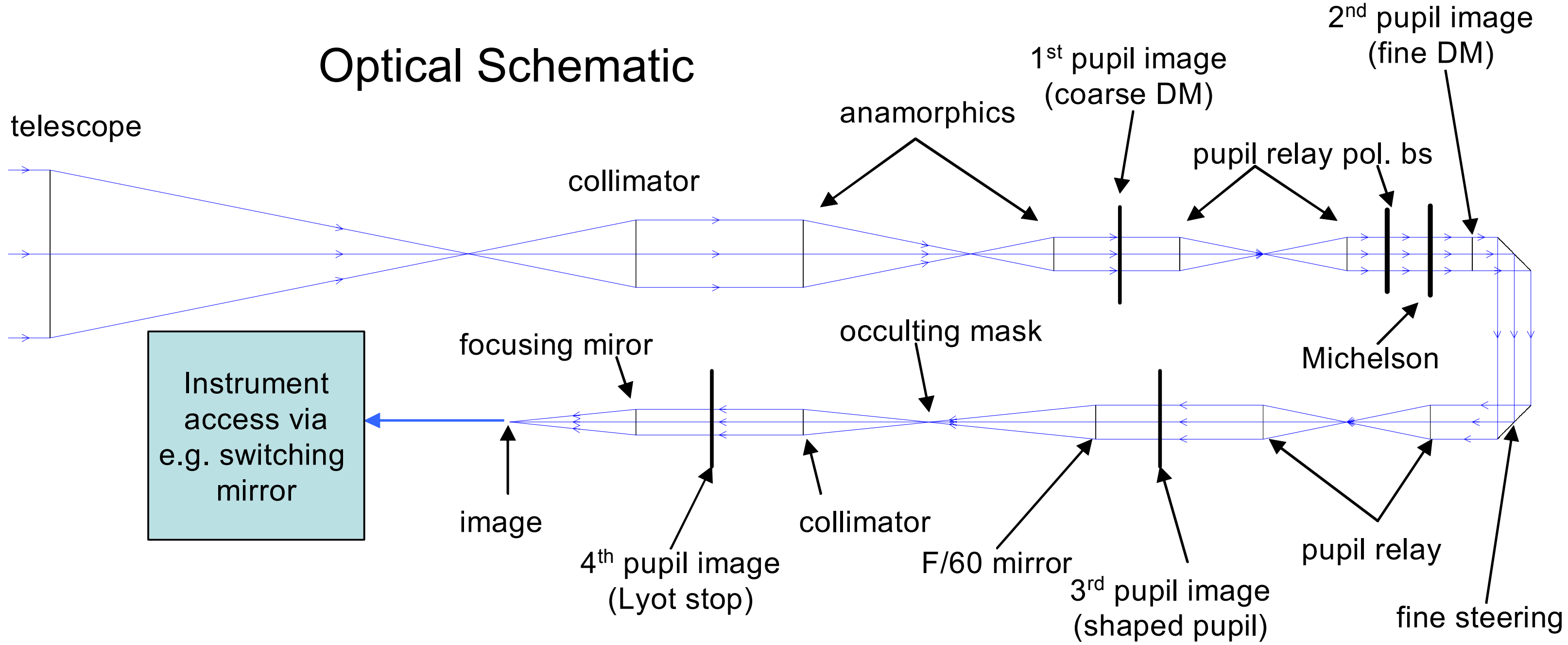

Optical Implementation

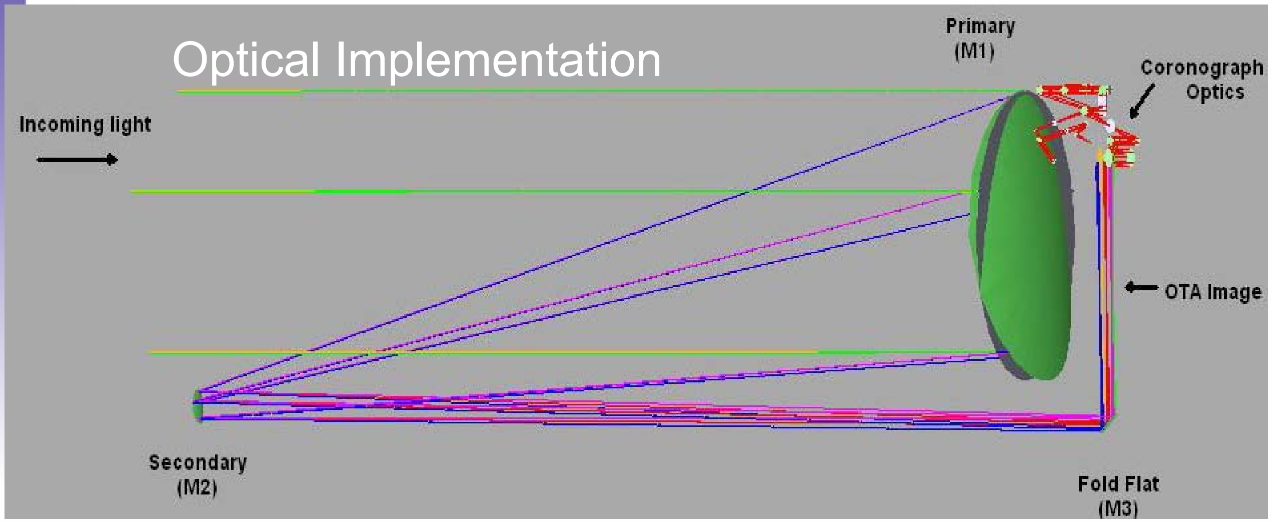

Magnified polychromatic spot diagram at final focus shows chromatic error fully suppressed.

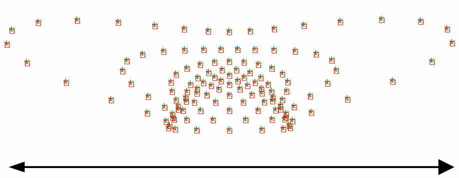

Executive Summary: Pointing Control Architecture

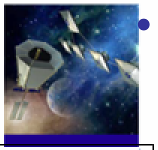

- Goal: meet error budget allocations
  - Fine pointing and coarse pointing modes
- Two architectures evaluated
  - Passive and Active
- Components based on current technology – flight heritage if poss.

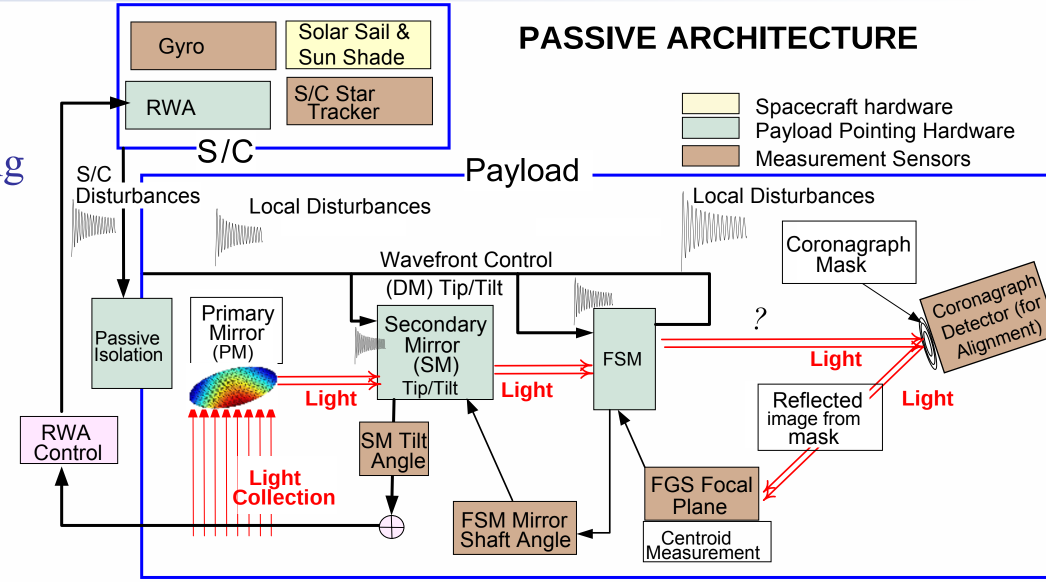

Reaction Wheel Assembly

Goodrich E-wheel

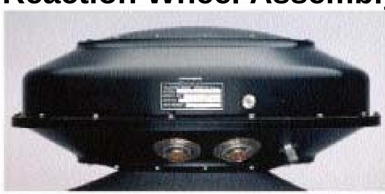

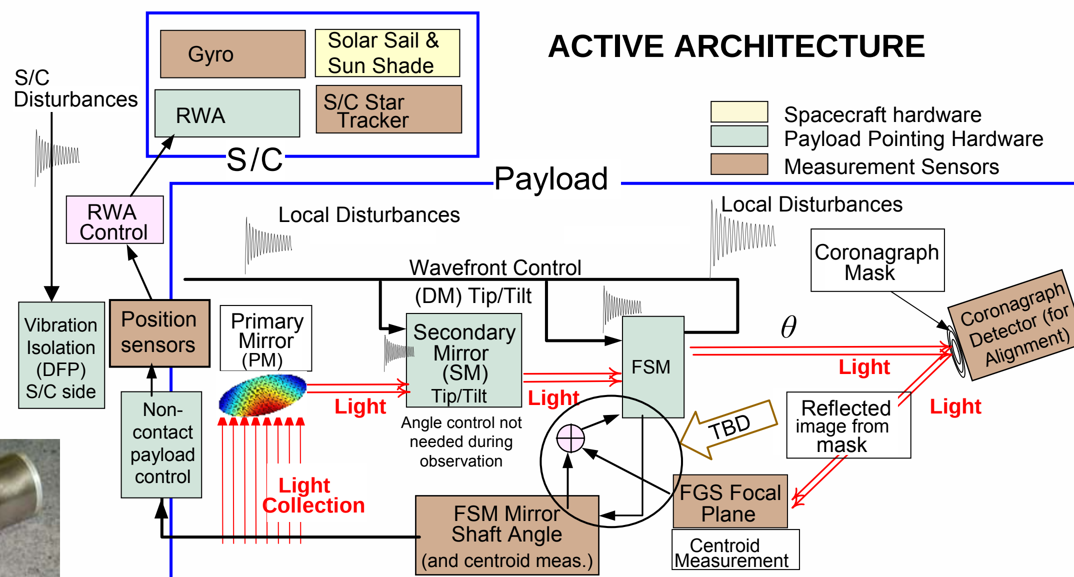

Secondary mirror tip/tilt assembly & actuator

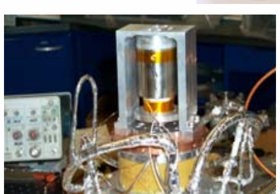

DFP single actuator assembly

Executive Summary: Mechanical System Configuration

Lockheed Martin
Ball Aerospace & Technologies Corp.
Northrop Grumman Space Technology
TC Technology
nightsky systems

TPF Terrestrial Planet Finder

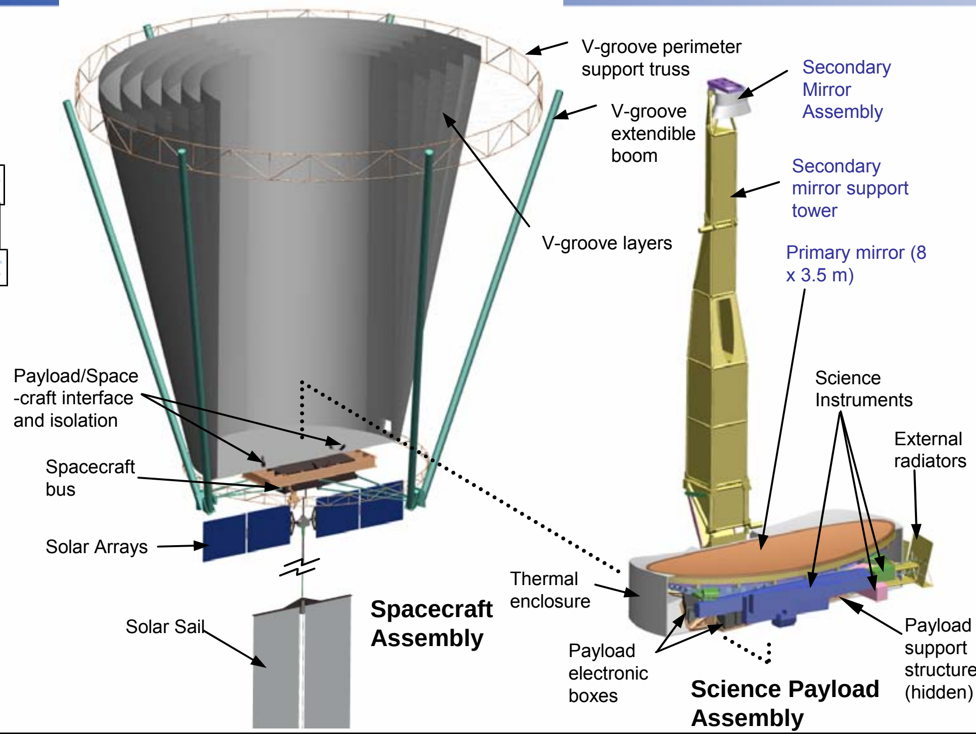

Science Payload Assembly

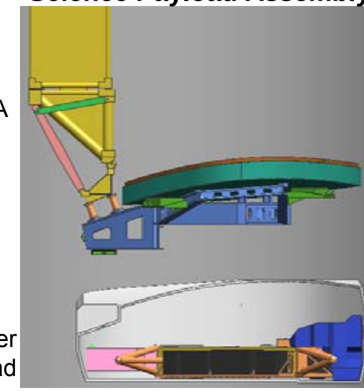

Interfaces and overview

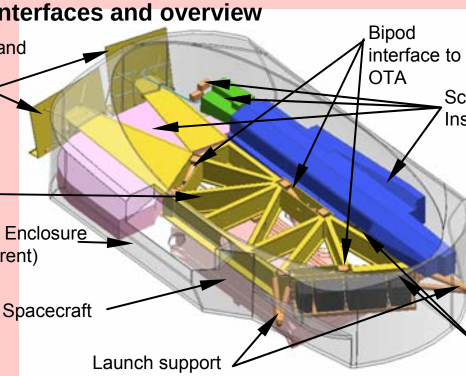

Non-OTA Science Payload

Instruments

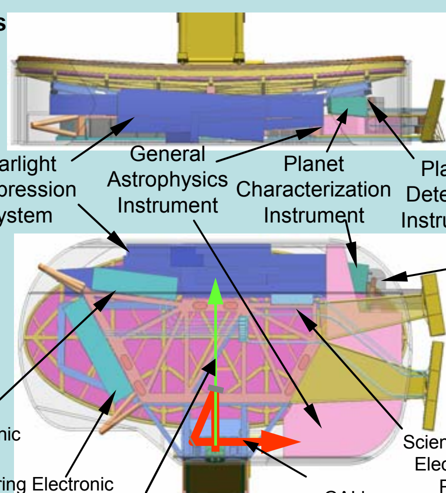

Thermal Control Hardware

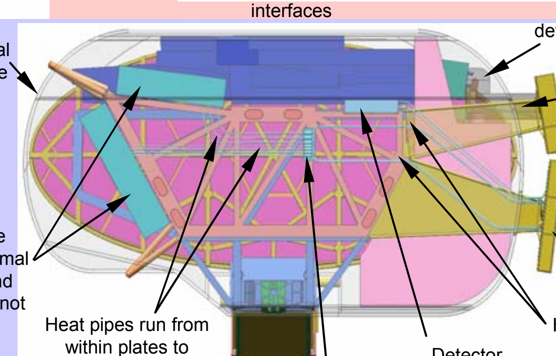

Executive Summary: Mechanical OTA Configuration

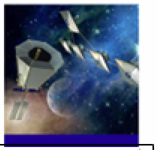

Lockheed Martin
Ball Aerospace & Technologies Corp.
Northrop Grumman Space Technology
TC Technology
nightsky systems

TPF Terrestrial Planet Finder

Deployable Tower
- hinged 4 segment deployable structure

Tertiary Mirror Assembly

Thermal control system

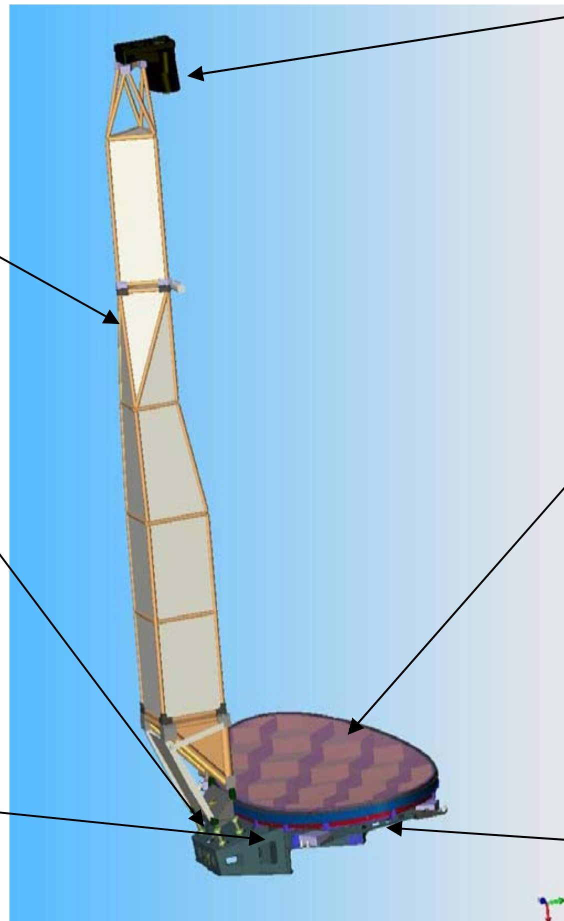

(Engler and Guzak)

Secondary Mirror Assembly
- .9m x .4m Secondary Mirror
- Pointing and control system
- Thermal control system
- Laser metrology reflectors

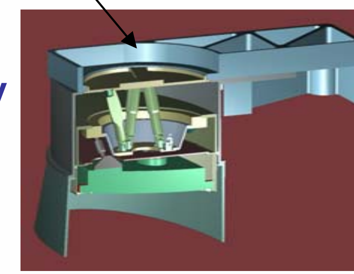

Primary Mirror Assembly
- 8mx3.5m Mirror
- Thermal control system
- Cover deployment system

Laser Metrology launchers

Aft Metering Structure

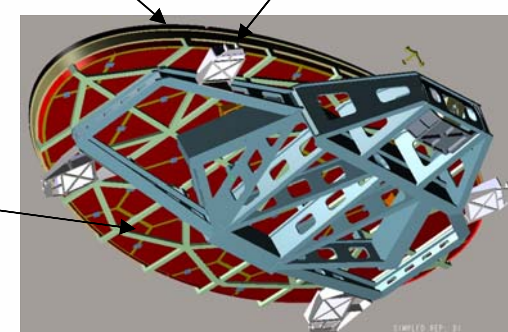

Executive Summary: Thermal Control Concept

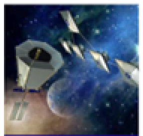

TC Technology

Terrestrial Planet Finder
TPF

- Includes a full array of design features available to provide the required thermal stability
- Relatively detailed full system thermal model
- Performance evaluation will guide the implementation of design features
- We are confident we can provide the needed thermal stability

Thermal Design Features

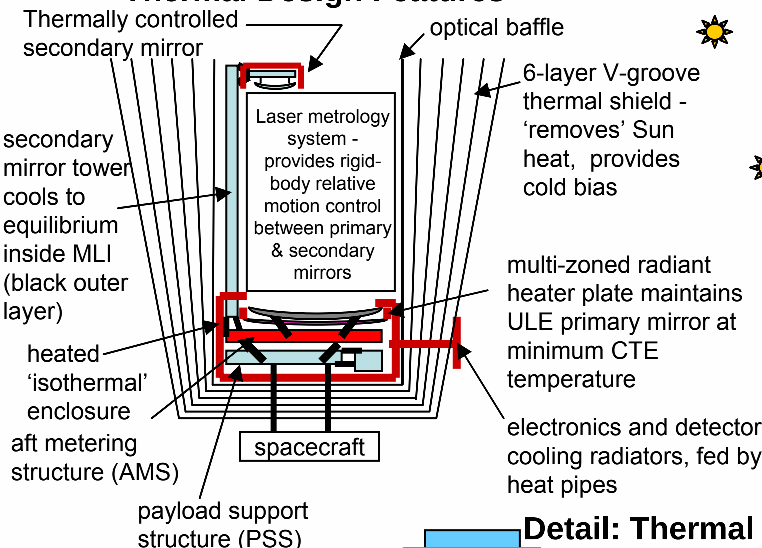

inside-to-out cold biasing provides for precision active thermal control

Field of View and Sun Position

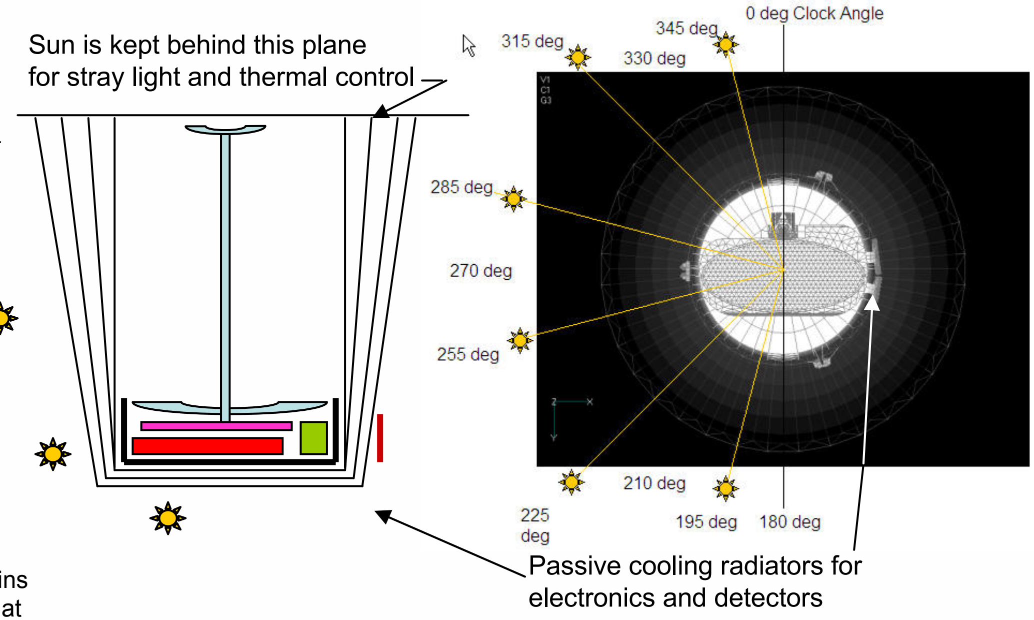

Detail: Thermal Enclosure

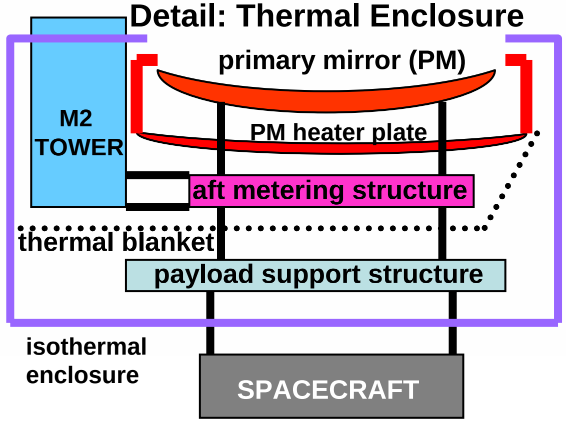

Detail: Electronics (and detector) Concept

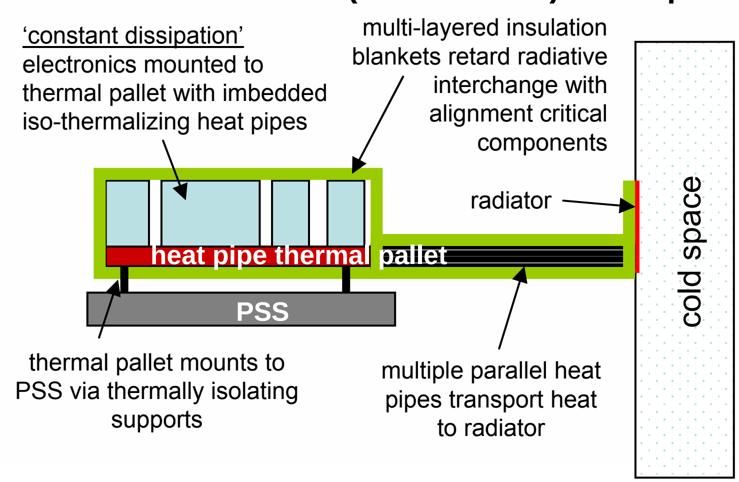

Executive Summary: Modeling Philosophy & Approach

One Design / One Model / One Mesh

- **Design/Analysis configuration control & management**
  - Models represent frozen design & no changes permitted during analysis cycle (as tempting as it may seem)
  - Exercise model thoroughly to understand improvements for next cycle
  - Design configuration managed through common file depository on TPF library w/ enforced documentation & nomenclature
- **One Model / One Mesh**
  - Same model geometry & mesh for all integrated systems analyses and disciplines ("***mid-fidelity model***")
  - Single discipline models may require ***high-fidelity models*** (e.g., PM launch stress), but remains a super-set of the mid-fidelity model
  - Trades analyses conducted separately on ***low-fidelity models*** for quick assessment
  - Optical design model forms basis for CAD/Thermal/Structural models
  - Same mesh reduces modeling errors due to numerical extrapolation & thermal/structural/optical mapping
  - Incorporate Modeling Uncertainty Factor (MUFs) when a credible basis exists (dynamics)

Priorities (in descending order of importance)

1. Estimate system performance & margins relative to the error budget (p.16)
   - Analyses of baseline design under nominal operating conditions
   - Assessments of off nominal design and/or operating conditions
   - Comparative analyses of alternate design options for trade studies p.18
2. Investigate performance sensitivity to driving system design considerations and constraints (p.17)
   - Perturb key design parameters and evaluate perf. improvements
   - Assessments traceable to baseline design models
3. Establish and refine derived key design requirements or constraints for elements, interfaces, and systems (p. 19)

Executive Summary: System Optical Performance Models

- Optical Sensitivity Matrices are created using models that predict contrast performance
- A high fidelity model was developed which includes:
  - An 8th order occulting mask and matching Lyot stop
  - Surface maps on all reflective optics
  - Rigid body motions on all optics up to the occulter
  - A 2DM Michelson WFC architecture
  - Broadband simulations
- Contrast was used as a metric of system performance for three cases:
  - 1.) Surface figure errors only
  - 2.) Surface figure errors with jitter induced by the reaction wheels
  - 3.) Surface figure errors with thermal misalignments
- System contrast performance: simulate performance of SSS in presence of representative static and dynamic system perturbations

Sample 2-D Performance Plots

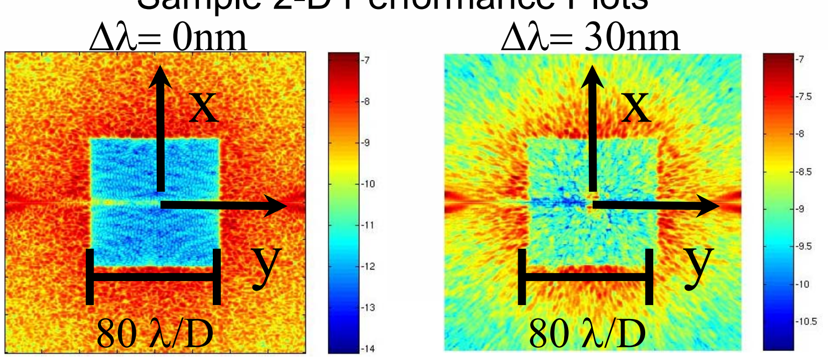

National Aeronautics and Space Administration
Jet Propulsion Laboratory
California Institute of Technology
Goddard Space Flight Center

Executive Summary: Thermal Performance Models and Analysis

Lockheed Martin
Ball Aerospace & Technologies Corp.
Northrop Grumman Space Technology
TC Technology
nightsky systems

TPF Terrestrial Planet Finder

- Evaluated Thermal Tools:
  - TSS/SindaG, TMG, IMOS
- Thermal Model & Run Information is provided
- Performance evaluation: Dither angle from 195° to 225° is worst case
- Evaluated Temperature Control Heater Powers

Dither Angle from 195° to 225° (worst case)

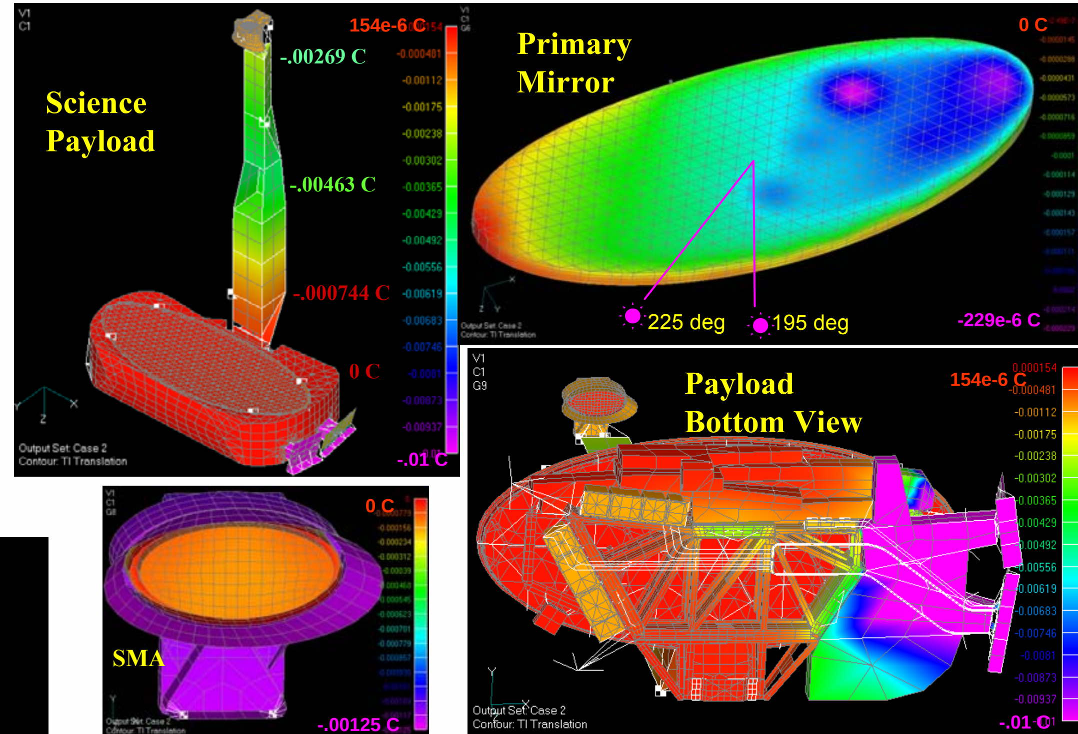

TMG Models

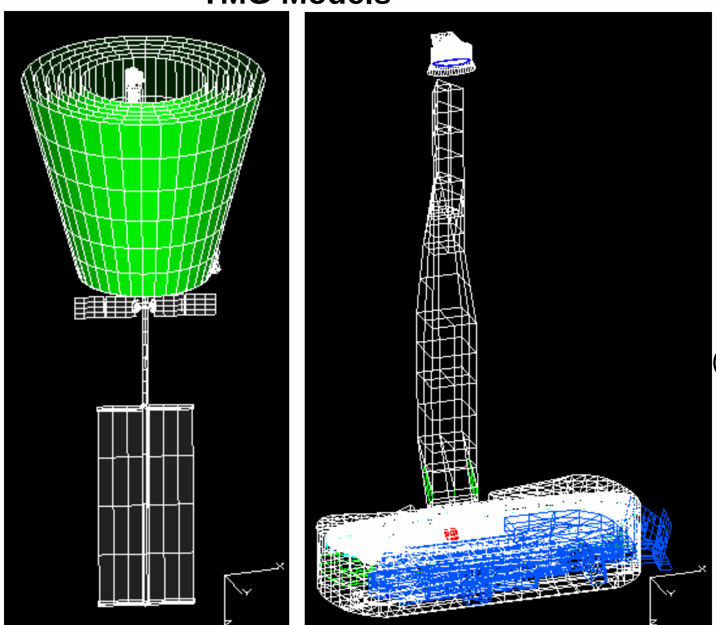

Transient results – all PM nodes, worst case dither

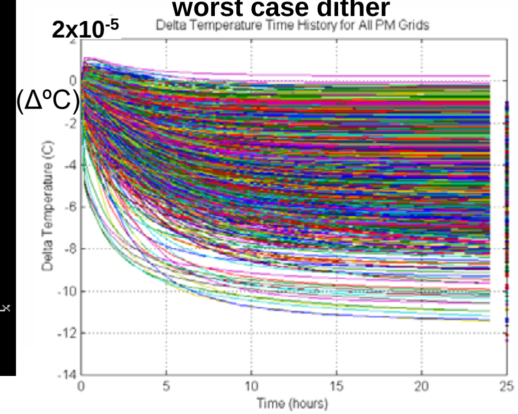

- Conclusions:
  - Even with worst case conditions, appear to be meeting requirements from Error Budget

Executive Summary: Structural Performance Models and Analysis

Lockheed Martin
Ball Aerospace & Technologies Corp.
Northrop Grumman Space Technology
TC Technology
nightsky systems

TPF Terrestrial Planet Finder

- **Currently, WFE's & Rigid Body motions of optics are within the error budget**
  - for thermal disturbance
- **Toolsets work well so far, and are getting better**
  - Looking forward to significant capability increase shortly
  - Lessons-learned: problems encountered & solved (or worked-around)
- **We need to account for CTE variation in PM**
  - Taking CTE variation into account generally results in higher WFEs than assuming uniform CTE
  - Initial calculations in work
- **Primary Mirror front-to-back delta-temperature drives distortion**
  - Focus & Astigmatism are biggest contributors to WFE
- **Design feasibility looks good: no major road-blocks**
  - Keep in mind the many idealizations made so far: more detail modeling to follow

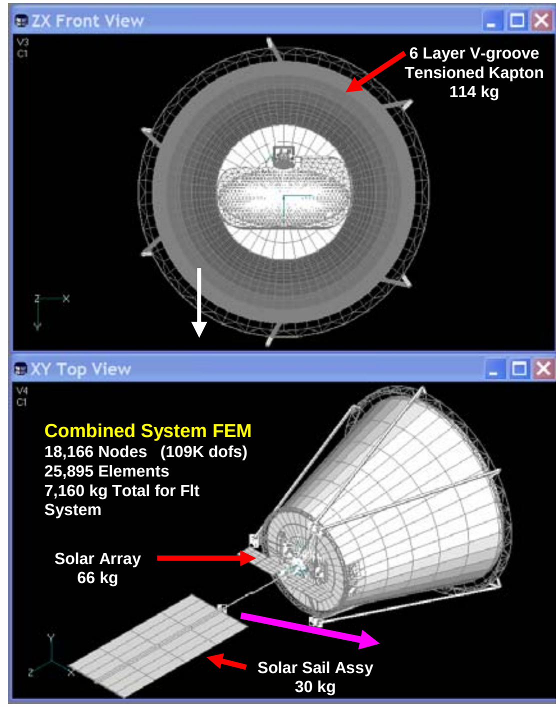

IDEALIZATIONS

- No hinges, latches or fittings modeled
- No temperature dependent properties
- Uniform properties for like materials
- Lumped & smeared masses for non-struct hardware to match mass-list
- Uniform, linearized model of tensioned membranes to capture geom stiffness

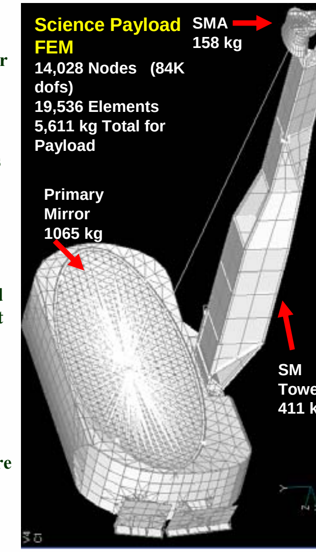

- Mid-Fi PM model captures overall dynamic & thermal distortion, but not local print-thru effects

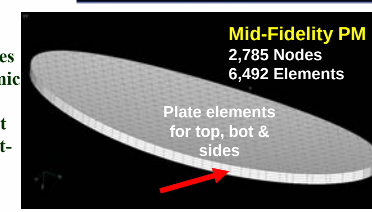

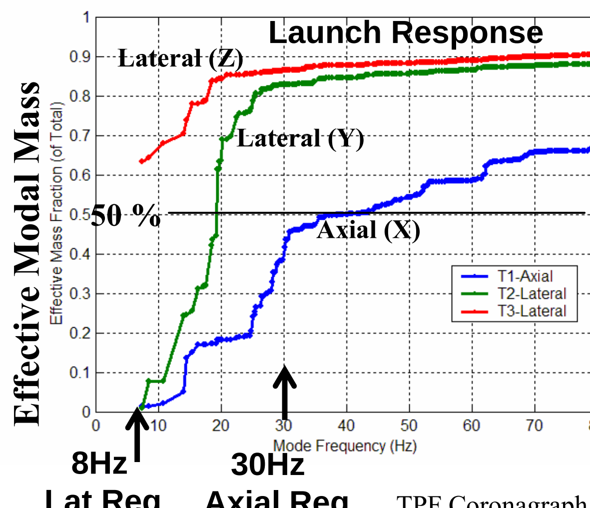

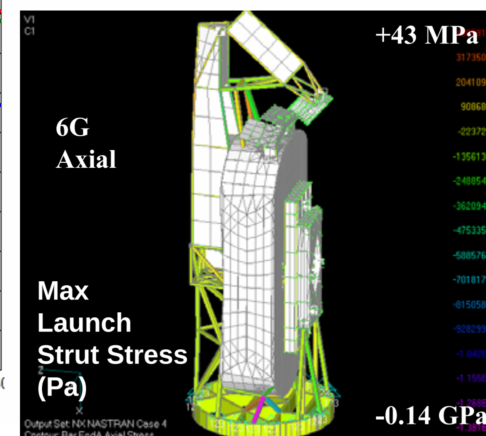

Executive Summary: OTA and PM Structural Performance Models and Analysis

- **The following structural analyses have been performed for the OTA and the PM:**
  - Developed the OTA structural model for use in the TPFC integrated system performance analysis
    - OTA structural model was developed and provided to JPL. The model was used in integrated dynamics and thermal performance analysis. On-orbit dynamics is acceptable for active design, but marginal for passive design. Thermal stability was found to be acceptable.
    - Developed low, mid, and high fidelity structural models of the PM to be used for various structural analyses.
  - Acoustics analysis to estimate load to PM from Delta IV-H fairing
    - AutoSEA analysis performed and estimated a max load of 10 G applied to the PM due to either a metal or composite fairing
  - OTA and PM dynamics
    - First OTA free-free mode was found to be 7.1 Hz, due to tower bending. First mode of the PM with its mount was found to be 20.6 Hz.
  - PM gravity sag for ground testing concern
    - Maximum deflection of the PM with its mount due to 1 G loading applied perpendicular to the mirror was found to be .473 mm. Optical performance due to gravity sag was also predicted.
  - PM launch load stress analysis
    - The analysis showed that the PM has a negative margin of safety for the flight baseline 1 design concept. However, an option to obtain a positive margin of safety in the PM is to add weight of 414 kg as well as 8 launch locks. Still investigating additional design alternatives.

- **Future structural analyses for the FB1 design of the OTA and the PM include:**
  - Weight optimization of the PM, AMS, and SMA.
  - Sensitivity to PM mount design, location, and stiffness
  - PM Quilting Effects (PM deformation due to thermal loads)
  - Stiffness analysis of SM tower due to stiffness of hinges/latches
  - PM open-back versus closed-back structural/thermal analysis.

- **The results of all these structural analyses will help in developing the design concept for the PM and OTA for the flight baseline 2 analyses.**

Executive Summary: ACS Analysis

- PCS operational concept and point designs defined
  - Flight heritage sensors, actuators, and control systems
  - Passive and active isolation point designs for suppression of RW disturbance
    - Passive design based on Honeywell D-Struts
    - Active based on Lockheed Martin Disturbance Free Payload
- Active system meets requirements
  - Significant margin (3-4 decades) for jitter under reaction wheel disturbance
  - Analyzed design options that "spend" margin to reduce cost
    - Hard mounted reaction wheels, payload pointing only (no actively controlled mirrors) for mask centration
- Passive system currently does not meet requirements
  - Design modifications that provide positive margin have been identified
    - Passive structural damping treatments, increased image control bandwidth
- Sensor/actuator noise contributions to jitter are being analyzed
  - Secondary Mirror position jitter is the largest source for the passive isolator design
- Work required to close out FB1
  - Analyze noise contributions to jitter for the active isolation design
  - Implement passive isolation design modifications and show positive margin
  - Mitigate Secondary Mirror noise contribution
  - Finalize recommendations for FB 2 design cycle

Executive Summary: Modeling Results

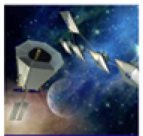

- Status: middle of cycle 2
  - Minimum Mission Concept was Cycle 1
  - Flight Baseline 1 is Cycle 2
- Initial analysis shows generally good environmental control with some issues
  - Primary Mirror launch loads
  - Mass
- These issues will be addressed as Cycle 2 is finished to guide Cycle 3
- In addition, for Cycle 3:
  - Optical Performance Modeling highlighted need to refine the design of the starlight suppression system
  - Need to re-evaluate primary mirror assembly

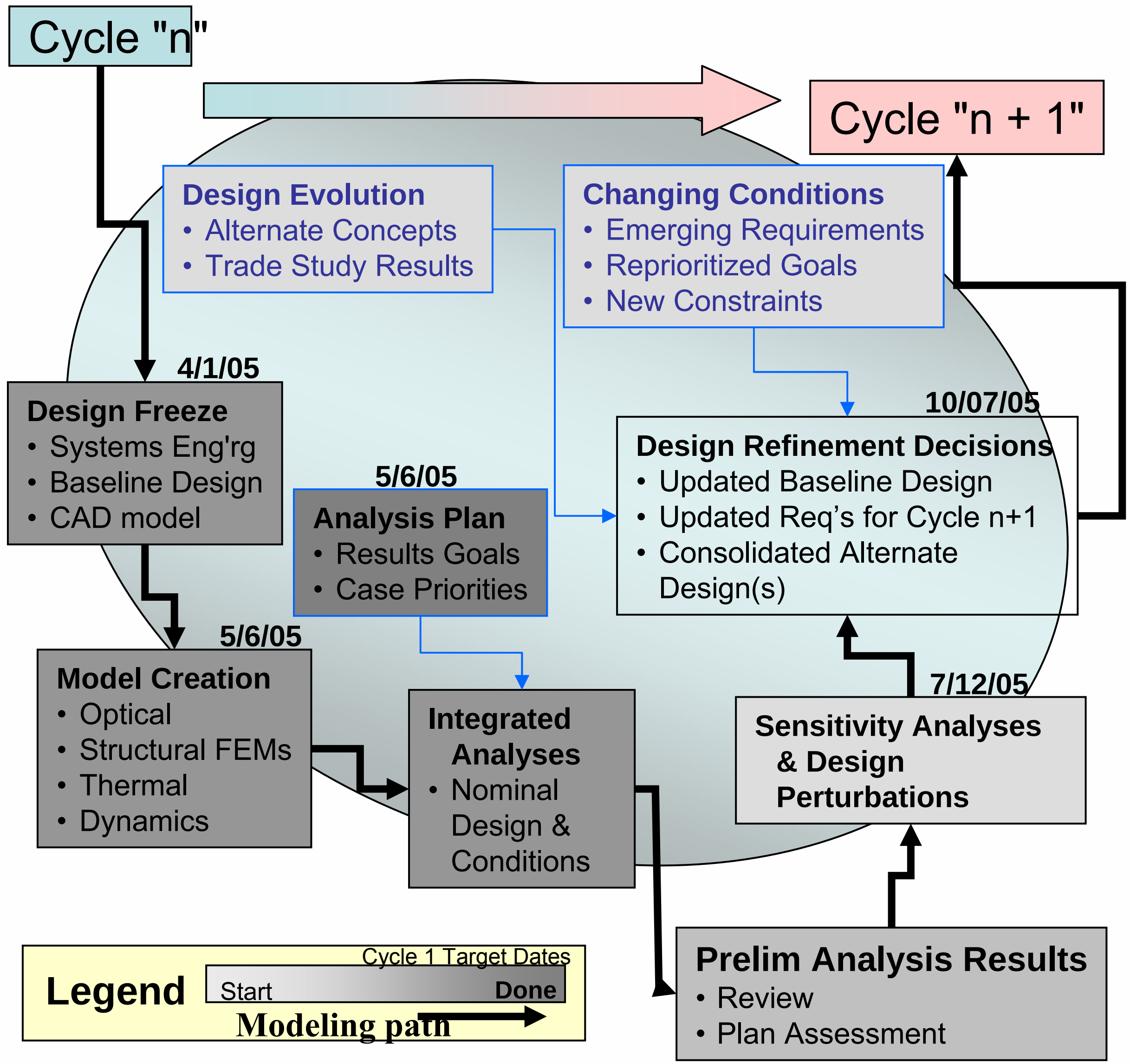

Executive Summary: Current trade studies for Flight Baseline 2 Cycle

Lockheed Martin
Ball Aerospace & Technologies Corp.
Northrop Grumman Space Technology
TC Technology
nightsky systems

TPF Terrestrial Planet Finder

PCS Trade Studies

- Reaction Wheels Trades
  - Location
  - Size
- Fine Guidance Sensor (FGS) design
  - Pick-off Location
  - FSM design (bandwidth, range of motion,)
  - FGS sensor model
- Payload Acquisition Camera Trade
  - Location
  - View of sky
  - Dynamic stability
- Active isolation
  - Roll sensor trade
  - Advantage of eliminating SM control system and possibly FGM control loop
- Solar Sail disturbance on S/C
- Map disturbances to contrast budget (provided preliminary results)
  - provides method directly looking at disturbance influences

Mass Reduction Trade Study

- Launch mass margin is below JPL suggested margin for entry into Phase B
  - –Self imposed goal >35% for pre-Phase A
- Many solutions identified for FB2 will reduce mass
- Exploring options to understand
  - – load paths & volumetric constraints
- Likely to reduce FB2 launch mass margin to >35%

Primary Mirror Shape Trade Study

- Pros
  - –TPFC can operate 2x faster!
  - –Narrower short axis is more enabling w.r.t. mechanical design
- Neutral
  - –Manufacturability
  - –Gravity Sag
- Cons
  - –2-4x more sensitive to aberrations
  - –Heavier PM
    - 8x2.8m would be about the same as baseline
- To Do
  - –Evaluate net efficiency versus aberration sensitivity impact on error budget and completeness

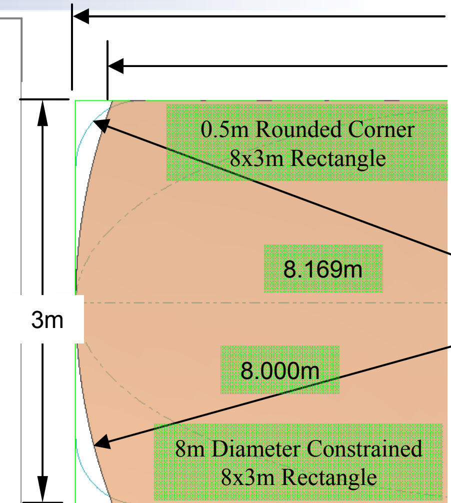

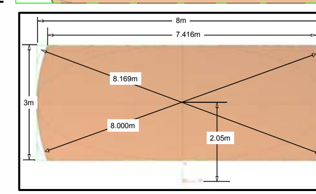

Open Back/Closed Back Trade Study

- Open back Primary Mirror configuration may have significant thermal performance advantage due to reduced thermal gradient through the mirror
- High Fidelity thermal models of two segments will be used to explore and compare thermal performance

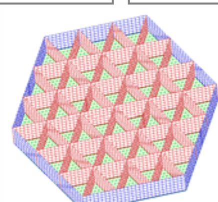

Open Back Segment Model

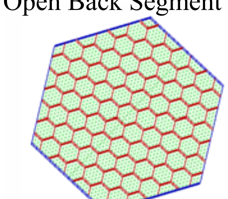

Closed Back Segment Model
(Rear Facesheet Removed)

Sun Shade Trade Study

- The 'sugarscoop' may be:
  - Easier to deploy
  - Perform better
- Performing top-level thermal comparison between the 'sugarscoop' and baseline conical configuration
- Simple models include:
  - sunshield
  - circular, continuous baffle
  - circular primary mirror
  - black boundary behind PM

'sugarscoop' shields flare circumferentially and axially, implying better rejection of perturbing solar energy

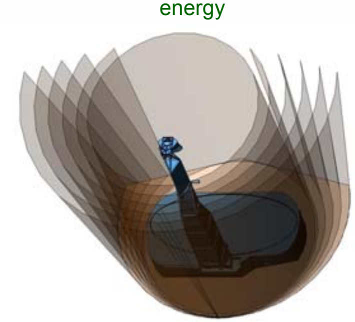

'sugarscoop' idea originated:
Northrop Grumman Astro Research

National Aeronautics and Space Administration
Jet Propulsion Laboratory
California Institute of Technology

Goddard Space Flight Center

TPF Terrestrial Planet Finder

Introduction
TPF Coronagraph
Flight Baseline 1
Design Presentation

Virginia Ford

Contributors: Tim Ho, Zeke Martinez, Richard Key, Jim Fanson

11-12 July 2005

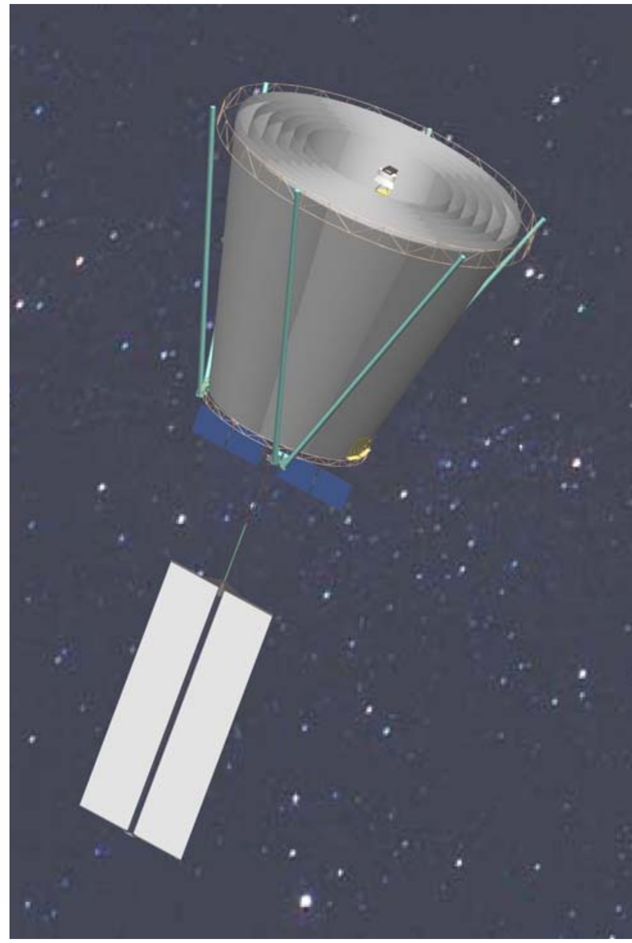

- TPF Coronagraph Design Team includes a nation-wide set of engineers from:
  - Jet Propulsion Laboratory
  - Goddard Space Flight Center
  - Ball Aerospace & Technology Corporation
  - Lockheed Martin
  - Northrop Grumman Corporation
  - with consultants from:
    - o TC Technology
    - o Nightsky Systems
    - o Swales
- This design presentation covers
  - Conceptual design developed for the first flight baseline mission
  - Modeling and analysis that has been done to understand the mission performance
  - Is intended to present status – not completed analysis

National Aeronautics and Space Administration
Jet Propulsion Laboratory
California Institute of Technology
Goddard Space Flight Center

Agenda

TPF Coronagraph FB1 Design Presentation
Room 410, Spitzer Science Center
California Institute of Technology, 1200 E. California Blvd, Pasadena
videocon: http://meetingplace.jpl.nasa.gov/a/86d05ace1a74dae63efc48e714275191
TPF Library location: https://tpf-lib.jpl.nasa.gov/tpf-lib/dscgi/ds.py/View/Collection-3137

Start Time	Topic	Presenter
07/11/05		
7:30 AM	**COFFEE**	
8:00 AM	Welcome	Fanson
8:10 AM	Introduction	Ford
8:35 AM	Mission Description	Ford
9:00 AM	Summary of Science Performance	Hunyadi
9:15 AM	System Error Budget - description and plans	Shaklan
10:00 AM	**BREAK**	
10:15 AM	System Optical Design	Shaklan/ Ohl
11:15 AM	System Pointing Control Architecture & Design	Alexander
12:00 PM	**LUNCH**	
1:15 PM	System Mechanical Design & Configuration	Ho
2:15 PM	OTA Mechanical Desgin & Configuration	Engler
2:45 PM	System Thermal Architecture & Design	Cafferty
3:30 PM	**BREAK**	
3:45 PM	OTA Thermal Architecture & Design	Fantano
4:15 PM	I&T Plans	Martino
5:00 PM	General Discussion & Feedback	All
7:00 PM	**GROUP DINNER**	

07/12/05		
8:00 AM	**BREAKFAST DISCUSSIONS**	All
9:30 AM	Modeling Introduction & Plans	Levine
10:00 AM	System Optical Models, Performance Results & Future Studies	Palacios
10:45 AM	System Thermal Models, Performance Results & Future Studies	Eug
11:30 AM	**LUNCH**	
12:45 PM	System Structural Models, Performance Results & Future Studies	Kissil
1:30 PM	Primary Mirror Structural Models, Performance Results & Future OTA Studies	Irish
2:00 PM	**BREAK**	
2:15 PM	ACS Models, Performance Results & Future Studies	Blaurock
3:00 PM	Summary of Analysis results & impact on future design	Levine
3:15 PM	Proposed FB2 configuration changes: ACS trade studies	Alexander
3:30 PM	Proposed FB2 configuration changes: primary mirror shape and structure trade study	Green
3:50 PM	Proposed FB2 configuration changes: sunshade trade study	Cafferty
4:10 PM	Proposed FB2 configuration changes: mass reduction trade studies	Ho/Engler
4:30 PM	Proposed FB2 configuration changes: open back vs closed back primary mirror structure	Fantano
4:50 PM	General Discussion & Feedback	All
5:30 PM	**ADJOURN**	

All the presentation files are located in the TPF library in collection 3137

The index of this document is based on the presentation sequence:

"Pre-Registered" Attendees (approx.)

TPF Terrestrial Planet Finder

IN PERSON				VIA TELECON	
1	Andrew Smith	27	Larry Dewell	1	Alice Liu
2	Andy Kissil	28	Lou Fantano	2	Ann Merwarth
3	Andy Kuhnert	29	Luis Marchant	3	Daniel Polis
4	Bala Balasubramanian	30	Marie Levine	4	David Mozurkewich
5	Bill Reeve	31	Mark Marley (Tues)	5	Ed Groth
6	Bob Brown	32	Marty Levine (AM)	6	Edward Groth
7	Bob Woodruff	33	Michael Krim	7	Gary Matthews
8	Brent Abbott	34	Neil Martin	8	Gary Mosier
9	Carl Blaurock	35	Paul Atcheson	9	Hiedi Hammel
10	Charley Noecker	36	Peter Feher	10	Jeremy Kasdin
11	Chuck Bowers	37	Peter Halverson	11	Joe Howard
12	Chuck Engler	38	Ray Ohl	12	Lia LaPiana
13	Dave Content	39	Richard Key	13	Manuel Quijada
14	Dave Palacios	40	Rob Egerman	14	Marty Levine (PM)
15	Dick Dyer	41	Roger Angel (Tues)	15	Michael Werner
16	Dominick Tennerelli	42	Sally Heap	16	Rick Lyon
17	Don Lindler	43	Sandra Irish	17	Roger Angel
18	Eug Kwack	44	Sarah Hunyadi	18	Roger Brissenden
19	Fernando Tolivar	45	Scott Horner	19	Ruth Carter
20	Garth Illingworth	46	Steve Kilston	20	Sara Seager
21	Harry Ferguson	47	Stuart Shaklan	21	Steve Ridgeway
22	Jim Alexander	48	Terry Cafferty	22	Steve Unwin
23	Jim Fanson	49	Tim Ho	23	Tom Williams
24	Jim Kasting	50	Tony Martino	24	Vern Weyers
25	Joe Green	51	Virginia Ford		
26	John Lou				

- The final attendance list included 62 people from NASA, JPL, Industry and Universities
- The number of people attending via telecon were not counted

TPF Coronagraph System Objectives

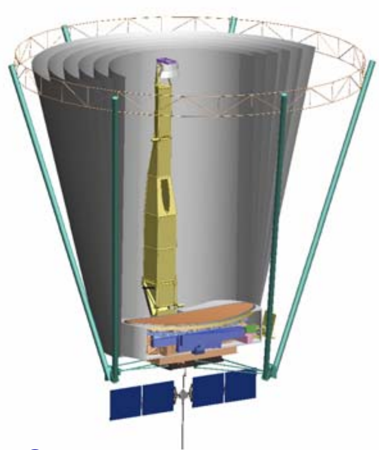

What? TPF Coronagraph Observatory

- Large very fine primary mirror
- Wave front sensing and control with Deformable Mirror and camera
- Starlight suppression – baseline via focal and pupil plane masks and stops
- Control of diffraction and polarization effects
- Very stable structural and thermal control
- Very accurate modeling of wavefront propagation, component effects, structural and thermal performance
- Integral Field Spectrometer
- Additional Astrophysics instruments

Why?

- By performing wavefront correction, the scatter and diffraction from the classic telescope can be adequately controlled so that faint light from a planet next to a star can be detected
- The light from a detected planet and re-visits can validate that a planet is found and be evaluated for spectral bio-signatures
- Fine quality telescope and imaging will be used for other astronomy

How?

- Develop and improve state-of-the art technology (test bed, DM, Mask & Stops, modeling tools)
- Model performance of components and verify through test bed experiments
- Fabricate large demonstration mirror to develop road map to meet TPF primary mirror reqts
- Analyze, develop and evaluate coronagraphic architectures and perform trades that lead to selection of optimum flight mission design

- This is a brief summary of the Terrestrial Planet Finder Coronagraph Project objectives.
  - Science Goals:
    - The primary goal is to detect Earth-like planets around other stars and measure the spectrum of that light to determine if the planets support life
    - A secondary goal is to use the required fine telescope for other astronomy
  - Technology Challenges:
    - We are looking for planets in the host star's habitable zone: where liquid water exists
      - This is temperature dependent – the zone radius and expanse is related to the brightness of the host star
      - The habitable zone is very close to the host star – much closer than any thing we have observed to date with telescopes
    - Earth-like planets are small and rocky – not gas giants like Jupiter or Saturn
      - They will be faint compared to the host star (brightness difference or contrast of 10^{-10})
      - No planets have yet been detected that meet these criterion
  - Technology Investigations:
    - A very specially-built telescope will be required that has adequate mirror quality and an active wavefront correction scheme
    - Starlight suppression technology is required beyond the state-of-the art to reduce the starlight by 10^{-10} so that the planet can be detected

TPF Coronagraph Current Life Cycle Schedule

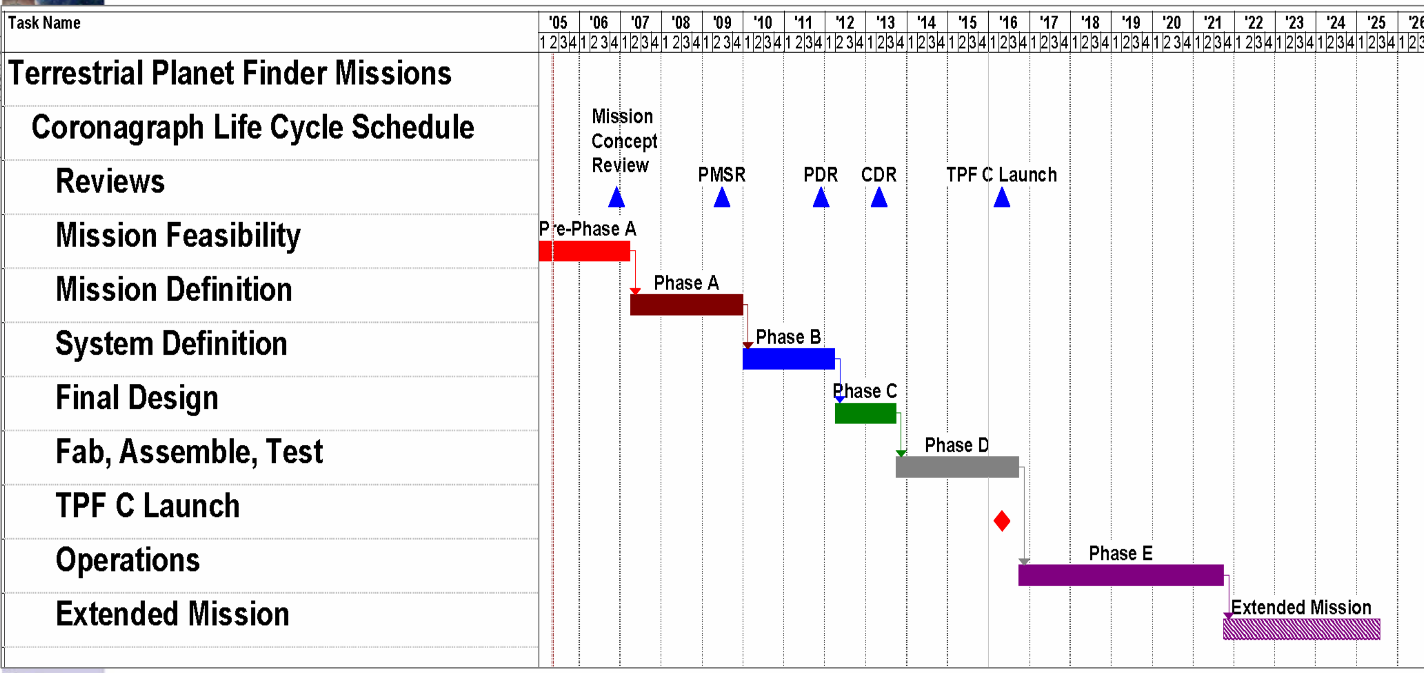

TPF

- TPF-C Schedule based on the NASA 2005 Proposed Operating Plan submission
- Launch in 2016
- Enter Phase A in 1st quarter 2007

National Aeronautics and Space Administration
Jet Propulsion Laboratory
California Institute of Technology
Goddard Space Flight Center

Entire TPF-C Effort
Pre-Phase A Schedule based on 2005 POP Budget

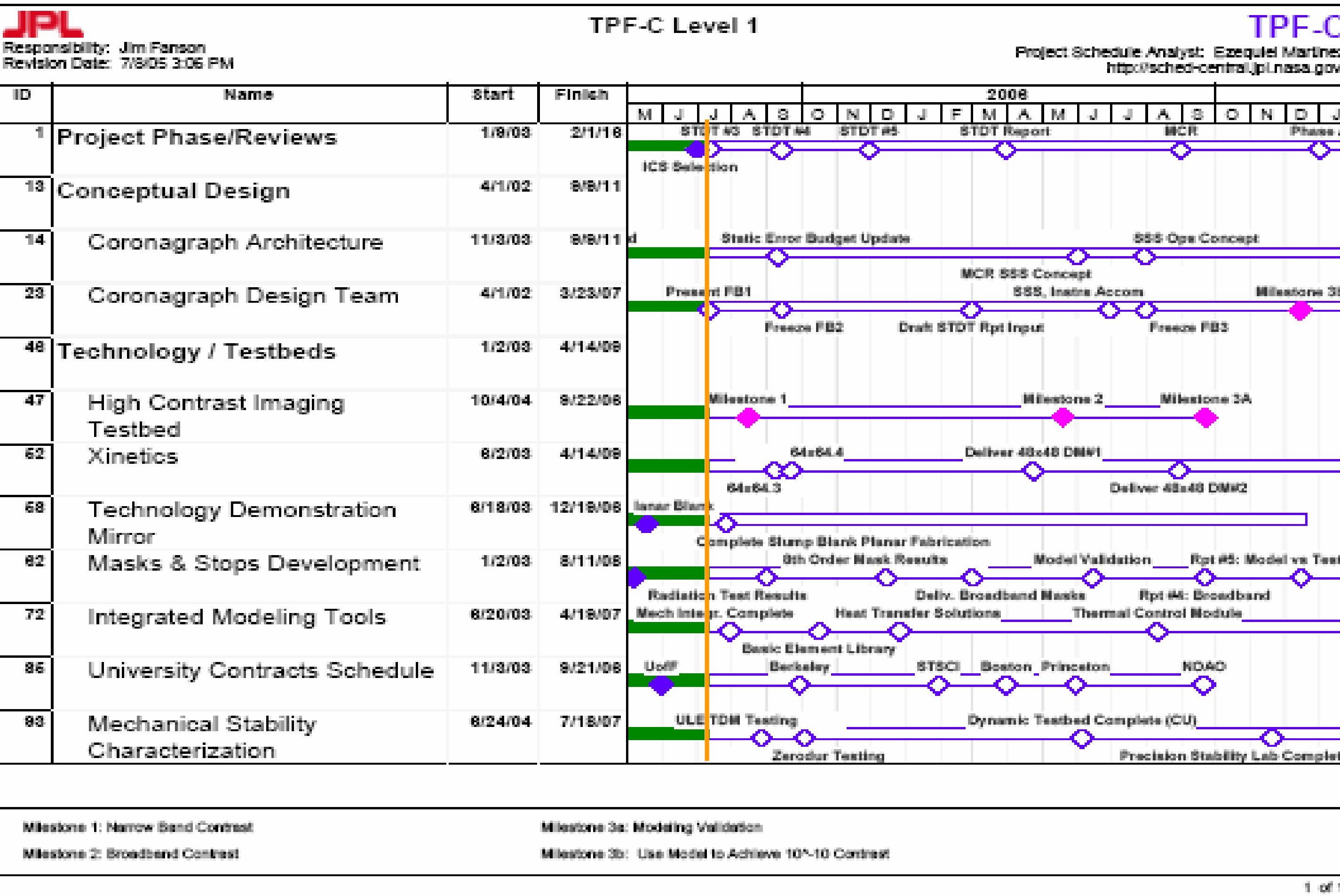

- **Four ◆ symbols indicate the critical milestones required to get into Phase A**
- **Milestone #1: Starlight Suppression**

Demonstrate that the High Contrast Imaging Testbed (HCIT) is capable of achieving a baseline contrast of 1x10-9 (goal 1x10-10) at a 4 l/D inner working angle, at l=785 nm and stable for at least one hour.

Planned Completion Date: Q3 FY05

- **Milestone #2: Broadband Starlight Suppression**

Demonstrate that the HCIT is capable of achieving a baseline contrast of 1x10-9 (goal 1x10-10) at a 4 l/D inner working angle over a 60 nm bandpass (goal 100 nm) with the center wavelength in the range of 0.5 µm to 0.8 µm.

Planned Completion Date: Q3 FY06

- **Milestone #3: Model Validation and Performance Feasibility**

3A: Demonstrate that starlight suppression performance predictions from high-fidelity optical models of the HCIT, utilizing measured data on specific testbed components, are consistent with actual measured results on the testbed. Correlation of model predictions with experimental testbed results validates models at a baseline contrast ratio of better than 1x10-9 (goal 1x10-10) over a 60 nm bandwidth.

Planned Completion Date: Q4 FY06

3B: Demonstrate, using the modeling approach validated against the HCIT performance combined with appropriate telescope models and the current mission error budget, that TPF-C could achieve a baseline contrast of 1x10-10 over the required optical bandwidth necessary for detecting Earth-like planets, characterizing their properties and assessing habitability.

Planned Completion Date: Q1 FY07

National Aeronautics and Space Administration
Jet Propulsion Laboratory
California Institute of Technology
Goddard Space Flight Center

TPF-C Design Cycle Schedule

	end date
Project Phases	
Pre Phase A	1/3/2007
Phase A	1/3/2010
Project Reviews and Meetings	
SWG/TIM	
STDT	
Mission Concept Review	9/15/2006
Major Project Milestones	
Design Concept Cycles	
Minimum Mission Design Concept	
Design Concept Development	1/15/2004
Freeze MM Baseline	1/20/2004
MM Modeling and Analysis	4/9/2004
Minimum Mission Report	4/22/2004
Flight Baseline 1 Design Concept	
Design Concept Development	1/20/2005
Freeze FB1 Baseline	1/20/2005
FB1 Modeling and Analysis	10/7/2005
Design Presentation	7/11/2005
Flight Baseline 2 Design Concept	
Design Concept Development	10/7/2005
Freeze FB2 Baseline	10/7/2005
FB2 Modeling and Analysis	2/15/2006
Mission Description Draft Inputs	2/15/2006
Flight Baseline 3 Design Concept	
Design Concept Development	7/28/2006
Freeze FB3 Baseline	7/28/2006
FB3 Modeling and Analysis	12/10/2006

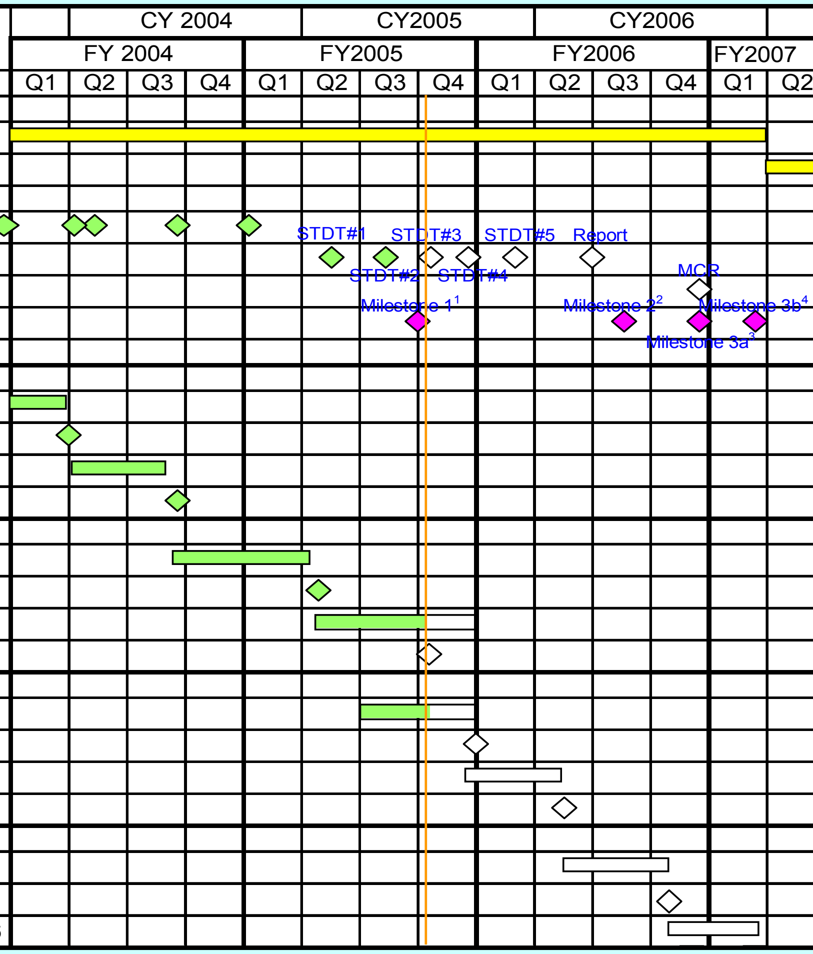

- Prior to entry into Phase A, we plan to conduct 4 design cycles:
  - Minimum Mission Design Concept (completed in 2004)
    - o Addressed minimum science requirements established in 2003
    - o Attempted to develop, model and analyze a system that could produce contrast adequate to find and characterize planets around 35 nearby stars
      - ➢Inner working angle 3λ/D, 6mx3.5m primary mirror, full conic sun-shade
      - ➢Full report in TPF library
        - https://tpf-lib.jpl.nasa.gov/tpf-lib/dscgi/ds.py/View/Collection-2410
  - Flight Baseline 1 Concept (FB1)
    - o Address updated Science Requirements – Flight Baseline
    - o Addressed systems flight issues
    - o Reduced system tolerances by adopting 4λ/D inner working angle, 6mx3.5m primary mirror, 8th order occulting mask
    - o Included heater hardware but not heater control
    - o Cursory definition of flight components requiring less technology development
  - Flight Baseline 2 Concept (FB2)
    - o Add heater control, refine design
    - o Add instrument accommodation detail to enable preparation of AO for instrument selection
  - Flight Baseline 3 Concept (FB3)
    - o Add instrument detail
    - o Refine design
    - o Meet milestone 3B

Goal for TPF-C Design Concept Cycles

Minimum Mission Concept
- Develop modeling and analysis process to enable contrast performance assessment with on-orbit thermal and dynamic perturbations
- Evaluate stability requirements and feasibility to meet them
- Cursory launch loads analysis

Cycle 1 – Flight Baseline 1 Design Concept (FB1)
- More Detailed Design
  - Include placeholder instruments, payload passive thermal control, Secondary Mirror assembly details, sun shade details, instruments, passive thermal control of payload
  - Larger, more difficult primary mirror with more detailed mounting
- Modeling advancement
  - Advance contrast performance modeling
  - Improve understanding of thermal and dynamic perturbations and model issues
- Launch loads analysis
- Determine thermal sensitivity leading towards active thermal control system design

Cycle 2 – Flight Baseline 2 Design Concept (FB2)
- Implement active thermal control
- Understand instrument accommodation issues
- Refine observatory design based on FB1 results and comments
- Reassess and advance modeling and contrast performance
- Prepare for AO for instrument selection

Cycle 3 - Flight Baseline 3 Design Concept (FB3)
- Meet contrast performance goal for Milestone 3b
- Evaluate and change concept and models as needed
- Update instrument accommodations and details

MINIMUM MISSION CONCEPT

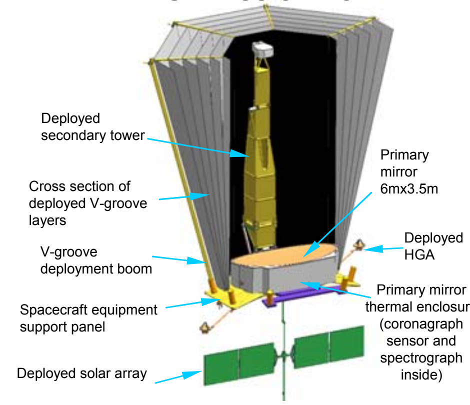

FLIGHT BASELINE 1 CONCEPT

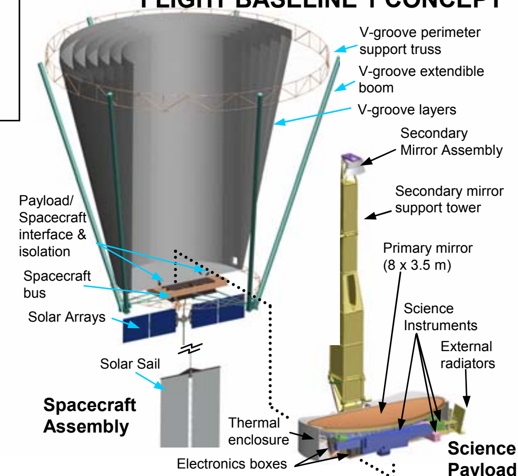

- Green coloring indicates what is completed
- White shows what is upcoming
- Minimum Mission Concept picture and Flight Baseline 1 Concept picture show some of the features and differences of the design concept as it has developed

Meeting Intended Results

- Inform TPF-C community of our status
  - Full two days worth of presentation
  - Some discussion time planned for each section
  - Comment forms are supplied to capture comments and topics for extended discussion
- Do not expect a flight-ready design concept
  - In pre-phase A need to work on advanced concepts and establish feasibility
  - We have limited resources:
    - Haven't spent much on standard engineering areas (our judgment)
      - Orbit, Launch, Spacecraft detail
      - I&T except in the telescope area
    - Some areas just aren't well covered
      - Software Definition
      - Ground support definition
- Do not expect to see a completed analysis
  - We are in final stages of FB1 analysis portion
  - Work is not complete but detailed schedule and plans are in place
  - Status is being presented
- Receive comments that will guide design choices for Flight Baseline 2
  - Please use comment forms to:
    - Capture your input correctly
    - Reduce extended discussion – keep to our schedule
  - FB2 choices are not finalized – we intend to use the comments we receive in our trade studies

Mission Description

Virginia Ford

Contributors: Doug Lisman, Peter Feher, Sarah Hunyadi, Architecture and Design Team

11-12 July 2005

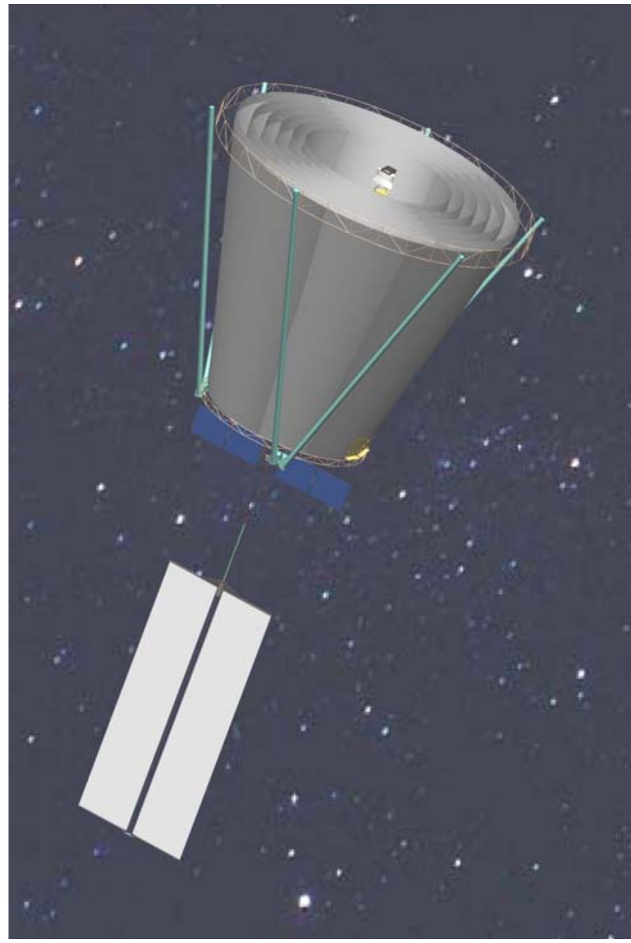

- Executive Summary:
  - Choices have been made for the mission and spacecraft that form the basis around which the observatory concept has been developed
  - The selected orbit is a Lissajous halo orbit around the L2 point
  - The field of regard and target star observation scenario define the limits of the thermal environment of the observatory
  - The resulting observatory concept is shown in a schematic defining the relationships between components

Mission and Spacecraft Choices for FB1

Lisman and Feher

	Parameter	Value	Comments
Mission	Duration required/goal	5/10 years	Resources for 10 years
	Orbit	L2	Direct trajectory
	Field of Regard	Sun angles > 95°	Potential earth/moon/planet constraints
	Required ΔV	60 m/s	
	Launch Energy (C_3)	-0.69 km^2/s^2	
	Launch Vehicle	EELV	
	Launch Fairing	5 m diameter	limits primary mirror short axis to ~3.5 m
	Launch Mass	9200 kg	
	Time to reach operating orbit	109 days	
	Ground Station	34m DSN Ka-Band	
	Downlink Data Rate	64Mbps	
Spacecraft	EOL Power	3kW	provided by solar arrays
	Reaction Wheels	6 Ithaco- E	
	Propellant	242 kg Hydrazine	
	Thrusters	12 20N	
	Hi Rate Downlink Frequency	Ka-Band	avg duration 2.5 hours per day
	Engineering Downlink Frequency	X-Band	
	Uplink Frequency	X-Band	
	Transmitter Power	50W	
	Hi Gain Antenna	43dB	0.5m patch array

- The table presents the choices for mission and spacecraft that create the framework of the Flight Baseline 1 design configuration
- The mission is based on orbiting around the sun in a Lissajous halo orbit around the L2 point

FB1 Estimated Mass

Lisman and Feher

Component	**Mass Estimate (kg)**	**% of Total Launch Mass**
Payload	5540	
Telescope	3440	43.5
Payload Support Subsystem	1508	19.1
Starlight Suppression Subsystem	412	5.2
Planet Detection Camera	10	0.13
Planet Characterization Spectrometer	20	0.3
General Astrophysics Instrument	150	1.9
Spacecraft	2374	30.0
Total Launch Mass	7914	
Launch Vehicle Capability	9200	
Launch Margin	**1336**	
Launch Margin (%)*	**14.4**	

Note: there is an upcoming presentation on mass reduction trade studies for FB2

*Defined as (LV Capability-Total Estimate)/Launch Capability

- This table presents the mass results from the CAD model of the FB1 concept
- Some margin is included in estimates for payload and telescope
- The desired launch margin percentage is 40% - analysis studies are in work to achieve this margin

FB1 Estimated Power Usage

Lisman and Feher

	Power Estimate (W)	% of Total Power
Payload	1049	51.2
Telescope including thermal control	664	32.4
Payload System Electronics and thermal control	156	7.6
Starlight Suppression Subsystem	87	4.2
Planet Detection Camera	2	0.1
Planet Characterization Spectrometer	40	2.0
General Astrophysics Instrument	100	4.9
Spacecraft	1000	48.8
Total Power	2049	
Available EOL Power	3000	
Power Margin (W)	**951**	
Power Margin (%)*	**32**	

*Defined as (Available Power-Total Estimate)/Available Power

- This table presents estimated electronic power estimates for FB1
- The desired power margin percentage is greater than 30%

FB1 Observing Scenario

Observation of each target star

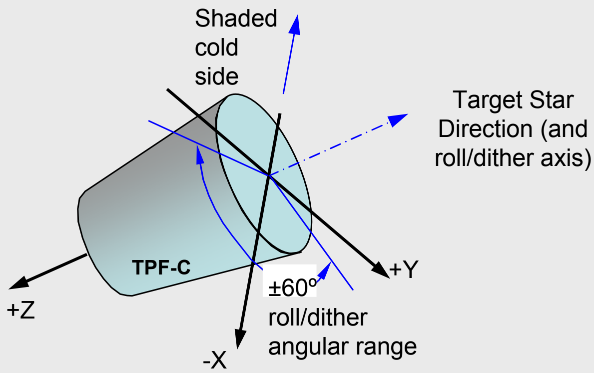

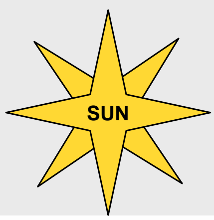

Observatory Field of Regard – Nearly full anti-sun semi-hemisphere

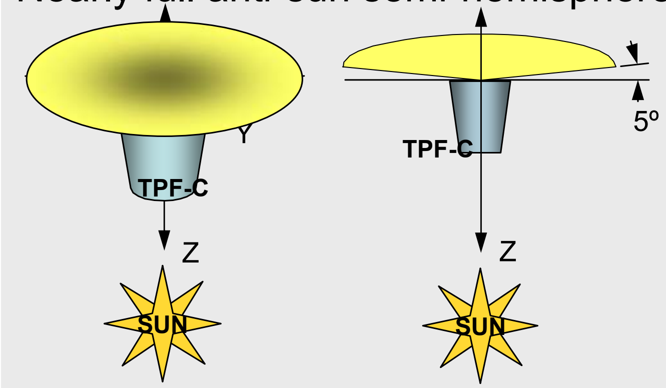

Discovery Scenario:

1. Acquire target star
2. Stabilize dynamics and collect light
3. Using Adaptive Optics, suppress star light
4. Dither 30 degrees
5. Stabilize dynamics and collect light
6. Subtract images
7. Roll to next 60 degree orientation
8. Repeat 2 through 6 two times

- Observatory Field of Regard:
  - The observatory is designed to examine stars in nearly the entire anti-sun semi hemisphere – a 5º margin is included. The field of regard includes all stars located in the cone defined as greater than or equal to 95º away from the sun. As the observatory travels around the sun, this field-of-regard will sweep the entire sphere of the universe, allowing observation of all star targets of interest during nearly 5 months of the year.
- Observation of each target star:
  - . During each star observation, the observatory will point at a star target. Once the dynamics are stabilized, the observatory will collect light. Using adaptive optics, the wavefront errors will be reduced until the starlight is suppressed adequately and an image will be taken. Next the observatory will "dither" about its pointing axis by 30 degrees. Once the dynamics are stabilized, the observatory will take an image in this new position. This image will be subtracted from the previous image to eliminate residual light scattered from the observatory (which will all move with the dither). Any planets present would then be detectable. Because the primary mirror is oblong, it is most sensitive along its long axis. In order to completely study the habitable zone around a star, the long axis has to be rotated to positions that are ±60º away from the starting point. This is accomplished by a "roll" along the pointing axis. At each new roll position, the adaptive optics are reset and then the image gathering is repeated, including the dither. With a 30º dither around 60º roll positions, the total angular rotation around the target direction axis is ±75º.
- The Field of Regard and target star Observation scenario create the thermal environment constraints of FB1.

Payload Mechanical Interfaces

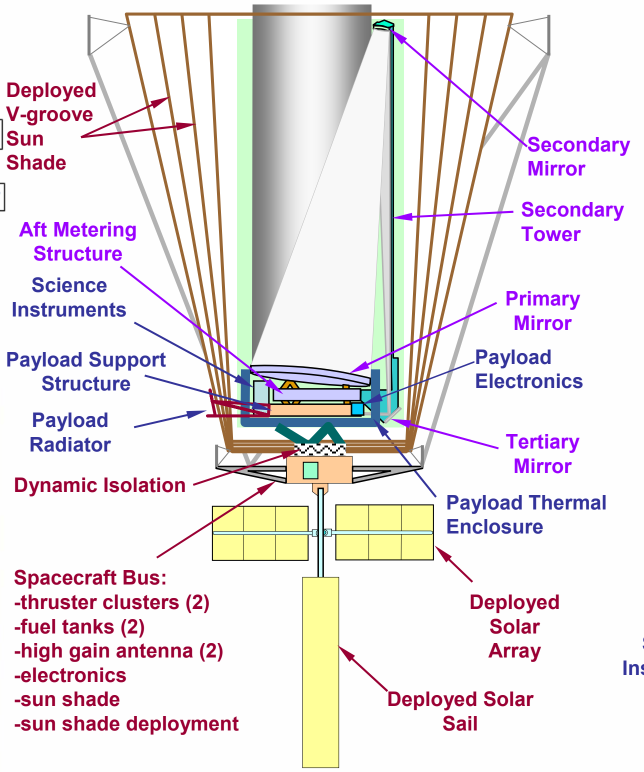

KEY
Spacecraft
Telescope
Other Payload

- Telescope
  - Primary, Secondary and Tertiary Mirror Assemblies
  - Secondary Mirror Tower
  - Aft Metering Structure
  - Thermal control hardware
  - Laser Metrology
- Payload Excluding Telescope
  - Structure mounting payload to Spacecraft through thermal and dynamic isolation components
  - Starlight Suppression System
  - Science Instruments
  - Thermal control components- heat pipes, radiators, Isothermal enclosure
  - Payload Electronics
- Spacecraft
  - Navigation components
    - Thrusters, Reaction Wheels, Solar sail, Fuel tanks
  - Communication components
  - Power system (solar panels)
  - Electronics
  - Sun shade

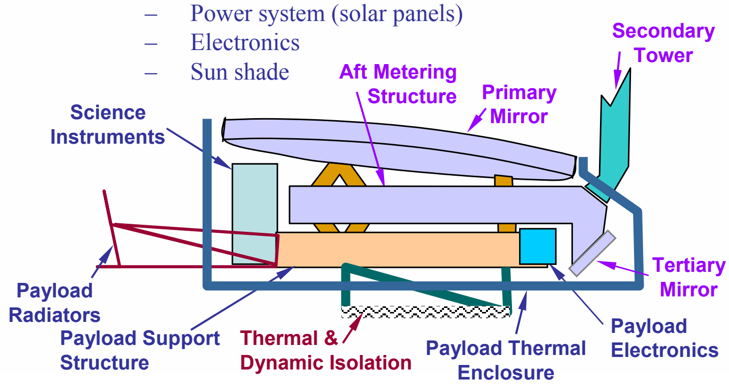

Terrestrial Planet Finder
TPF

- Schematic of FB1
  - Spacecraft:
    - o Sunshade:
      - ➢ Large deployable conic shaped v-groove layers which insulate the payload from the changing sun angles during the observational scenarios
      - ➢ Maximizes the opportunity to view target stars multiple times during one year so that planets will have time to orbit into a favorable position out from behind the star.
      - ➢ Structurally attached to the spacecraft through deployable arms and booms
      - ➢ Any dynamic snaps or warping of the sunshade structures will be filtered through the spacecraft before reaching the sensitive payload.
    - o Other spacecraft components:
      - ➢ Dynamic isolation – either passively or active isolation. Both options were analyzed.
      - ➢ Also: thruster clusters, orbit maintenance fuel tanks, communications antennas, and reaction wheels, solar panels and solar sail
  - Payload:
    - o Telescope:
      - ➢ Primary, Secondary, Tertiary mirror assemblies and supporting structures
      - ➢ Laser metrology monitoring relative position of primary mirror to secondary mirror
      - ➢ Thermal control heaters, and related electronics
    - o Other Payload:
      - ➢ Structure mounting payload to spacecraft
      - ➢ Starlight Suppression System
      - ➢ Science Instruments
      - ➢ Thermal control hardware: isothermal enclosure, heatpipes, radiators, electronics
      - ➢ Electronics

Trade studies – pg 1

	Agreed on study - incorporate in FB2	Requires analysis results - Decide prior to FB2 Freeze	Defer to FB3	After FB#3 (Phase A)
1.0	**Mission - orbit detail, ΔV, Launch Vehicles, mission duration**			
	may pad ΔV to be conservative			
2.0	**Starlight Suppression System alternatives**			
2.1	**Consider alternates to dither maneuver for speckle removal (per NRA concepts)**			
2.2	**Consider series DMs, remove beam-splitters, redundancy**			
2.3				
2.4	**Consider increasing OWA for giant planets with larger DM, FOV for dust disk observations**			
2.5	**Consider longer wavelength observations (per NRA concepts) up to about 0.9µm**			
2.6	**Evaluate anamorphic optics compared to larger DM**			
3	**Instruments accommodations**			
4	**Pointing and Control - active vs passive dynamic isolation**			
4.1	**Define frequency range and control loop bandwidths, assess compatibility with actuator capabilities**			
4.2	**Evaluate necessity of secondary mirror steering, pending capability of payload vibration isolator**			
4.3	**Evaluate mounting of payload Payload Acquisition Camera, evaluate changes to reaction wheels**			

TC Technology

nightsky systems

TPF Terrestrial Planet Finder

- These trade studies are in work to evaluate future flight baseline design options

Trade studies – pg 2

	Agreed on study - incorporate in FB2	Requires analysis results - Decide prior to FB2 Freeze	Defer to FB3	After FB#3 (Phase A)
5	Primary Mirror			
5.1	Consider shape changes - increased depth and 8x3m race-track vs elliptical PM shape			
5.2	Open vs. Closed back PM structure evaluation			
5.3	Evaluate PM actuators vs. Coarse DM			
5.4	Resolve PM launch load issues - configuration change to reduce loads or add dampers/absorbers			
6	Mass Management			
6.1	Redesign thermal enclosure/Secondary Tower/AMS/LD5 boxes - mass efficient stiffness, add 4 arcmin FOV			
6.2	Add mass estimates for: launch constraints, dust covers, ballast, identify load bearing mass			
6.3	Evaluate mass sensitivity to: PM frequency, vibration control, SM actuation, metrology, solar sail			
7	Solar Array - Consider alternatives			
8	Solar Sail - improve design for better torque balance			
9	Sunshade - consider alternatives, add degradation features, trade performance against stowing/deploying issues			

TPF Terrestrial Planet Finder

National Aeronautics and Space Administration
Jet Propulsion Laboratory
California Institute of Technology
Goddard Space Flight Center

Trade studies – pg 3

	Agreed on study - incorporate in FB2	Requires analysis results - Decide prior to FB2 Freeze	Defer to FB3	After FB#3 (Phase A)
10	**Stray Light - develop concept for telescope baffles, add vanes, deployment issues**			
11	**Define viewing constraints from earth, moon, Jupiter, etc.- characterize vs. orbit size/position**			
11.1	**Contamination: understand requirements, add covers on exposed optics as required**			
12	**Thermal Control - incorporate active thermal control**			
12.1	**Consider thermal configuration changes - electronics mounting, heat pipe dynamics, alternate approaches**			
13	**I&T design issues**			
13.1	**Select OTA test configuration, incorporate features in flight design**			
13.2	**Understand required flight jitter requirement - use to evaluate chamber availability and testing capability**			
13.3	**Understand required flight thermal gradient requirements - use to evaluate chamber availability and testing capability**			
13.4	**Trade optical concepts for OTA tests - sub-aperture test requirements, model system, define requirements**			
14	**Software Definition**			
15	**Ground Segment Definition**			

TPF Terrestrial Planet Finder

TC Technology

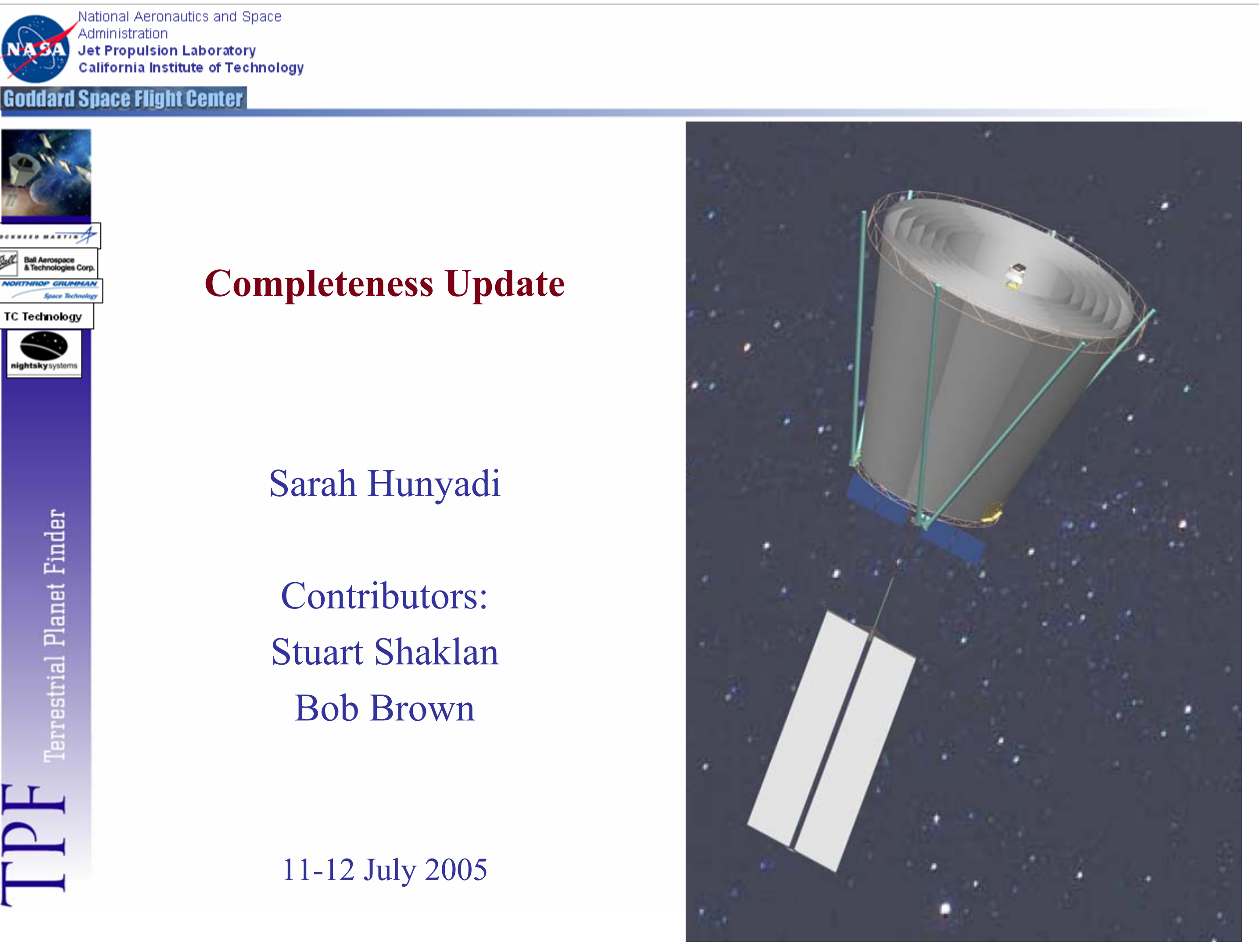

- The purpose of this presentation is to set the stage for our current requirement of instrument sensitivity at delta magnitude = 25 , and to show you the work we are planning to do to better define the optimal instrument performance parameters.

Overview

TPF Terrestrial Planet Finder

- Update of ongoing completeness analysis with Stuart Shaklan and Bob Brown
- Change from circular to elliptical orbits
- Synchronization of integration times
- Optimization of single visit completeness
  - Bob Brown employs an auction optimization
  - JPL employs an efficiency cutoff optimization
  - These two are shown to be equivalent
- Now using best estimate system throughput
- First iteration of program completeness optimization

- Completeness is defined as the portion of a star's habisphere that is visbible to a TPF-C observation.
- In order to measure completeness, we populate a star's habisphere with a large number of planets and we determine which of those planets are visible to TPF-C given magnitude and IWA constraints.
- We have also snychronized JPL integration times with those of Bob Brown and we will be presenting completeness results with the current best estimate of system throughput based on the current coronograph.
- In addition, the map for program completeness with be outlined.

Completeness

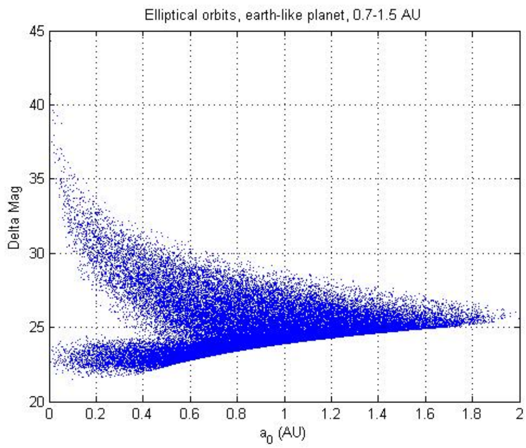

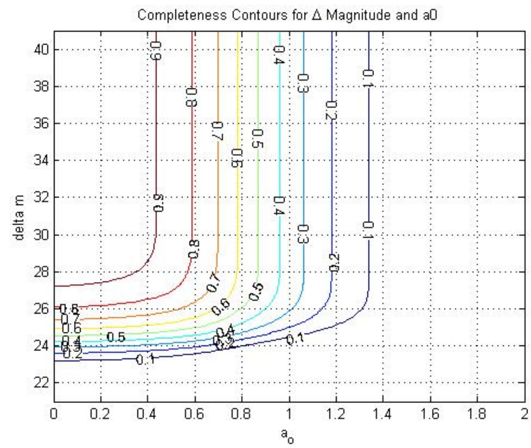

- Elliptical orbits extend range of habitable zone orbits
- Integrate elliptical planet distribution over a_0 and IWA to obtain completeness contours
- Contours are shifted for stellar luminosity and distance to obtain completeness vs. delta magnitude
- Noise and flux calculations give integration time vs. delta magnitude

- The chart on the upper right gives the planetary distribution over uniformly spaced elliptical orbits for planets that populate the habisphere of a star. The chart is shown for the case of earth like planets around L=1 star but can be read for stars of all luminosities. Ellipticity spreads out the range of habitable zone orbits beyond 1.5 AU
- a0=projected inner working angle = inner working distance
- Given an inner working distance and a delta magnitude cutoff, a completeness at these parameters for a given star can be determined. This can be shown as a point in the chart on the upper left. A collection of these points gives the contours shown in the chart. Again, this chart can be shifted from L=1 to any stellar luminosity. Therefore completeness curves over delta magnitude can be obtained for every star.
- Integration time vs. delta magnitude can be obtained from noise and flux calculations
- Thus a curve for completeness over time can be obtained for every star

Single Visit Auction Comparison – for detection of earth-equivalent planets

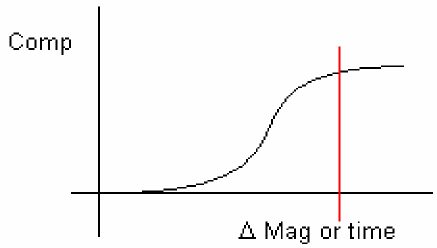

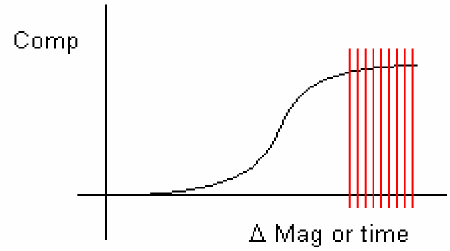

- JPL optimization uses an iterated efficiency cutoff factor to eliminate all time from star that falls below the efficiency cutoff.
- Brown optimization cuts time from a star, hour by hour, based on lowest incremental efficiency.

Both programs then optimize over number of hours cut, keeping one year of integration time to obtain the maximum cumulative completeness.

	JPL		Brown	
ΔMag	# Stars	# Planets	#Stars	#Planets
25	138	32.60	135.21	32.59
25.5	125	38.29	122.77	38.32
26	115	41.10	113	40.96
27	114	42.16	106	41.04

- The upper two charts show hypothetical completeness curves over time.
- The goal of the auction completeness optimization is to cut integration time from stars that are not as productive to obtain the highest cumulative completeness (which is equivalent in the following charts to number of planets).
- One method of performing this optimization is by looking at incremental completeness over time or incremental efficiency.
- On the two charts above the red lines indicate the difference between two different, but equivalent optimizations.
- For each optimization, integration time is cut from the back end of a stellar completeness curve on those stars that are lower in productivity.
- The chart on the right shows the Bob Brown optimization. In this optimization time is cut one hour at a time from a star in the list based on lowest incremental efficiency for that hour of time. This time removal occurs until a certain quantity of hours are removed – indicated on this chart by the last red line.
- On the left is the JPL efficiency cutoff optimization. For this optimization all the time for a given incremental efficiency below the cutoff is removed from the star. The efficiency cutoff begins at a value of zero (equivalent to the delta mag = 25 case) and is then incremented until the time removed from the star list is greater than an hour cutoff allotment.
- Each program then sorts the stars remaining in the list after the auction by highest overall efficiency and retains the stars that allow one year of integration time. This allows optimization over both incremental and overall efficiency.
- As you can see the results obtained from the JPL optimization and the Brown optimization are very similar.

New Throughput Parameters

Old Assumptions

- SNR=10
- IWA= 0.057 arcsec
- 0° dither
- Lyot throughput = 50%
- System throughput = 21%
- Total throughput w/ CCD QE = 17.0%
- Circular orbits

New Assumptions

- SNR=5
- IWA= 0.0655 arcsec
- 30° dither
- Lyot throughput = 34%
- System throughput = 10.8%
- Total throughput w/ CCD QE = 8.64%
- Elliptical orbits

Common Parameters

- Telescope = 8x3.5 m ellipse
- CCD QE = 0.8
- Integration time = 1 year
- Central wavelength = 550 nm
- Bandpass = 110 nm
- 3 rolls

- These are the new parameters based on new throughput numbers which now include anti-reflective coatings, dielectric beam splitter materials and polarizations.
- Total throughput decreases by a factor of 2, but the SNR also decreases by a factor of two. With background limited sources this would imply a decrease in integration time by a factor of two. For those sources that are not background limited, the integration times would be lower with the new assumptions, but not by a factor of 2.
- The inner working angle differs due to the decrease in available inner working angle with dither and roll maneuvers. With more rolls, the inner working angle increases. We take the 50% point at 3 rolls to be the inner working angle for this case – see backup slides for more details.

Preliminary Parameter Auction Results

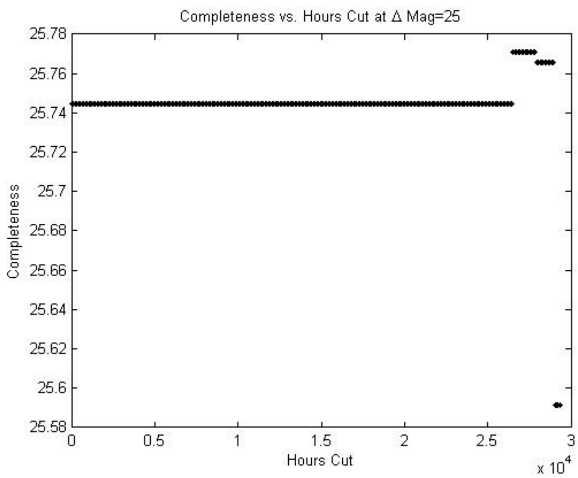

ΔMag = 25

- Planets = 25.771 (JPL)
- Planets = 26.13 (Brown)
- Participating Stars = 146
- Little improvement over ΔMag=25 (flat line)

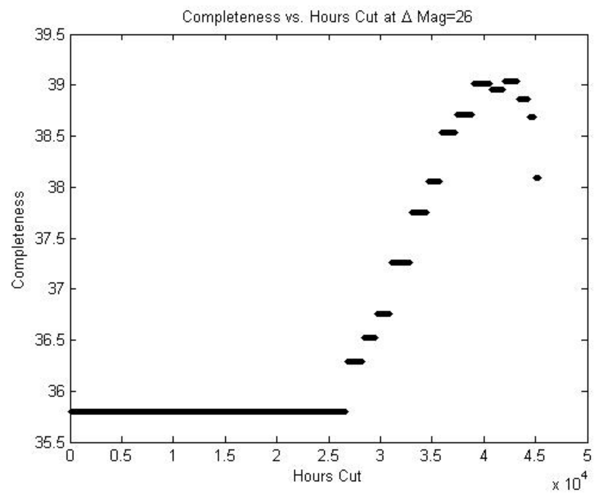

ΔMag = 26

- Planets = 39.038
- Participating Stars = 126
- Significant improvement over ΔMag=25

- Will be preliminary until we correlate with Bob Brown's results. However the results on the delta magnitude=25 case are very close.
- These are new results for the efficiency cutoff optimization. The plots show hours cut on the x-axis and cumulative completeness (number of planets found) on the y-axis for different limiting delta magnitudes.
- The graph is not continuous because it shows different levels of efficiency cutoff. The lines are flat because for that set of hour cut allotments the stars that are included in the optimization are the same
- For the case of delta magnitude = 25, the line remains flat at the cutoff for stars at delta mag=25. There is minimal gain from optimizing at this delta magnitude.
- However, for delta magnitude = 26 there is substantial increase in the number of planets found at delta mag = 25 and the optimization gives a much better result than the delta mag=26 cutoff.
- Moving the requirements to delta mag=26 could show a large improvement in the number of planets found, but program completeness will need to be completed first.

National Aeronautics and Space Administration
Jet Propulsion Laboratory
California Institute of Technology
Goddard Space Flight Center

ΔMag=25 and ΔMag=26 Comparison

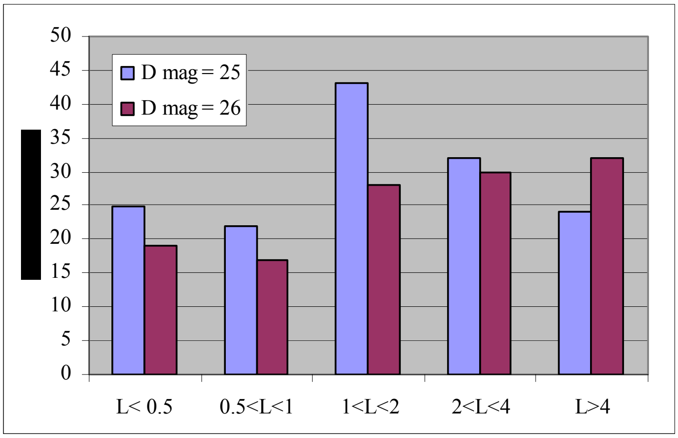

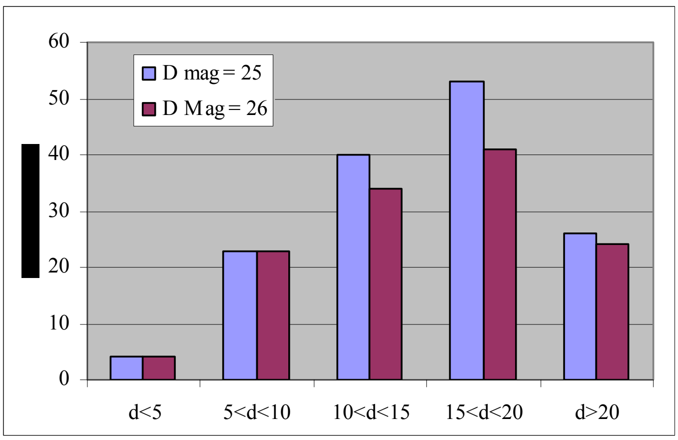

- ΔMag=25
  - 146 stars
  - 25.77 planets
- ΔMag=26
  - 126 star
  - 39.04 planets
- For ΔMag=26 more high luminosity stars are visited
- Fewer number of stars, but much higher planet count
- Can view stars deeper and observe planets that are 2x fainter

Terrestrial Planet Finder
TPF

- These two charts compare the characteristics of the stars that were observed with the auction at delta mag =25 and delta mag = 26. The blue bars in both graphs are for delta mag = 25 and maroon are for dmag=26
- The top chart bins the stars into 5 luminosity classes – from less than 0.5 to greater than 4 Lbol.
- The bottom chart bins the stars into 5 distance classes – from less than 5 parsecs to greater than 20 parsecs.
- For delta mag = 26, more higher luminosity stars made the cut because you can observe deeper with fainter planets to obtain better overall completeness.
- At delta mag = 26, proportionally more distant stars are visible.

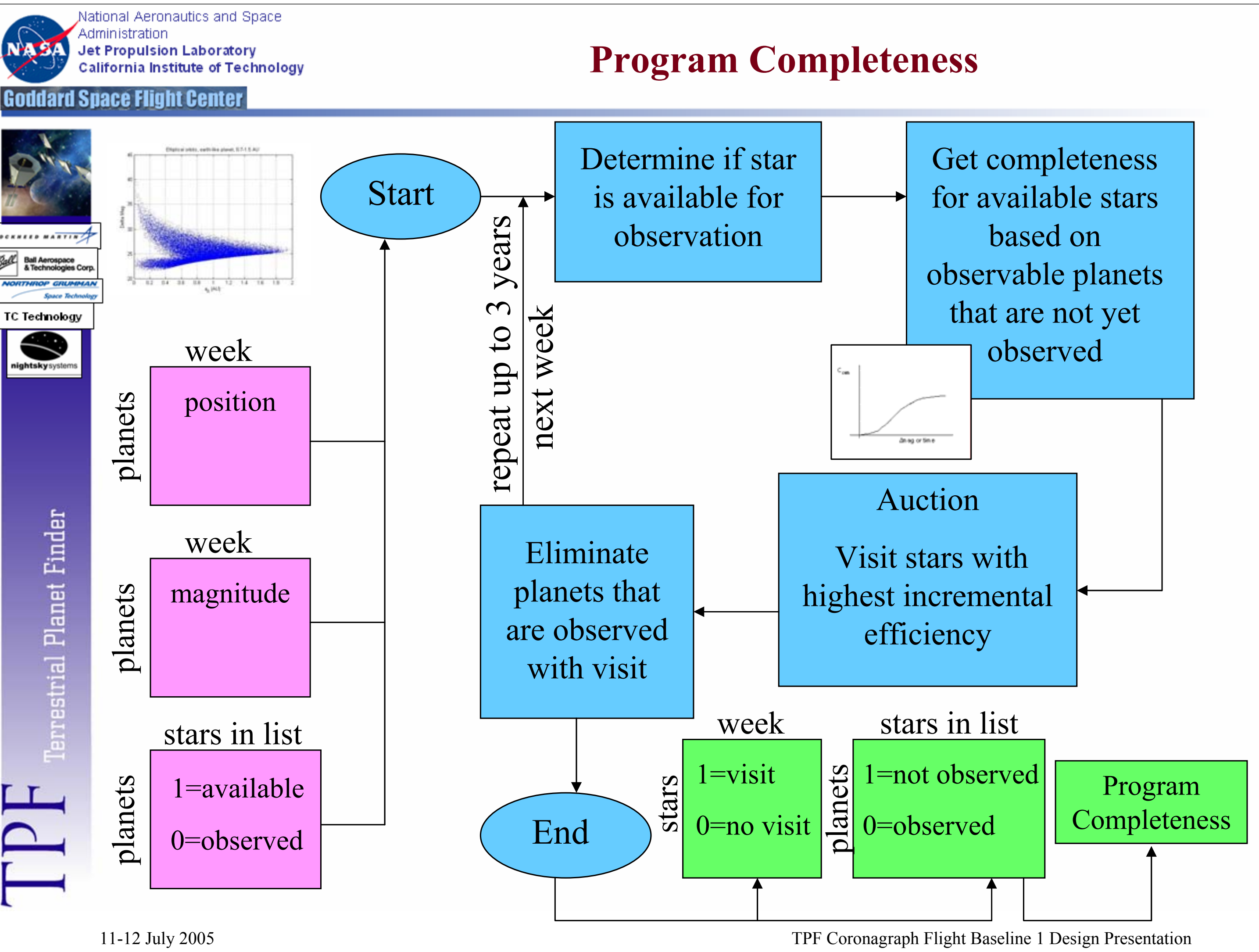

- Outline of program completeness.
- We being with three matrices shown in pink. These are obtained by taking the distribution of planets shown earlier and propagating this distribution through time. This gives the top two matrices – that of planet position and magnitude for a given time (in this case, a week) The third input keeps track of the 10,000 planets used in this analysis and determines if those planets were observed through the program. It begins out as a matrix of ones.
- The program then takes these inputs and moves along this loop. The first procedure is to determine if the star is visible for a given time frame. If the star is visible, the program then obtains a completeness curve over time, based on the number of planets in the beginning sample that have not yet been viewed.
- For the first week all planets are available for viewing so the completeness curve is the same as that given for single visit completeness. Once the completeness curves for participating stars have been obtained, the program runs an auction to keep the stars with the highest incremental efficiency.
- For the stars that make it through the auction, the planets that were observed in this new observation are removed from the list of possible planets. This feeds back into the completeness curves in part 2.
- This loop of visiting, obtaining a completeness curve, auctioning and removing viewed planets occurs for up to a three year observing program.
- At the end of the program there are three outputs shown in green. One is a list of visits – if the star was visited or not, the second is a list of planets that were viewed (0) or not viewed (1) for every star. By summing this matrix – program completeness numbers can be obtained.

Backup Slides

IWA – 0° dither

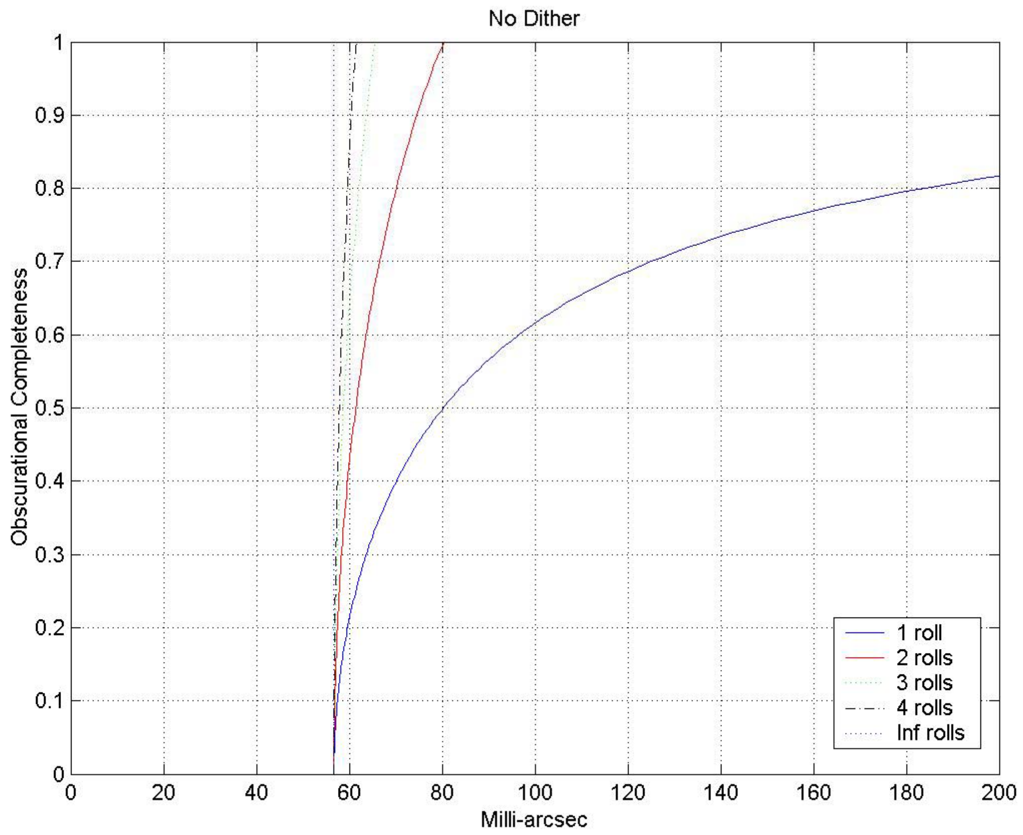
No Dither
Obscurational Completeness
Milli-arcsec
0
0.1
0.2
0.3
0.4
0.5
0.6
0.7
0.8
0.9
1
0
20
40
60
80
100
120
140
160
180
200
1 roll
2 rolls
3 rolls
4 rolls
Inf rolls

IWA - 30° dither

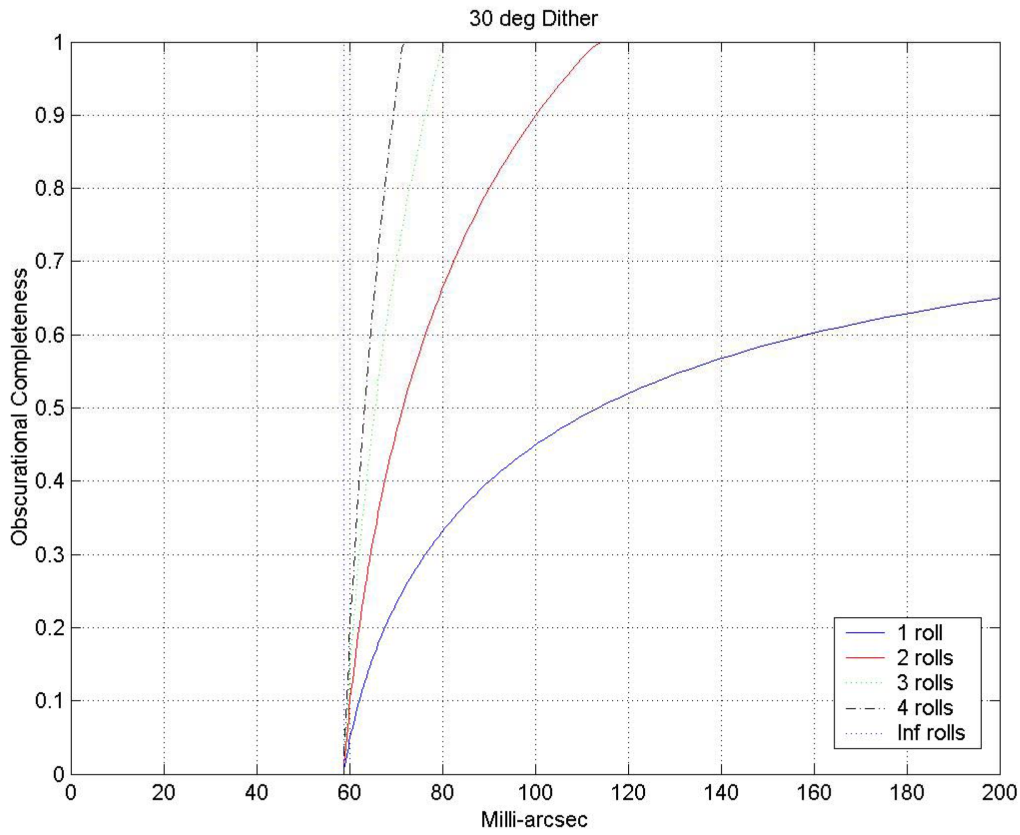

Completeness Summary

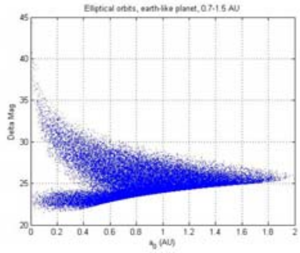

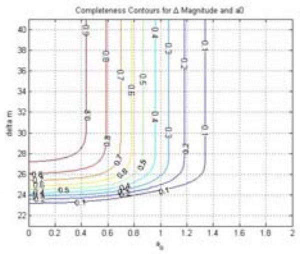

- Elliptical planetary orbits expand range of habitable planets
- Probability distribution of planets gives completeness contours
- Completeness curves are optimized for highest planet count with auction optimization

Equivalent Optimizations

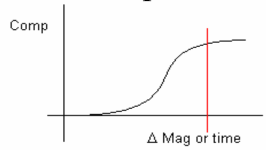

JPL

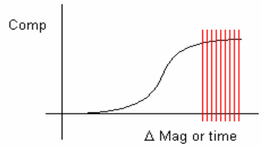

Brown

	JPL		Brown	
ΔMag	# Stars	# Planets	#Stars	#Planets
25	138	32.60	135.21	32.59
25.5	125	38.29	122.77	38.32
26	115	41.10	113	40.96
27	114	42.16	106	41.04

Optimized Results at ΔMag=25 and ΔMag=26

ΔMag=25

- Planets = 25.771 (JPL)
- Planets = 26.13 (Brown)
- Participating Stars = 146
- Limited improvement over Δmag=25 cutoff

ΔMag=26

- Planets = 39.038
- Participating Stars = 126
- Great improvement over both Δmag=25 cutoff and Δmag=26 cutoff

National Aeronautics and Space Administration
Jet Propulsion Laboratory
California Institute of Technology
Goddard Space Flight Center

TPF Terrestrial Planet Finder

TPF-C Error Budget: Description and Plans

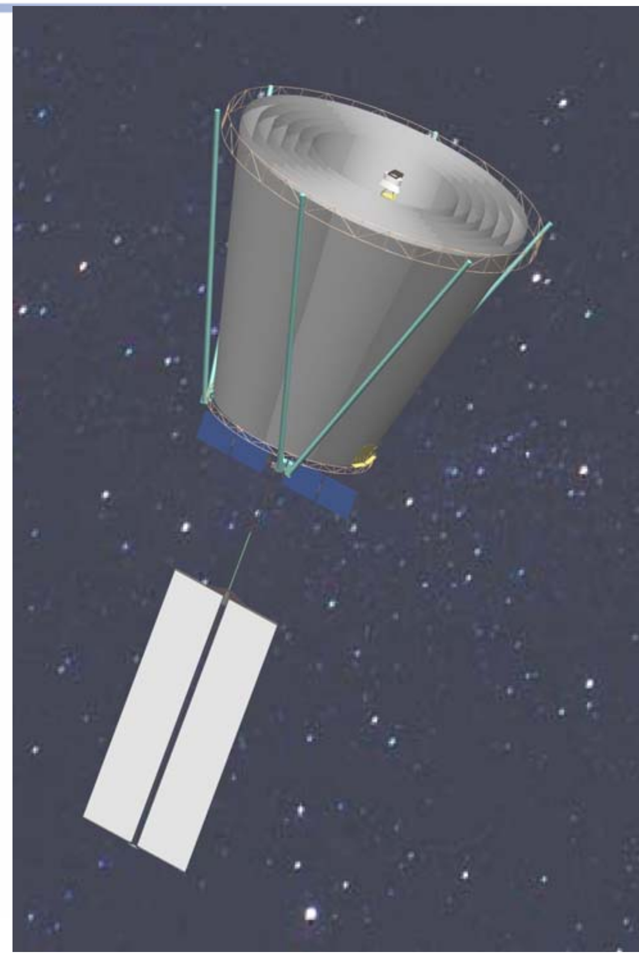

Stuart Shaklan

Contributors:
Luis Marchen
Joseph Green
Oliver Lay
David Palacios

11-12 July 2005

- Detailed information pertinent to this presentation can be found in the following paper:
  - S. B. Shaklan, L. F. Marchen, J. J. Green, and O. P. Lay, “The Terrestrial Planet Finder Coronagraph Dynamics Error Budget,” Proc. SPIE vol 5905 (San Diego, 2005).

High-Level Requirements

Lockheed Martin
Ball Aerospace & Technologies Corp.
Northrop Grumman Space Technology
TC Technology
nightsky systems

TPF Terrestrial Planet Finder

Table 1. TPF-Coronagraph Contrast Error Budget Requirements.

	Requirement	Comment
Static Contrast	6.00E-11	Coherent Terms
Contrast Stability	2.00E-11	Thermal + Jitter
Instrument Stray Light	1.50E-11	Incoherent light
Inner Working Angle	$4\ \lambda/D_{long}$	57 mas at λ=550 nm, D_{long} = 8 m
Outer Working Angle	$48\ \lambda/D_{short}$	1.5 arcsec at λ=550 nm, D_{short} = 3.5 m
Bandpass	500-800 nm	Separate observ. in three 100 nm bands.

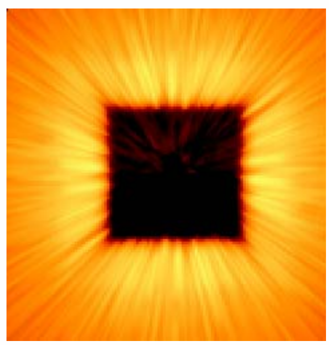

•

The contrast error budget (CEB) specifies the level and stability of scattered light in the dark hole. The scattered light level is expressed in terms of instrument contrast, where contrast is defined as the integrated scattered light in a diffraction-limited resolution spot, normalized by the coronagraph mask throughput, and divided by the light from the star that would be present without a coronagraph mask. A rigorous definition is given in Green & Shaklan (2003). Table 1 gives the working requirements as of June, 2005.

•The contrast level and stability are both functions of position in the image plane. We have found that the dynamic evolution of low-order aberrations and the predominance of low-order imperfections in the optics have their largest impact at the IWA. In the rest of this paper, we evaluate the contrast error budget at the IWA. The dynamic (though not necessarily the static) contrast levels are smaller at larger working angles. We have not yet performed a detailed study of contrast stability at the OWA, though it is expected to be small compared to the IWA.

Static and Dynamic Terms

$$\text{Contrast} = I_s + \langle I_d \rangle$$
$$\text{Stability} = \text{sqrt}(2 I_s \langle I_d \rangle + \langle I_d^2 \rangle)$$

I_s = Static Contrast	I_d = Dynamic Contrast
Wave Front Sensing Wave Front Control Gravity Sag Prediction Print Through Coating Uniformity Polarization Mask Transmission Stray Light Micrometeoroids Contamination	Pointing Stability Thermal and Jitter Motion of optics Beam Walk Aberrations Bending of optics Aberrations
Every item is unknown territory, new technology. Most are bandwidth-dependent	Solve with Design and Engineering, linear modeling. Bandwidth independent.

- This presentation focuses on Dynamic terms. These are the terms that lead to a change in image plane contrast.
- We can tolerate static contrast that is as large as the exozodi background (perhaps as large as 1e-9) as long as the dynamic terms remain below 1e-11. The problem is that the larger the static terms, the more sensitive we are to changes in the state of the system. The stability equation shows that the product of static and dynamic contrast drive the error budget.
- Static contrast is much more difficult to model than dynamic contrast. Static contrast requires detailed, rigorous diffraction propagators operating broadband. The dynamics terms are all differential – diffraction ringing and similar effects are second order. We can model dynamics terms with standard linear sensitivity models generated by ray-trace codes and Fourier conjugate plane (Fraunhofer) propagators.

Error Budget Models

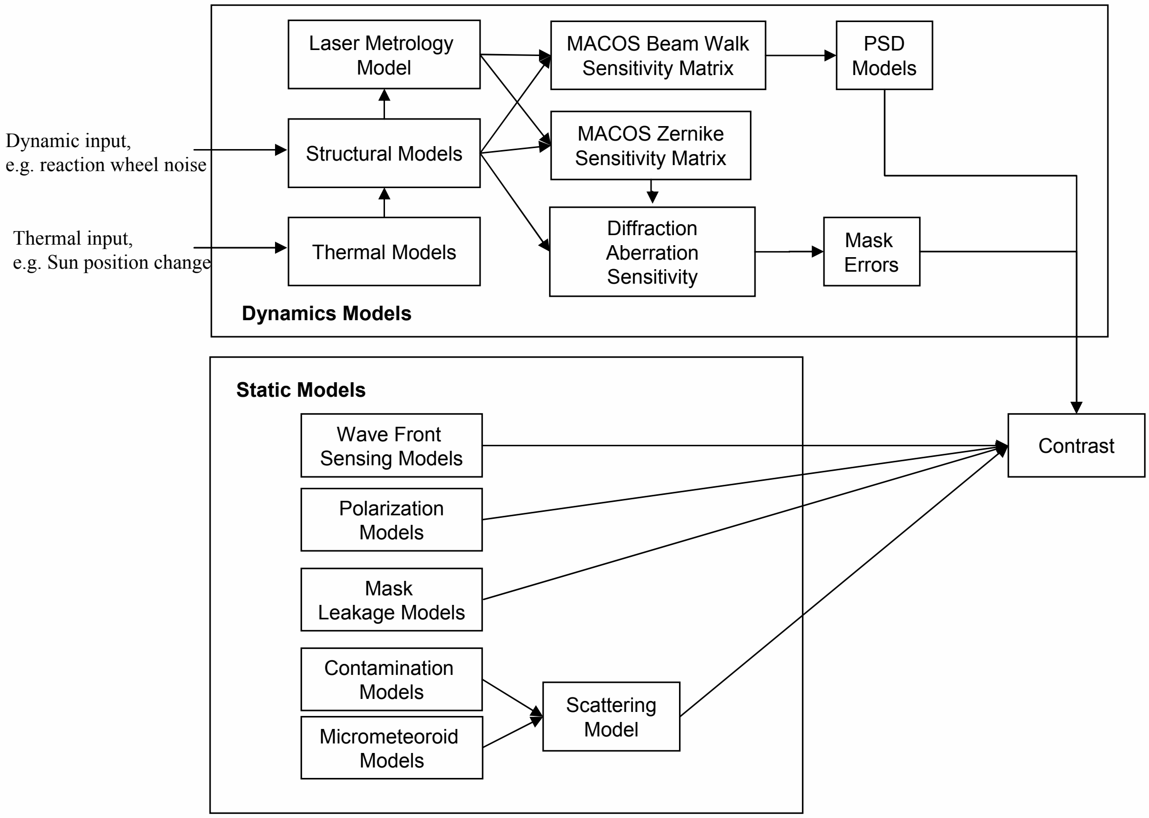

Figure 3. Models used to calculate static and dynamic contrast.

- A Fraunhofer pupil-to-image plane model is used for calculating image plane contrast as a function of wavefront components for ideal coronagraph designs as well as coronagraphs with mask transmission errors. The wavefront components are decomposed into Zernike polynomials that are orthogonal over circular and elliptical apertures. This is called the 'diffraction aberration sensitivity' model.
- A MACOS13-based aberration sensitivity model determines the Zernike mode amplitudes when any optical component is moved over 6 degrees of freedom (DOF). This model is the 'Zernike sensitivity matrix.' The telescope and coronagraph optics are described in separate papers.
- The model of the laser metrology system between the primary and secondary mirrors is based on a simple linear point-to-point analysis of the metrology beams to determine beam length sensitivity to the 6 degree-of-freedom (6-DOF) motion of the secondary. We use ray tracing of the TPF-C telescope to determine aberration sensitivity versus motion of the secondary mirror. These two models are combined to yield the aberration sensitivity versus metrology beam lengths. The coronagraph model determines image plane contrast as a function of aberrations. We can thus determine by combining the linear ray trace and coronagraph models, the image plane contrast versus metrology beam length deviations12.
- Static error models, as noted above, are based on Fresnel diffraction analysis and include broad-band multi-DM wave front control systems. Coronagraph mask errors include phase and amplitude transmission errors measured in the laboratory, and theoretical models based on detailed electromagnetic calculations of mask transmission (for binary masks). We have also modeled the expected distribution of micrometeoroid damage to the primary mirror. We are currently studying scatter from particle contamination to determine what fraction of the forward and backward scattered light can be compensated by the DMs. Standard polarization ray-tracing is used to determine polarization amplitude and phase non-uniformity in the off-axis system, but we have not yet performed modeling of polarization effects arising from coating non-uniformities.

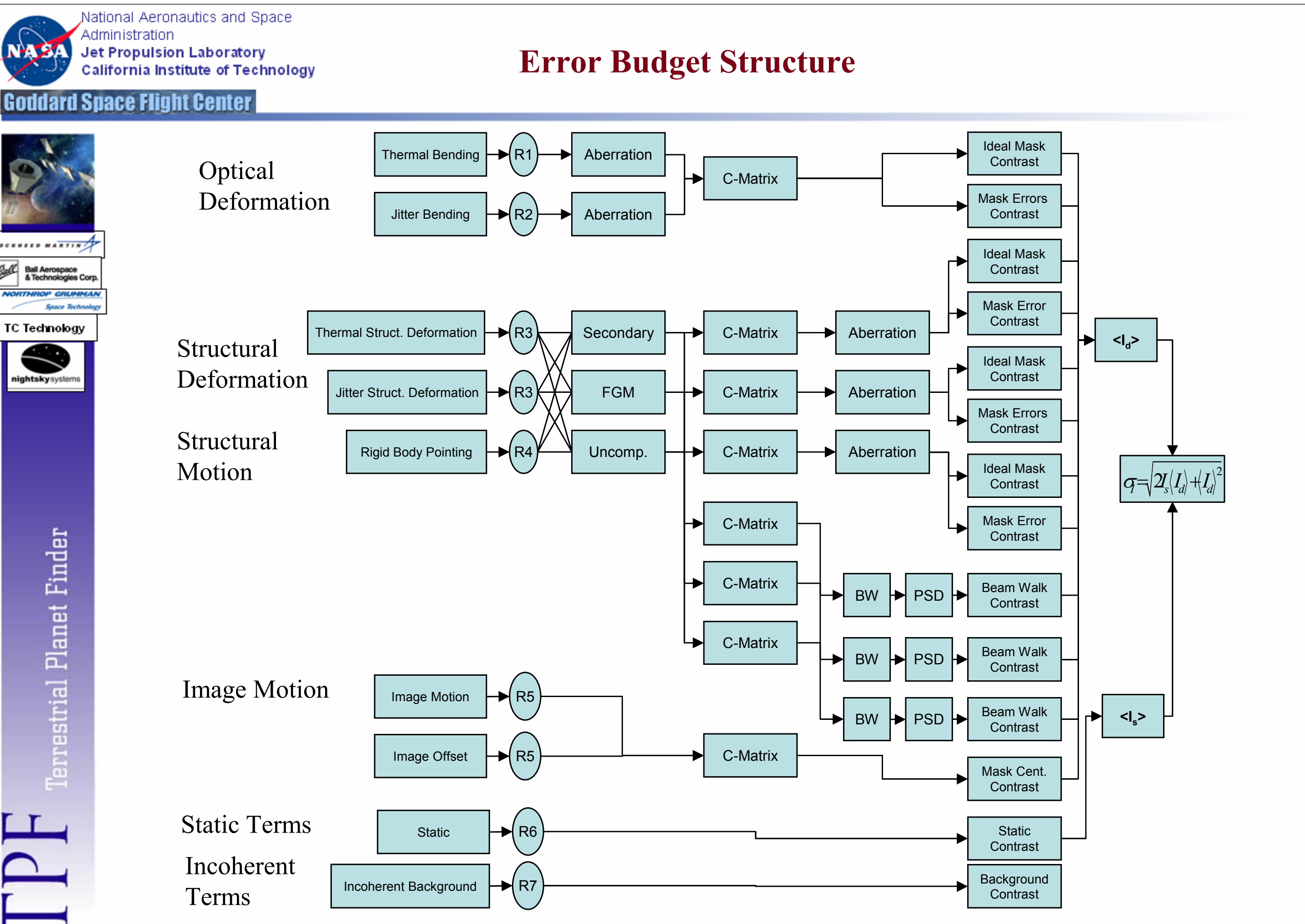

Figure 1. Error Budget Structure. 'C-matrix' is a sensitivity matrix or equation.
R1-R7 are multiplicative reserve factors.

- There are 4 main categories of dynamics terms (Optical deformation, structural deformation, structural motion, image motion), coherent static terms, and incoherent static terms (stray light, e.g. from particulate contamination).
- Motions are allocated to dynamics terms. These are multipled by reserve factors (all set to 2 in the CEB) before being applied to sensitivity matricies.
- Structural motion (rigid body pointing) and structural deformation (relative motions of rigid-body optics) lead to beam walk and aberrations. A 3-stage pointing control system (see later slide) minimizes beam walk and image motion on the mask. Each stage requires a separate sensitivity matrix.
- Wherever an aberration occurs, two errors are calculated. The first is leakage of the aberration around an ideal mask. The second is leakage directly through a mask imperfection.
- The PSD boxes are power spectral densities for various optics (see later slide).
- Contrast is energy: contrast terms add linearly: they do not add as root-sum-squared quantities.

Beam Walk Model

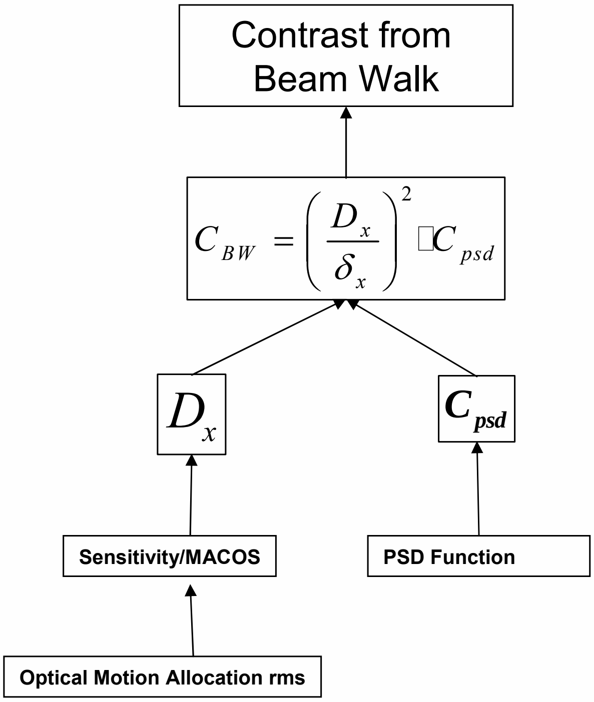

$$C_{psd} = \left(\frac{2\pi}{\lambda} \cdot \sqrt{ \iint 16\pi^2 (\delta_x k_x)^2 \cdot \left[\frac{A}{1 + \left(\frac{\sqrt{k_x^2 + k_y^2}}{k_0} \right)^n} \right] dk_x dk_y } \right)^2$$

Figure 4. Beam walk calculation. C_{psd} is the contrast for a unit value of beam walk, δ_x at a spatial frequency (image plane position) of k_x.. D_x is the beam walk calculated from linear sensitivity matrices applied to allocated translation and tilt motions.

- See C. Noecker, Proc. SPIE Vol 5905 (San Diego, 2005) for further details.

Control Systems

- 3-tiered pointing control
  - Rigid body pointing using reaction wheels or Disturbance-Free Payload
  - Secondary mirror tip/tilt (~ 1 Hz)
  - Fine-guiding mirror (several Hz)
- PM-SM Laser Metrology and Hexapod
  - Measures and compensates for thermal motion of secondary relative to primary.

- If the secondary is held fixed, the rigid body pointing requirement is ~ 0.4 mas (1 sigma)
- Tilting the secondary mirror to control low-bandwidth pointing errors allow relaxation of the rigid body pointing error requirement to 4 mas (1 sigma).

- A laser metrology system monitors the spacing and shear between the primary and secondary mirrors. It is required to operate at 25 nm (1 sigma).

Pointing Control

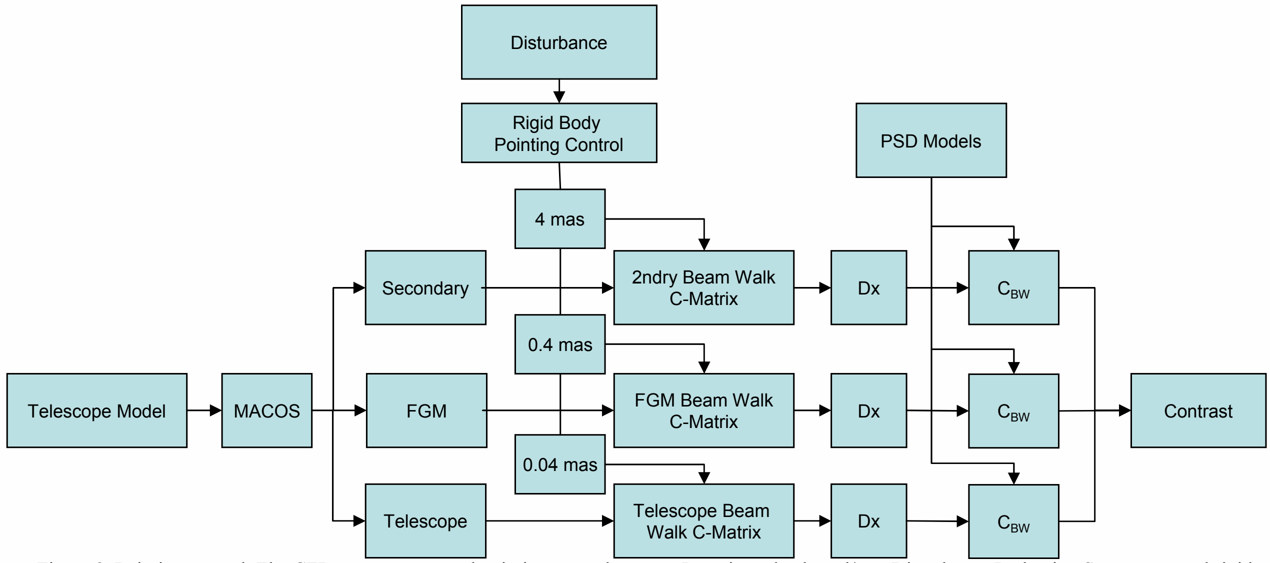

Figure 2. Pointing control. The CEB assumes a nested pointing control system. Reaction wheels and/or a Disturbance Reduction System control rigid body motions to 4 mas (1 sigma). The telescope secondary mirror tips and tilts to compensate the 4 mas motion but has a residual due to bandwidth limitation of 0.4 mas. A fine guiding mirror in the SSS likewise compensates for the 0.4 mas motion leaving 0.04 mas uncompensated.

Error Budget Screen Shot

Error Budget

			4 λ/D
Final Contrast	=	WFE +Background	5.63E-11
σ_I	=	$\sqrt{2 I_s \langle I_d \rangle + \langle I_d \rangle^2}$	2.00E-11
<I>	=	<Id> + <Is> Total Contrast	4.13E-11
<Id>	=	Jitter/Thermal Error+Bending of Optics+Rigid Body+Image Position	5.14E-12

Bending of Optics Jitter/Thermal (Includes Reserve)	1.72E-12
Jitter/Thermal Structural Deformation Aberrations and Beam Walk (Includes Reserve)	1.49E-12
Image Position Offset and Image Jitter (Includes Reserve	6.37E-13
Rigid Body Pointing (Includes Reserve)	1.29E-12
IS = Static Error (Includes Reserve)	3.62E-11
Background Error	1.50E-11

Jitter/Thermal Reserve (Beam Walk and Structural)				2.00
Reserve Factor Bending of Optics				2.00
Reserve Factor (Image Position Jitter and Offset)				2.00
Reserve Factor Mask Transmission Errors				2.00
Reserve Factor Rigid Body Pointing				2.00
Reserve Factor for WFS/C				2.00
Reserve Factor Amplitude Uniformity				2.00
Reserve Factor Polarization Leakage				2.00
FGM-Residual				0.10
Secondary-Residual				0.10
			No Reserve	Reserve
ΔM	The no reserve ΔM can be changed here		5.00E-04	1.00E-03

ON
FGM ON/OFF

ON
Secondary ON/OFF

- This is a screen shot of the main error budget page, an excel spreadsheet.
- Note the switches at the bottom: we can push the 'button' to turn the secondary mirror and fine guiding mirrors on an off. Logic in the spreadsheet then applies the appropriate sensitivity matrices to the beam motion and aberrations.

Turn off 2ndary Mirror Pointing Control

Error Budget

		4 λ/D
Final Contrast =	**WFE +Background**	**2.19E-10**
$\sigma_I = \sqrt{2 I_s \langle I_d \rangle + \langle I_d \rangle^2}$		**2.00E-10** ←
<I> = <Id> + <Is>	**Total Contrast**	**2.04E-10**
<Id> =	**Jitter/Thermal Error+Bending of Optics+Rigid Body+Image Position**	**1.67E-10**
Bending of Optics Jitter/Thermal (Includes Reserve)		**1.72E-12**
Jitter/Thermal Structural Deformation Aberrations and Beam Walk (Includes Reserve)		**3.63E-11**
Image Position Offset and Image Jitter (Includes Reserve		**6.37E-13**
Rigid Body Pointing (Includes Reserve)		**1.29E-10**
IS = **Static Error (Includes Reserve)**		**3.62E-11**
Background Error		**1.50E-11**

		No Reserve	Reserve
Jitter/Thermal Reserve (Beam Walk and Structural)			2.00
Reserve Factor Bending of Optics			2.00
Reserve Factor (Image Position Jitter and Offset)			2.00
Reserve Factor Mask Transmission Errors			2.00
Reserve Factor Rigid Body Pointing			2.00
Reserve Factor for WFS/C			2.00
Reserve Factor Amplitude Uniformity			2.00
Reserve Factor Polarization Leakage			2.00
FGM-Residual			0.10
Secondary-Residual			0.10
ΔM	The no reserve ΔM can be changed here	5.00E-04	1.00E-03

ON	OFF
FGM ON/OFF	Secondary ON/OFF

- When we turn the secondary mirror off, passing 4 mas of rigid body pointing errors through the telescope, the contrast stability increases by an order of magnitude.
- This is caused by beam walk on the small optics preceeding the coronagraph mask.

Power Spectral Density of Optics

- Fold mirrors 1 and 2 are ‘super fold’
- First off-axis-parabola is ‘Super OAP’
- Cylindrical mirrors are ‘anamporphic’
- DM is r.s.s. of all optics. K0 is scaled value from PM (8 m scaled to 10 cm)

Table 2: PSD specifications for optics modeled in the CEB.

	Primary	Secondary	Fold	Super Fold	OAP	Super OAP	Anamorphic 1	Anamorphic 2	DM
D (m)	8.02	0.83	0.1	0.1	0.1	0.1	0.23	0.10	0.10
k0 (cy/m)	4	4	10	10	10	10	10	10	320
A (m^4)	9.60E-19	9.60E-19	1.25E-20	7.58E-21	1.25E-20	1.09E-20	5E-20	7.5E-20	8.52E-22
n	3	3	3	3	3	3	3	3	3
RMS WF	8.51E-09	9.55E-09	2.15E-09	1.67E-09	2.15E-09	2.00E-09	5.24E-09	5.27E-09	1.62E-08

- Here are the parameters of the power spectral densities assumed for optics in the system. The PSD equation appears in slide 6 (Beam Walk calculation).
- Note that several optics assume better than 2 nm rms wave front (better than 1 nm rms surface).

National Aeronautics and Space Administration
Jet Propulsion Laboratory
California Institute of Technology

Goddard Space Flight Center

Key Dynamics Requirements

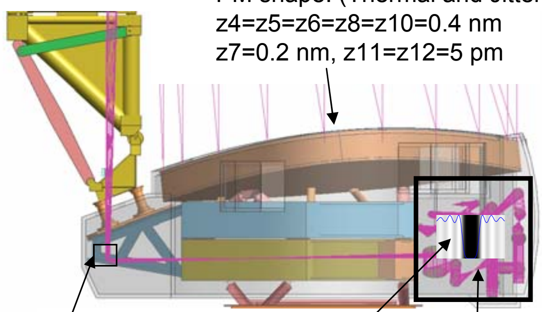

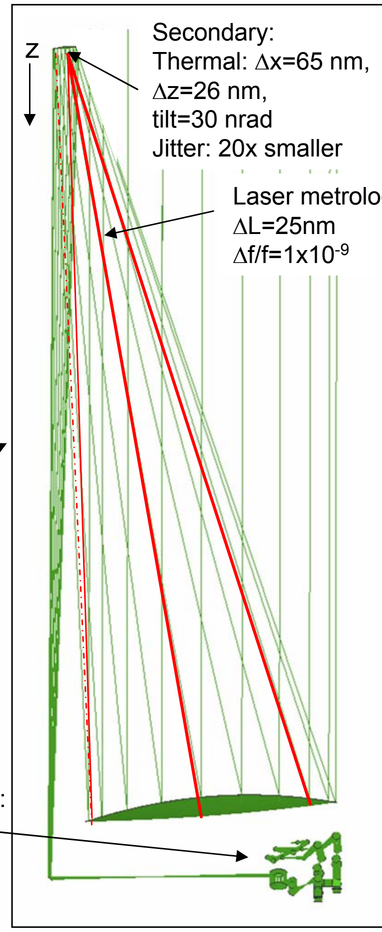

Figure 5. We identify the major engineering requirements to meet the dynamic error budget. Thermally induced translations lead to beam walk that is partially compensated by the secondary mirror. Jitter is partially compensated by the fine guiding mirror.

TPF Terrestrial Planet Finder

- Here we point out the key dynamics requirements derived from the error budget contrast allocations.

Contrast Roll Up

Table 4: Rolled up Dynamic Contrast Contributors

Perturbation	Contributor	Nature	Contrast	Fraction
Structural Defomation	Beam Walk	Thermal	8.29E-13	16.12%
		Jitter	6.33E-13	12.31%
	Aberrations	Thermal	3.28E-14	0.64%
		Jitter	4.43E-17	0.00%
Bending of Optics	Aberrations	Thermal	8.60E-13	16.72%
		Jitter	8.60E-13	16.72%
Pointing	Beam Walk		1.29E-12	25.10%
	Image Motion		9.04E-14	1.76%
	Mask Error		5.46E-13	10.63%
SUM			5.14E-12	

- Table 4 is a roll-up of dynamic contrast contributors, including bending of the optics, beam walk across all optics, and pointing errors. The roll-up is based on allocations of engineering requirements (e.g. allowed motion of a given optic, allowed bending of an optic) applied throughout the system. Allocations were derived from extensive modeling efforts on a previous 6-meter version of TPF-C.
- The largest grouped contributor to image plane contrast is beam walk caused by pointing errors. The majority of this occurs on the first five mirrors following the secondary mirror, near the Cassegrain focus. The walk is due to 0.4 mas of pointing error that remains uncompensated by the secondary mirror. (Recall that the secondary corrects up to 4 mas of rigid body pointing, but 0.4 mas is at frequencies beyond the secondary mirror control bandwidth.) The first two folds and the first off-axis parabola have 'Super Fold' and 'Super OAP' PSDs , while the cylindrical optics are about 2.5 times worse. To reduce the beam walk, we must adopt a combination of better pointing and better optical surfaces. Note that if the secondary mirror is not used in the pointing control loop, and if rigid body pointing stability is s = 4 mas, there is 10x more beam walk on these optics, resulting in contrast of 1.3x10-10 (and the overall dynamic contrast going to 1.67x10-10).
- The single largest contrast term in the error budget is the 'Mask Error' term at the bottom of Table 4. As noted above, this term is the leakage of light that is offset by 0.3 mas with 0.3 mas random pointing error, through a mask with a 5x10-4 transmission error at 4 l/D. We expect that it will be challenging to build a mask to this level of precision. The leakage falls off as the square of the pointing error , so a reduction in pointing error will relax the mask requirement.

Contrast and Contrast Stability

Error Budget

		4 λ/D
Final Contrast =	**WFE +Background**	**5.63E-11**
$\sigma_I = \sqrt{2 I_s \langle I_d \rangle + \langle I_d \rangle^2}$		**2.00E-11** ←
<I> = <Id> + <Is>	**Total Contrast**	**4.13E-11**
<Id> =	**Jitter/Thermal Error+Bending of Optics+Rigid Body+Image Position**	**5.14E-12** ←
Bending of Optics Jitter/Thermal (Includes Reserve)		**1.72E-12**
Jitter/Thermal Structural Deformation Aberrations and Beam Walk (Includes Reserve)		**1.49E-12**
Image Position Offset and Image Jitter (Includes Reserve		**6.37E-13**
Rigid Body Pointing (Includes Reserve)		**1.29E-12**
IS **= Static Error (Includes Reserve)**		**3.62E-11** ←
Background Error		**1.50E-11**

Jitter/Thermal Reserve (Beam Walk and Structural)		2.00
Reserve Factor Bending of Optics		2.00
Reserve Factor (Image Position Jitter and Offset)		2.00
Reserve Factor Mask Transmission Errors		2.00
Reserve Factor Rigid Body Pointing		2.00
Reserve Factor for WFS/C		2.00
Reserve Factor Amplitude Uniformity		2.00
Reserve Factor Polarization Leakage		2.00
FGM-Residual		0.10
Secondary-Residual		0.10
	No Reserve	**Reserve**
ΔM — The no reserve ΔM can be changed here	5.00E-04	1.00E-03

ON **FGM ON/OFF** **ON** **Secondary ON/OFF**

- We point out that dynamic terms by themselves are small: 5.14e-12. When combined with static terms, they lead to contrast stability of 2e-11.

Static Terms: Work in Progress

- SPIE 5905, San Diego August 2005
  - "Coronagraph Mask Tolerances For Exo-Earth Detection," Oliver Lay et al.
    - Broad band limitations in binary mask design, 2-DM control
  - "Measurement of Wavefront Phase Delay and Optical Density in Apodized Coronagrapic Mask Materials," P. Halverson et al.
    - HEBS masks, broad band response
  - "Polarization-Compensating Protective Coatings for TPF-Coronagraph Optics to Control Contrast Degrading Cross-Polarization Leakage" K. Balasubramanian et al.
    - Broad-band polarization control

Plans

- Re-evaluate requirements
  - Set limiting_delta_magnitude = 26?
  - 2-3x change in structural stability requirements
- Static Error Budget
  - Broad-band limitations
  - Gravity Sag
  - Chromatic Mask Errors
  - Mask Polarization Effects
- Incoherent Light
  - Stray light study underway at GSFC (Ed Frenier)
- Dynamic Error Budget
  - Re-allocate to match modeling results
- Detection vs. Characterization
  - Same structure, but characterization requirements may be more challenging because spectral line depth is small (signal contrast << 1E-10).

- A change in limiting delta magnitude may result from ongoing ‘photometric and obscurational completeness’ studies (see R. Brown, ApJ 2005).
- We are now placing our emphasis on the static error budget. The following pages are back-up slides related to control of static wave contrast.

OTA and Starlight Suppression System

Zakos Mouroulis

Contributors:
Ray Ohl
Stuart Shaklan
Joe Green
Bala Balasubramanian

11-12 July 2005

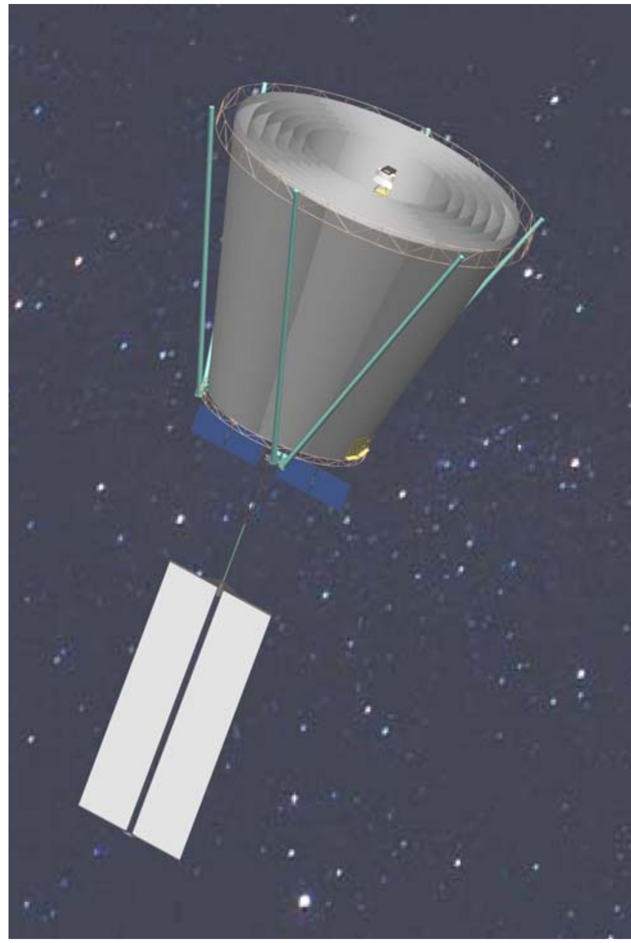

OTA optical concept

Perspective view of ray trace (~YZ plane) showing off-axis direction

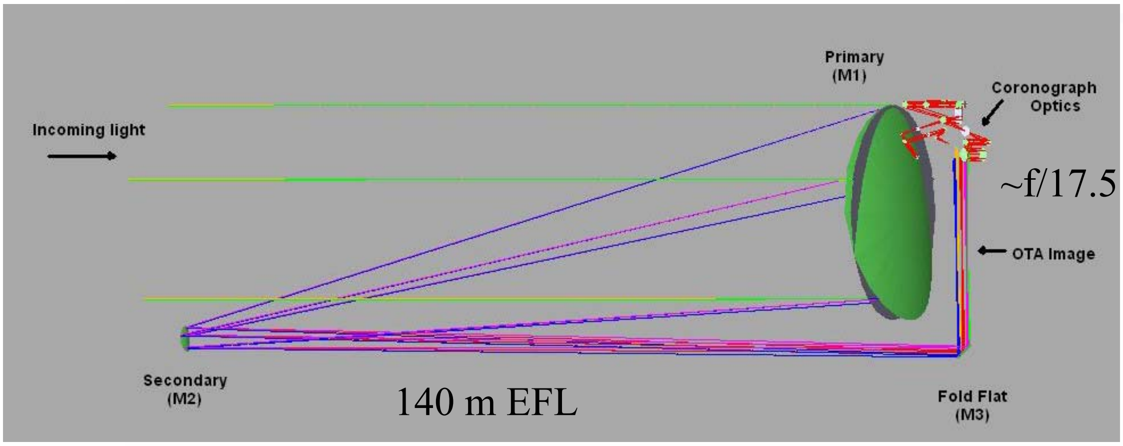

Name	Physical size		Off-axis distance (mm)	R (mm), f/#	k
	X (mm)	Y (mm)			
PM	8000	3500	2300	26750, 3.82	-1.00189
SM (convex)	890	425	237	3041, 4.13	-1.49
M3	290	310		:	

- Ritchey-Chrétien telescope
- 2 powered mirrors (PM, SM) and 1 flat (M3)
- PM and SM are hyperbolic, SM is convex
- Curved focal surface
- Off-axis aperture (in YZ plane)
- Astigmatism is the primary off-axis aberration
- Coating: protected silver

On-going trade studies

- Optical prescription: Gregorian vs. ~Cassegrain
  - Alignment sensitivities
  - Polarization
  - Stray light
  - Convex mirror fabrication/testing
  - Packaging
  - OTA wavefront correction

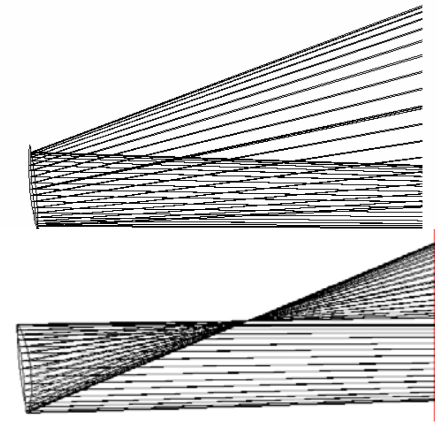

- PM mirror design
  - Blank material: Zerodur (Schott) vs. ULE (Corning)
  - OTA wavefront correction: PM actuators vs. "coarse DM" in coronagraph
  - Open-back vs. closed-back optimized blank

Starlight Suppression System

- "Expanded" Lyot coronagraph, with four pupil locations: coarse DM, fine DM, shaped pupil, Lyot mask
- Anamorphic optics provide circular beam cross section onto coarse DM and beyond
- Polarizing beamsplitter arrangement provides two distinct coronagraphs (paths)
- Two fine DMs per path in a Michelson arrangement for amplitude and phase correction
- System comprises only collimating and focusing mirrors, with aberrations corrected everywhere along the optical train at the level of ~0.001λ
- Options under consideration include removing polarizing elements and also possibly the Michelson, leading towards an all-reflective, single path system

System Block Diagram

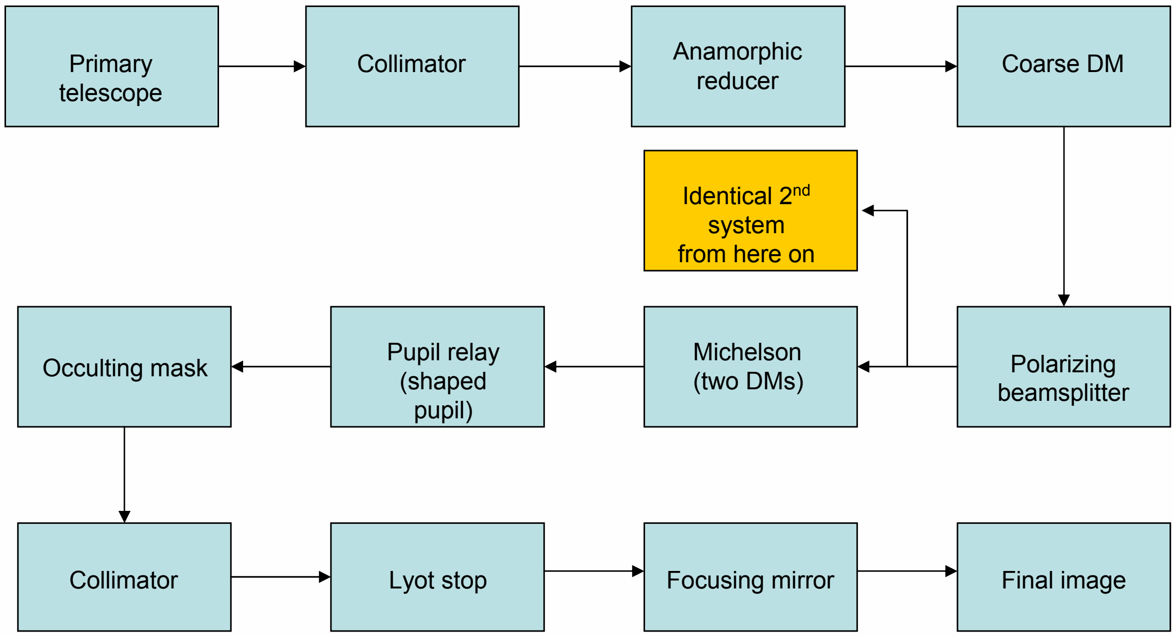

System Schematic

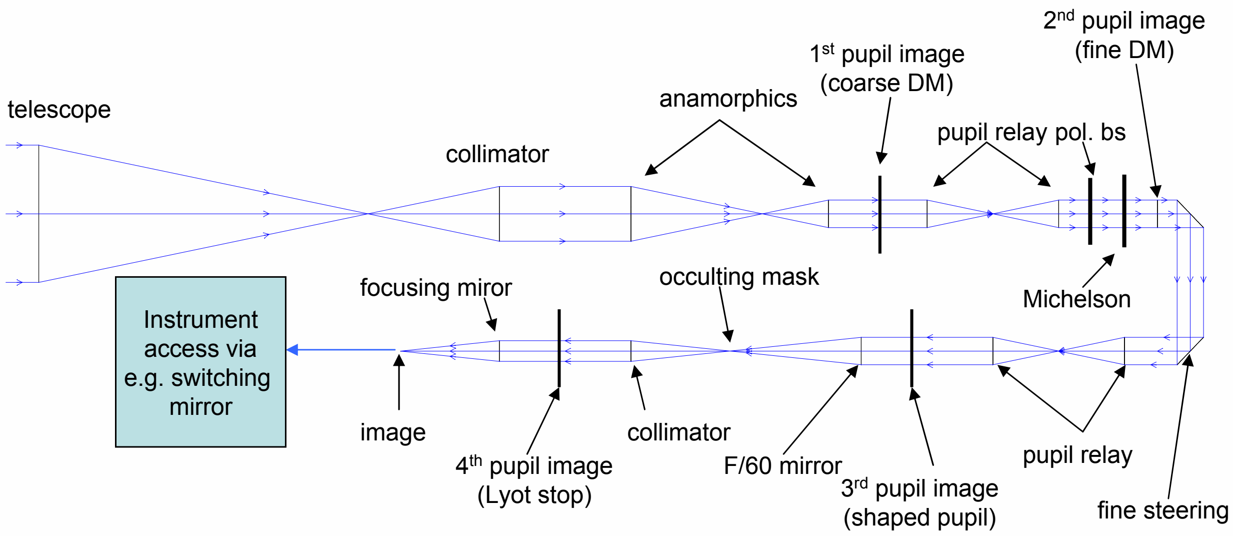

- shows the number of pupil locations, intermediate foci, collimated spaces
- not all optical elements identified
- beam diameters & focal lengths not to scale
- mirrors shown as perfect lenses

Three views of the SSS accommodation behind the telescope primary

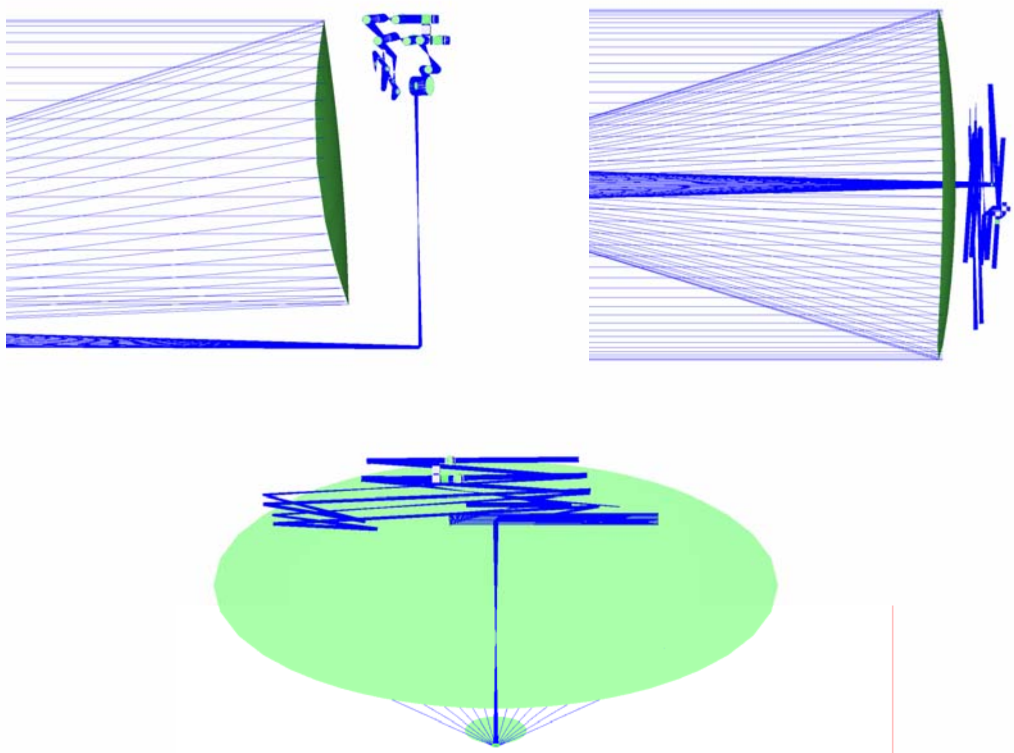

Optical layout (single path)

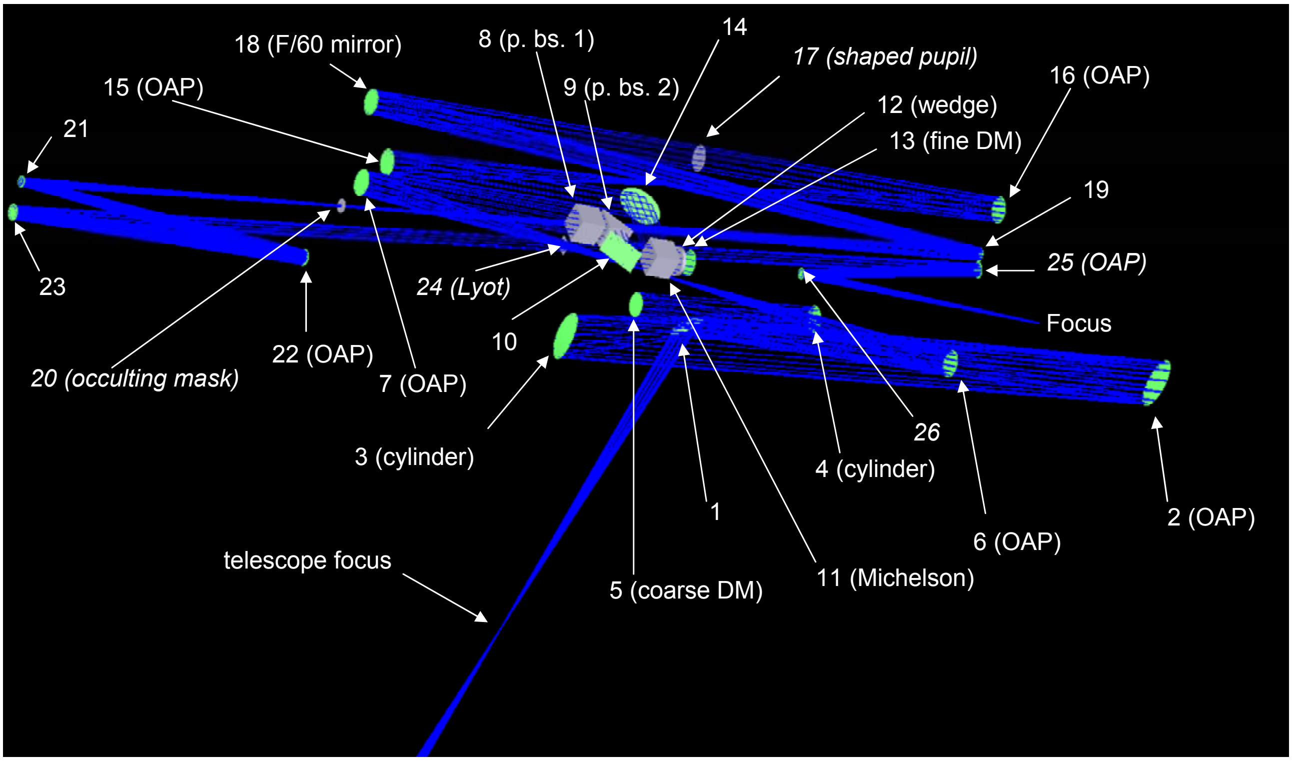

All powered mirrors are off-axis parabolas (OAP). Elements not otherwise identified are flat fold mirrors. Numbering of elements follows the light (same as table on p. 7.)
Shows one polarization path and a single path through the Michelson (one fine DM).

Optical layout (all paths)

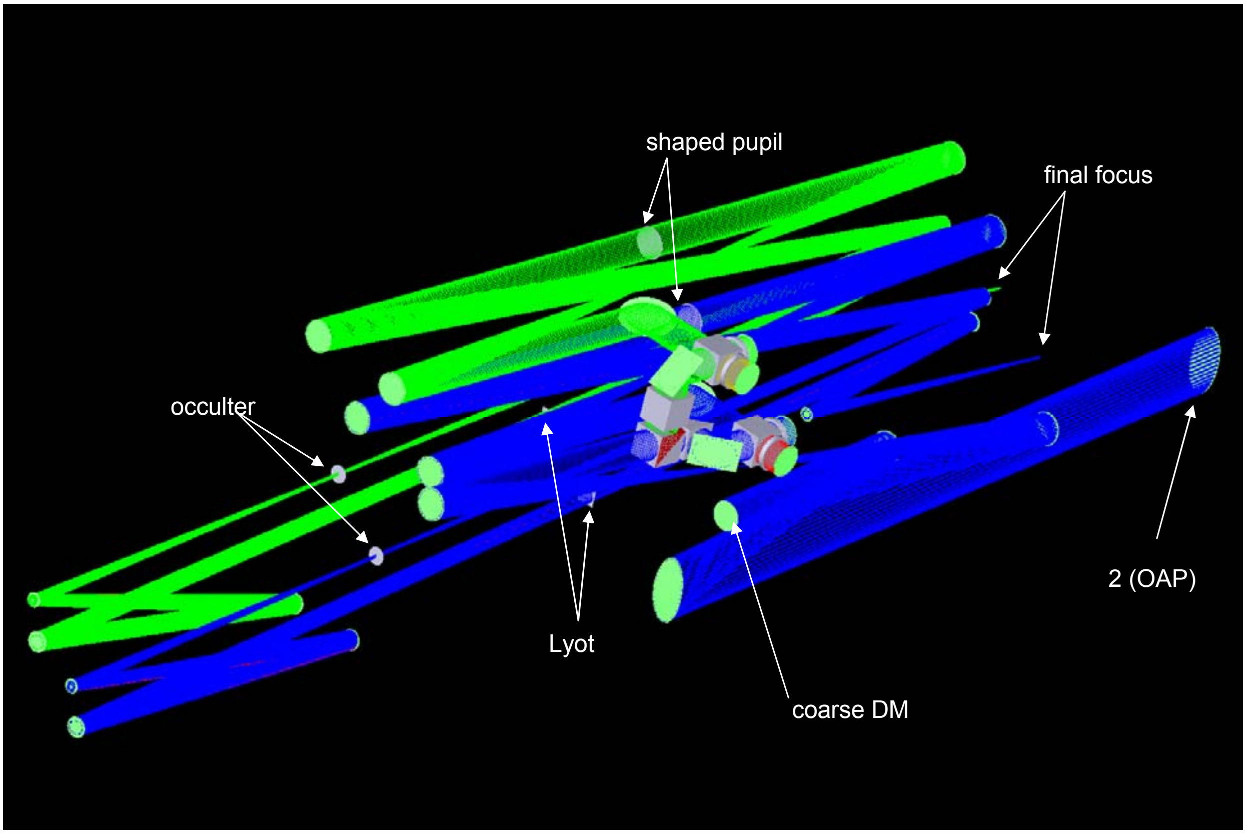

Shows both polarizations and two fine DMs per path (complete Michelson arrangement)
Second polarization path shown in green. Starts at element #2 of previous slide.

Element listing

Element #	Type	Focal length (mm)	Approx. beam footprint (mm)	Function
1	Flat mirror		140x46	Fold
2	Parabolic mirror	4000	230x100	Collimator
3	Cylindrical mirror	800	230x100	Anamorphic reducer (1)
4	Cylindrical mirror	350	100 Ø	Anamorphic reducer (2)
5	Deformable mirror		100 Ø	***Coarse DM***
6	Parabolic mirror	1500	100 Ø	Pupil relay (1)
7	Parabolic mirror	1500	100 Ø	Pupil relay (2)
8	Polarizing beamsplitter (1)		100 Ø	Separates polarizations
9	Polarizing beamsplitter (2)		100 Ø	Increases unwanted beam extinction
10	Flat mirror		140x100	Fold/fine steering
11	Beamsplitter		100 Ø	Michelson
12	Wedge		100 Ø	Chromatic correction
13	Deformable mirror		100 Ø	***Fine DM***
12	Wedge		100 Ø	Same as 12(return path)
11	Beamsplitter		100 Ø	Michelson (return path)
14	Flat mirror		100x140	Fold/fine steering
15	Parabolic mirror	1500	100 Ø	Pupil relay (1)
16	Parabolic mirror	1500	100 Ø	Pupil relay (2)
17	Optional mask		100 Ø	***Shaped Pupil***
18	Parabolic mirror	6000	100 Ø	F/60 to occulting mask
19	Flat mirror		56 Ø	Fold
20	Mask			***Occulting mask***
21	Flat mirror		35x30	Fold
22	Parabolic mirror	3000	55x60	Collimator
23	Flat mirror		52 Ø	Fold
24	Stop		50 Ø	***Lyot stop***
25	Parabolic mirror	2000	52 Ø	Focusing
26	Flat mirror		35x32	Fold
27				Final focus

Principle of the anamorphic reducer

(a): non-imaging direction (b): imaging direction

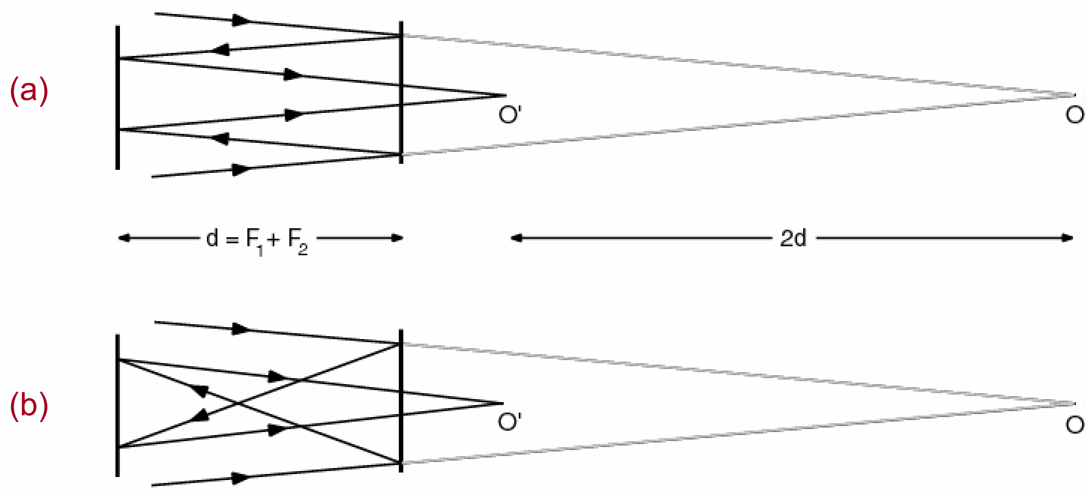

Original pupil image is at O. After insertion of reducer, it is imaged at O' for both directions. Shown here with ideal thin mirrors. In (a) rays appear to follow the law of reflection since the mirror has no power. In (b), the mirror has power.

Effect of the anamorphic reducer

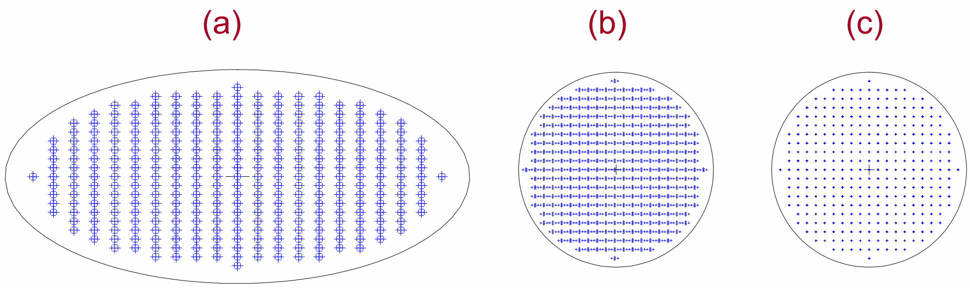

Beam footprints at (a): first cylindrical mirror, (b) second cylindrical mirror, (c) coarse DM

Each dot in (c) represents ray intersections from all field points, which are closely coincident, indicating good pupil imagery. In (a) and (b) which are far from a pupil location, the ray intersections are smeared forming a near continuum.

Polarizing beamsplitter approach

Crystal:

- High extinction and broadband well beyond 1000 nm
- Serious aperture size restriction (<~2”) necessitates re-imaging to 4” DM
- Cannot be polished well enough at arbitrary angles
- Not optimum for constructing wedges

(Not feasible)

Thin film:

- Not high extinction, needs extra polarizer (or 2nd cube)
- A lot of glass, requires extreme control of optical quality
- Can be made to size
- Sufficiently broadband for 500-800 nm, very challenging (impossible?) beyond
- Can make arbitrary wedge angles easily for controlling chromatic shift

(Baseline)

Wire grid:

- Not high extinction, needs two in series
- Sufficiently broadband, even to 1000 nm
- Can be made on high quality fused silica substrates
- Can make arbitrary wedge angles
- Not yet demonstrated at large sizes needed

(probably best future approach as technology matures)

Polarizing beamsplitter performance

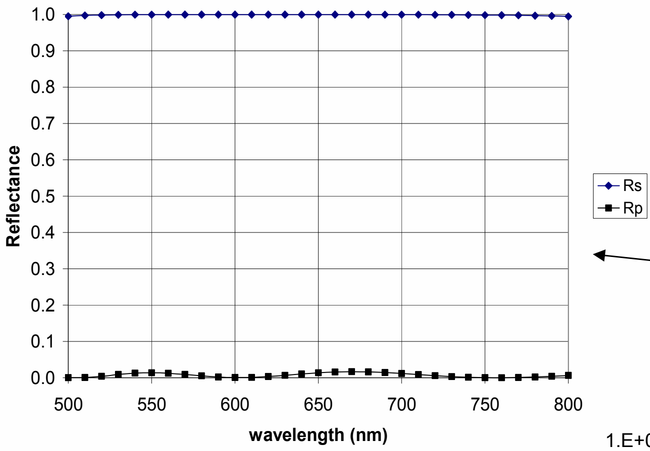

Based on a preliminary 10-layer MgF_2/TiO_2 design sandwiched in LaK glass.

s and p reflectances for a single cube

Transmittance of two crossed cubes. Top curve has a minimum value of 98.3%. Leakage component is below 1e-4 throughout.

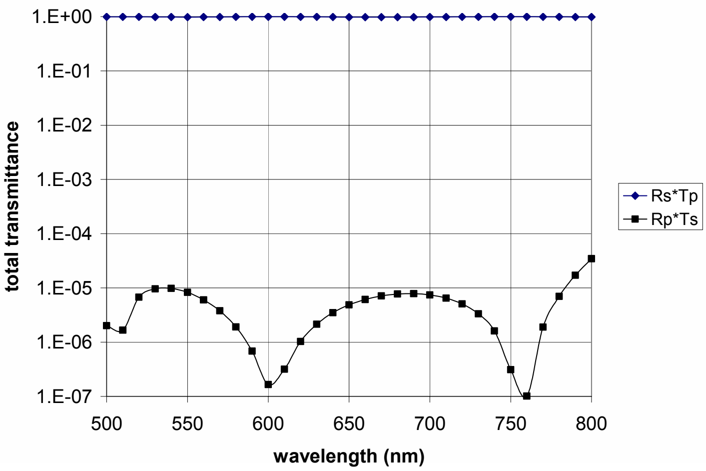

Polarizing beamsplitter design

"Cubes" are quasi-cubes to avoid ghosts:

surface	*Angle (deg)*
front	-0.2
rear	0.2
air gap	0.6
last	0.4

- First cube wedge: -0.2º, second cube wedge 0.4º
- Air gap compensates for wedge fabrication error.

Chromatic compensation (through two pol. bs quasi-cubes):

Angular displacement: << 1 nrad

Linear displacement: ~0.1 µm

These angles are semi-arbitrary, compensation can be achieved with any (small) initial angle.

If wire grid polarizers prove to be a better solution, chromatic compensation can be achieved in different ways (next).

Michelson vs. Mach Zehnder for DM arrangement

Choice is driven primarily by wedge (beamsplitter) design and compactness

Compensating wedge options

M-Z

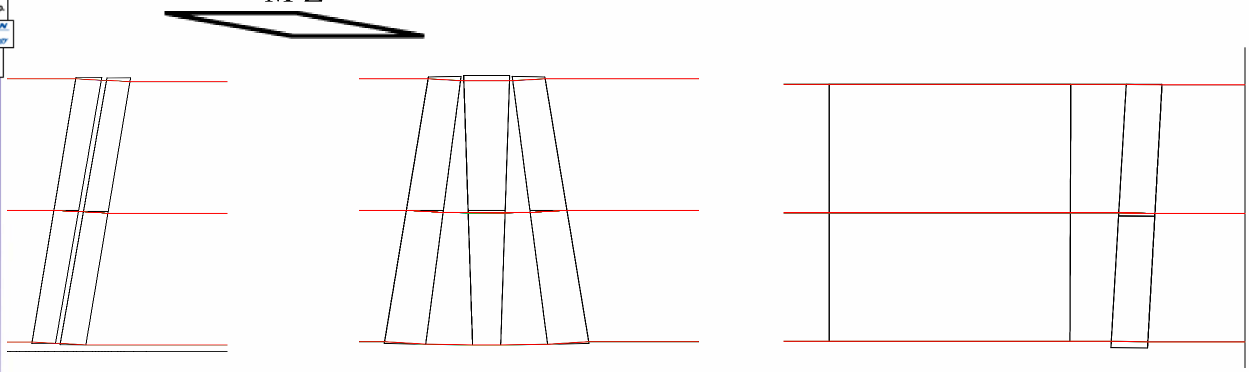

Double wedge (1st surface refl.)

Triple wedge (1st surface refl.)

Quasi-cube plus wedge (immersed reflection, 45°)

	Double wedge	*Triple wedge*	*Quasi-cube*
Linear dispersion	27 μm	0.1 μm	6 μm
Angular dispersion	<< 1 nrad	0.8 nrad	<< 1 nrad

Michelson with quasi-cube plus wedge chosen

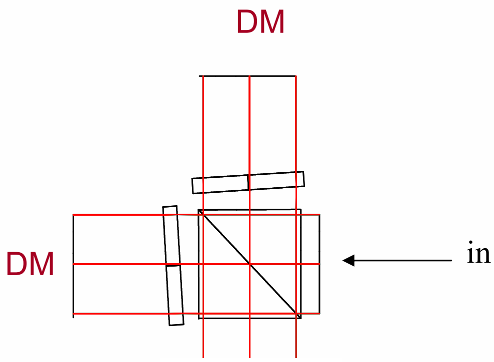

Cube and prism have wedge angles of 0.2°, "air" gap has a wedge angle of ~3.3°.

Material is fused silica

Symmetric design

Complete pol. b/s and Michelson assembly

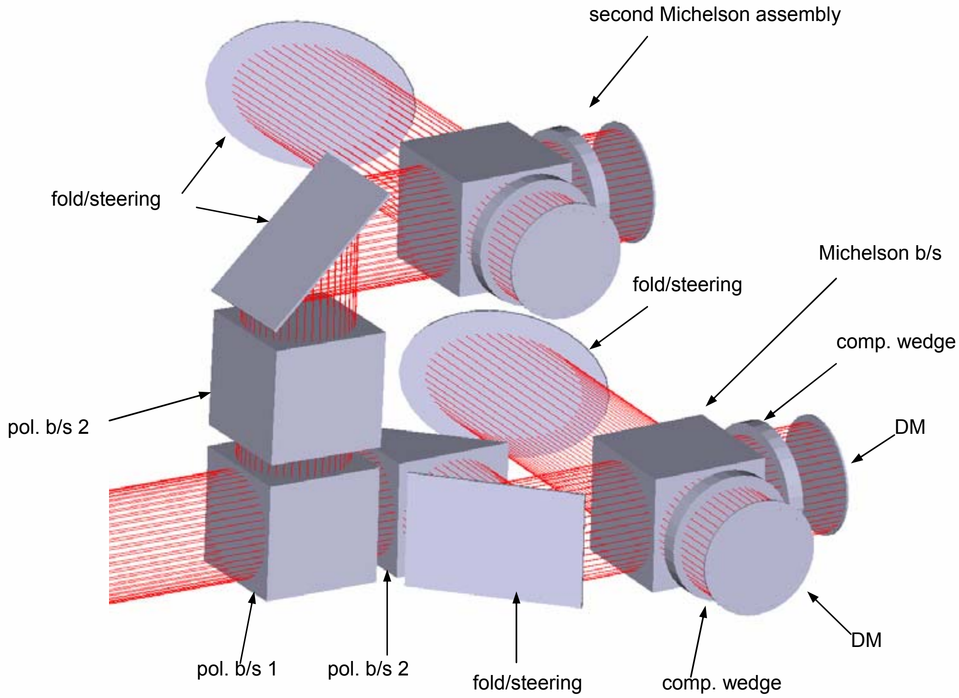

Design performance

Spot diagrams shown inside the corresponding Airy disk size for the middle of the field and the worst-case 2” field location.

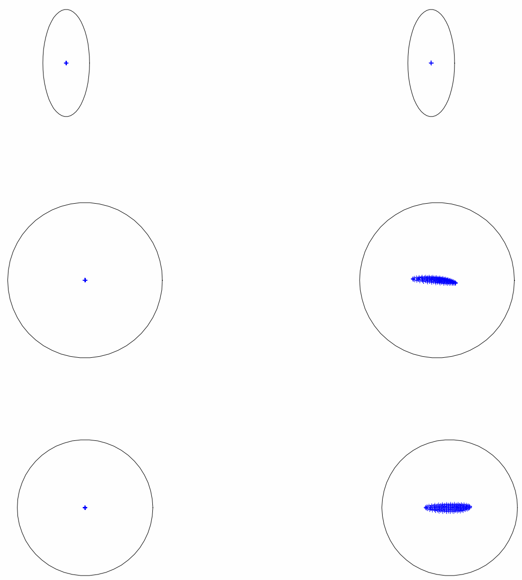

Telescope focus

Occulting mask

Final focus

Center of field has only telescope residual aberration. Edge of field gradually degrades as more OAPs are added along the way.

Design performance

	Field position	Strehl ratio	rms aberration (waves @ 500 nm))
Telescope focus	center	1.000	0.0001
	2"	1.000	0.0004
Occulting mask	center	1.000	0.0001
	2"	0.986	0.0145
Final focus	center	1.000	0.0001
	2"	0.974	0.0295

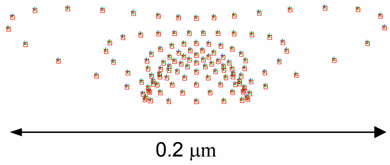

Magnified polychromatic spot diagram at final focus shows chromatic error fully suppressed.

System Pointing Control Architecture & Design

James Alexander

Contributors:
Alice Liu (GSFC)
Carl Blaurock (Nightsky Systems)
Larry Dewell (LMCO)

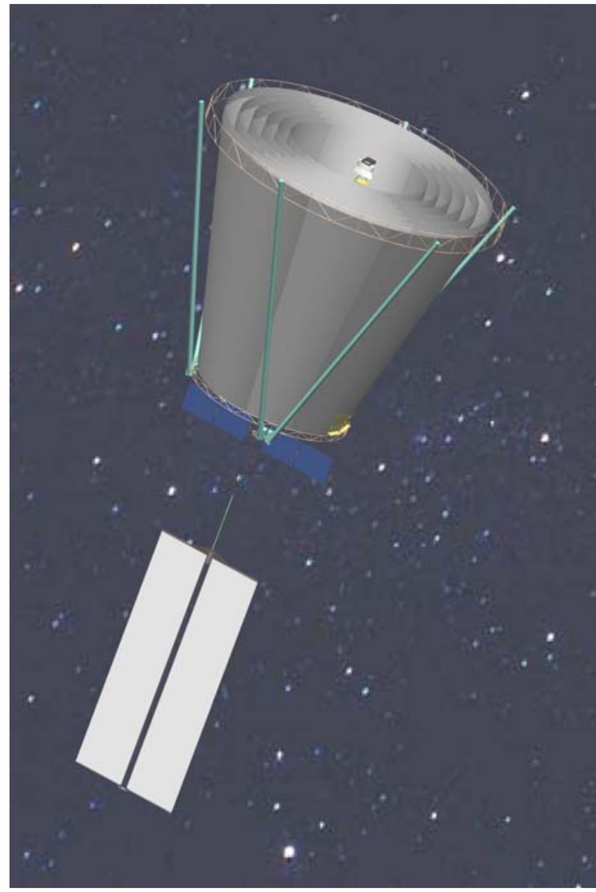

11-12 July 2005

Outline

- Pointing Control System (PCS) Overview
  - Objectives
  - Vibration isolation architectures
  - Requirements
  - Operational modes
- Pointing Control System Design
  - Actuator description
  - Sensor descriptions

•The PCS (Pointing control system) covers the entire pointing of the coronagraph.

–This includes the Spacecraft (S/C) ACS, (the S/C also known as the support module) which has gyros, reaction wheels and star trackers.

–This presentation gives a high level view of the architecture, requirements, and highlights the approaches for achieving the tight pointing requirements.

•The Payload Module (where the coronagraph and other science instruments reside) is isolated from the S/C by either an active (the current baseline) or passive isolation system, along with sensors to provide a better estimate of the actual pointing of the coronagraph and other instruments on the payload.

Flight Baseline 1 Design Objectives

- Create PCS designs to meet error budget requirements
- Develop operational concepts from coarse to fine pointing modes
- Selected hardware based on current technology and flight heritage
- Chosen two baseline architectures for analysis
  - Passive isolation system
  - Active isolation system

•Cycle I develop a set of requirements and analysis approaches to analysis pointing performance, focusing primarily on how to reduce vibrations transmitted to the payload and how to compensate for those which are transmitted.

•Hardware selected was based on hardware that either is fully mature, or in an advanced state of development (TRL 5 or highter), or hardware that is a reasonable extrapolation from existing hardware (e.g., the payload acquisition star cameras described later).

•Two baseline approaches were selected, with the key difference being the isolation system. The passive isolation (no active control) is mature in development. The active approach, the analysis for which is based on the Lockheed Disturbance Free Payload (DFP), is currently at TRL 5, meaning that it has been testing in the laboratory in an environment reasonably consistent (vacuum, temperature) with the flight environment.

Two Approaches to Vibration Isolation

- Two-stage passive isolation design
  - First stage on reaction wheel assembly
    - Isolator struts modeled on Honeywell D-strut
    - 1.5Hz target frequency
  - Second stage at bus-payload interface
    - 1Hz target frequency
  - Selected modal damping
- Active isolation design
  - Disturbance free payload (DFP) architecture (Lockheed Martin)
  - Instrument payload and spacecraft bus connected only by cables
  - Payload/spacecraft non-contact actuators and payload attitude sensors provide precision inertial pointing of payload by reacting against mass of spacecraft
    - 0.5 Hz target payload pointing bandwidth
  - Spacecraft attitude control driven to maintain non-contact actuator finite stroke/gap
    - 0.015 Hz target relative attitude control bandwidth

- Note that vibration can be induced on the payload by transmission through the isolator, by mechanisms on the payload side, thermal gradients, external torques, and by transmission across cables connected to both the S/C and Payload Module (such as power cables)
- The Active Isolation is expected to provide a higher degree of isolation because of the magnetic coupling (no physical contact) between the S/C and Payload for the isolation, hence less compensation will be required on the payload.

Passive Architecture

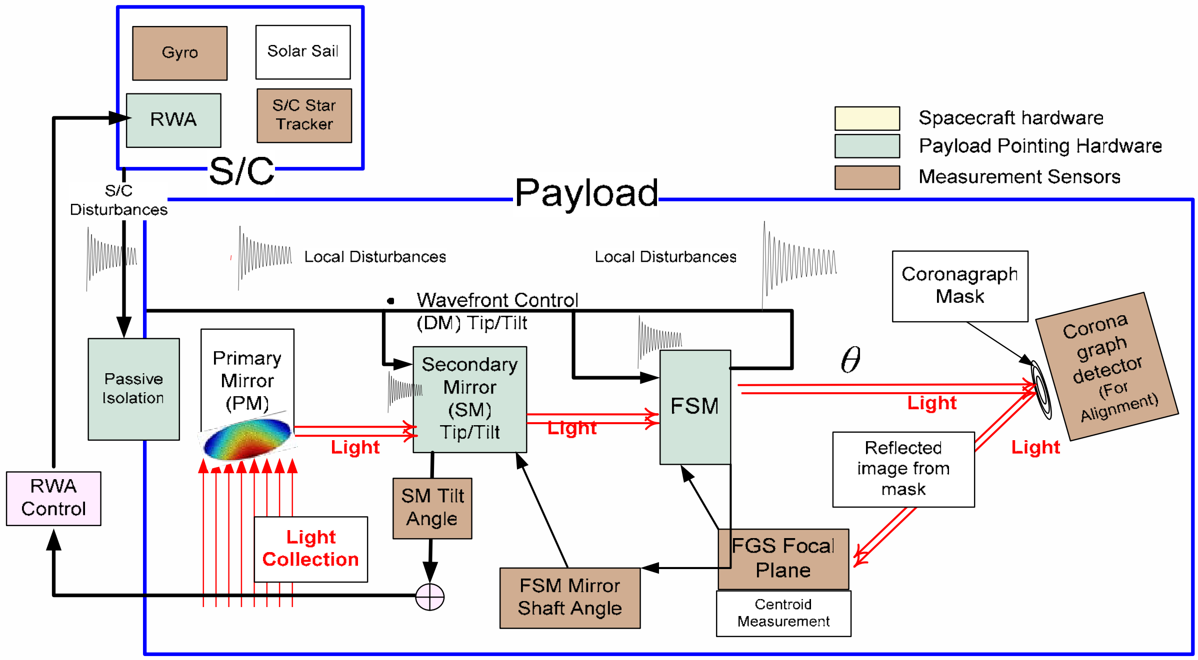

- Use of passive isolation requires RWA, SM, and FSM control for maintaining pointing control. Note that the reaction wheels must point the entire S/C

- Overall architecture takes light from the coronagraph star, uses RWA to point the S/C, Secondary mirror to maintain beam walk control on telescope, and FSM to take out high frequency pointing errors. Light from the coronagraph star is reflected from the coronagraph mask surface for feedback to the detector.
- The Feedback to the Reaction wheels is the secondary mirror pointing angle relative to the Payload frame. The feedback to the secondary mirror pointing is the FSM angled (shaft angle). This implementation (based on mechanical pointing angles) keeps the Payload beamwalk and alignment within requirements.
- Note that other schemes /implementation for the FGS implementation will be evaluated in the next cycle.

Active Architecture

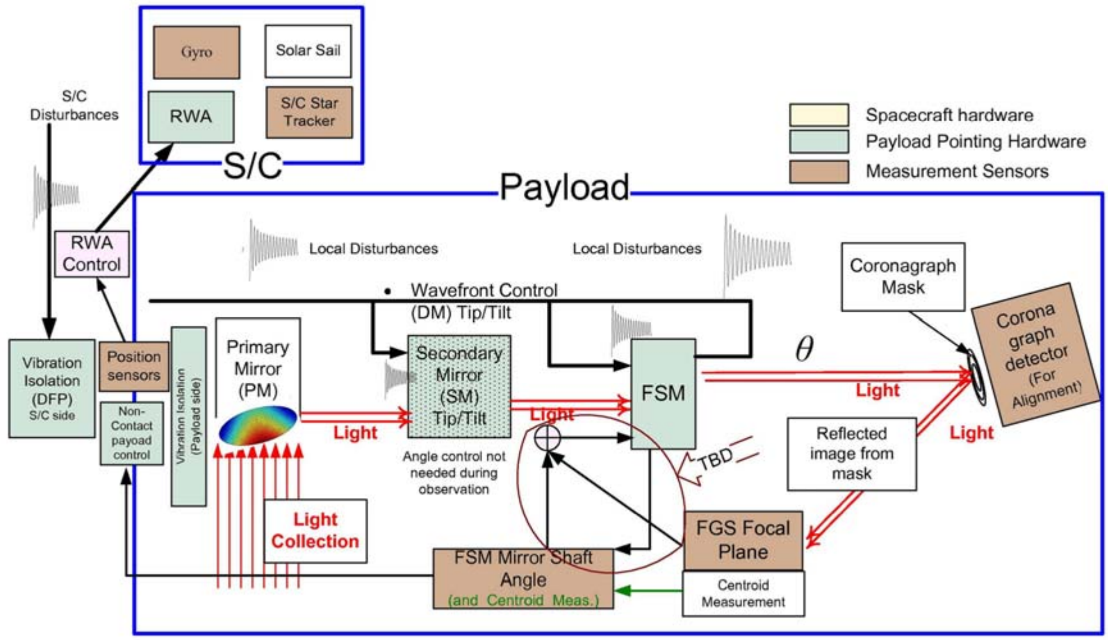

- Current Analysis shows that both SM and FSM control not needed during observation, but only the output from the FGS focal plane. The green arrow replaces the circled area.
  - The current architecture is still showing the FSM loop until the noise models have been more developed.
  - Both the FSM and SM control are required for the case of passive isolation
- Note that the active isolation position sensors are used to drive reaction wheel control

TPF Terrestrial Planet Finder

- After acquiring the coronagraph acquisition star, the DFP stabilizes the payload pointing using feedback directly from the FGS is used to point the payload using the DFP. The misalignment between the Payload and S/C is sensed by actuator sensors and is feedback to the RWAs to keep the overall pointing within the roughly 1 degree pointing capability of the DFP.
- In this mode of operation, the secondary mirror is expected to not be pointed for tip/tilt control. Current analysis shows that even the FSM control may not be needed during the observation. However, the FSM loop is still shown in the architecture until all the noise sources have been analyzed.
- See slide 16 for block diagram emphasing DFP.

PCS Requirement – Contrast and Optic Performance

- Top level contrast requirements

Beam Walk	LOS	LOS mask error	Structure Deformation	SD mask error	PM deformation	PM def. mask error	**Total contrast**
1.90E-12	9.04E-14	5.46E-13	2.75E-17	1.64E-17	8.55E-13	5.19E-15	**3.40E-12**

- Opto-mechanical responses:
  - Image position (line-of-sight (LOS) errors)
    - Image jitter (σ) <= 0.3 mas (1σ)
    - Image offset (Ω) <= 0.3 mas
  - Beamwalk on each optic identified in error budget
    - Beamwalk due to pointing (after all control loops closed) <= 0.04 mas
  - Zernike amplitudes (aberrations): structure deformation and deformation of optic

$$C_{pointing} = c_1\sigma^4\Omega^4 + c_2\sigma^6\Omega^2 + c_3\sigma^2\Omega^6 + c_4\sigma^8 + c_5\Omega^8$$

Zernike mode	SD Aberr (nm)	PM Aberr. (nm)
4	4.78E-02	4.00E-01
5	6.21E-03	4.00E-01
6	4.58E-02	4.00E-01
7	2.50E-03	2.00E-01
8	6.00E-03	4.00E-01
9	3.48E-03	3.00E-01
10	4.41E-03	4.00E-01
11	1.29E-04	5.00E-03
12	1.44E-04	5.00E-03
13	3.77E-05	5.00E-03
14	7.95E-05	5.00E-03
15	4.56E-05	5.00E-03

- These requirements are from a rather complicated error budget. The key result to note for the coronagraph is that the ultimate goal is to achieve the best contrast, which is the circled number in the side --- jitter, pointing error, etc all contribute to this number. The small the circled number, the better.

PCS Requirement – Physical motions

- Physical motions
  - Rotation and translation requirements on first 3 optics following PM and coronagraph box

	Rx (nrad)	Ry (nrad)	Rz (nrad)	Tx (nm)	Ty (nm)	Tz (nm)
SM	1.829	1.216	5.226	2.643	5.518	1.076
Fold 1 (M3)	10.050	10.050	10.050	100.500	100.500	100.500
Fold 2 (M4)	10.050	10.050	10.050	100.500	100.500	100.500
Coronagraph Box	10.050	10.050	10.050	10.050	10.050	10.050

  - Rigid body pointing
    - X/Y axis (tip/tilt) jitter < 4 mas (1σ)
    - Z axis (around LOS) ~ 1asec (1σ)
- Operational efficiency requirement: slew/settle time for a 30 degree dither must be completed in 30 minutes

- No comments on this slide

National Aeronautics and Space Administration
Jet Propulsion Laboratory
California Institute of Technology
Goddard Space Flight Center

Acquisition Layout

Terrestrial Planet Finder
TPF

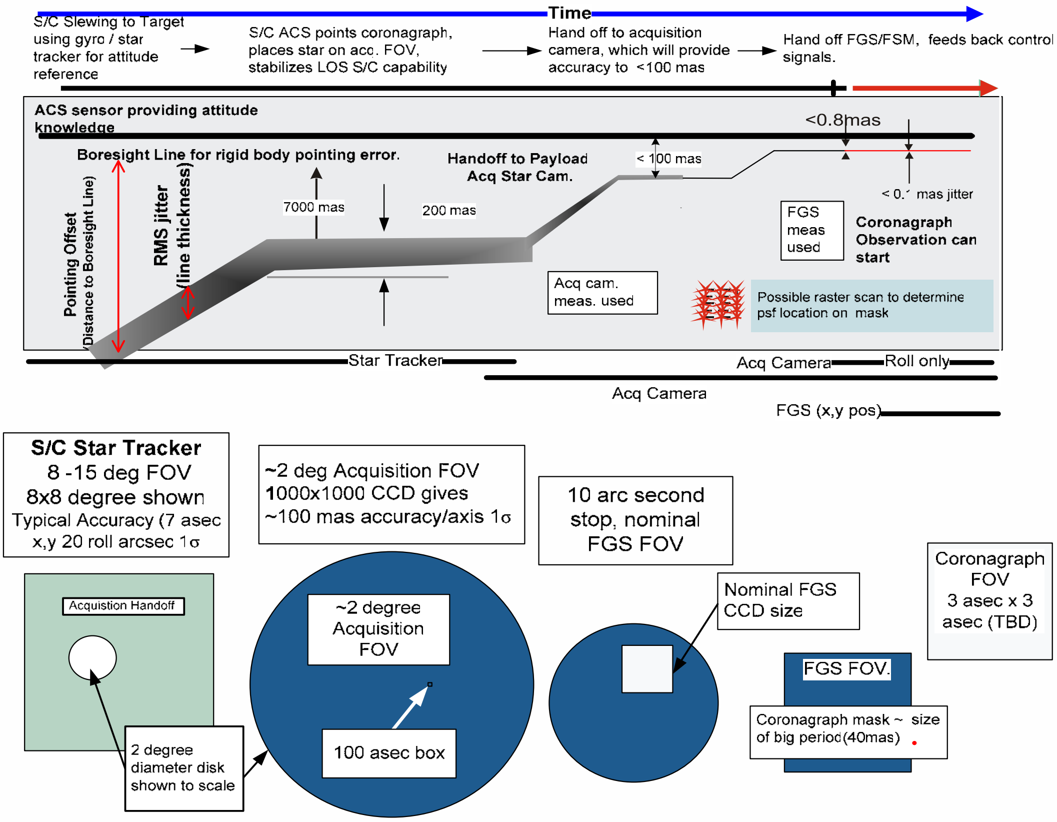

- Because of the very small FOV of the coronagraph, (the mask is < 0.1 arcsecond wide), very tight attitude knowledge is required to place a star (the coronagraph star) on the mask.
- The S/C star trackers are "loosely" coupled to the payload through the isolation system. Using the reaction wheels and S/C star tracker, we should be able to point the payload to better than 60 arcseconds (3 sigma) + alignment errors +errors introduced by the alignment of the payload to S/C.
- A payload star acquisition camera (PSAC) of > 1 degree will be large enough FOV for the handoff. The larger FOV shown is to obtain the needed star coverage.
- Note that there are actually PSAC, both active, with FOV's separated by at least 30 degrees to provide the three axis attitude knowledge on the payload.

Operational Modes

- Coarse Mode
  - Rigid body slewing and coarse pointing
  - Requirement:
    - Accuracy 7 asec
    - Coarse pointing stability <1 asec (1σ)
  - Primary stability in coarse mode from the gyros.
- Acquisition Mode
  - Guide star image to fine guidance sensor (FGS) field of view (FOV)
  - Requirement:
    - Accuracy better than 1 asec
    - Stability from Payload Star Acquisition Camera (PSAC) <100 mas (1σ)
    - Accuracy limited by alignment stability to coronagraph
- Fine Pointing Mode
  - Stabilize image position on mask using fine guidance mirror (FGM) or fine steering mirror (FSM)
  - Requirements: contrast, optical performances, and physical motions (see error budget)

- This section development in more detail the operations hinted at on page 7, the previous page, for each of the isolation systems.
- The accuracy shown are what are expected from our baseline system. Recall that the PSAC is actually a pair of FOV's.
- The coarse, acquisition and fine pointing modes are discussed for the passive isolation system (next 4 slides).
- For the active isolation system, the coarse, acquisition, and fine pointing modes are treated the same; as a result, only the fine pointing mode is shown, but in greater detail (2 slides, following passive isolation description)

Coarse Mode – Passive System

- 3-axis inertially stabilized attitude control system (ACS)
- Actuators: 6 reaction wheels (RW) to point observatory (payload + spacecraft support module)
- Sensors/estimators: Kalman filter on gyros (IRU) and star trackers (ST) signals to provide 3-axis attitude inf

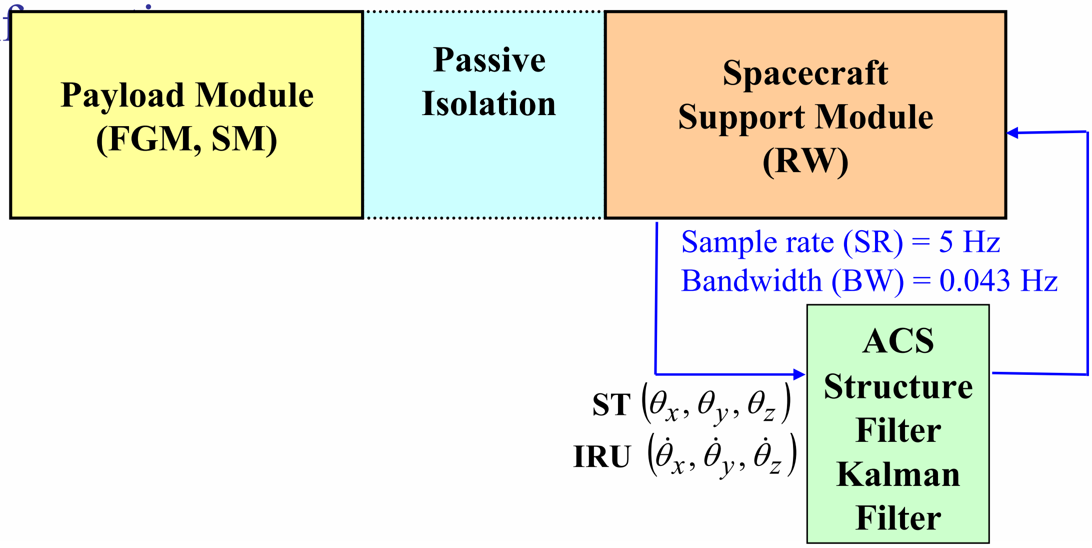

- Coarse mode uses the reaction wheels to point the S/C to where the coronagraph star should fall on the coronagraph. Feedback is directly to the reaction wheels; uses S/C star trackers for attitude knowledge.

Acquisition Mode – Passive System

- Similar to coarse mode with tighter pointing and sensing requirements
- Actuators: 6 reaction wheels
- Sensors: payload star acquisition cameras (PSACs) provide 3-axis attitude information and rate derivation

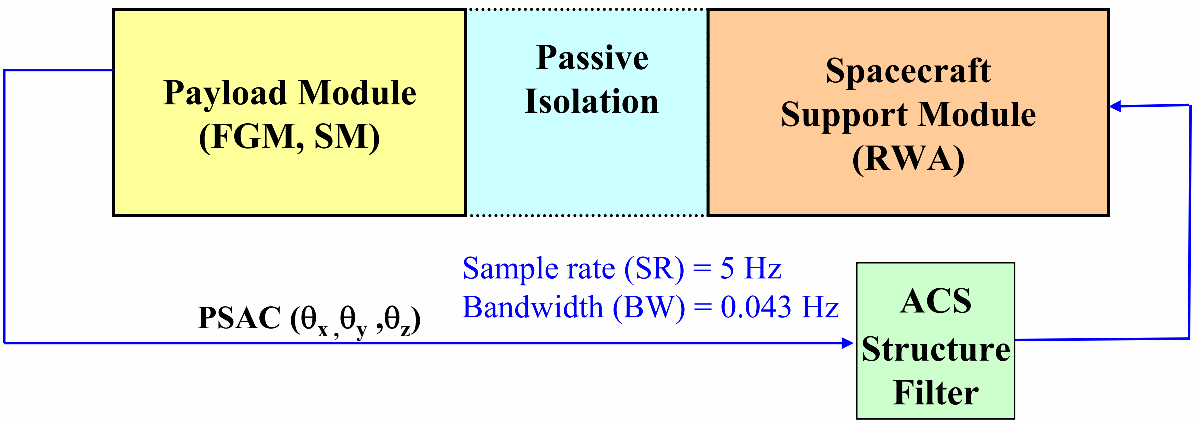

- Acquisition mode uses the reaction wheels to point the S/C to where the coronagraph star should fall on the coronagraph. Feedback is directly to the reaction wheels; similar to the coarse mode except PSAC is used instead of S/C star trackers.

Fine Pointing Mode – Passive System

- Rigid body fine pointing (ACS)
  - Reduce low frequency and constant external disturbances
  - Actuator: 6 reaction wheels
  - Sensor: PSAC used only for roll information (θ_z) around LOS, and SM motions (feedback from position) used for θ_x and θ_y information
- Secondary mirror control (SMC)
  - Compensate for thermal drift between Payload Modules and Spacecraft Support Module
  - Provide additional tip/tilt pointing correction
  - Actuators: 6-axis hexapod actuator
  - Sensor: laser metrology, tip/tilt angles of FGM
- Image motion control (IMC)
  - Attenuates high frequency θ_x and θ_y errors
  - Actuators: fine guidance mirror (FGM)
  - Sensor: fine guidance sensor (FGS)

TPF Terrestrial Planet Finder

- Vibrations reduced by letting Payload settle; assumed a damping of 0.1%
- S/C must point Payload using reaction wheel control. Uncompensated error (due to low bandwidth of S/C ACS is taken out by secondary mirror. Finally the fine steering mirror (FSM, also referred to as the Fine Guidance Mirror, or FGM) is used to perform high bandwidth control. Measurements from the fine guidance sensor (FGC or FGS) are used to provide the attitude information needed to control the FSM.
- The control system then relies on three dependent loops. S/C pointing, secondary mirror pointing, and fine guidance pointing. See description on next slide.

Fine Pointing Mode – Passive System

- Features three "staged" control systems
  - Rigid body control off-loads secondary mirror control
  - Secondary mirror control off-loads fine guidance mirror control
- Other control loops
  - Wheel speed control (WSC) compensates for wheel drag torque
  - SM hexapod control uses laser metrology feedback signals to stabilize low frequency (thermal drift) motions between SM and PM

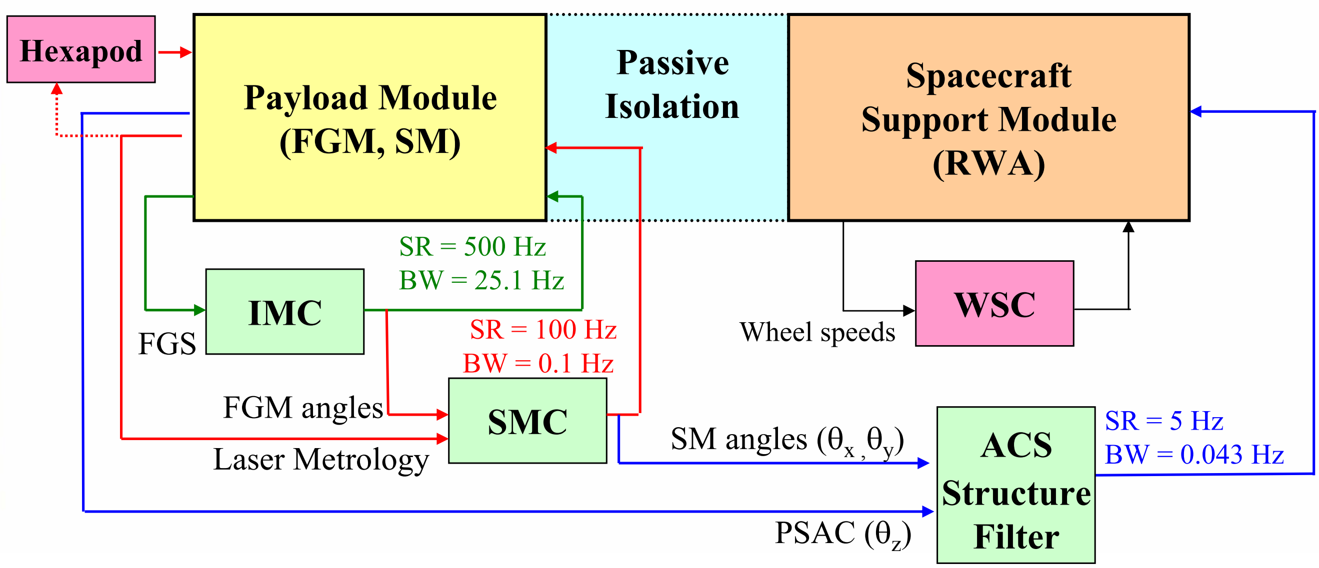

- See passive architecture, slide 5.

Fine Pointing – Active System

- 3-axis inertially-stabilized control system for Payload Module, using Payload Module FGS and PSAC and DFP non-contact actuators
- FGM line-of-sight control not necessary
- Sec. translation control to maintain Prim-Sec. trans. align.
- S/C Support Module inertial attitude control and Payload Module-S/C Support Module relative translation control using IF sensors to maintain interface stroke/gap

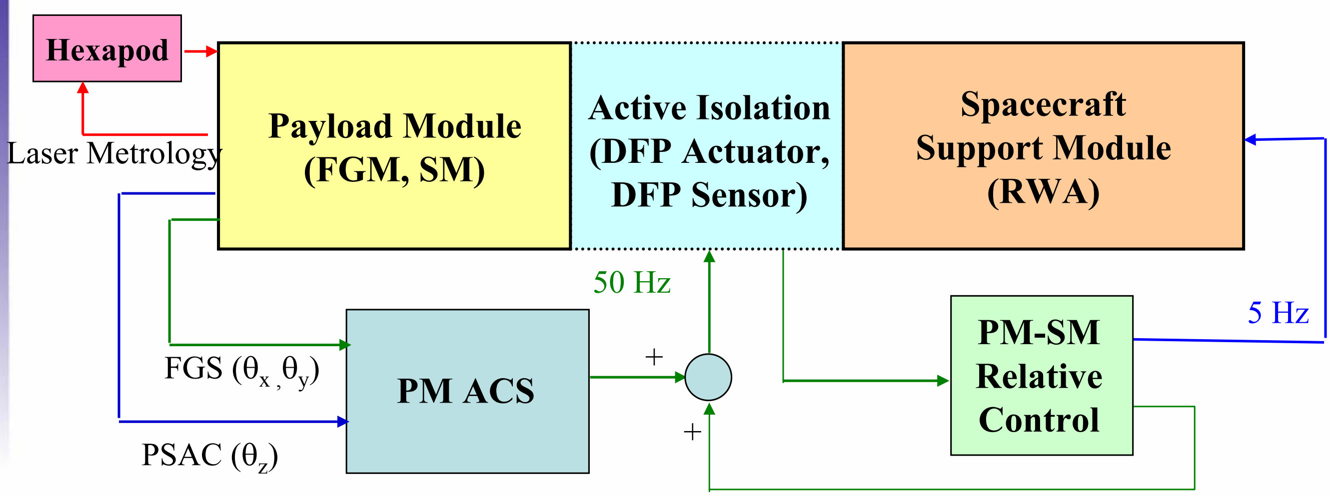

- The fine pointing in the active system relies on direct feedback from the FGS (fine guidance sensor). See active architecture, slide 6.

Pointing Modes (Acquisition, Coarse, Fine) – Active system

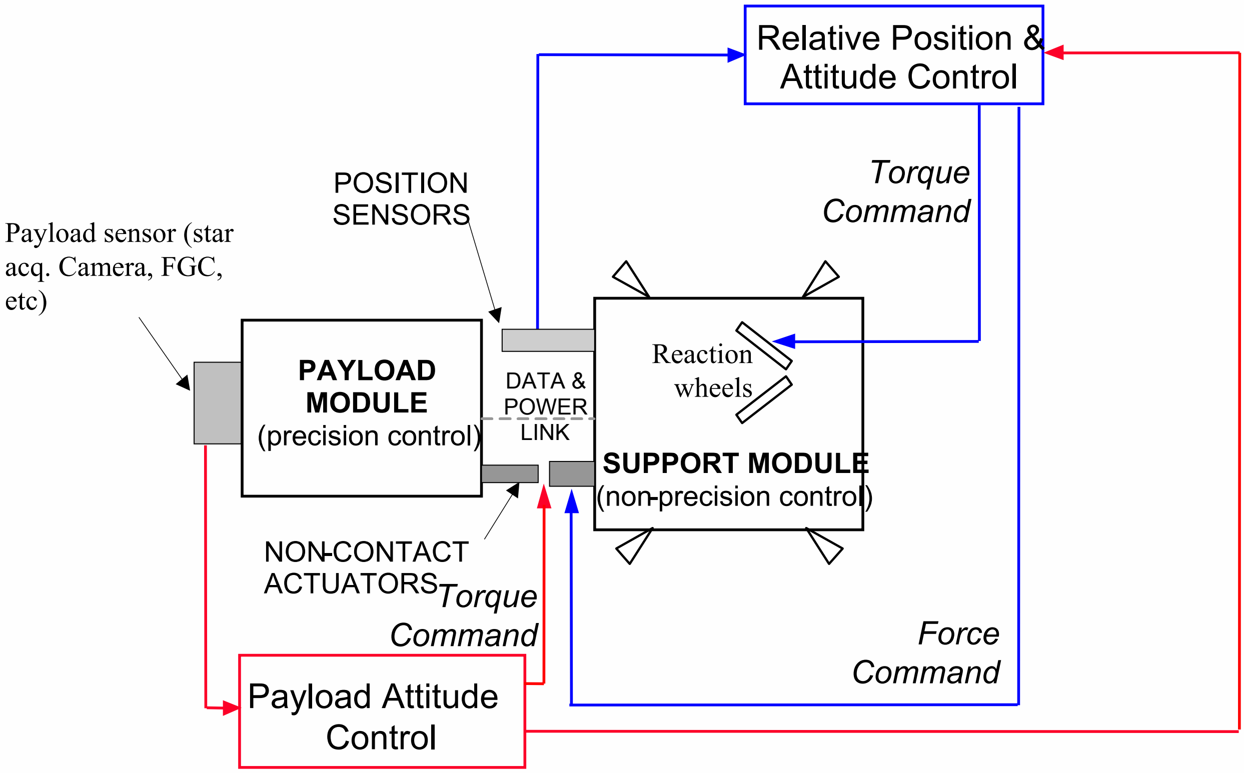

- This shows a cartoon of the hardware configuration of the DFP. See architecture slide for description (slide 6)

Representative Actuator Descriptions - Spacecraft

- Reaction wheel assembly
  - Collected wheel information from Goodrich, Honeywell, and Teldix
  - Baseline six Goodrich wheels
- Wheel performance specs
  - Torque limit = 0.3 Nm
  - Momentum limit = 50 Nms
- Wheel Disturbances
  - Harmonic disturbances – included 8 harmonics from Goodrich data
  - Torque quantization (16-bit D/A)
  - Torque noise ~6.4e-4 N-m/$Hz^{1/2}$ (0.1-1 Hz)
  - Nonlinear drag torque and torque ripple effects

Goodrich E-wheel

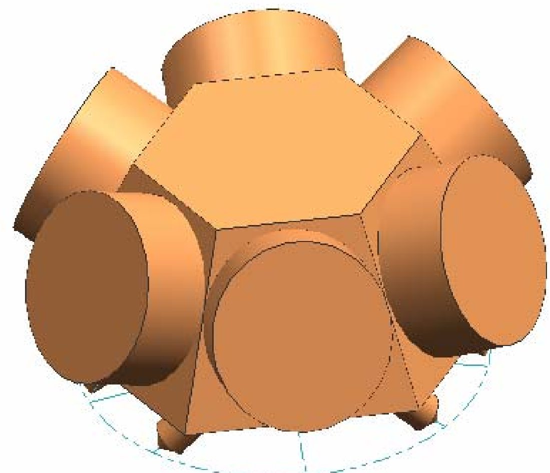

Figure by Tim Ho

- The hardware shown here is used in the current baseline for analysis purposes. This does not imply that it has been selected for the mission, but only to show existence of suitable hardware.

Representative Actuator Descriptions - Payload

- Secondary Mirror (SM)
  - Six axis hexapod
  - Piezoelectric actuators
  - 100Hz first mode
  - Correct for relative position and rotation between primary and secondary mirror
  - Stroke ≈ 200 nm
- Fast steering mirror (FSM)
  - Two-axes tip/tilt mirror
  - Small range of motion
  - Consider re-actuated design to reduce disturbances
  - Uses fine guidance camera for feedback signals
  - Stroke ≈ 100 asec

PI six-axis hexapod

- The above pictures are only used to show the viewer what the equipment might look like, and should be taken as “clip art”, since they are not of the correct size or performance as shown.

National Aeronautics and Space Administration
Jet Propulsion Laboratory
California Institute of Technology
Goddard Space Flight Center

Active System Actuator – DFP

TPF Terrestrial Planet Finder

TC Technology

DFP single actuator assembly

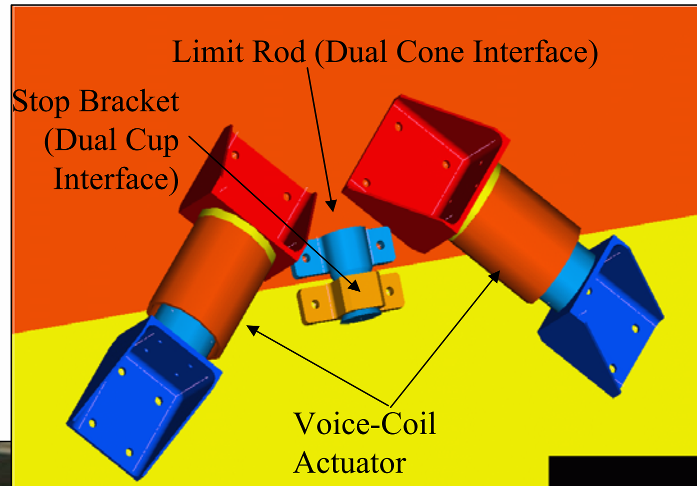

DFP typical mechanical design

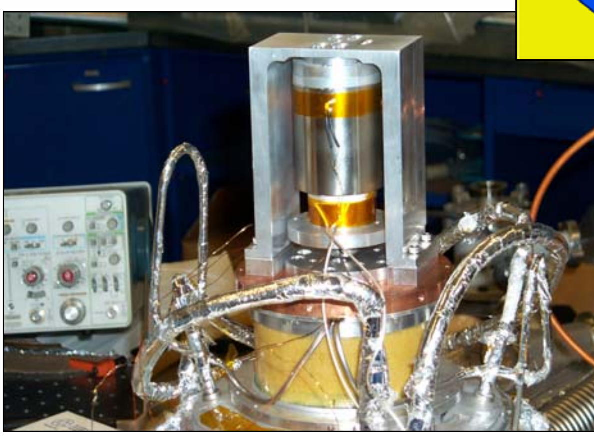

DFP actuator cryogenic testing

- This shows the DFP key components, and the testing of the DFP in the laboratory. Note that the DFP used 3 pair of voice coil actuators, as illustrated in the upper right panel.

Representative Sensor Descriptions - Spacecraft

- Star tracker
  - 8-15 deg FOV
  - (5, 5, 20) arcsec 1σ
  - Update rate ~10 Hz
- Gyros
  - 2-3 axis IRU
  - SKIRU D-II
    - $\sigma_u = 1.33\text{e-}5$ arcsec/sec$^{1.5}$
    - $\sigma_v = 0.019$ arcsec/sec$^{0.5}$
    - Max rate = 2 deg/sec
  - Update rate > 2 Hz
- Wheel tachometer
  - Digital pulse outputs (less noisy than analog outputs)
  - Performance depends on pulse resolution of the wheel (72 pulses/rev for E-wheel)

Ball CT-602

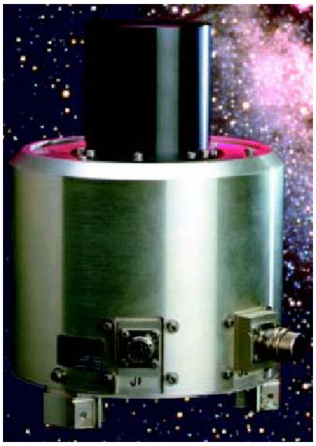

SKIRU D-II

- Redundant - Three-Axis IRU
- No-Single-Point of Failure
- NASA Standard

- Typical S/C equipment used for study. Will provide needed performance, but other hardware may ultimately be used.

Payload Star Acquisition Camera Concept

- Payload Star Acquisition Camera System
  - Pair of star trackers (sep angle > 30deg) -- Based on SIRTF/AXAF high precision type star cameras
    - Narrow FOV (2 -5 degrees), collecting optics ~10cm, multiple star tracking;
    - Provide full sky coverage, current design shows looking through baffle
    - Sample at 5 Hz
  - Will bridge gap between star tracker accuracy and coronagraph occulting spot
  - Could also be used for guiding for ancillary science at less precision than the coronagraph mode. Expected relative accuracy better than 100mas
- Acquisition camera current placement (diagram Tim Ho). Cycle 2 will revisit placement.

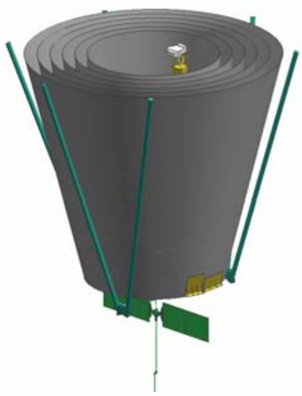

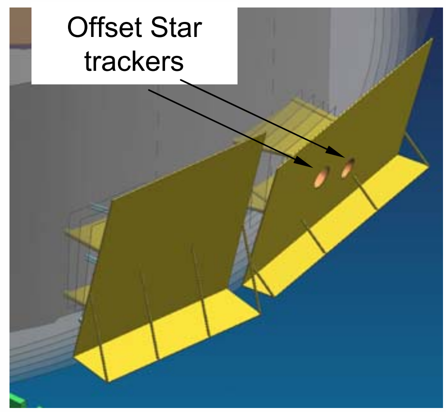

- PSAC (Payload Star Acquisition Camera) System is two camera system, pointing roughly 30 degrees separation, mounted on the payload. Separation of the FOV's gives 3 axes high accuracy. The basic design provides performance consistent (within reasonable extrapolation based on aperture size) with current high precision star trackers such as have been flown on SIRTF and Chandra.
- The choice of FOV is a trade between star coverage and pixel size resolution. Fewer stars at higher accuracy makes the star selection easier, but may not give full sky pointing coverage. The current assumption is a 10 cm collection aperture; (the optical design becomes more complicated maintaining the same aperture with the wider FOV).
- The acquisition camera provides roll information during the fine pointing mode.
- With the 10cm aperture, the pointing of each camera at the galactic poles is limited to about 25mas 1 sigma pointing jitter (assuming a 5 Hz sampling rate and assuming a 5 degree FOV), and all stars above limiting magnitude tracked. Larger aperture or better star availability (away from the poles) could improve the jitter performance. The accuracy (averaged over multiple frames) relative to the coronagraph will be better than 0.3 arcseconds after calibration.
- Calibration will be updatable after each observation. Thermal drift will be the limitation.

Fine Guiding System Concept

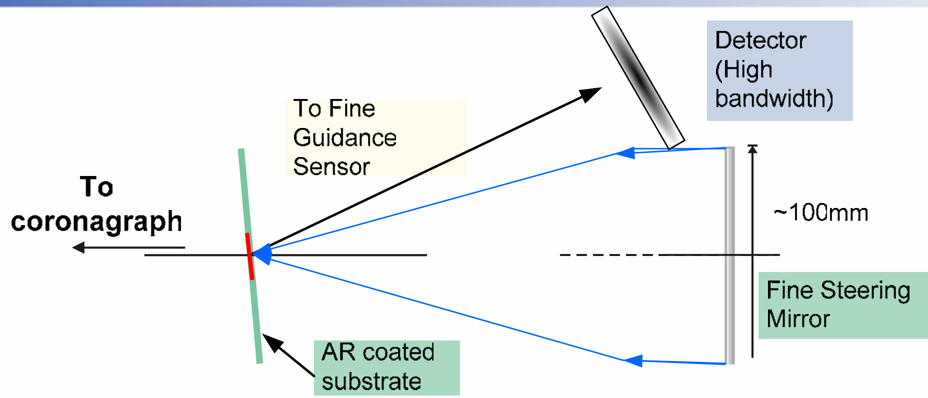

<u>Coronagraph plane mask & supporting substrate</u>
Reflection from coronagraph mask backside or from AR coating on the substrate – at least 1% light returned. Assumes AR coating extends over to full field at the focal plane mask

<u>FSM</u>
Located near DM
Bandwidth ~ 8 to 40Hz
Stabilize image to ~ 0.03 mas
Resolution ~ 0.01 mas on sky

- Current concept
- Light reflected will return ~ 1% of light hitting.
- Detector pixels expected to subtend ~ 1mas to 10 mas

- The FGC is a combination of a FGM and a tracking sensor. The fine guidance mirror controls star location on the coronagraph mask, with the goal of preventing the central star light from leaking past the mask, with a requirement of 0.3mas offset to minimize the light leakage. Additionally there is a jitter requirement of 0.04mas rms (in the direction of the long axis) control error to reduce the effects of beamwalk. The coronagraph target star light is collected by the 22 square meter primary mirror. The FGC will make use of some of the rejected light. The sketch (Fig 2) shows how the light goes through the primary-secondary mirror combination, is steered by an FSM to the coronagraph, where the light is then reflected off the surface of the substrate holding the mask, and returned to a detector for measurement of a star centroid.

Fine Guidance Sensor

- Fine Guidance Camera System
  - Tracks from the star signal rejected from the coronagraph
    - Signal provided from coronagraph target stars ~7 mag.
      - *Mirror 8m x 3.5m --- large collection area*
      - $\lambda_{0.6}/D_{8m}$ *= 15.5mas. NEA requirement ~ 1/400 of* $\lambda_{0.6}/D_{8m}$ *in long axis*
      - $\lambda_{0.6}/D_{3.5m}$ *= 35.3mas gives PSF parameters*
  - Angular measurement requirement on FGS driven by NEA requirement
  - FOV ~3 asec (3 to 10)
  - Fine guidance system designed by GSFC
  - FSM used for both image stabilization and determining maximum contrast alignment
    - possibly not needed during observation with active isolation
  - System must meet tight stability requirements
    - (LOS image jitter $1\sigma = 0.3$ mas, beamwalk pointing jitter $1\sigma = 40$ microarcsec as shown in current error budget (sampled at 100 Hz to 500Hz, TBR)

TPF Terrestrial Planet Finder

- The frame rate and accuracy and star magnitude have been selected to support the 0.04 mas jitter. If the pointing requirement were a 4mas requirement, the signal to noise requirement becomes a lot looser, and that roughly a factor of 10,000 less information is required, which translates into roughly 10 stellar magnitudes, assuming the same platform jitter and ignoring the larger contribution of detector noise, which could allow the FGS to be used, in some circumstances, as part of the pointing of the GAI with a much dimmer star.

Active System Sensor: DFP Interface Sensors

Sensors based on Inductive (Eddy-Current) Sensor Technology (mature, proven)

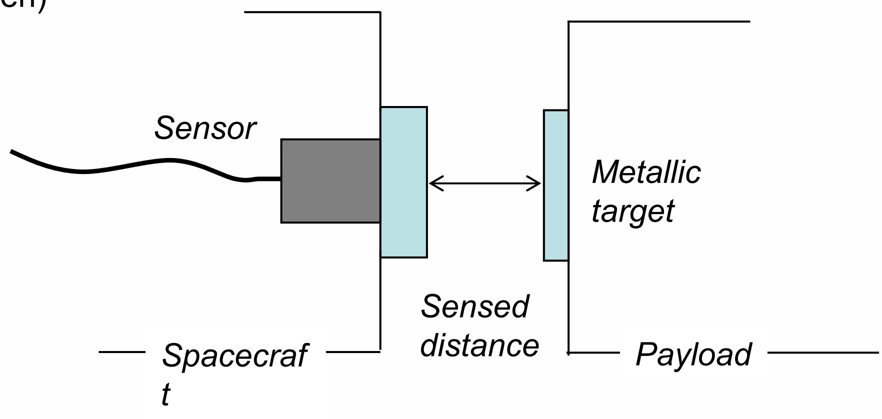

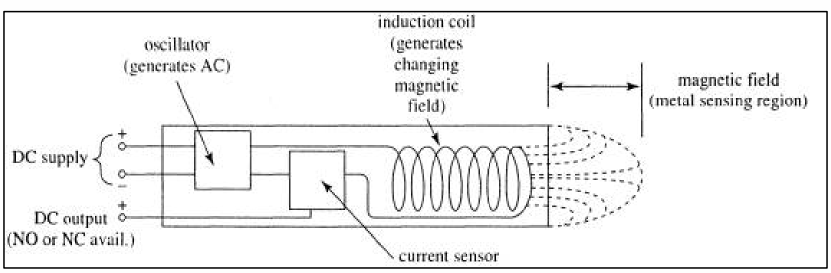

Candidate sensor: Kaman 26U	
Size	1 in. D., 1.5 in. L.
Range	±4 mm
Resolution	1-3 µm
Nonlinearity	8 µm

- With the DFP, the spacecraft and payload are not structurally connected; there are non-contact actuators at the spacecraft-payload interface. The payload is equipped with an a fine guidance sensor that is used to derive an attitude error signal of the payload relative to a desired attitude. The non-contact actuators are commanded based on this attitude error producing a relative torque between the payload and the spacecraft. The payload "pushes" against the rotational inertia of the spacecraft to perform inertial attitude control.

- Because the non-contact actuators have a finite stroke and gap over which they can operate, the interface is also equipped with non-contact sensors that sense relative attitude and translation of the payload with respect to the spacecraft. The relative attitude measurement is used as an error measurement to derive a commanded torque to the spacecraft; in this sense, the spacecraft is commanded to "follow" the payload to manage the interface actuator constraints.

Backup Slides

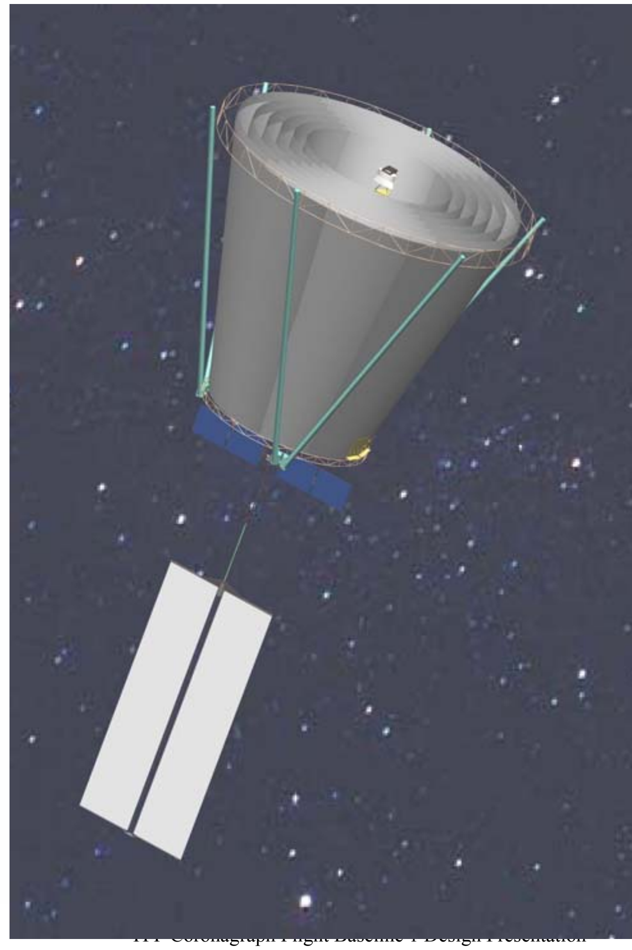

Coarse Mode - Active System

- 3-axis inertially-stabilized control system for S/C Support Module, using S/C Support Module star tracker and DFP non-contact actuators
- S/C Support Module inertial attitude control and Payload Module–S/C Support Module relative translation control using interface sensors to control interface stroke/gap

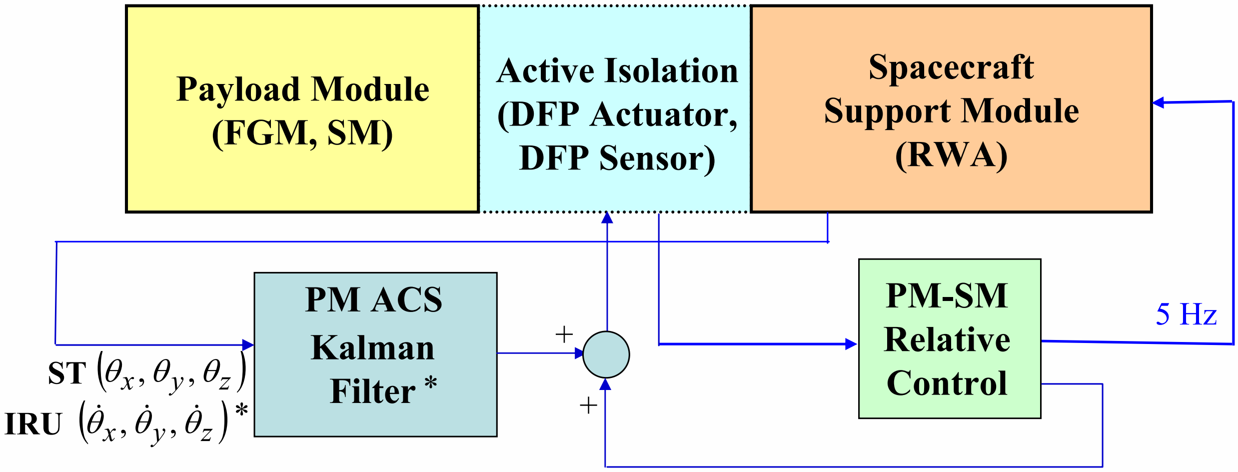

* PM Inertial rate sensor usage depends on sample rate of PM star trackers

Acquisition Mode – Active System

- 3-axis inertially-stabilized control system for Payload Module, using Payload star Acq camera and DFP non-contact actuators
- S/C Support Module inertial attitude control and Payload module-S/C relative translation control using interface non-contact sensors to maintain interface stroke/gap

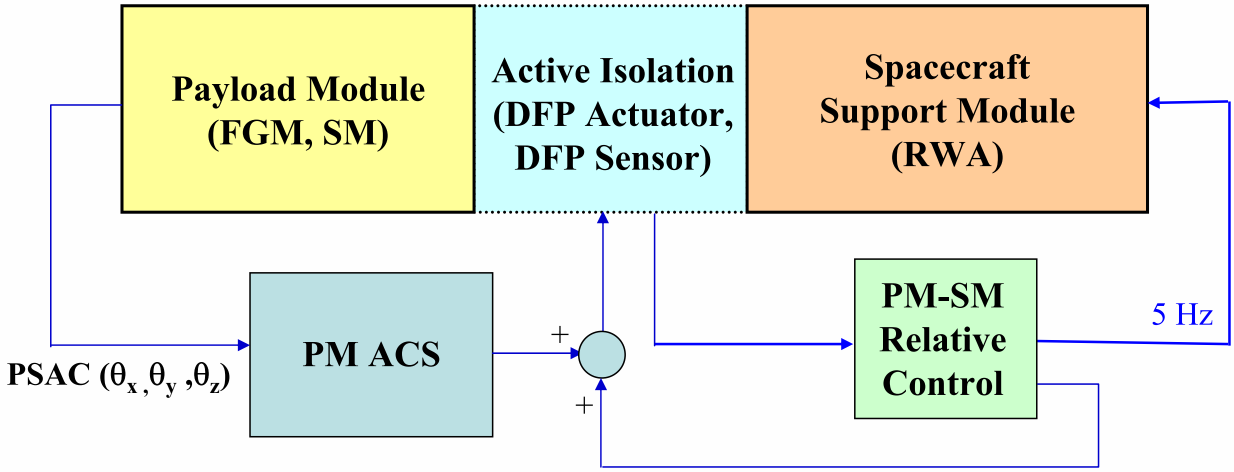

DFP Payload-Spacecraft Interface

- DFP Interface volume
  - Three separate brackets requiring a volume of less than 2500 cm^3 each (21cm x 11cm x 10 cm)
- DFP Interface depth, d, can be as small as 5 mm
  - Shown in the picture with d = 60-mm
- Total DFP Interface mass
  - About 30 kg, including electronics boxes and launch locks

View of DFP Interface on DFP 3D Testbed

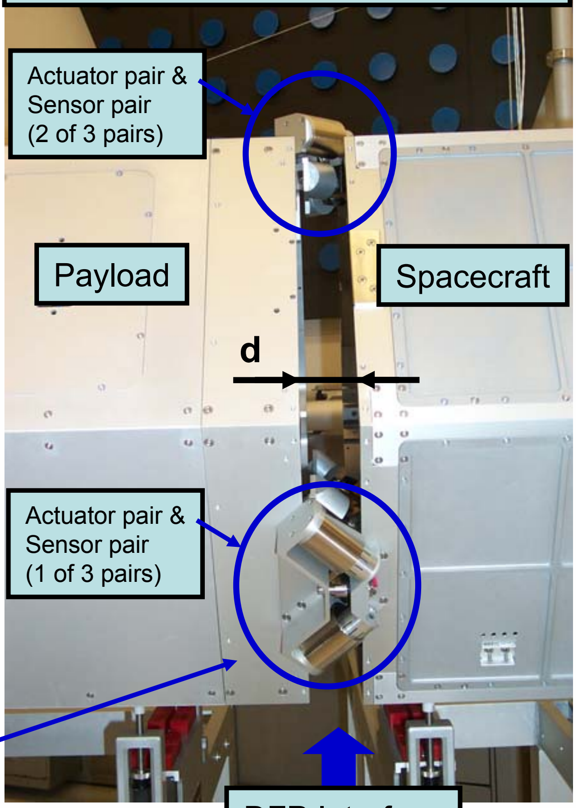

Full size sensors and actuators for large space system

Sensor Descriptions – DFP

- Current sensor selection: Inductive proximity sensor
  - Mature, proven technology
  - Models are available for cryogenic operation
  - Flight heritage
  - Candidate sensor: Kaman 26U
    - Sensor head dimensions: 1 in. Dia., 1.5 in. long
    - ±4 mm range
    - 0.8 µm resolution p-p (zero displacement – noise limited @ 10Hz bandwidth)
    - 3.8 µm resolution p-p (full scale displacement – noise limited @ 10Hz bandwidth)
    - Non-linearity: 8 µm (peak over full range)
- Alternative sensor technologies under evaluation
  - Capacitive sensors (flight heritage, and cryogenic operation)
  - Optical sensors

TC Technology

nightsky systems

TPF Terrestrial Planet Finder

System Design and Configuration

Timothy Ho

Contributors:

T. Cafferty, C. Engler, V. Ford, P. Feher, A. Kissil, E. Kwack, P. Mouroulis, D. Lisman

11-12 July 2005

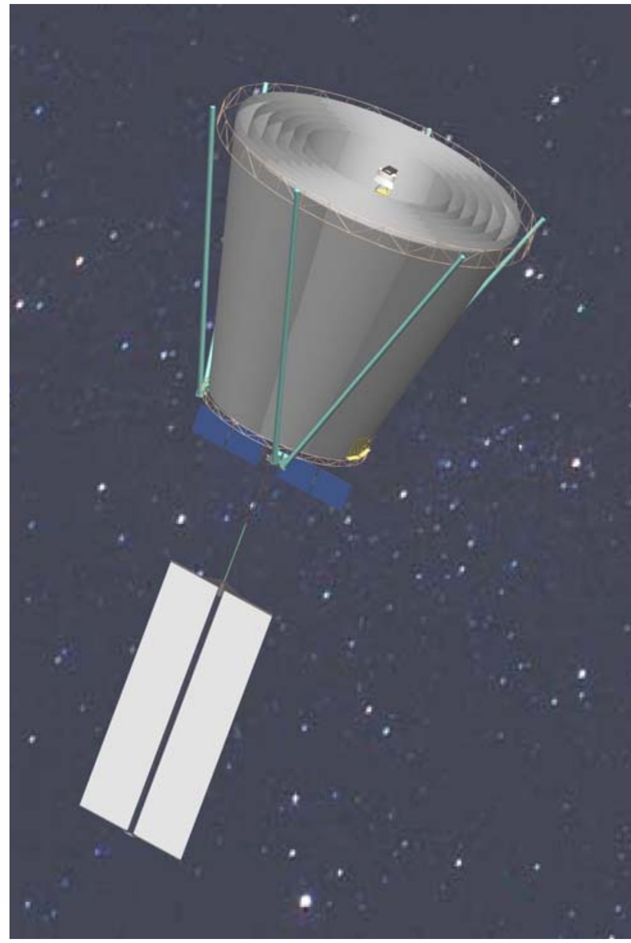

Topics

- Deployed Configuration Overview / Science Payload
- Optical Telescope Assembly / Payload Support / Spacecraft Interfaces
- Optical Prescription Path
- Payload Support Assembly
  - Payload Support Structure
  - Instrument Locations
  - Payload Thermal Control
- Spacecraft Assembly
  - Bus / Reaction Wheels / Tanks
  - V-groove
  - Solar Array and Solar Sail
- Stowed Launch Configuration

Deployed Configuration Overview

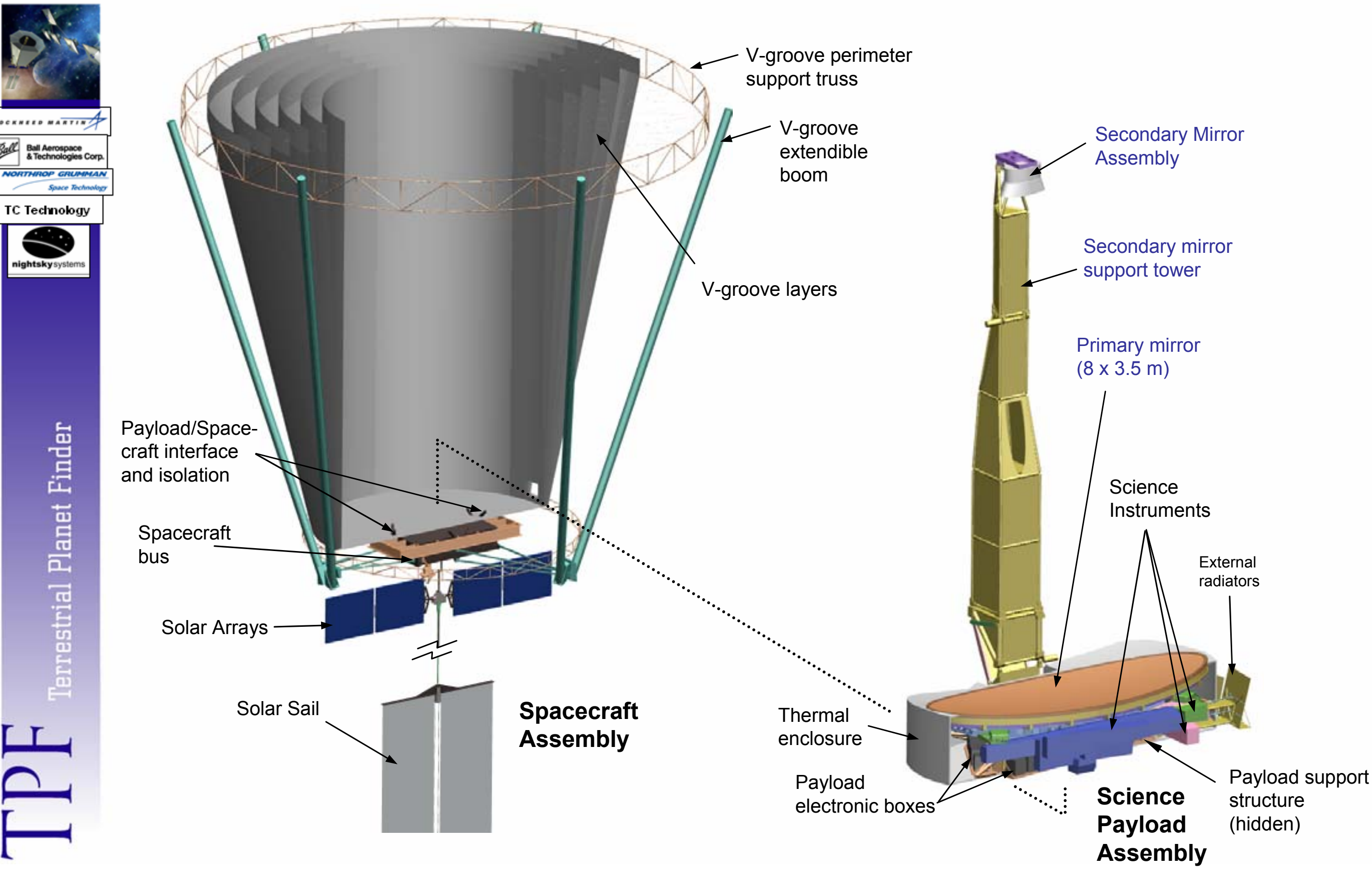

- This slide shows the two major assemblies of the flight system. The complete flight system is called the Observatory. The low frequency sail, sunshade, and solar arrays and reaction wheels are supported by the spacecraft bus. Instruments, telescope, payload electronics, and payload thermal control are part of the science payload assembly. The division of the two assemblies is made at the isolation stage between the spacecraft and science payload. The isolation stage is the only interface between the two assemblies and effectively isolates the jitter and vibration sensitive components in the payload from the spacecraft. Cabling across the interface has been minimized by placing several electronics boxes in the science payload assembly.

Science Payload Assembly

OTA
(Optical Tele-scope Assembly)
-Primary
-Secondary
-Tertiary
-Structural and thermal control support structure for mirrors
-Laser metrology

Payload Support Assm
-Instruments
-Electronic boxes
-Thermal control for detectors & e-boxes
-OTA Support
-Spacecraft I/F

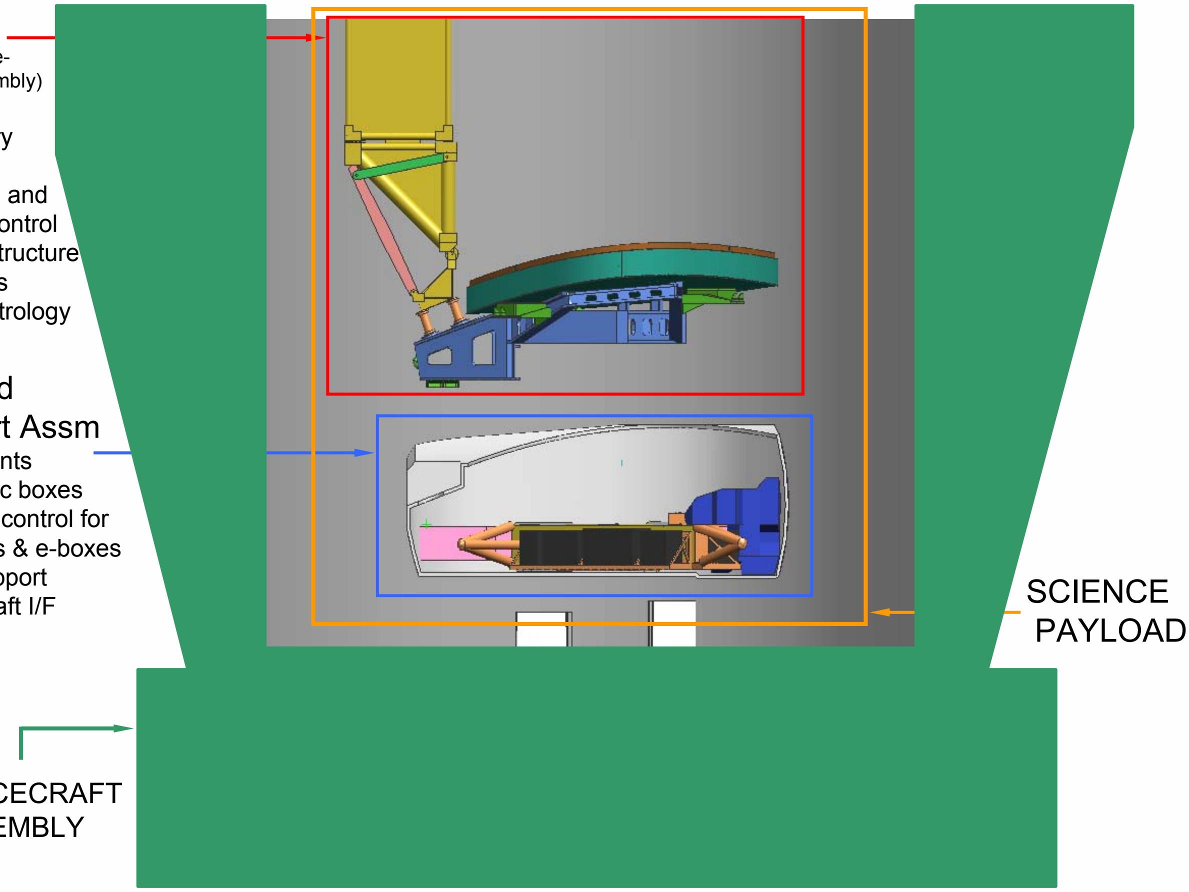

- This slide shows the break down of the Science Payload Assembly. The Science Payload Assembly (orange box) is composed of two sub-assemblies – the Optical Telescope Assembly (OTA) (red box) and the Payload Support Assembly (blue box). The OTA consists of the primary, seconday, and tertiary mirrors, the structural and thermal support for those mirrors, and the laser metrology system. Details of the OTA design will be presented as part of Chuck Engler's presentation. The Payload Support Assembly consists of the instruments and electronic boxes and associated thermal control which are all attached to a main supporting structure called the Payload Support Structure (PSS). The OTA and spacecraft interface to the PSS.

OTA / Payload Support / Spacecraft Interfaces

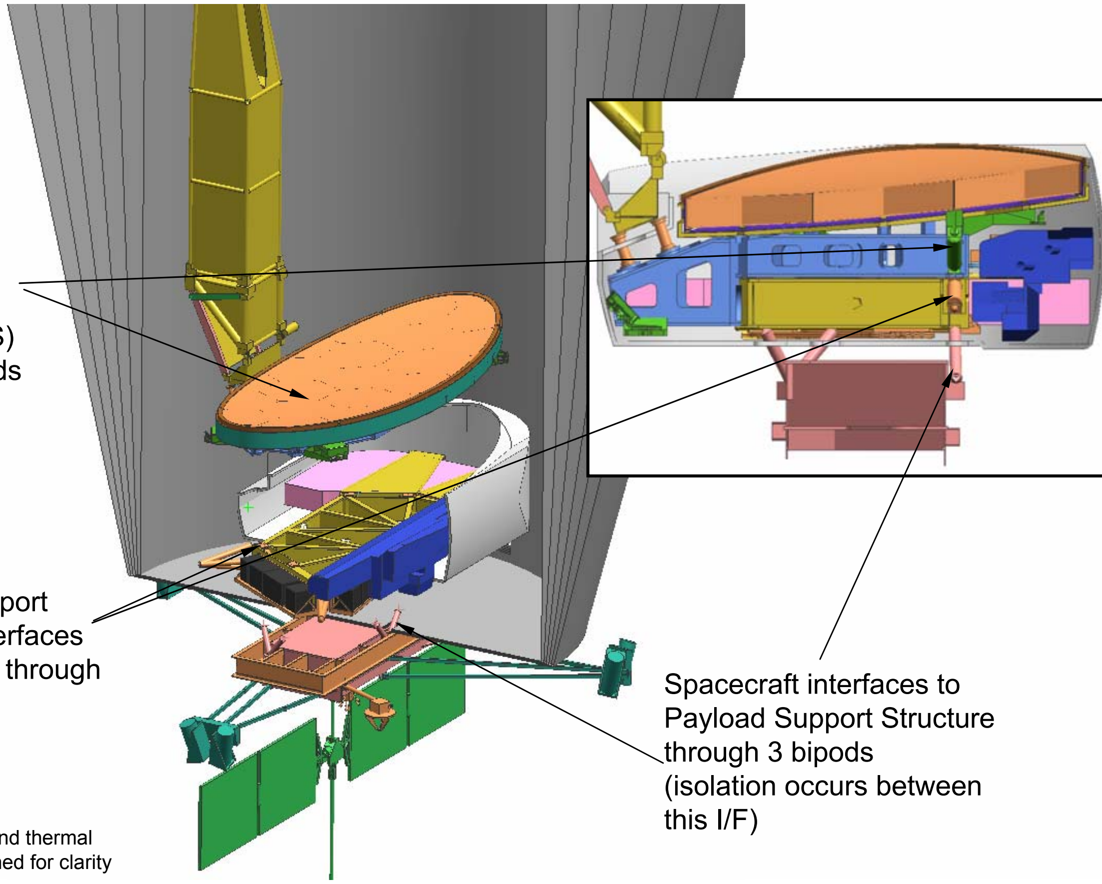

- This slide describes how the interfaces between the major components are configured.

Optical Prescription Path

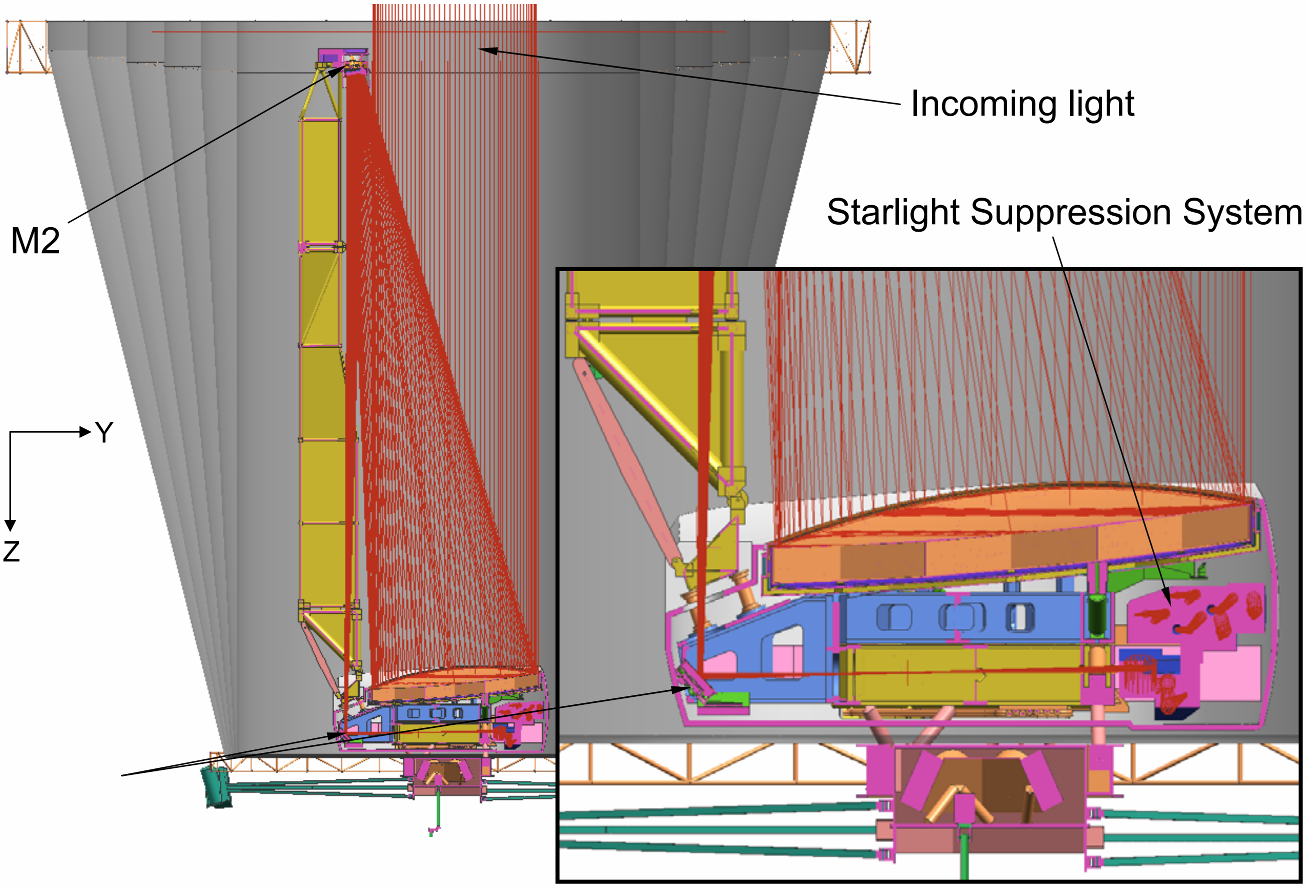

- This slide shows the optical prescription overlayed onto the mechanical configuration. It shows how the telescope folds the light under the primary mirror, through the PSS, to position the starlight suppression system along the minor axis at the outer edge.

Payload Support Assembly

Payload Support Structure & Attachments

- The Payload Support Structure (PSS) is the main interface to the OTA and spacecraft
- Supports the science instruments, payload electronics, thermal control radiators/heat pipes and the thermal enclosure
- A main load carrying interface to the launch shroud PAF
- Provides a clean interface to OTA

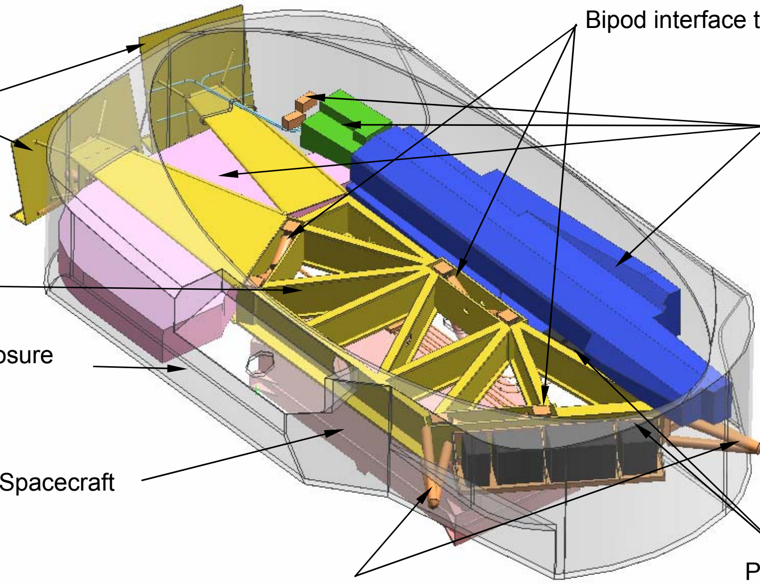

- This slide details the Payload Support Assembly and the PSS interfaces and its role as a support structure.

Placeholder Science Instrument Locations

- Not preferred choices for instrument concepts
- Used to understand accommodation requirements
- From tertiary mirror of telescope, a pickoff mirror sends :
  - Outer portion (red arrow) of the beam to the GAI (assumed 10 arcsec – 4 arcmin)
    - Beam height limitation for GAI: 30 cm
  - Inner portion of the beam to the SSS (green arrow)
  - Light delivered to detection and characterization instruments through SSS

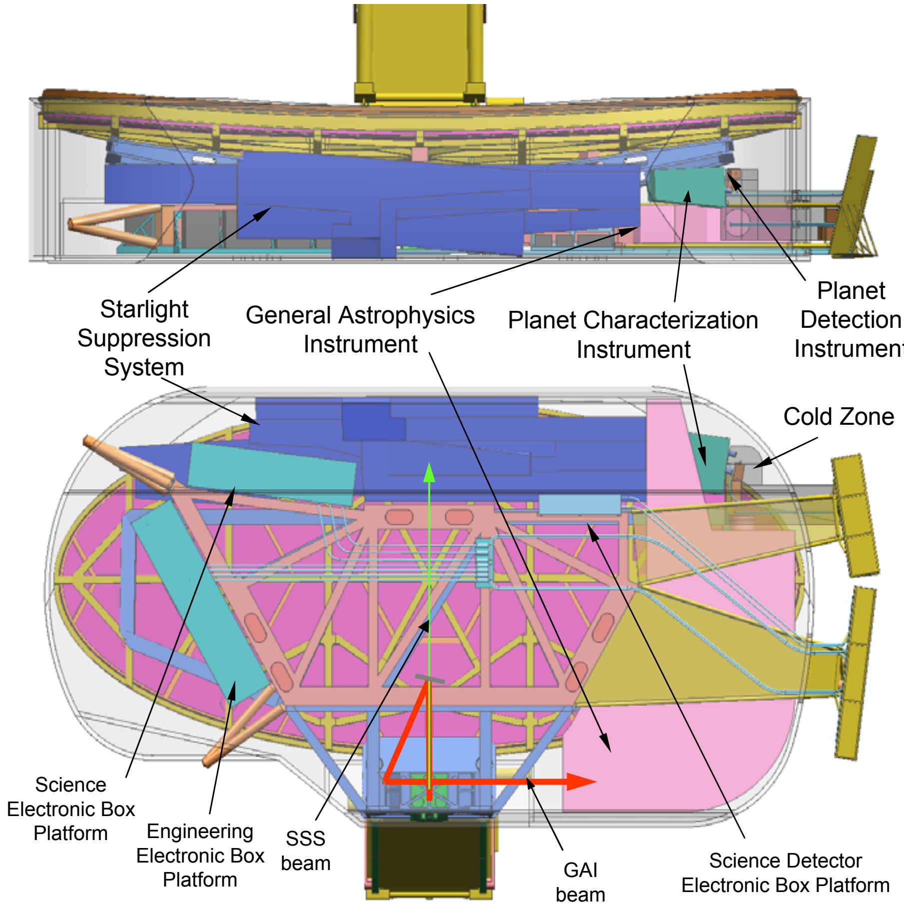

- This slide shows where the science instruments are located. A picture of the actual beam paths of the instruments can be found in the back-up slides at the end of this slide package.

Payload Thermal Control

- Isothermal Enclosure surrounds warm portion of payload:
  - 290K – 305K
- Cold zone enclosing detectors isolated from warm zone:
  - assumed temperature: -100C±5C

Placeholder Detector	Cooling power (assumed)
GAI	12 Watts
Detection	5 Watts
Characterization	8 Watts

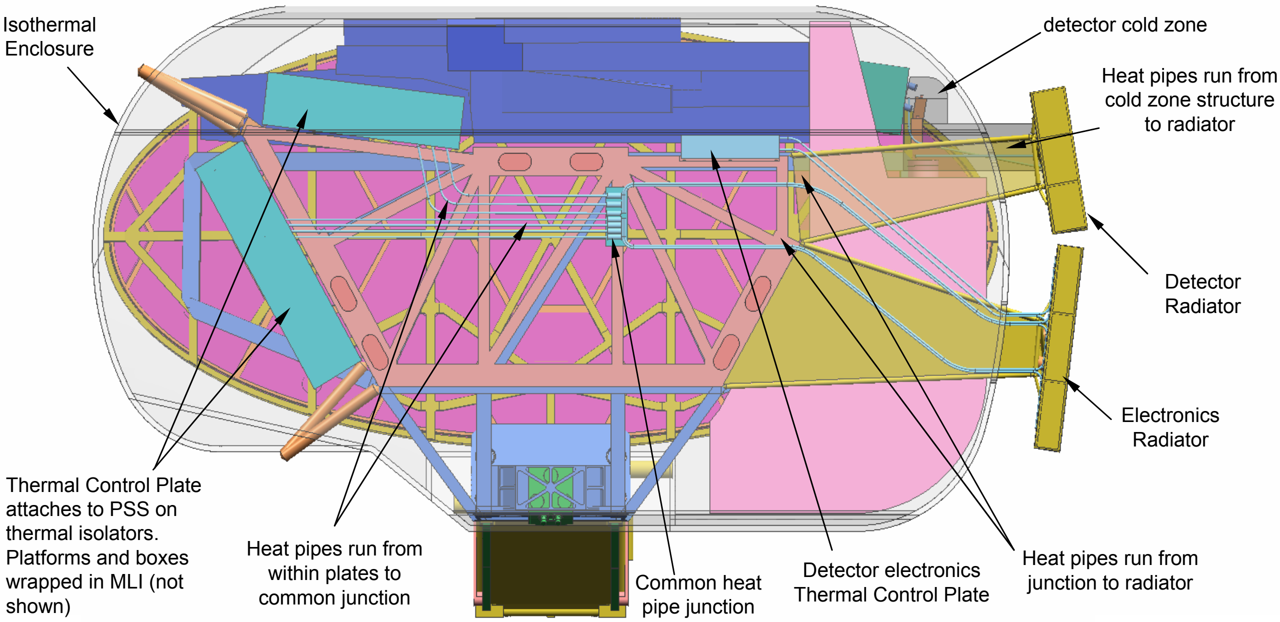

- This slide details the passive thermal control system for the electronic boxes and instrument detectors. A system of heat pipes runs from within the thermally isolated electronic box platforms to an external radiator. There are a total of 9 heat pipes for the electronic box thermal control. The instrument detectors are also cooled by heat pipes and run to a separate external radiator. There are a total of 4 heat pipes for the instruments. Both radiators protrude outside of the v-groove.

Spacecraft Assembly

Spacecraft Bus

- Spacecraft houses the reaction wheels and propellant tanks
- Supports thrusters, antenna, v-groove system, solar array and solar sail
- In the load path for launch

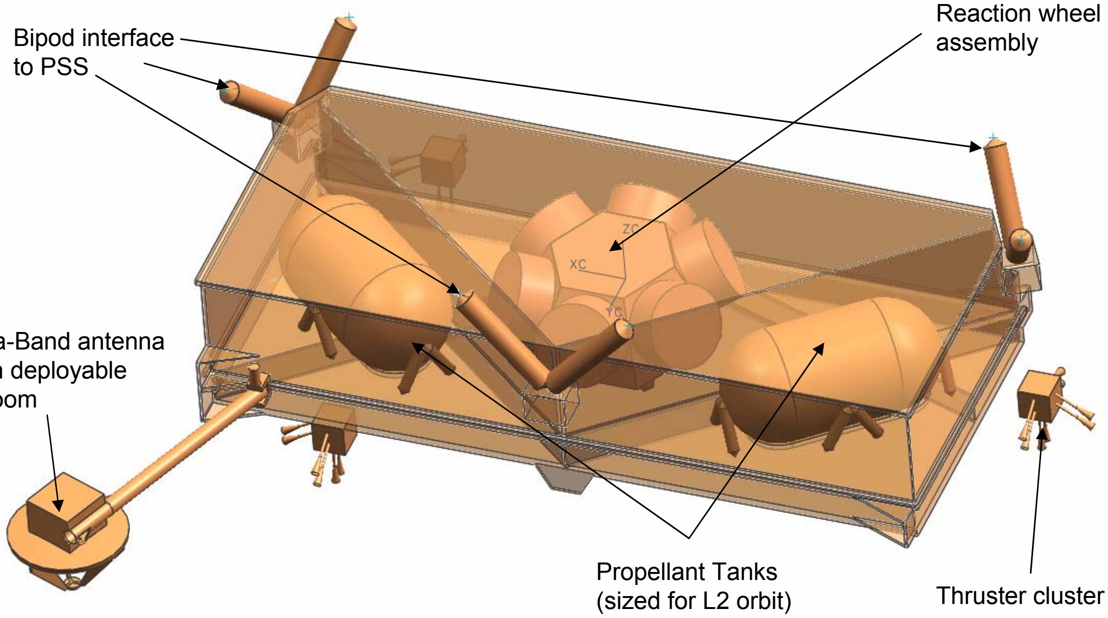

- This slide shows how the spacecraft bus is configured with the reaction wheels in the center and the propellant tanks symetrically placed on opposite sides of the reaction wheels. Thruster clusters supported off spacecraft and v-groove support structure (not shown)

V-groove

- V-groove is supported off the spacecraft bus
- Extendible booms are deployed and supported on tripod structures
- Perimeter trusses support the ends of the v-groove
- 6 layers separated by 3 degrees between layers and 50mm separation at base

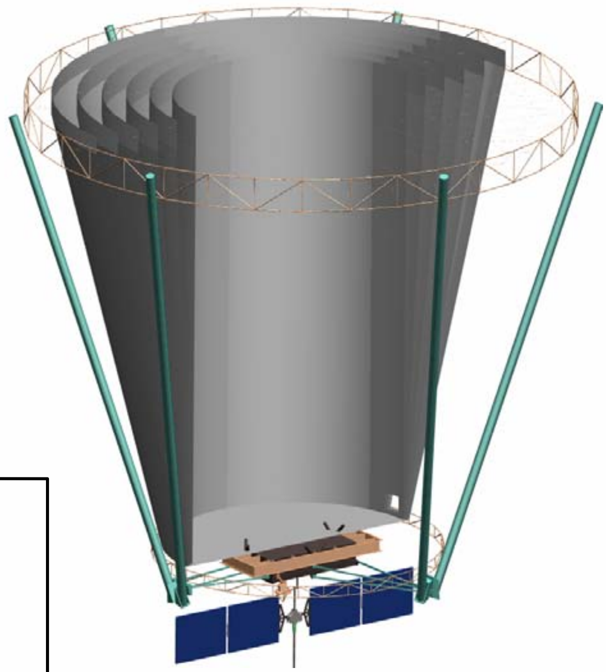

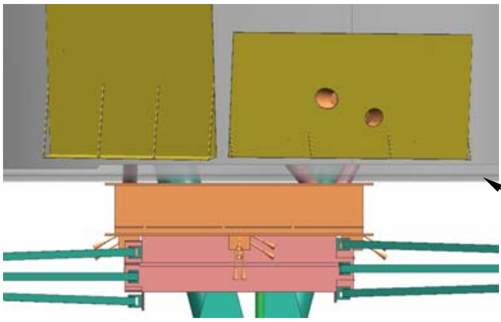

V-GROOVE CLOSEOUT:
6 flat layers occupy 50mm in height – remaining gap left for blanketing

- This slide briefly discusses the configuration of the v-groove sunshade and closeout.

Solar Array and Sail

- Solar array
  - Panel size: 2m x 1.5m
  - Total area: 12 m^2
  - Power: 3000 W
  - 2 DOF
- Solar Sail
  - Length: 14 m
  - Width: 6.36m
  - 1 DOF
- Both are utilized to balance solar pressure – distances and lengths calculated
- Sail centerline is aligned with v-groove centerline

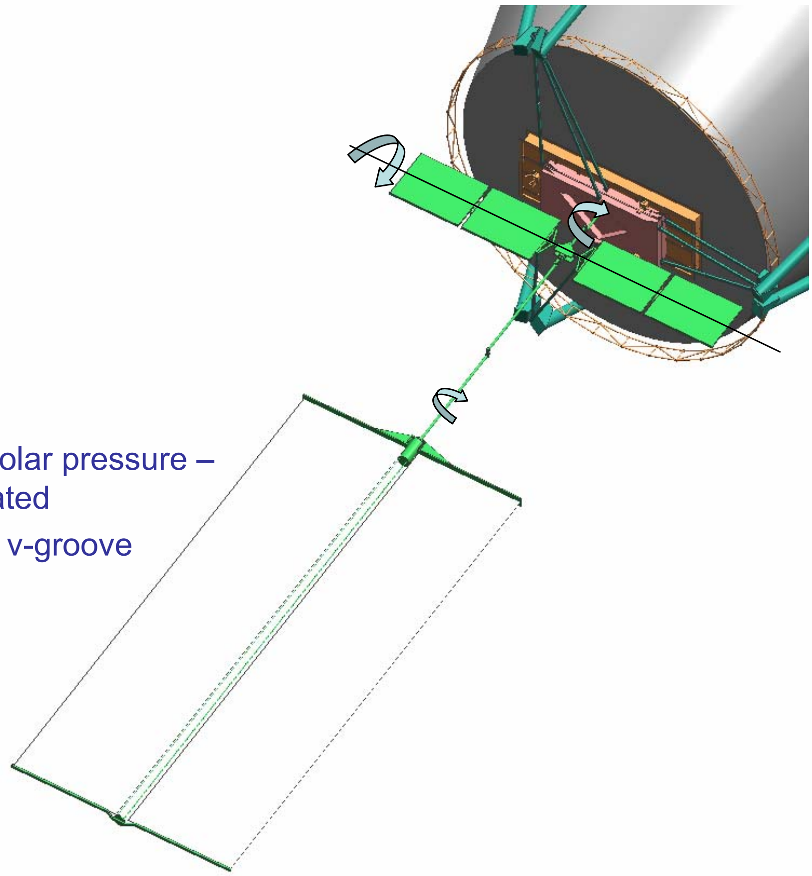

- This slide gives a few parameters of the solar array and solar sail configuration and purpose.

Stowed Launch Configuration

National Aeronautics and Space Administration
Jet Propulsion Laboratory
California Institute of Technology
Goddard Space Flight Center

Launch Load Path Schematic

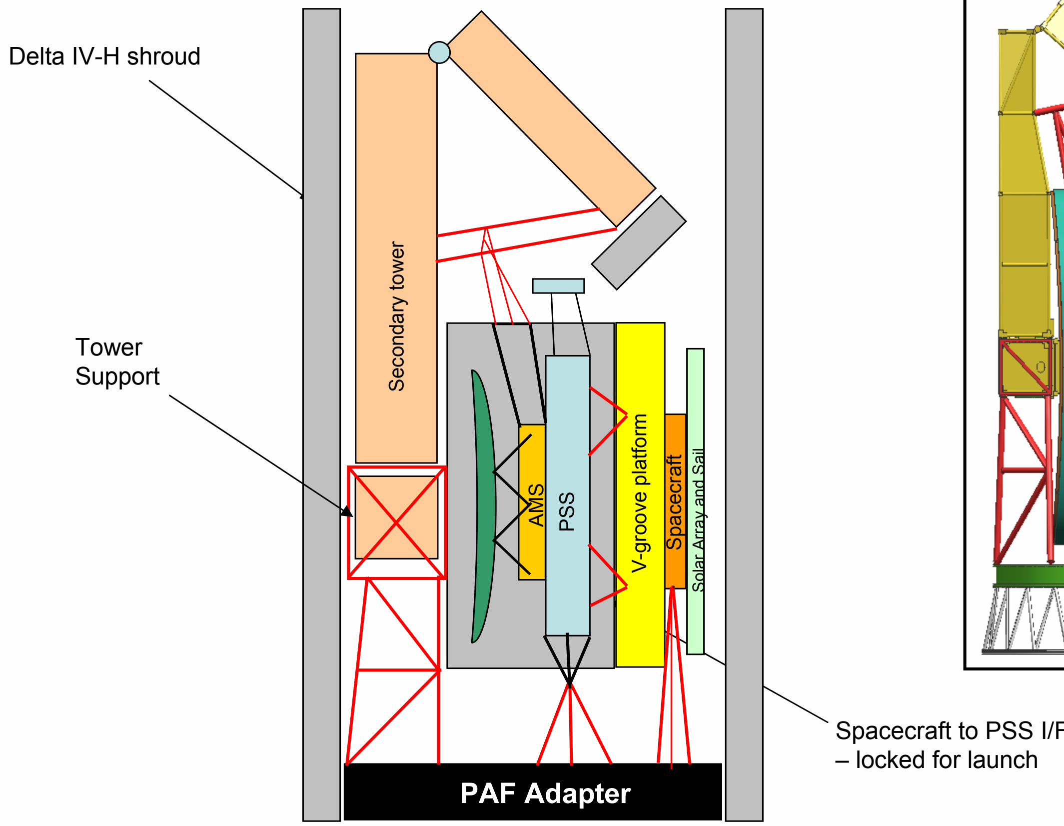

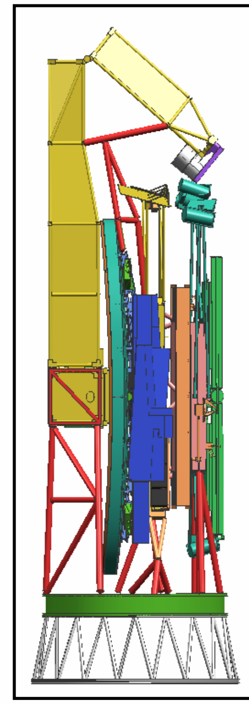

Terrestrial Planet Finder
TPF

- This slide shows a schematic of the launch support and load paths. The solar array and sail fold up close to the spacecraft. The vgroove sunshade, canister and arms stowed. The tower folds along 3 orthogonal axes.
- The tower is supported by a structure to the PAF. The tip of the tower is tied back to the tower itself and also to the AMS. The mirror and spacecraft are attached together which is then supported to the PAF through the PSS and spacecraft on bipod/tripod structures. The view on the right (thermal enclosure not shown) is the flight stowed configuration corresponding to the schematic.

Stowed Configuration in Shroud

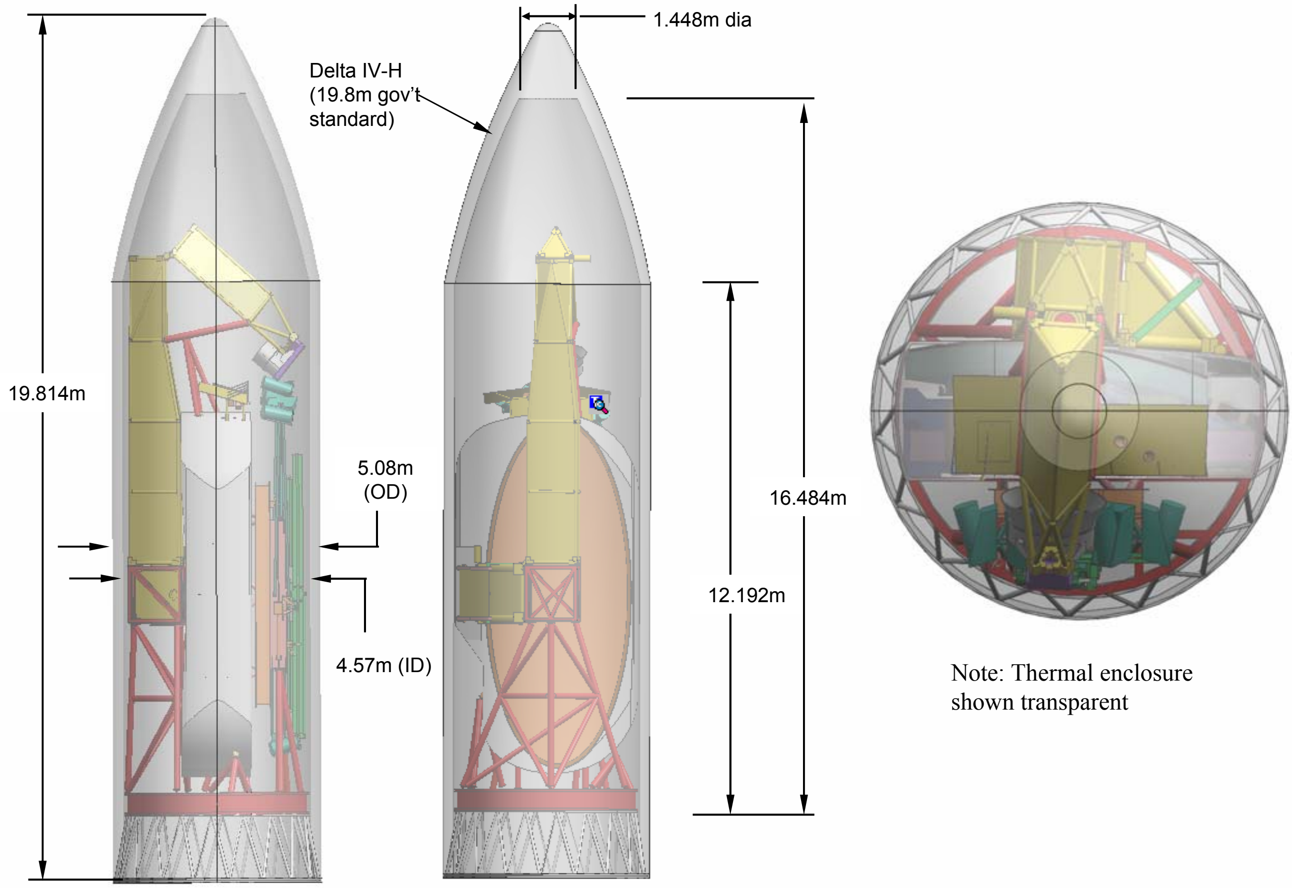

- This slide shows the clearance to the launch vehicle shroud of the stowed configuration. Shroud dimensions are shown. The diameter of the shroud is the limiting constraint on the system.

Summary

- Many different concerns were considered throughout the design
  - CG and CP
  - Vibration isolation interface
  - Assembly integration and accessibility
  - Stowed configuration
  - Thermal and structural concerns
- Launch shroud diameter limits the stack-up height of components

Back up slides

Payload Computing and Electronics Philosophy

Assumed Electronic box sizes: (W x H x L) cm

1) OTA MCE - 36 x 38 x 24
2) Payload System Elex – 36 x 38 x 48
3) Laser Metrology – 40 x 40 x 68
4) OTA Thermal Control – 36 x 38 x 38
5) Planet characterization – 36 x 38 x 36
6) Planet detection – 36 x 38 x 48
7) Fine DM controller – 36 x 38 x 36
8) GAI – 36 x 38 x 24
9) Planet Detection Detector electronics– 12 x 12 x 18
10) Planet Characterization Detector electronics– 12 x 12 x 18
11) GAI Detector electronics– 12 x 12 x 36

- Instruments responsible for science data computing including data compression
- Spacecraft will provide data storage and downlink
- All instrument electronics mounted on payload side to minimize cabling stiffness (thus dynamic perturbation exchange)
- Instrument electronics not required to be co-located with optics assemblies mounted on payload-provided thermal control plate
- All boxes include redundancy except for the GAI

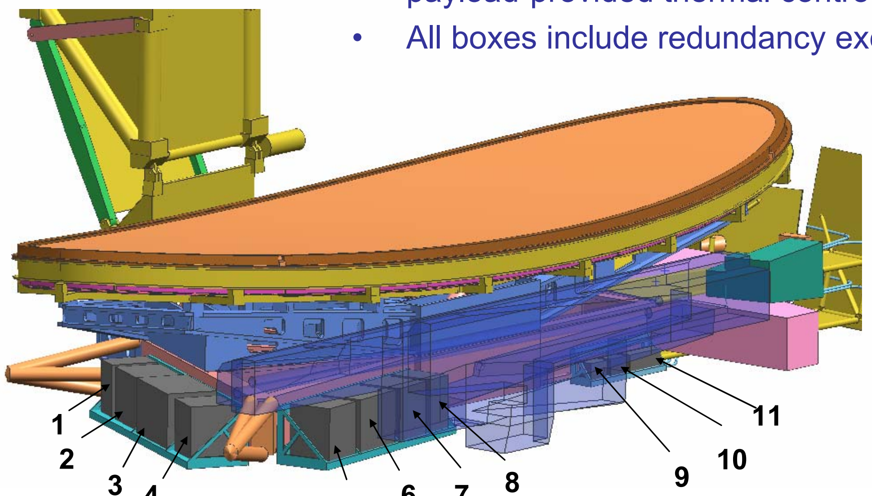

Note: Thermal enclosure not shown, SSS shown transparent blue

Placeholder Instrument Beam Paths

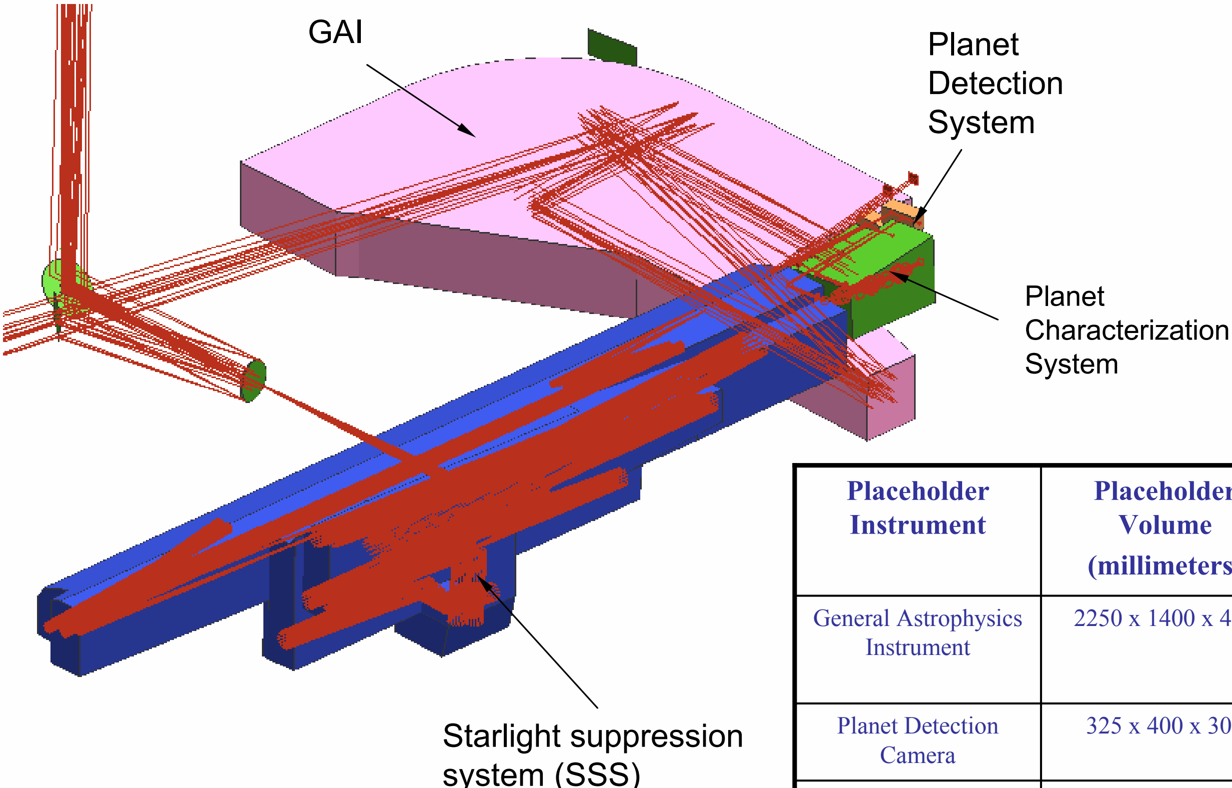

Notes:
1) Beam paths highlighted in red

Placeholder Instrument	Placeholder Volume (millimeters)
General Astrophysics Instrument	2250 x 1400 x 400
Planet Detection Camera	325 x 400 x 300
Planet Characterization Instrument	750 x 400 x 300

Thermal Enclosure

- The thermal enclosure completely surrounds the primary mirror and encloses everything behind the mirror.
- Maintains a stable temperature within the cavity
- Attaches to PSS.
- Cutouts for light beam, spacecraft interface, SM tower, and radiator support structure

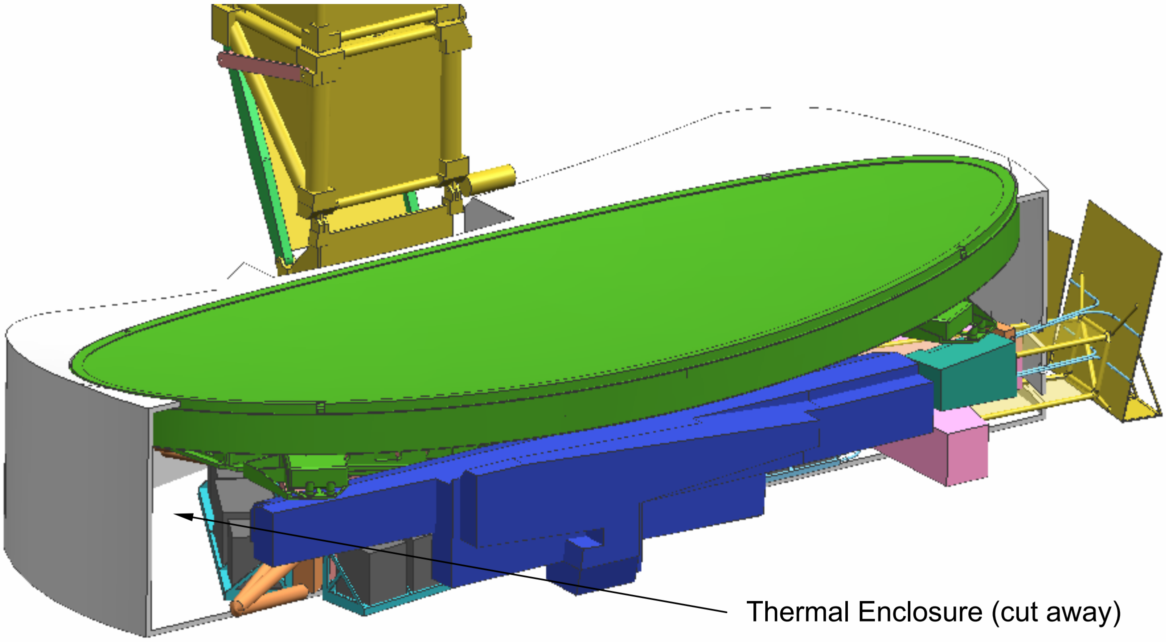

- This slide shows how the thermal enclosure surrounds the primary mirror and all the components behind the mirror.

Thermal Enclosure Details

Cutouts for light beam, spacecraft interface, SM tower, and radiator support structure

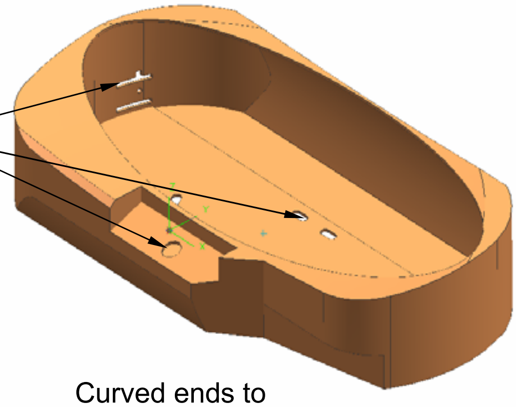

Rounded corners follow the v-groove

GAI requires larger volume

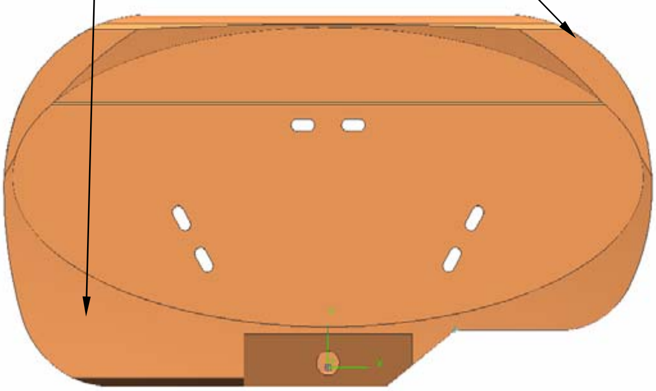

Curved ends to follow the launch shroud

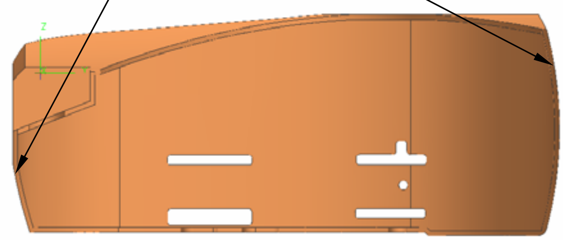

X-section

Radiator locations outside v-groove

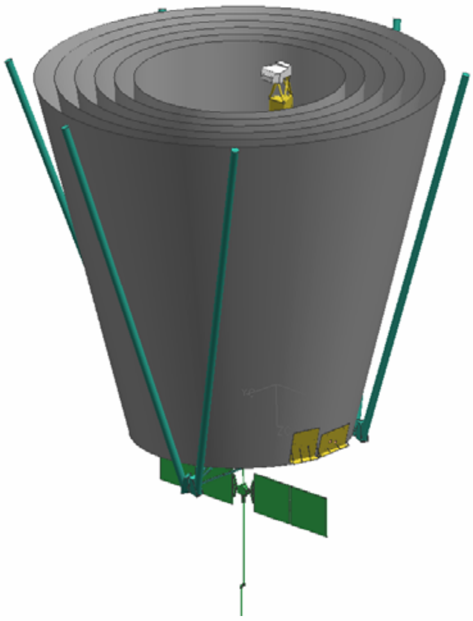

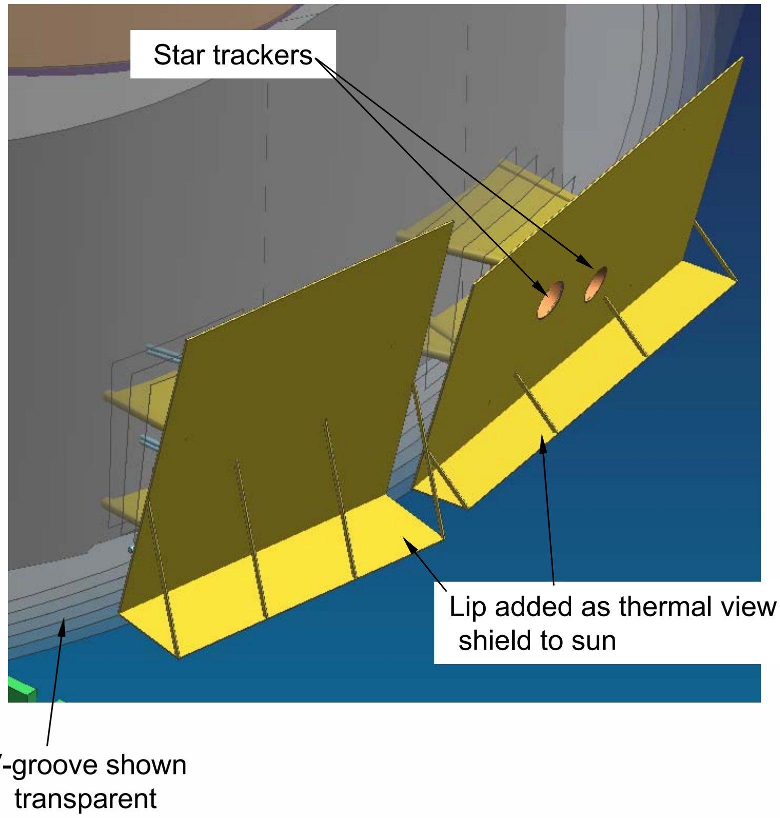

V-groove deployment canister details

- Canister deployment similar to JWST secondary deployment

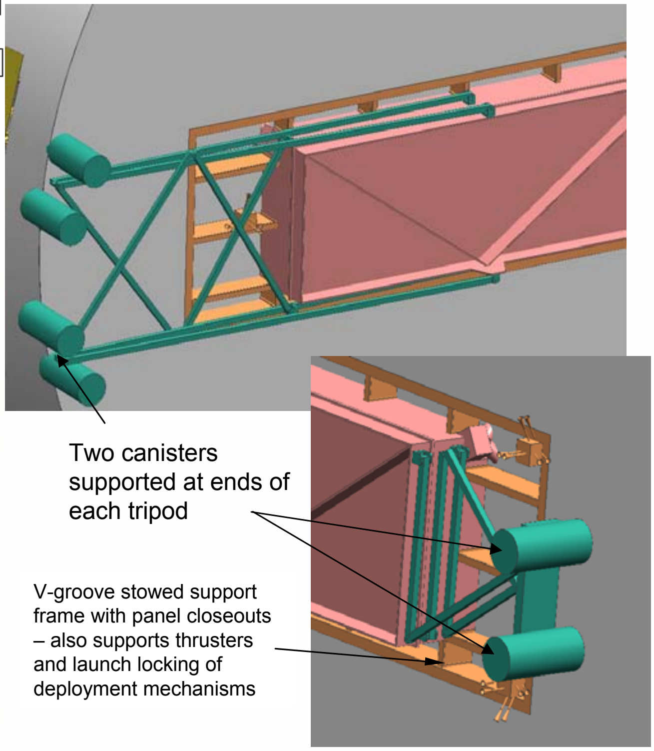

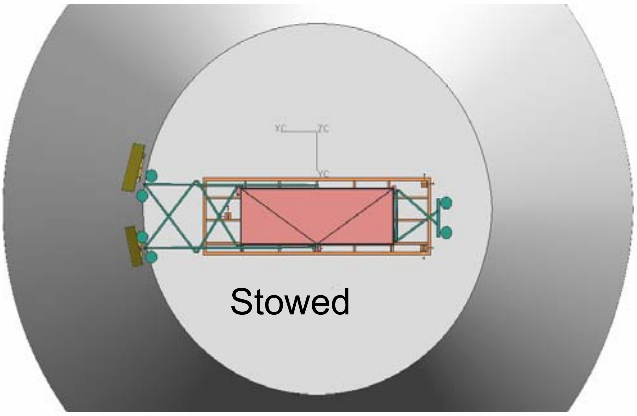

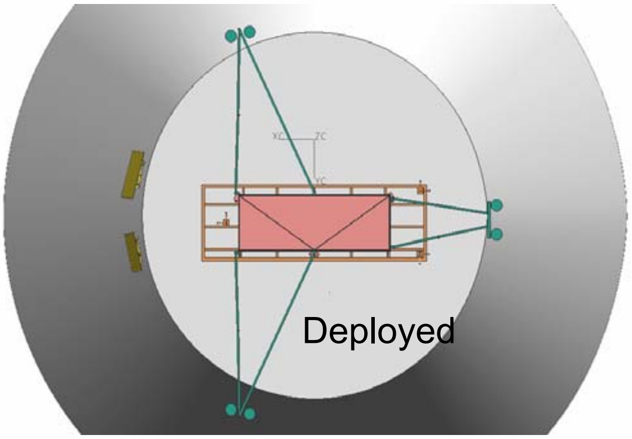

Solar Array and Sail Stowed

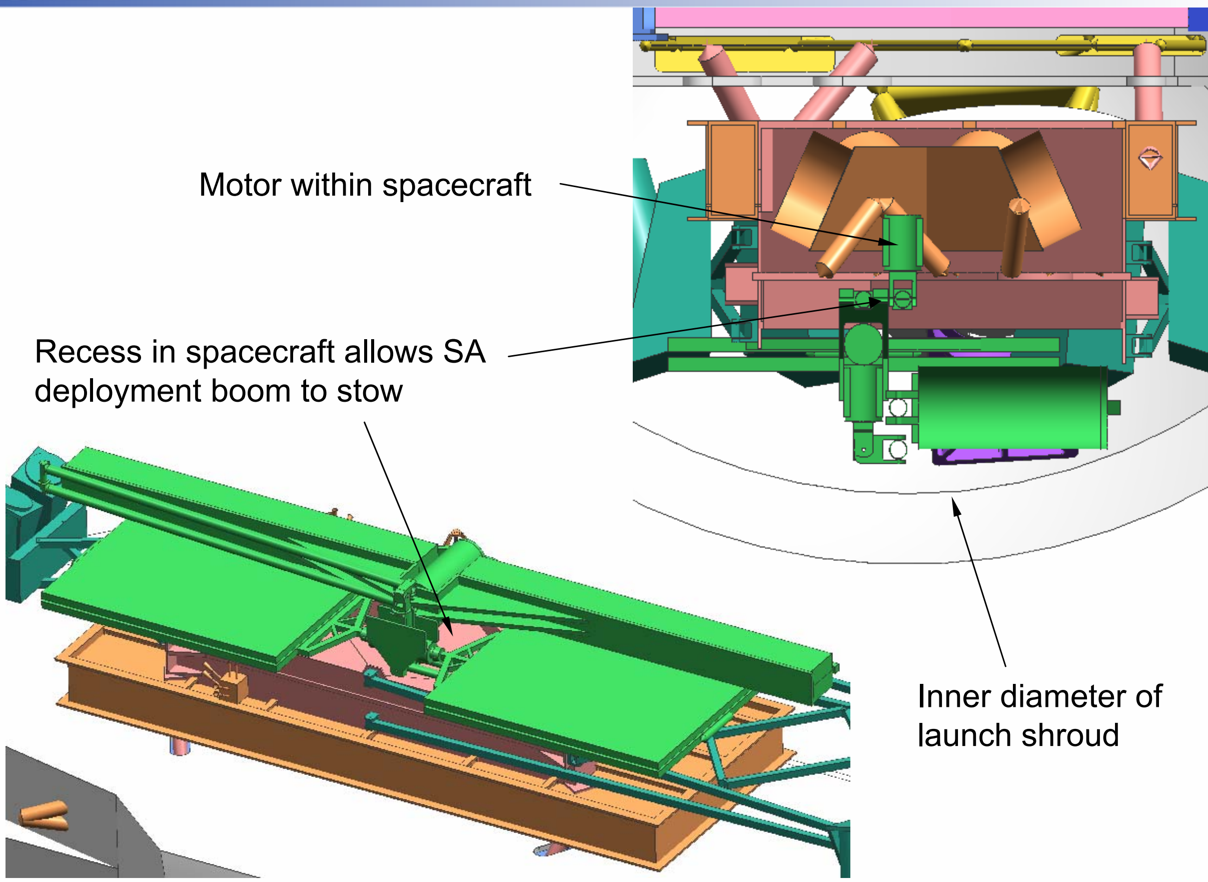

Deployment Sequence

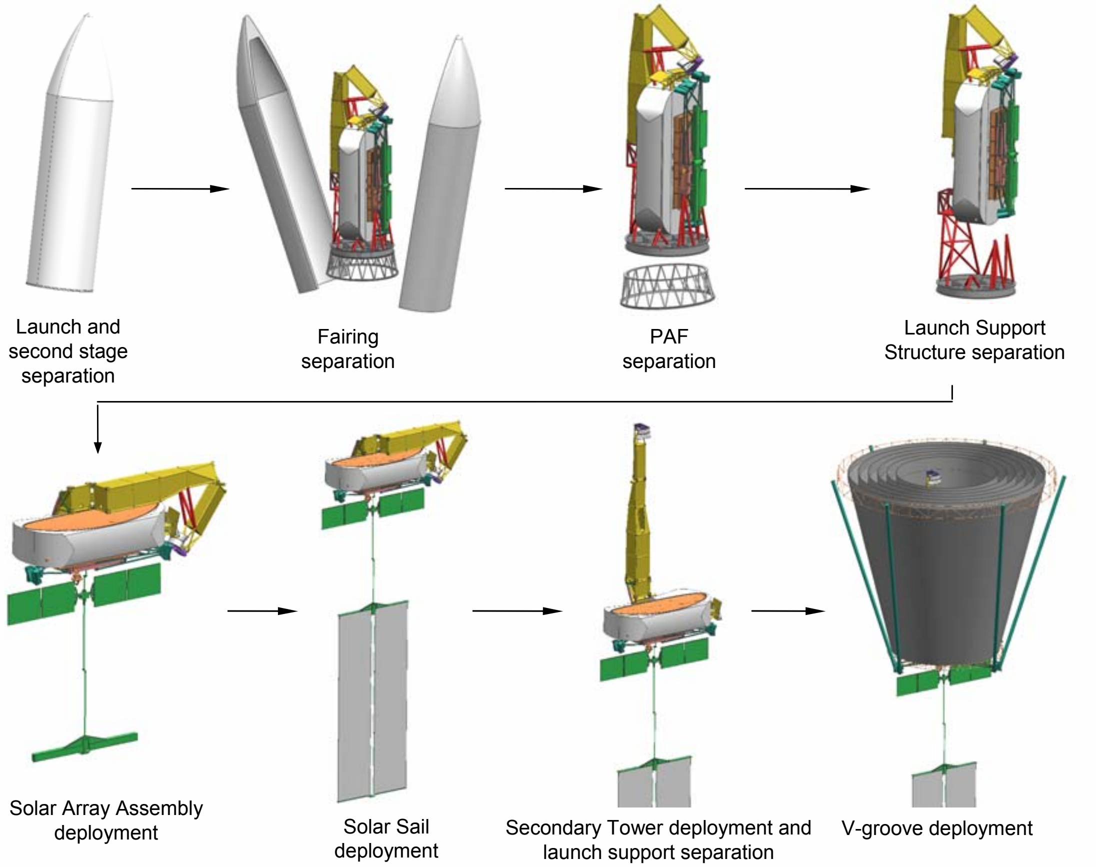

- This slide shows the coarse deployment sequence of the flight vehicle from stowed to deployed.

OTA Mechanical Design and Configuration FB1

Charles Engler
Electromechanical Systems
GSFC

Contributors:
Jeff Guzek
-Design Interface Inc.

11-12 July 2005

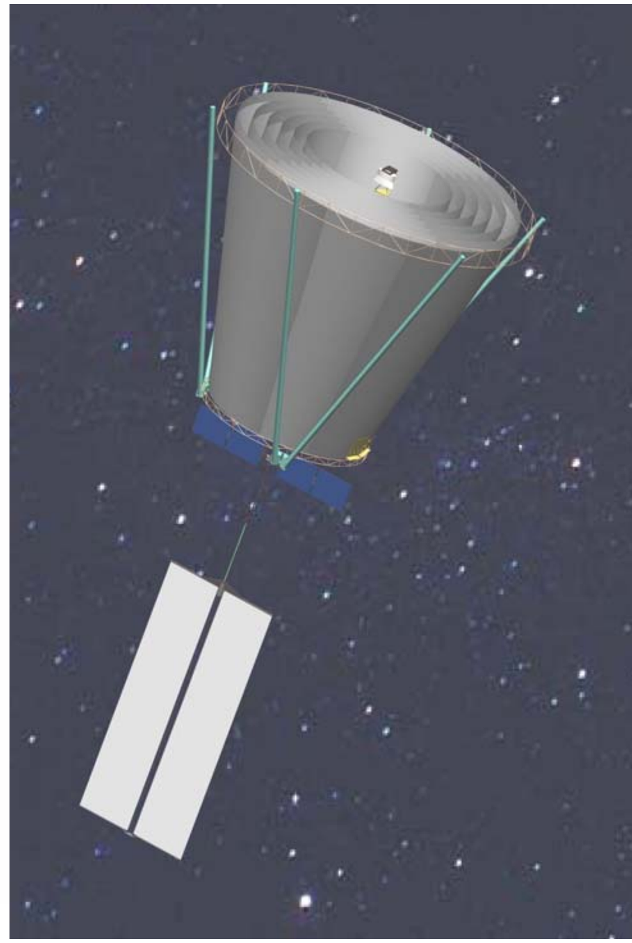

Optical Telescope Assembly FB1

TC Technology
Terrestrial Planet Finder
TPF

- Major subassemblies

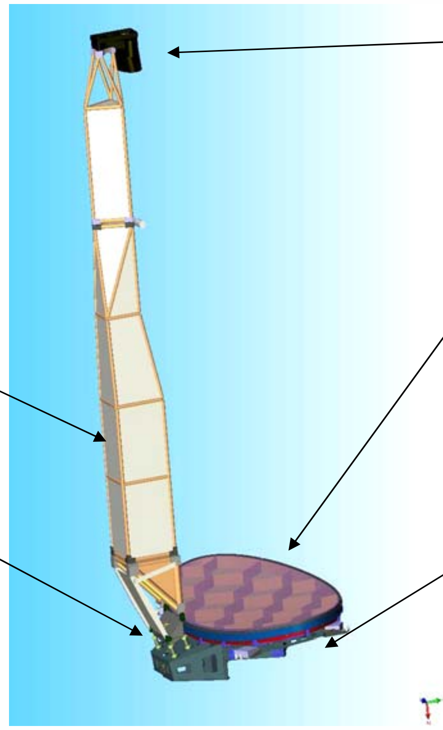

Secondary Mirror Assembly
- .9m x .4m Secondary Mirror
- Pointing and control system
- Thermal control system

Primary Mirror Assembly
- 8mx3.5m Mirror
- Thermal control system
- Cover deployment system

Deployable Tower
- 4 segment
- M55J composite

Third Mirror Assembly
- .3mx.3m Mirror
- Pointing and control system
- Thermal control system

Aft Metering Structure
- Meters focal distance of PM, SM, M3
- Support thermal control system

- SMA features a six-axis hexapod for pointing and control
  - Coarse positioning to 25 nanometers
  - Fine positioning to 7 nanometers or better

Primary Mirror Assembly FB1

- Estimated Mass FB1: 2626 Kg
- 8m x 3.5m Primary Mirror 1065kg
- Aft metering structure
  - M55J Composite material
  - Supports (meters) PM,SMA,M3
  - PM bipod structure
  - LD5 Box support
- PM thermal control system
  - Composite Rib Structure supporting PM thermal control system.
  - Composite petals for thermal control of individual mirror cells.
  - Thermal blanketing

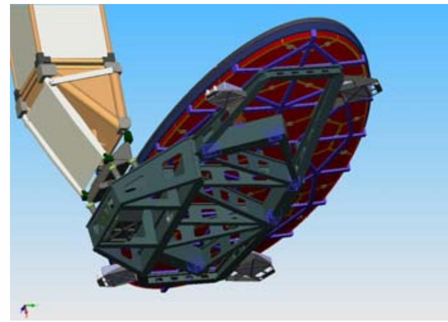

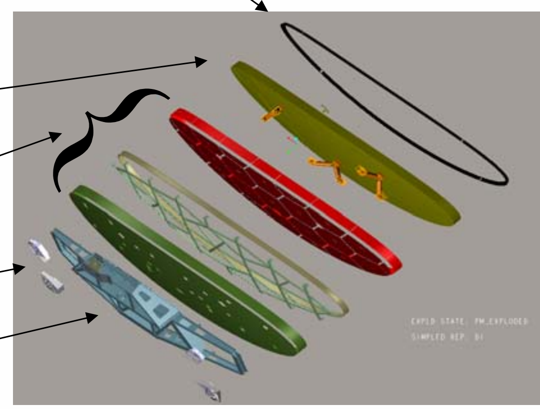

- {{

Secondary Mirror Assembly FB1

- Estimated weight FB1: 146 Kg

SM support structure to tower

Three Bipod supports minimize stresses into mirror

Mirror thermal control system

.9m x .4m Secondary Mirror
17.7 Kg (70% light weighted)

Optical mask

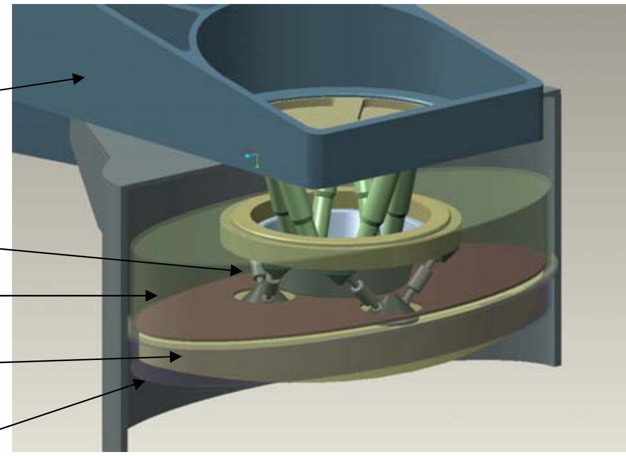

Mirror pointing and control system
- Two-stage hexapod
- Coarse stage:
  - Travel: +/- 25mm
  - Repeatable: +/- 100 nanometers
- Fine stage:
  - Stroke: +/- 200 nanometers
  - Resolution: TBD

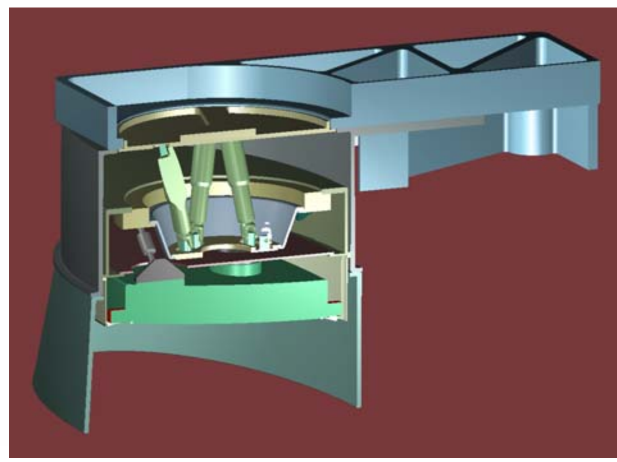

M3 Mirror Assembly FB1

- Estimated weight FB1: 20 Kg

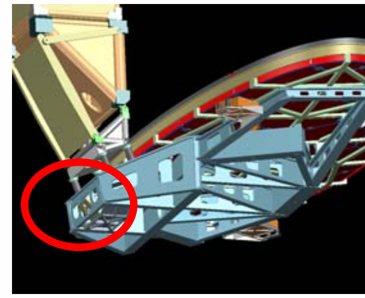

Optical mask

.3m x .3m Tertiary mirror
5 Kg (50% light weighting)

Mirror thermal control system

Three Bipod supports minimize stresses into mirror

Mirror pointing & control system
Tip,Tilt, Focus mechanism
Rubicon-type actuator
6 mm stroke, 9 nm resolution

Support Cradle to AMS

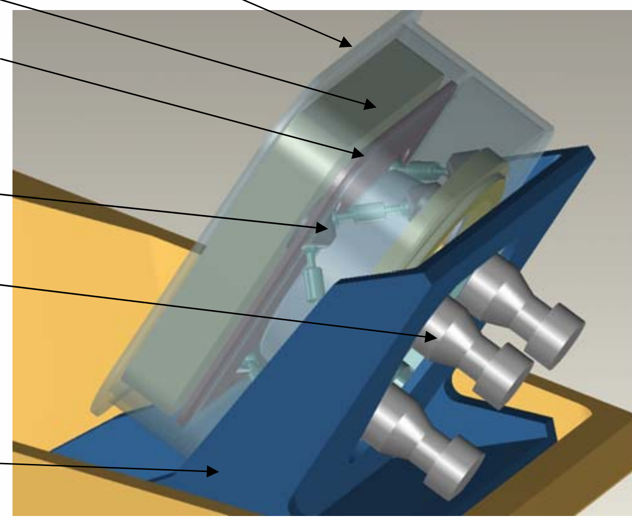

Secondary Tower FB1

- Estimated mass FB1: 197 Kg
- Metering structure featuring a 12m deployable boom
- Four segments deploy from stow position and lock after deployment
- Composite truss configuration
- Provision for accommodating the Optics Path through the lower half of the assembly

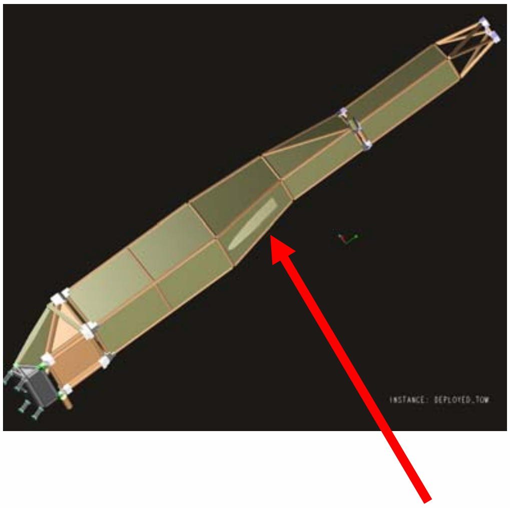

Summary- OTA Mechanical Configuration FB1

- Integrated team approach:
  - **GSFC Thermal, Optical, Structural and Systems involvement**
  - **GSFC and JPL mechanical design collaboration**
- Established working concepts for all major subassemblies
- Solid FB1 development efforts will result in substantial improvements to the OTA for FB2

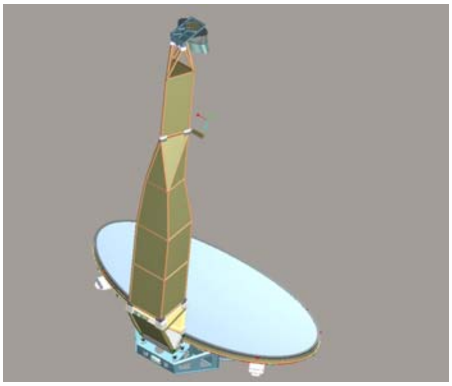

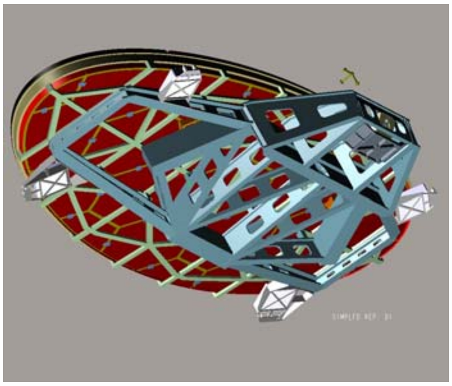

System Thermal Architecture and Design

Terry Cafferty
TC Technology

Contributor: Eug Kwack

11-12 July 2005

TPF Terrestrial Planet Finder

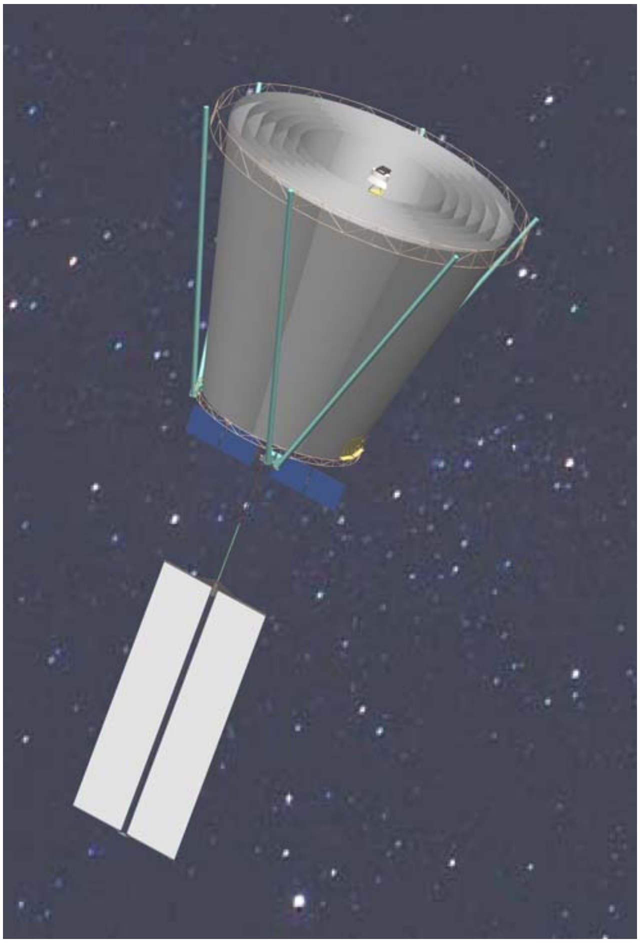

- Early in the TPF-Coronagraph program, due to funding limitations, a fundamental decision was made to select one baseline approach to carry forward as a pathfinder into more detailed analysis. The two basic architectural approaches revolved around the sunshade design and the location of gimbals. One option was to gimbal the observatory behind a flat, JWST-style sunshade. The other option was to gimbal only the solar panels behind an observatory that is essentially rigidly attached to the spacecraft bus. We chose the latter as our baseline.

Thermal Control Architecture Topics

TC Technology

Terrestrial Planet Finder
TPF

1. the thermal challenge of TPF-Coronagraph
   – extreme dimensional stability for long periods with a moving Sun
2. observation scenario drives thermal architecture
   – summarize observation scenario and how it determines thermal reqmts
3. baseline overall thermal design approach
   – cocoon V-groove shield, nested boxes, cold biasing, potential for active control
4. we limit where the Sun can be
   – stray light, thermal stability, and passive cooling enabled
5. the V-groove sunshade
   – 'removing the Sun', features, operating principles, options
6. behind the primary mirror
   – nested components, thermal damping, active control potential, power dissipation
7. electronics cooling
   – electronics thermal pallet, isolation, heat pipes, radiator, active option
8. detector cooling
   – ~ -100 C, ethane heat pipes, shielded cold radiator, active option

- TPF Coronagraph requires long exposures to gather enough photons to form an image. And for speckle removal, it is essential that the observatory be rotated (or 'dithered') about the boresight axis to form a second image, so that the two images can be combined.
- TPF-Coronagraph includes features (a laser metrology driven hexapod on the secondary mount, as well as downstream deformable mirrors) to take out wavefront errors and optical distortions prior to beginning an observation sequence. And it is reasonable to assume that the environmentally induced disturbances are constant for a given orientation. But when the environmental (solar) orientation changes during a dither, then the disturbance directions change. So it is not the shape of the optical system at the beginning of an observation that is critical, but rather the transient distortions induced by the dither.
- Since the exposure times for both images are very long, the optical system must remain dimensionally stable in the extreme. During the 'dither' between the two images, the primary thermal effect is that the Sun moves in its position relative to the observatory. Therefore, the thermal control system must be capable, in effect, of 'removing' the Sun as a disturbance.
- The primary thermal feature implemented to 'remove the Sun' is the multi-layered V-groove shield, which has the job of reflecting the Sun's disturbance away to cold space to such an effect that the size of the disturbance arriving at the observatory is small enough that dimensional stability is maintained. This passive design feature is essential for controlling solar-induced disturbances coming into the front face of the primary mirror, since there is no conventiently implemented active means of controlling such disturbances.

The TPF-Coronagraph Thermal Challenge

- milli-Kelvin or better temperature stability
- many-hour observation
- 30-degree dither
  (moves the Sun midway through the total observation)

- cooling for instrument detectors at ~ -100 C
- cooling for observatory electronics
- cooling for science instruments

- control transient thermal inputs
- control internal power fluctuations
- limit active thermal control system instabilities
- control spacecraft thermal transients

- This chart summarizes the basic tasks of the thermal control system.
- In addition to providing extreme thermal stability of the optics, the system must also accomplish a number of important tasks, each one of which imposes its own set of disturbance laibilities.
- For example, cooling instrument detectors to ~-100 C implies a large thermal gradient between the cold transport system and the relatively warm surrounding alignment-critical structure, with the accompanying necessity to keep these temperature levels from cross-contamination.
- Further, we have chosen as our baseline to house observatory electronics on the observatory side of the spacecraft/observatory interface. These electronics must be designed, operated, mounted, cooled and cabled in a manner such that their operation does not thermally perturb the observatory during critical observations.
- Because the laser metrology system actively compensates for rigid-body motions between the secondary mirror and the primary mirror, somewhat larger transient temperature variations within the secondary mirror support tower can be tolerated, up to a level consistent with the compensatory limits of the laser metrology system and the secondary mirror support actuators it drives.

The Observation Sequence

defines the primary task of the thermal control system

1. slew observatory to acquire new target

2. settle into thermo-mechanical equilibrium in a fixed clocking orientation about the boresight axis
   - quick settling is good (maximizes observation time)

3. correct wavefront with deformable mirror(s)

4. build up initial image (in thermally stable environment)

5. dither 30 degrees about the boresight axis
   - Sun 'moves' 30 degrees

6. build up speckle subtraction image
   - multiple hours in destabilized thermal environment
   - quick settling is potentially bad (conflict with step 2)

- The observation sequence 'moves the Sun' thirty degrees about the boresight axis halfway through the process of building up a final image from which speckles have been removed. This solar movement , without effective means for 'removing it', has the potential to completely destroy the optical alignment of the system. The most important aspect of the thermal control system, then, is the necessity to effectively remove the Sun from the observatory's operating environment. Once this is accomplished, the perturbing strength of the remaining disturbances is much smaller.
- TPF Coronagraph requires long exposures to gather enough photons to form an image. And for speckle removal, it is essential that the observatory be rotated about the boresight axis to form a second image, so that the two images can be combined.
- TPF-Coronagraph includes features (laser metrology driven hexapod on the secondary mount, as well as downstream deformable mirrors) to take out wavefront errors and optical distortions prior to beginning an observation sequence. And it is reasonable to assume that the environmentally induced disturbances are constant for a given orientation. But when the orientation changes during a dither, then the disturbances change. So it is not the shape of the optical system at the beginning of an observation that is critical, but rather the transient distortions induced by the dither.
- Since the exposure times for both images are very long, the optical system must remain dimensionally stable in the extreme. During the 'dither' between the two images, the primary thermal effect is that the Sun moves in its position relative to the observatory. Therefore, the thermal control system must be capable, in effect, of 'removing' the Sun as a disturbance.
- Following the re-pointing of the observatory to a new target star, we want (since we wish to maximize observation time) the observatory to settle quickly into its new (environmentally induced) 'shape', so that the first image can be built up. But following the dither for speckle removal, we would like the effects of thermal distortion to appear slowly, so that there is time to build up the speckle removal image before the distortion becomes too great. In the best case, the thermal control system would perform so well that the steady-state thermal distortion following the dither is small enough that the system distortion is always under critical limits.

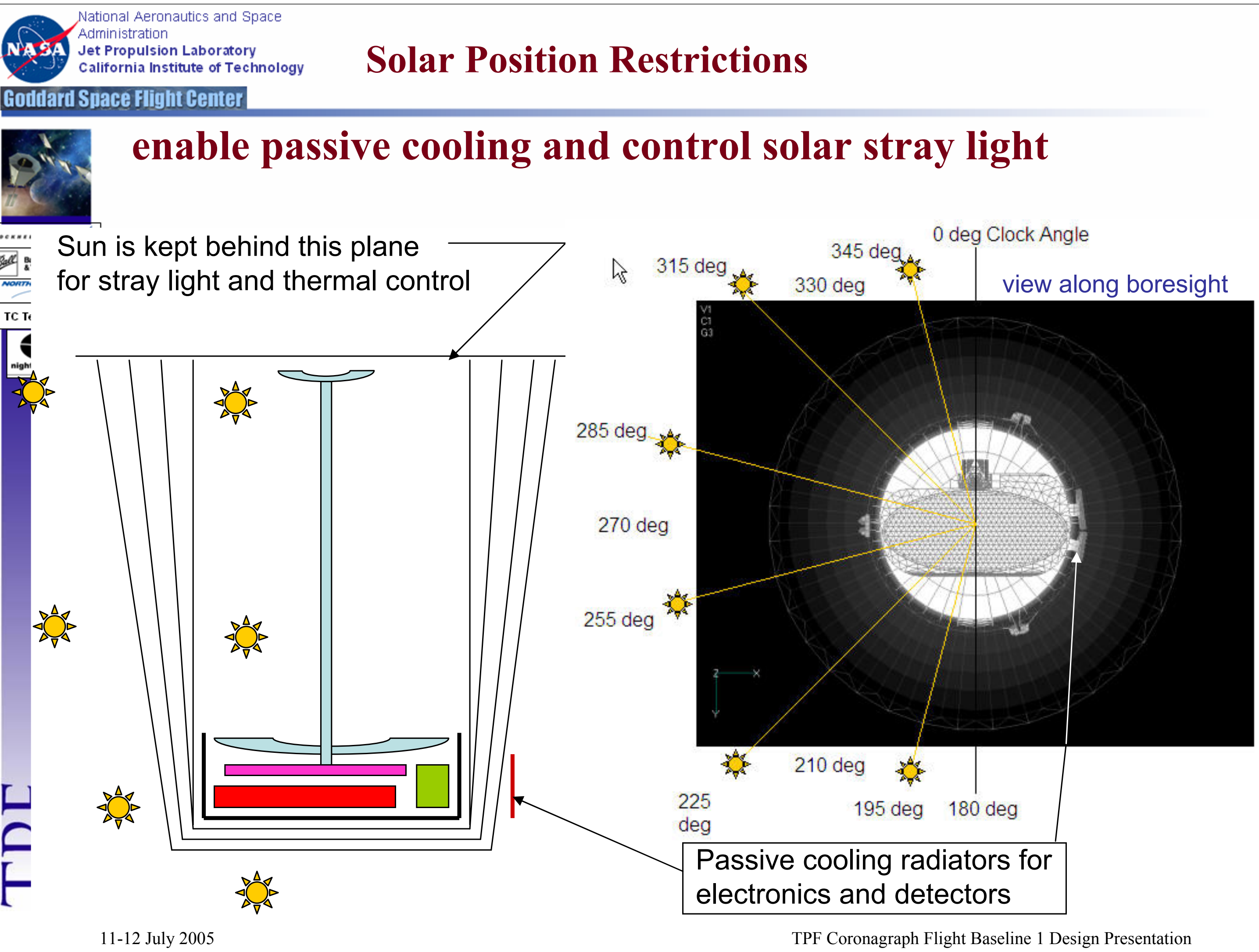

- In order to control in-band stray light, our operational scenario limits where the Sun can be during observations. We do not allow the Sun to illuminate the inside of the baffle surrounding the telescope. This also provides a hemisphere of stable cold space into which the potentially disturbing solar energy can be rejected through the openings in the V-groove shield assembly.
- The view on the right shows the limits on solar position about the boresight axis. There are three basic orientations of the observatory about this axis with respect to the sun: 210, 270 and 330 degrees. Dithers are made across the total 30 degree angle defined by plus and minus 15 degrees about each of these basic orientations.
- By limiting the position of the Sun about the boresight axis in this manner, we open up a view to cold space for our passive radiators, which we use to cool our warm electronics and to cool our cold instrument detectors.

Overall Thermal Architecture

passive and active features combine to provide required thermal stability

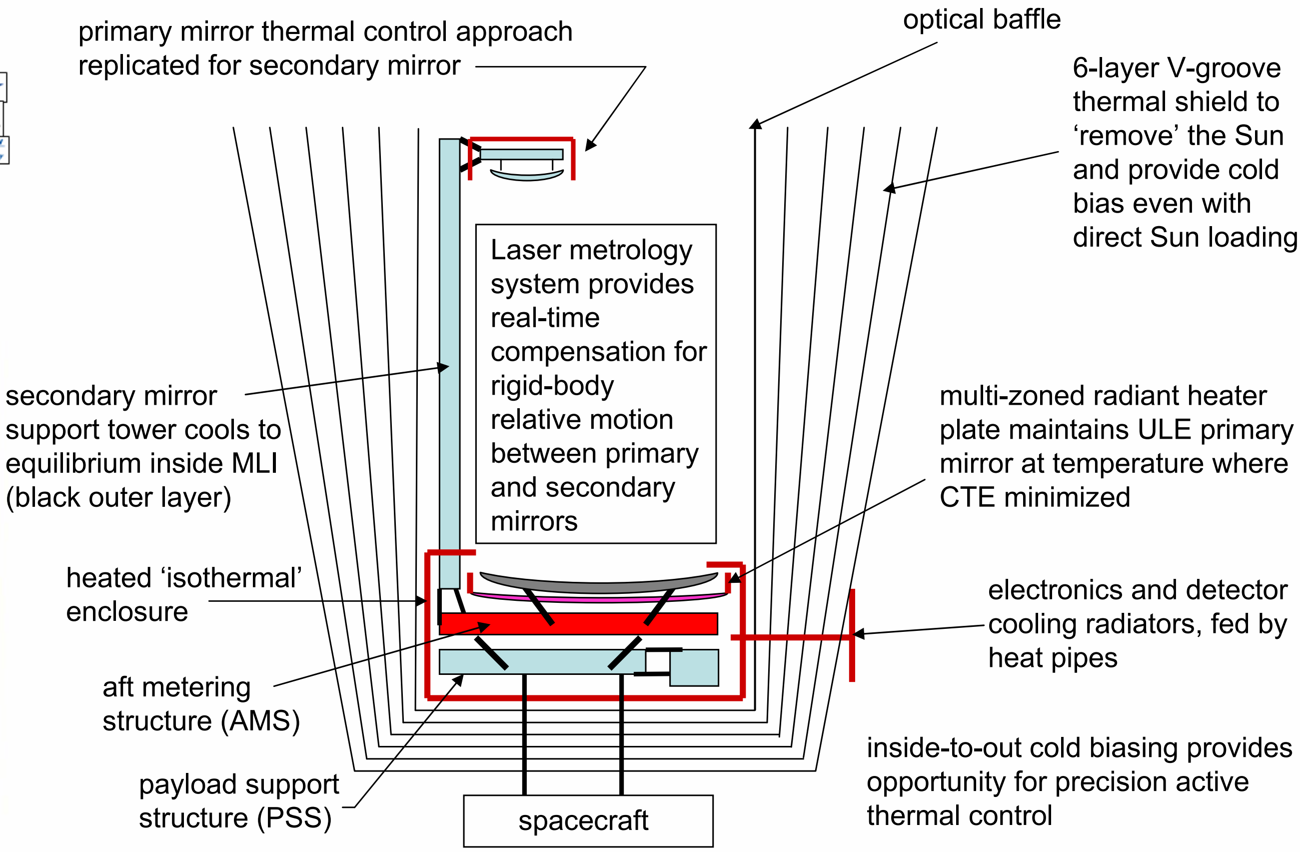

- This chart schematically shows the basic thermal control features for the baseline architecture. These features are discussed in greater detail on other slides and corresponding notes.

Six-layer Conical V-groove Sunshield

critical to primary mirror thermal stability

- outer surface silvered Teflon second-surface mirror, T ~ 220 K EOL max in full Sun
- intermediate surfaces IR-specular aluminum on Kapton film, emittance ~ 0.03
- 3 degrees axial divergence between layers
- 200 degree circumferential temperature difference in outer layer reduced by axial and circumferential radiant tunneling
- circumferential gradient at any axial position in baffle ~0.1 degree
- controls (transient) radiative loading on optically active side of primary mirror
- also considering alternative shapes (flat, ‘sugar scoop’) and active control on intermediate layer(s)

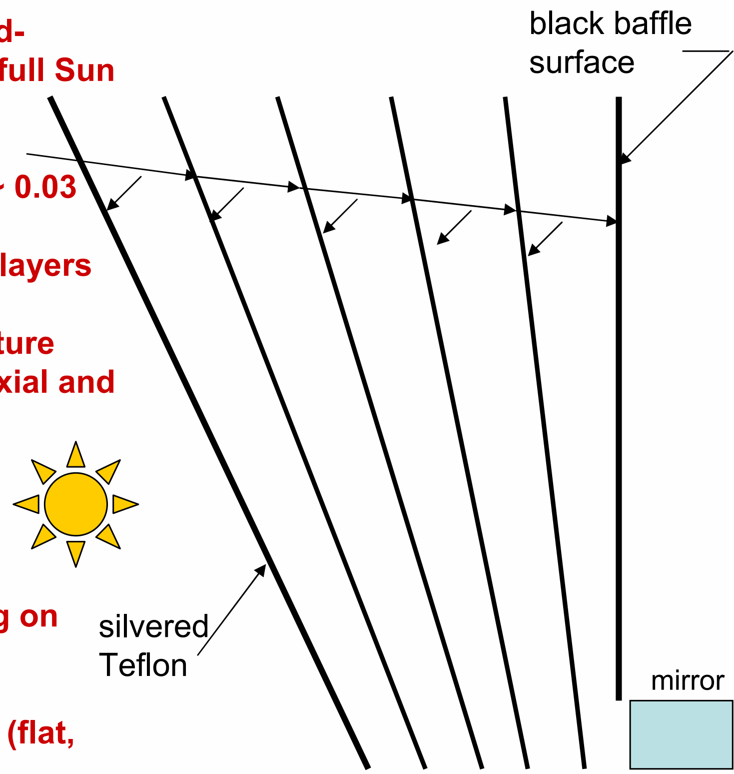

- Shows the basic features of the V-groove sunshield assembly. The exterior surface is silvered teflon second-surface mirror, which combines low solar absorptance with high infrared emittance, passively reducing the temperature gradient in the othermost layer of the sunshield, from the hot side to the cold side. This temperature rediction ripples through to the innermost layer, the baffle.
- The innermost surface is blackened for in-band stray light control
- All intermediate surfaces are specular pure aluminum, vapor deposited on a plastic substrate, probably polyimide or Kapton.
- The highly reflective surfaces and the geometry act together to distribute the disturbing energy curcumferentially and reject the bulk of it to spece, so that the amount of disturbance arriving at the baffle, which radiatively influences the face of the primary mirror, is drastically reduced.
- Other shapes (in addition to the baseline conical shape) are under consideration, driven primarily by the need to deploy the sunshade and accommodate the electronics and detector cooling radiators. One alternate configuration, dubbed the ‘sugar scoop’, looks very promising and may become our baseline for the next design iteration.

Behind the Primary Mirror

multiple features enhance thermal stability during long observations

- primary mirror is heated radiatively by a multi-zoned heater plate…to a bulk temperature corresponding to minimal ULE CTE
- design is cold biased from the PM heater plate 'out', to provide active control authority over all elements

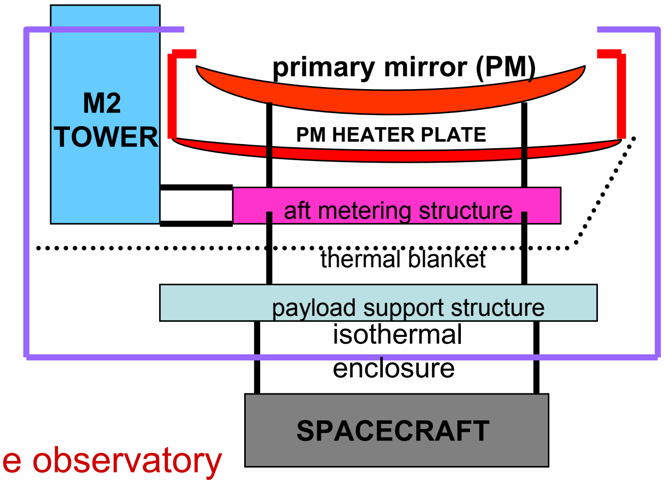

- spacecraft is cold biased relative to the observatory
- SM tower allowed to cool to equilibrium, inside its thermal blankets
- multi-layered insulation (MLI) at interface between AMS and PSS
- nested configuration provides natural damping of outside disturbances
- potential to selectively implement precision active thermal control (as suggested by detailed examination of transient thermal model output)

TPF Terrestrial Planet Finder

- The optics are heated to near room temperature because the ULE glass that is used to make them has minimal coefficient of thermal expansion (CTE) at a particular temperaturenear room temperature, and because the system will be ground tested at that temperature. In orbit, the telescope would tend to cool to an equilibrium temperature well below room temperature, so heat must be added.
- The primary mirror is the optical element that is most sensitive to thermal transients; we have designed the system so that there is a multi-zoned heater plate behind the primary mirror, to allow us to maintain different segements of the primary mirror (each of which will have an optimal temperature with respect to minimizing CTE) at slightly different temperatures. The coupling between this multi-zoned heater plate and the primary mirror is radiative, to avoid point conductive loading or directly applying heaters to the back of the mirror.
- Because we have implemented a laser metrology system between the primary and secondary mirrors, the system will continuously move the secondary mirror on an actively controlled hexapod to maintain the optimal secondary mirror position with respect to the primary mirror in 6 axes (3 linear and 3 angular), even during observations. For this reason, we are allowing the graphite-epoxy secondar mirror tower to cool to equilibrium, and not maintaining it near room temperature. The secondary mirror tower is mounted by thermally isolating tubes from the primary mirror's aft metering structure (AMS).
- For controlling disturbances coming from behind the primary mirror, we have built in a number of features, including a cold-biasing from inside to out, so that there is the possibility of actively controlling (with heaters) disturbances traveling from the outside in. Such heaters might be implemented either in a constant-power mode, or in a feedback controlled mode. We have also built in a 'nested boxes' approach, with successive layers separated by low-thermal-conductance supports, so that the system is naturally thermally damped against transient disturbance traveling from outside in.

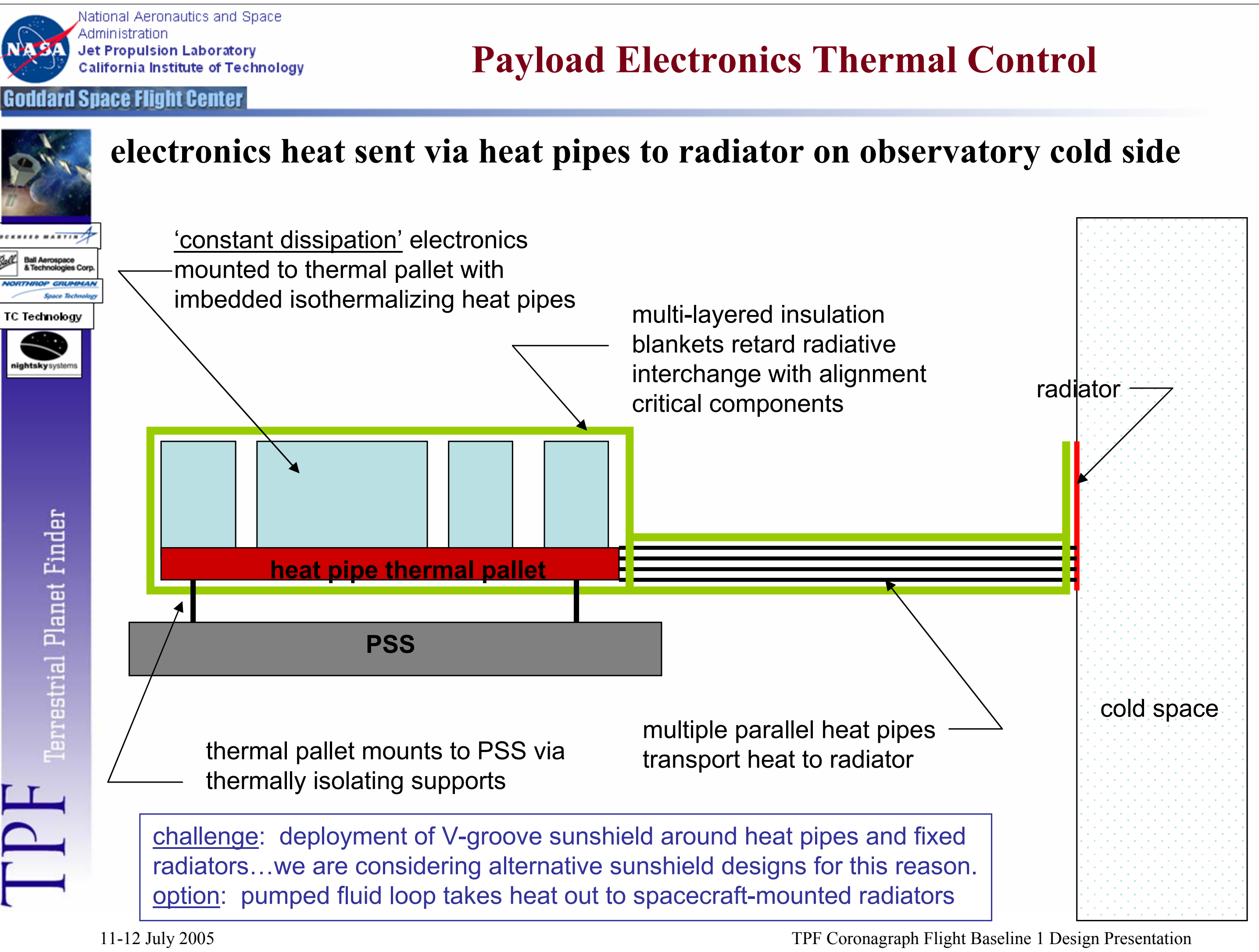

- The bulk of all observatory electronics will be mounted to a thermal pallet which is structurally tied to the payload support structure (PSS) using thermally isolating materials.
- The thermal pallet will be kept nearly isothermal using multiple imbedded heat pipes.
- Great care will be taken to ensure that the power dissipation associated with the electronics is as constant as possible during observations.
- Heat from the electronics is transported from the thermal pallet to the passive radiator on the cold side of the observatory using multiple parallel transport heat pipes of a conventional nature.
- A high-performance multi-layered insulation (MLI) blanket is used to keep the electronics from radiative communication with the surrounding alignment-critical structure.
- An option we are considering would make use of a pumped fluid loop to remove electronics power to the spacecraft side for radiative rejection to space. We have not chosen this option as our baseline because we are concerned that the fluid transfer lines would transmit excessive vibrational disturbances to the observatory.

Thermal Control for Science Detectors

detectors cooled to ~ 170 K by ethane heat pipes feeding a fixed radiator on observatory cold side

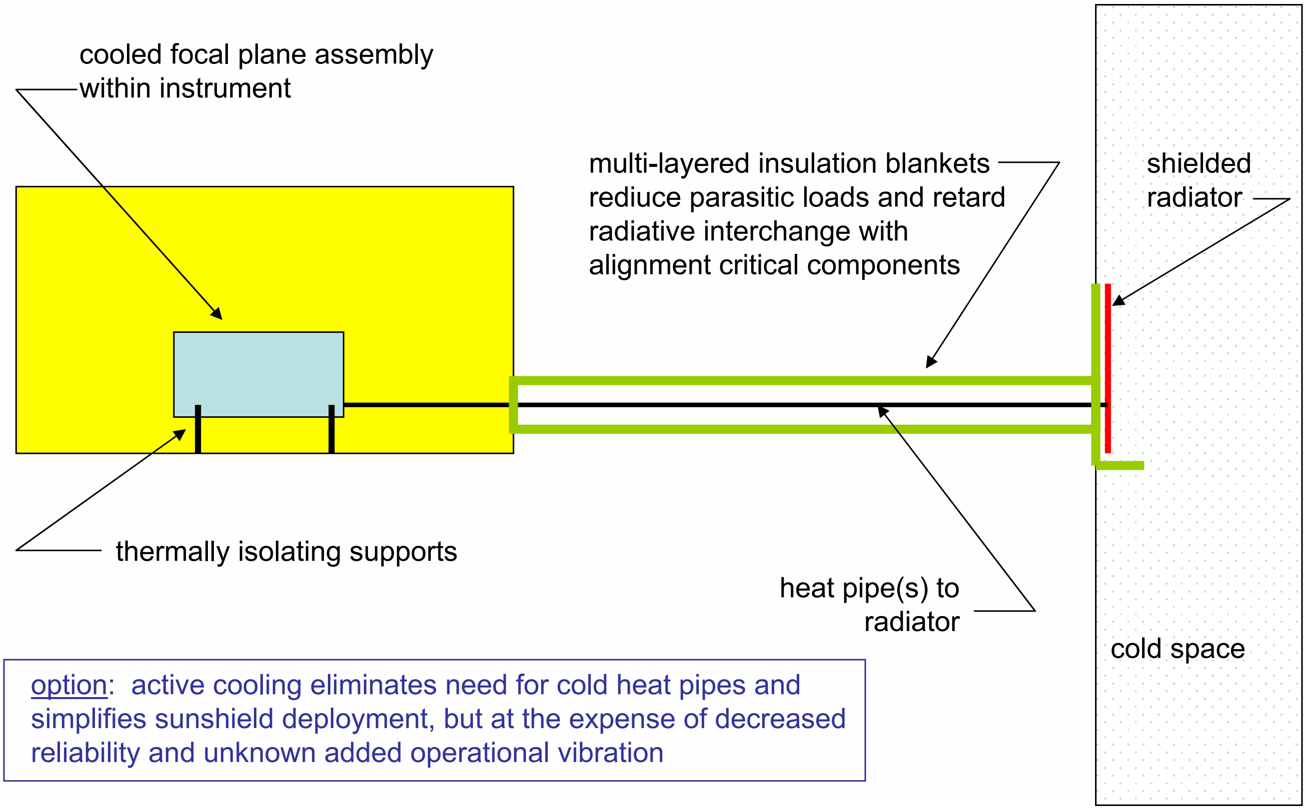

- Heat loads (active and parasitic) arriving at the instruments' cooled focal plane assemblies will be removed by conventional heat pipes to a thermally isolated passive radiator mounted on the cold side of the observatory.
- Great care will be taken to ensure that the power dissipation associated with the various focal planes is as constant as possible during observations
- A high-performance multi-layered insulation (MLI) blanket is used to keep the cryogenically cooled assembly from radiative communication with the surrounding alignment-critical structure.
- An option (not currently under consideration) would make use of an active (turbo-Brayton) cryocooler to remove detector heat to the spacecraft side for radiative rejection to space. W have not chosen this option as our baseline because we are concerned that the cryocooler working fluid transfer lines might (along with the cryocooler itself) transmit vibrational disturbances to the observatory.

Thermal Architecture and Design

summary

- we have a full array of design features available to us to provide the required thermal stability
- we now have a relatively detailed full system thermal model
- we are exercising that model in a logical fashion to evaluate performance and guide the implementation of design features
- we are confident we can provide the needed thermal stability

- The first aspect we wanted to verify is the ability of the sunshield to control solar induced disturbances transmitted radiatively to the face of the primary mirror. We are satisfied this is well in hand.
- The next step is to release the structure behind the primary mirror from boundary node constraints, and to replace the constant temperatuyre boundary imposition with constant power heater dissipation. Once this is done, we will repeat our disturbance scenarios and assess the effects of the dither amneuvers on transient system wavefront error. We have a very detailed thermal/structural/optical model with which to make this assessment.
- We may discover that the constant-power heater approach is insufficient to maintain the required thermal stability, in which case we would begin investigating selective implementation of active (ffedback) thermal control on our heaters.
- The detailed thermal/structural/optical model is essential to the understanding of the disturbance sources and paths (and for determining the best ‘fixes’).
- When we began this investigation, the thermal task seemed overwhelming and next to impossible, but at this point we are cautiously convinced we have built in the necessary design options so that we can systematically discover a way to make the system work thermally to the required stability.

Optical Telescope Assembly

Thermal Sub-System

Louis Fantano

Contributors:
Cliff Jackson

11-12 July 2005

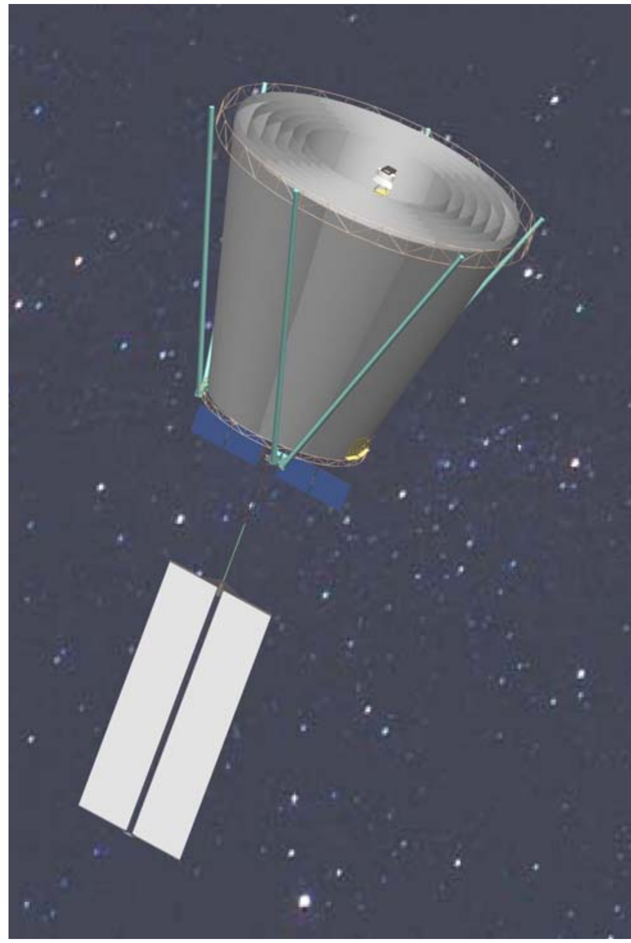

Presentation Outline

- Thermal Design Schematic
- Radiation Thermal Control Strategy
- Conduction Thermal Control Strategy
- Thermal Design Implementation
- OTA Dissipated Power Estimate
- OTA Thermal Sub-System Status

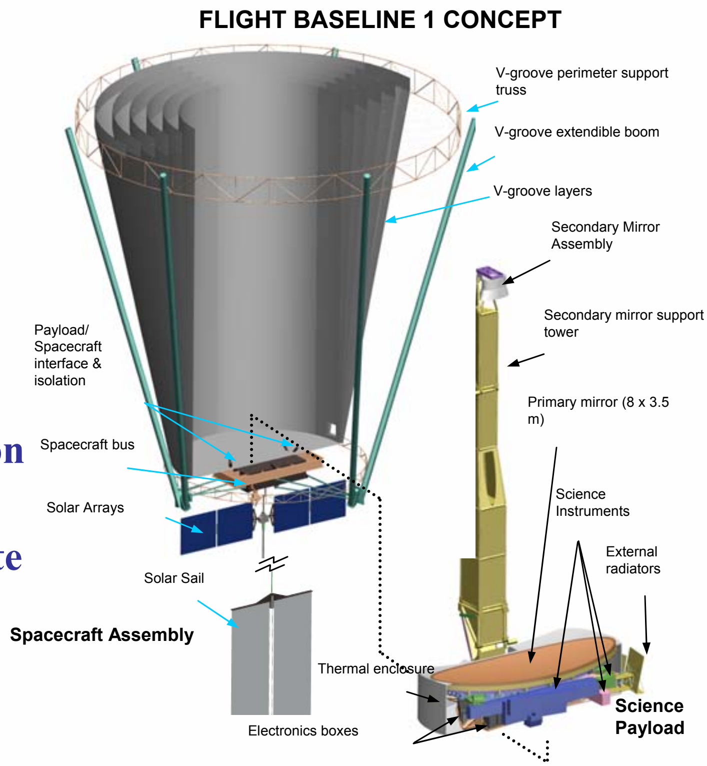

Thermal Design Schematic

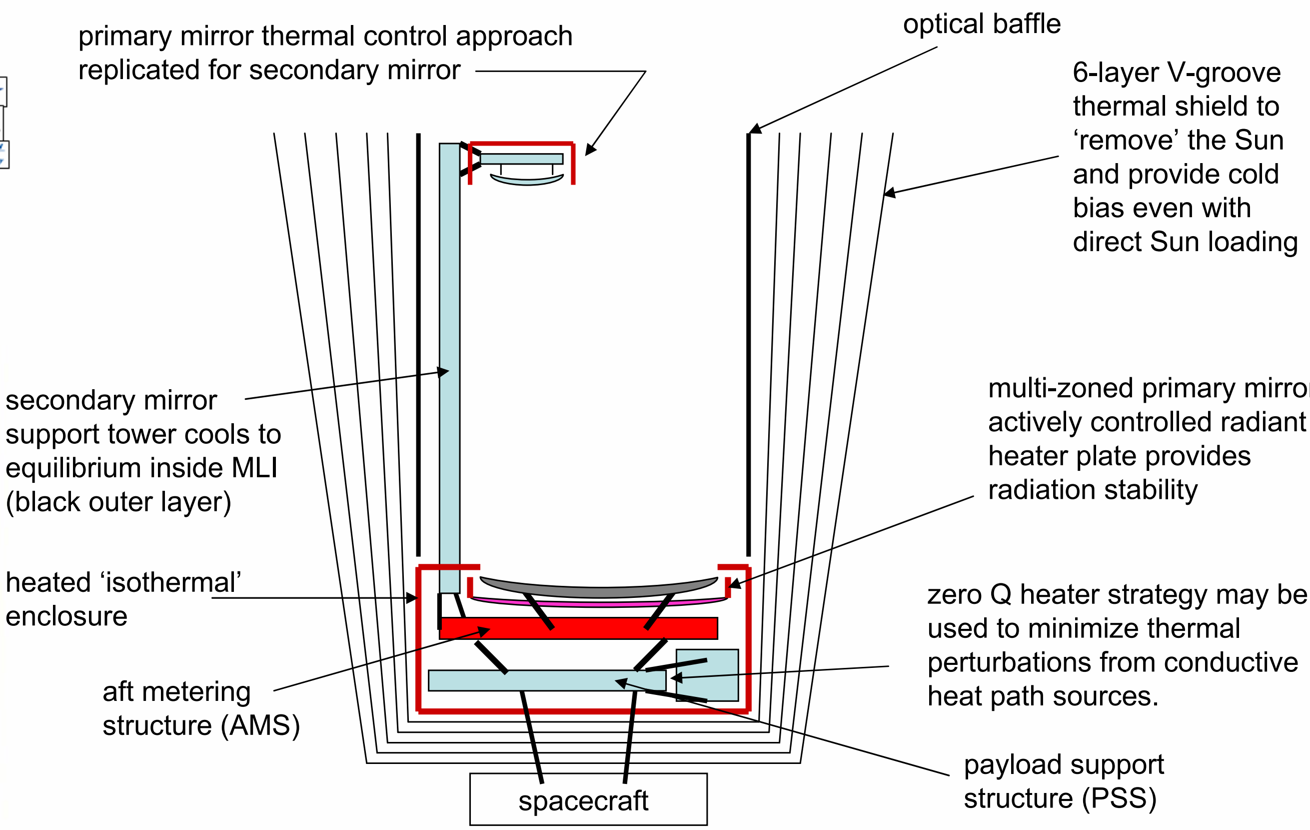

OTA thermal design development is driven by the fact that ULE optical elements have poor thermal conductance properties and are highly sensitive to any hardware that may be brought in to contact with it. In addition, the overriding TPF thermal requirement is to maintain optical element temperature stability over extended time durations. Consequently, the best thermal design approach is to control the radiation environment that surrounds each optical element to be stable and to control all thermal conductive interfaces for near zero heat flow. This is the approach that has been chosen and implemented.

Radiation Thermal Control Strategy

- OTA radiation thermal control is achieved via a combination of passive and active thermal control techniques.
  - Heaters and Temperature Sensors
  - Thermal Control Electronics
- The PMA and SMA are thermally controlled by forming a temperature-stable radiation environment around each element's perimeter and rear using K1100 composite panels as temperature control zones.
- All TPF-C OTA electronics boxes, with the exception of the LD5 boxes, are mounted to the JPL-provided Engineering Electronics Thermal Plate.

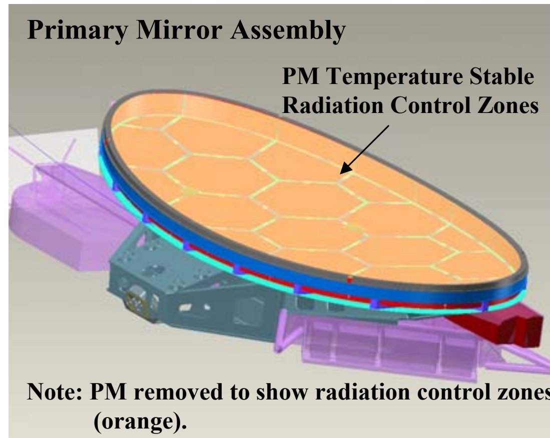

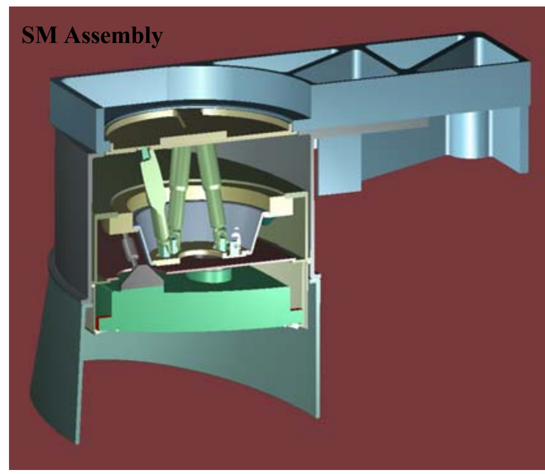

- The principal thermal design driver for OTA optical components is temperature stability. Changes in optical element and bench temperatures during planet detection and characterization campaigns may cause mechanical distortions that can affect telescope performance.
- OTA thermal control is achieved combining passive and active thermal control techniques, including the use of heaters (and sensors as needed) to maintain desired temperatures. Optical elements are thermally controlled by radiation control zones that surround each element's perimeter and rear. Heaters are also used at key conductive interfaces to achieve near zero heat flow through each respective interface to provide stable thermal boundary conditions to the OTA.
- Low and constant LD5 box power dissipation (3 W) enables its heat to be radiated to the local surroundings. All other TPF-C OTA electronics boxes are mounted to the JPL-provided Engineering Electronics Thermal Plate. Thermal control for these boxes will be provided as part of JPL's overall PSS thermal design. In addition, the JPL contribution will include the Isothermal Enclosure MLI/heaters around the AMS which provides a stable thermal environment for the PMA.

Conduction Thermal Control Strategy

TC Technology

Terrestrial Planet Finder
TPF

Zero Q Conductive Interface Heater Strategy

- Goal – Achieve near zero heat flow at key conduction interfaces while minimizing power required to do so.
- All key conduction interfaces may employ a zero heat flow (Zero-Q) thermal control strategy to achieve temperature stability based on analyses results. The following are candidate conduction interfaces that might employ the Zero-Q heater strategy:
  - SMA / SST Isolation Struts
  - SMA-Bipod / Secondary Mirror
  - PMA / SST-Isolation-Struts
  - PMA-Bipod / Primary Mirror

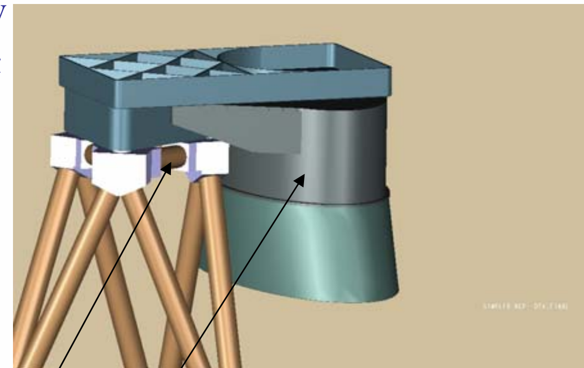

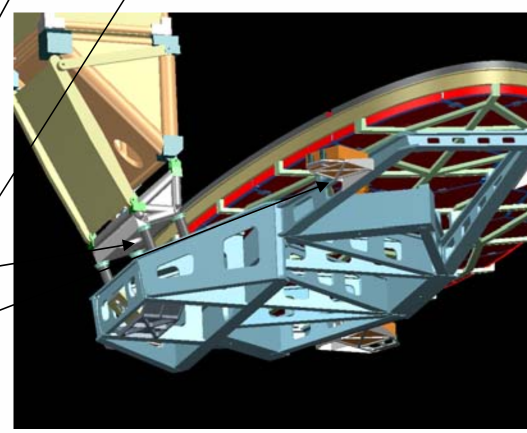

- Each Zero Q conductive interface is characterized by poor thermally conducting bipod or isolation strut materials (Titanium or MJ55 composite). The length of a bipod/strut is insulated with MLI to minimize the radiation coupling to the surrounding environment. A 1- to 3-inch wide high resistance heater is adhered at the bipod/strut center and circumscribes its perimeter. This heater is overlaid with 3-mil aluminum foil tape. One temperature sensor (the control sensor) is located at the end of the bipod/strut adjoining the temperature-stability-critical element, and another temperature sensor is located on the side of the heater closest to the control sensor.
- Thermal analyses of the operational observing scenario will be performed to determine the direction of the bipod/strut temperature gradient assuming a fully insulated bipod/strut. The Zero-Q thermal control strategy requires that the bipod/strut end opposite the temperature-stability-critical end be cooler so that heat can be applied at the center to achieve near zero heat flow. Based on thermal analyses results for each specific location, a window may have to be sized and cut out of the MLI to ensure that the desired bipod/strut temperature distribution is achieved. If the local thermal environment is not cooler than the control temperature and the temperature-critical bipod/strut side is cooler than the non-critical side, then the control sensor will be located to the non-critical side.
- Thermal control electronics support three modes of operation. The three modes are temperature control, fixed power control, and active dual sensor zero-Q temperature feed back control. The temperature control mode maintains selected sensors at specified temperatures. The fixed power control mode applies a fixed constant power to a heater. The active temperature feed back control mode actively regulates heater power to achieve near zero heat flow by matching the temperatures of specially selected thermal sensors.

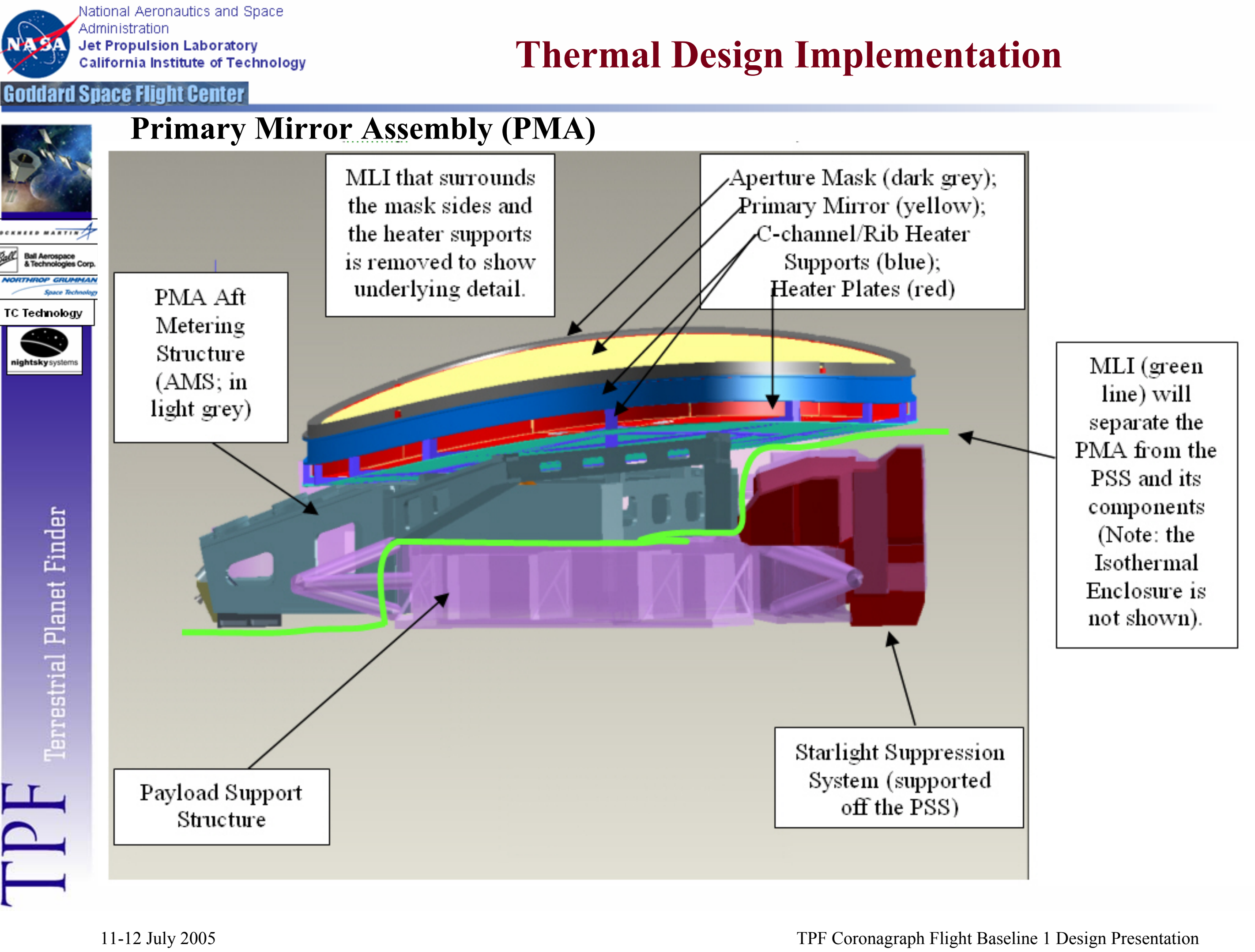

- The GSFC supplied PMA includes the AMS structure and the components supported off it, whereas the JPL supplied hardware assemblies include the various assemblies below the AMS structure that are supported by the PSS. A multi-layer insulation (MLI) blanket is located beneath the AMS structure to provide a near adiabatic interface between GSFC- and JPL-provided mechanical assemblies (this is in addition to the Isothermal Enclosure blankets/heaters that surround both the PMA and the PSS).
- Each hexagonal shaped primary mirror segment (23 total) has a dedicated thermal control zone. Twenty three (23) separate thermal control zones are located one inch behind the primary mirror (one per segment) and sixteen (16) thermal control zones are located around the periphery of the PM (one per segment, set back 0.5 inches) to control the mirrors radiation environment. Each thermal control zone is comprised of K1100 quasi-isotropic (QI) composite material in which K1100 fibers within each panel are laid up at a 45 degree angle to obtain equal thermal conductivity in both x and y directions. Each panel is an eighth inch thick. Kapton-Inconel heaters are applied to the rear side of each thermal control zone (interrupted only by structural support points) to achieve near-uniform heat application to each thermal control zone. These heaters can be controlled either in fixed power or fixed temperature modes selectable from the ground.

Thermal Design Implementation

Top Down PMA View showing the Iso-Thermal Enclosure (IE; white). PM segments made visible through partially transparent PM Front Face

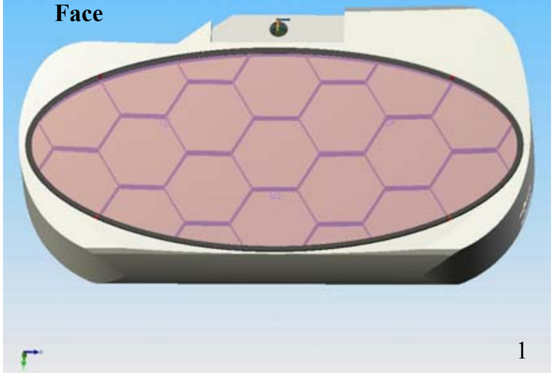

1

Same View with IE & PM removed. Note green MLI visible through gaps between rear thermal control heater zones (red).

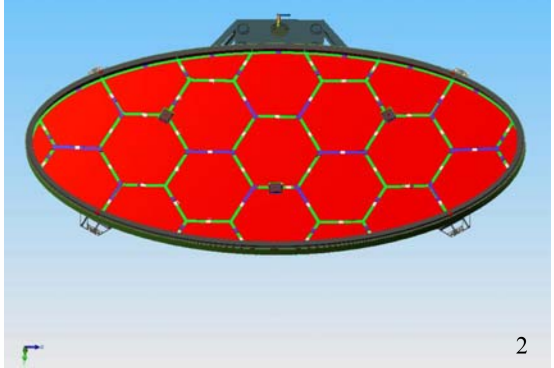

2

MLI, bipods, and aft PM heater zones removed. Note the four (4) LD5 boxes.

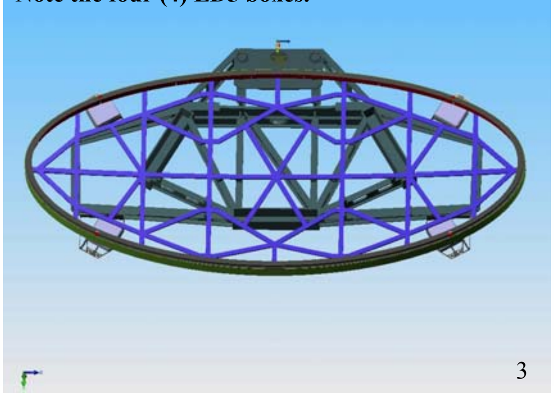

3

View of MLI (green) that surrounds PM heater zones.

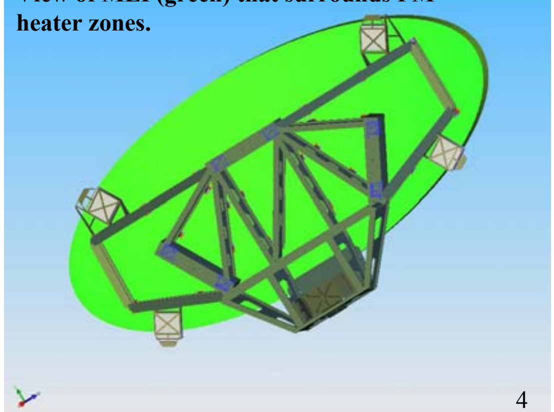

4

- MLI blankets (12 double sided VDA layers with 3-mil thick kapton inner and outer layers) are located behind the mechanical rib/c-channel supporting structure (and also extend above the c-channel to cover the PM aperture mask exterior, with any area extending above the Isothermal Enclosure having a black kapton outer layer). A two inch gap separates the aft PM heater plates from each other to accommodate potential placement of primary mirror actuators in a future design cycle. These gaps are left open for the baseline thermal analysis, but may be closed out with MLI. The thermal heater plates are mechanically supported by M55J (or equivalent) composite rib/c-channel structure, and are attached to this structure with G10 isolators (one per aft heater plate, and 2 per side heater plate). The low thermal conductance associated with this M55J/G10 combination, along with the advantageous A/L geometry of the ribs, provides effective thermal isolation between each thermal control zone. But, low thermal conductivity titanium connectors attach the aft heater plates (not the side heater plates) to each other to provide structural support, and will result in some additional thermal coupling between the aft zones.

Thermal Design Implementation

M3 Fold Flat

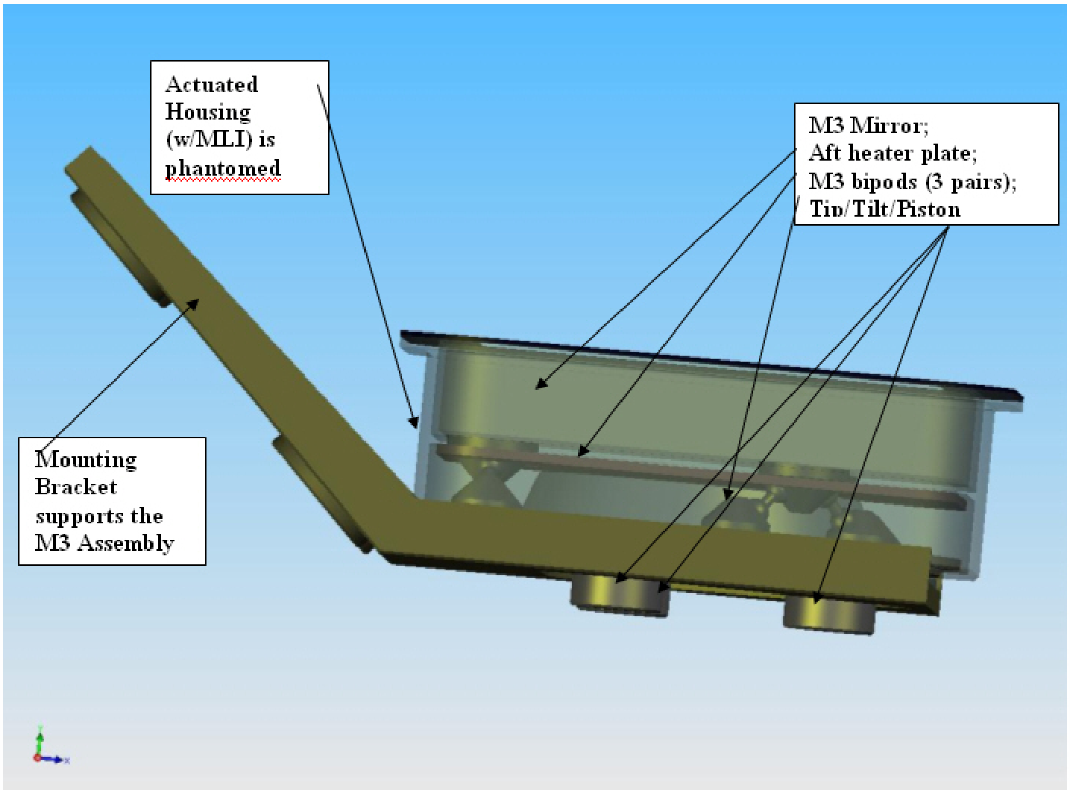

- The M3 mirror thermal design concept is shown. A single K1100 thermal control zone is located behind the mirror and is supported off the surrounding actuated M3 housing. A kapton-inconel heater strip is mounted to it and provides an even heat distribution along the panel. No heater control zone is provided around the mirror perimeter. However, a thermally adiabatic skirt formed via an MLI blanket with a 3-mil inner kapton layer and a black kapton outer layer (otherwise the same construction as used for the PM thermal bathtub blankets) is wrapped around and behind the M3 housing to minimize internal thermal gradients.

Thermal Design Implementation

Secondary Mirror Assembly (SMA)

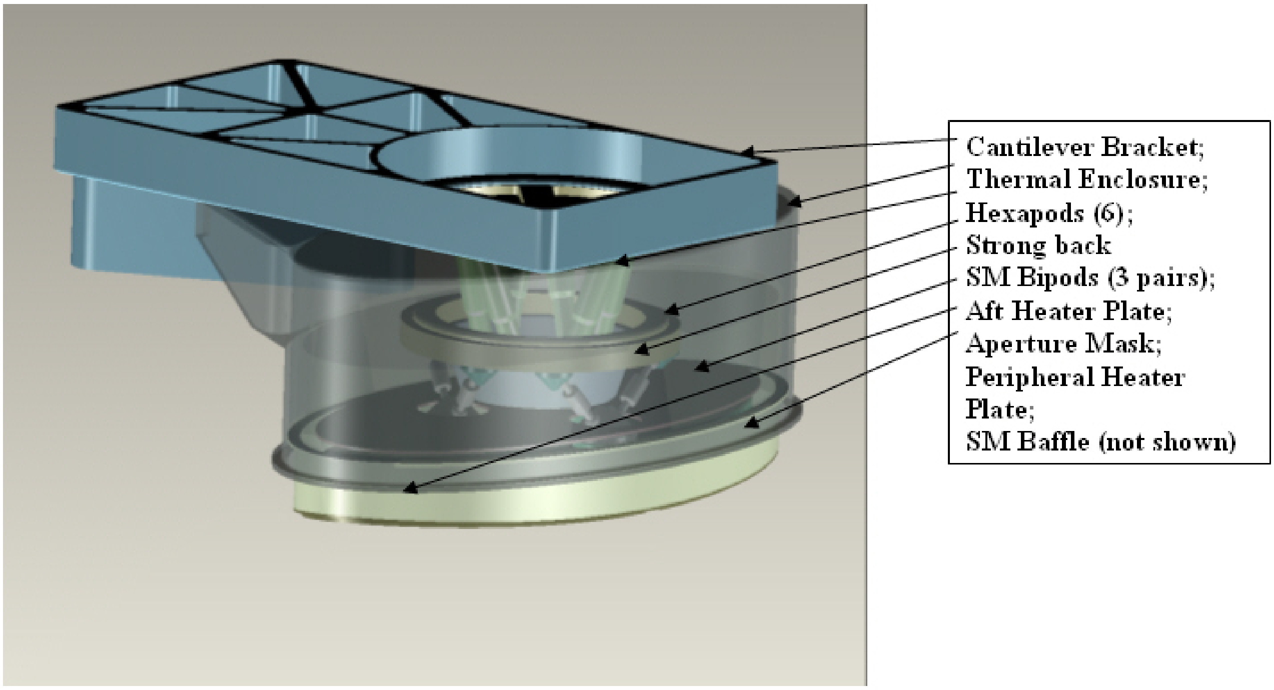

- The figure illustrates a cutaway view of the SMA. A dedicated eighth inch thick K1100 heater plate is located directly behind the secondary mirror. A kapton-inconel heater applied to the back of this panel evenly distributes the applied heat. No MLI blanket is located directly behind this thermal control zone, as this heater is also going to warm the hexapod assembly area.
- An additional curved eighth inch thick K1100 heater cylinder surrounds the SM perimeter at a uniform distance (~35 mm) from the mirror’s edge. A kapton-inconel heater applied to the outside of this heater cylinder provides the necessary uniform heating. No MLI blanket is provided directly on this heater plate, but the directly adjacent thermal housing that surrounds it is fully insulated and closes out the sides of the cylinder. The hexapod assembly and cantilever bracket closes out the back of the volume.
- The secondary mirror and associated components are contained in an enclosure to limit heat loss. The bipod struts that support the secondary mirror off the strong back structure are insulated with 6-layer MLI including 1 and 1.6 -mil kapton inner and outer layers, respectively, and have Zero-Q heaters applied under the MLI. The 14-layer enclosure exterior MLI has a 3-mil black kapton outer layer which is specified for stray light purposes. The side of the enclosure that faces deep space in the optical axis direction has a small dedicated radiator to provide enclosure cold bias. This radiator has a heater applied to it so that the enclosure temperature can be regulated to achieve the required temperature distribution.

OTA Estimated Power Dissipation

	OTA Observing Mode Power Dissipation			
	#	Estimated Power W	Total W	Power Fluctuation Delta W / 8 Hrs
Electronic Boxes				
LD5 Laser Boxes	4	3	12	~ 0
TSCE Box	1	56	56	~ 0
MCE Box	1	20	20	Duty Cycle TBD
LME Box	1	6	6	~ 0
Other Components				
SMA Coarse Actuators	6	TBD	TBD	~ 0
SMA Fine Actuators	6	TBD	TBD	Duty Cycle TBD
M3 Actuators	3	TBD	TBD	~ 0
Total Component Power			**94**	
Heater Power		TBD	TBD	TBD

- The power dissipation values presented represent the best estimates available. It is critical that the power dissipated by the LD5 Laser boxes does not increase since the LD5 thermal control approach relies on radiation exchange to the surrounding environment.

OTA Thermal Sub-System Status

- The proposed OTA thermal control system qualitatively provides an extremely stable thermal environment to TPF OTA optical elements.

- The quantitative thermal performance associated with the proposed design is being modeled and preliminary thermal performance results are encouraging.

National Aeronautics and Space Administration
Jet Propulsion Laboratory
California Institute of Technology
Goddard Space Flight Center

TC Technology

TPF Terrestrial Planet Finder

Integration, Test, and Verification Plans

Anthony J. Martino

Andrew Smith
Michael Krim
Joe Pitman

11-12 July 2005

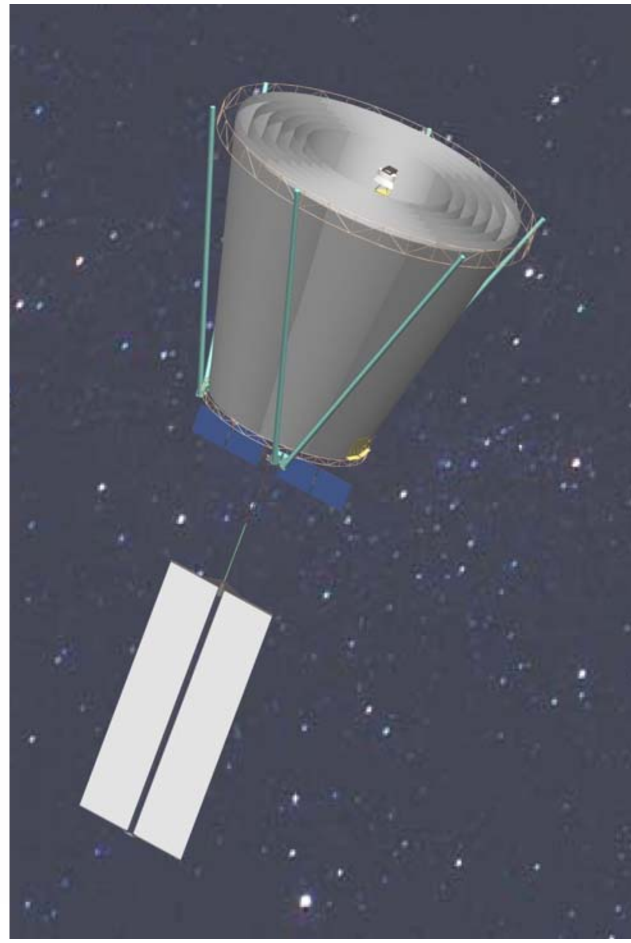

- A description of the current state of plans for integration, test, and verification of TPF-C.
- Integration and test discussions began in May. This document captures a preliminary plan.

Outline

- Requirements Levels
- Verification Matrix example
- Verification overview: telescope assembly
- Primary mirror verification and test
- Overall integration and test flow
- Future Work

- Backup charts: more detailed I&T flows

- High-level description of the integration, verification, and test program.
- Final, detailed requiriements are still being worked out, and will be for some time. Integration and test plans are proceeding based on reasonable assumptions about what the requirements will be.
- Presenting an overview of how the requirements will break down, with, as an example, a detailed look at part of the requirements matrix for the telescope.
- Followed by a top-level description of the logical flow from test through analysis to verified requirements for the telescope assembly, and then the primary mirror. These are likely to be among the most challenging I&T tasks.
- Then a very high-level description of I&T flow for the entire mission, followed by a description of the next steps in the integration, test, and verification planning effort.

Requirement Levels

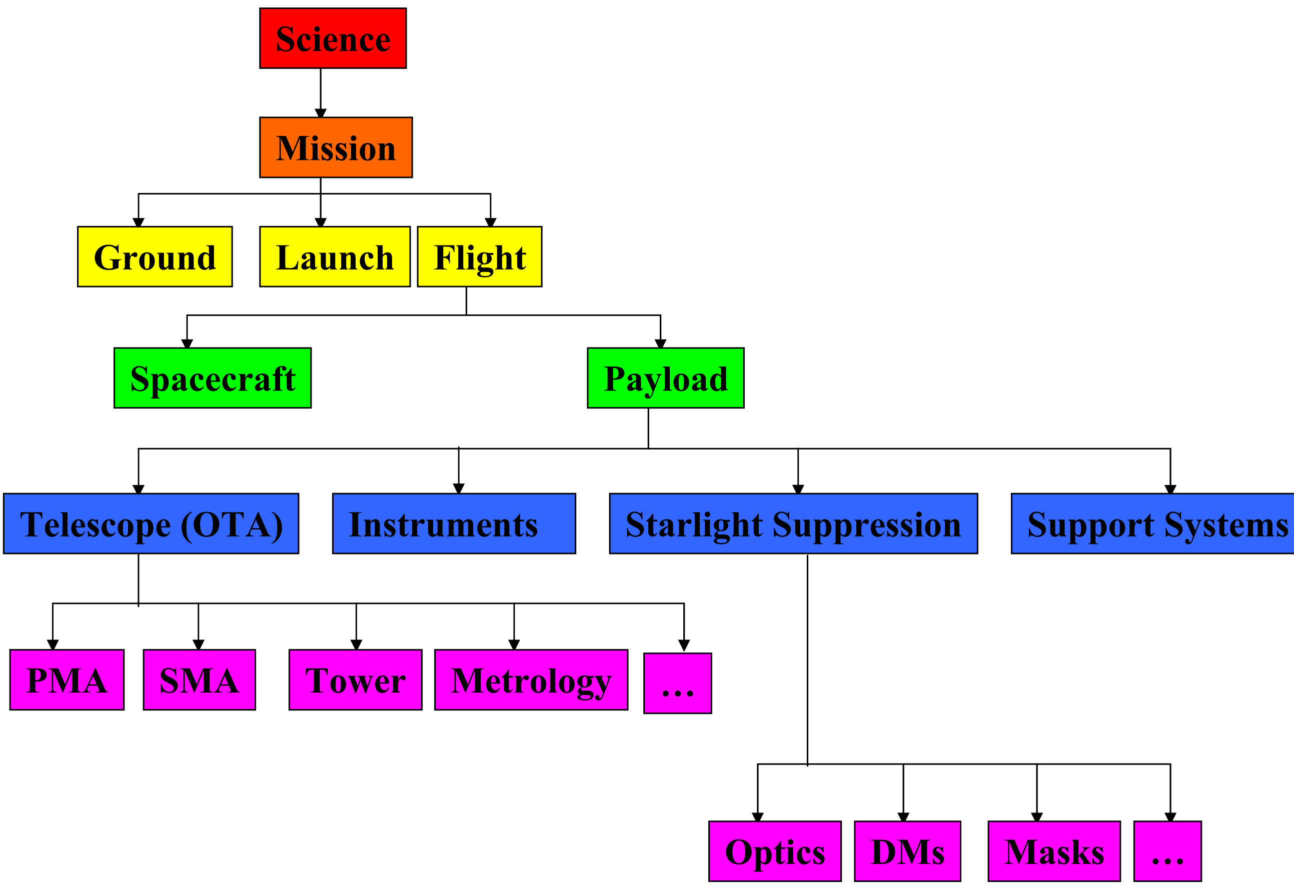

TPF Terrestrial Planet Finder

- This is how we envision the requirements breaking down.
- The science requirements, which are still being defined, will drive the requirements for the mission. The present baseline design for the mission is based on a preliminary set of science requirements.
- I&T planning to this point has concentrated on the payload, and in particular, the Optical Telescope Assembly (OTA). That is considered to be the most challenging task, because testing to the required precision may be beyond the capability of facilities that will reasonably be available.
- The OTA comprises the Primary Mirror Assembly (PMA) which includes the primary mirror and its associated structure and thermal control, Secondary Mirror Assembly (SMA), a tower that supports the secondary, a metrology subsystem that controls the spatial relation between the primary and secondary, and various support subsystems. We will be taking a closer look later in the presentation.
- Extensive integration, test, and verification activities will take place at the subsystem level before work at the higher levels begins.
- Similarly, other systems like the Starlight Suppression System will have requirements, and IT&V plans starting at low levels and working up to a verified system.

Verification Matrix (section)

REQUIREMENTS	TEST	ANALYSIS		COMMENTS
3.3.1 OTA				
3.3.1.1 OTA level requirements				
3.3.1.1.1 *First order optical properti*				
3.3.1.1.1.1 Magnification	x			
3.3.1.1.1.2 Field of view	x			
3.3.1.1.1.3 Effective focal length	x			
3.3.1.1.1.4 Focal ratios	x			
3.3.1.1.1.5 Focus location	x			
3.3.1.1.2 *Resolution*				
3.3.1.1.2.1 Major axis		x		Based on full-aperture measurements of idividual elements and subaperture end-to-end measurements.
3.3.1.1.2.2 Minor axis		x		Based on full-aperture measurements of idividual elements and subaperture end-to-end measurements.
3.3.1.1.3 *Wavefront*				
3.3.1.1.3.1 Dynamic		x		Combines sub-aperture ene-to-end measurements made in an environment that comes as close as possible to predicted flight mechanical and thermal disturbances with CTE and disturbance response measurements of individual elements, subscale OTA testbed measur
3.3.1.1.3.2 Static		x		Combines multiple sub-aperture end-to-end measurements. Compare with verified model.
3.3.1.1.4 *Contrast contribution*		x		Based on measurements with GSE coronagraph and HCIT results.
3.3.1.1.5 *Pointing*	x			Verification of secondary mirror contribution to pointing control
3.3.1.2 Primary mirror assembly				
3.3.1.2.1 *PMA level requirements*				
3.3.1.2.1.1 Surface figure				
3.3.1.2.1.1.1 static		x		Center-of-curvature measurement of PM surface figure using gravity off-loading support and model of residual figure error.
3.3.1.2.1.1.2 dynamic		x		Combines surface figure measurements made under over-driven thermal and mechanical loading conditions with measurements of subscale PMA response to flight-like environmental loading.
3.3.1.2.1.2 Alignment	x			Alignment with metering structure.
3.3.1.2.2 *Primary mirror*				
3.3.1.2.2.1 First order optical pro	x			
3.3.1.2.2.2 Mechanical Properties				
3.3.1.2.2.2.1 Mass	x			
3.3.1.2.2.2.2 Dimensions	x			
3.3.1.2.2.3 Reflectance	x			
3.3.1.2.2.4 Thermal properties				
3.3.1.2.2.4.1 CTE distribution		x		Based on measured surface figure response to applied thermal perturbations. Compare to direct measurements of samples from ULE

- This is a section of the verification matrix, showing requirements at the Optical Telescope Assembly (OTA) level, the Primary Mirror Assembly (PMA) level, and the primary mirror itself.
- For each requirement, our current judgement is shown as to whether we will be able to verify the requirement by test, or we will have to verify it by analysis.
- The most basic requirements are shown as verified by test, but the more demanding requirements will be verified by analysis. This is based on assumptions that our ability to relieve gravity sag, and to duplicate the on-orbit thermal and vibration environments, will fall short of what is necessary to directly verify the on-orbit requirements. We plan to investigate the truth of these assumptions.
- We also assume here that full-aperture end-to-end testing will not be feasible, and we will have to verify optical performance requirements by use of a model derived from sub-aperture tests. We also plan to investigate the trade between full-aperture and sub-aperture testing.

National Aeronautics and Space Administration
Jet Propulsion Laboratory
California Institute of Technology
Goddard Space Flight Center

Verification Overview: OTA

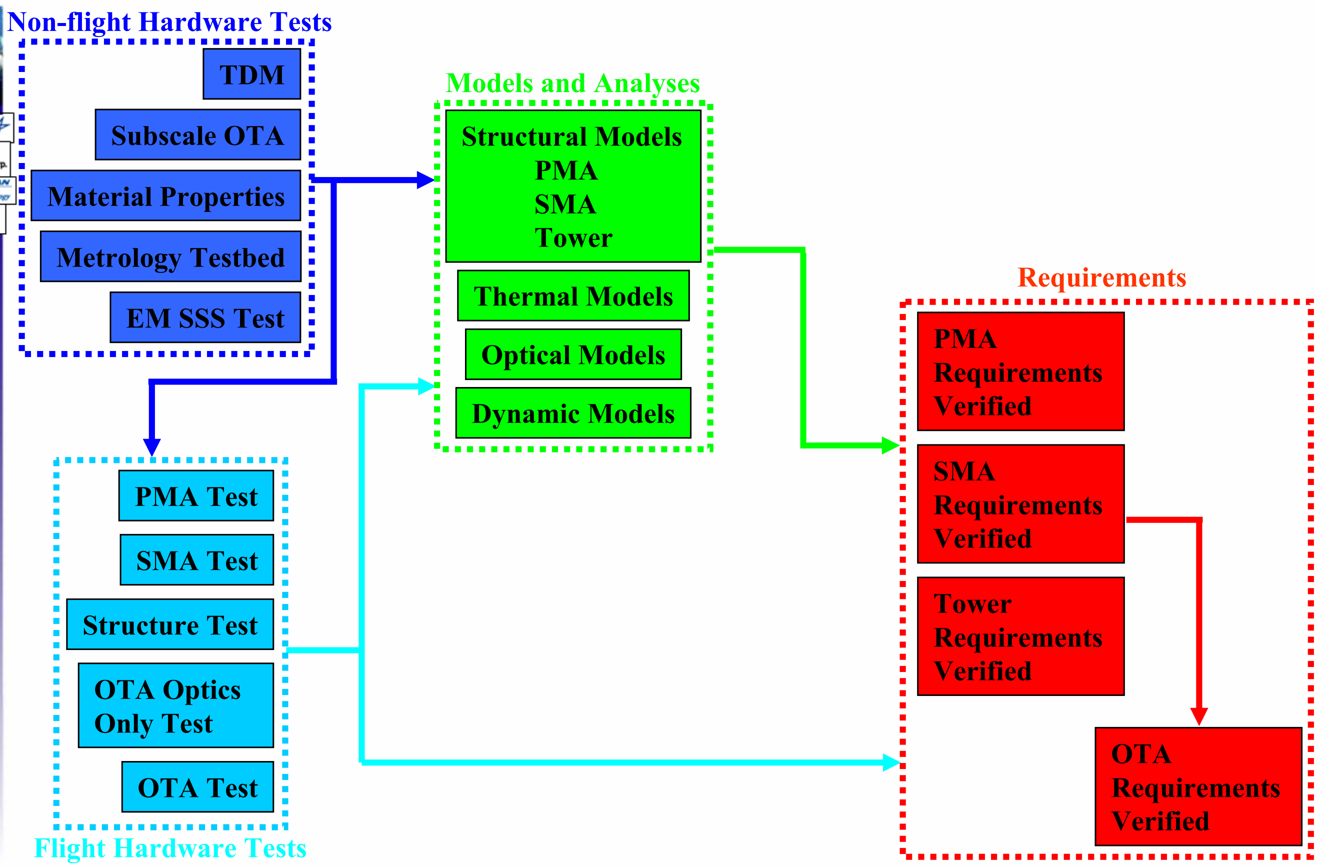

TPF Terrestrial Planet Finder

- Here we see the relation between tests, measurements, or experiments on non-flight hardware, tests on flight hardware, and models and analyses as they relate to the verification that the product meets the requirements.
- Non-flight hardware tests include
  - the Technology Demonstration Mirror (now in production),
  - a subscale Optical Telescope Assembly that will demonstrate properties of the primary mirror not covered by the TDM, and will also be used to test the temperature control and metrology concepts
  - Several testbeds that measure, with an unprecedented precision, certain properties of the materials we are considering. These include thermal expansion coefficients and optical scattering properties.
  - A testbed devoted to the metrology subsystem that controls the relative positions of the primary and secondary mirrors. It will demonstrate laser stability and closed-loop control of a hexapod actuator with the required precision
- Flight hardware tests are shown as groups:
  - tests of the primary mirror assembly, secondary mirror assembly, and structures at the subsystem level
  - Optical tests of the PMA and SMA using a super-stable, non-flight structure to hold them together
  - Tests of the integrated OTA, first without and then with an engineering model starlight suppression system
  - In a few cases, these flight hardware tests directly verify requirements. In most cases, however, flight hardware tests will provide parameters for models.
- Structural, thermal, optical, and dynamic models, integrated together, will provide predictions, with the necessary precision, of the on-orbit performance of the OTA that will verify the requirements that cannot be tested directly.
  - Models will be validated by data from non-flight hardware tests. In particular, it is necessary to prove that the models have the required precision.
  - Tests of flight hardware will provide parameters that will be input to the models
- Many of the same tests and models will verify requirements at the subsystem (PMA, SMA, tower, …) levels and at the system (OTA) level.
- This is a fairly high-level view. The planning process has already gone to a much lower level

Verification Example: Primary Mirror Assembly

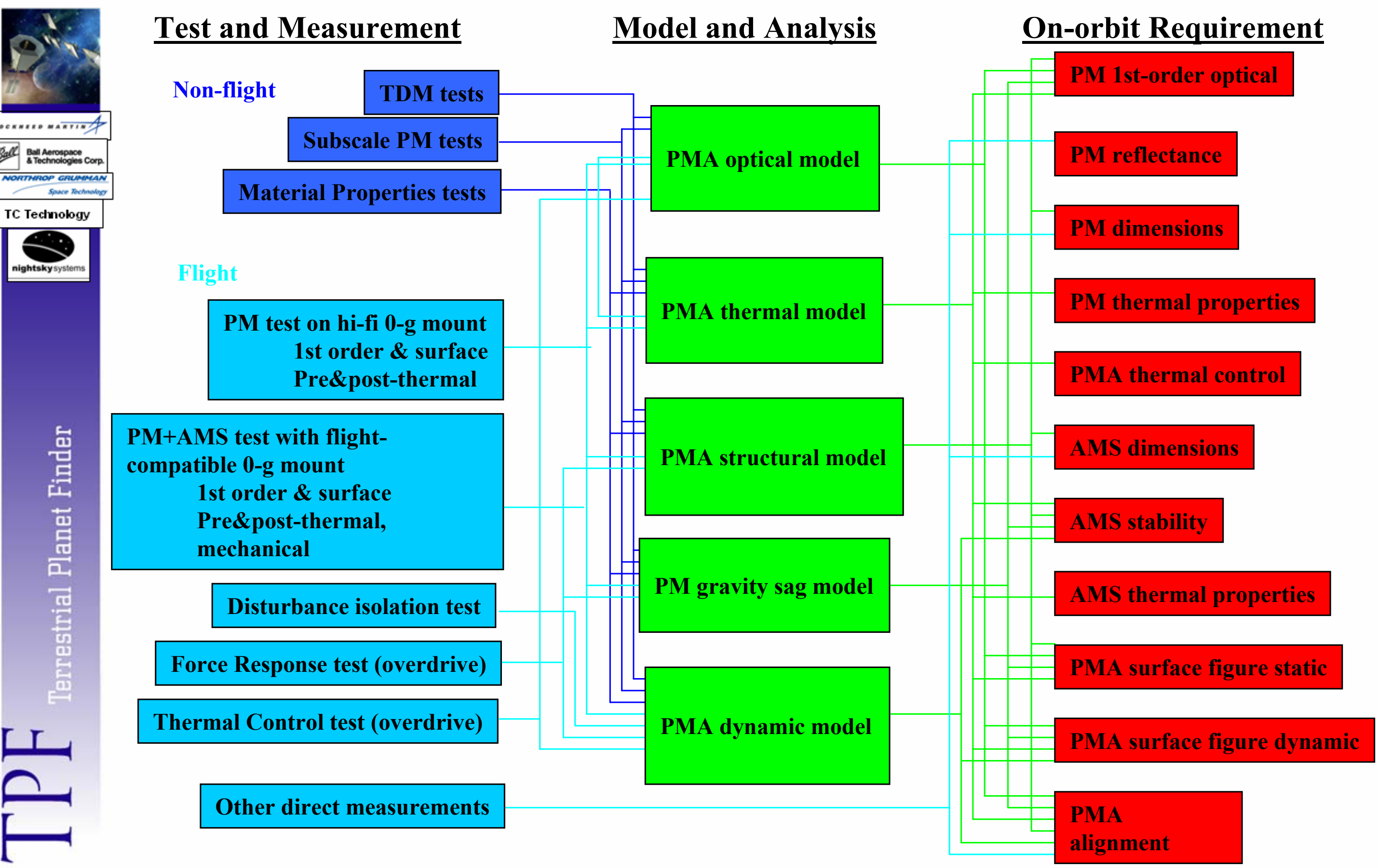

- Here is a much more detailed look at one part of the flow seen in the previous chart, focusing on the primary mirror assembly. Again we see tests on non-flight hardware, tests on flight hardware, models, and requirements.
- Note the scarcity of direct paths from measurement to verified requirement. Almost all the paths go through models. This area, the primary mirror assembly, may be the most difficult to test because of the very large size (8x3m) combined with extreme precision (nanometers). Only very basic properties of the primary mirror can be verified directly. Even verification of the first-order optical properties will likely need to use a gravity-sag model to achieve the required precision with respect to on-orbit performance. “Zero-g” mounting during test will minimize the gap between test and on-orbit environment that the model will have to span.
- Overdriving during test will provide parameters for the models. We will then rely on the models to provide precision below the noise level of the tests.

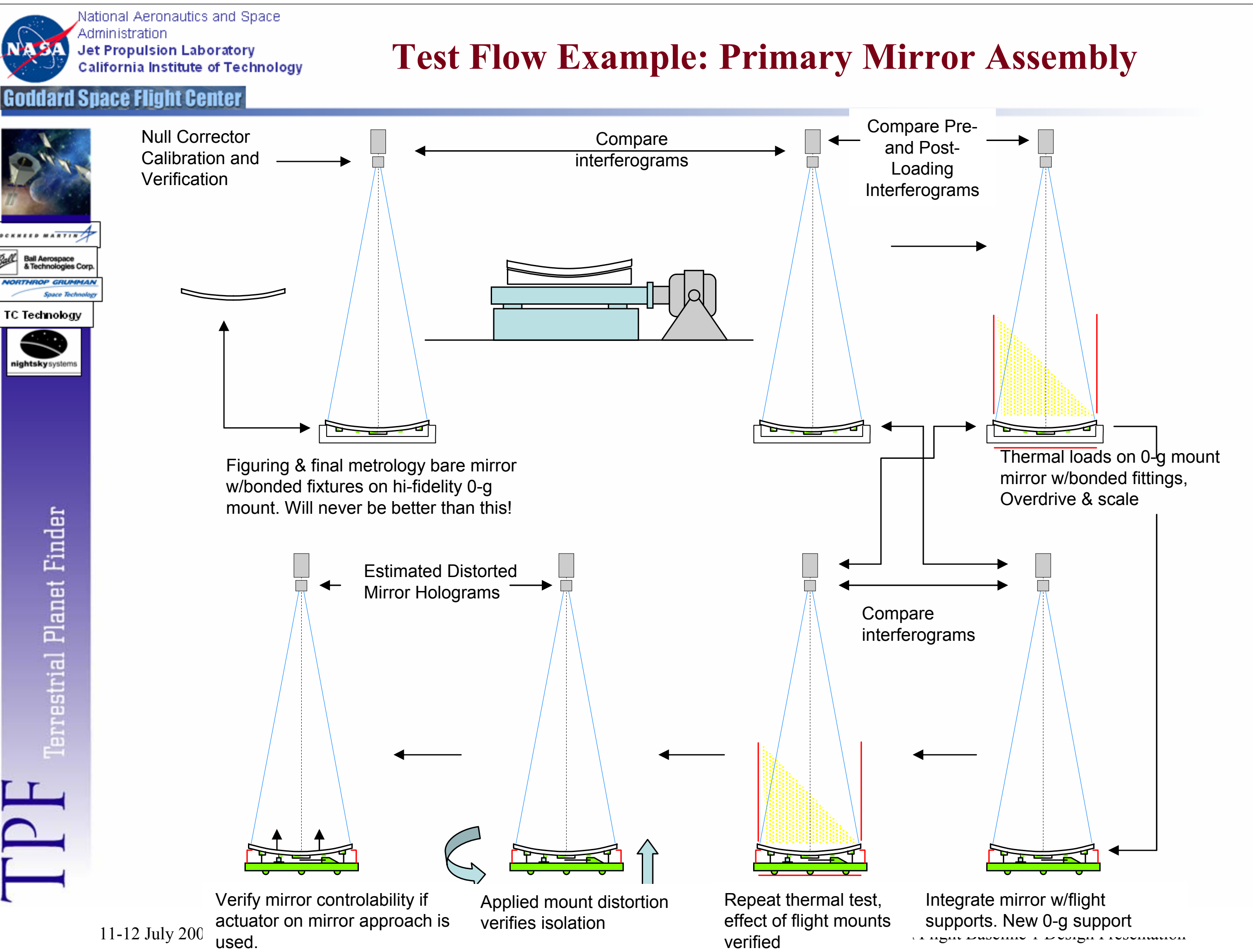

- This chart represents the lowest level of I&T planning done to date. Here we see a sequence of activities for the primary mirror assembly. Similar diagrams, for other phases of payload I&T, can be found in the backup charts.
- Figuring and final metrology of the primary mirror are done on the best possible zero-g mount, which is not necessarily compatible with the flight mounting scheme.
- The mirror, on the high-fidelity 0-g mount, is subjected to mechanical and thermal loads, and its optical performance (measured with an interferometer at the center of curvature) is measured. These measurements are as close as we will see on the ground to the on-orbit performance of the mirror, and will be used as inputs to the integrated structural-thermal-optical model.
- After the mirror is integrated with its flight supports (the Aft Metering Structure (AMS) and Payload Support Structure (PSS) or substitute, a different gravity-offloading scheme will be used. It is assumed that this will not be as effective as the high-fidelity zero-g mount.
- The thermal loading test will be repeated, to observe the effect of the flight mounts
- Known forces will be applied to the mount to validate the model's predictions of how the mirror will respond

National Aeronautics and Space Administration
Jet Propulsion Laboratory
California Institute of Technology
Goddard Space Flight Center

I&T Flow Overview

TPF Terrestrial Planet Finder

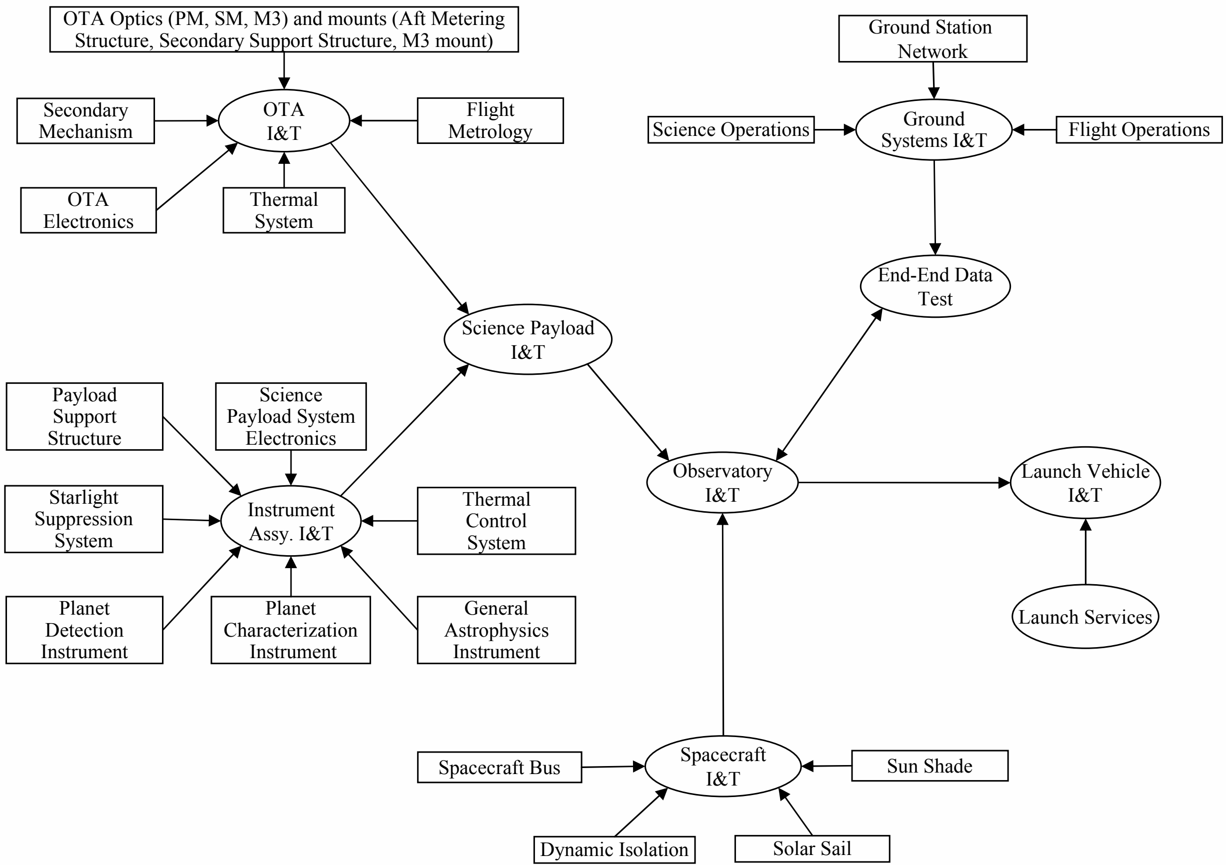

- Here we see a possible flow of integration and test for the entire mission
- The Optical Telescope Assembly is integrated as a unit.
- The instruments and starlight suppression system are integrated together; then the resulting assembly is integrated with the telescope assembly to form the science payload.
- The science payload is brought together with the spacecraft to form the observatory, which is then brought together with the launch vehicle.
- The ground systems are integrated together, then tested with the observatory.

Future Work

- Complete requirements definition and fill in verification matrix.
- Trade verification by analysis against test to rely on test as much as is feasible.
- Develop more detailed plans for the test and analysis programs.
- Detailed I&T planning to date has concentrated on the Optical Telescope Assembly. Planning will be extended to include the entire payload, the flight segment and the mission.

- As the science requirements mature, requirements for the hardware implementation will be defined more completely and in greater detail.
- Our knowledge of what is feasible to test will also improve, allowing us to define more clearly the extent to which requirements can be verified by test, and to what extent we will depend on analysis to verify that requirements will be met on orbit. As this becomes more clear, actual plans for hardware testing will become more concrete.
- In particular, plans will become better defined for testing the primary mirrror.
- Eventually, plans for I&T of the rest of the mission will catch up with plans for telescope I&T.

Backup Charts

Matching, Verifying and Integrating the SMA

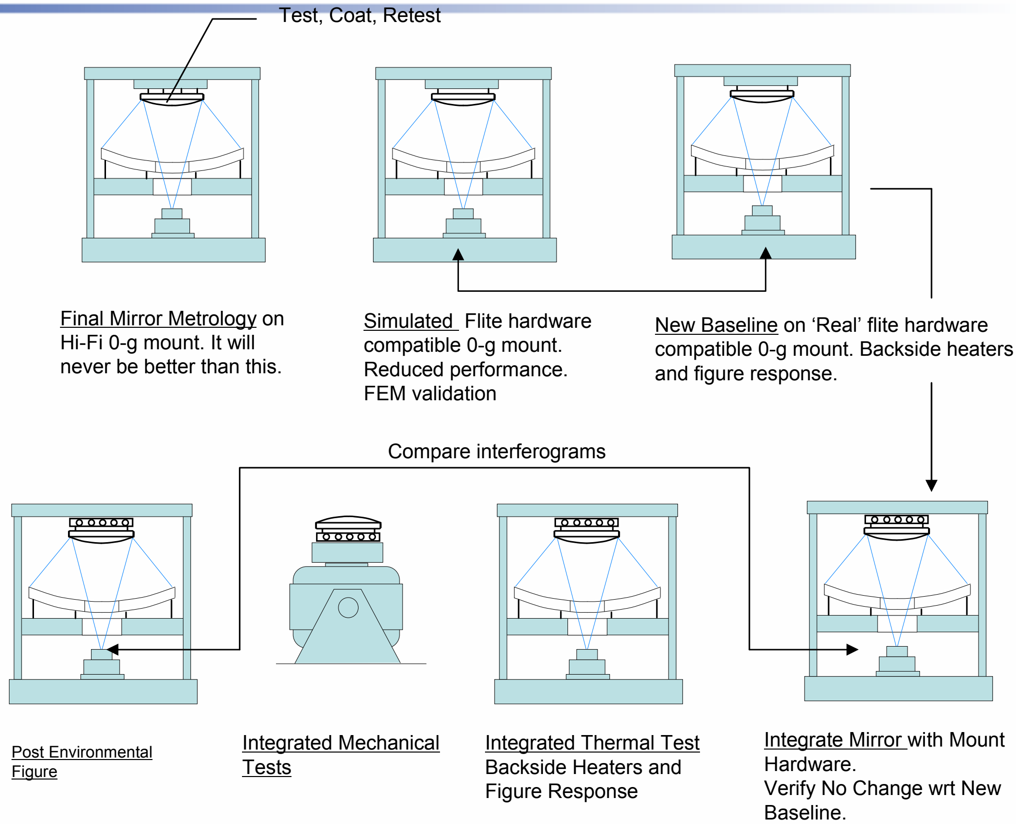

Primary Mirror Thermal Control

Flight level control demonstrated at sub-scale level

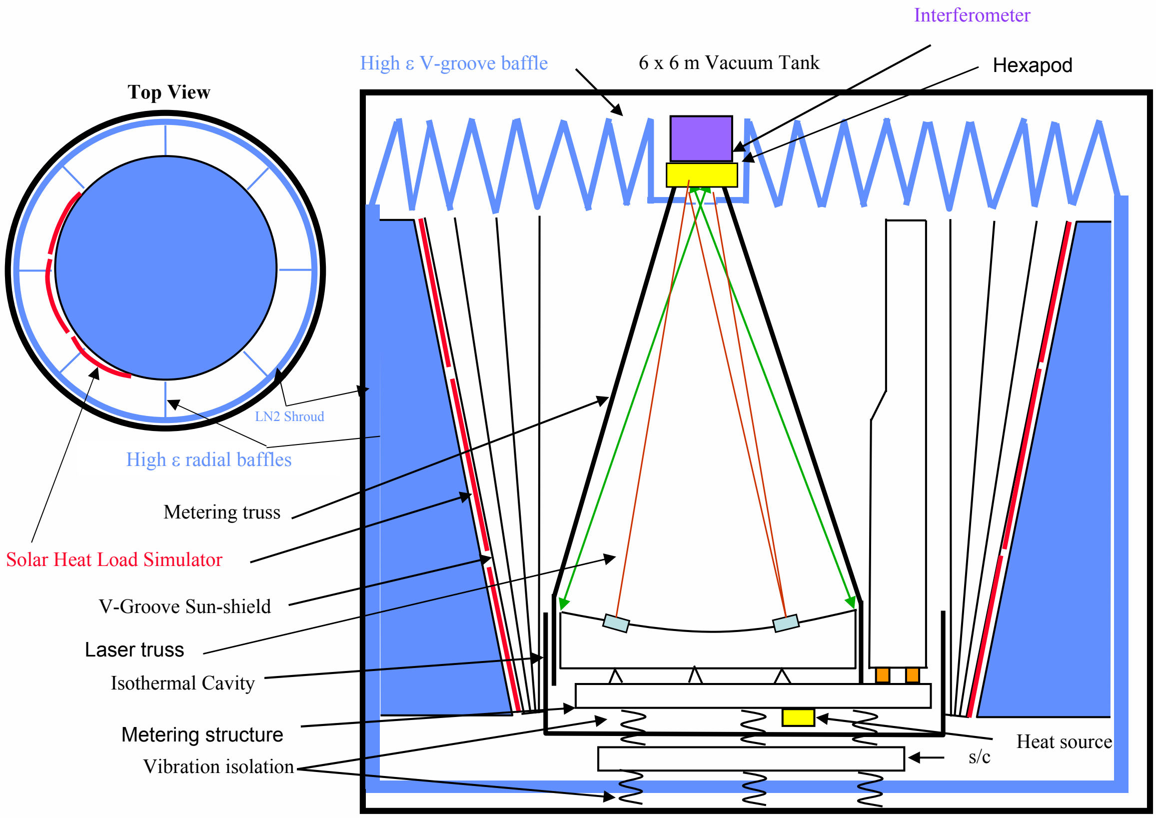

Structural Tests and Optical Component Integration

Deployed Modes (in 2 or More
  Orientations to discern any gravity dependence)
  Response to RWA noise and damping (2 or More orientations …)
Stowed Modes
  Above All leads to verified structural model
  Stowed Sine Transients, Acoustics
Deployments

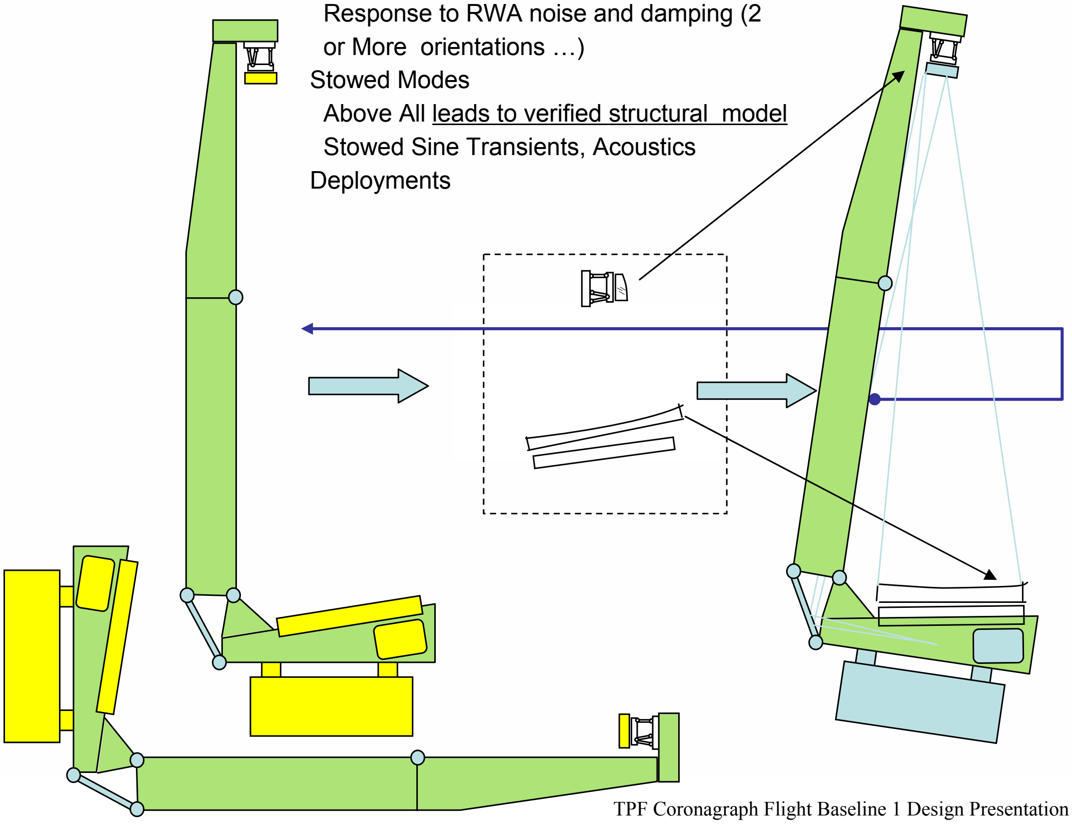

A Candidate Hardware Visualization

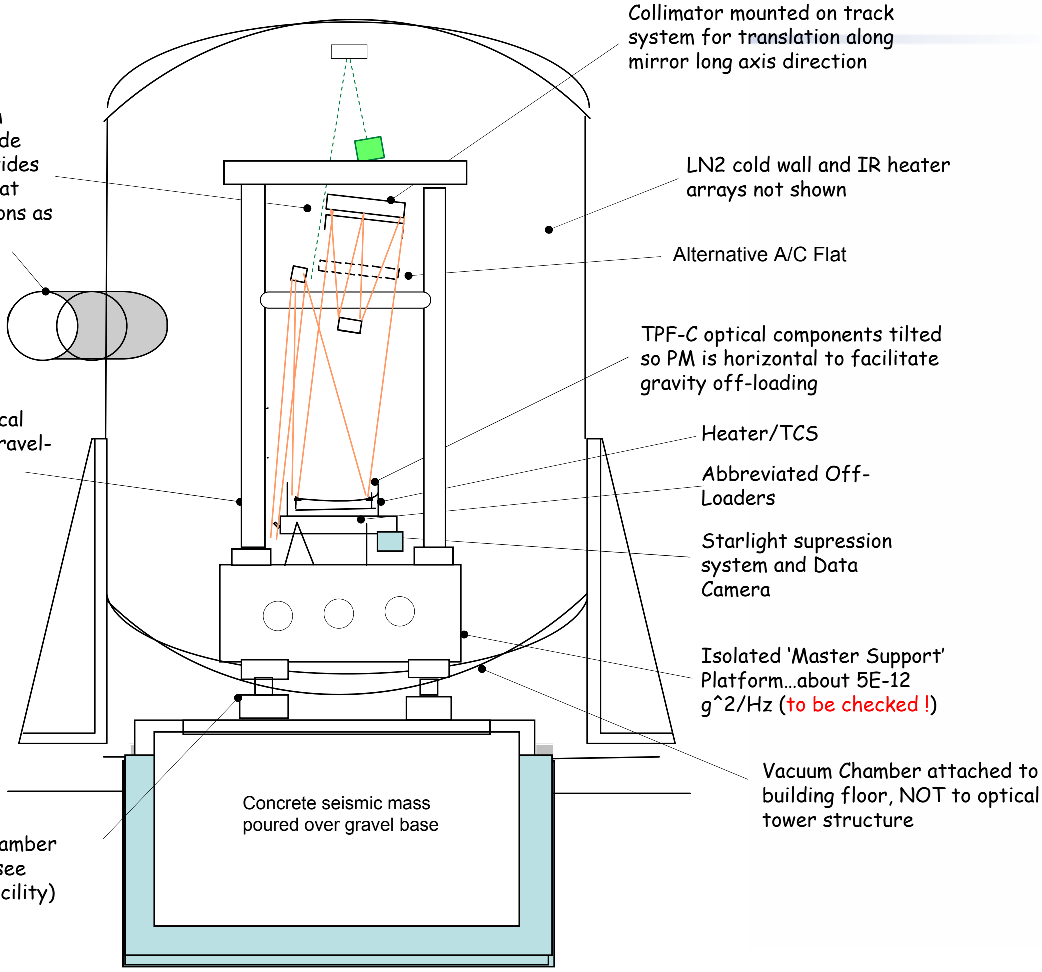

OTA-to-Coronagraph Interface Verification

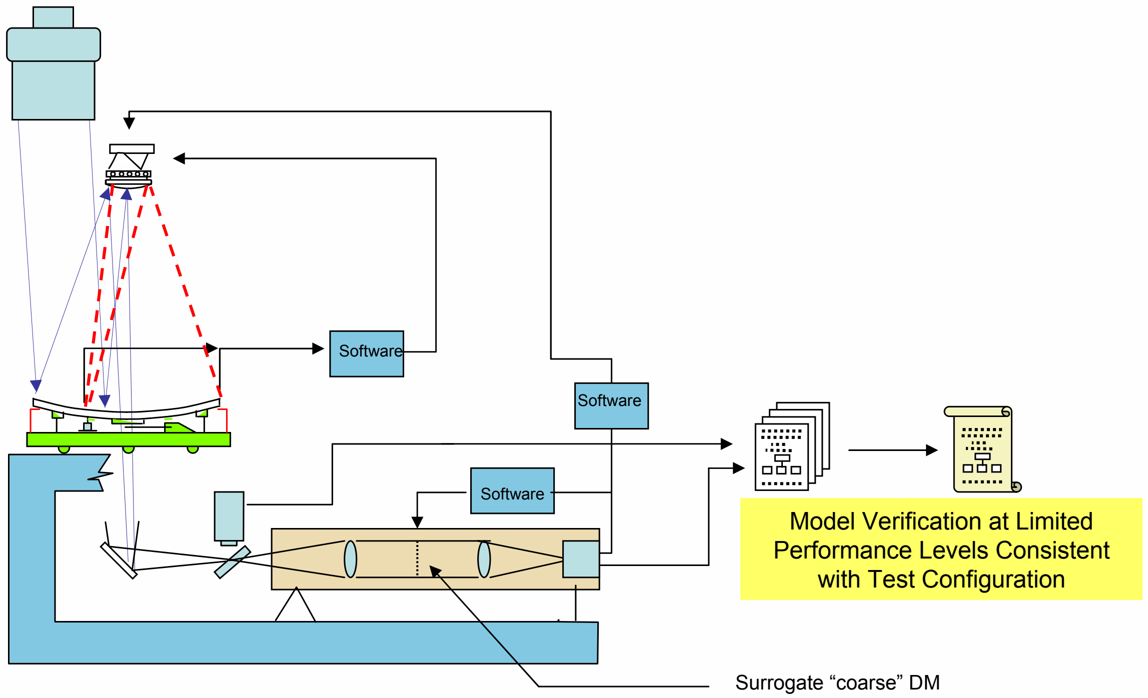

TPF Terrestrial Planet Finder

OTA Optics-Only Verification
Matched PM/SM Using Verifiable Test Equipment

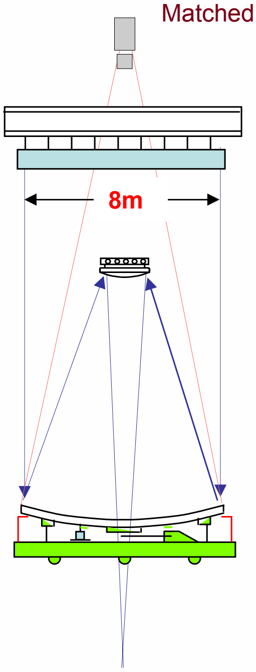

Full Aperture to be Traded with Partial Aperture Illumination
- Test Objectives
- Direct performance measurements or model validation
- Cost and Schedule

Current Assessment is that partial aperture more practical

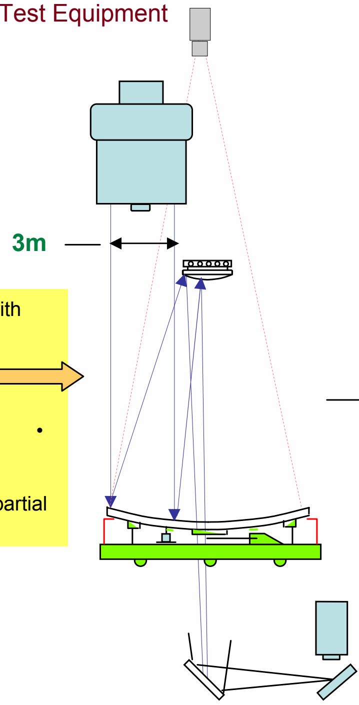

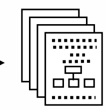

Test Configuration Model

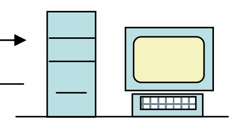

Validated test configuration model using as-built/measured component data.
Feed results into system level performance model.

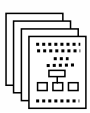

OTA-to-Coronagraph Interface Verification

OTA level Requirements

Measure in completed telescope & correlate with model
- effective focal length
- field of view
- back focus
- static wavefront quality

Measure SMA response to ±5mas simulated pointing fluctuation at f/60 focus. (Linear motion = ±5 μm and 12μm along orthogonal axes.)

Assumptions:
1. Optical measurements made at room temperature in vacuum.
2. Only thermal balance tests are made at LN2 temperatures. (Collimator removed.)

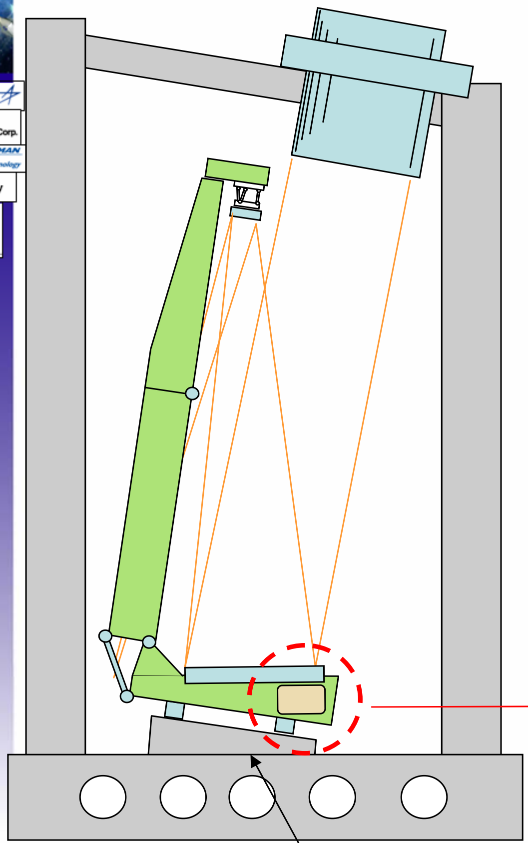

Diagnostic optics package. Same optical & mechanical interface as coronagraph

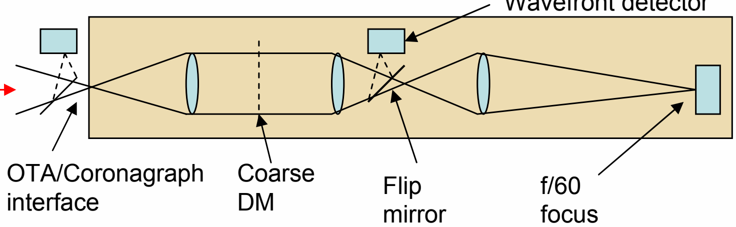

Suggested OTA – Coronagraph System Test.

The OTA is mated with a high fidelity copy of the front end optics of the cornagraph. (Front-end optics include all optics up to the deformable mirrors.) A test is made to establish that the wavefront at the entrance pupil of the Star Supression System (SSS) will be within the capture range of the deformable mirrors and that the pupil image will be located correctly on the deformable mirrors. If these goals are achieved then it can be inferred that the combined OTA/coronagraph will provide the required contrast when the flight coronagraph is mated to the OTA..

Assumptions:

1. The flight front-end optics will relay the light in the OTA image properly to the SSS.
2. Given that the wavefront presented to the SSS is within the capture range of the deformable mirrors the SSS will produce the required contrast.

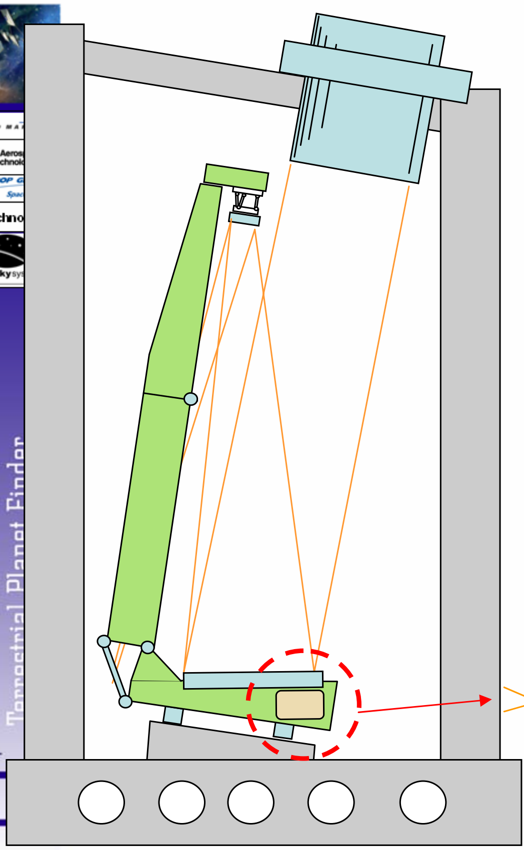

Copy of front-end coronagraph optics. Includes fold mirrors, collimators, anamorphic optics & relay optics. Duplicates with high fidelity mechanical and optical interface with OTA & Star Supression System.

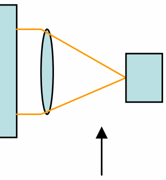

Wavefront detector

National Aeronautics and Space Administration
Jet Propulsion Laboratory
California Institute of Technology
Goddard Space Flight Center

TC Technology

Terrestrial Planet Finder
TPF

Modeling Introduction & Plans

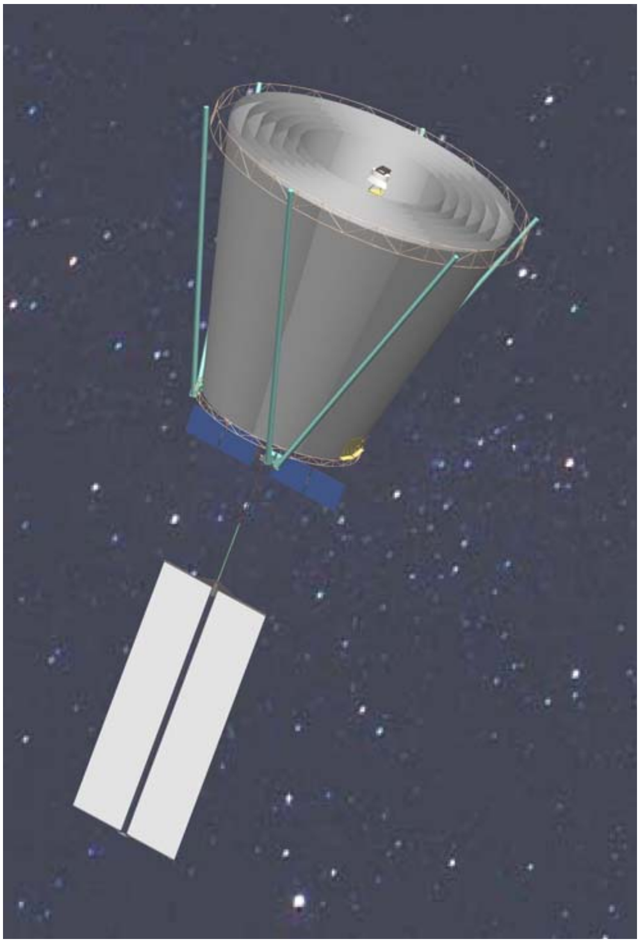

Marie Levine

Contributors:
Modeling Team

11-12 July 2005

Content

- Iterative Design/Analysis Cycle Process
- Modeling Approach & Philosophy
- Cycle1 Analysis Goals, Products & Schedule
- Cycle1 Baseline Design for Core analyses
- Preliminary Tasks
- Current Status

(see backup slides for details of the modeling plan)

Design & Analysis Cycles through Project Phases: Not a linear process

PDR-CDR

Pre-Phase A → Phase B-C → Phase D

Explore Design Options
Trade-off Requirements
Optimize Performance
Identify Technology

Detailed Design Completed
Requirements Defined
Verification & Validation Planned
Technology Demonstrated

Flight Models Validated
As-Built System Verified

Increasing model fidelity & complexity

Iterative Design/Analysis Cycle Process

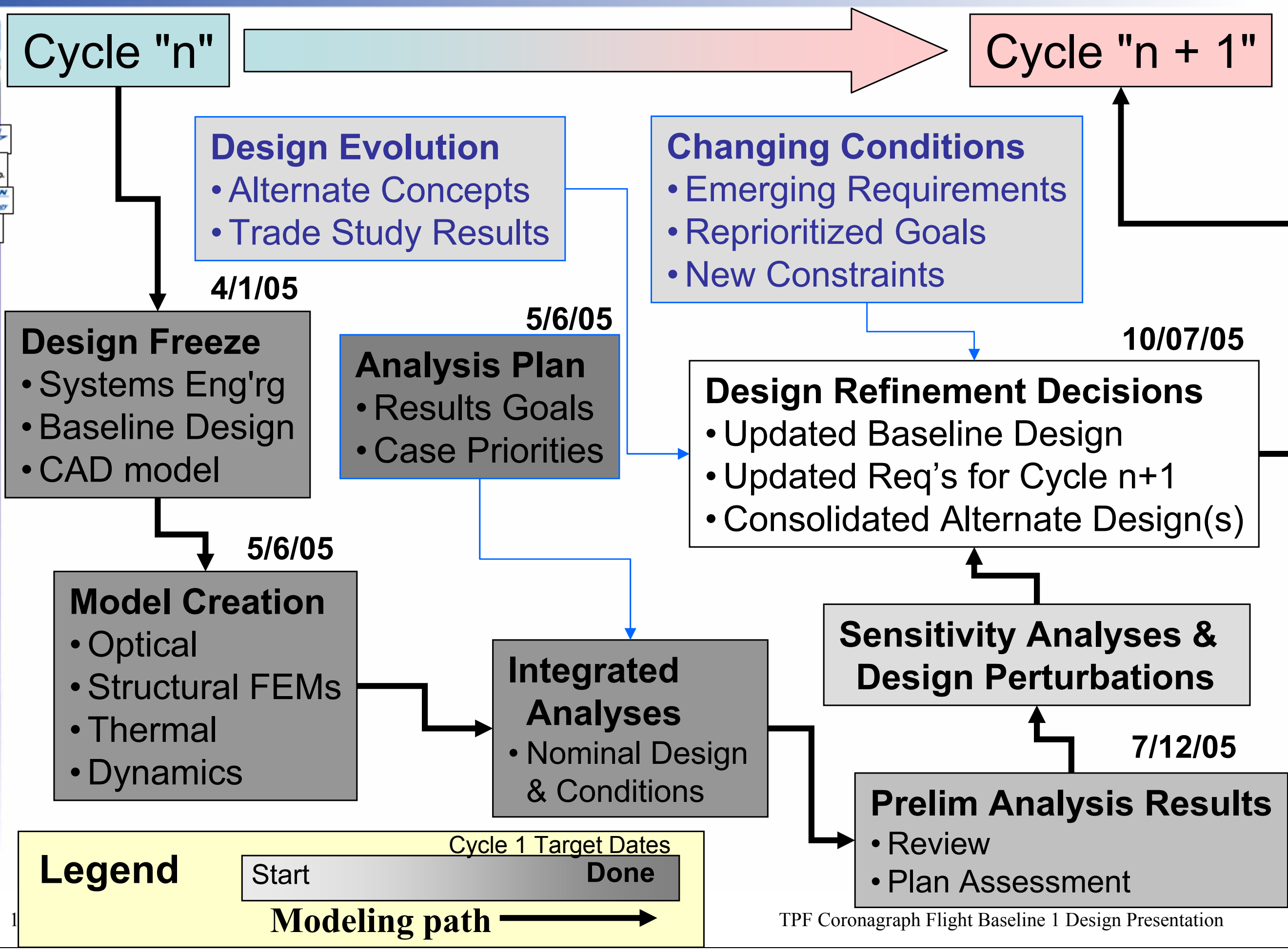

Preliminary Tasks: "Cycle 0"

- Multi-center team coordination & communications:
  - New team starting this year, w/ some position changes
    - Get new team members up to speed about TPFC
    - Introduce and enforce modeling philosophy
  - Learning how to work together effectively
    - Establish modeling plans across disciplines & centers
      - Management coordination & progress tracking
    - Agree on modeling tools (esp. CAD & thermal)
      - Develop model transfer protocol
    - Establish communications
      - Across the country at many locations
      - Define meetings & attendance
      - Learn to use videoconferencing

- Modeling tool validation
  - Thermal (TMG): issues with limits of code accuracy, model size, …
  - Optical (MACOS): code de-bugging, diffraction propagation, …

Modeling Approach & Philosophy: *One Design / One Model / One Mesh*

- **Design/Analysis configuration control & management**
  - Models represent frozen design & no changes permitted during analysis cycle (as tempting as it may seem)
  - Exercise model thoroughly to understand improvements for next cycle
  - Design configuration managed through common file depository on TPF library w/ enforced documentation & nomenclature

- **One Model / One Mesh**
  - Same model geometry & mesh for all integrated systems analyses and disciplines ("***mid-fidelity model***")
  - Single discipline models may require ***high-fidelity models*** (e.g., PM launch stress), but remains a super-set of the mid-fidelity model
  - Trades analyses conducted separately on ***low-fidelity models*** for quick assessment
  - Optical design model forms basis for CAD/Thermal/Structural models
  - Same mesh reduces modeling errors due to numerical extrapolation & thermal/structural/optical mapping
  - Incorporate Modeling Uncertainty Factor (MUFs) when a credible basis exists (dynamics)

Integrated Modeling & Analysis Process

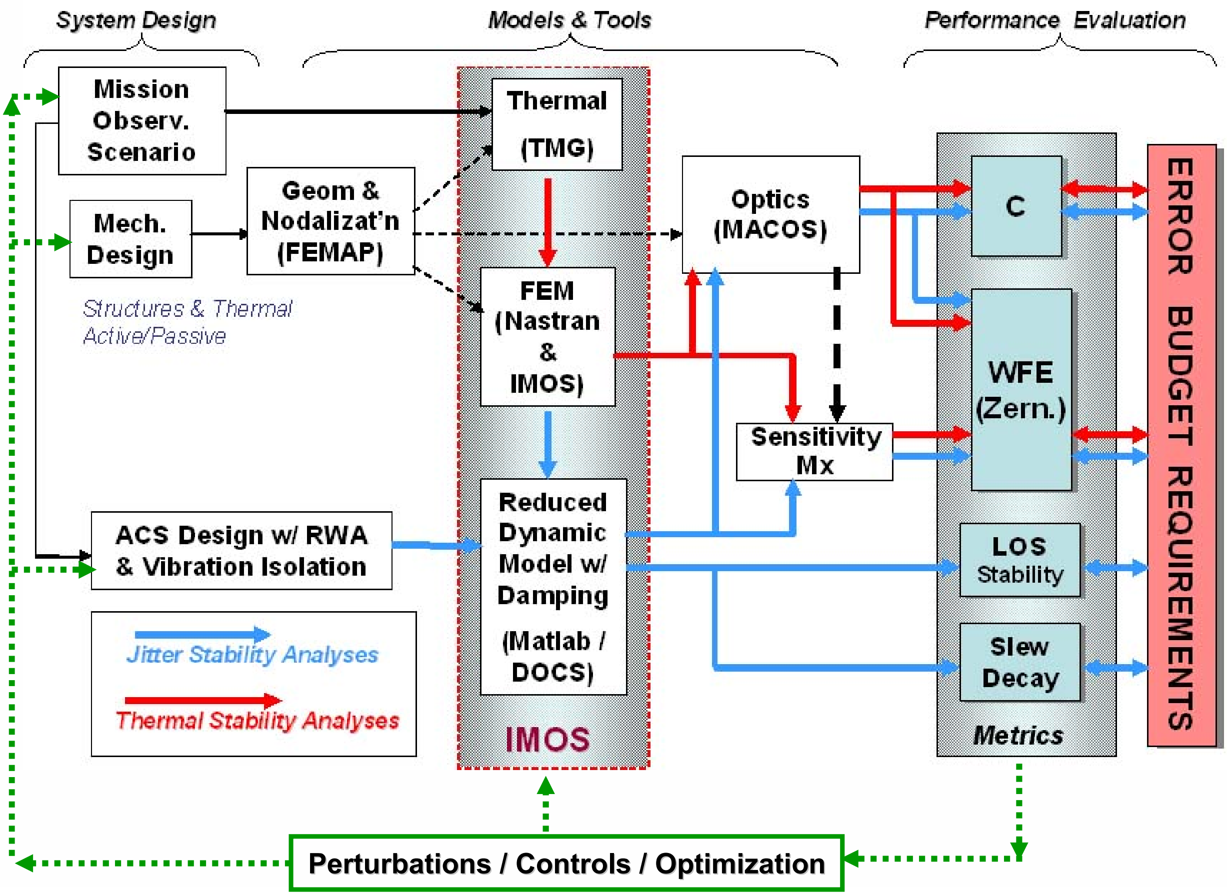

Cycle 1 Analysis Results Goals

Priorities (in descending order of importance)

1. Estimate system performance & margins relative to the error budget (p.16)
   - Analyses of baseline design under nominal operating conditions
   - Assessments of off nominal design and/or operating conditions
   - Comparative analyses of alternate design options for trade studies p.18

2. Investigate performance sensitivity to driving system design considerations and constraints (p.17)
   - Perturb key design parameters and evaluate perf. improvements
   - Assessments traceable to baseline design models

3. Establish and refine derived key design requirements or constraints for elements, interfaces, and systems (p. 19)

Cycle 1 Modeling & Analysis Products

Models

③ done

1. Assemble & verify integrated system model of baseline design
   - Deployed system configuration (Mid-Fidelity common model for all disciplines)
   - Launch mechanical configuration (Simplified system, Hi-Fi PM quasi-static stress)
   - Preliminary stray light assessment

③ in work

2. Preliminary models of alternate designs for trade studies
   - Good for cursory structural, thermal or optical analyses to mitigate margin problems or optimize performance

Analyses

③ almost done

1. Performance margins results for following
   - Deployed system WFE & Contrast stability under nominal conditions
   - Pointing control system performance
   - Stowed launch performance & stress margins

③ in work

2. Performance sensitivity results for deployed system WFE & Contrast stability sensitivity to:

   Optical bandwidth, CTE variations, OTA mass distribution, PMA mount/launch lock configuration, System fundamental frequencies, SMA control system performance, PMA TCS (Thermal Control System) variability and to sunshield effective emissivity ….

③ to be done

3. Derived key design requirements or constraints for following:
   - Vibration isolation and SMA control requirements
   - Deployed system fundamental frequencies
   - Deployed system PMA TCS stability requirement
   - Etc …

Cycle 1 Schedule Summary

ID	Name
1	TPF-C Flight Baseline Analysis Cycle 1 : FB1
2	FB1 FLIGHT DESIGN & ANALYSIS
3	FB1 Design Definition
9	OTA CAD Model
51	Coronagraph & S/C CAD Model
52	System CAD Model, Operation
53	Freeze Baseline Design
54	Launch Model
57	Material Properties Defined, Design Information For Modeling
58	Build FE Mesh
65	STDT #1
68	Build & Verify Models
78	Define Observational Scenario: Nominal & Bounding Performance
79	Initial Model Outputs & Deliverables
84	Integrated Analysis: Nominal Performance
85	System Temperatures
93	Thermal Distortion to WFE
98	Deliver Nastran temps & distortions to OTA
99	PCS & Dynamics
100	Jitter to WFE studies from RWA imbalance
103	Rigid Body / LOS Performance
110	Optical & WFSC
125	Planet Detection Simulation
126	System Studies
127	System Structures
128	System launch analysis
137	System Sensitivities & Requirements
141	Mech Design Options for Cycle 2
146	Launch-to-orbit commissioning
153	System Thermal Stability and Control (SM, AMS, PSS, …)
168	PCS Sensitivities & Requirements
172	Optics
183	OTA Studies
184	PM Performance
193	OTA Design Options for Cycle 2
200	Straylight Analysis
201	FB2 Start
202	STDTAnalysis Presentation

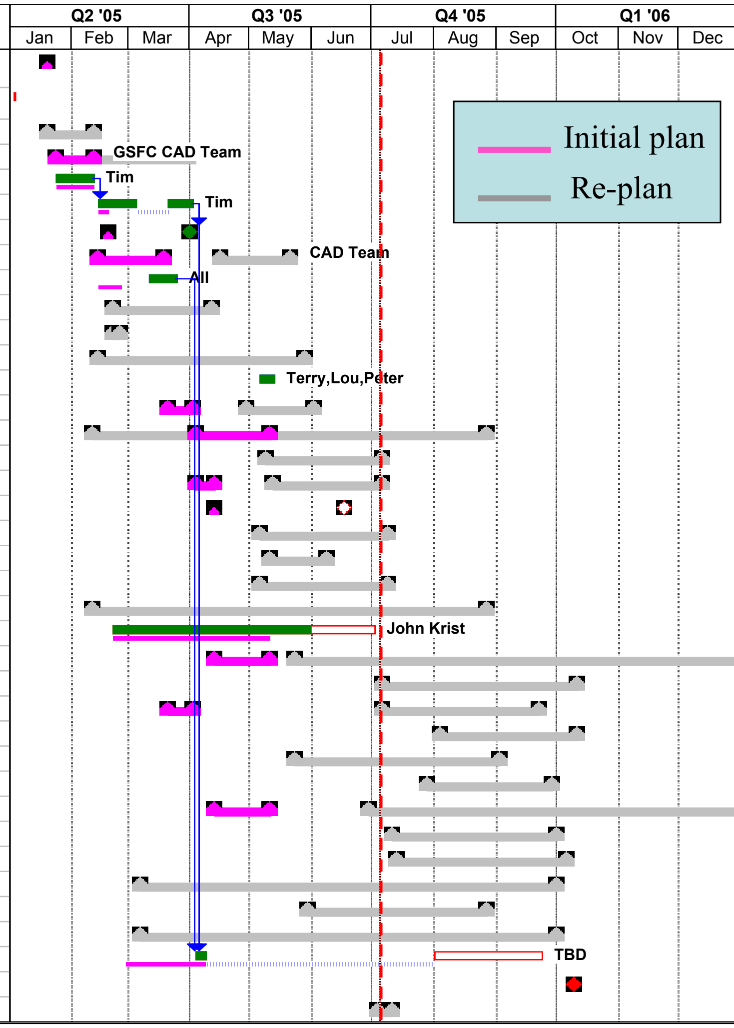

- Summary of the FB1 Schedule
- Detailed schedule has 200 task entries: defines task predecessors, task deliverables, workforce assignments, duration, critical path
- Task progress is tracked at weekly modeling telecons, and schedule is updated regularly
- Learning as we go: needed to re-plan to make up for preliminary tasks prior to start of FB1 modeling & analysis

Cycle 1 Design for Core Analyses

Configuration BV1d-D frozen 4/1/05

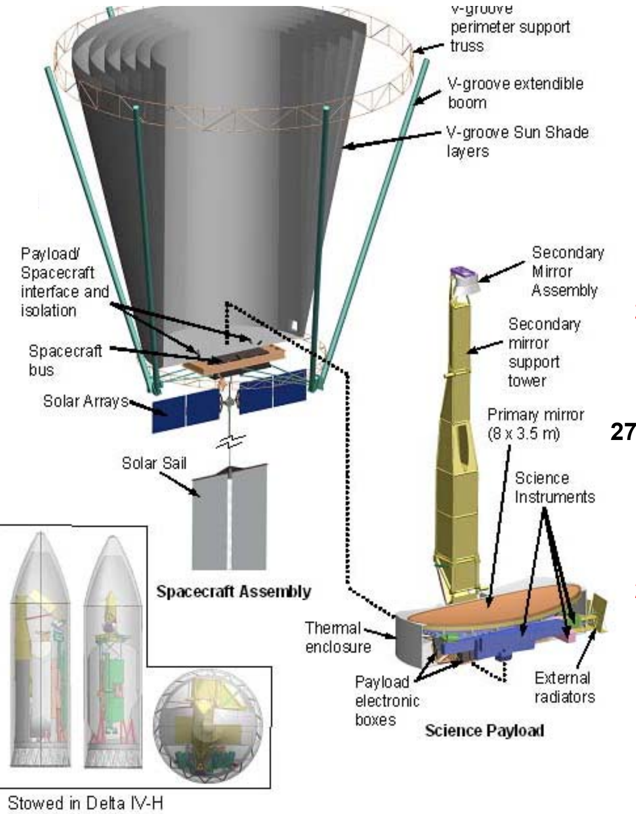

Nominal Observing Angles

60° roll with ± 15° dithers

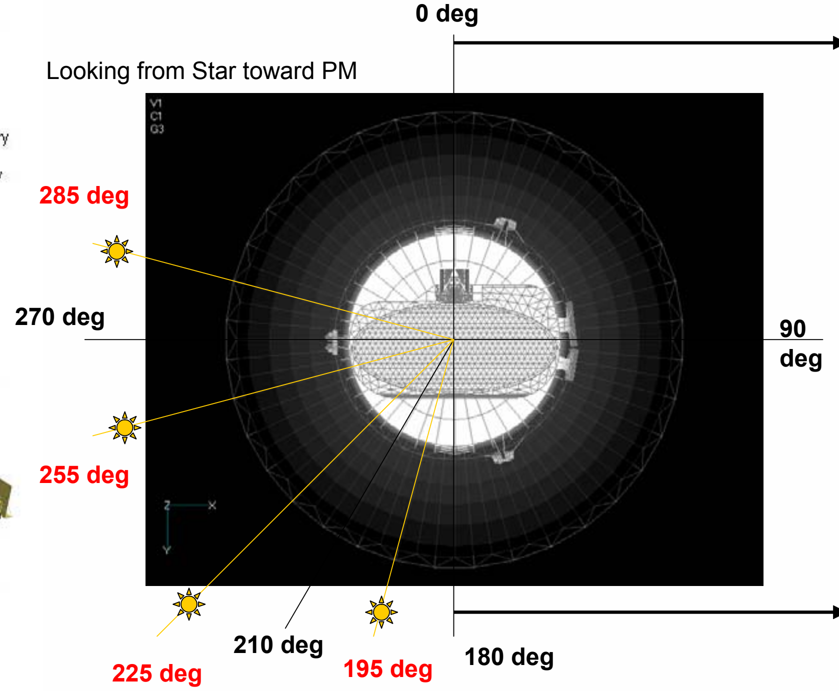

Reminder

- This is work in progress and not all tasks are completed to evaluate Cycle 1 design and formulate Cycle 2

… But

  - *there is an extensive plan that delineates the path to completing Cycle1 into Cycle 2. Still 2½ months to go!*
  - *Tasks are on schedule and progressing as planned*

- The preliminary results look very promising especially for on-orbit performance, some aspects of launch design still need to be worked out

…. But

  - *we are diligently working through the problems and are investigating solutions as necessary*
  - *The designs will be improved and models become more detailed as we move towards Phase A.*

- We are open to suggestions and recommendations

BACKUP SLIDES

Nomenclature

- **Cycle n** = the period starting with the definition of an updated design concept and ending with completion of its performance evaluation and alternate design option assessments.
- **Model** = numerical representation of the design
- **Analysis** = exercising the model to environmental conditions to extract performance metrics of interest
- **Model Verification** = model conforms to what was designed and interfaces with each component as expected (e.g., model consistency checks)
- **Model Validation** = demonstration that model predicts the behavior of the intended design & physics (e.g.test correlation)

Current Status

- Cycle 1 plans defined and tracked, Cycle 2+ plans in progress
- Effective team communication & model exchange established
- All FB1 models complete
  - Integrated FB1 design stowed & deployed
  - Discipline models verified
- FB1 nominal performance evaluation complete
  - Deployed WFE and Contrast stability to thermal and jitter environment
  - ACS pointing margins
  - Launch stress evaluation
- Performance sensitivity studies in progress
  - CTE variations, fundamental frequencies vs mass vs optical performance, optical bandwidth effects, mounts & launch restraints, …
- Key control design requirements not yet quantified
- Where performance is marginal alternate designs & trade studies have been proposed/planned and analyses in progress

Analyses for Performance & Margins

Priorities (in descending order of importance)

1. Deployed condition thermal/structural induced optical errors
   - System errors (e.g., rigid body motion driven WFE)
   - Optics figure error (e.g. quilting of PM w/ high fidelity model)
2. Deployed condition jitter margins
3. Deployed condition pointing control and stability margins
4. Stowed condition launch load margins
   - System analyses of significant contributing modes
   - Quasi-static stress analyses of PMA
5. Deployed condition PM thermal control margins
6. Ground test condition margins for PM figure verification approach – includes 1-G sag

Analyses of Performance Sensitivities

Priorities (in descending order of importance)

1. Deployed optical performance sensitivity to key design parameters: e.g., uncertainties in material properties (nominal, variations), mass & frequencies, temperature variations (bulk, gradients), sunshield v-groove separation / circularity/ emissivity, mounting/support features ….
2. ACS performance sensitivity to sensor noise, mass props, vib isolation,…
3. Deployed System/SM tower fundamental modes sensitivity to uncertainties in System/SMA mass, material properties, deploy/lock mechanism stiffness, etc
4. Mass margin sensitivity to SMTA f_n, PMA f_n (stowed, on-orbit), active/passive isolation, SMA stroke, mount/support features, ….
5. Deployed and ground condition PM modal content sensitivity to uncertainties in PM mass, PM build, PM mounting, thermal states
6. Deployed condition PM thermal/structural deformation sensitivities to uncertainties in thermal control (spatial, temporal), thermal gradients, …
7. Deployed condition OTA optical error sensitivities to sunshield effectiveness uncertainties (BOL/EOL, degradation, etc)
8. Optical performance sensitivity to BOL/EOL degradation, wavelength,

Key Trades Supported by Analyses

1. Closed-back vs open-backed
2. RWA design option trades
3. PM architecture: elliptical vs race track
4. PMA launch support
5. Sunshield architecture: conic vs sugar scoop
6. PMA core segmentation (hex versus square)
7. Actuated PMA versus coarse DM
8. Sunshield circularity

Analyses to Derive Key Requirements

Priorities (in descending order of importance)

1. Derived mechanical properties from thermo-optical performance: e.g., CTE (bulk and variability) constraints or temperature gradients
2. Thermal control requirements
   - Constant temperature boundary, Constant power boundary, Discrete heater locations
3. SMA position stability & control requirements
4. Vibration isolation requirements
5. Deployed condition frequency constraints
   - SMTA , PMA, Sunshield , Solar Array and Solar Sail fundamentals
6. Stowed PM requirement for mounts & launch lock supports
7. Sunshield effective emissivity
8. Ground test condition bounds on isolated OTA assembly stability (jitter & thermal environment)
9. Ground test PM requirement for figure actuators, if any
10. Modeling error margin allocation
11. Others TBD

Cycle 1 Alternate Concepts for Analysis

Alternate Design Concepts for Cursory Analyses

1. Passive vs dynamic isolation
2. Racetrack monolithic PMA
3. 8x3m mirror
4. Sugar-scoop sunshade concept
5. PM mounts & launch locks
6. Lightweighted SMA
7. OTA baffle concept
8. Active thermal control layer in sunshield

TC Technology

TPF Terrestrial Planet Finder

TPFC System Performance Model

Dr. David M. Palacios

Contributors:
Phillip Dumont
Joe Green

11-12 July 2005

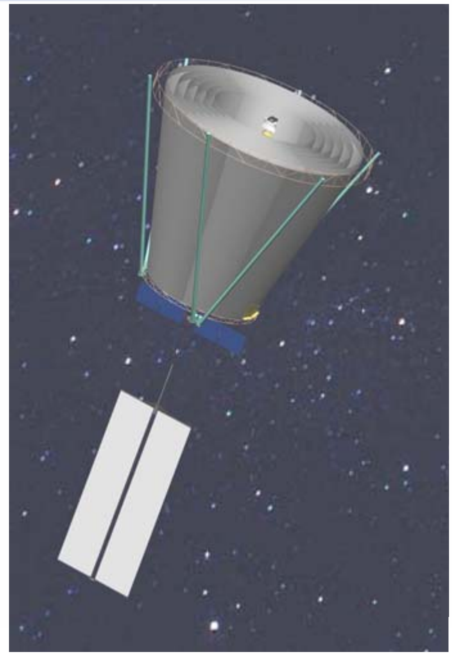

National Aeronautics and Space Administration
Jet Propulsion Laboratory
California Institute of Technology
Goddard Space Flight Center

Performance Modeling Capabilities

TPF Terrestrial Planet Finder

- Folded model with near field diffraction between important surfaces up to the Occulter. (using MACOS package)
- 8th-order mask and matching Lyot stop are implemented
- Surface maps applied on all reflective optics
- Rigid body motions of all optics with 6 degrees of freedom
- Model contains a 2DM Michelson WFC architecture with a full dark hole iterative nulling algorithm
- Broadband simulations
- Model can also include shaped pupil masks and amplitude aberrations without position perturbation capability
- Outputs contrast as a final metric of system performance

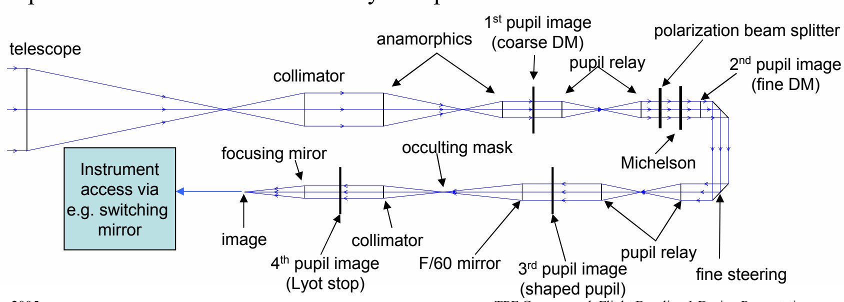

- MACOS software package provides near-field diffraction propagation between components in a realistically folded model. It also provides a clean interface to thermal and dynamic perturbations via a NASTRAN format, as well as Matlab interfaces for patches to specially handled areas.
- Currently the occulting mask and Lyot stop are modeled as ideal elements. Errors have been measured and will be added to the model in the next few months.
- Surface maps that are applied to all reflective optics are consistent with the error budget and with identified capabilities
- Rigid body motions enable the model to capture sensitivity to static errors and dynamic perturbations
- The 2DM Michelson arrangement allows both phase and amplitude correction over the square dark hole
- Both single wavelength and broadband wavelength light were simulated
- Additional components can easily be added such as shaped pupil masks and amplitude aberrations
- The contrast at the image is used as the final metric of the system performance

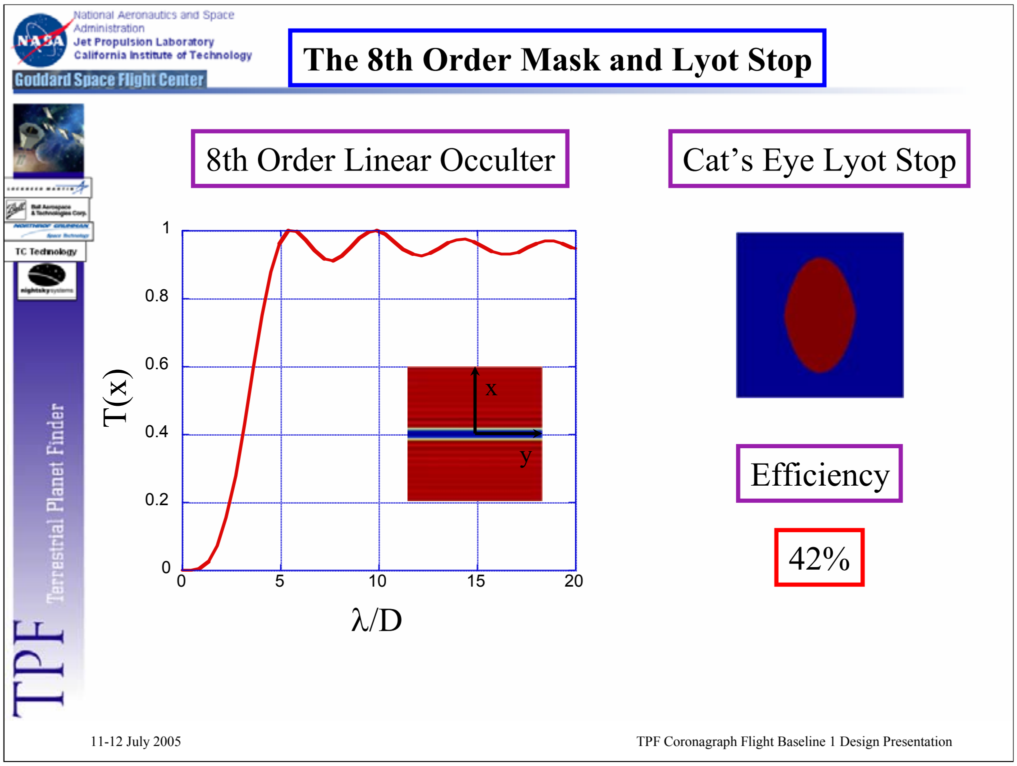

- Mask and stop properties that were used:
- \- The 8th order linear occulter depicted in this slide is approximately 20% oversized from the optimal design given by Shaklan et al. in their 2005 APJ paper which has been accepted for publication.
- \- The Lyot stop also has a slightly smaller size but still obtains a 42% planet signal throughput.

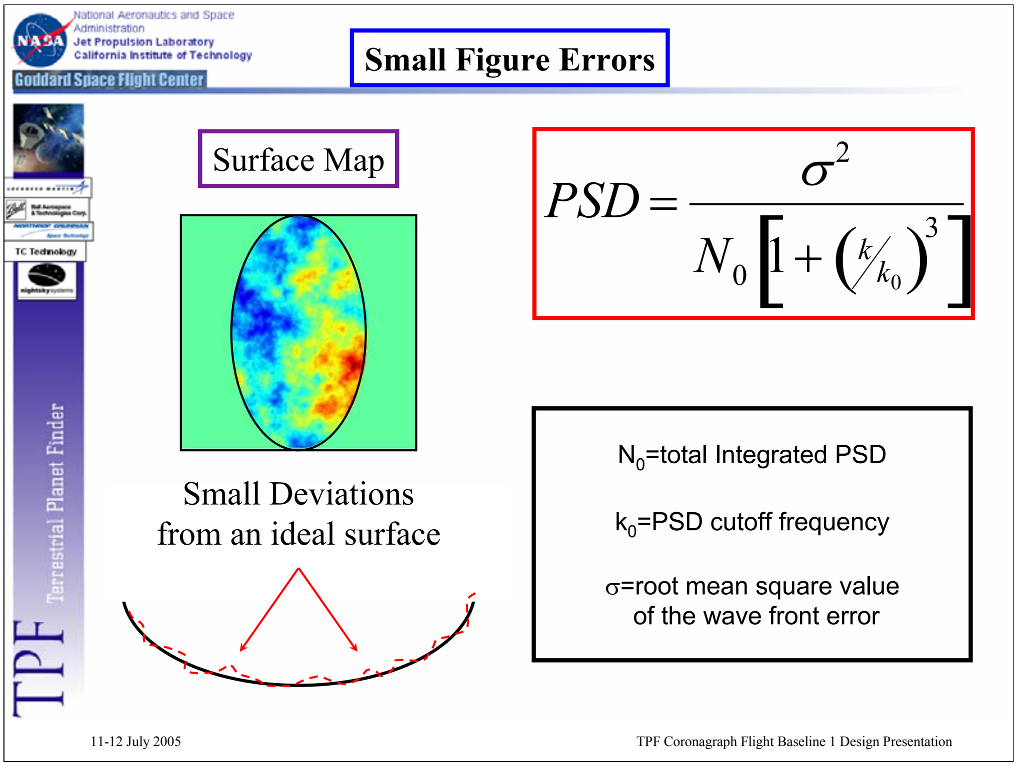

- Small Figure errors ranging from 1-10nm wave-front error, were placed on each reflective surface in the prescription up to the occulting mask.
- For example: The Primary mirror had a power spectral density function (PSD) describing its surface with, k_0=4cycles/m, σ=4.26nm (surface error).
- When light is reflected from a surface, the induced wave-front error is twice the surface error.

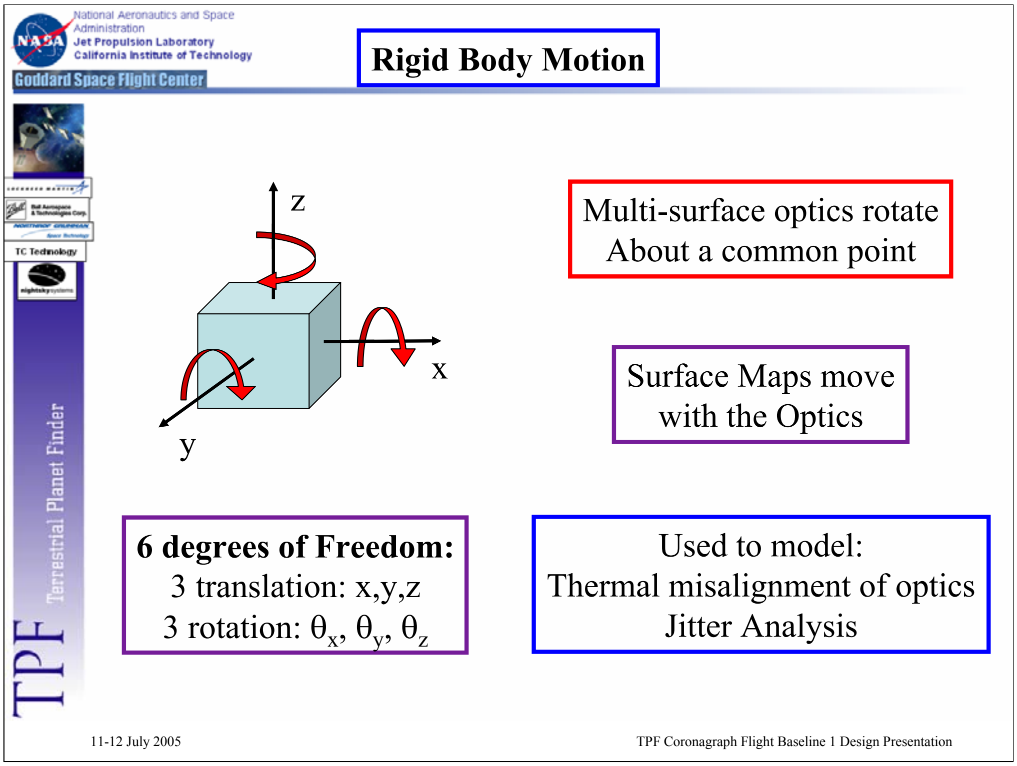

- The positions of all optics up to the occulting mask can be perturbed with 6 degree-of-freedom, rigid motion with the exception of the occulting mask and the deformable mirror.

- Presently we can only place optical path difference surface maps onto surfaces to be perturbed. Amplitude errors can be placed onto surfaces but cannot be moved.

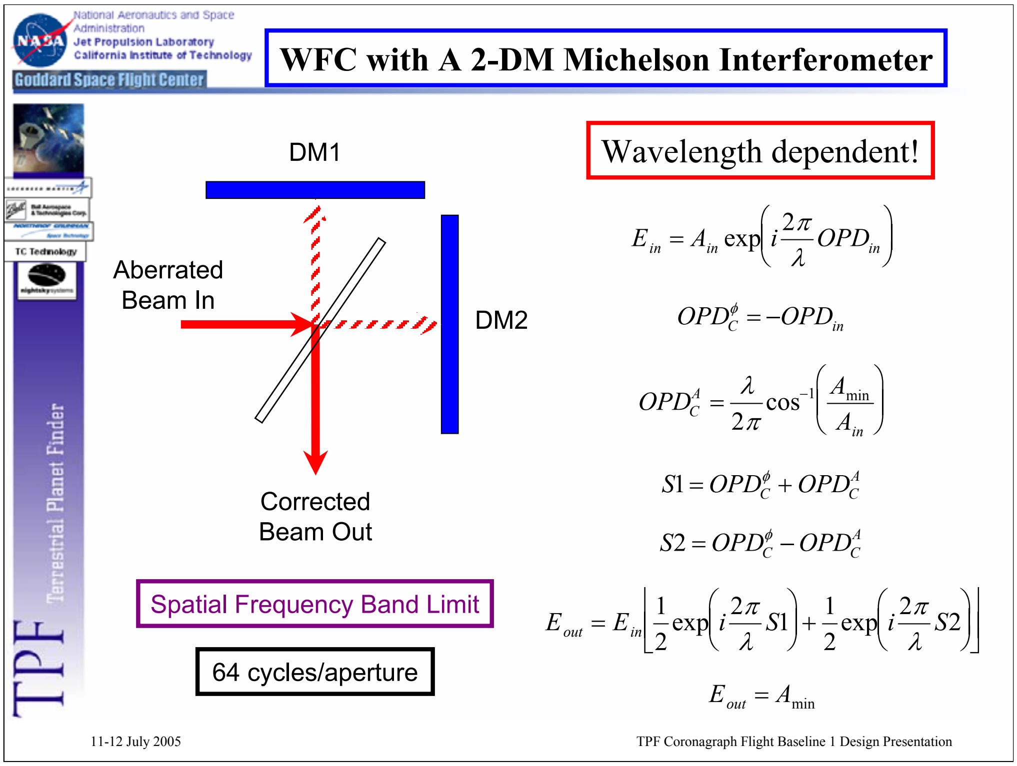

- The 2DM Michelson configuration was modeled in MATLAB outside of MACOS. The iterated solution is then applied as a complex amplitude mask to the DM surface in the prescription.
- The DMs are ideal and are described by a band-passed spatial frequency representation instead of an influence function representation. This is equivalent to assuming perfect Sinc(r) functions for influence functions.
- The amplitude correction in this technique is wavelength dependent and was not optimized to correct for broadband operation.

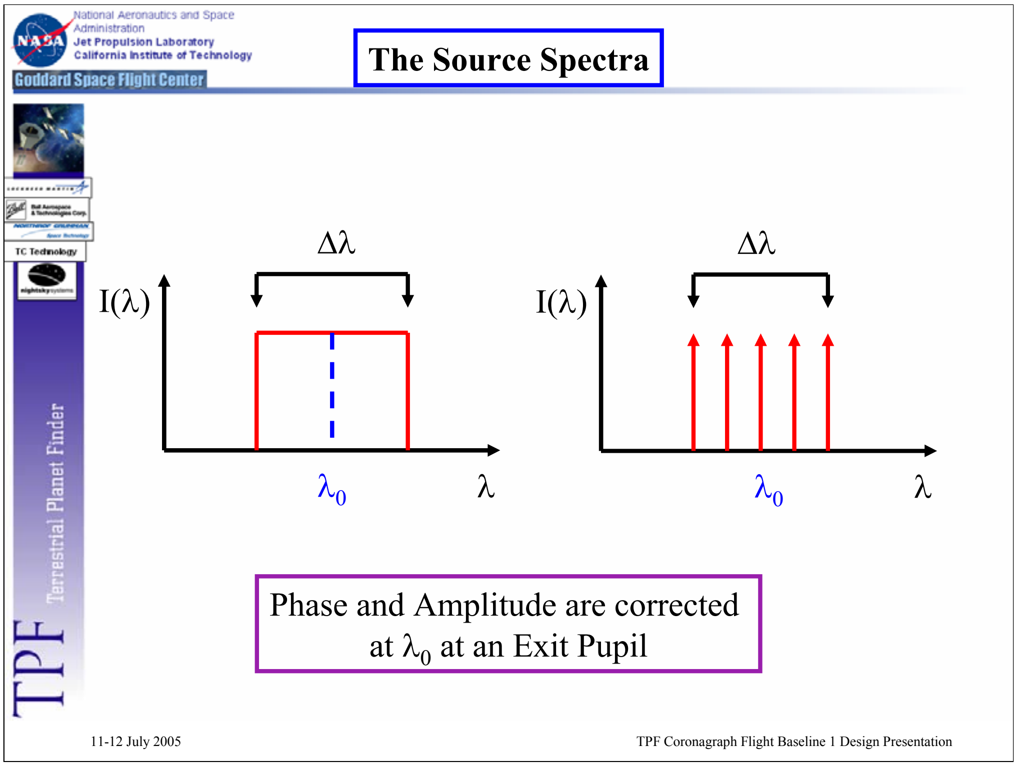

- - The source spectra was represented as a flat top function although any spectra could be represented.
- The spectrum was represented by 5 discrete wavelengths. This could be increased for higher spectral resolution but increases simulation run time dramatically.
- The central wavelength was used to determine the correcting surfaces for the wave-front control. This may not be the optimal solution.

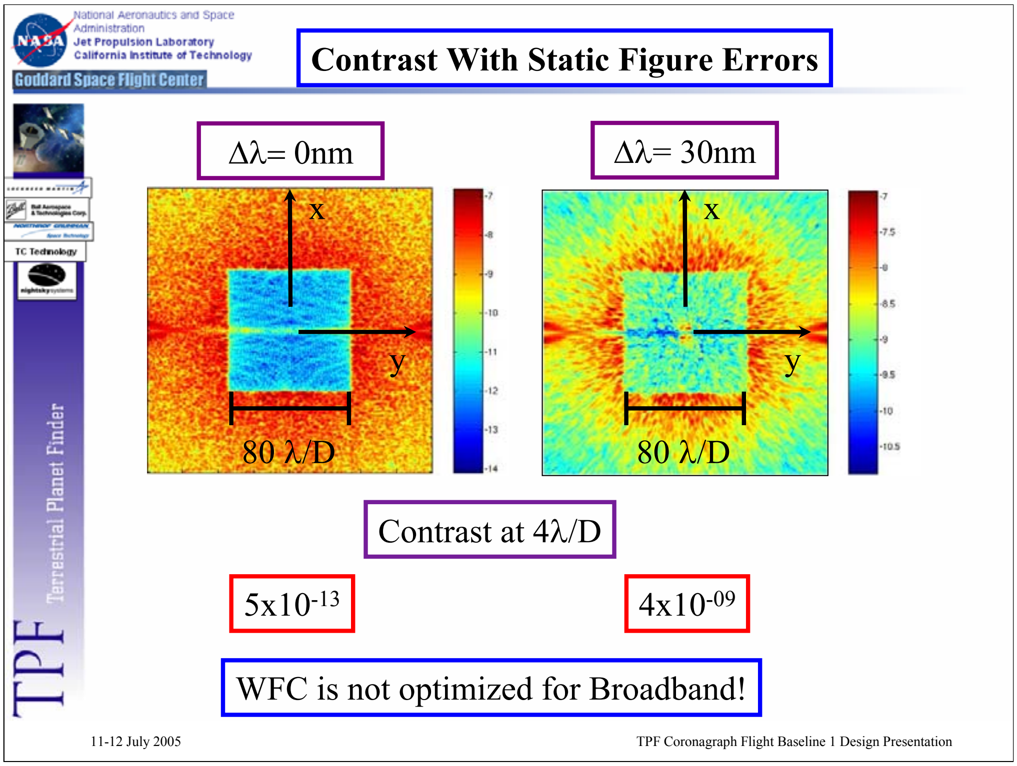

- This slide was produced with no dynamic errors just the static figure errors applied.
- With this non-optimized WFC scheme and a spectral bandpass of $\Delta\lambda$=30nm, we are not meeting our contrast requirements. However, we are easily meeting the requirements in the monochromatic case.
- Broadband optimization may improve the contrast for this system. Fully understanding the role spectral bandwidth plays in limiting contrast will lead to alternate solutions

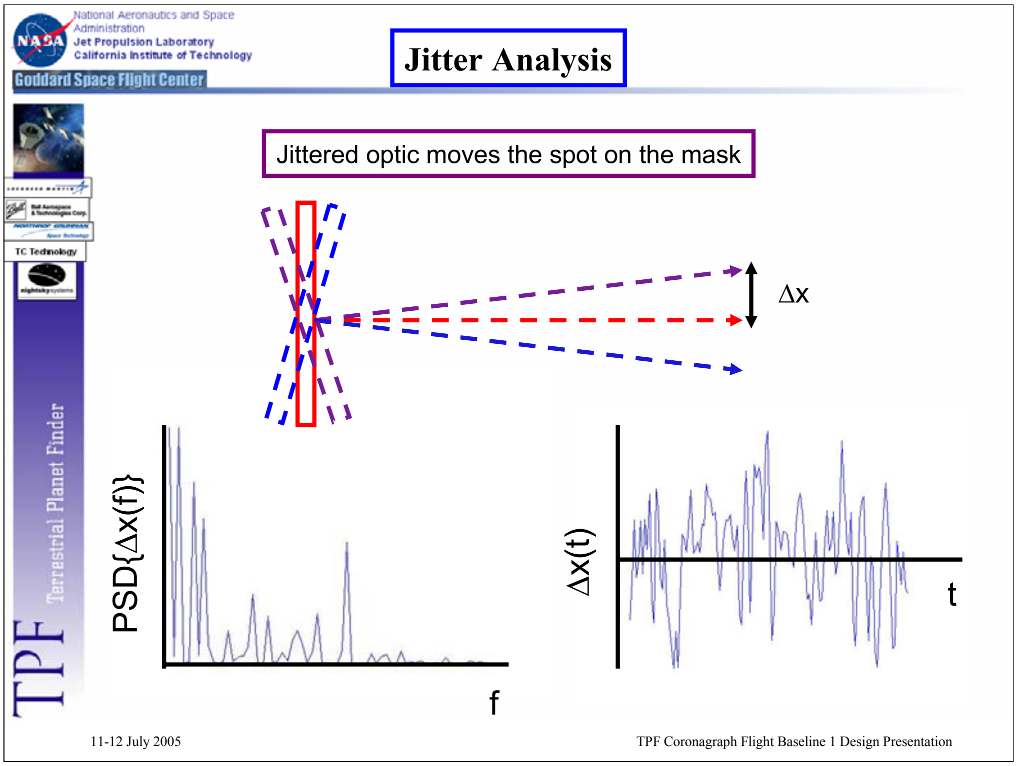

- The dynamic perturbations to the optics due to Jitter were applied to each optic up to the occulter with the exception of the DM and the occulting mask.
- The optics were allowed to move with 6 degrees of freedom in both the positive and negative or clockwise and counterclockwise directions.
- A time series was constructed by picking the worst case frequency of vibration applied to the optic for each degree of freedom.

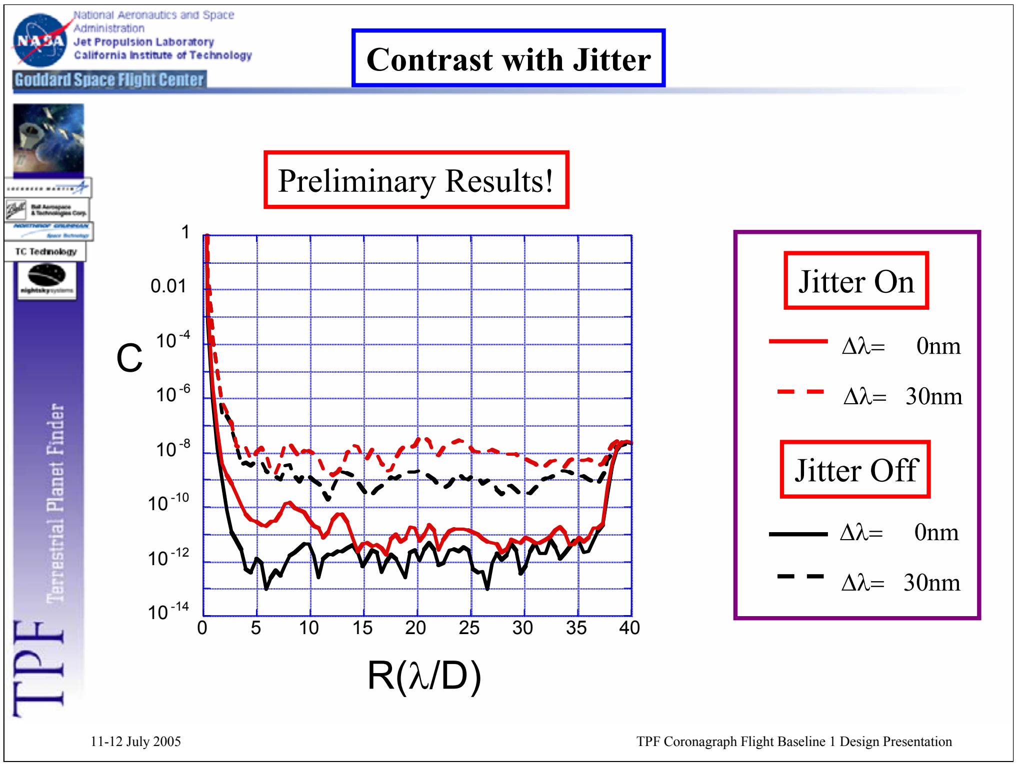

- These results are preliminary, but show the proper behavior for contrast degradation due to jitter.
- Note, the inner angles closer to the star are degraded worse than the outer working angles as expected.
- The broadband results were little affected by jitter, demonstrating the dominance of figure errors in broadband contrast degradation.

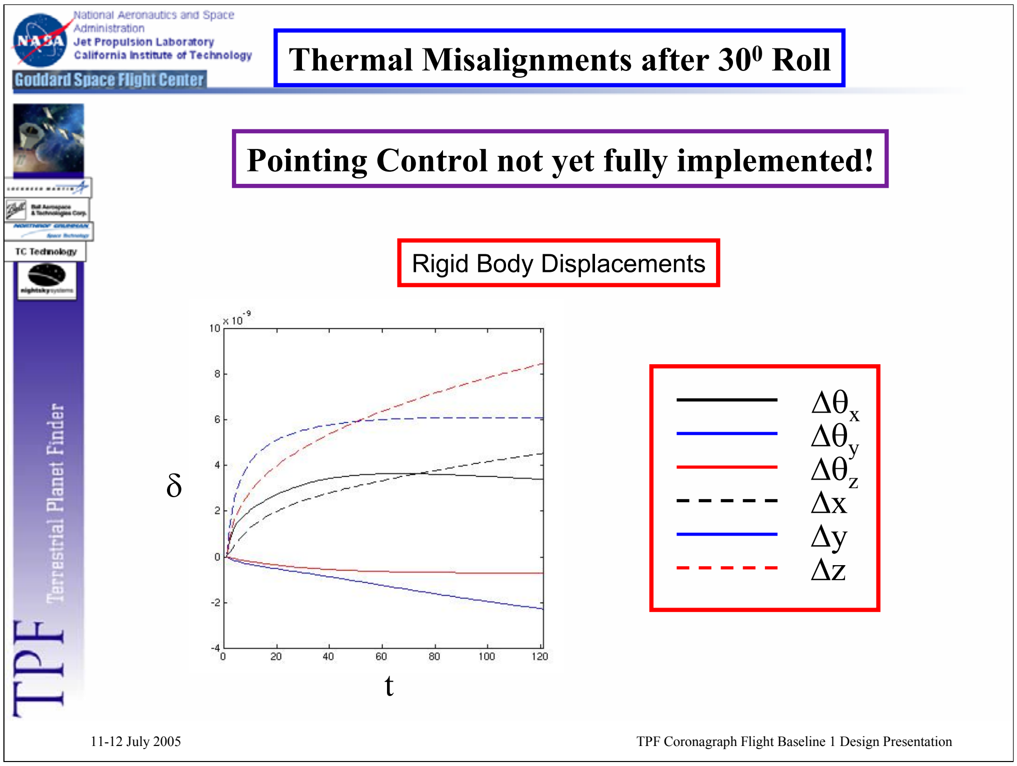

- These are preliminary results – control algorithms are in work and will be added by the end of Cycle 1.
- These are the transient thermal–induced misalignment of optics after a 30^0 roll over a 24 hour time period. These results do not include any active control.
- The passive pointing control is also not properly implemented. As you can see in the example, the optics relax to a misaligned state, which is not compensated over the 24 hour measurement.

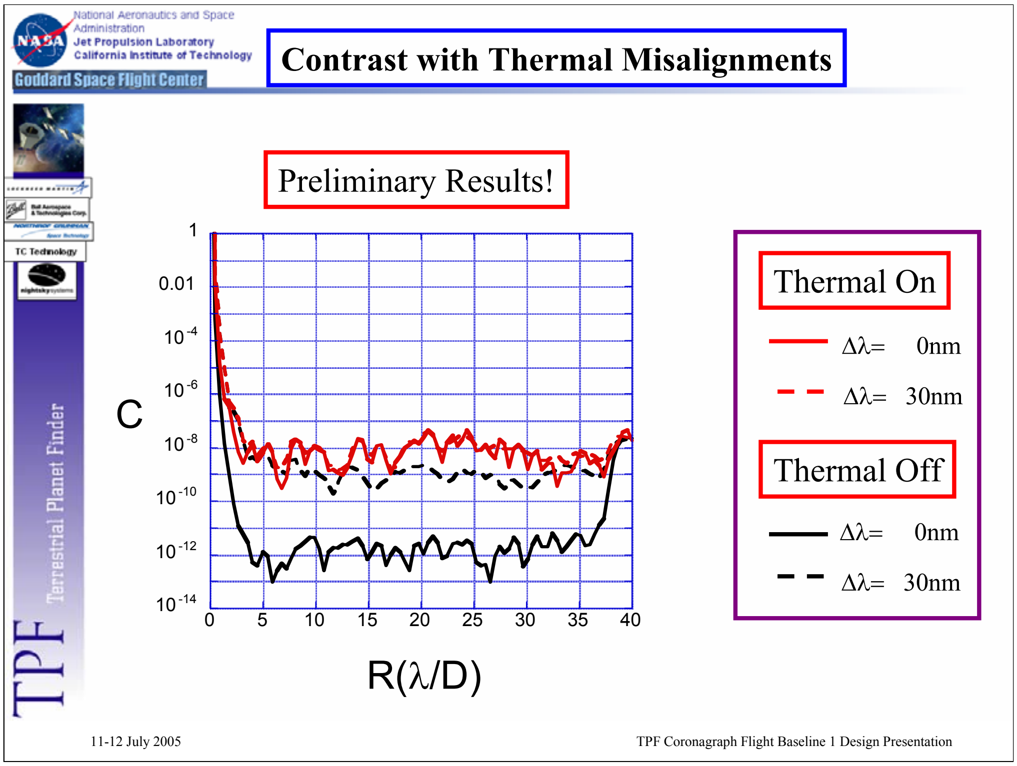

- The contrast depicted here is generated over the full 24 hour time period and does not necessarily represent a particular mission operation scenario.
- These are preliminary results without pointing control. The poor contrast results are not representative of actual operation but are just a first attempt at modeling thermal effects. The modeling will be improved over the next few months to capture the operational scenario and the thermal effects more accurately.

Future Work

Model Upgrades

- Reduced Noise Floor is the first priority
- Inclusion of Mask Errors
- Proper modeling of Cylindrical Optics
- Add pointing control correction
- Inclusion of amplitude errors without position perturbation capability

Future Studies

- Thermal and Jitter analysis with deformations on the Primary Mirror
- Broadband WFC optimization
- Error Budget Validation

System Thermal Modeling & Performance

Eug Kwack

Contributors:

Michael Saeger (ATA), Andy Kissil, Tim Ho, Terry Cafferty

11-12 July 2005

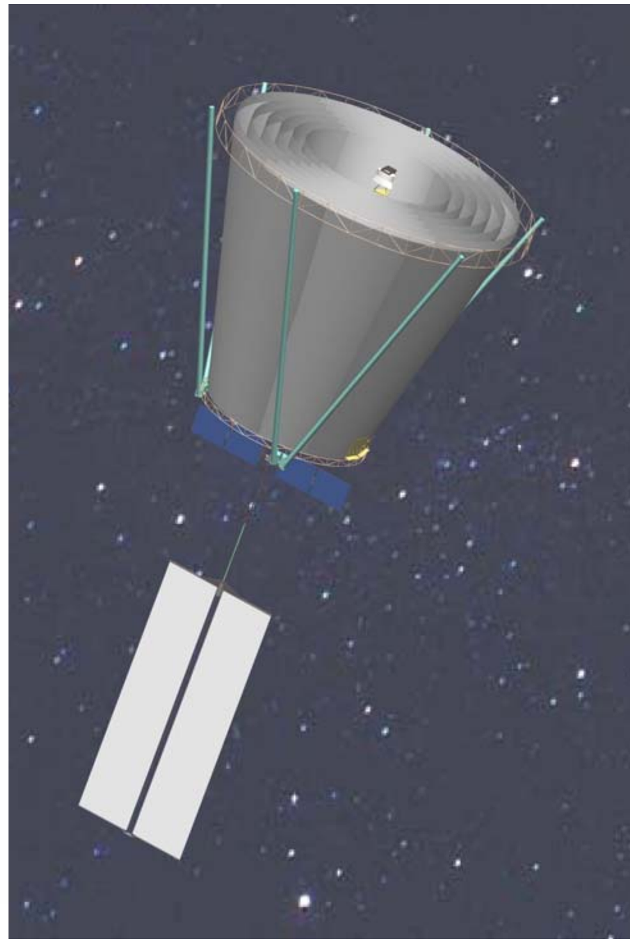

Outline

- Thermal Tools
  - TSS/SindaG, TMG, IMOS
- Thermal Models and Run Information
- Steady Results at 195 deg Sun Angle
- Delta-Temperatures for 30 deg Dither
  - Temperature differences between two steady-states of the beginning and end following a 30 deg Dither
  - Transient Results of PM during 30 deg Dither
- Temperature Control Heater Powers
- Conclusions and Future Work

Thermal Tools used

- TSS/SindaG and TMG
  - TSS: Thermal Synthesizer System
  - SINDA: System Improved Numerical Differencing Analyzer
  - TMG: Thermal Model Generator
  - A simplified model was used to investigate the effects of specularity, spacing between layers and angle between layers of sun shield. Both TMG and TSS/SindaG were used.
  - In FB1 study, TMG is used for faster run time and better data exchanges with other tools.
  - Double precision version of TMG is available (I-DEAS11)
  - Eventually IMOS (Integrated Modeling Optics Software) will be used once it is ready.

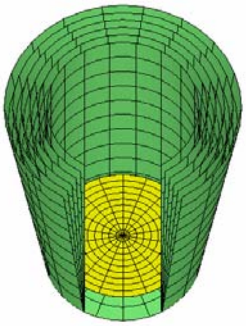

TMG Thermal Model

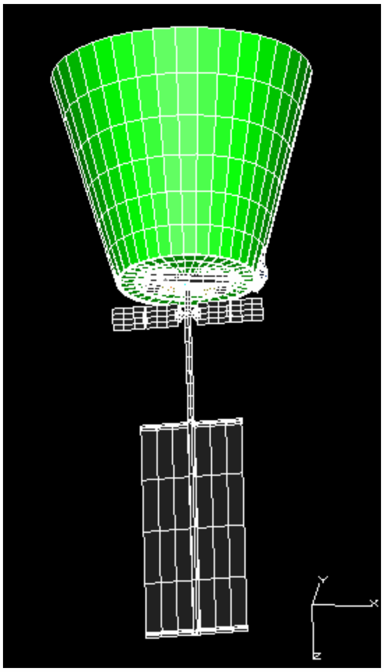

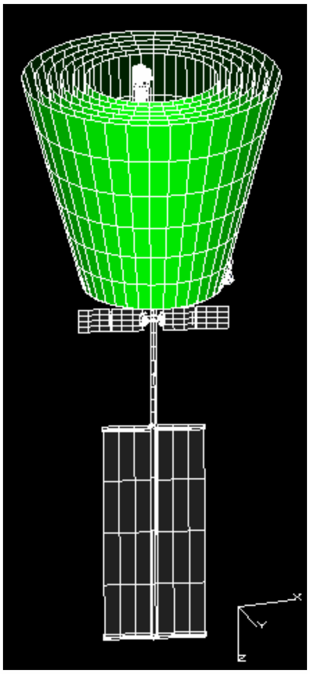

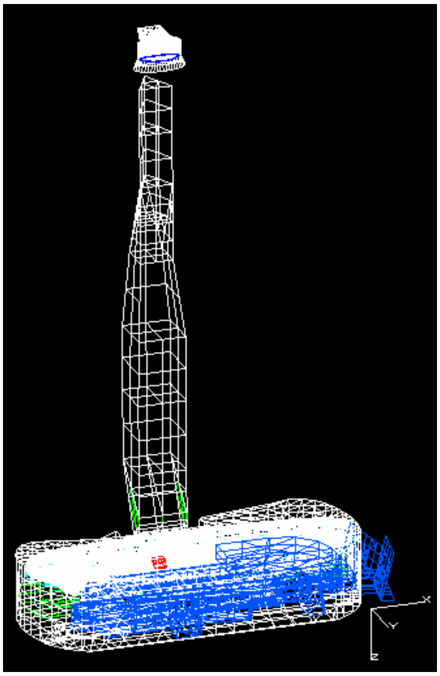

Number of Nodes: 18,180
Number of Elements: 39,517 (2,654 beams, 3,662 solids, 32,201 thin shells)

Temperature Control Heaters

Heaters	Set Temp*, °C
PM Bot Heaters	22
PM Side Heaters	22
SM Top Heaters	22
SM Side Heaters	22
M3 Back heaters	22
Thermal Enclosure Heaters	17
SST Mounting Beam Heaters	17

*** In FB1, constant temperature BC's are imposed.**

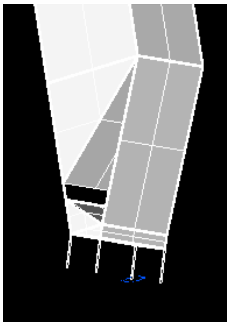

SST Mounting Beam Heaters

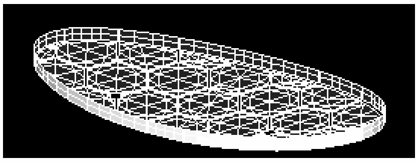

Primary Mirror (PM) Heaters

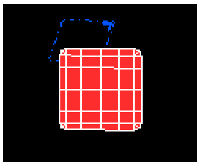

Tertiary Mirror (M3) Heaters

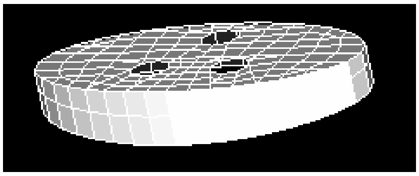

Secondary Mirror (SM) Heaters

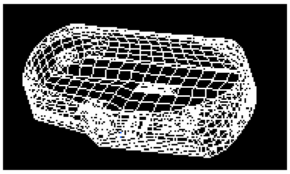

Thermal Enclosure Heaters

Clock Angle Definition from Andy

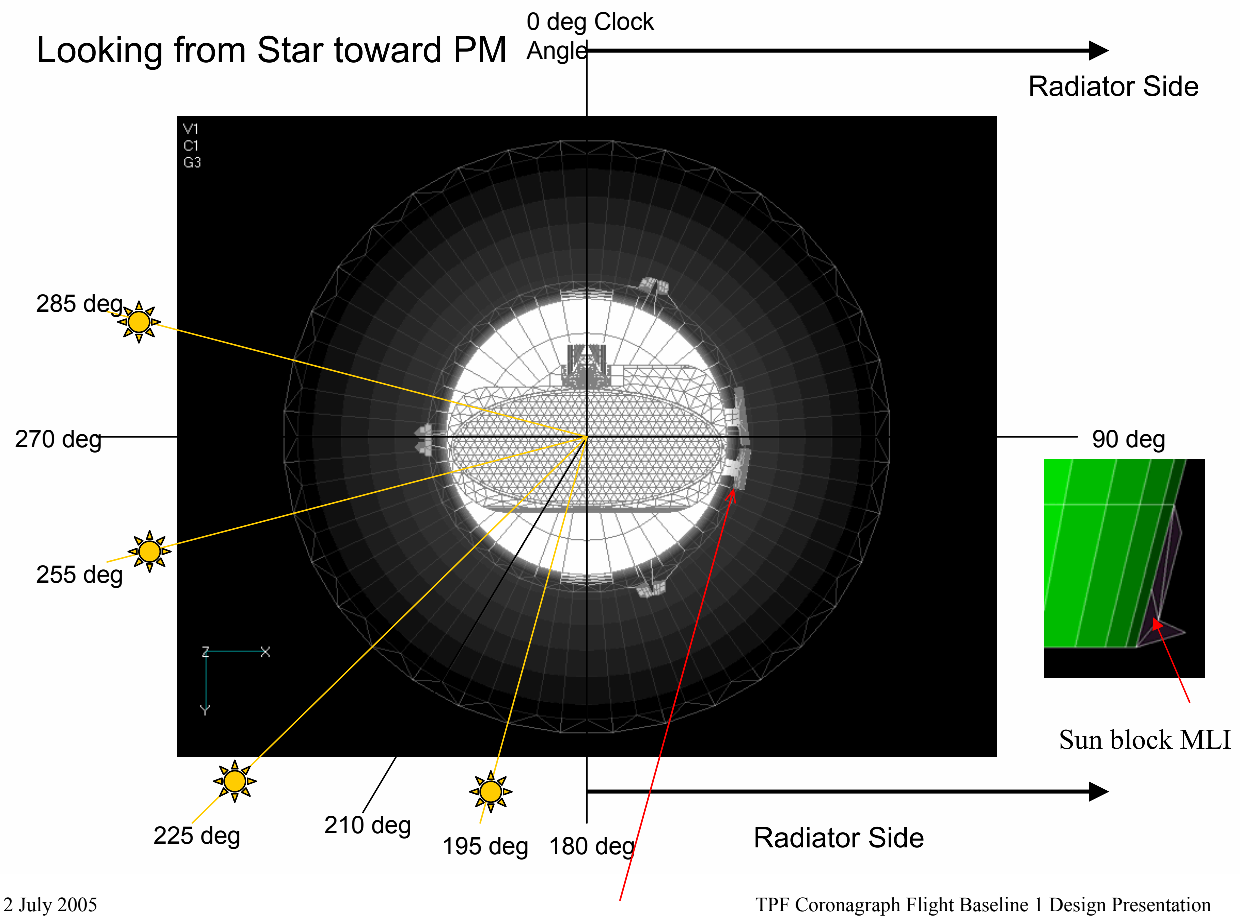

Run Information with Thermal Community Workstation

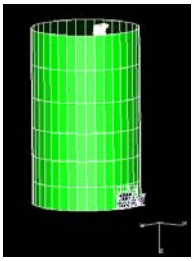

Internal Enclosure

External Enclosure

	Internal Enclosure	External Enclosure	Solution Elapsed Time	Radiation Conductor
Run #1	Diffuse(Hemicube)	Diffuse(Hemicube)	3 hr 30 min	4,718,407
Run #2	Diffuse (ec=0.05)	Specular (ec=0.05)	2 days 23 hr 58 min	7,320,528
Run #3	Diffuse (ec=0.02)	Specular (ec=0.02)	6 days 7 hr 57 min	8,086,053

* Old Thermal Community Workstation: Dell Precision Work station 530 (2.2 Ghz)
  TMG: Version 11.0.321

* New Thermal Community Workstation: Dell Precision Work station 670 (3.6 Ghz)
  TMG: Version 11.0.684
  Solution Elapsed Time for Run#3: 3days 19 hours

Temperatures for 195deg Sun Angle

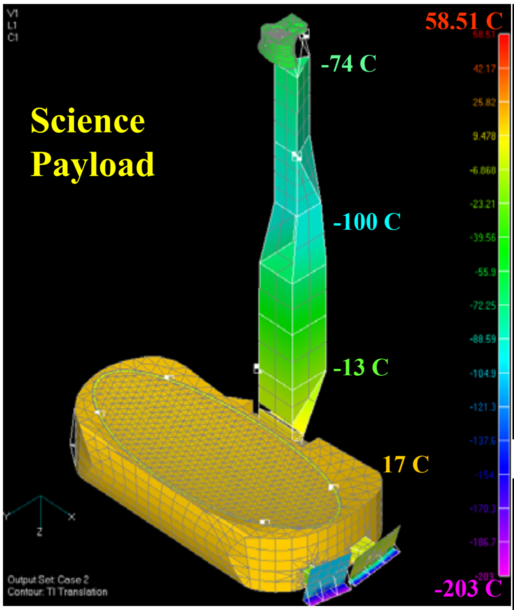

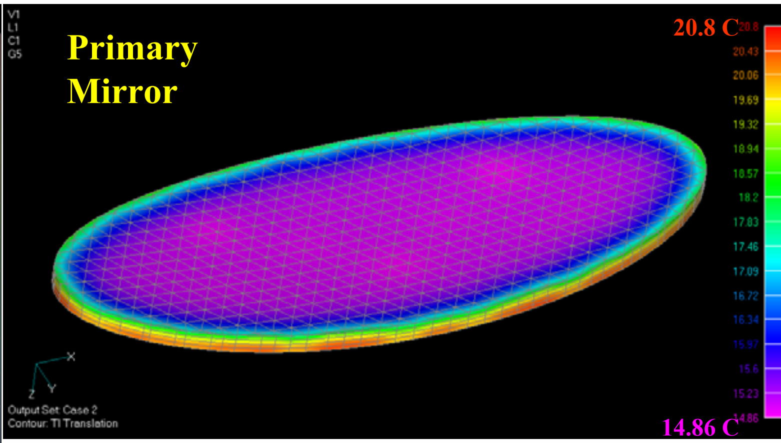

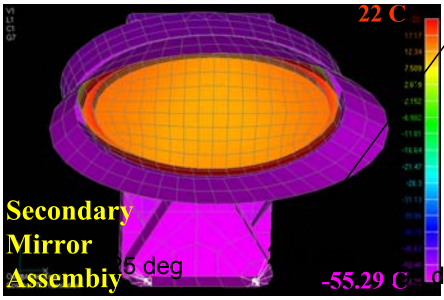

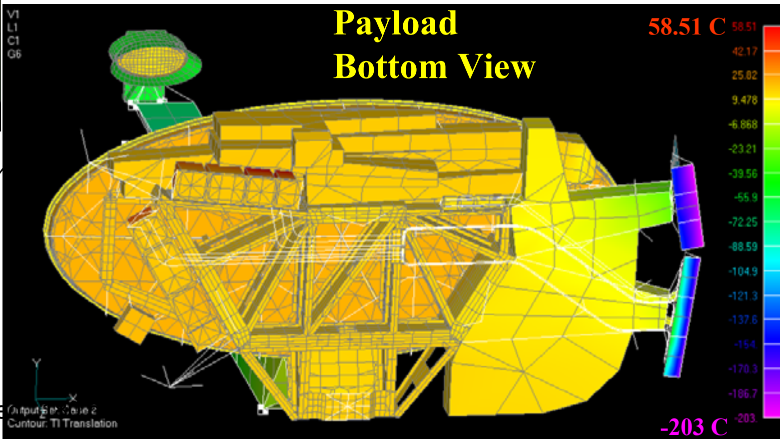

Temperatures for 195deg Sun Angle

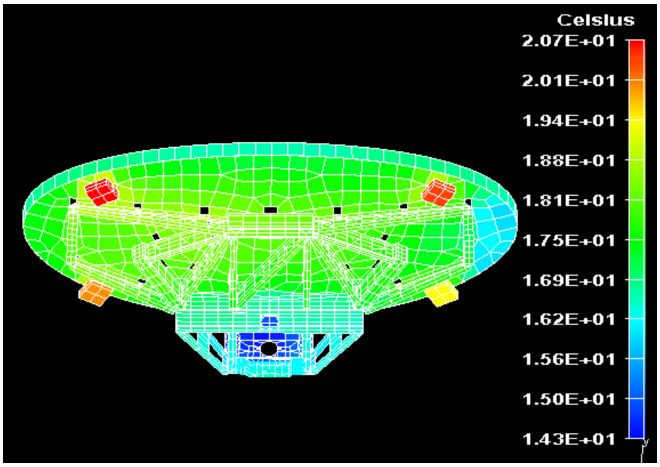

Temperatures of OTA laser electronics are from 19 to 21^{o}C only by radiative cooling from chasses

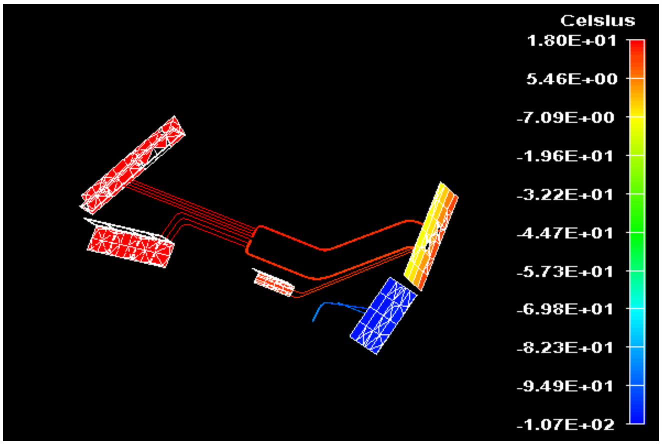

Most PSA electronic mounting plate temperatures are maintained below 18^{o}C by combination of heat pipes and a radiator

Delta-Temps for 30 deg Dither (Steady-State, 195-225 deg): Hemi-Hemi

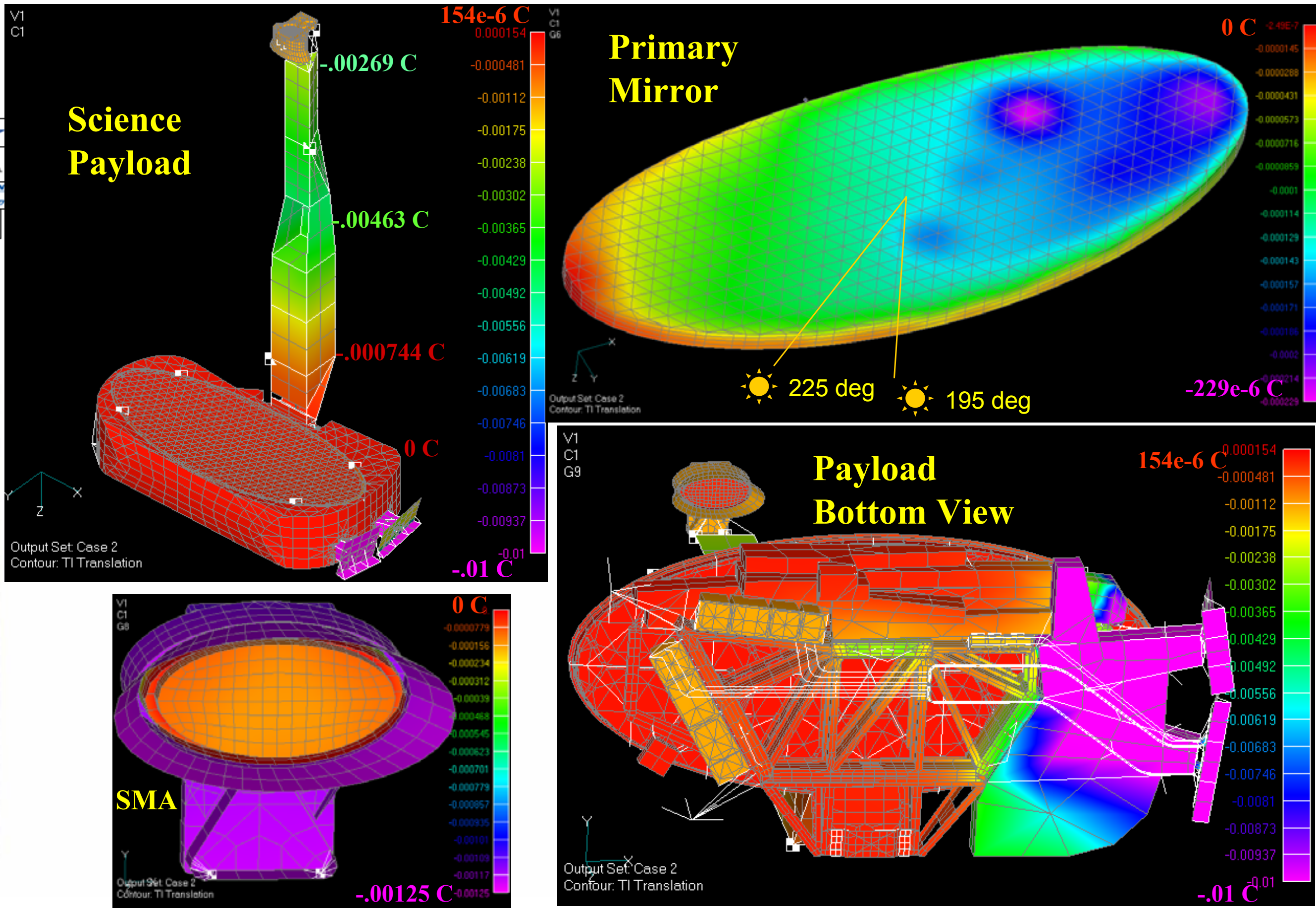

Delta-Temps for 30 deg Dither (Steady-State, 255-285 deg): Hemi-Hemi

285 deg

255 deg

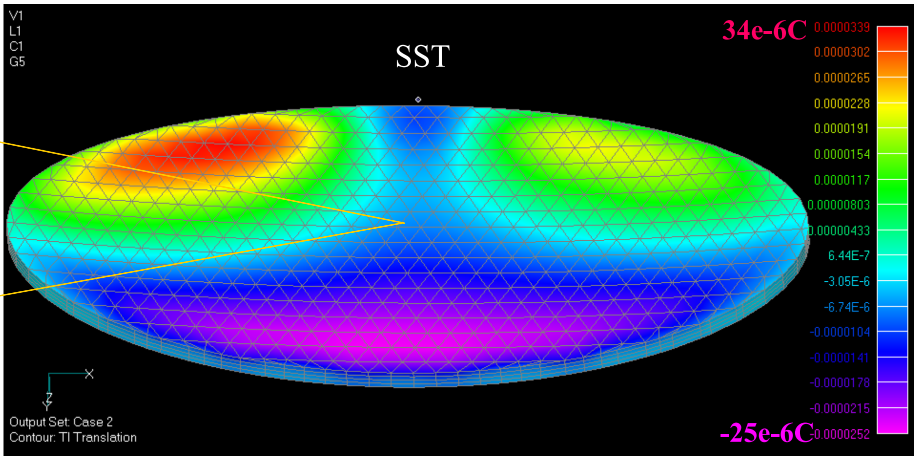

PM front

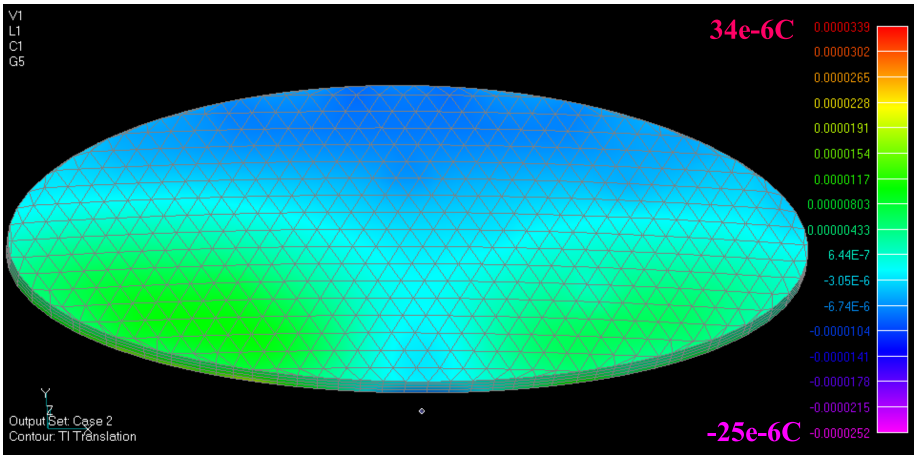

PM back

Delta-Temp Time-History: Averaged Temp of PM 30 deg Dither (195 to 225 deg)

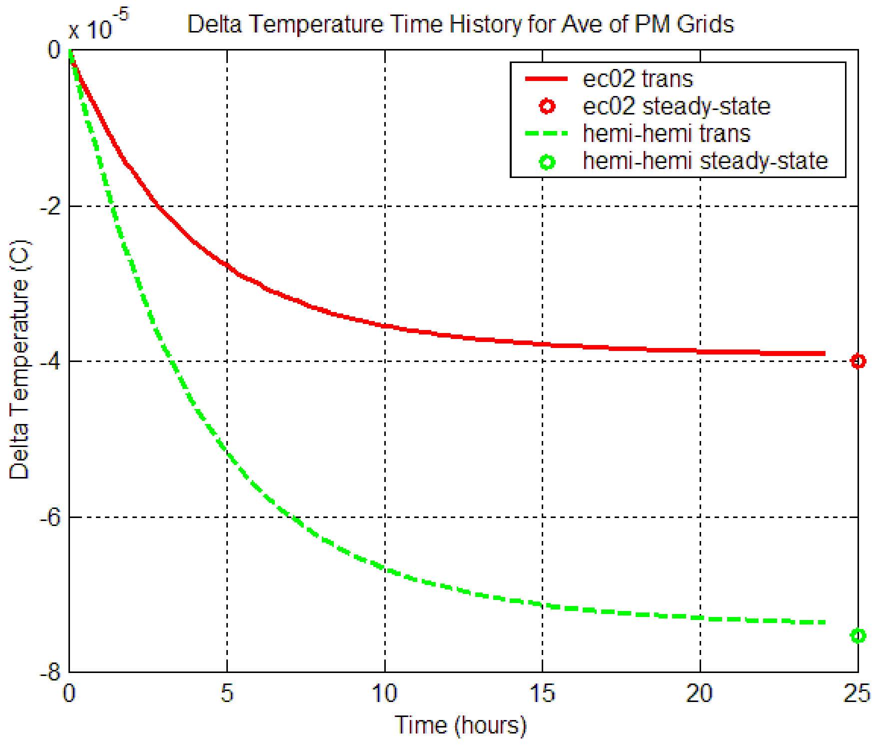

Temperature Control Heater Powers
255 deg Sun Angle

Heaters	Set Temp, ^oC	power*, w
PM Bot Heaters	22	336.78
PM Side Heaters	22	389.69
SM Top Heaters	22	14.29
SM Side Heaters	22	17.25
M3 Back heaters	22	0.88
Thermal Enclosure Heaters	17	622.29
SST Mounting Heaters	17	13.60
Total		1394.78

* powers required to maintain heaters at set temperatures

Heater Temperatures with constant powers 255 deg Sun Angle

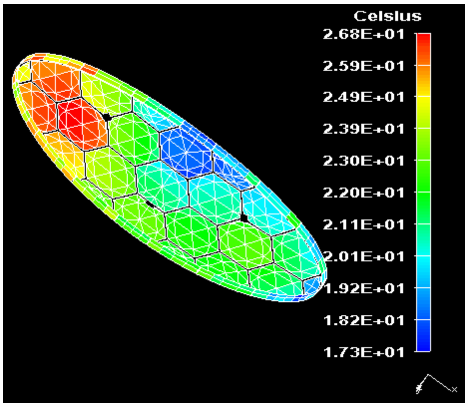

Primary Mirror Heaters

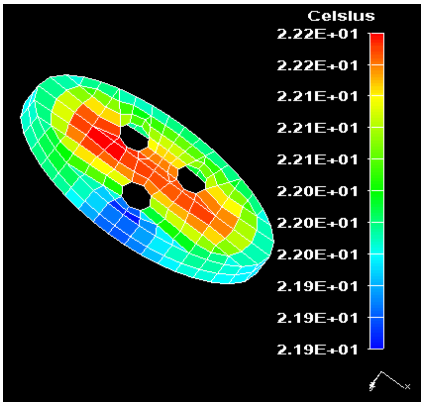

Secondary Mirror Heaters

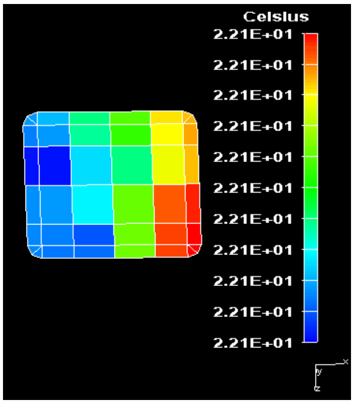

Tertiary Mirror Heaters

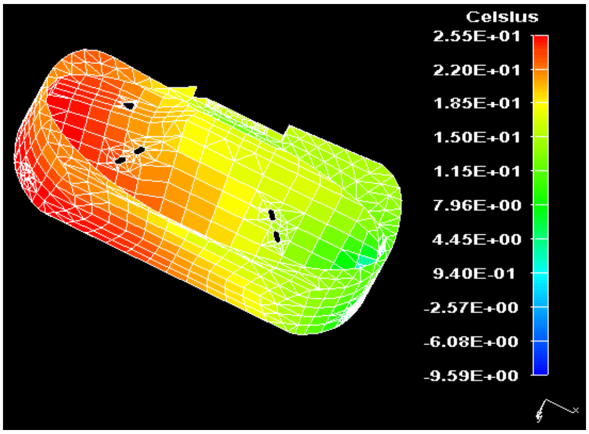

Thermal Enclosure Heaters

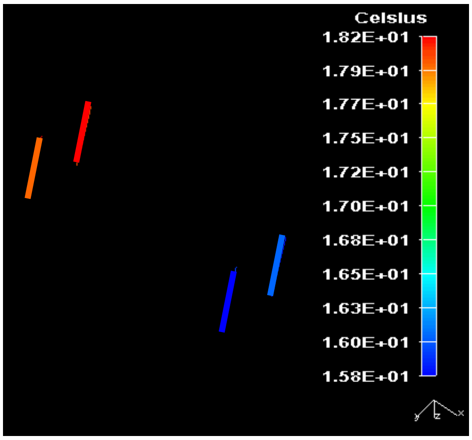

SST Mounting Beam Heaters

Wrap-Up

Conclusions

- Lessons-learned on TMG
  - Large numbers should not be used for labeling of elements: elements were relabeled using small numbers.
  - Algorithm to calculate nodal temperatures from element temperatures should be improved: nodal temperatures were recalculated by Andy using Matlab.
  - Some elements such as rigids, rods and lump masses should not be used: replaced by non-geometric elements
- Sun shield (v-grooves) works beautifully.
- Mounting plates for PSA electronics are maintained at room temp by combination of heat pipes and radiators. OTA laser electronics heat is successfully dissipated by radiation
- The 195-225 deg Dither produces much higher temperature disturbances than the 255-285 case. However, computed WFE's of the 195-225 deg Dither **with constant temp at heaters** are below requirements level.
- So far, there is no major show stopper.

Future Studies

- Sun locations behind Telescope (including shadowing)
- Transient results with constant heater powers instead of constant heater temperatures
- Thermal optical property changes during mission
- Proceed to FB2 design and modeling

National Aeronautics and Space Administration
Jet Propulsion Laboratory
California Institute of Technology
Goddard Space Flight Center

Delta-Temp Time-History
30 deg Dither (195 to 225 deg)

Faster "Hemi-Hemi" Method

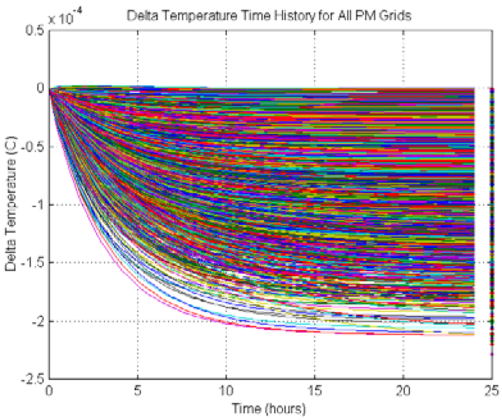

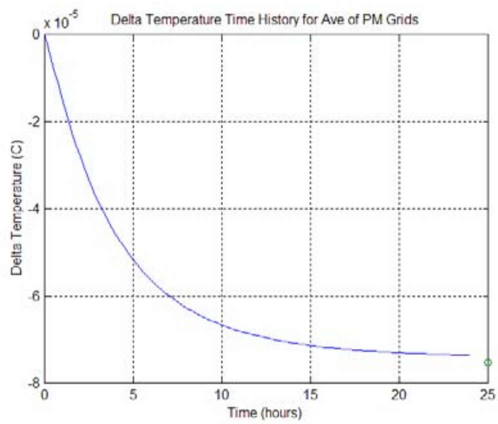

Rigorous, Slower Method (EC=0.02)

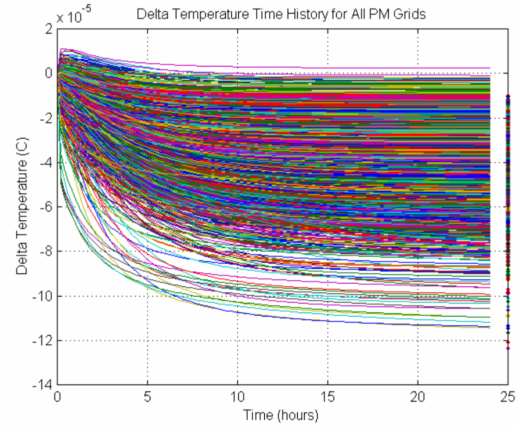

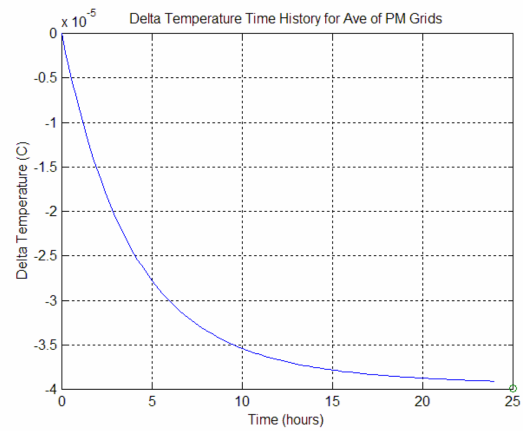

T during 30 deg. Dither from 255 to 285 deg roll

Integration control method: backward
Time step: 180 s
Convergence dT: 10^{-6}

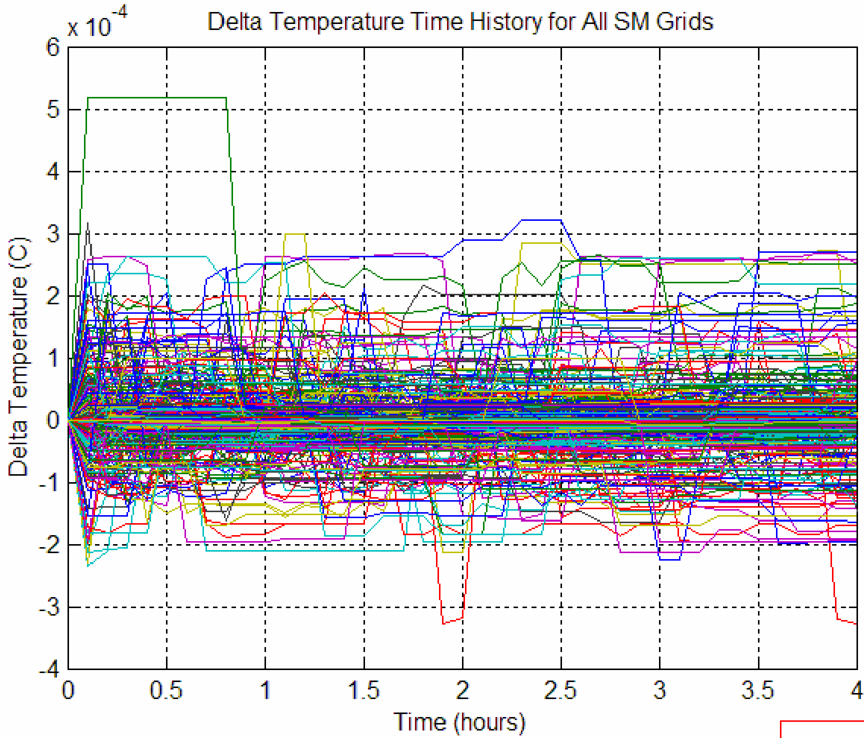

Back-Up

Maximum PM Temperature Changes during Sun moving from +Y to –Y: Specularity

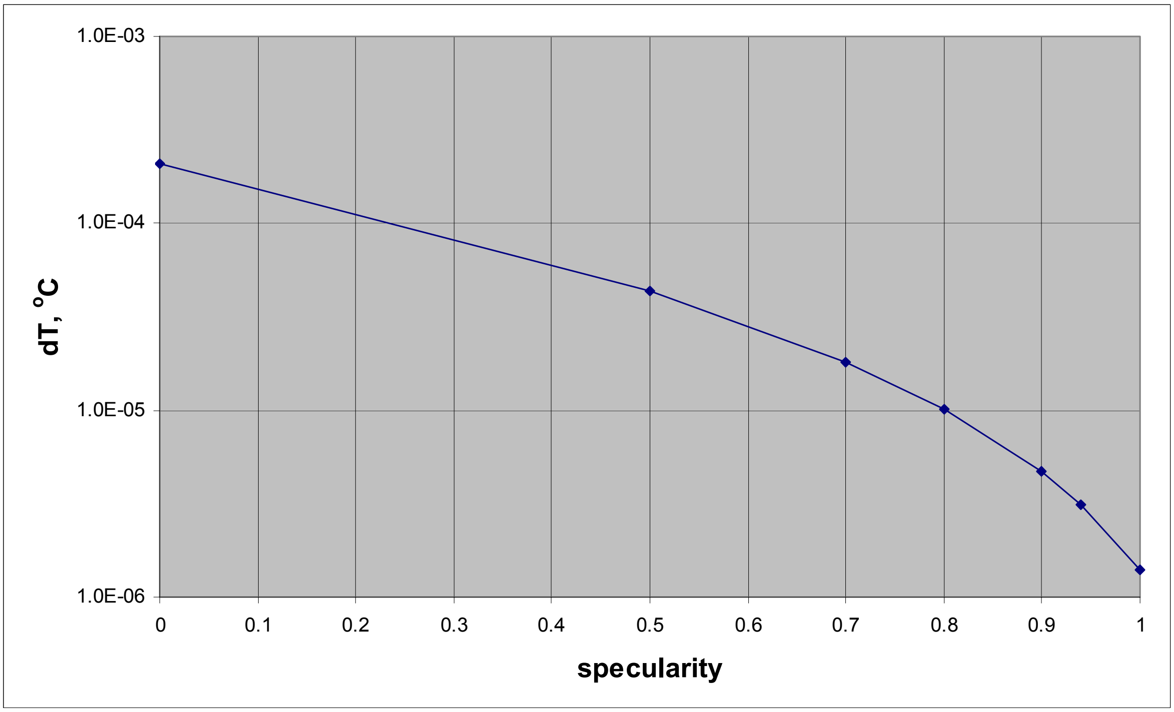

* angle between layers θ = 3deg., gap = 5 cm

Maximum PM Temperature Changes during Sun moving from +Y to –Y: Angle θ

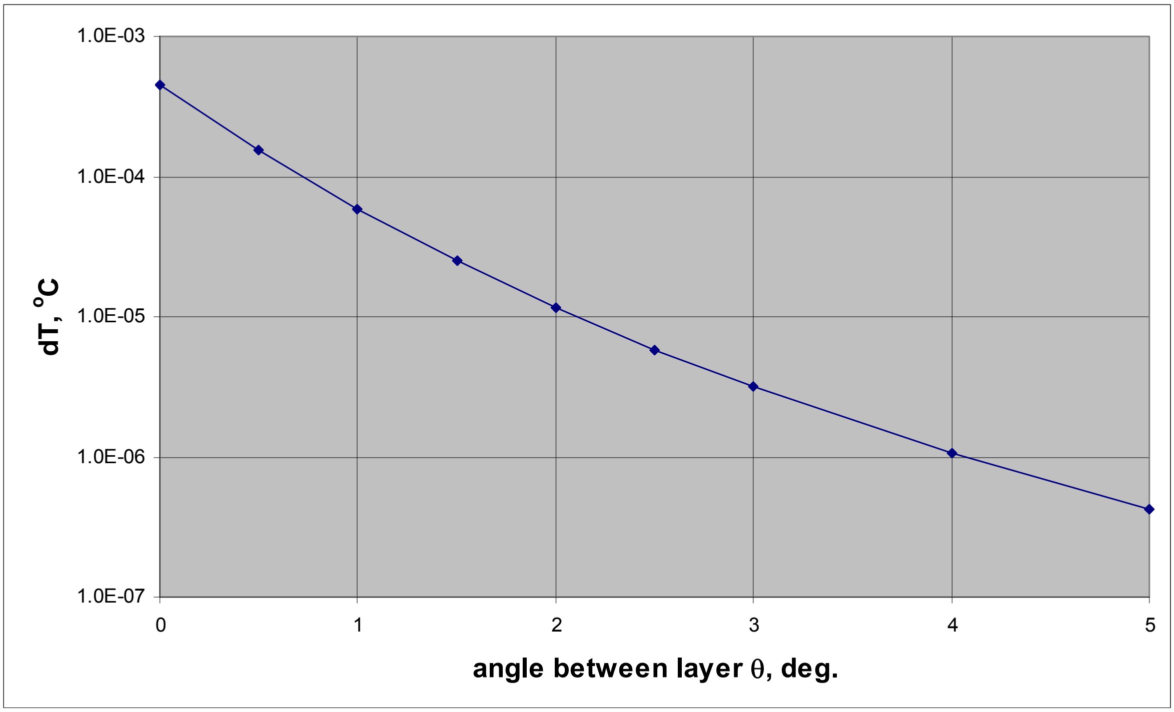

* specularity s = 0.94, gap = 5cm

Maximum PM Temperature Changes during Sun moving from +Y to –Y: Gap

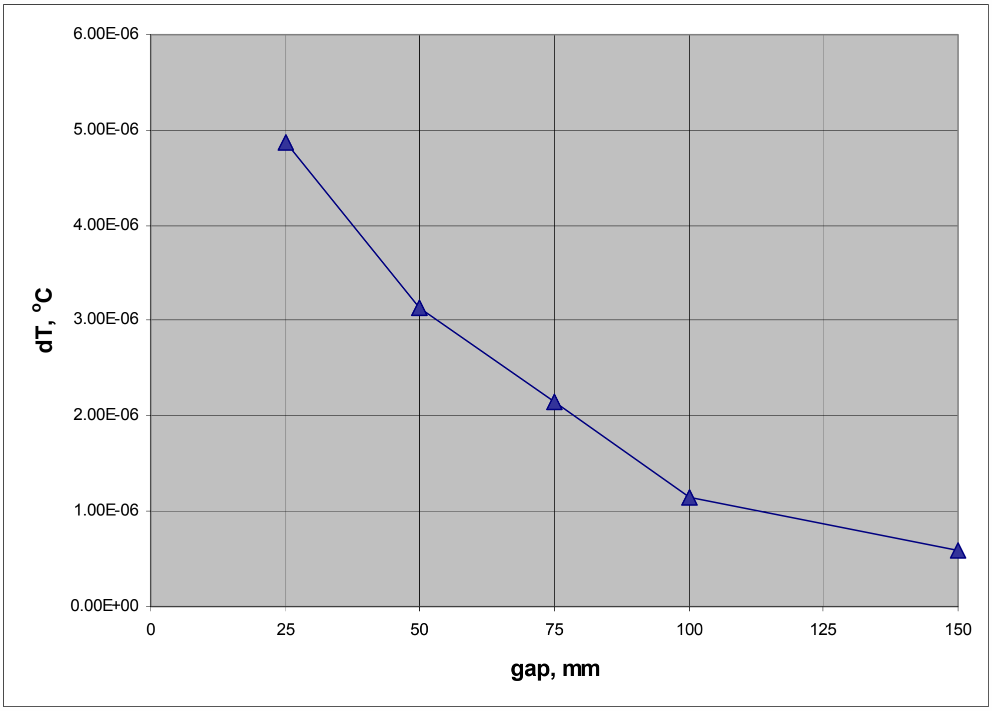

* angle between layers θ = 3deg., specularity s = 0.94

PM Temperatures with thick cylinderical TE: TMG and TSS/SINDAG

	s = 0.94 TMG	s = 0.94 TSS/SINDAG
PM avged Temp, Sun @ +X	17.363056	17.362549
PM avged Temp, Sun @ -X	17.363056	17.362549
PM min Temp, Sun @ +X	17.326949	17.327987
PM max Temp, Sun @ +X	17.480773	17.476815
PM max dT during Sun from +X to -X	-1.528E-06/ 1.526E-06	-2.710E-06/ 2.710E-06

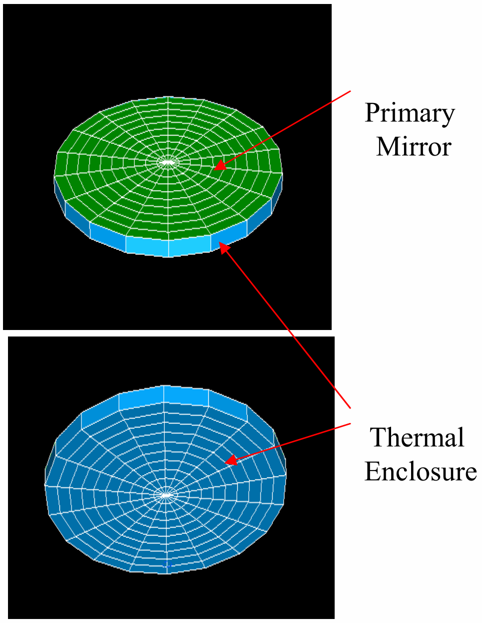

Effects of Meshing of Sun Shades

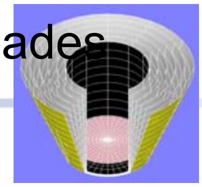
12x10

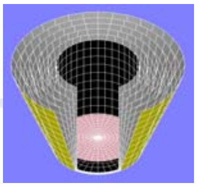
36x10

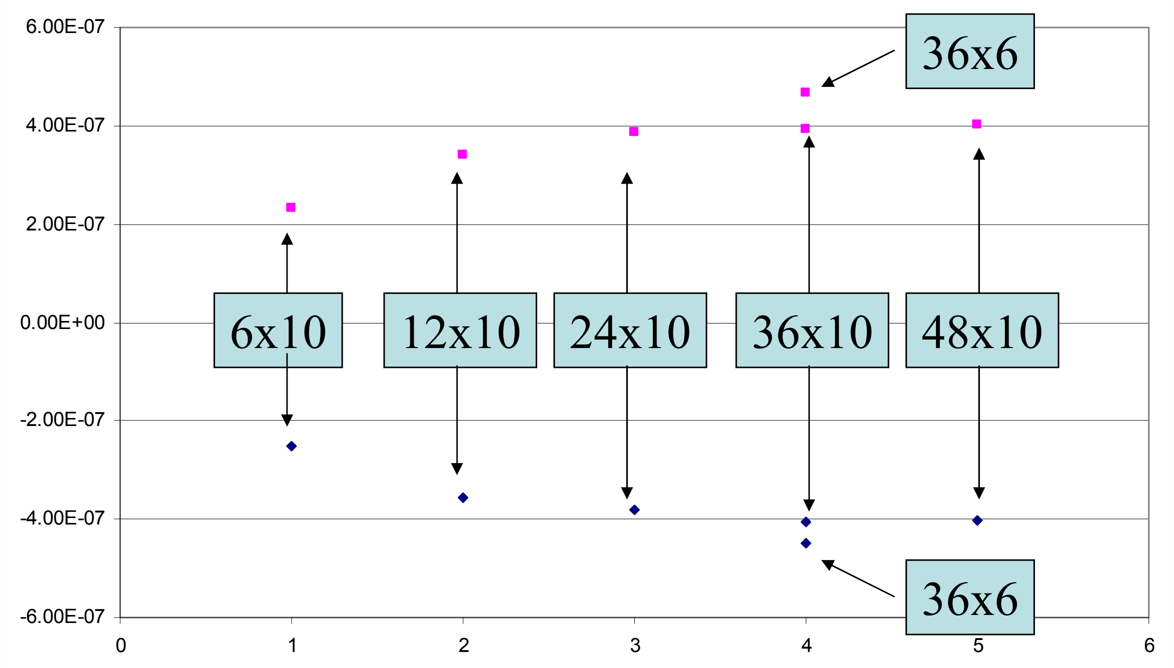

dT = max. temperature rises and drops in PM during 30 deg. dither

Sun Shield Temperatures: 255 deg roll

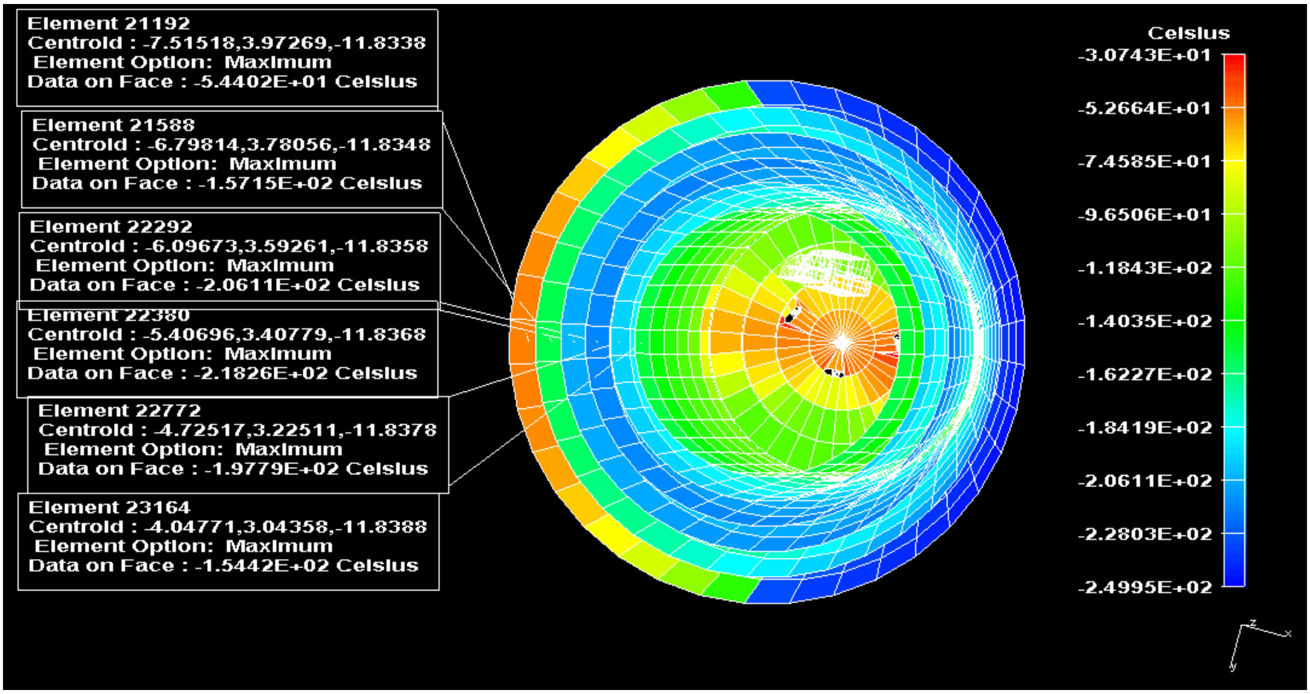

Back-Up

Sun Shield Temperatures: 255 deg roll

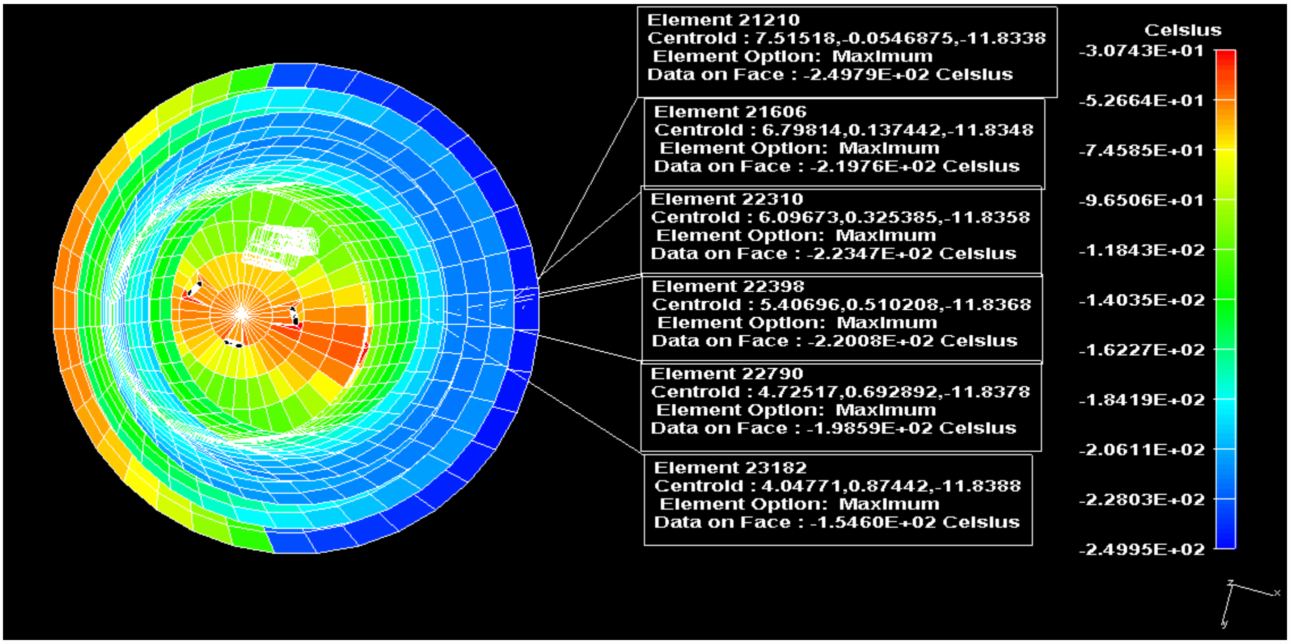

Back-Up

Sun Shield Temperatures: 255 deg roll

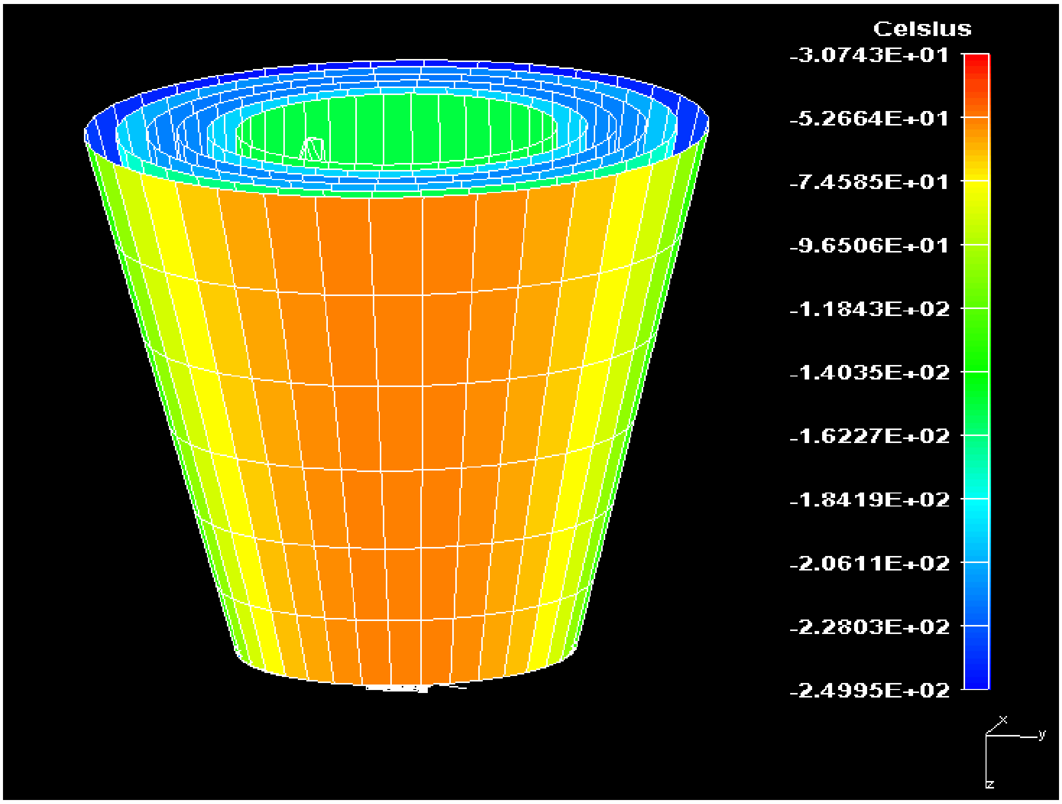

Back-Up

PM, Bipods and AMS Temperatures: 255 deg Roll

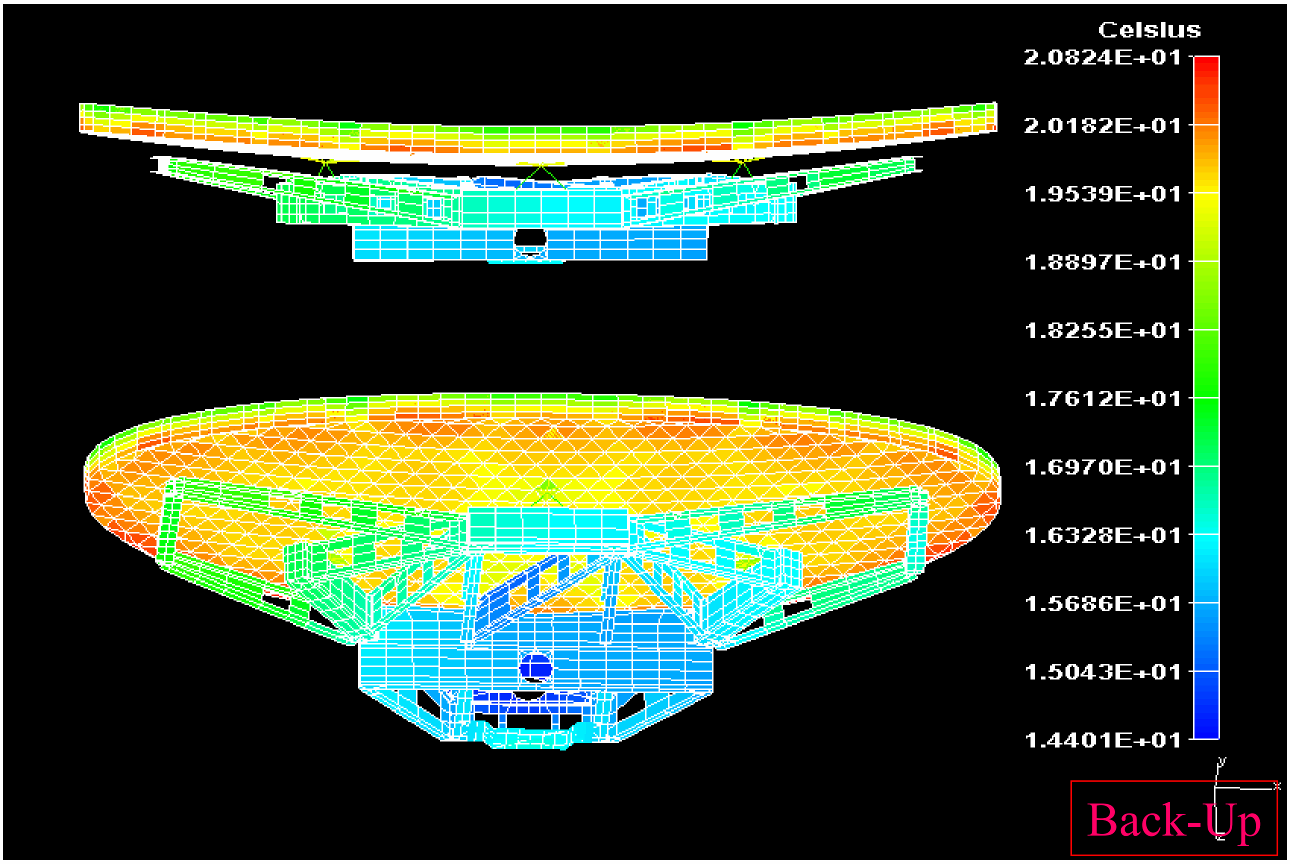

AMS View to Baffle through Holes in Thermal Enclosure

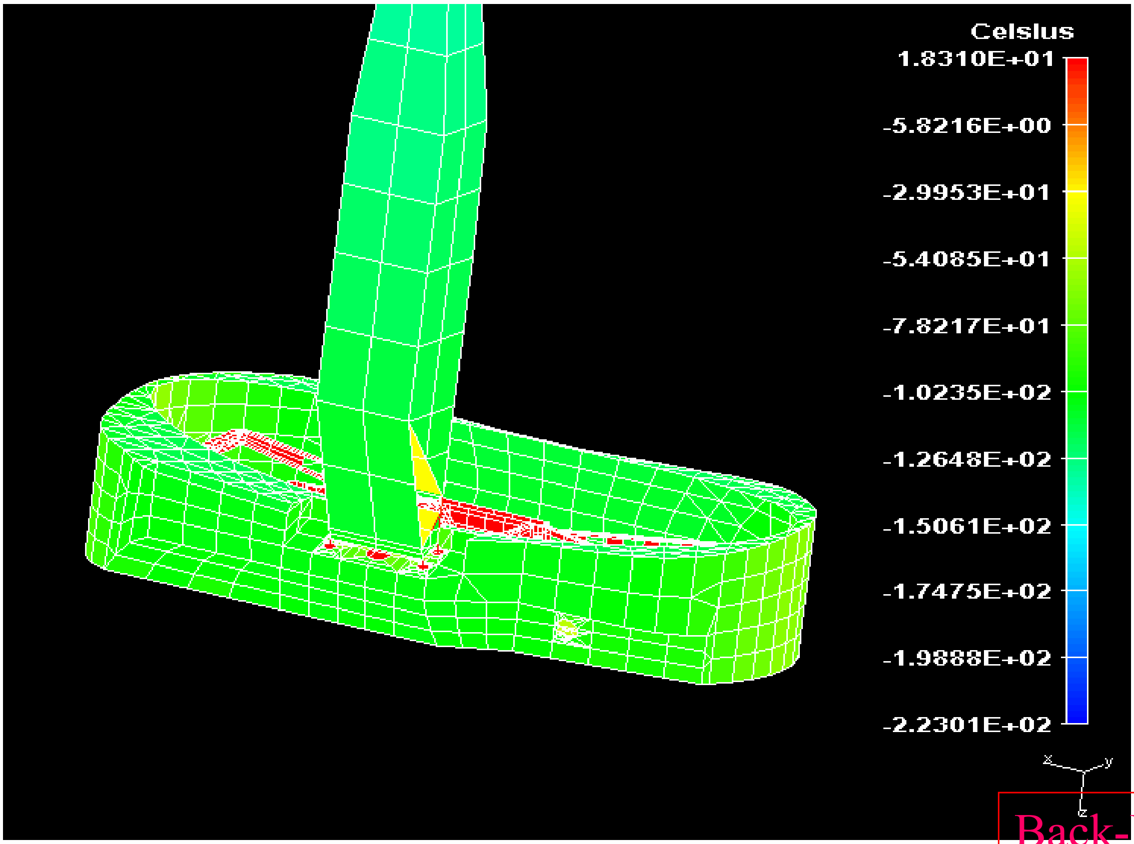

Back-Up

National Aeronautics and Space Administration
Jet Propulsion Laboratory
California Institute of Technology
Goddard Space Flight Center

PM Heaters, Mask and C-Channel Temperatures: 255 deg Roll

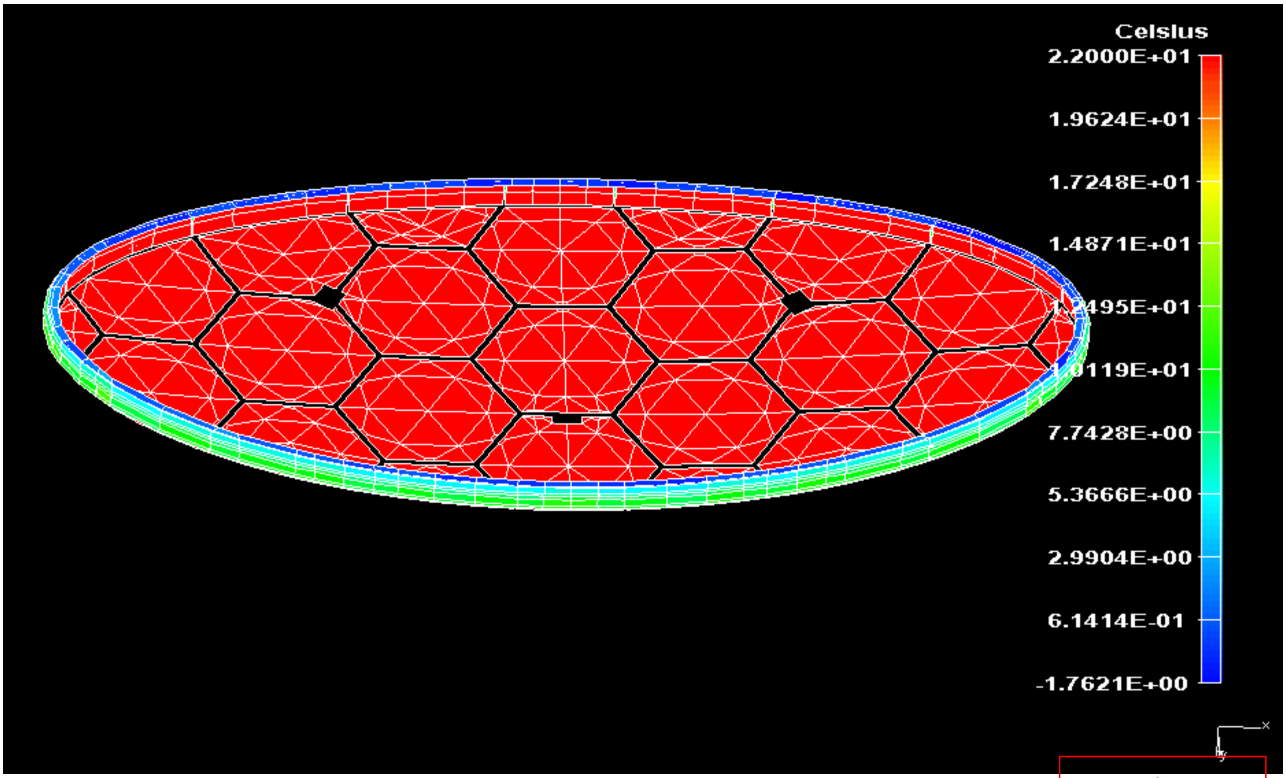

Back-Up

Terrestrial Planet Finder
TPF

SST Temperatures: 255 deg Roll

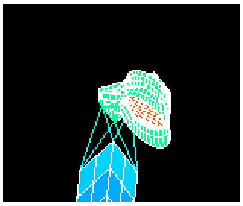

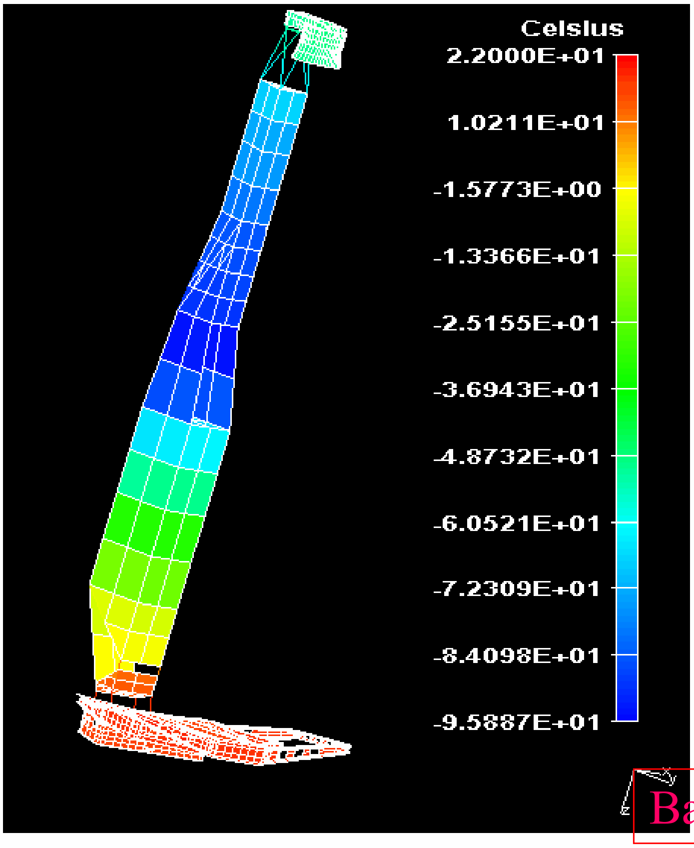

Back-Up

SMA, SST and TE MLI Temperatures: 255 deg Roll

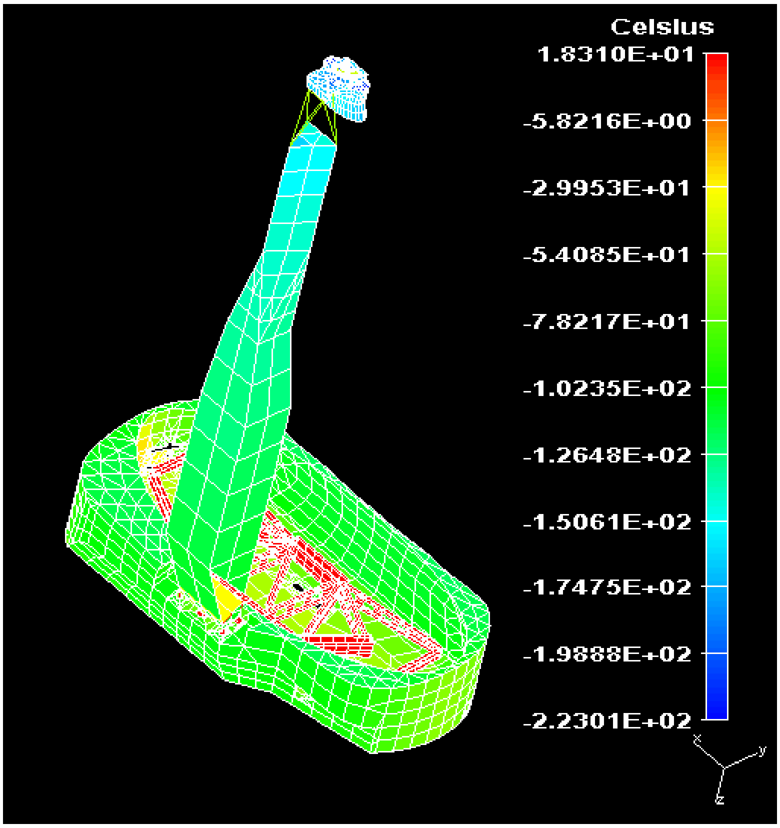

Back-Up

SMA Temperatures (outer cover removed): 255 deg Roll

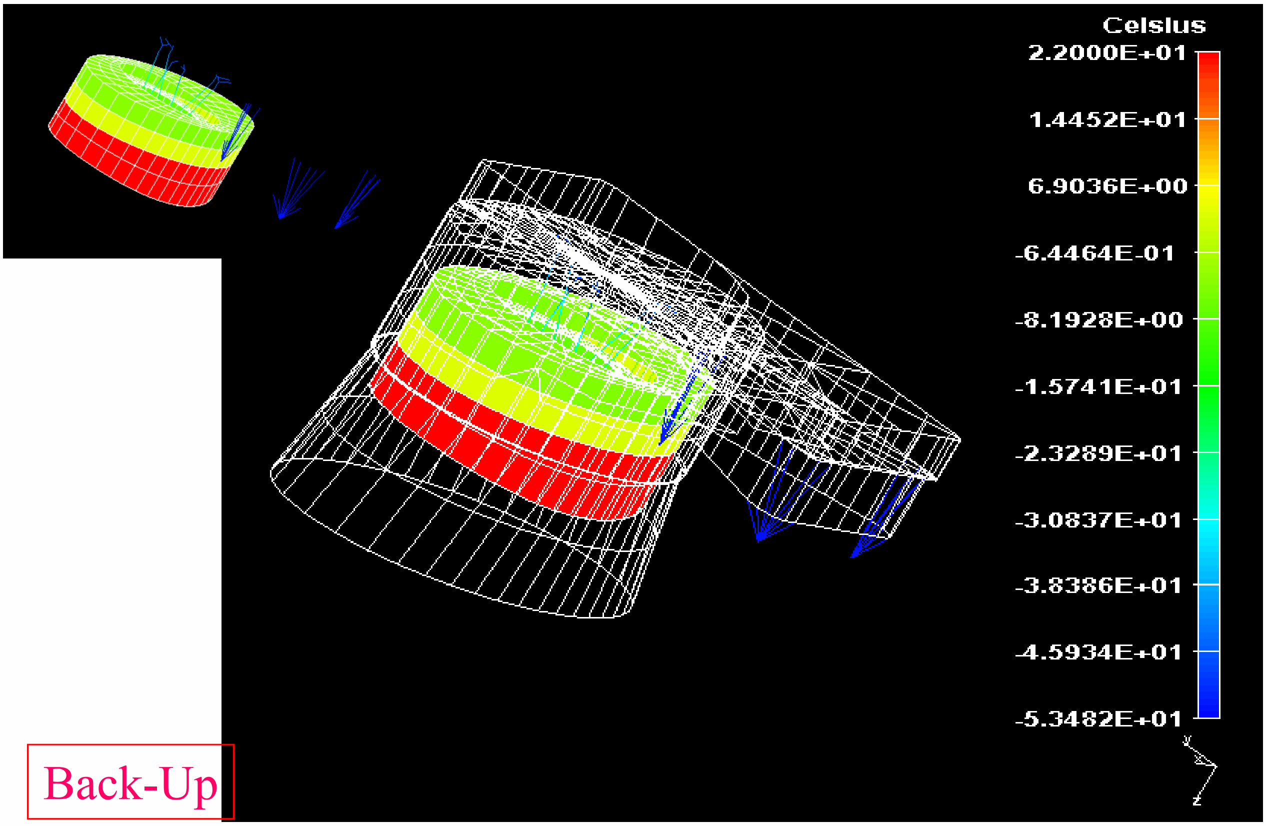

Back-Up

SMA Temperatures (outer cover removed): 255 deg Roll

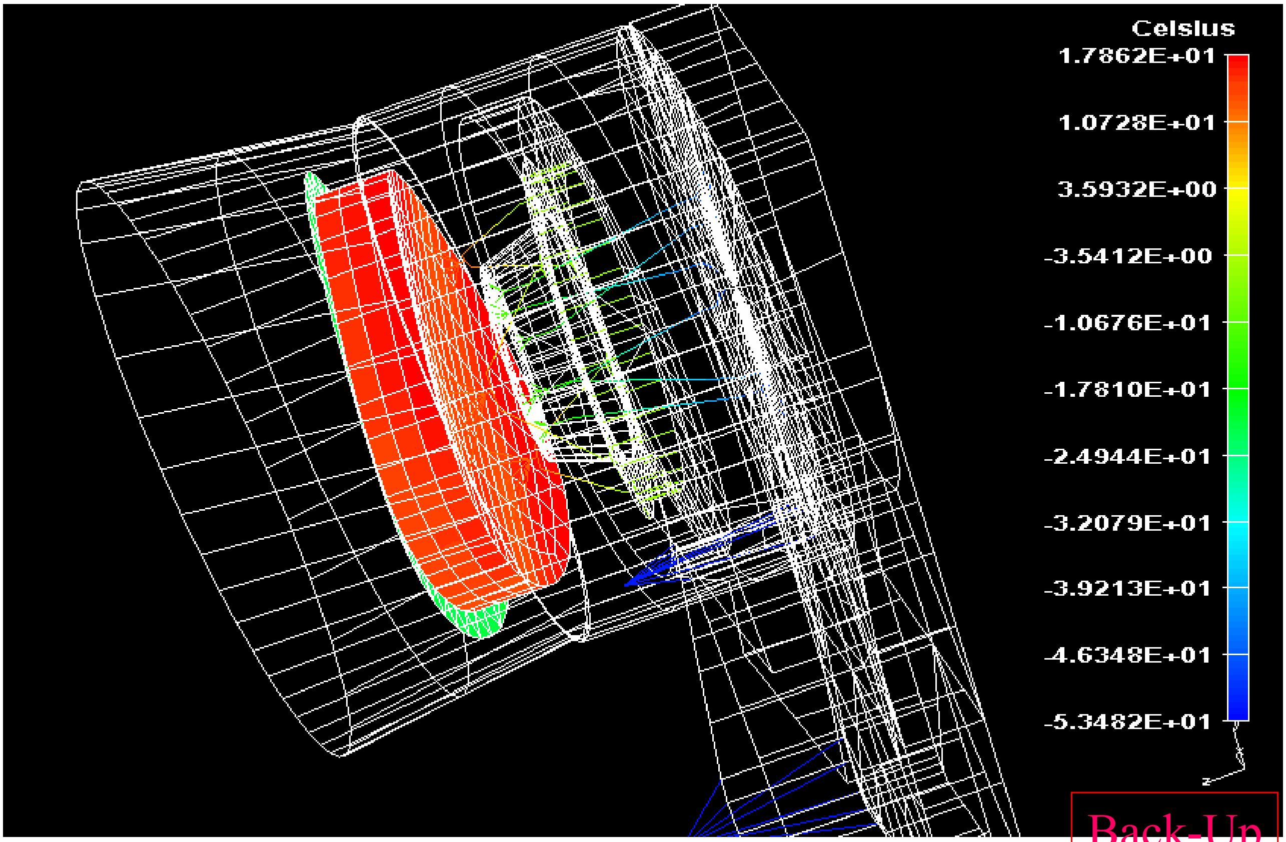

Back-Up

SM Heaters and SM Support Ring Temperatures: 255 deg Roll

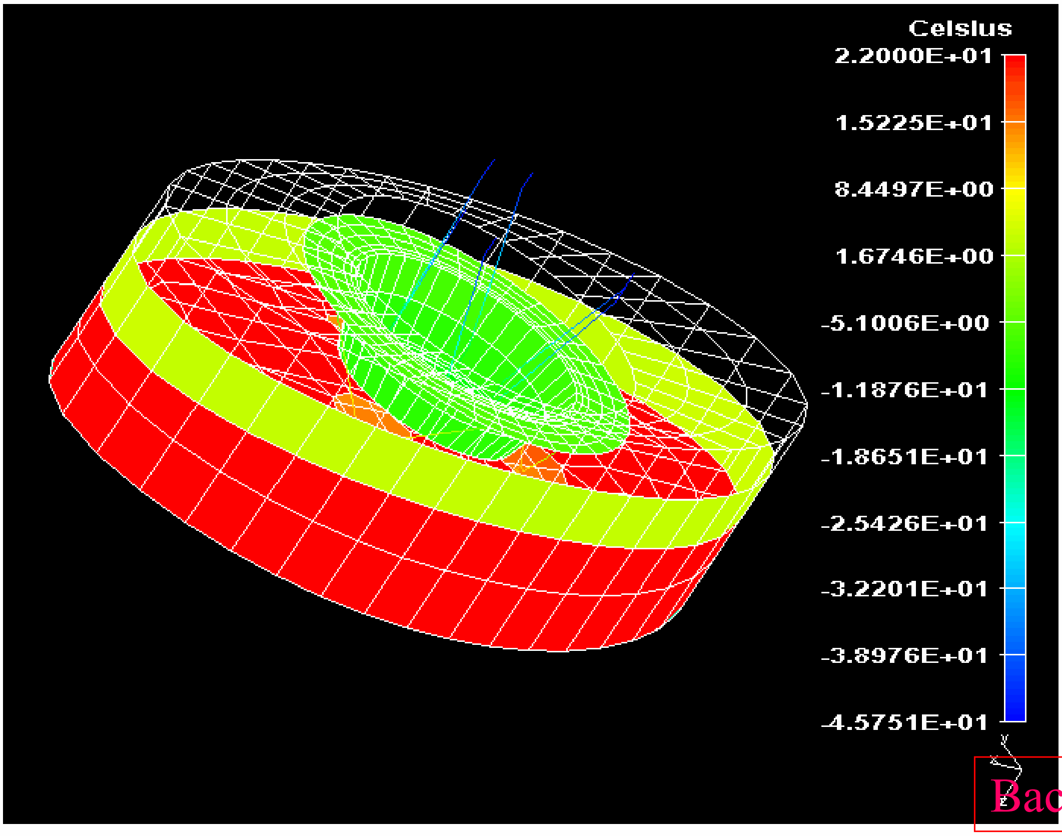

Back-Up

SM, SM Support Ring and Hexapod Temperatures: 255 deg Roll

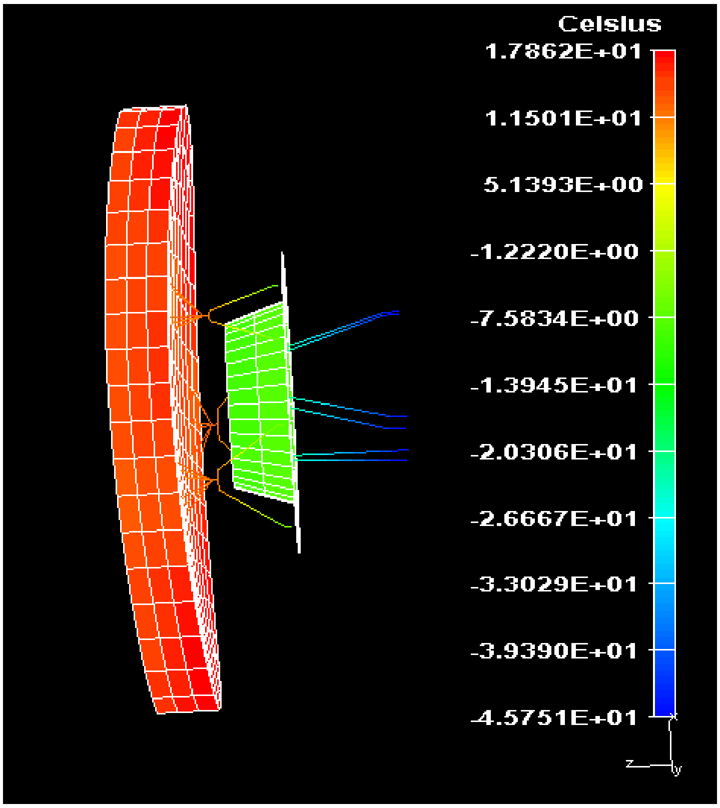

Back-Up

SM Temperatures: 255 deg Roll

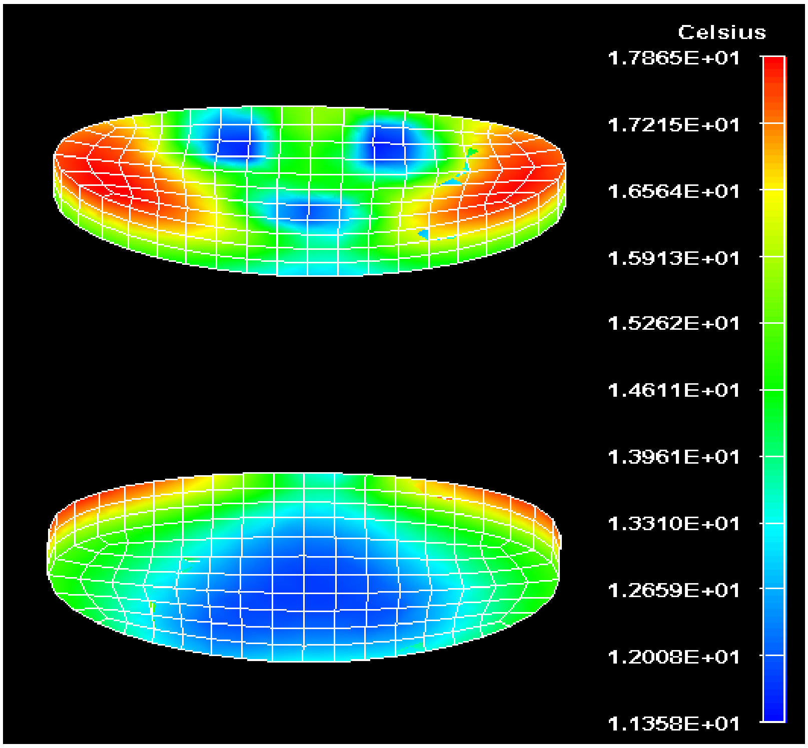

Back-Up

dT of SM during 30 deg. Dither: Hemi-Hemi

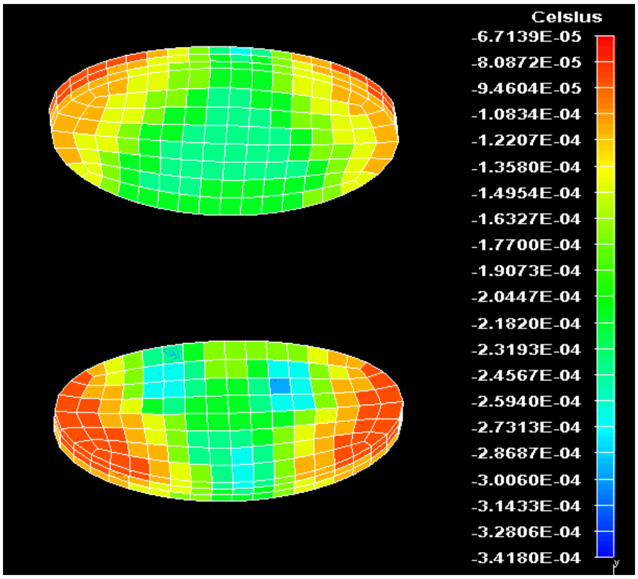

from 195 to 225 deg

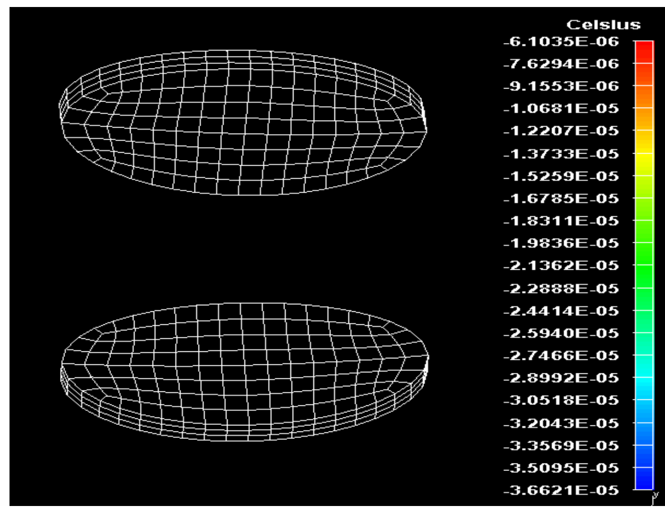

from 255 to 285 deg

Back-Up

Terrestrial Planet Finder
TPF

PSS, Electronic Mounting Plate Temperatures: 255 deg Roll

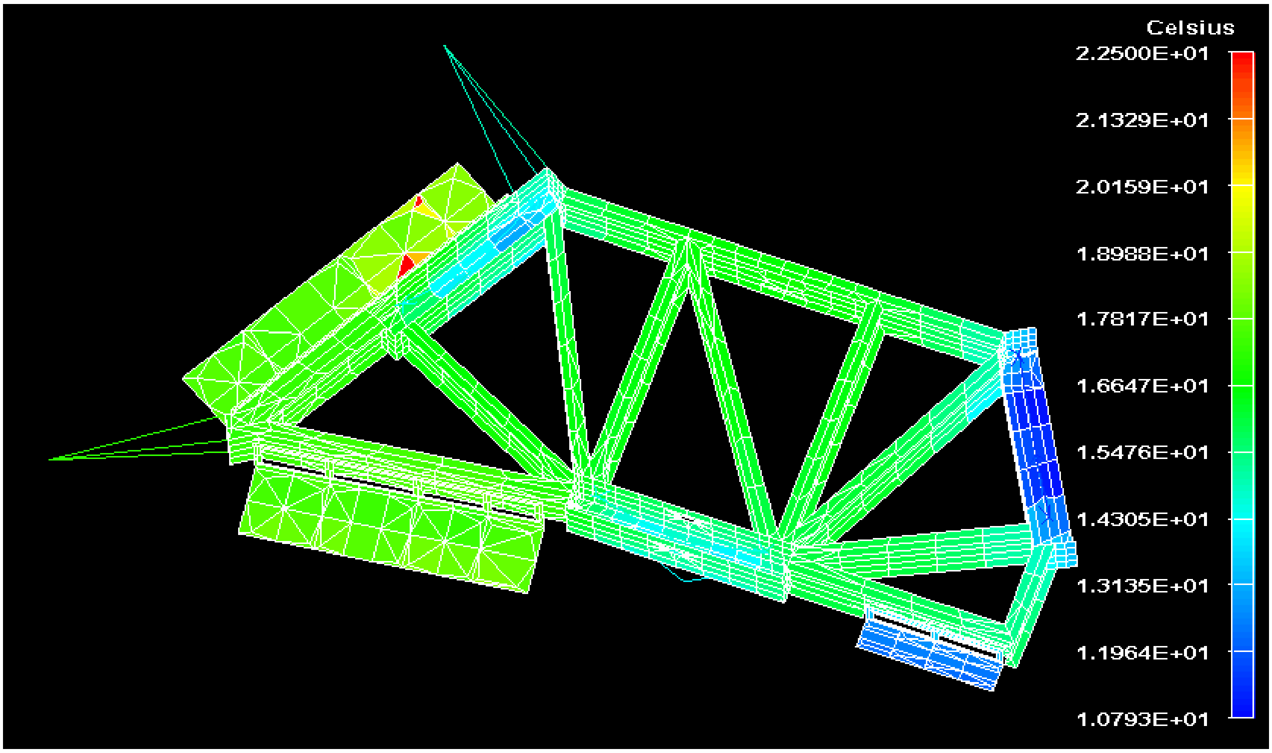

Back-Up

PSS and Electronic Chasses Temperatures: 255 deg Roll

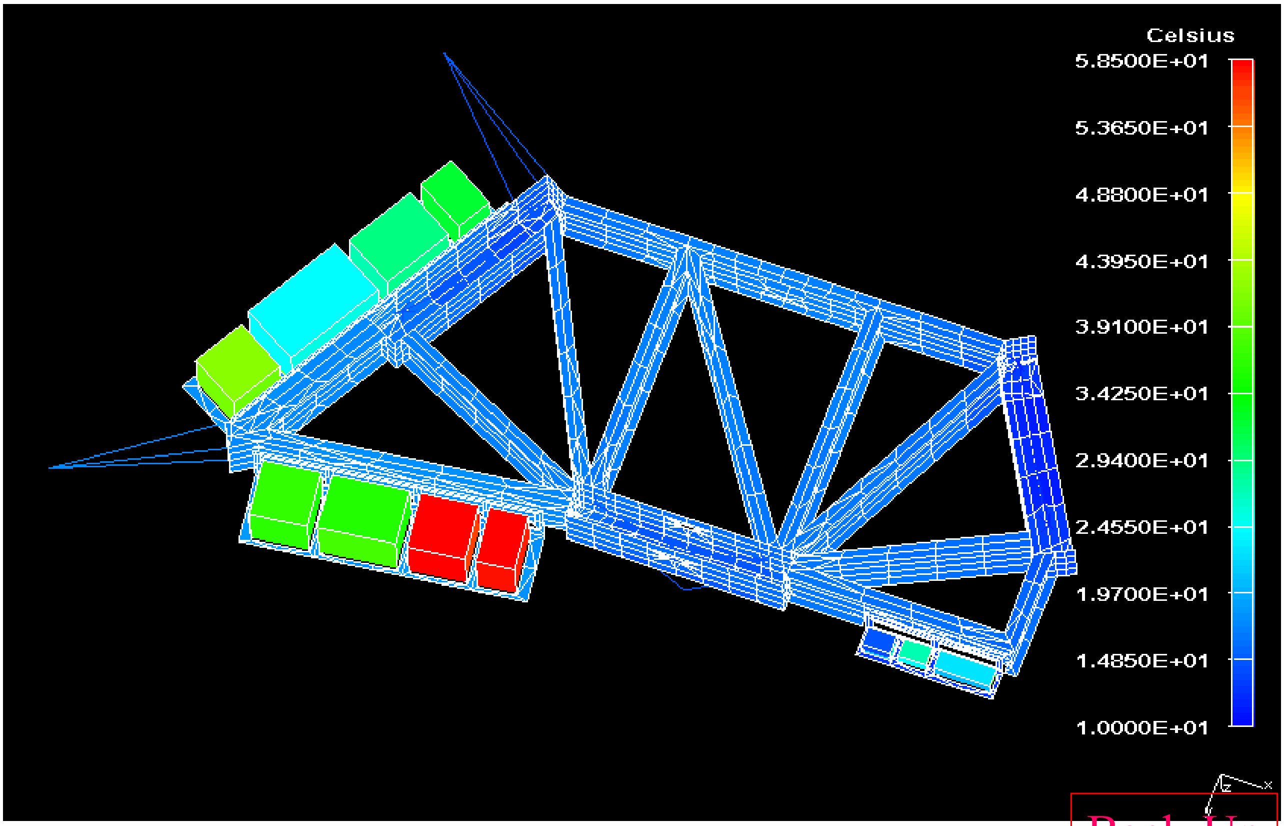

Back-Up

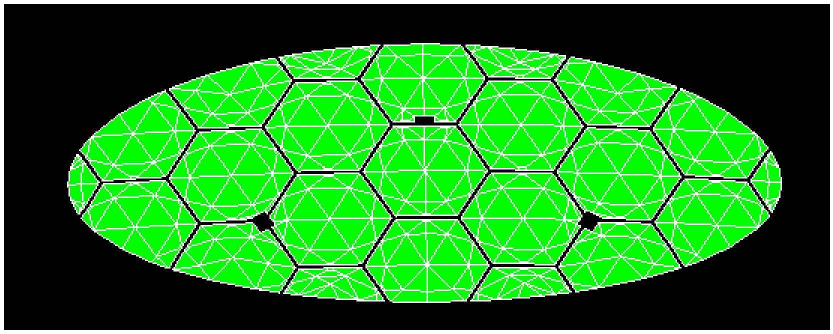

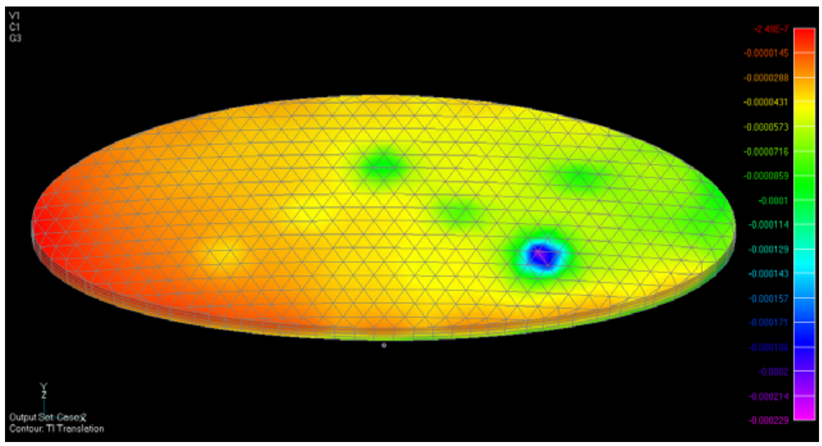
V1
C1
G3
-2.49E-7
-0.0000145
-0.0000288
-0.0000431
-0.0000573
-0.0000716
-0.0000859
-0.0001
-0.000114
-0.000129
-0.000143
-0.000157
-0.000171
-0.000186
-0.0002
-0.000214
-0.000229
Output Set: Case2
Contour: T1 Translation

dT* of Optical Telescope Assembly (OTA) during 30 deg. Dither: Hemi-Hemi

from 195 to 225 deg

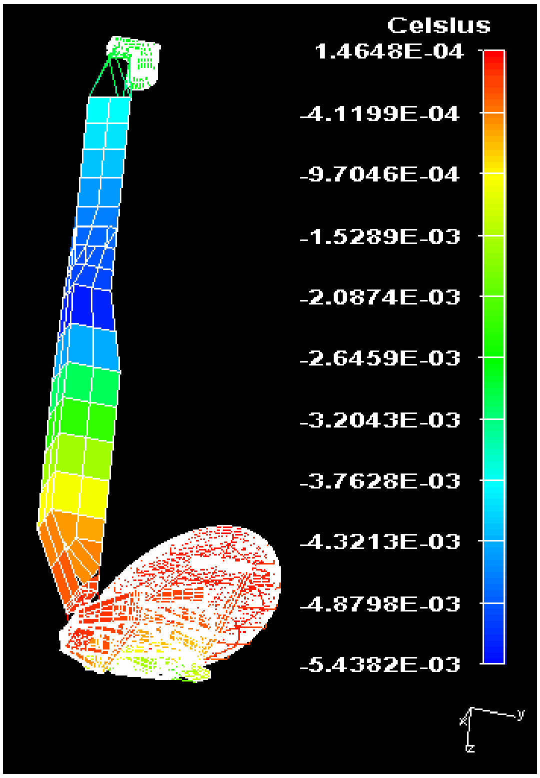

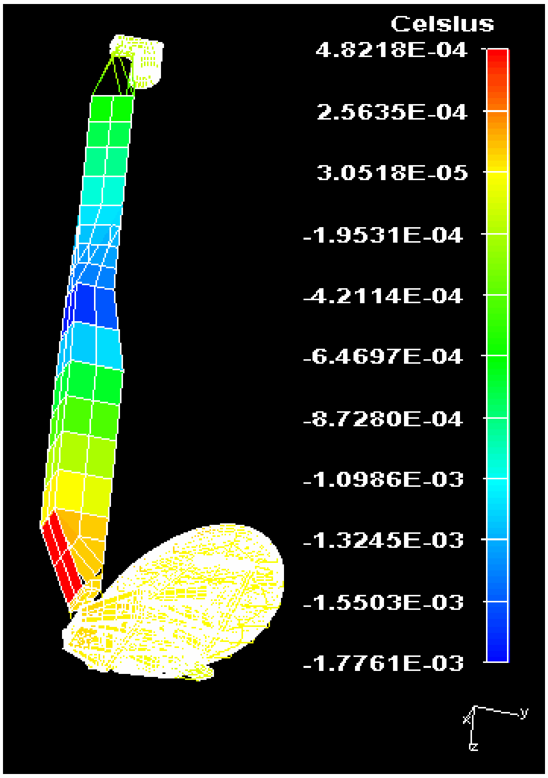

from 255 to 285 deg

* dT is the temp difference between two steady states

dT* of Aft Metering Structure (AMS)and Laser E Boxes during 30 deg. Dither: Hemi-Hemi

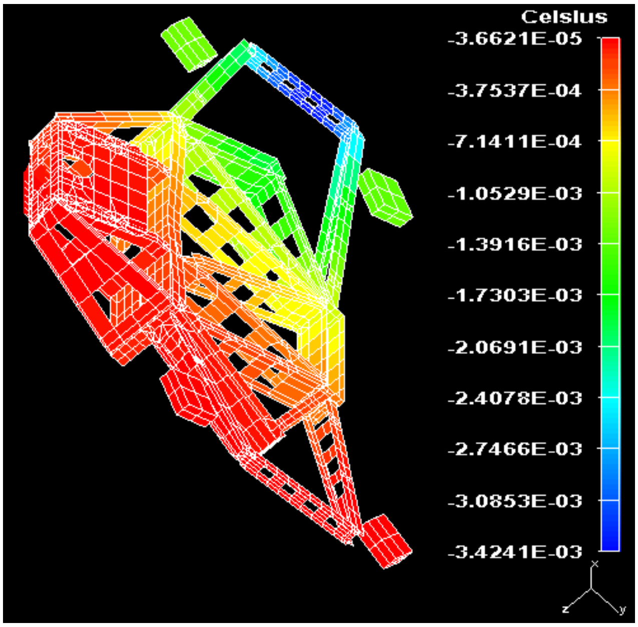

from 195 to 225 deg roll

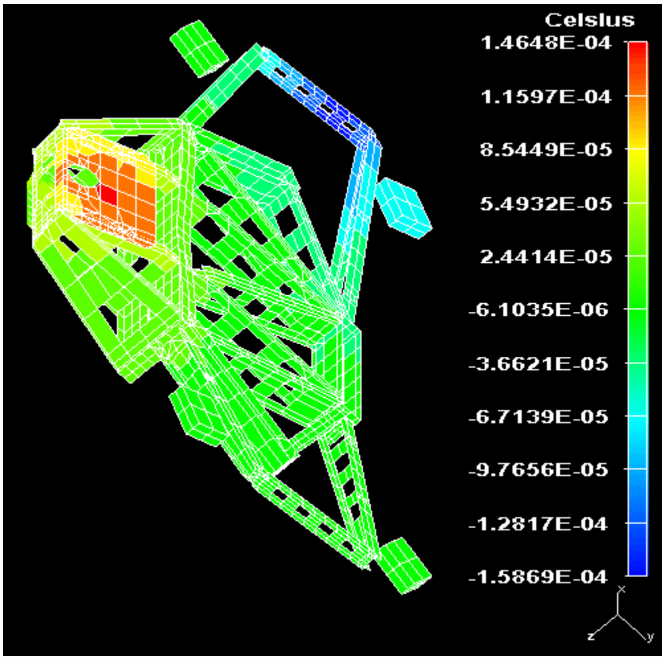

from 255 to 285 deg roll

* dT is the temp difference between two steady states

dT* of Electronics and Payload Support Structure (PSS) during 30 deg. Dither: Hemi-Hemi

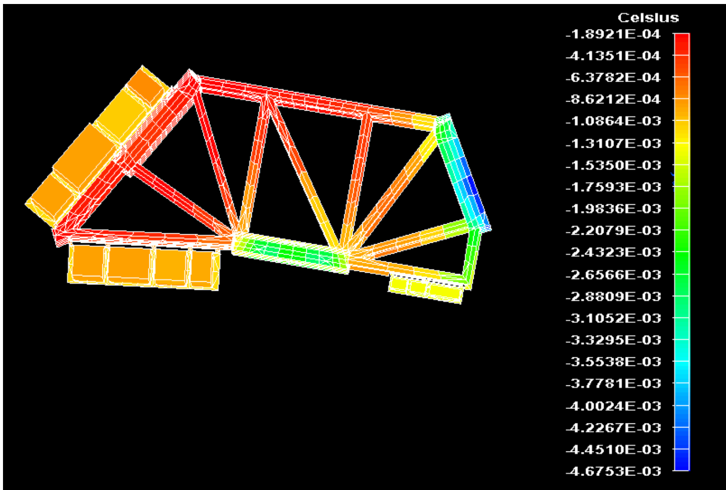

from 195 to 225 deg

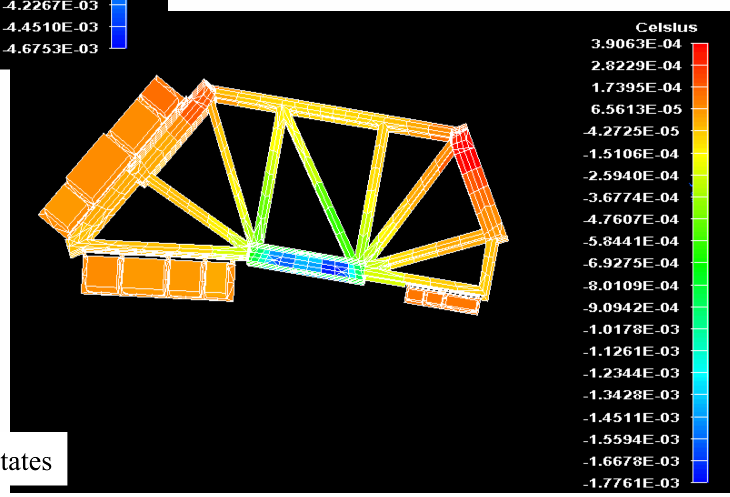

from 255 to 285 deg

Back-Up

* dT is the temp difference between two steady states

Sun at 75 deg to the optic(telescope) axis

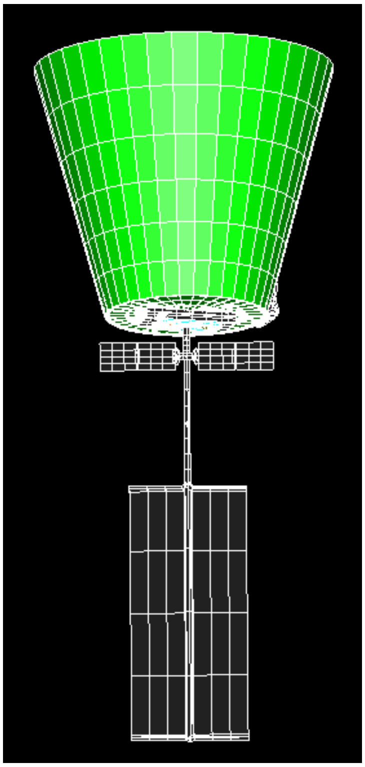

195 deg roll

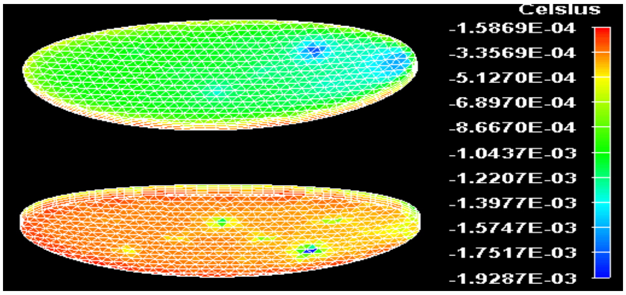

dT during 30 deg Dither from 195 to 225 deg: Hemi-Hemi

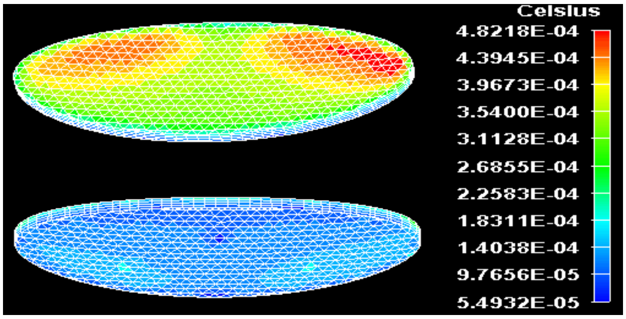

dT during 30 deg Dither from 255 to 285 deg: Hemi-Hemi

Back-Up

Sun at 75 deg to the optic(telescope) axis

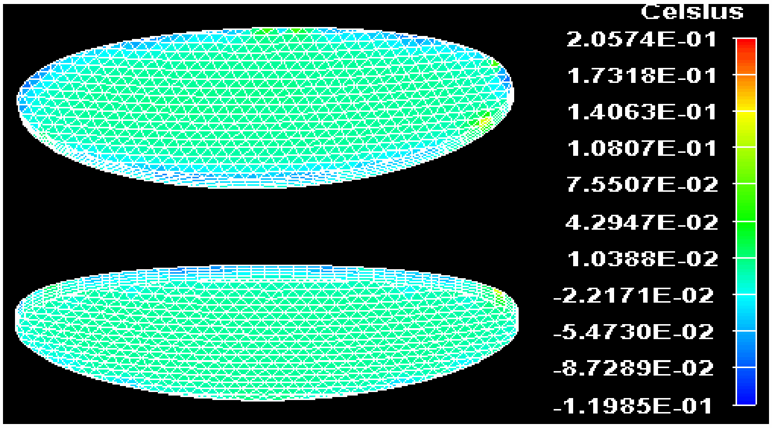

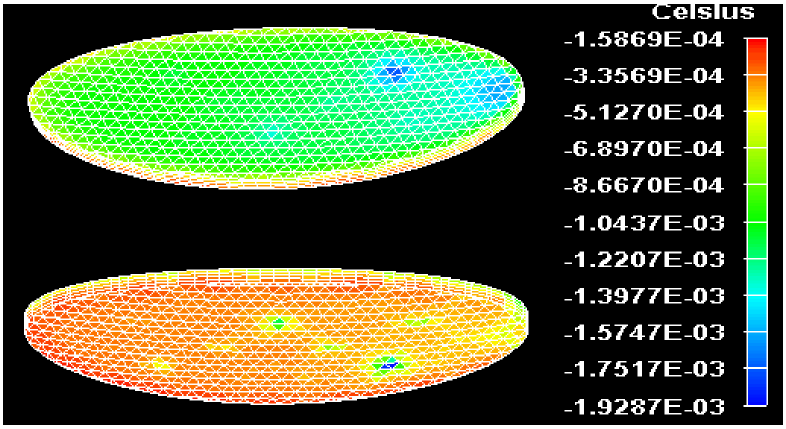

Back-Up

TPF Terrestrial Planet Finder

System Structural Modeling & Performance

Andy Kissil

Contributors:
Eug Kwack, Tim Ho, Sandra Irish, Ichung Weng

11-12 July 2005

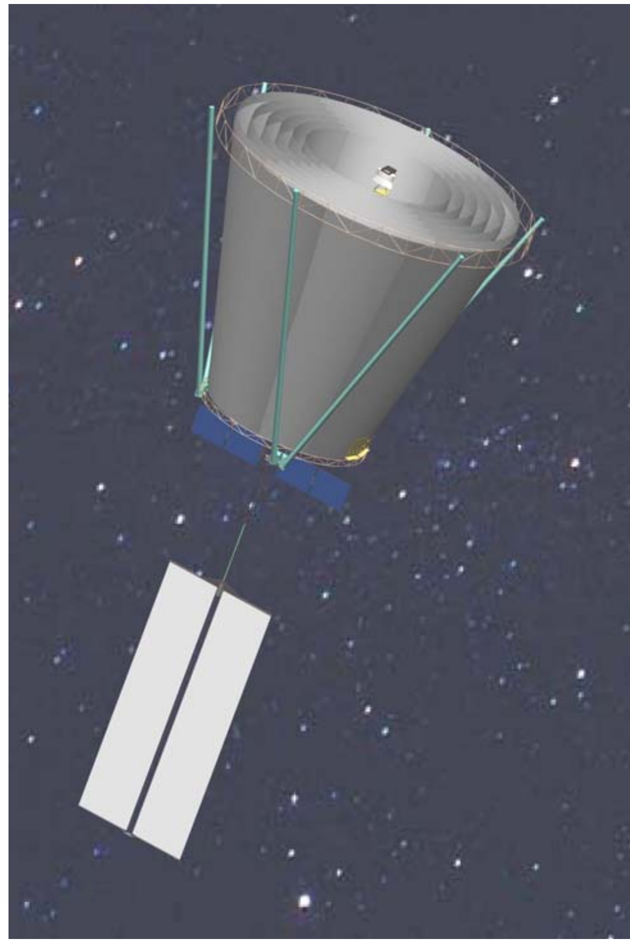

Summary

- Snap-shot of work to date & current status
  - A lot Accomplished, but work is still in-progress
- FEM overview
  - Model fidelity: size/complexity, mass, idealizations
  - Materials
- System performance to-date looks very promising
  - Constant CTE (Coefficient of thermal expansion)
    - WFE due to Primary Mirror Distortion
    - Relative Motion of Rigid Optics
  - Variable CTE
    - WFE due to Primary Mirror Distortion
- System Launch Analysis
- Conclusions & Future Work
  - Computed WFE's & RB motions for thermal disturbance are within error budget

Combined System & Science Payload Finite Element Models Overview

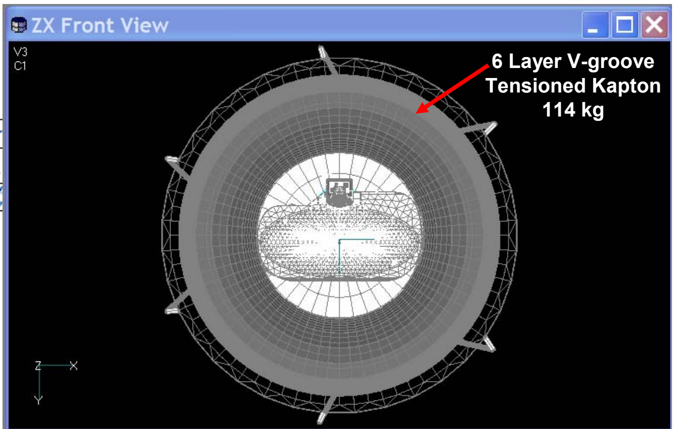

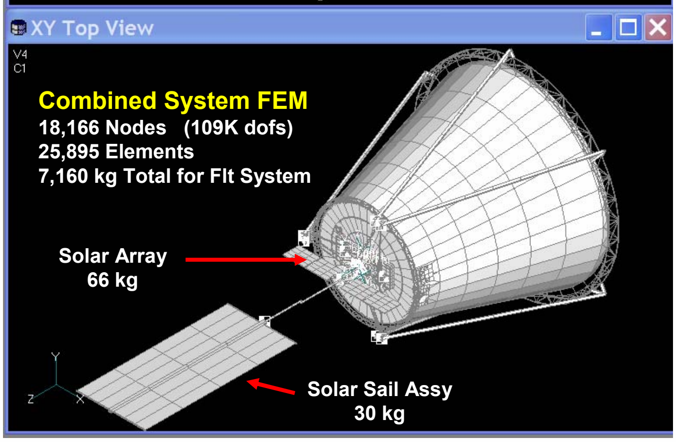

Terrestrial Planet Finder

TPF

IDEALIZATIONS

- No hinges, latches or fittings modeled
- No temperature dependent properties
- Uniform properties for like materials
- Lumped & smeared masses for non-struct hardware to match mass-list
- Uniform, linearized model of tensioned membranes to capture geom stiffness

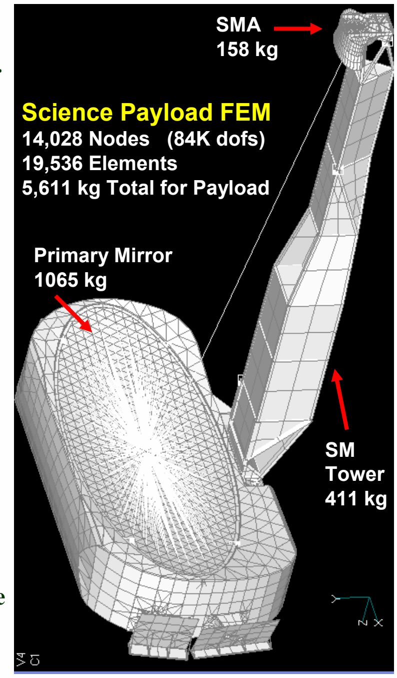

- Mid-Fi PM model captures overall dynamic & thermal distortion, but not local print-thru effects

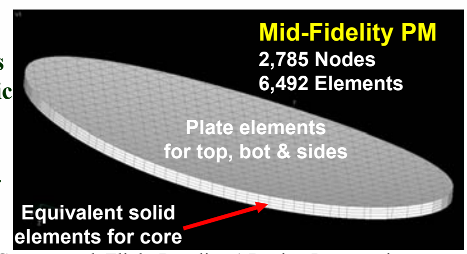

- GSFC modeled the OTA, and JPL modeled the rest of the system & integrated with OTA
- Model is fairly high-level: does not include joint details, fittings, or temperature dependent properties
- The tensioned V-groove sunshield & solar sail are included in the linearized FEM
- There are 2 FEM versions: one with passive isolation between S/C & Payload; and other with two separate free-bodies, connected with an active isolation system
- Mid-Fidelity PM FEM is good for thermal & dynamic response analysis, but cannot capture cell print-thru or detail stresses: Hi-Fi model is used for detail analysis

Slide 273

AK2 Andrew Kissil, 7/5/2005

Detailed View of Science Payload & Spacecraft Bus FEM

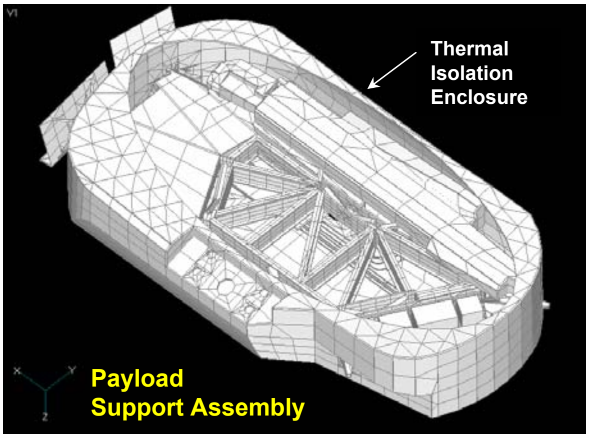

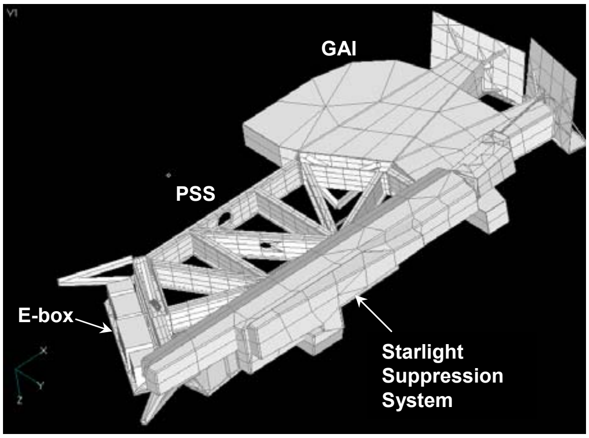

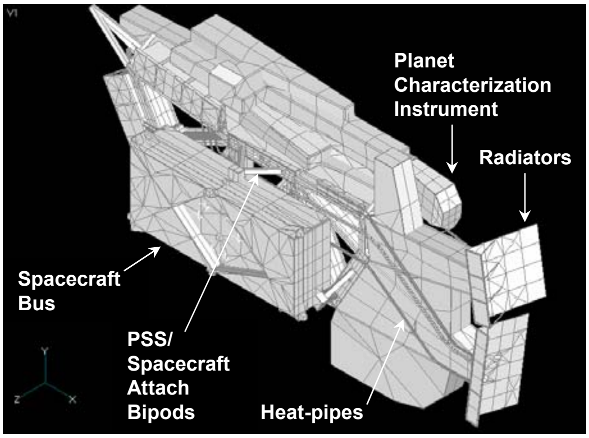

Typical Materials (no temp dep modeled)

ULE Glass: nom CTE= 10 ppb/C, 2210 kg/m^3
M55J/954 CFRP: nom CTE= -250 ppb/C, 1633 kg/m^3
K1100/954 CFRP: nom CTE= -300 ppb/C, 1886 kg/m^3

Mass Summary for Items Shown

Thermal Enclosure = 479 kg
PSS = 368 kg
Starlight Suppression Sys = 422 kg
General Astrophysics Instr = 150 kg
Planet Characterization Instr = 20 kg
Spacecraft Bus = 833 kg

TPF Terrestrial Planet Finder

- The Thermal Isolation Enclosure (the size of a School Bus) is made from isotropic K1100/954 composite: high thermal conductivity, and good stiffness to weight ratio
- PSS is the backbone support structure for Payload Assembly, supporting instruments and OTA
- The PSS & many other support components are made from M55J/954 composite: good strength & decent thermal expansion behavior

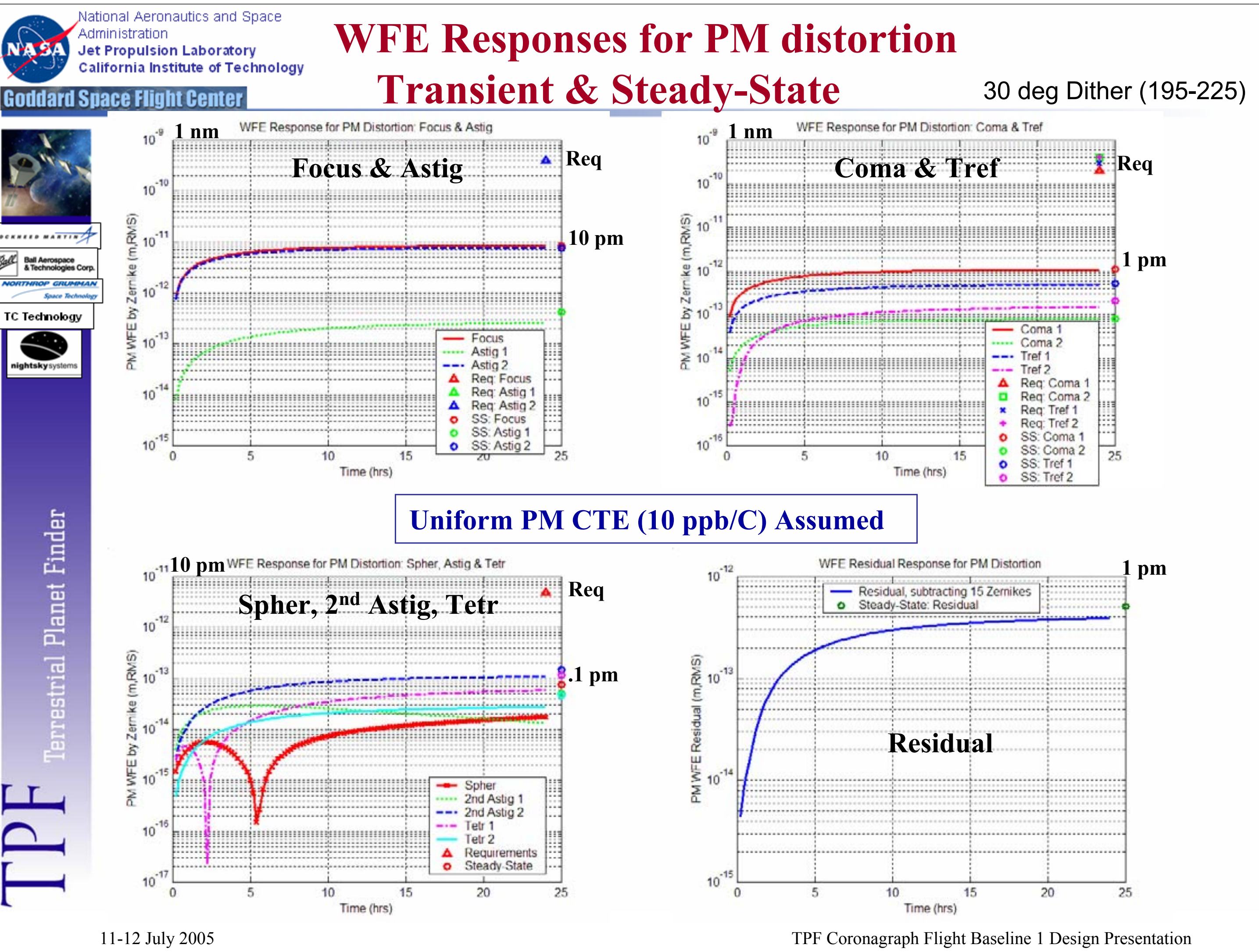

- These WFE responses were computed using a uniform CTE assumption (10ppb/C) for the Primary Mirror material
- The steady-state responses are indicated by the circles at the right edge of each plot
- We are within the error budget requirement levels, which are indicated by symbols in the upper right of each plot
- The residual response level is small enough to indicate that we are carrying enough Zernike terms in our analysis (currently 15)

Focus & Astig Vary with Changes in PM Front-Back Delta-Temp

30 deg Dither (195-225)

Terrestrial Planet Finder

TPF

WFE Response is Dominated by Circular Focus: Bending of PM Induced by Changes in Front-to-Back Delta-Temp

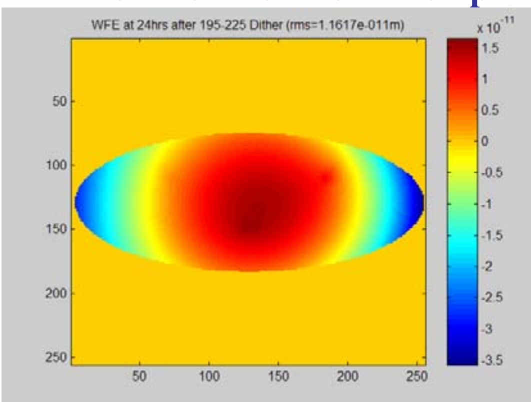

WFE= 11.6 pm rms @ 24 hrs after Dither

~100nm rms / deg C

Slope Verified by Independent Front-Back Delta-Temp Only Run

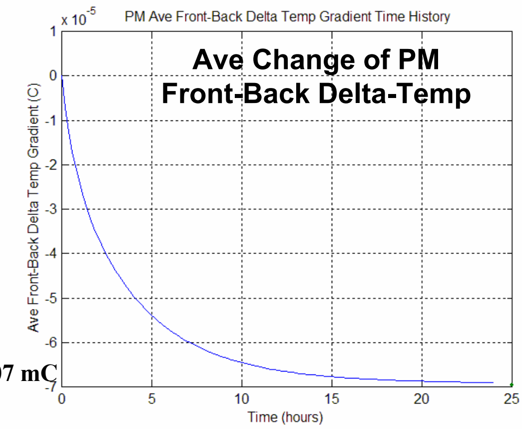

Uniform PM CTE (10 ppb/C) Assumed

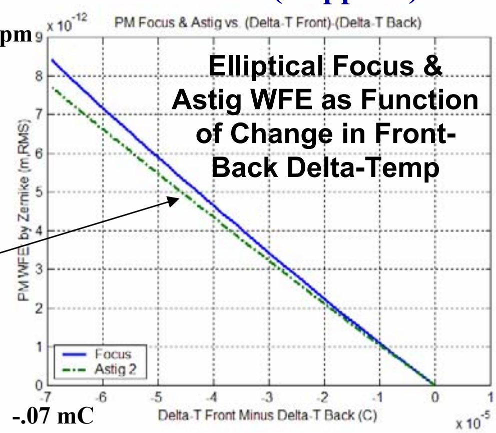

- WFE map, dominated by circular focus, indicates distortion consistent with an overall front-to-back temperature change
- Circular focus maps primarily into focus & astigmatism for elliptical Zernikes
- Ran a separate analysis with ideal changes in front-to-back delta-temps, corroborating the above assertion

Relative Motion of Rigid Optics

Open-Loop Response
30 deg Dither (195-225)

All Optics Motions are Relative to Primary Mirror

Motion Budget Values Derived from Beam-Walk Effects

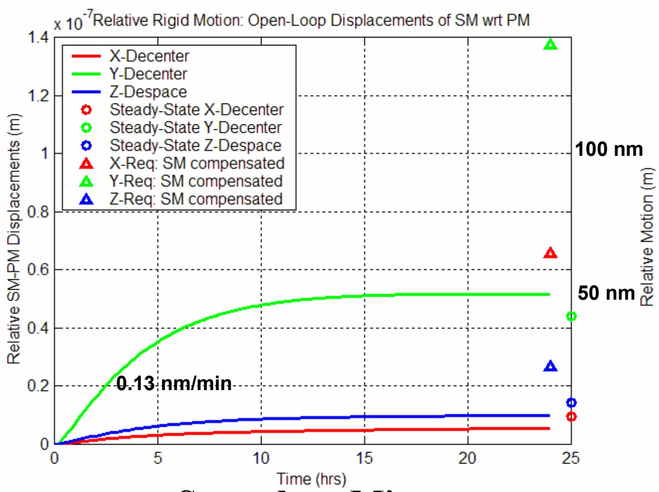

Secondary Mirror

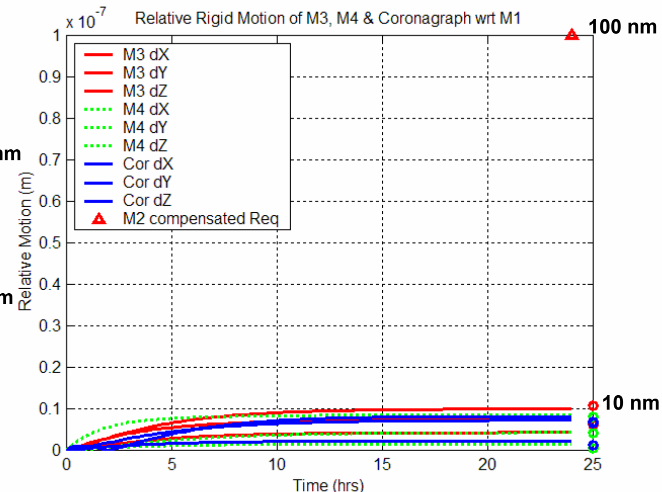

M3, M4 & Coronagraph Box

- **All rigid optics motions are within error budget**
- **M3 & M4 are the first two fold mirrors in train**
- **Assumed constant CTEs (will look at effects of CTE variability)**
- **No hinges, latches or fittings modeled yet**

Terrestrial Planet Finder
TPF

- The relative rigid body motion of the individual optics effects beam-walk
- Our analysis shows that we are within the current error budget allocations
- The secondary mirror motion can be compensated for with it’s 6dof actuator (& metrology system), however, these motions were small enough not to need compensation
- Future studies will add more analysis detail to address idealizations made thus far

Monte-Carlo Study of Primary Mirror CTE Variation

- **Modeling & Analysis done using IMOS: generated 1000 Random (with structure) element CTE distributions**
- **Each of the 92 regions (23 segs x 4 layers) of the mirror were given CTE variations four functions: bias, side to side, radial & axial**
- **Function parameter values randomly set consistent with TDM CTE Specifications**

TDM PDR CTE Specs

(used by Kodak)

INITIAL MIRROR CTE TOLERANCES		
No.	Description	Tolerance (ppb/C)
1	Weighted Blank Average	+/- 10
2	Core Segment Axial Gradient	+/- 10
3	Core Segment Radial Range	< 15
4	Max Core Segment-Segment Average Delta	< 10
5	Face Plate Axial Gradient	+/- 5
6	Face Plates Pt-to-Pt Difference	< 5
7	(Face Plate Average) - (Core Segment Average)	+5 to +15

Overall CTE Statistics for PM

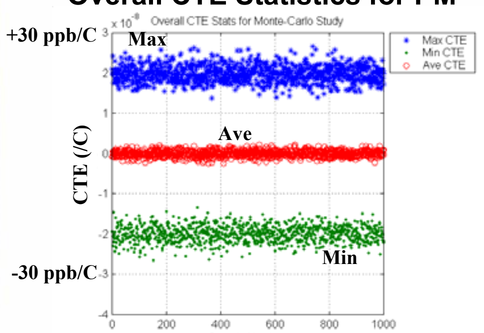

Sample CTE Distribution (1 of 1000)

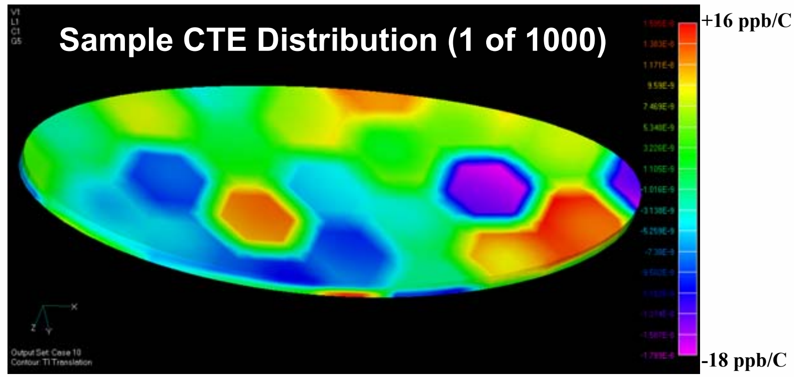

- Analysis was performed using an IMOS model, in which the element CTE's were factored out (IMOS greatly simplifies data handling for the 1000 load cases)
- The parameter ranges used in association with the 4 functions were consistent with the TDM (Tech Devel Mirror) CTE tolerances
- Overall, the CTE's varied within +/- 30 ppb, even though the variation within an individual boule is tighter
- The lower right image shows color contours of the CTE distribution for one of the 1000 trial sets

National Aeronautics and Space Administration
Jet Propulsion Laboratory
California Institute of Technology
Goddard Space Flight Center

Monte-Carlo Study of Primary Mirror CTE Variation

TC Technology

TPF Terrestrial Planet Finder

Steady-State Dither Results
30 deg Dither (195-225)

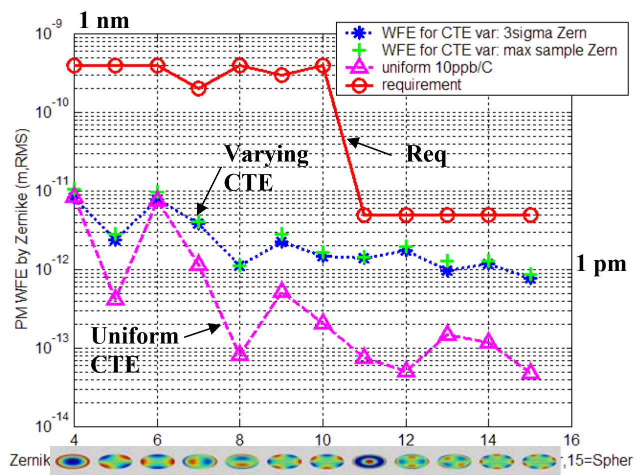

- **Current WFE performance is within error budget** (more conditions consid in future)

  Can be significantly improved with segment positioning based on measured CTEs
- **Need to consider CTE variability**: uniform CTE assumption is not conservative
- Can determine allowable **PM CTE tolerances** with this type of analysis

- So far, all the computed WFE's are within the error budget
- Results for uniform CTE assumption are not conservative: i.e. they generally underestimate the WFE
- We still need to look at Sun positions behind Telescope, including shadowing effects
- We also still need to address CTE temperature dependence
- If needed, we can significantly improve performance with segment positioning based on CTE measurements of the actual boules, as demonstrated in the Minimum Mission Study

System Launch Analysis

Normal Mode Frequency

LV Payload Req (Delta IV-H): 8Hz Lat, 30Hz Axial

Computed from FEM: 7.4Hz Lat, ~25Hz Axial
Close to req freq - can be improved

Non-compliance is not a big issue - CLA

Stress (Combined 6G Axial & 0.5G Lateral, Quasi-static)

Check that stresses are not excessive

PSS (M55J): ~**0.06 GPa** (**9 ksi**) (~45 ksi Allow)

Strut (K1100): ~**0.14 GPa** (**19 ksi**) (~36 ksi Allow)

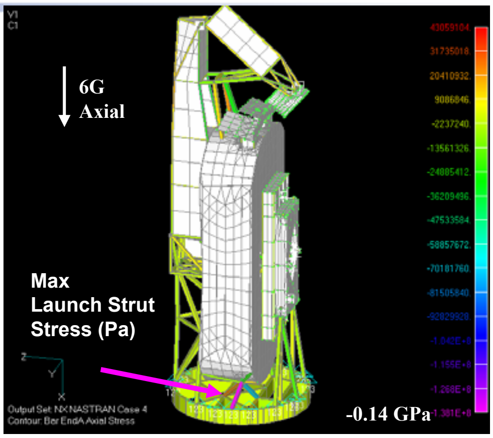

Max PSS Stress (Pa)

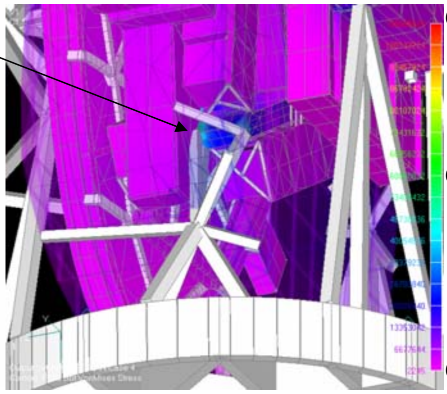

0.1 GPa
0.06 GPa
0 GPa

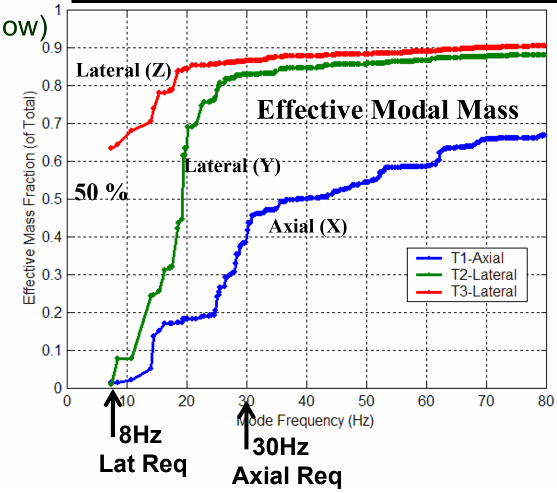

TPF Terrestrial Planet Finder

- This is our first iteration for the launch support design
- Computed frequencies for stowed configuration are close to, but slightly below LV requirements
- The frequencies can be increased with standard engineering practices for design improvement
- Stresses are at reasonable levels, and can be reduced even more without drastic design changes

Wrap-Up

Conclusions

- **Toolsets work well**, and are getting better (looking forward to significant capability increase shortly)
  Lessons-learned: problems encountered & solved (or temporarily worked-around)
- **Currently, all computed WFE's & RB motions for thermal disturbance are within error budget**
- **We need to account for CTE variation in PM:** Taking CTE variation into account generally results in higher WFEs than assuming uniform CTE of 10 ppb/C
- **Focus & Astigmatism are biggest contributors to WFE**
  Due to changes in PM front-to-back delta-temps
- **Design feasibility looks good: no major road-blocks**
  Keep in mind the many idealizations made so far (snapshot): more detail modeling to follow

Future Studies

- Look at effects of **Sun locations** behind Telescope (including shadowing), and **heater power control**
- **Optimize launch support structure**: reduce mass & increase stiffness
- **Optimize whole Fight System**: reduce mass & improve performance
  Look at **material trades, variability & light-weight sections**
- **Quantify analysis tool accuracy & precision** (Testbed correlation will provide ultimate validation)
- Proceed to **FB2 Design & Modeling, and more detail** added

✓Toolsets have worked well overall, requiring some modifications as we go along, and improvements are in the works

✓So far, our analysis demonstrates design feasibility, but we still need to address additional levels of analysis detail

✓We need to account for CTE variation in PM to properly predict performance

✓PM front-to-back delta temps dominate thermal induced WFE

✓Future improvements to FB1 are straight-forward good engineering practices (no leaps of faith required)

Backup Slides

Temperatures for 195deg Sun Angle (deg C)

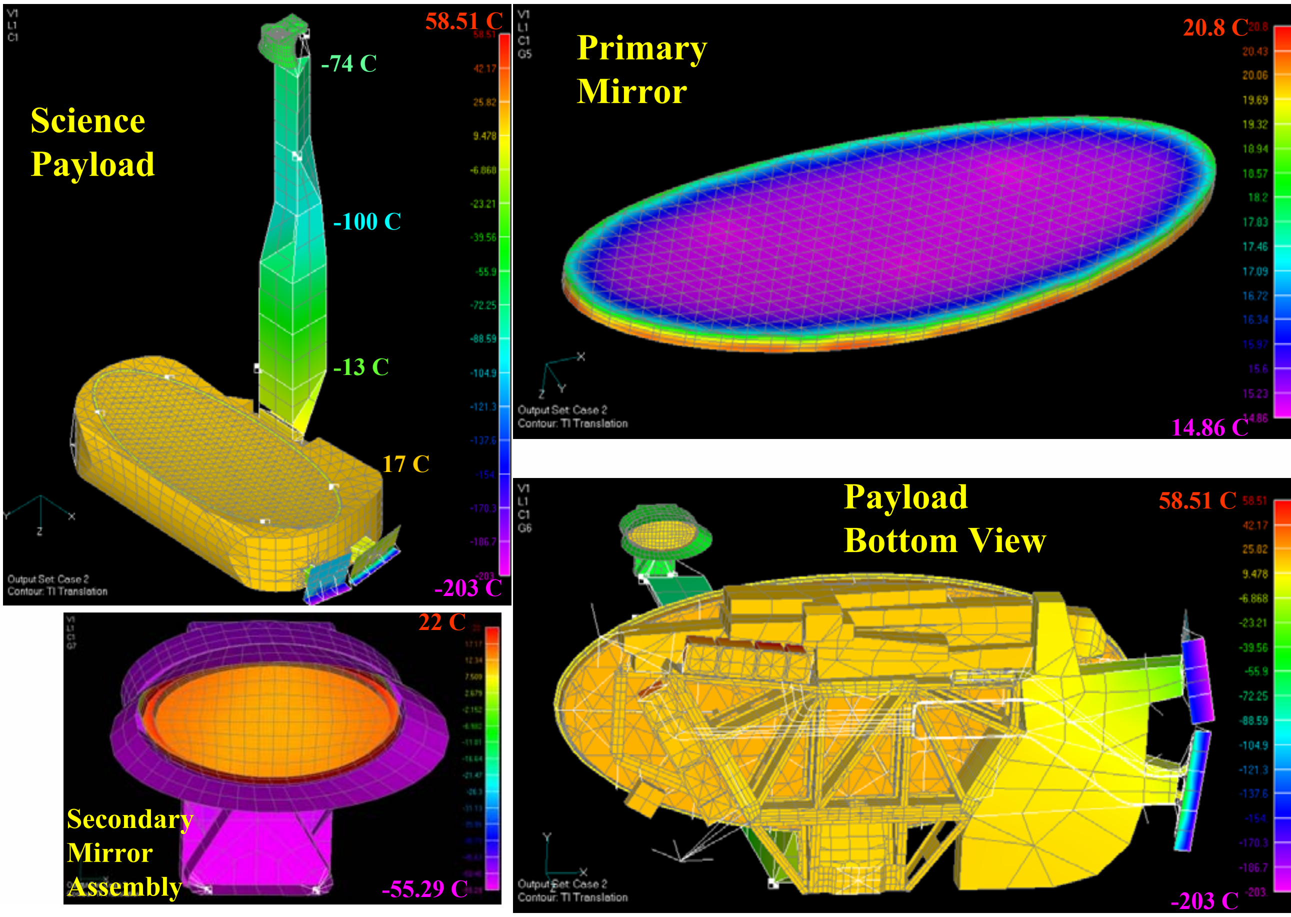

- Coldest temperature occurs on the radiator, as it should
- Intermediate cold-spot occurs at mid-span of SM tower, as expected
- PM has ~6 deg C temperature variation: cold center, and warmer toward the edge & bottom heaters

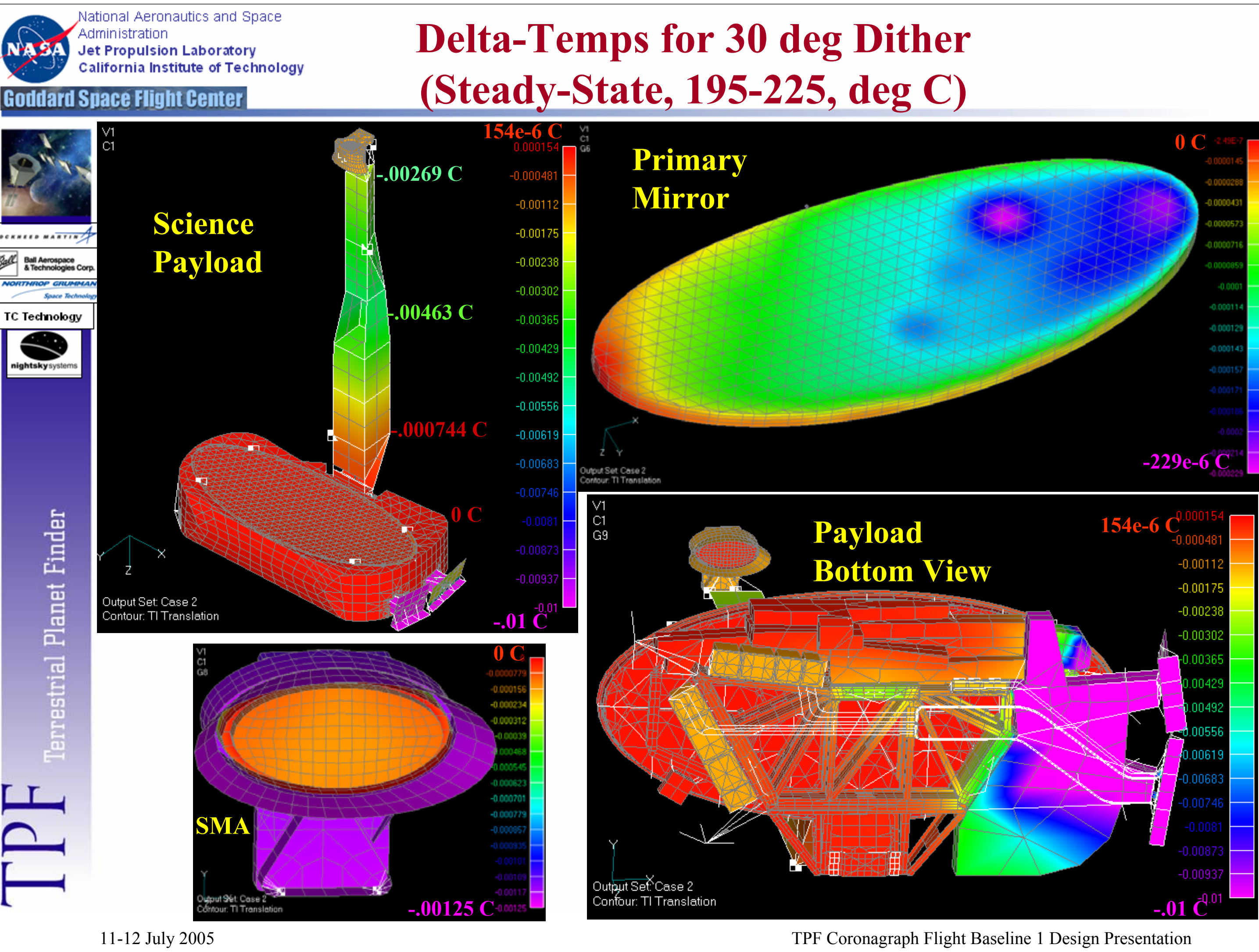

- Overall, largest delta temps occur at the radiators
- Bottom right pic shows large temperature changes are occurring in the region of the radiator support structure
- Upper right indicates that these large delta-temps are influencing the PM via the closest bipod

In-Orbit Performance with Thermal Disturbance from Dither Maneuver

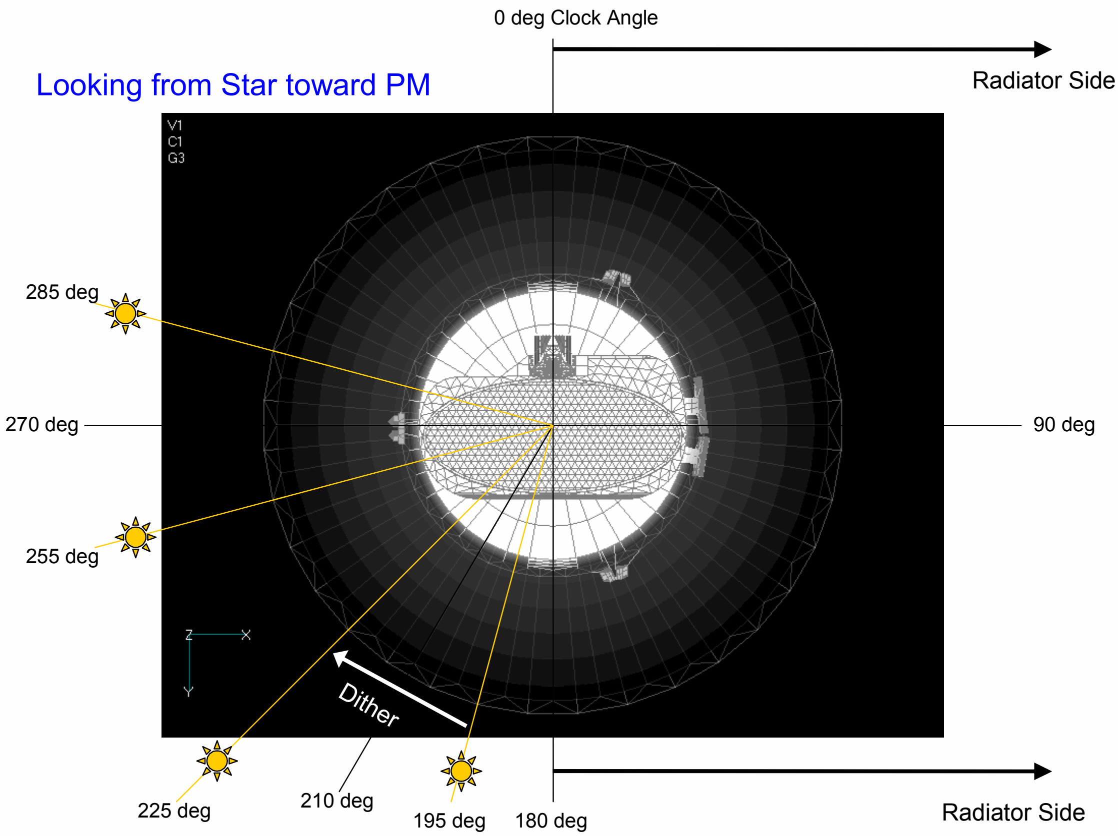

- This picture shows a view looking from the target star toward the PM, with the SM tower in the 12:00 position
- We refer to Sun orientations angles with 0 deg at 12:00, and increasing in the clockwise direction as viewed here (the Sun angle will never be in the 0-180 deg range)
- Three 30 deg dithers are currently required for the planet detection process: 60 degrees apart
- So far, we have analyzed two dither scenarios: 195-225 & 255-285, both with the Sunlight coming from a direction normal to the bore-sight

Monte-Carlo Study of Primary Mirror CTE Variation

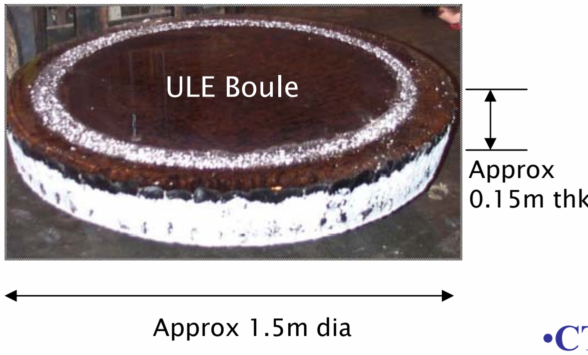

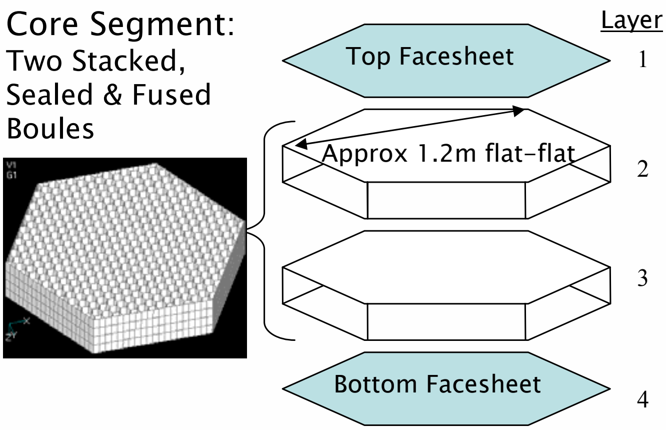

- **CTE was varied by region**
- **There are 92 regions used**
  - 4 layers x 23 segments
- **CTE variation functions used:**
  - **Bias** or piston
  - **Side to side** variation along x & y dir
  - **Radial** (in xy plane)
  - **Axial** (along z-dir)

TPF Terrestrial Planet Finder

- Consider each core segment to be constructed by stacking, sealing & fusing two boules
- CTE was randomly varied using 4 functions for each of the 92 regions within the mirror

Delta-Temps for 30 deg Dither (195-225, deg C)

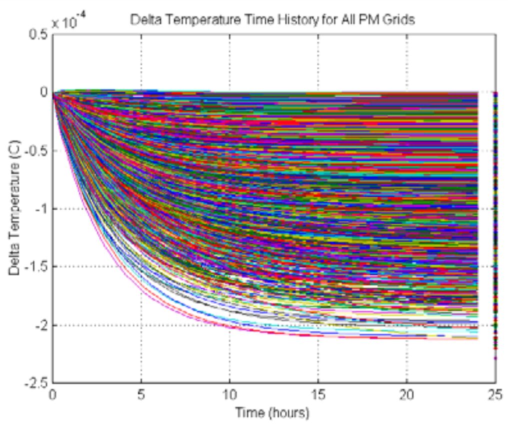

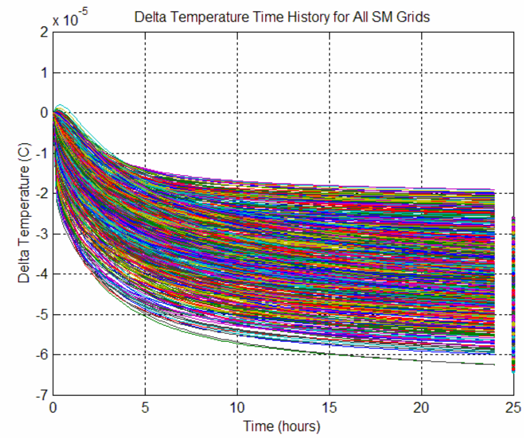

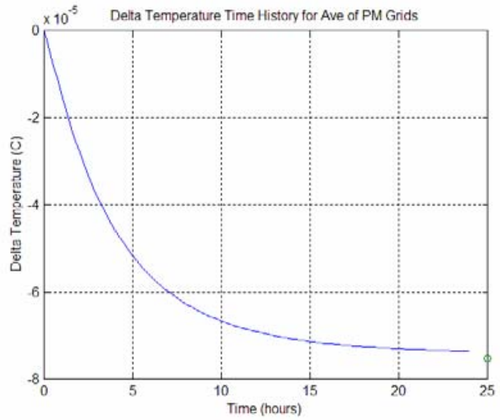

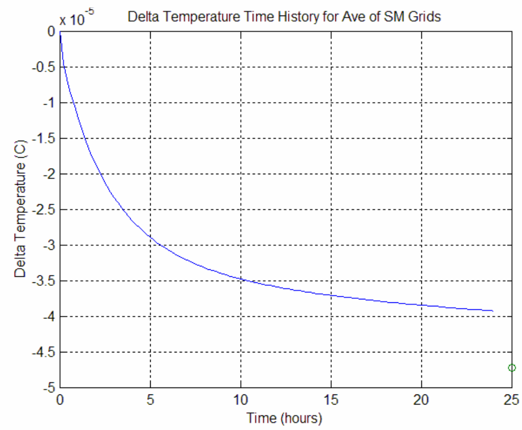

Monte-Carlo Study of Primary Mirror CTE Variation

Steady-State Dither Results Comparison

30 deg Dither (**255-285**)

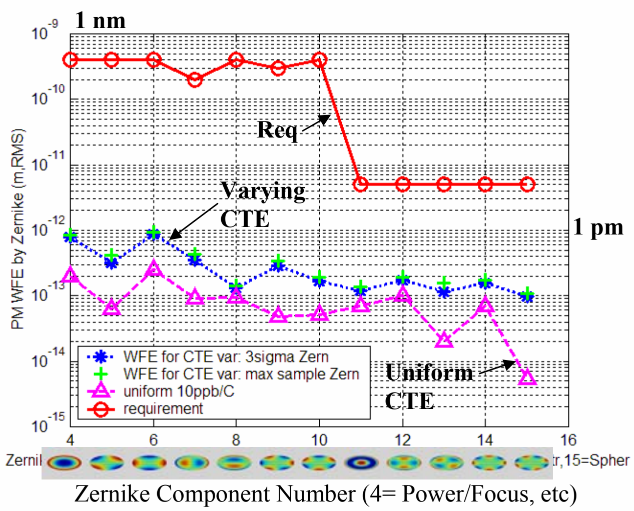

30 deg Dither (**195-225**)

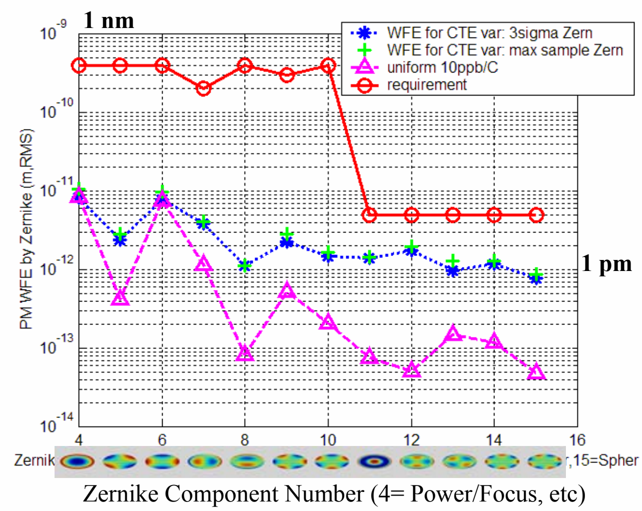

- **Current WFE performance is within error budget** (more conditions consid in future)

  Can be significantly improved with segment positioning based on measured CTEs
- **Need to consider CTE variability**: uniform CTE assumption is not conservative
- Can determine allowable **CTE tolerances** with this type of analysis

TPF Terrestrial Planet Finder

- Results for uniform CTE assumption are not conservative: i.e. they generally underestimate the WFE
- So far, all the computed WFE's are within error budget
- We still need to look at Sun positions behind Telescope, including shadowing effects

Primary & Secondary Mirror Temps for 285deg Sun Angle

Temps in deg C

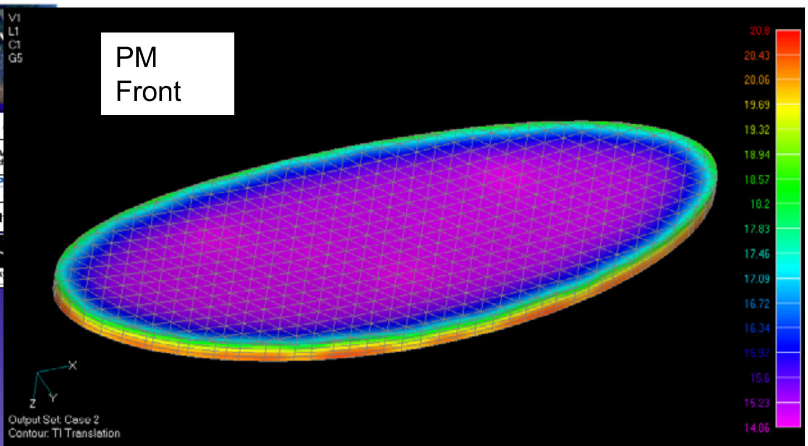

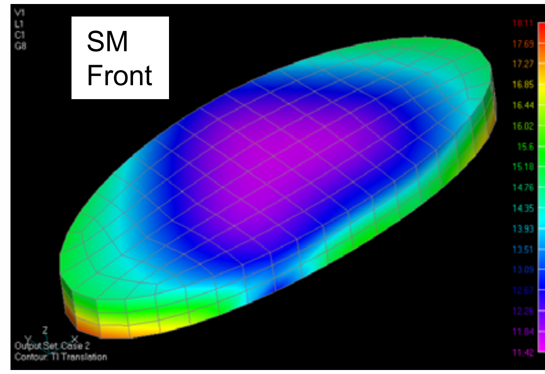

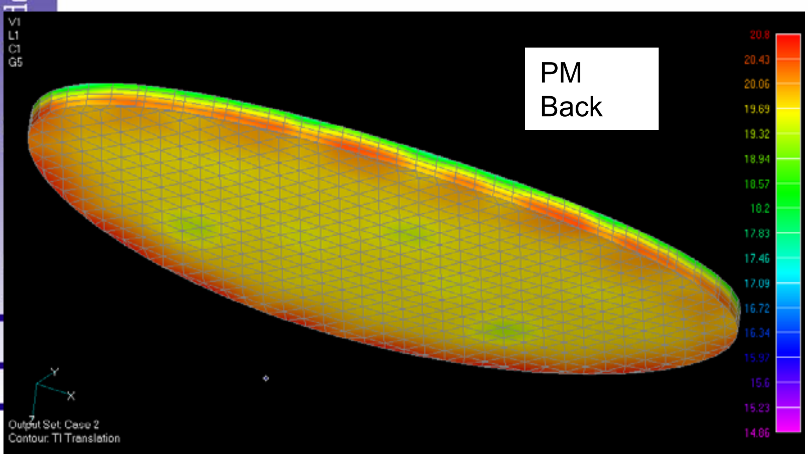

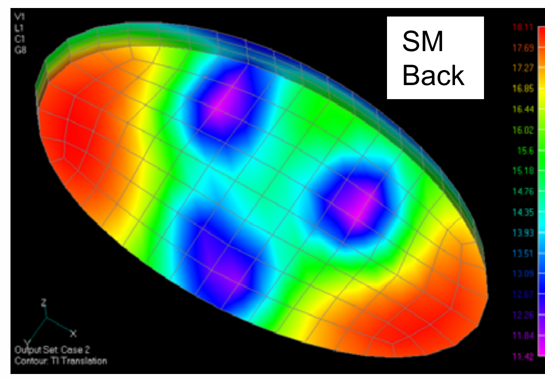

TPF Terrestrial Planet Finder

Delta Temp Contours

30 deg Dither (255 to 285 deg)

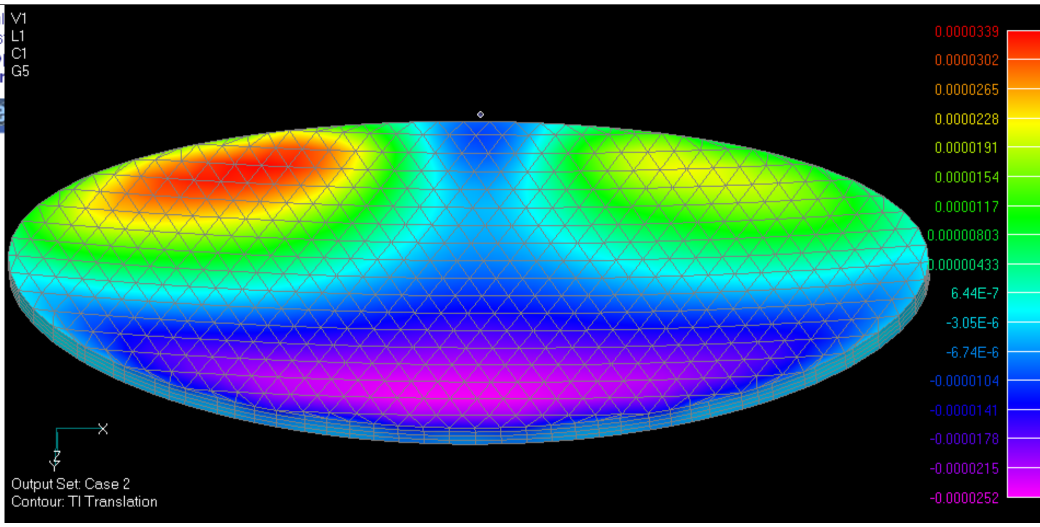

Steady-State

PM Front

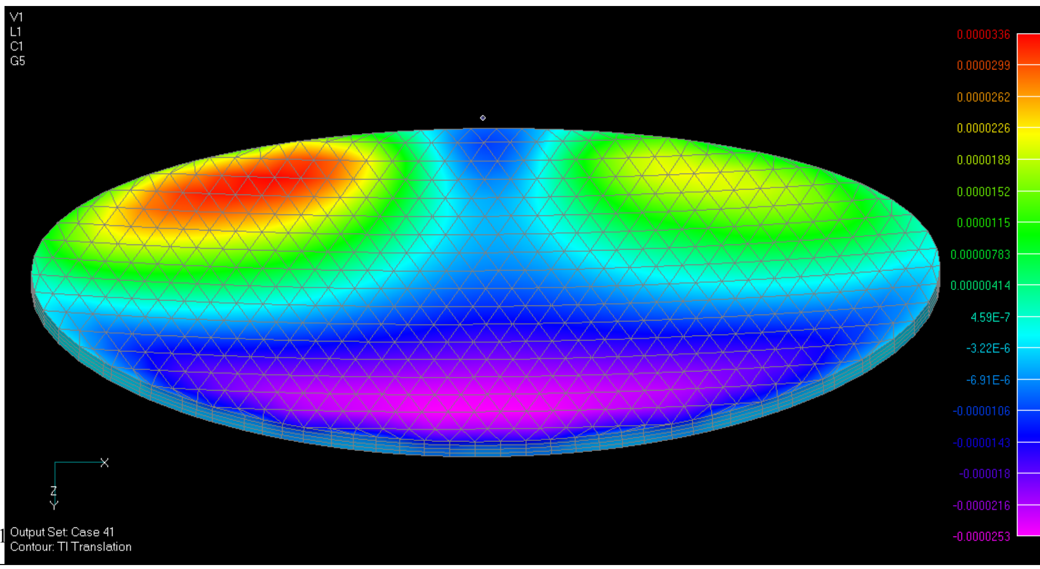

Transient after 24 hrs

Click picture to run animation of Delta Temp Contour Change over Time

30 deg Dither (255 to 285)

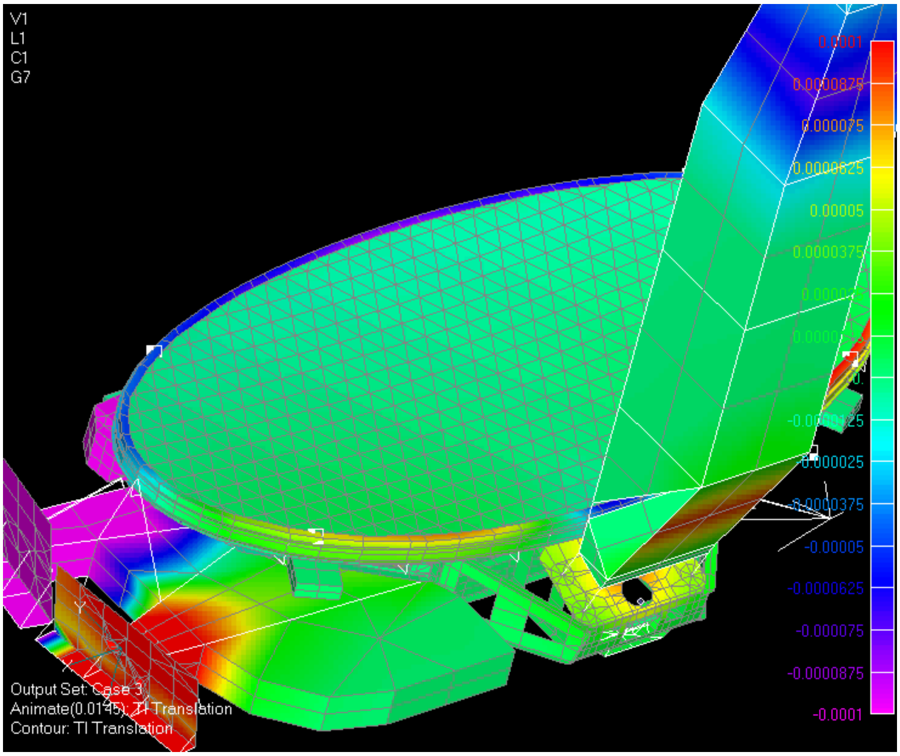

Click picture to run animation of Delta Temp Contour Change over Time

30 deg Dither (255 to 285)

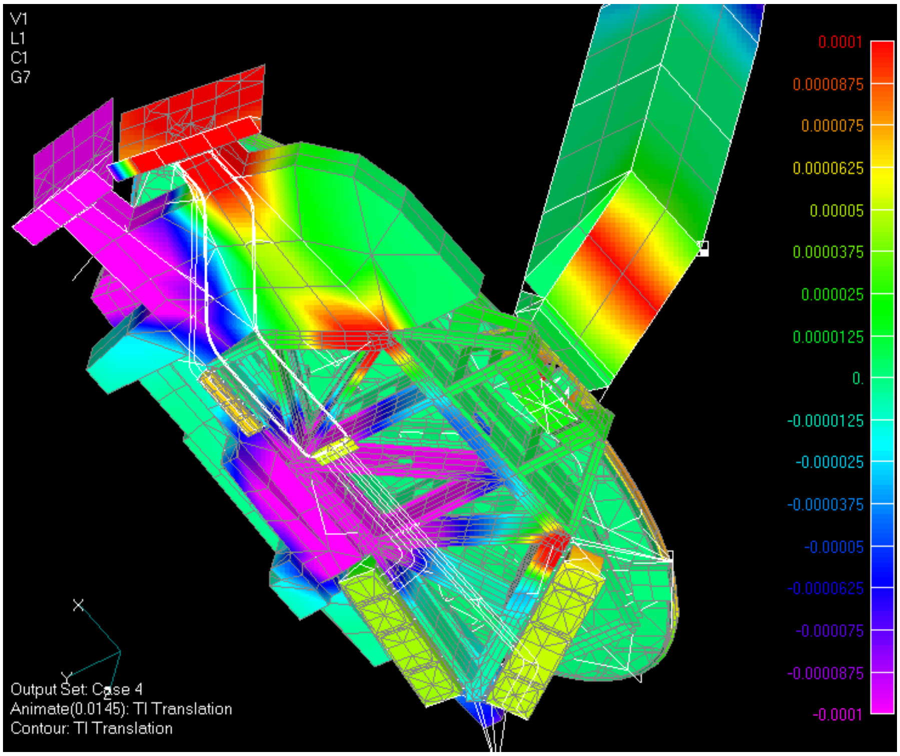

Combined System Normal Modes Used for Dynamic Response Analysis

- Very high modal density, due to presence of sunshield and solar sail

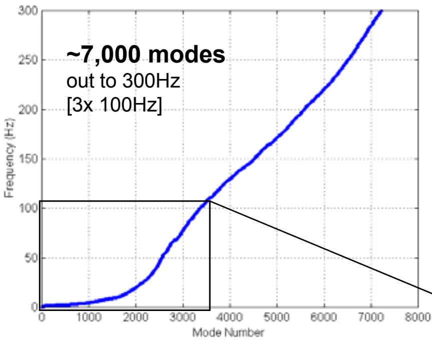

Fraction of Modal Strain Energy in Shield/Sail Assy

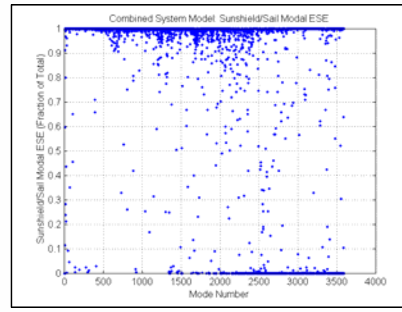

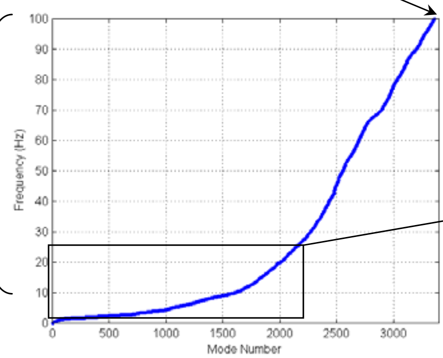

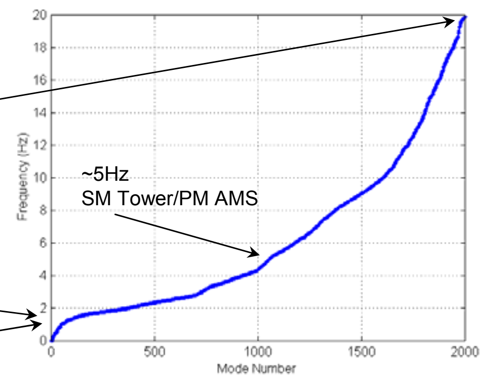

TPF Terrestrial Planet Finder

Primary Mirror (PM) Structural Models, Performance Results, & Future OTA Studies

Sandra Irish/GSFC

Contributors:
Ichung Weng/Swales Aerospace
Jeff Pattison/GSFC
Erik Benedetti/GSFC

11-12 July 2005

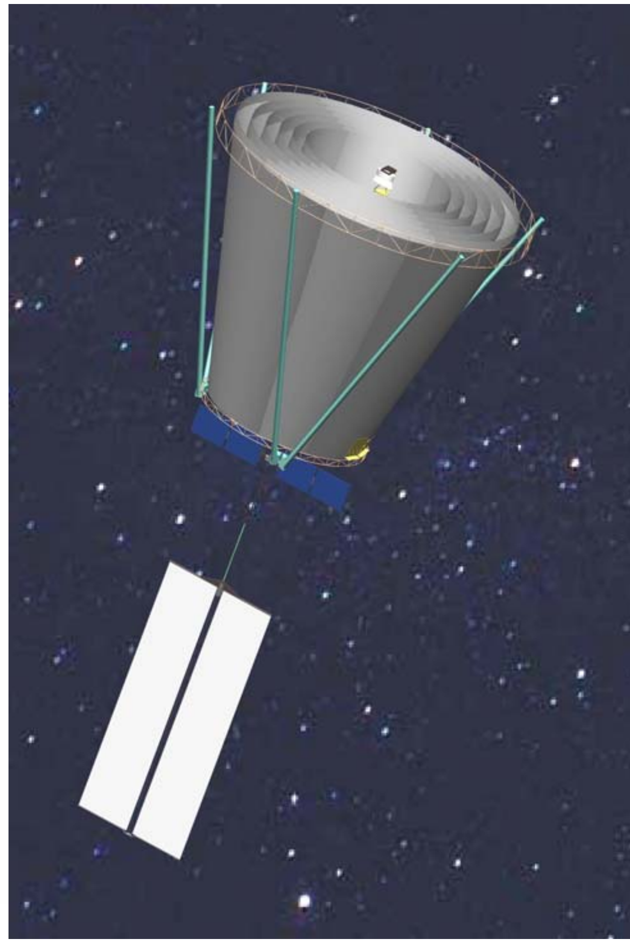

- This presentation will focus on the structural models and structural analysis that are being performed for the TPFC primary mirror (PM). In addition, future analysis that are planned for the OTA and the PM will be discussed. This work is being presented by Sandra Irish, OTA Structural Analyst, who works in the Mechanical Systems Analysis and Simulation Branch at GSFC. Other contributors to this work include, Ichung Weng, who is a structural analyst at Swales Aerospace, and Jeff Pattison and Erik Benedeitti, who are also structural analysts from GSFC.

Executive Summary for the Primary Mirror (PM) Structural Models, Performance Results, & Future OTA Studies

- **The following structural analyses have been performed for the OTA and the PM:**
  - Developed the OTA structural model for use in the TPFC integrated system performance analysis
    - OTA structural model was developed and provided to JPL. The model was used in integrated dynamics and thermal performance analysis. On-orbit dynamics is acceptable for active design, but marginal for passive design. Thermal stability was found to be acceptable.
    - Developed low, mid, and high fidelity structural models of the PM to be used for various structural analyses.
  - Acoustics analysis to estimate load to PM from Delta IV-H fairing
    - AutoSEA analysis performed and estimated a max load of 10 G applied to the PM due to either a metal or composite fairing
  - OTA and PM dynamics
    - First OTA free-free mode was found to be 7.1 Hz, due to tower bending. First mode of the PM with its mount was found to be 20.6 Hz.
  - PM gravity sag for ground testing concern
    - Maximum deflection of the PM with its mount due to 1 G loading applied perpendicular to the mirror was found to be .473 mm. Optical performance due to gravity sag was also predicted.
  - PM launch load stress analysis
    - The analysis showed that the PM has a negative margin of safety for the flight baseline 1 design concept. However, an option to obtain a positive margin of safety in the PM is to add weight of 414 kg as well as 8 launch locks. Still investigating additional design alternatives.

- **Future structural analyses for the FB1 design of the OTA and the PM include:**
  - Weight optimization of the PM, AMS, and SMA.
  - Sensitivity to PM mount design, location, and stiffness
  - PM Quilting Effects (PM deformation due to thermal loads)
  - Stiffness analysis of SM tower due to stiffness of hinges/latches
  - PM open-back versus closed-back structural/thermal analysis.

- **The results of all these structural analyses will help in developing the design concept for the PM and OTA for the flight baseline 2 analyses.**

- This chart is a top level summary of the structural analysis work that has been performed for the flight baseline 1 design of the OTA and PM and the future structural analysis work that will be performed. The first bullet lists the structural analyses that have been completed. The statements in red give a very brief summary of the results of that particular analysis. The second bullet lists the structural analyses that still need to be completed. The results of all these analyses will provide meaningful information that will be used to tailor the mechanical design that will be studied for flight baseline 2.

Outline of Presentation

- Objectives
- PM Structural Models
- Gravity Sag
- Dynamics Analysis
- Launch Loads and Acoustics Analysis
- Stress Analysis due to Launch Loads
- Future PM and OTA Studies
- Conclusion

- This chart explains the topics that will be discussed in this presentation. The presentation will start with a discussion of the purpose of the PM structural analyses, then discuss the results of the analyses that have been performed, and finally, the presentation will discuss the future analyses that are planned. The picture in the lower right hand corner shows the CAD model of the PM and its mounts. This is the hardware that will be discussed in this presentation.

Objectives

Structural analyses are being performed to:

- Develop the OTA structural model for use in the TPFC integrated system performance analysis
- Show structural performance of the PM due to Delta IV-Heavy loads (both acoustics and liftoff)
- Show optical performance of the PM due to gravity sag and thermal loading
- Show that the OTA and PM have adequate stiffness to meet on-orbit performance and launch loading
- Develop weight optimized structural designs

- This chart discusses the purpose of performing structural analyses for the PM and mount design. An OTA structural model is developed so that it can be included in the TPFC integrated system performance analysis. Structural analysis is being performed to show that the PM can survive launch on a Delta IV-Heavy vehicle, to predict the gravity sag of the PM, and to predict the deformations of the PM due to thermal loading. Also, dynamics analysis is being performed to estimate the first significant frequency of the OTA and the PM to show that is will meet the stiffness requirement for both on-orbit performance and the launch environment. Finally, structural analysis is being performed in order to obtain weight optimized structures.

PM Structural Models

- PM Low-Fidelity Structural Model
  - Description: Flat plate model to represent PM and bar elements to represent mounts
  - Purpose: Acoustics analysis and trade studies

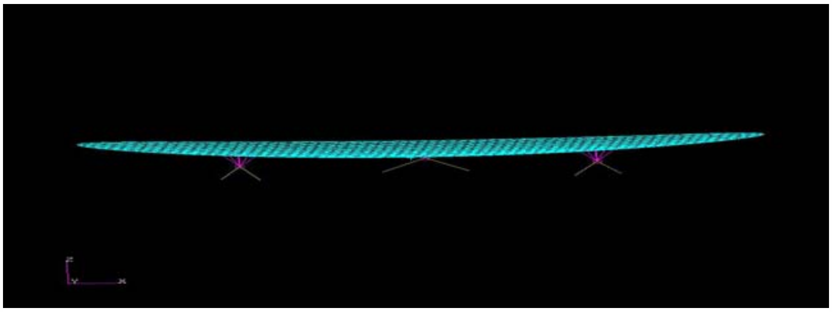

- PM Mid-Fidelity Structural Model
  - Description: Solid model to represent PM and bar and spring elements to represent mounts
  - Purpose: TPFC system dynamics and thermal analyses, and trade studies

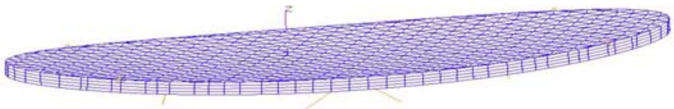

- PM High-Fidelity Structural Model
  - Description: Detailed plate model that represents all core and mirror segment geometry and detailed bar and solid elements to represent the mounts
  - Purpose: PM gravity sag, stress analysis, weight optimization studies

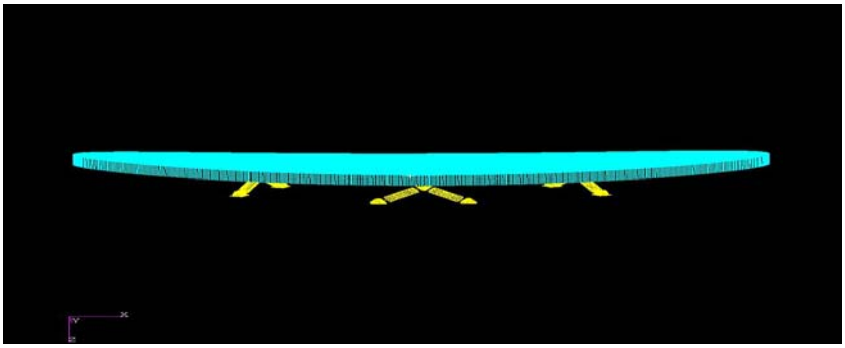

- This chart shows that various types of structural models are used to perform many different types of structural analyses for the PM and its mount design. The PM low-fidelity structural model consists of a flat plate with bar elements to represent the mounts. It is used for acoustics analysis and trade studies. The PM mid-fidelity structural model consists of plate and solid elements to represent the mirror and spring and bar elements to represent the mounts. This model is used for the TPFC integrated system dynamics and thermal analyses. The PM high-fidelity structural model consists of plate elements that represent all aspects (facesheets and all cells of the core) of the mirror and bar and solid elements to represent the mounts. This model is used for detailed PM analyses such as gravity sag, stress analysis and weight optimization studies.

PM High-Fidelity Structural Model: Model Overview

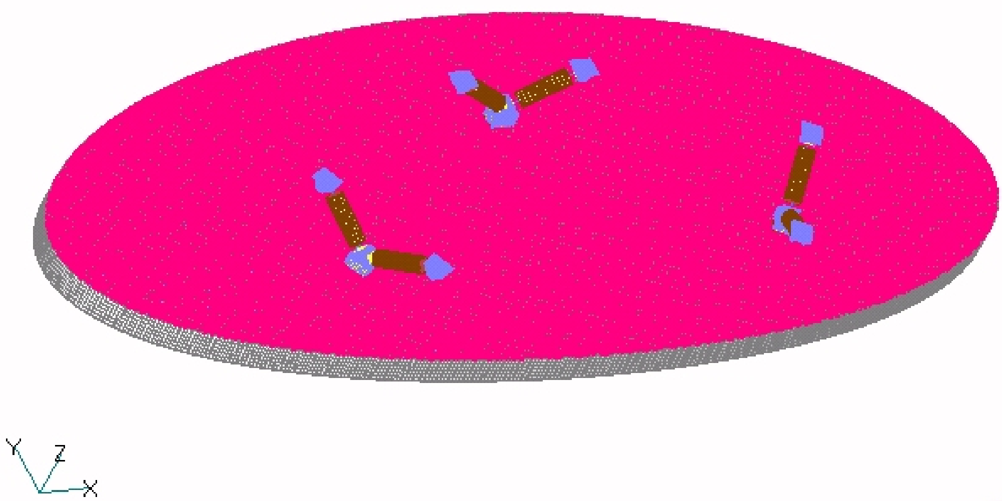

Sub-system	CBAR	CQUAD / CTRIA	CQUADR/ CTRIAR	CHEXA/ CPENTA/ CTETRA	RBE3
PM	0	285,472	0	0	0
Bipod	96	0	240	15,248	24
TOTAL	96	285,472	240	15,248	24

TOTAL ELEMENTS **301,080**
TOTAL NODES **189,786**

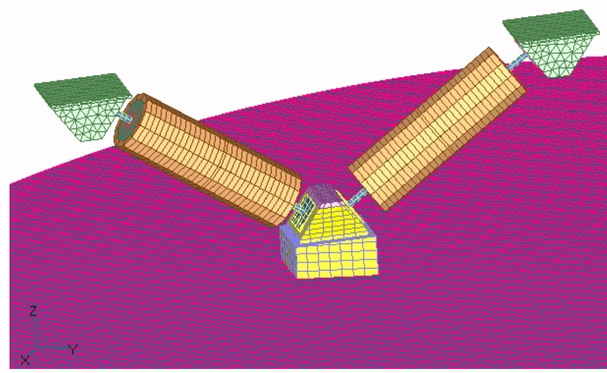

- This chart shows an overview of the PM high-fidelity structural model. The model is very detailed with elements to represent each cell of the hexagonal core, and front facesheet and back facesheet of the PM. Also, the mounts are modeled as bar and solid elements to closely represent its flight baseline 1 design. The model contains over 300,000 elements and over 189,000 node points.

PM High-Fidelity Structural Model: PM Parameters

177196 grids
285472 elements
PM material is ULE.

Outer dimensions: 8.0 m x 3.5 m x .25 m
Facesheet thickness: 7.3 mm
Backsheet thickness: 7.3 mm
Top of core thickness: 3.0 mm
Core thickness: 1.5 mm
Top of segment struts thickness: 6.0 mm
Segment struts thickness: 3.0 mm
Perimeter thickness: 3.0 mm
Model Weight: 1065.9 kg

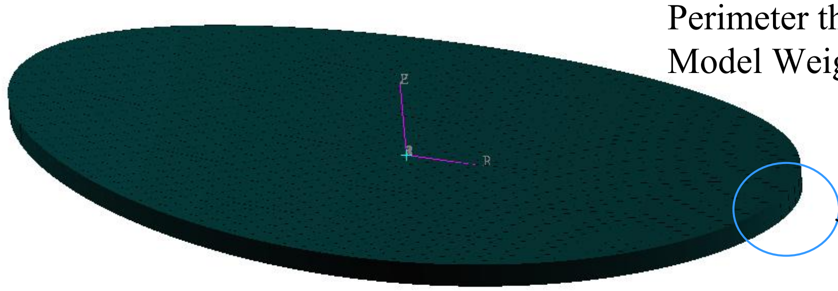

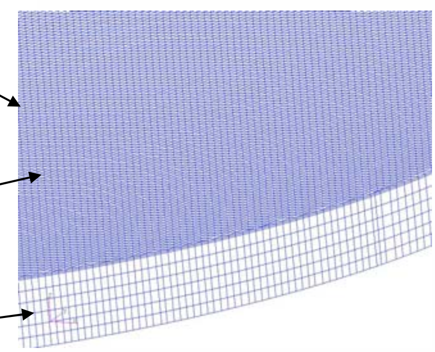

- This chart shows the thicknesses used for the various parts of the PM flight baseline 1 design. The mirror is made of ULE glass and it is 90% lightweighted, but it still weighs 1065.9 kg. All dimensions chosen for this baseline design are such that it can be manufacturd by currently available processes.

PM High-Fidelity Structural Model: PM Hex Core

Core
(shown with segment struts
and without perimeter)

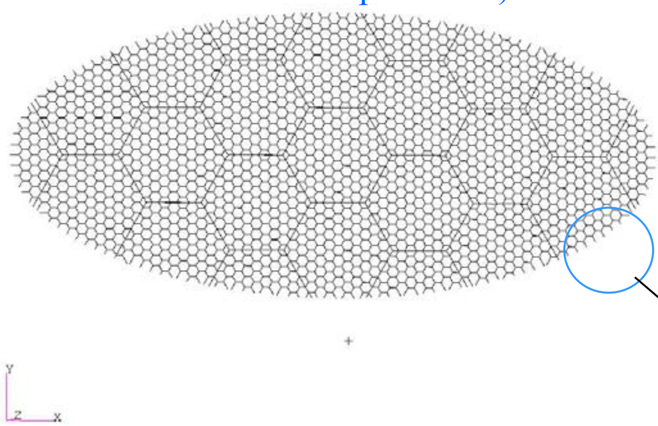

Hex Core
Wall Thickness is 1.5 mm

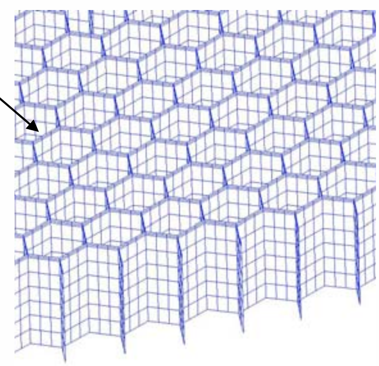

- This chart shows the hexagonal core of the PM flight baseline 1 design. Each cell of the core has been modeled in order to obtain an adequate stiffness representation of the PM.

PM High-Fidelity Structural Model: Mount Parameters

Total:
12790 grids
15608 elements

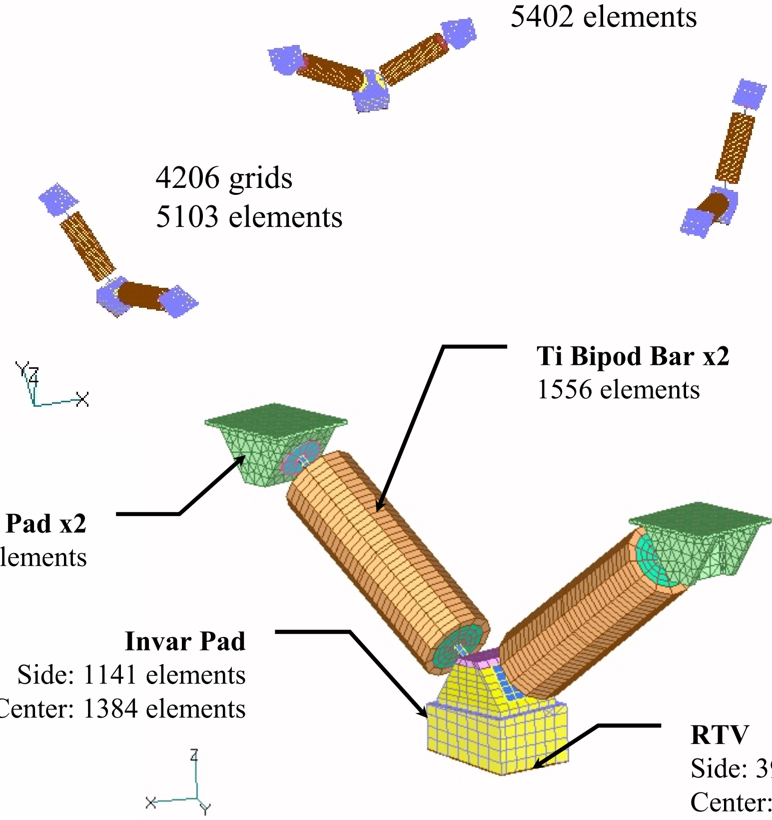

- This charts shows the details of the structural model of the PM mounts. There are three bipod assemblies. Each assembly consists of Invar pads that are connected by a Ti bipod. The Invar pad (shown in yellow) mounts to the PM using 1 mm thick RTV. The Invar pads (shown in green) mount to the AMS structure, directly above the bipods of the PSS.

PM High-Fidelity Structural Model: Weight

TPFC Primary Mirror and Bipod Assembly FEM Weight Breakdown			
Component	**Material**	**FEM Weight (Kg)**	**Solid Model Weight* (Kg)**
Primary Mirror Optic	ULE	1065.94	1066.00
Bipod Pads	Invar	127.95	117.50
Bipod Strut	Titanium	67.38	72.30
Total		**1261.27**	**1255.80**

- This charts shows a comparison of the CAD weight and the finite element model (FEM) weight. It shows that there is good agreement between the CAD and the FEM representations. The total weight represented in the FEM is 1261.27 kg.

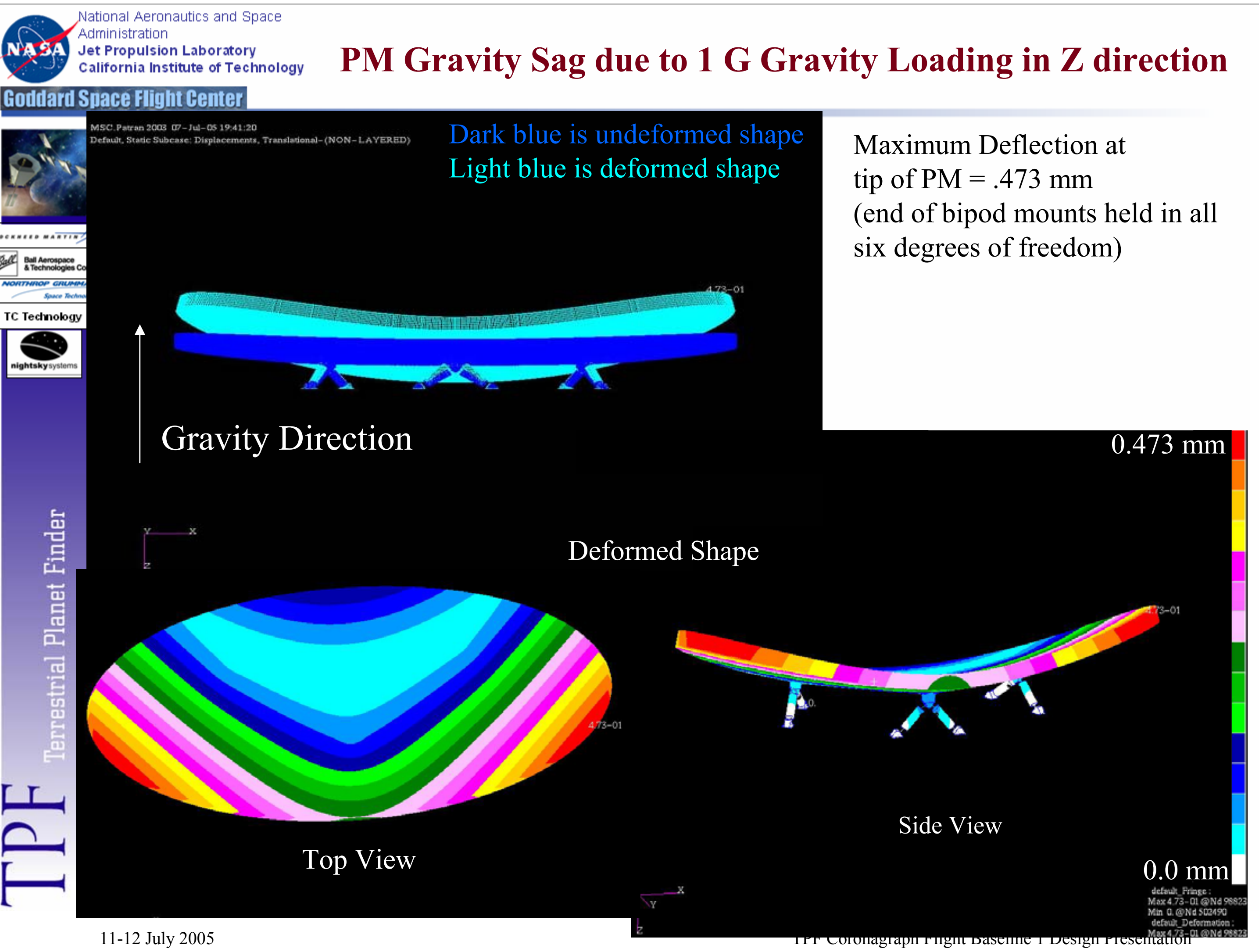

- This chart shows that for the flight baseline 1 design, the maximum deflection due to 1 G load applied in the Z direction was found to be .473 mm. This is the estimated deformation that will need to be off-loaded on the ground in order to perform optical measurements during ground testing. The pictures show different views of the deformation. The red area is the largest deformation.

PM Optical Performance due to 1 G Gravity Loading in Z direction

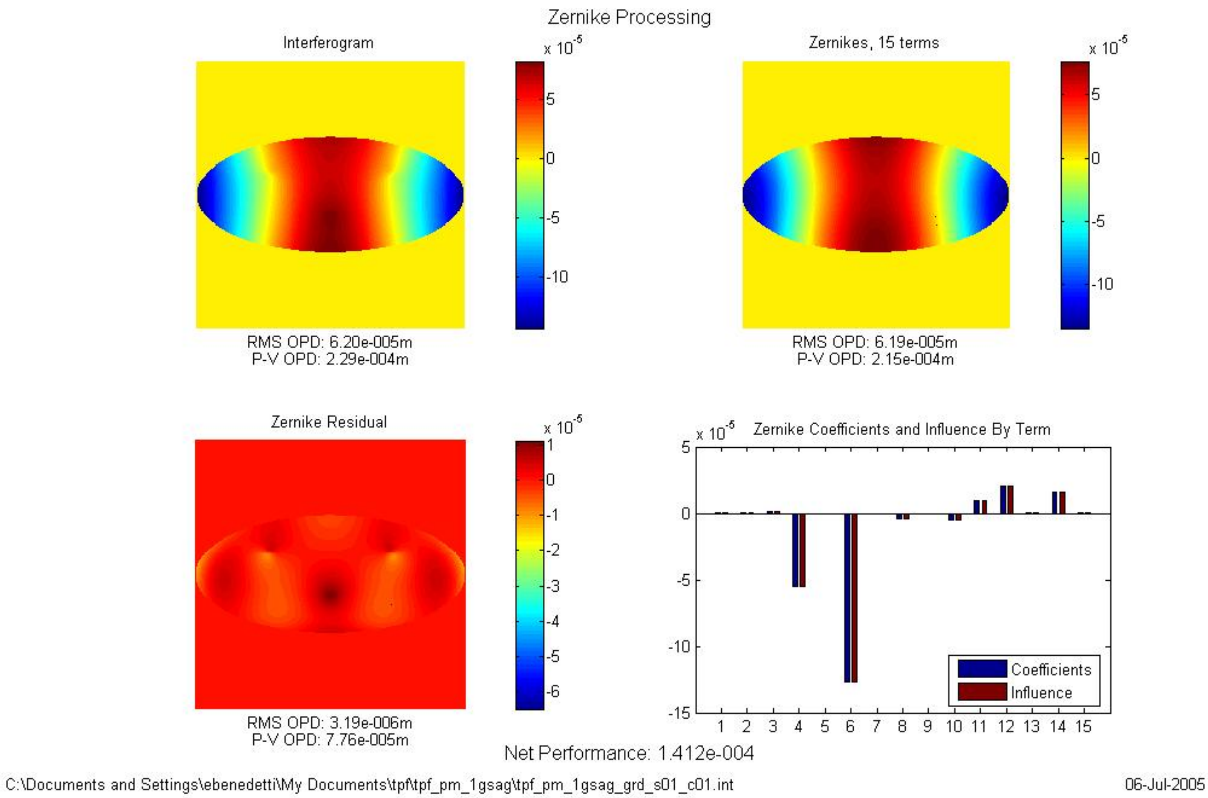

- This chart shows the optical performance due to the 1 G gravity loading after rigid body motion and tilt has been removed. RMS error and Peak-to-Valley number is shown as well as the Zernike coefficients.

PM Dynamics Analysis

PM Bipod model was held at base of Invar pad.
First mode is 20.65 Hz (RTV thickness 1 mm)

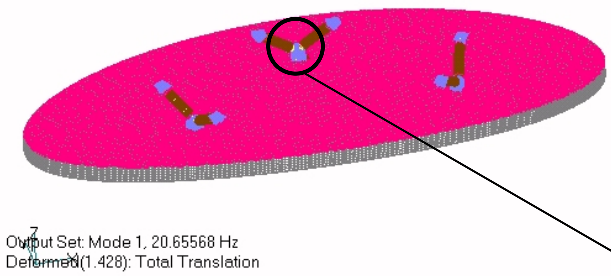

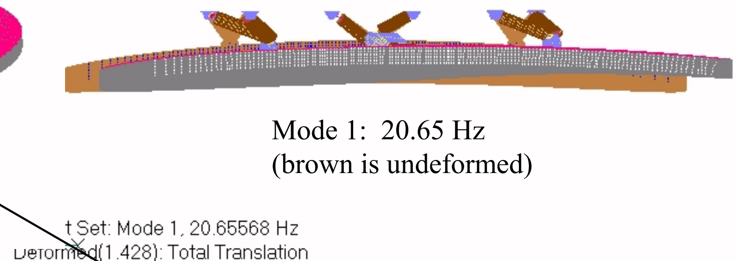

Mode 1: 20.65 Hz
(brown is undeformed)

Baseline Design

Mode	Frequency (Hz)
1	20.65
2	21.14
3	29.56

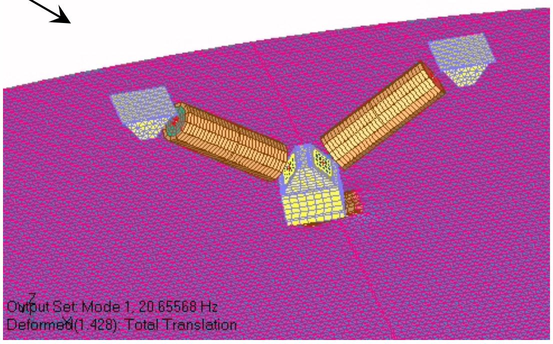

- This chart shows that the fundamental frequency of the PM with its bipod mounts is 20.65 Hz. The mode shape for this frequency is the primary mirror bending as well as lateral motion of the mounts. The boundary condition for this analysis is with the bottom of the bipods held in all six degrees of freedom.

Launch Loads

PM stress analysis used Delta IV-Heavy load factors.

- Quasi-static load:
  - 6G in X & .5G in -Z
  - 6G in X & .5G in Y
- Acoustics load: 10G in Z (acoustics analysis performed to obtain this load level)

Materials	ULE	RTV	Invar	Titanium (Ti-6Al-4V)
Allowable	15.2 Mpa/2200 psi (tensile)	2.1 Mpa/300 psi (tensile) 1.2 Mpa/173 psi (shear)	461.9 Mpa/67 ksi (ultimate) 262.0 Mpa/38 ksi (yield) 96.5 Mpa/14 ksi (microyield, 1ppm plastic deformation)	896.3 Mpa/130 ksi (ultimate) 827.4 Mpa/120 ksi (yield)
Source for Allowable	ITT TDM baseline	ITT TDM baseline	Daniel Polis NASA code 541	MIL-HBK-5H
Factor of Safety (FS)	3.0 5.0 (analysis only)	2.0	1.4 (ultimate) 1.25 (yield)	1.4 (ultimate) 1.25 (yield)
Source for FS	NASA-STD-5001	NASA-STD-5001	NASA-STD-5001	NASA-STD-5001

Terrestrial Planet Finder
TPF

- This chart shows the launch loads, allowable strengths of materials and safety factors currently being used for the PM stress analysis. The loads are based on the Delta IV loads manual and on acoustics analysis. (The details of the acoustics analysis performed to obtain the 10 G load is shown in one of the backup slides of this presentation.) The allowable strengths of the ULE and RTV are the same that are being used for the Technology Demonstration Mirror (TDM) progrom. All factors of safety are based on the recommendations listed in NASA-STD-5001.

PM Stress Analysis: Flight Baseline 1 Results

Baseline Design

Component	Peak Stress (Mpa/ksi) Quasi-static Load (6 G in X, .5 G Z) Acoustic Load (10 G in Z)	Margins of Safety
PM ULE	151.8/22.02 66.71/9.68	**-.97** **-.92**
RTV	20.64 / 2.99 (tensile) 6.16/.89 (tensile)	**-.95** **-.83**
Ti bar	403.5/58.5 469.4/68.08	.59 (ultimate) / .64 (yield) .36 (ultimate) / .41 (yield)
Invar Mount	50.52 / 7.33 70.47 / 10.22	5.53 (ultimate) / 3.15 (yield) 3.68 (ultimate) / 1.97 (yield)

Note:

1. PM/Bipod structural model (baseline design) weights 1261.4 kg comparing 1255.8 kg of solid model.
2. Margins for Invar are based on nominal ultimate/yield allowable.

- This chart shows the stress analysis results from applying the liftoff loads and acoustics loads to the PM and its mounts. The results show a negative margin for the PM and the bond material, which is RTV for the flight baseline design. The margins are positive for the mount hardware.

PM Stress Analysis: Flight Baseline 1 Results

Terrestrial Planet Finder
TPF

6G in X & .5G in -Z

151.8 Mpa = 22.02 ksi

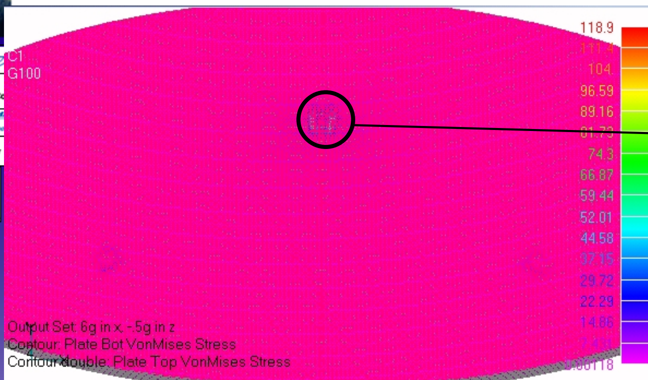

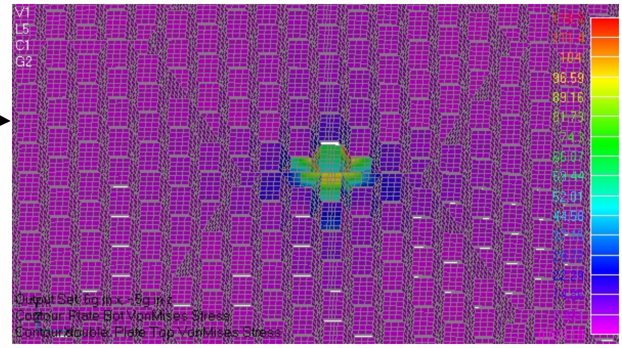

10G in -Z

66.71 Mpa = 9.68 ksi

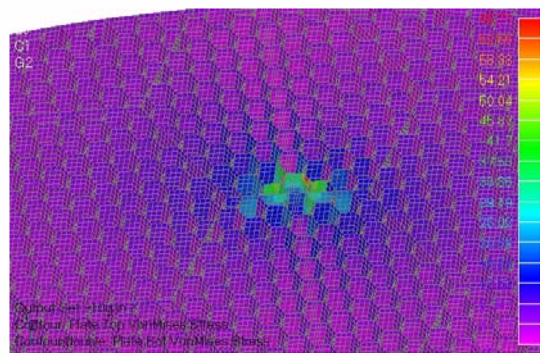

- This chart shows the stress distribution in the PM. The pictures on the left are the stresses in the facesheet and the pictures on the right are the stresses in the core. These stresses are very high and will exceed the allowable strength of the ULE.

National Aeronautics and Space Administration
Jet Propulsion Laboratory
California Institute of Technology
Goddard Space Flight Center

PM Stress Analysis: Mod 5 to Flight Baseline 1 Design

Mod. 5 (best case from previous analysis) :

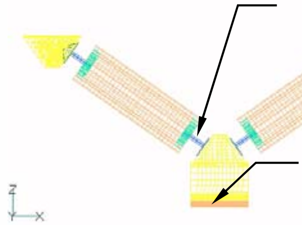

Increased Ti bar diameter from 12.7 to 25.4 mm

Changed RTV to Invar

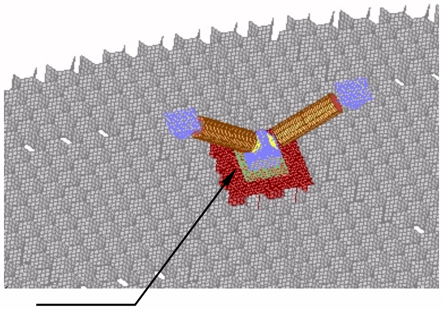

Increased PM wall thickness to 14.6mm in red colored area 18.5”x19.5” (included 9.8”x10.2” PM mounted area).

Configuration	Δ Weigh (kg)	PM Stress Quasi-static (MS) Acoustic (MS) (Mpa/ksi)	RTV stress Quasi-static (MS) Acoustic (MS) (Mpa/ksi)	Ti bar stress Quasi-static (MS) Acoustic (MS) (Mpa/ksi)	Invar Mount stress Quasi-static (MS) Acoustic (MS) (Mpa/ksi)
Baseline design	-	151.8/22.02 (-.97) 66.71/9.68 (-.92)	20.64 / 2.99 (-.95) 6.16/.89 (tensile) (-.83)	403.5/58.5 (.59/.64) 469.4/68.08 (.36/.41)	50.52 / 7.33 (5.53/3.15) 70.47 / 10.22 (3.68/1.97)
Modification 5	+122.3	13.04/1.89 (-.61) 17.14/2.49 (-.71)	N/A	98.73/14.32 (5.48/5.7) 131.9/19.13(3.85/4.02)	73.33 / 10.46 (3.57/1.91) 94.32 / 13.68 (2.50/1.22)

TPF Terrestrial Planet Finder

- Since the flight baseline 1 design for the PM showed a negative margin of safety, modifications to the design were considered. These modifications included adding stiffness to the areas behind and around the mount locations. The best case was modification 5 and the results for this case are shown in this chart. Notice that the margins of safety are getting better, but unfortunately, still negative.

PM Stress Analysis: Mod 5 to Flight Baseline 1 Design

6G in X & .5G in -Z

12.4 Mpa in Core

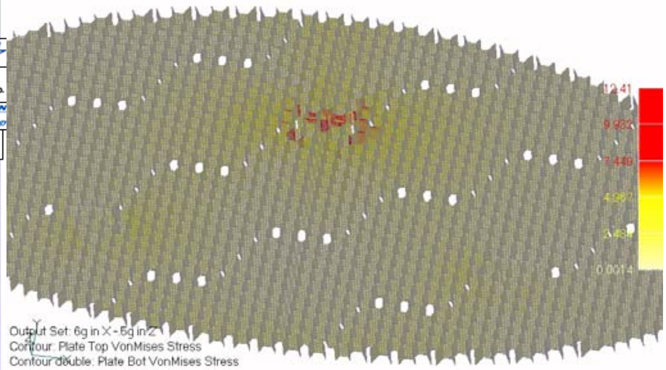

13.0 Mpa in back facesheet

10G in -Z

17.1 Mpa in Core

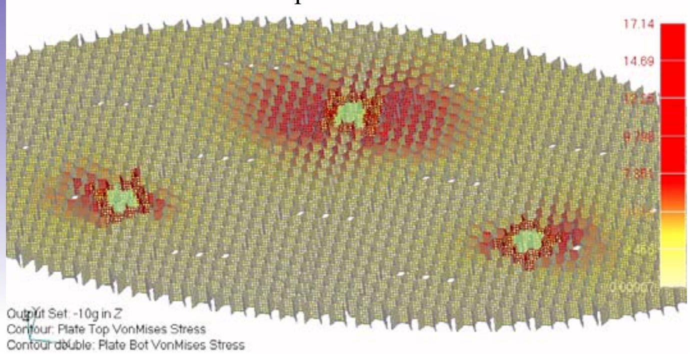

13.4 Mpa in back facesheet

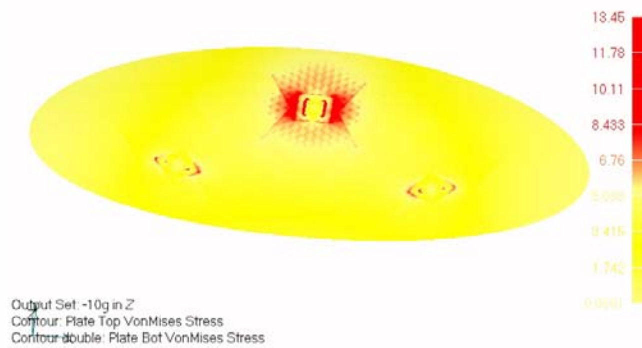

- This chart shows the stress distribution in the PM for modification 5. The pictures on the left are the stresses in the core and the pictures on the right are the stresses in the facesheet. Note, these stresses still exceed the allowable strength of the ULE. It is required that the stress in the ULE be less than 5.0 Mpa (which is the allowable strength of the ULE divided by the Factor of Safety of 3.0).

PM Stress Analysis

- PM Stress Analysis Peer Review was held to discuss possible solutions to achieve positive margin of safety in the PM for launch loads.
- Comments and suggestions include:
  - Category 1: Modifications to PM and mount that do not require major design changes to the OTA or other TPFC hardware
    - Perform a trade study to look at bipod angle (need to reduce moment into PM)
    - Change shape of Invar mount pad, ie. Hex, shorter and tapered at edges
    - When including additional stiffness in the PM behind the mount region, apply a gradual thickness change as you move out from center of mount area
  - Category 2: Modifications that would require major design changes to the OTA or other TPFC hardware (possible changes for Flight Baseline 2 design)
    - Perform a trade study to determine optimal mount locations and bipod angle, also don't rule out a 4-pt mount
    - Adding launch locks (see next slide for details), try center launch lock
    - Look into stronger adhesive (possible affect to optical performance)
    - Consider alternate manufacturing process for ULE at mount area

- A peer review was held to obtain comments and suggestions on the PM and mount design that would help the PM to pass the launch load requirement. The peer review consisted of experts in mechanical design, mechanical analysis and opto-mechanical mount design. This chart lists the top suggestions provided by the peer review members. These suggestions are listed by category 1 and category 2 modifications. Category 1 changes would not require major design changes to the OTA or other TPFC hardware. Category 2 changes would require major design changes to the OTA or TPFC hardware. These suggestions are currently being evaluated and additional analyses are being performed.

PM Stress Analysis: Modification to Improve Design (Mod 5-8)

Mod 5-8 includes 414 kg of additional weight and 8 launch locks.

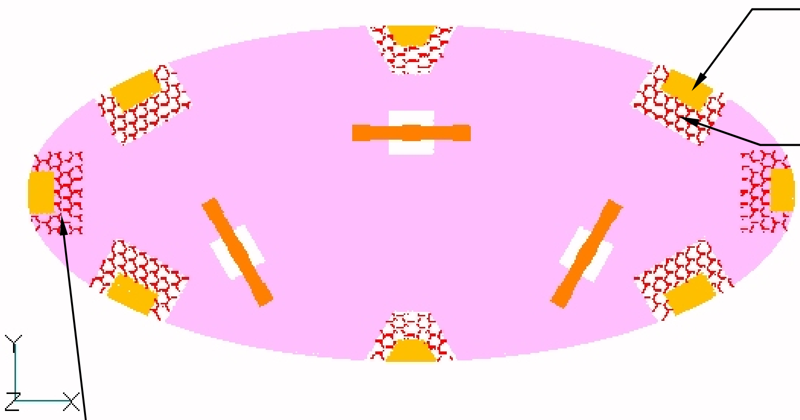

479 x 277mm (18.8” x 10.9”). Wall thickness is 42mm (include both side facesheet)

870 x 583mm (34.2” x 22.9”) (exclude 479 x 277 mm area). Core thickness is 6 mm. Both side facesheet thickness is 7.3mm.

867 x 582mm (34.1” x 22.9”). Core thickness is 4 mm. Back facesheet thickness is 5 mm. Front facesheet is 7.3 mm.

10G in -Z

Stress in PM Core

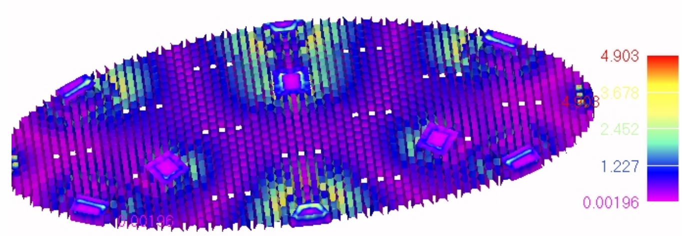

4.9 Mpa = .71 ksi

- This chart shows the results from applying 8 launch locks to the PM launch design. With 8 launch locks and an additional 414 kg of weight, this design shows positive margin of safety in the PM. The stresses in the PM were found to be less than 5.0 Mpa. This is just one option that would allow the PM to pass the launch load requirement. Other options are being evaluated.

Future PM and OTA Trade Studies

- Weight Optimization of PM, AMS and SMA. (Started PM optimization, see table below.)

Configuration	Weight (kg) (Baseline weight is 1065.94 kg)	Fundamental Frequency (Hz)*	1 G Z Deformation (mm)
Baseline: FS = BS = 7.3 mm	-	30.19	.289
FS = 7.3 mm, BS =5.0 mm	-112.56	29.77	.298
FS = 7.3 mm, BS = 3.0 mm	-210.44	28.49	.330
FS = BS = 5.0 mm	-225.12	29.35	.309

*For optimization study, model is only PM without mounts. PM is held at mount locations in all six degrees of freedom.

- Sensitivity to PM mount design, location, and stiffness
- PM Quilting Effects (PM deformation due to thermal loads)
- Stiffness analysis of SM tower due to stiffness of hinges/latches

- PM open-back versus closed-back structural/thermal analysis. (Structural models are created for this study, see pictures below.)

Closed-back hex core

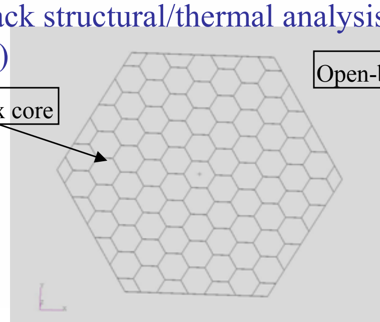

Open-back triangle core

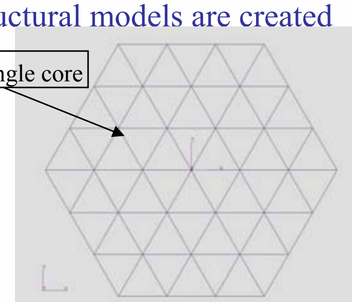

- This chart discusses the future structural analyses that are planned for the PM and OTA. Several of the analyses have begun, such as the weight optimization of the PM and the open-back versus closed-back structural/thermal study. For the PM weight optimization, the structural results are presented for modifying the facesheet and backsheet thicknesses; however, the optical performance for each of these cases has not yet been completed. Also, additional cases are being considered. For the open-back versus closed-back structural/thermal study, the structural models have been developed and verified and the thermal loading is still being developed. Other studies that are being performed include, the optical sensitivity to the PM mount design, location and stiffness, the PM quilting effects, and the stiffness of the SM tower due to the stiffness of hinges and latches.

Conclusion

- PM and mount flight baseline 1 design was analyzed and found acceptable for stiffness and gravity sag, however, the design did not meet the launch load requirement. Only the inclusion of launch locks and additional weight were demonstrated to meet this requirement, however additional alternatives will be analyzed.
- Future studies will continue to investigate the PM launch loads issue and look into weight reduction of the PM and OTA designs.

- This chart briefly summarizes the structural analysis work performed for the PM and the future studies that are planned for the PM and OTA. The analyses completed include dynamics, gravity sag and stress analysis due to launch loads. One of the concerns at this time is that the FB1 PM design has negative margin of safety for the launch environment. Future studies will investigate this issue as well as perform other structural analyses for the PM and OTA.

Backup Slides

National Aeronautics and Space Administration
Jet Propulsion Laboratory
California Institute of Technology
Goddard Space Flight Center

PM Acoustics Analysis

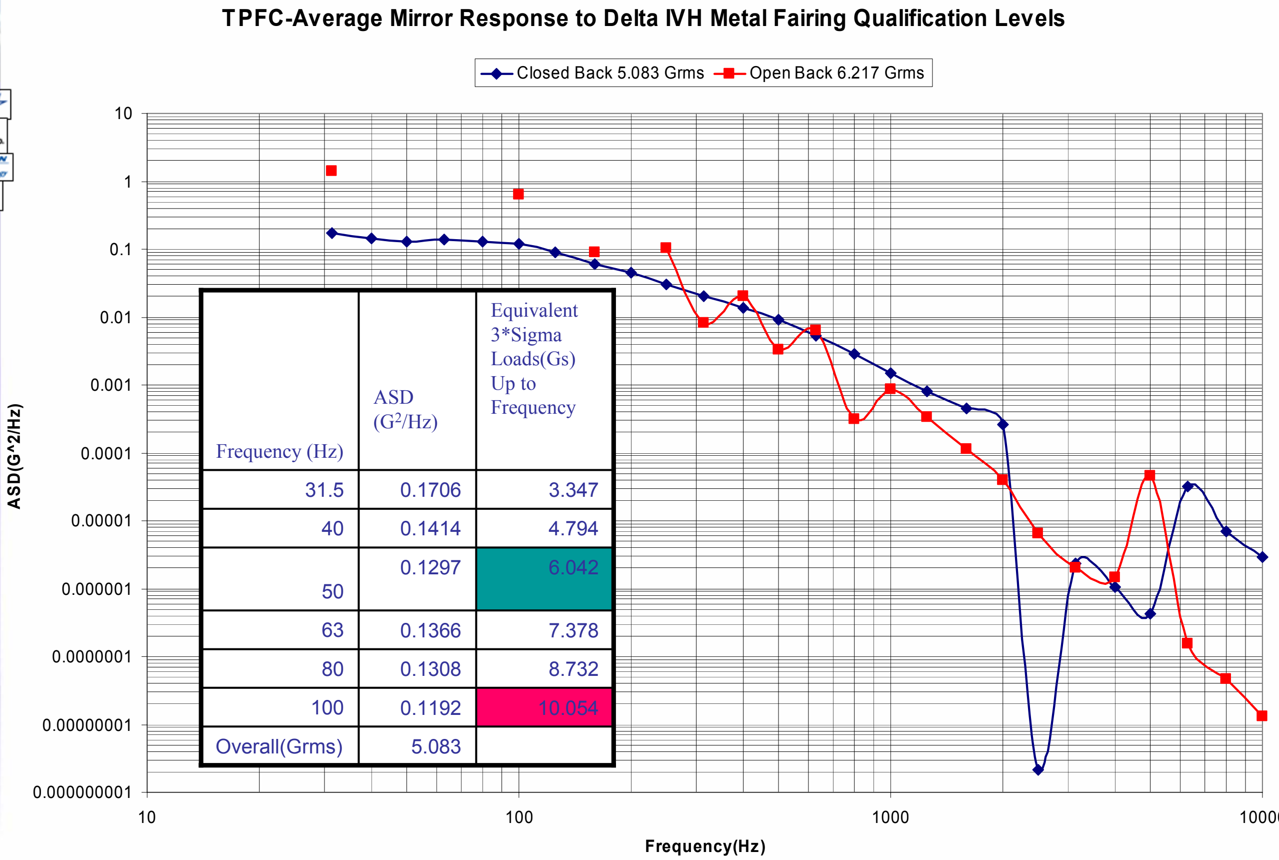

Frequency (Hz)	ASD (G^2/Hz)	Equivalent 3*Sigma Loads(Gs) Up to Frequency
31.5	0.1706	3.347
40	0.1414	4.794
50	0.1297	6.042
63	0.1366	7.378
80	0.1308	8.732
100	0.1192	10.054
Overall(Grms)	5.083	

Terrestrial Planet Finder
TPF

- This charts shows the response of the PM due to the Delta IV-Heavy acoustics loading from the metal fairing. These are qualification levels and a damping of .5% was used in the analysis. Also, the acoustics loading from the composite fairing was considered in the analysis. Including all modes up to 100 Hz, the total load on the PM due to acoustics from the metal fairing is 10.05 Gs.

PM Stress Analysis: Flight Baseline 1 Results

6G in X & .5G in -Z

RTV (center bipod)

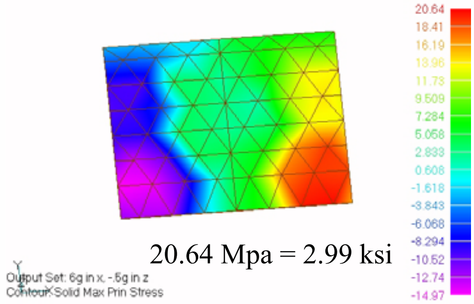

20.64 Mpa = 2.99 ksi

6G in X & .5G in -Z

Invar Mount (center bipod)

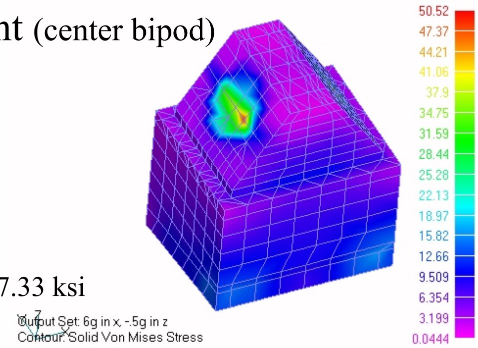

50.52 Mpa = 7.33 ksi

10G in -Z

RTV (center bipod)

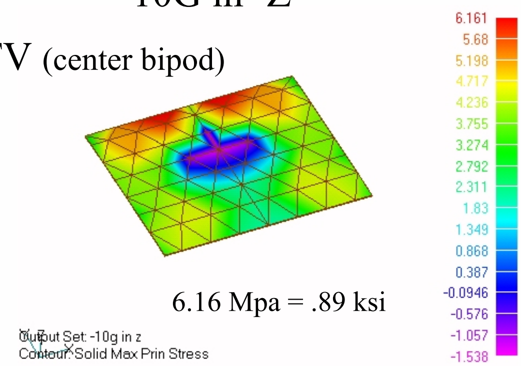

6.16 Mpa = .89 ksi

10G in -Z

Invar Mount (center bipod)

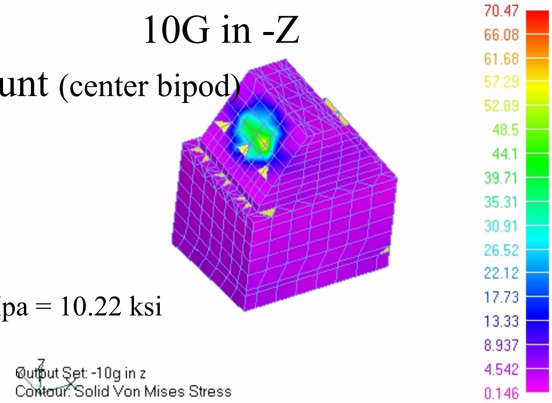

70.47 Mpa = 10.22 ksi

- This chart shows the stress distribution in the RTV and in the Invar mount closest to the PM for the flight baseline 1 design configuration.

PM Stress Analysis: Flight Baseline 1 Results

Ti Bar (center bipod)

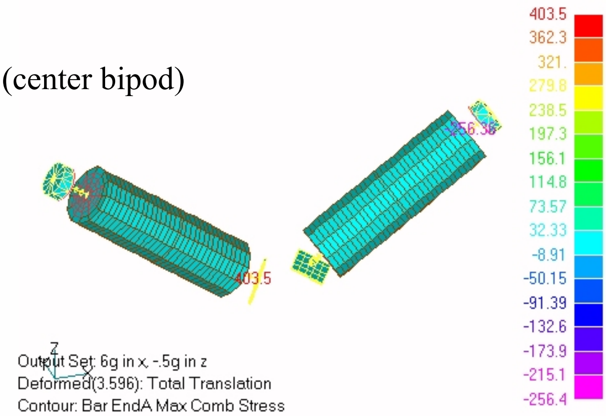

6G in X & .5G in -Z

403.5 Mpa = 58.5 ksi

Ti Bar (center bipod)

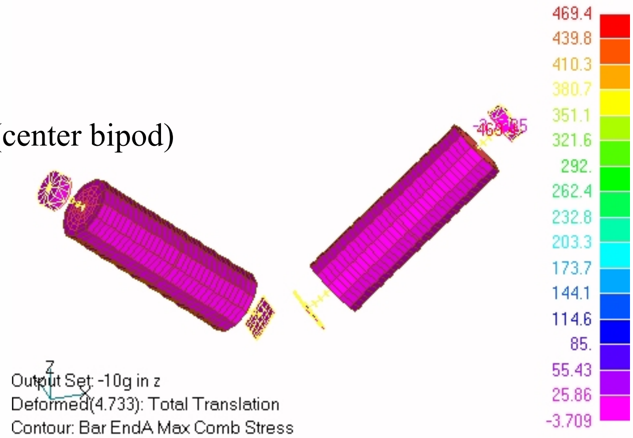

10G in -Z

469.4 Mpa = 68.08 ksi

- This chart shows the stress distribution in the bipods for the flight baseline 1 design configuration.

Lockheed Martin
Ball Aerospace & Technologies Corp.
Northrop Grumman Space Technology
TC Technology
nightsky systems

TPF Terrestrial Planet Finder

ACS Models, Performance Results & Future Studies

Carl Blaurock (Nightsky Systems)
Contributors:
Larry Dewell (LMCO)
Alice Liu (GSFC)
James Alexander (JPL)

11-12 July 2005

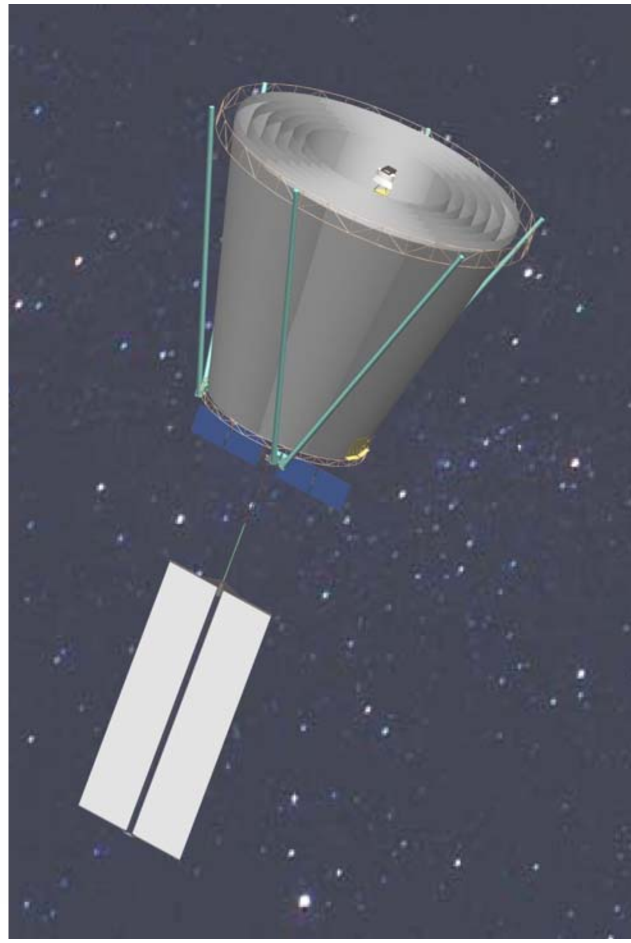

- The Attitude Control System (ACS) is also referred to as the Pointing Control System (PCS) in order to emphasize the fact that it's responsible not only for the rigid-body attitude control of the spacecraft, but for the stability of the image on the detector in the presence of dynamics-induced jitter

Outline

- Objectives and methodology
- Integrated dynamics model
  - Structure
  - Optics
  - Disturbance sources
  - Uncertainty modeling
  - Control/isolation point design
    - Passive
    - Active
- Nominal performance
- Sensitivity results
- Slew/settle performance for 30 degree dither

- The PCS team is responsible for verifying the jitter performance of the design (the contributions of structural dynamics to contrast loss)
- Many aspects of the design are uncertain
  - Structural stiffness, mass, and damping
  - Disturbance spectra
  - Isolator performance
  - Etc
- Need an appropriate (controlled) level of conservatism without making the job impossible
- The analysis philosophy is to identify as many nonidealities as practicable, then model them with as much fidelity as possible
  - Minimize “unknown unknowns” that need to be accounted for with factor of safety
- The integrated model is the mechanism for bringing all of the nonidealities together

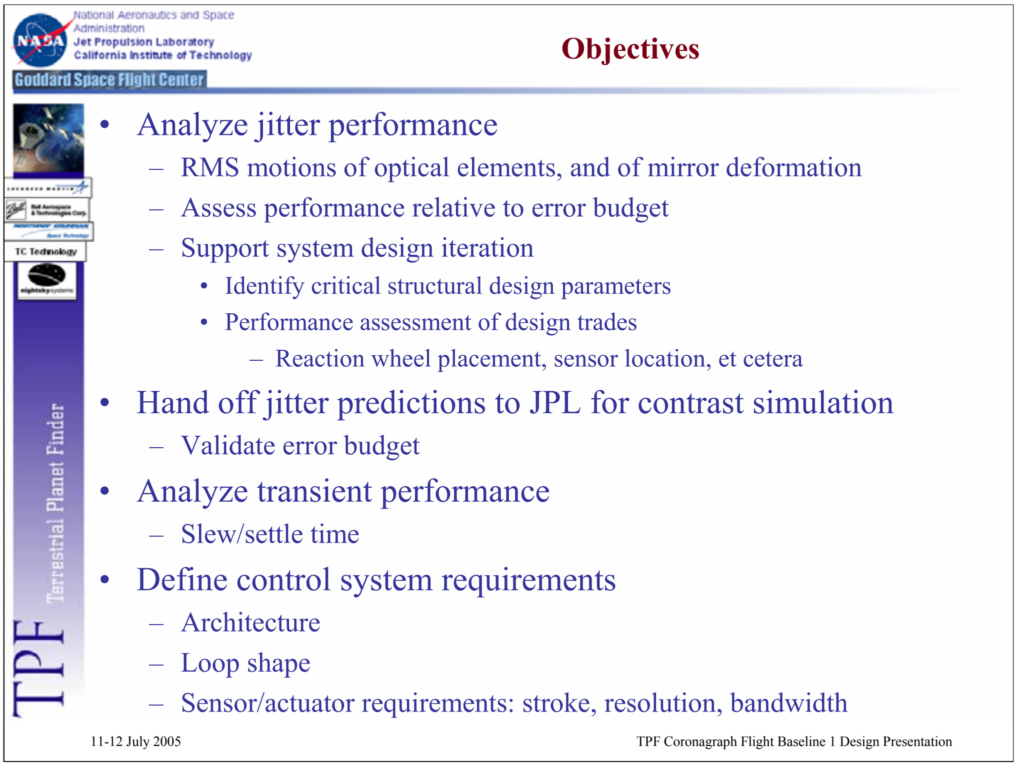

- The responsibilities of the PCS group are to:
  - Design the Pointing Control System to meet the jitter components of the error budget (or to minimize jitter induced contrast, if the error budget cannot be met for the current design)
  - Generate jitter predictions: specifically rigid-body motion of the optics, and deformation of the optics
- "Customers" for our data are
  - The optical simulation team: they predict contrast in the presence of the jitter predictions we provide
  - The structural designers: they can redesign the system to reduce the response at particular frequencies
  - The error budgeting team: they can change the budget to reflect our predictions
    - Re-allocate requirements
    - Another example is the 8th order mask, which makes the PCS control system requirements much looser compared to a 4th order mask
  - The design team: we tell them
    - What sensors and actuators are needed, and where they go
    - The impact of design decisions on the jitter performance of the instrument
    - The slew/settle time which impacts efficiency

Integrated dynamics model

- Fully coupled dynamic model from disturbance inputs to optical performance
  - Disturbance models to represent physical disturbances
    - Reaction wheel imbalance
    - Sensor noise
    - Actuator noise
  - Structural model of observatory dynamics
  - Active control systems
  - Optical models map physical motions to optical response
- Two integrated models are used
  - High order linear model for analysis of high-bandwidth disturbances
    - 1000-2000 modes
    - Disturbance-Optics-Controls-Structures (DOCS) Toolbox in MATLAB
  - Low order nonlinear model for transient response simulation
    - 35 modes, Simulink®
  - Cross validation of predictions
    - Common design vector

- Jitter response is an inherently coupled process
  - Disturbances flow through the structure, to perturb the optical response, which is measured by sensors, and corrected by actuators that act on the structure
  - The integrated model captures all of these processes, with associated errors and uncertainties
- Many of the disturbance sources are not well characterized, so we use the analysis to tell us which ones are important for TPFC
  - Engineering judgement to identify the strongest design drivers (reaction wheel imbalance)
  - Simpler approximations of error sources that we want to account for but do not expect to drive the design (sensor noises)
  - When analysis shows that one of the simpler approximations shows an exceedance, we improve the model of that disturbance (and redesign if the analysis still shows an exceedance)
- Nonlinear time domain model to predict transient response, to look at phenomena that are inherently nonlinear (large angle slews) and to confirm linear models of “weak” nonlinear phenomena (e.g. quantization)
- Linear model to analyze responses that inherently drive many modes, to design controllers, and to perform design sweeps that require many (100’s-1000’s) performance evaluations

Structure

- Structural models provided by JPL in the form of a Normal Modes model
  - Andy Kissil (Sandra Irish et. al. at GSFC provide the telescope model)
  - 3 structural models are used
    - Passive isolation (between payload and Support Module)
    - Active isolation with reaction wheel assembly isolator (payload and Support Module are completely separate)
    - Active isolation with hard mounted RWA
- Modal damping vector defined using Strain Energy Fractions
  - Best damping estimate with knockdown

$$\zeta_i = \sum_j F_{ij} \zeta_j$$

- Converted to state space model using input/output node definitions
  - Projection equations used to decompose optical node motions consistent with the error budget
    - Deformation of the primary: tip/tilt removed
    - Structural deformation: rigid motion of the optics relative to the primary
    - Rigid Body Pointing: all 21 optics moving "rigidly", ie no relative motion
- Full order models have ~7200 modes 0-300Hz
- Three reduced order models are used
  - Medium: ~2000 modes, used for analysis
  - Small: ~1000 modes, used for design
  - Slew: ~30 dominant LOS modes 0-10Hz

Component damping

Component	Best estimate	Knock down	Nominal value
Payload isolator	5%	2	2.5%
RWA isolator	5%	1.2	4.17%
Sunshield	1%	3	0.33%
Bus	0.5%	5	0.1%
OTA	0.5%	5	0.1%

- Multiple structural models required to support active/passive isolation trade
- Structural damping has a strong influence on jitter response, but at the same time is difficult to predict
  - We want to design to a given level of conservatism, but anything beyond that makes the design more difficult without buying down any additional risk
  - Damping model is designed to capture the phenomena we can count on to help us (e.g. damping in the isolator will damp the payload as well) with designed-in conservatism (knockdown factors)
- State space model describes structural response from physical disturbance inputs to optical element motions (outputs)
  - Outputs are computed consistent with the terms in the error budget
- Model reduction is used to improve the analysis efficiency
  - Reduced model sizes allow better evaluation of the trade space (more designs)
  - Reduction algorithms maintain the input-to-output prediction accuracy of the models

Optics

- Optical models are provided in the form of linear sensitivity matrices that map structural node motions to optical response (JPL/Phillip Dumont)
  - Centroid on mask (LOS)
  - Beam walk on all 21 optics
    - Post processed to enforce zero beam walk on the DM
      - Beam walk is defined by the chief ray, which by definition has zero beam walk on the DM
  - Structural deformation aberrations
    - WFE at the mask due to rigid optics motions
  - Optical deformation aberrations
    - WFE at the mask due to deformation of the primary
      - The SM, M3, and M4 are meshed but were considered rigid for this cycle

- Linear optical sensitivity matrices are an efficient way to compute optical response
  - No need to run optical analyses “on-line” during a jitter analysis
  - Optical motions are small enough that the assumption of linearity is justified
- Optical performances are the same as used in the error budget
- We’ll be doing optical deformation aberrations for the SM, M3, and M4 mirror surfaces in the next design cycle

Disturbance sources: RW

- The baseline design uses 6 Goodrich E wheels in a pyramid
- The reaction wheels are modeled as a sum of sinusoidal disturbances acting at harmonics of the wheelspeed

$$d(t) = \sum_{i=1}^{N_h} C_i f_{\mathrm{rw}}^2 \sin(2\pi h_i f_{\mathrm{rw}} t + \phi_i)$$

- Disturbance coefficients are derived from curve fits to force/torque vs RPM data
- Disturbance fundamental corresponds to static/dynamic imbalance
  - 0.273 g-cm, 21.4 g-cm^2
  - Easily achievable with Fine Balancing option
- The structural/optical response is computed by RSS'ing the responses from each force/moment component from each wheel

$$d(j\omega_i) = C_i f_{\mathrm{rw}}^2 \delta(j\omega_i) e^{j\phi_i}$$

$$z(\Omega) = \sqrt{\frac{1}{\sqrt{2}} \sum_{i=1}^{N_h} \left|G_{zd}(j\omega_i)\right|^2 \left|d(j\omega_i)\right|^2}$$

- The response is scaled to approximate 2 of the 6 wheels spinning at the same speed
- Maximum wheelspeed is 3850 RPM (64 RPS)
  - Minimum wheelspeed 3RPS if jitter performance requires it

- The reaction wheels are the largest magnitude disturbance, and drive the design to use some type of isolation (passive or active)
  - Approach is to have a dynamically "noisy" side (the support module) that the wheels are mounted to, and a "quiet" side where the optics are located (the payload)
- The wheels create disturbances at the fundamental due to imbalance, and at sub/super-harmonics due to bearing imperfections
  - Can be modeled as a sum of sines
  - Imbalance disturbances can be modeled analytically, but harmonics are dependent on the particular wheel design and need to be experimentally determined
  - Harmonics are generally much smaller
- Assumption of 2 wheels at the same speed is conservative, since wheel momentum can be traded between the six wheels to avoid 2 or more at the same speed
- Wheelspeed lower bound is required by the passive isolator design, since there is disturbance amplification near the isolator break frequency
  - Active design requires no lower bound, potentially doubling momentum capacity
  - wheel stiction imparts an impulsive disturbance when the wheel speed goes through zero, and the jitter response to this has not been performed

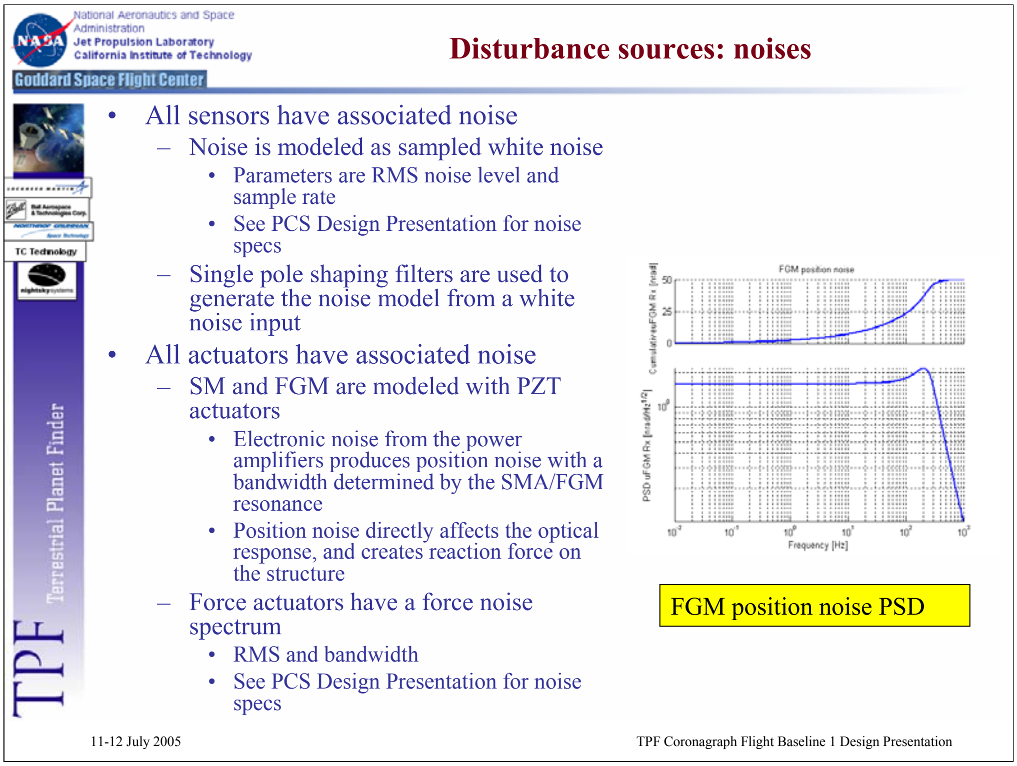

- Sensor and actuator noises are significantly lower magnitude than the wheelspeed, but potentially problematic since they act directly on the payload
  - Do not benefit from the ~4 or more decades of attenuation provided by the isolation
- Linear frequency domain analysis is continuous-time, so shaping filters are used to approximate sampled sensor noise
- Secondary Mirror and Fine Guidance Mirror are actuated with piezoelectrics (PZTs) which are position control devices, so electrical noise from the amplifiers results in position jitter
  - The actuators will respond up to their mechanical resonance frequency, and then roll off, resulting in a bandlimited position jitter
  - Manufacturers' specifications for position jitter are typically given as an RMS equivalent angle
  - The reaction force on the structure is potentially a larger problem that the optical jitter that results from motion of the optic, since the structure can dynamically amplify the force when it excites a structural mode

Uncertainty modeling

- The performance predictions include a Model Uncertainty Factor (MUF) that applies a frequency dependent gain to the response prediction
  - Approach developed by Bob O'Donnell (Veridian), Tupper Hyde (GSFC), and SIM JPL
- The MUF is developed on a component basis then assembled together
  - Defined as a dB gain then RSS'ed
- Component MUFs are functions of
  - Frequency
    - Low frequency response is usually predicted more accurately than high frequency
    - The TPFC MUF is constant 0-20Hz, increases linearly to 40Hz, then is constant to infinity
  - Model maturity
    - Component MUFs are higher for models that have no test heritage, and decrease for models that have component, subsystem, and system level testing

	Modal Gain MUF (gain …uses dB info for calcs)																	
	Below Break									Above Break								
Component	Net	Analysis Only		Component Test		Subsystem Test		Element / Observatory Test		Net	Analysis Only		Component Test		Subsystem Test		Element / Observatory Test	
RWA Disturbance	1.413	1.9953	0	1.4125	1	1.0593	0	1.0351		1.585	1.9953	0	1.5849	1	1.3725	0	1.05	
RWA Isolators	1.259	1.2589	1	1.122		1.0593		1.0351		1.585	1.5849	1	1.5849	0	1.3725	0	1.05	
Bus	1.995	1.9953	1	1.122		1.0593		1.0351		3.981	3.9811	1	1.5849	0	1.3725	0	1.05	
AMS Isolator	1.259	1.2589	1	1.122		1.0593		1.0351		1.585	1.5849	1	1.5849	0	1.3725	0	1.05	
Instrument	1.995	1.9953	1	1.122		1.0593		1.0351		3.981	3.9811	1	1.5849	0	1.3725	0	1.05	
Optical Performance	1.122	1.122	1	1.0593		1.0351		1.0233		1.122	1.122	1	1.0593	0	1.0351	0	1.05	
Product of MUF	2.98	3.47		1.52		1.14		1.08		8.28	8.80		2.80		2.03		1.29	

- MUFs are chosen to account for uncertainties in the modal response magnitudes of the structure
  - Errors in the predicted mode shape for a particular mode will cause errors in the amount of motion generated by a disturbance in that mode, and in the resulting motion of the optics from that mode
  - Has nothing to do with damping; damping uncertainty is handled with a separate knockdown factor as described earlier
- System is broken up into components, and each component is given its own MUF
  - The MUF for a structural component is larger at high frequency, since the prediction error is likely to be greater
  - The MUF for a component is reduced when test data is used to verify predictions of the response of that component
- Component errors may increase or decrease the optical response, so the component MUFs are RSSed to compute the system MUF

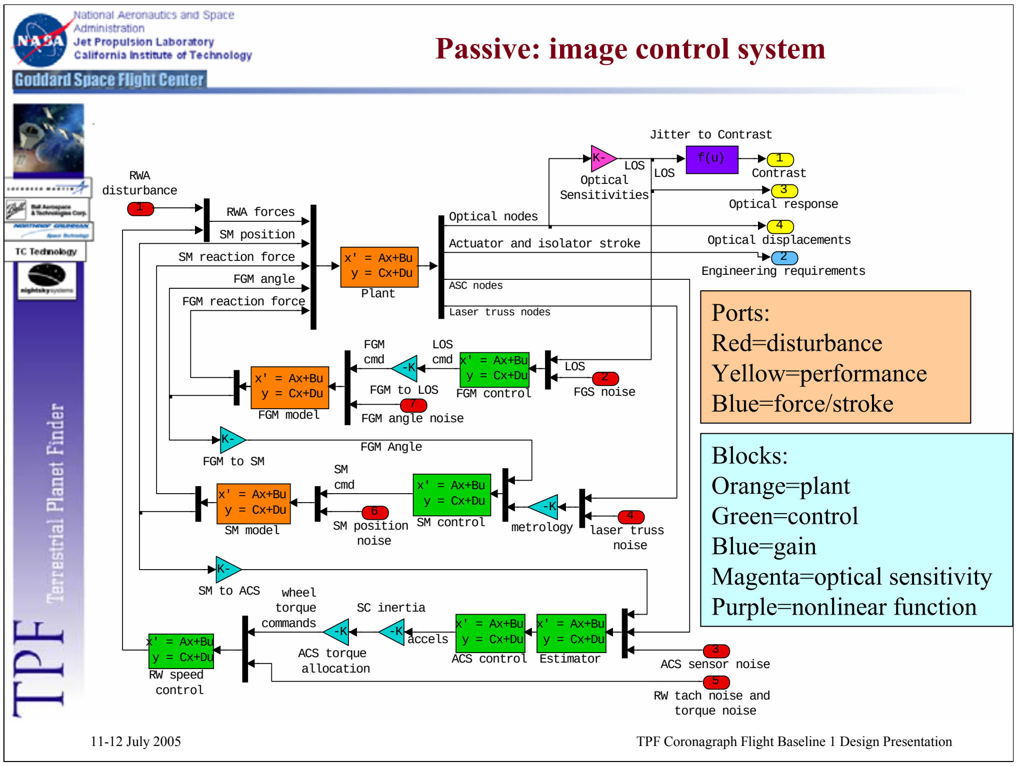

- The integrated model for the passive isolation design maps disturbances (red) to performances that can be compared to the error budget (yellow) and also provides design information (blue)
- The image control system is implemented as a staged design
  - The FGM acts to position the target star on the mask, as sensed by the FGS
  - The SM offloads the FGM (senses the FGM angle and tip/tilts to an angle that will zero the FGM angle)
  - The ACS controller offloads the SM (senses SM tip/tilt and generates reaction wheel torques to move the spacecraft to an attitude that zeros the SM tip/tilt)
- The other 4 axes of the SM are controlled to maintain the SM-PM relative position
- The reaction wheels are controlled using a local speed servo to reject spin axis disturbances
  - There is an associated tachometer sensor noise
- The bottom row of blocks is on the support module (noisy side) and everything above is on the payload (quiet side)

Passive system point design

TPF Terrestrial Planet Finder

- The passive design uses a two-stage passive isolator plus a three-stage image control system
  - The passive isolator consists of a 1.5Hz isolator on the Reaction Wheel Assembly, and a 1 Hz isolator between the payload and Support Module
- The image control system is designed using classical loop shaping techniques
  - Simple controllers with minimal parameters are used to enable rapid design sweeps
  - 6dB gain margin and 30 degrees phase margin are enforced for all loops
- The FGM and SM compensators are second order low pass filters with a lead network at cross over

Control loop	Parameter	Value	Sample Freq.	Margins	Bandwidth
FGM	Break freq. Lead	1 Hz 45º	500 Hz	7.01dB 25.6º	25.1 Hz
SM	Break freq. Lead	0.001 Hz 45º	100 Hz	49.11dB 45.7º	0.1 Hz
ACS	Crossover Integral T.C. ratio Estimator freq. Elliptical order Elliptical ripple Elliptical atten. Elliptical freq.	0.016Hz 0.075 10Hz 3 1dB 30dB 0.56	5Hz	9.3 dB 34.8º	0.043 Hz
RW speed control	Bandwidth Lead	1Hz 60º	100 Hz		1 Hz

- The ACS uses an inertia compensated PID design adapted from the NGST Yardstick design
- Reaction wheel speed control
  - Spin axis disturbances can be controlled with feedback from a tachometer
    - Torque noise, drag torque
  - Tachometer noise introduces additional error
  - Integral compensator with 1Hz bandwidth is used for the point design

- The passive system uses two stages of passive isolation that are built into the structural model
  - Important since this captures many of the non-idealities that limit isolator performance
- Image control system is designed using flight-traceable design techniques and realistic margins
  - Somewhat simplified SM/FGM controllers to accommodate design sweeps
  - Other control architectures could give better performance, this is just a starting point

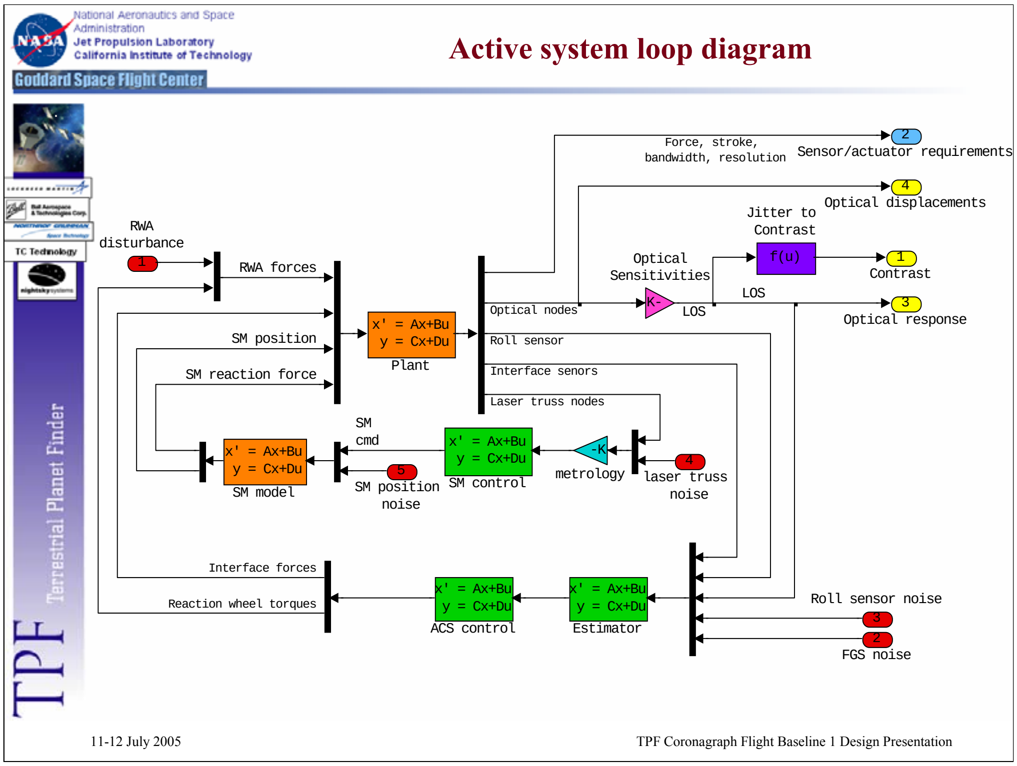

- Analysis results show that the active system can point the payload with the required accuracy, without the need for the FGM and SM, so these loops were disabled
  - Fewer actuators means fewer noise sources
- The SM controller is still required to maintain SM-PM alignment
- The active and passive integrated models are built with common components
  - Such as the optical sensitivity matrices, RW disturbance models, …
  - Only the plant dynamics and the control systems are changed
  - The resulting integrated models are then analyzed using the same code
- On this chart, the dividing line between the quiet payload and noisy support module goes through the ACS control blocks
  - The interface forces that point the payload are driven only from sensors on the quiet side
  - There is only a weak mechanical connection between the support module and payload (they are essentially formation flying)
  - So there is very little disturbance transferred across the interface, this is the key to the active system performance

National Aeronautics and Space Administration
Jet Propulsion Laboratory
California Institute of Technology
Goddard Space Flight Center

Active system point design

TC Technology

TPF Terrestrial Planet Finder

- Non-contact active isolation and pointing
  - Non-contact actuators (NCAs) impart relative force between payload and support module (0.5Hz bandwidth) to control payload inertial attitude
    - Fine Guidance Sensor for pitch/yaw
    - Payload Star Acquisition Camera for roll
    - Interface relative translation
  - Reaction wheels control payload/support module relative angle to maintain requisite interface stroke and gap
  - Pointing is only a function of quiet side (payload) sensors
    - Insensitive to support module disturbances and dynamics
- Interface is shorted by
  - Power/data cabling
    - Adds a stiffness
    - 100 N/m, 100 N-m/rad is used for the nominal results
    - 10x higher than best estimate
  - Back-EMF of the NCAs
    - Rate dependent relative force

- The active isolation system uses a Lockheed Martin technology called Disturbance Free Payload (DFP)
  - Non-contacting voice coil actuators are used to point the payload
  - The reaction wheels are used at very low bandwidth to keep the non-contacting actuators within stroke limits
- The connection across the interface is shorted by a power/data cable with compliance and the back-EMF in the actuators
  - The power/data cable stiffness is conservative, based on best estimates of cable stiffness (with reasonable destiffening measures applied)
  - The back-EMF is a best estimate (ie is not conservative)

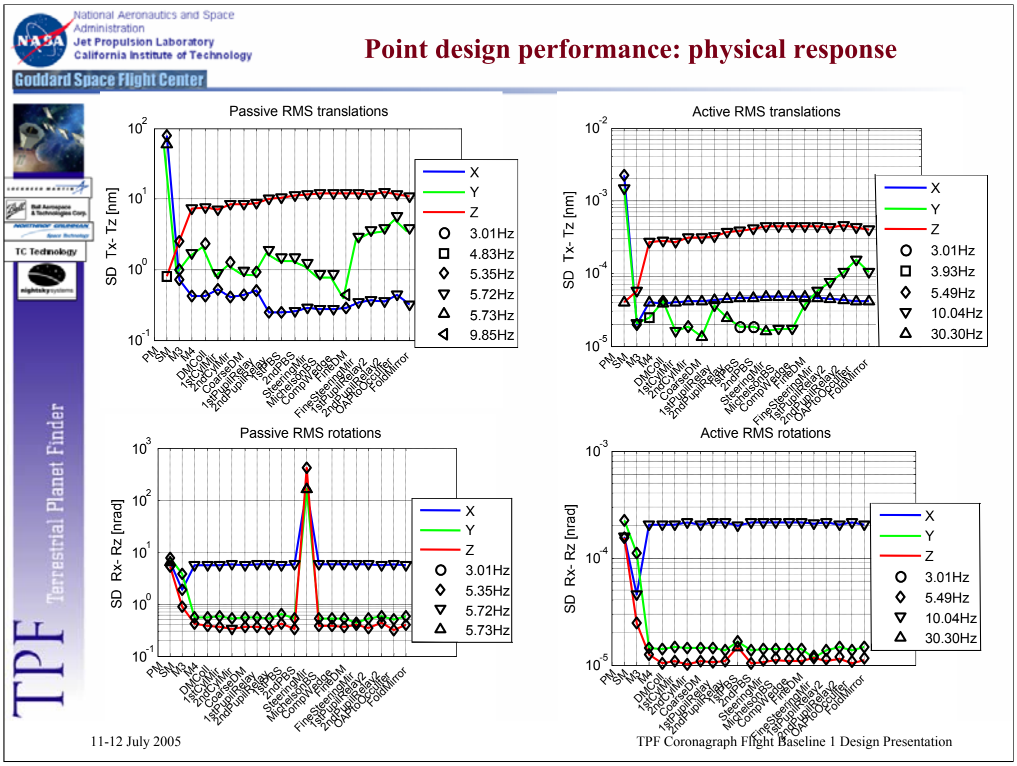

- The plots show the worst-case motions of the optics, over reaction wheel speed
  - The top plots show RMS translation, in 3 axes
  - The bottom plots show RMS rotations
  - The symbols call out the wheel speed at which the worst-case response occurs
  - The passive system plots are on the right, and active on the left
  - Motion is relative to the PM, so no PM response is shown
- The passive system optical responses are significantly over requirements for the SM, but within requirements for the downstream optics
  - The SM exceedances are at 5.35 and 5.75 Hz, which are the frequencies of the Secondary Support Tower first bending modes
- The passive system shows large angular excursions of the Fine Steering Mirror, produced by the control system as it keeps the target star positioned on the mask
  - The SM control system doesn't generate much motion since the bandwidth is well below the frequency of vibration
- The active system response is well below requirements in translation and rotation (and does not exhibit the Fine Steering Mirror rotation since the active design does not require that mirror for pointing performance)

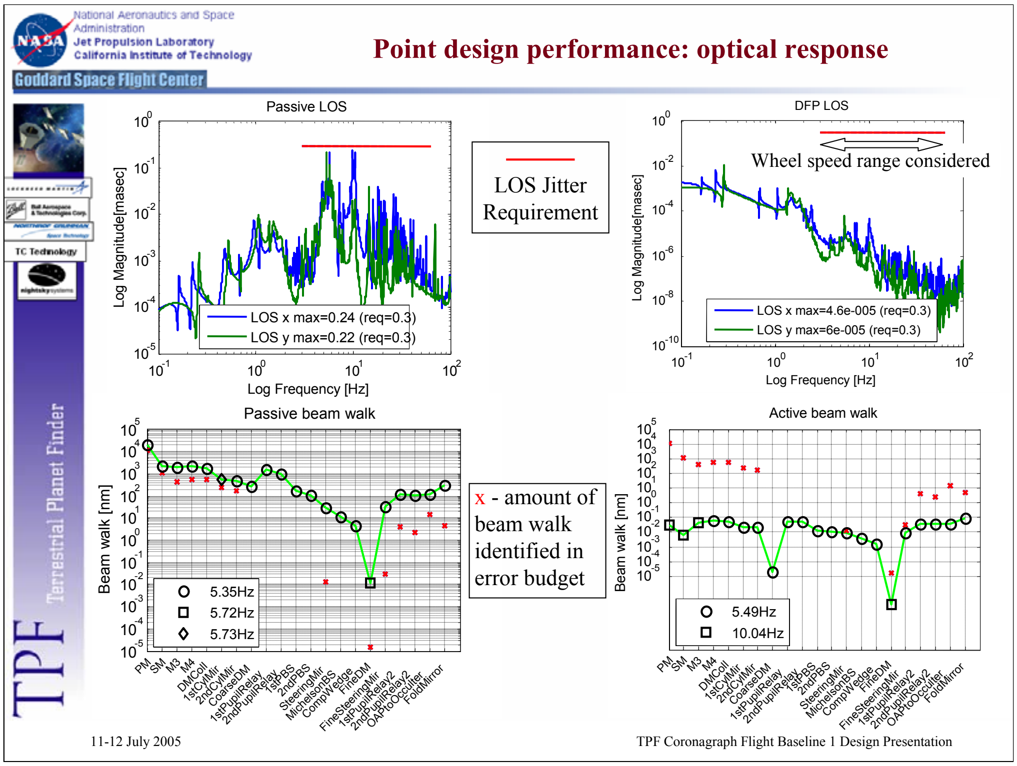

- The top plots show the predicted LOS for the passive (right) and active (left) designs, in mill-arcseconds
  - The curves give RMS LOS versus wheelspeed in rev/sec
  - The red bar is the requirement
  - Both designs meet requirements
    - o By design for the passive system, since the IMC was tuned to suppress LOS just below requirements
- The bottom plots show RMS beam walk for the passive (left) and active (right) designs
  - The active design shows more beam walk than was identified in the error budget
  - This will lead to larger beam walk contrast
  - Again the exceedances occur at the Secondary Tower first bending modes
- The active beam walk shows significantly less beam walk

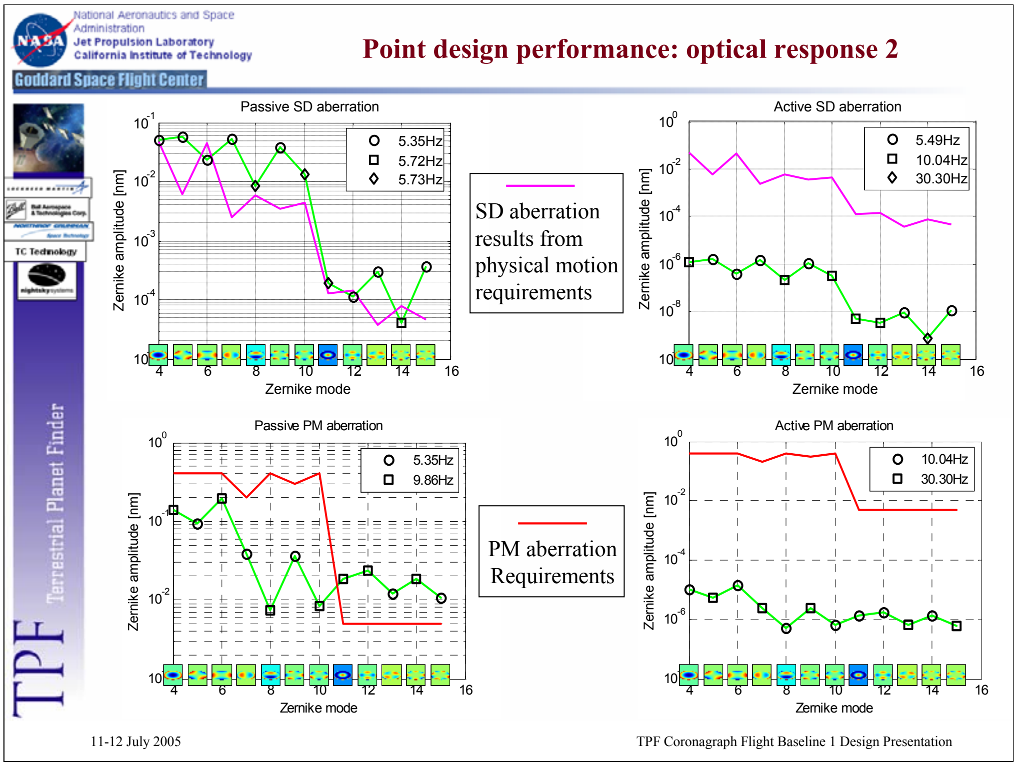

- The top plots show the aberration (wave front error), in terms of RMS Zernike amplitudes in nanometers, for the passive (left) and active (right) designs
  - The passive response is more than that computed in the error budget
  - This is not a big concern since the contrast contribution is very low
  - The passive design is well below requirements
- The bottom plots show the RMS Zernike amplitudes due to PM deformation for the passive (left) and active (right) designs
  - The passive design meets the low order Zernike requirements, but exceeds the higher Zernike mode requirements
  - The active system meets all requirements

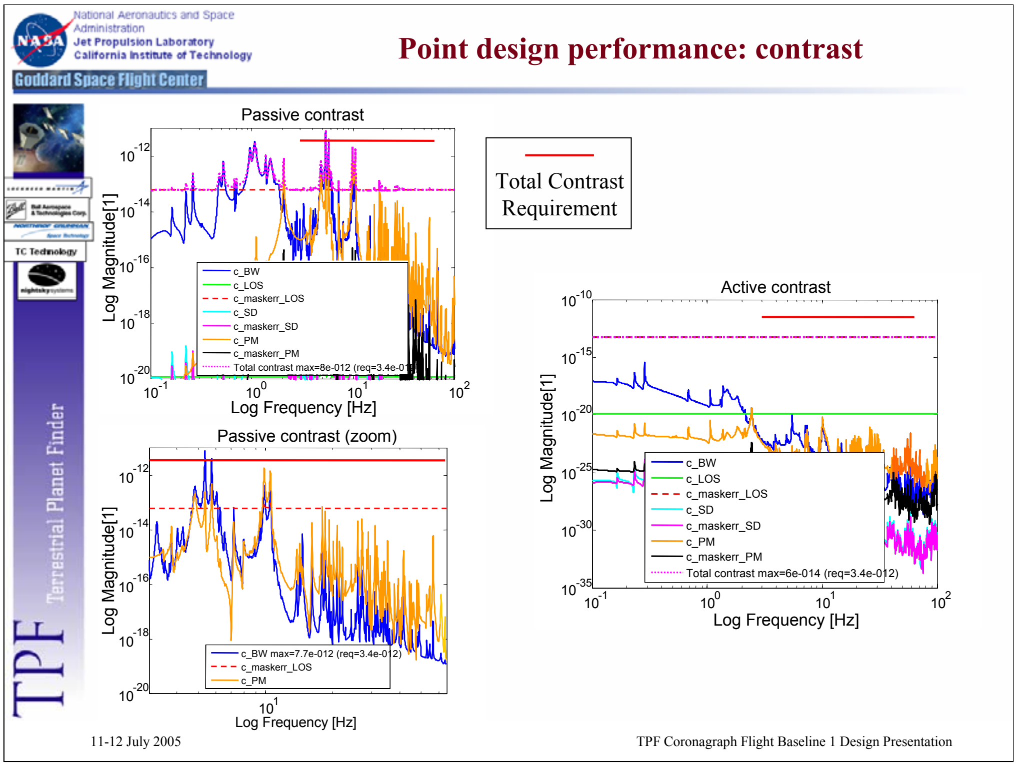

- The top left plot shows the contrast versus wheelspeed for the passive design, by contribution, along with the requirement (red bar)
  - The system exceeds the contribution requirement around 5.35 Hz
- The bottom left plot shows the contrast contributions versus wheelspeed from the beam walk and PM deformation
  - The exceedance is due to beam walk at 5.35 Hz
  - The physical optical motions also showed exceedances at 5.75 Hz, but they do not cause a contrast exceedance due to the correlation between optical motions
- The right plot shows the contrast versus wheelspeed for the active design
  - The contrast requirement is met for all frequencies
  - The total contrast is dominated by LOS mask error, which in turn is dominated by static offset of the star on the mask
    - Contrast is a coupled function of LOS jitter and offset, with a term that is a function only of offset
    - When LOS jitter is small, the offset term dominates and appears as a static contrast degradation
    - No analysis has been done to determine what the true drivers and magnitude of the offset are, this analysis assumes the error budget value of 0.3 masec

Sensitivities: contrast vs. damping

	Passive 0.1%	Passive 0.5%	Active 0.1%	Active 0.5%	Contrast Req
Beam walk	7.7e-12	2.6e-12	1.2e-20	1.1e-22	1.9e-12
LOS	8.1e-17	5.7e-18	1.2e-20	1.2e-20	9e-14
LOS mask error	9.7e-14	7.4e-14	6e-14	6e-14	5.5e-13
Structural deformation	1.6e-16	3.4e-17	3.3e-26	1.8e-27	2.8e-17
SD mask error	7.9e-17	2.7e-17	5.3e-26	6e-28	1.7e-17
PM deformation	1.8e-12	6.6e-13	5.9e-21	8.9e-21	8.5e-13
PM deform. mask error	4.9e-16	1.8e-16	2.6e-24	1.3e-23	5.2e-15
Total contrast	9.5e-12	3.3e-12	6e-14	6e-14	3.4e-12

TPF Terrestrial Planet Finder

- The conservatism of the 0.1% structural damping assumption was checked by re-analyzing the system at the best estimate damping level of 0.5%
- The table shows the contrast contributions for the passive system at 0.1% and 0.5% damping, the active system at 0.1% and 0.5%, and the requirement for each contribution
- The passive design still does not meet requirements at the higher damping level
  - The design conservatism is not driving the passive system design
- The active system contast is dominated by the LOS offset term, so is not a function of damping

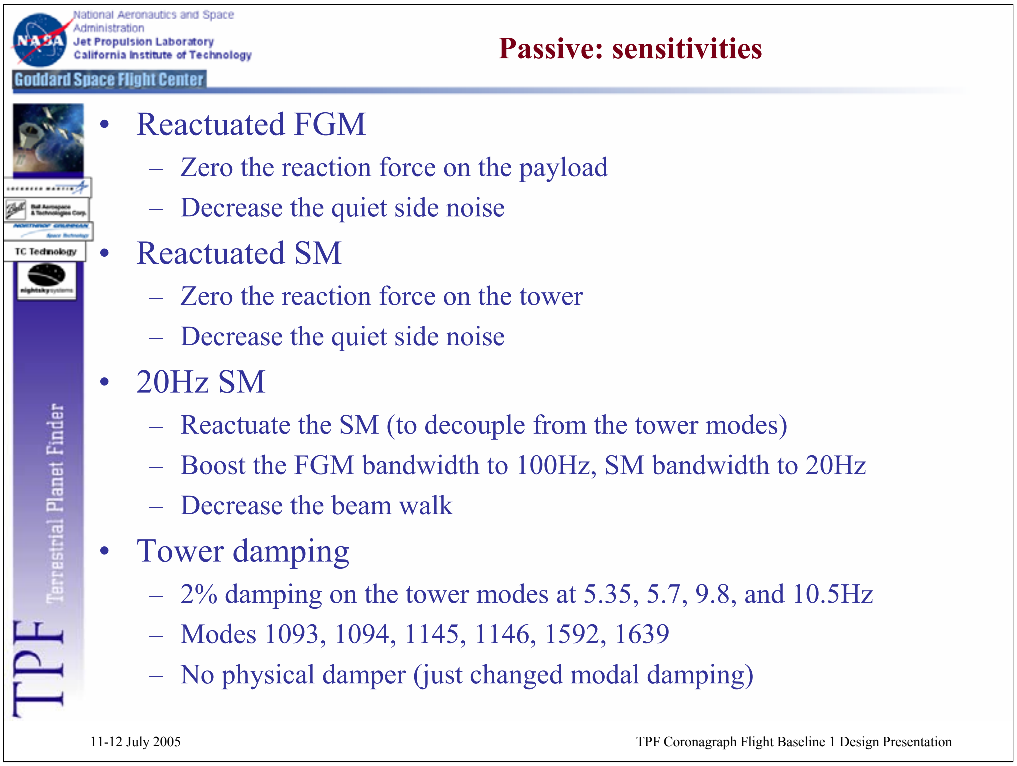

- Sensitivities of the passive system to various design parameters were examined in order to identify a passive design that would meet requirements
- Reactuation (or momentum compensation) is a technique that drives an equivalent mass 180 degrees out of phase with the moving component, to produce near-zero net force on the structure
- Reactuation of the FGM and SM were considered
  - The SM would be difficult to reactuate since it would require the addition of mass on the top of the Secondary tower, detrimentally lowering its frequency, and the SM assembly is already over its mass budget
  - However it is the primary source of contrast degradation so was not rejected out of hand
- The SM can reduce beam walk on the downstream optics when used as a pointing actuator, and beam walk is currently the limiting factor in the passive design, so an SM controller that suppresses the 5.35Hz response could reduce the system contrast to below the requirements
  - The SM bandwidth is limited by spillover instability due to the structural modes, so the SM must be decoupled from these modes (reactuation is one approach, a soft-mount to the tower is another)
- Passive damping of the tower would also reduce the 5.35Hz response

Passive sensitivities: RWA to contrast

	Nominal	Reactuated FGM	Reactuated SM	Reactuated SM + 20Hz SM	2% Twr Damping	Contrast Req
Beam walk	7.8e-12	7.8e-12	8.5e-12	5e-14	3.7e-13	1.9e-12
LOS	7.7e-17	7.7e-17	1.1e-16	1.2e-20	1e-19	9e-14
LOS mask error	9.7e-14	9.7e-14	1e-13	6e-14	6.3e-14	5.5e-13
Structural deformation	1.6e-16	1.6e-16	1.9e-16	8.1e-18	3.6e-18	2.8e-17
SD mask error	8e-17	8e-17	8.7e-17	1.1e-17	2.7e-18	1.7e-17
PM deformation	1.8e-12	1.8e-12	2e-12	2e-12	2.1e-13	8.5e-13
PM deform. mask error	4.8e-16	4.8e-16	5.5e-16	5.5e-16	9.6e-17	5.2e-15
Total contrast	9.6e-12	9.6e-12	1.1e-11	2.1e-12	6.4e-13	3.4e-12

TC Technology

TPF Terrestrial Planet Finder

- The analysis shows that both the 20Hz SM, and the tower passive damping, could meet the contrast requirements

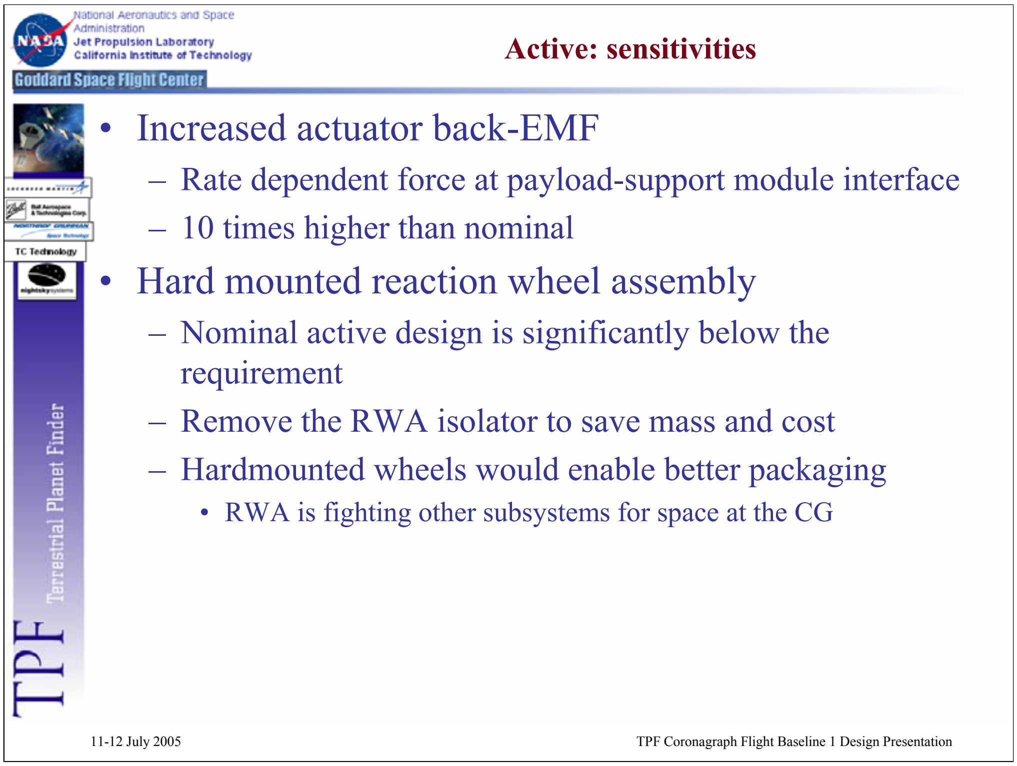

- The active system back-EMF was non-conservative, so a conservative number was analyzed
- The active system performs significantly better than requirements, suggesting that the Reaction Wheel Assembly isolation could be removed (causing the response to get larger) but still be within requirements

National Aeronautics and Space Administration
Jet Propulsion Laboratory
California Institute of Technology
Goddard Space Flight Center

Active sensitivities: RWA to contrast

	Nominal	x10 back EMF	Hardmount RWA	Contrast Req
Beam walk	5.7e-18	5.7e-18	3.8e-16	1.9e-12
LOS	1.2e-20	1.2e-20	1.2e-20	9e-14
LOS mask error	6e-14	6e-14	6e-14	5.5e-13
Structural deformation	2.7e-24	2.7e-24	3.1e-23	2.8e-17
SD mask error	1.6e-24	1.6e-24	6.2e-24	1.7e-17
PM deformation	1.7e-20	2e-20	7.2e-17	8.5e-13
PM deform. mask error	2e-23	2.4e-23	6.3e-20	5.2e-15
Total contrast	6e-14	6e-14	6.1e-14	3.4e-12

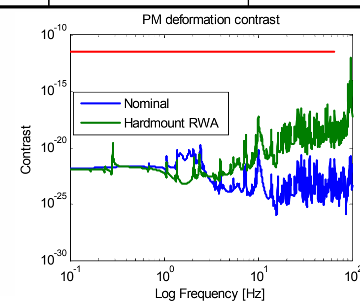

TPF Terrestrial Planet Finder

- The table shows the contrast by contribution for the nominal passive design, the larger back-EMF, and for the hardmounted RWA
- In all cases the active system still meets requirements
- The figure shows the contrast versus wheelspeed for the nominal active design (blue) against the hardmounted RWA design (green)
  - The hardmounted RWA response shows significantly more response at higher frequency, since the RWA isolation is removed
  - The requirement is still met, withing the speed limits of the wheel

Nonlinear Time Simulations

- Create time simulation that complements DOCS linear system analysis and incorporates nonlinearities in real system
- Perform jitter analysis due to nonlinear actuator and sensor effects (see backup slides)
  - RWA drag torque
  - RWA tachometer measurements
- Estimate slew/settle time for dithers
  - Updated 6 wheel configuration
  - Simulate acquisition sequence from coarse mode to fine observing mode

- The time simulation is being used to assess the transient response of the system, and assess the effects of nonlinearities
- The following section shows a simulation of a dither manuever, in which the payload is rolled 30 degrees about the line of sight
  - The telescope starts with the star locked in the FGS in fine pointing mode
  - The telescope then rolls around the line of sight in coarse pointing mode
  - The acqusition sensors are then used to bring the star back into the FGS in acquisition mode
  - The fine pointing mode then locks the star to the FGS once again
- The simulation is for the passive isolation design
  - The active system will be evaluated for the same slew

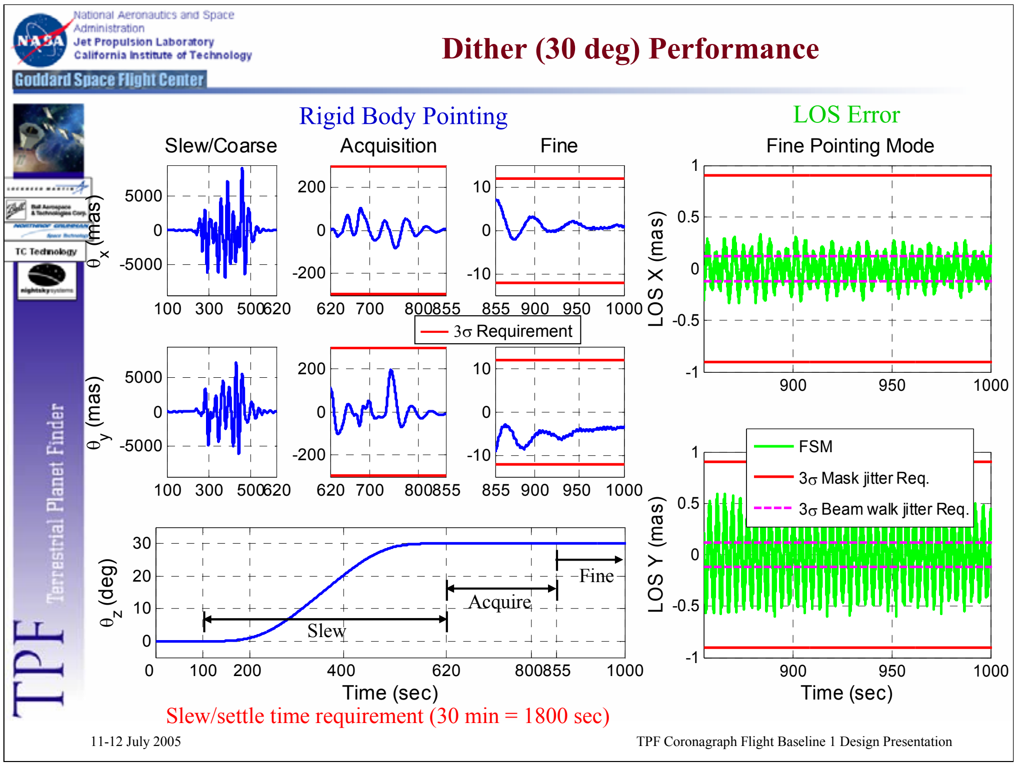

- The bottom left plot shows the roll angle of the telescope during the dither manuever, during the slew, acquisition, and fine pointing modes
- The top left 2x3 grid of plots shows the X and Y rigid body pointing performance of the telescope for each mode
  - The plots are on different scales since the angles are much smaller in fine pointing mode
  - The red lines show 3-sigma requirements
  - The rigid body pointing is within requirements for all modes, and the system settles to within requirements within 855 seconds
    - o The settling time is well within the 1800 second requirement
- The two right plots show the position of the centroid on the mask (in units of angle on the sky) during fine pointing mode
  - The tachometer noise from the wheel speed control loop is exciting a 0.26Hz mode, causing LOS jitter

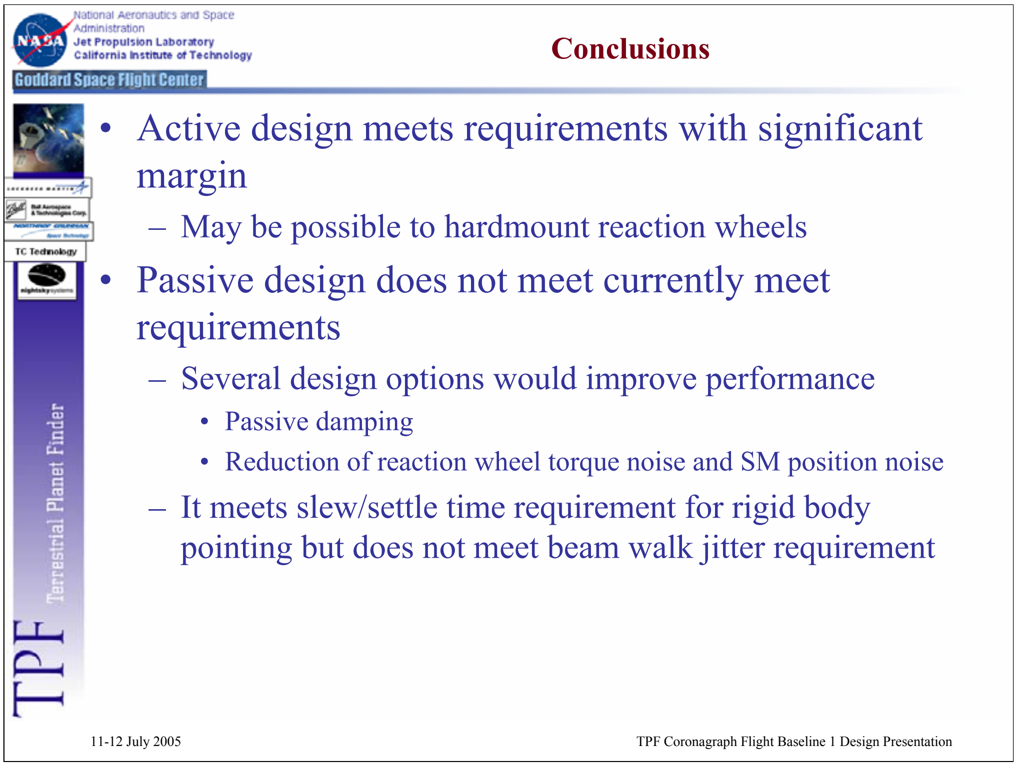

- The analysis results show that the active system can provide significant margin
  - The RWA isolation could be removed, with an attendant cost reduction
- The passive system can meet requirements with some low cost/risk modifications
  - Passive design is a particularly attractive option, and additionally buys down significantly the risk of unexpectedly low system damping
- At this stage it is likely that both systems are feasible
- The performance advantages of the active system must be traded carefully against the greater maturity of the passive system

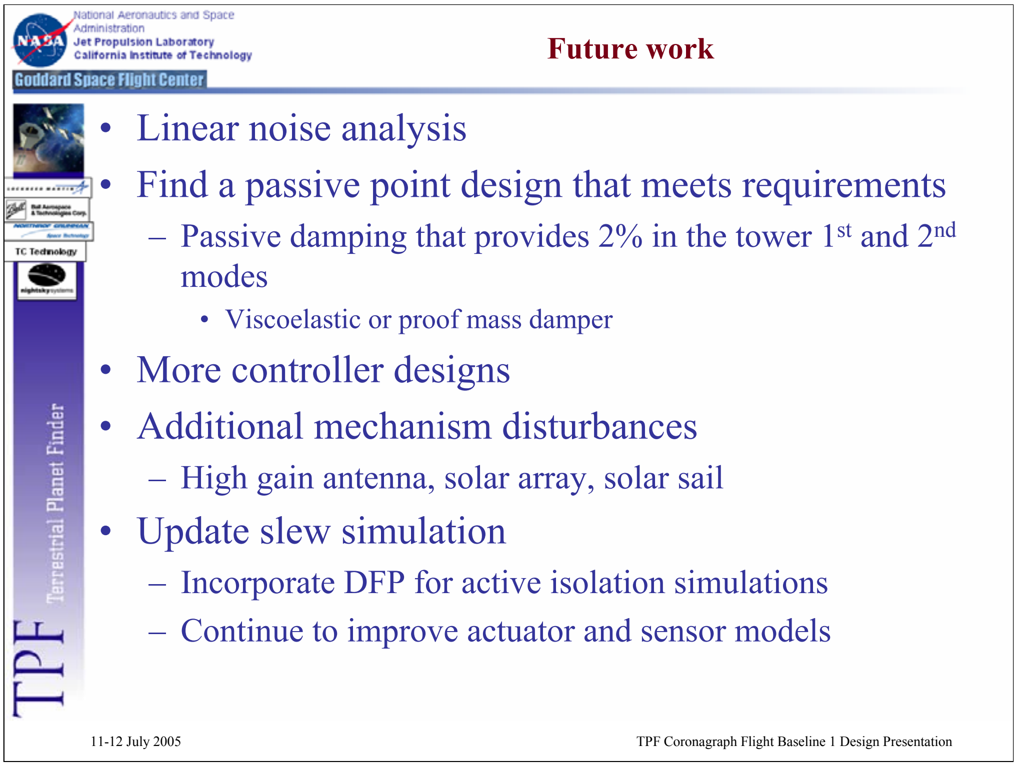

- The jitter due to sensor/actuator noise must be evaluated
  - This is of particular interest for the active design since it may dominate the jitter response
  - The passive design needs to allow for the noise jitter
- Different controller designs may more optimally balance disturbance suppression with sensor noise contribution
- The baseline observation scenario assumes that all of the mechanisms are fixed during observation
  - This limits observation time since the wheel momentum must be dumped periodically by the solar sail (although this limit may be less pressing than the thermal distortion-induced observation time)
  - It may be possible to slew the antenna, solar array, and or solar sails during observation
  - This would give more operational flexibility

TPF Terrestrial Planet Finder

Backup Slides

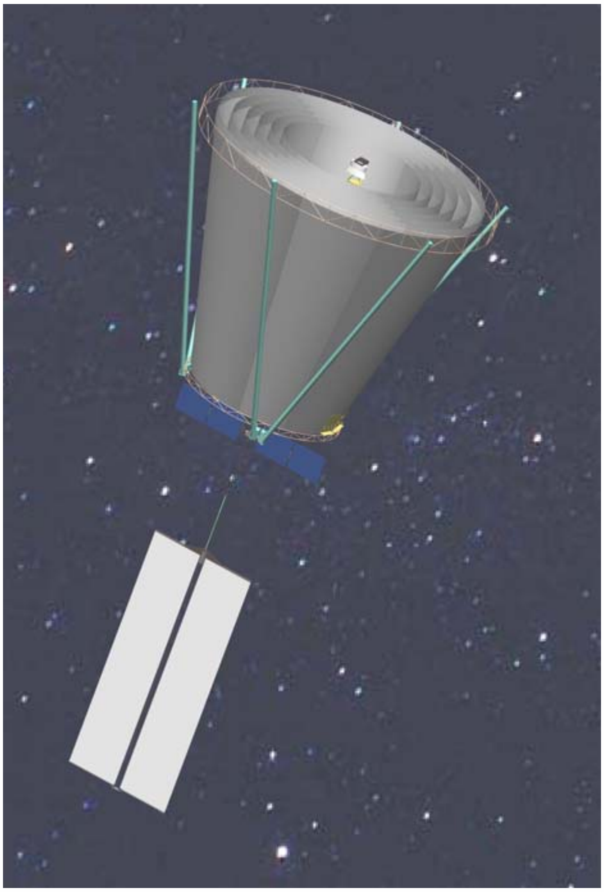

Simulation Model Descriptions

- Nonlinear time simulation is created in Simulink, modified from JWST Yardstick model
  – Captures nonlinear attitude rigid body dynamics (gyroscopic effects)
  – Include a reduced set of significant flexible modes (35 modes)
  – LOS and beam walk sensitivities are currently implemented
  – Same controller, vibration isolation, actuator, and sensor models are implemented as the DOCS linear model
- Slew control design description
  – PD controller plus acceleration feedforward
  – Structure filter used to reduce flexible mode responses and settling time
- Disturbances
  – RWA: imbalances, torque quantization, drag torque, and torque noise
  – Sensor noises: gyro, star tracker, PSAC, FGS, orientation of FGM, orientation of SM, and tachometer quantization

- Time simulation model has some commonalities with the linear simulation model used to conduct the RWA jitter analysis
- Some nonlinear effects that can be added or removed to assess their effect
- Coarse mode control system

Wheel Drag Effects

- Drag torque
  - Model is a curve fit from vendor data (MAP, TRMM)

$$T_{\text{drag}} = \alpha \operatorname{atan}(\beta H_{\text{rw}}^{\gamma}) \qquad \alpha = 0.341 \qquad \beta = 0.0399$$

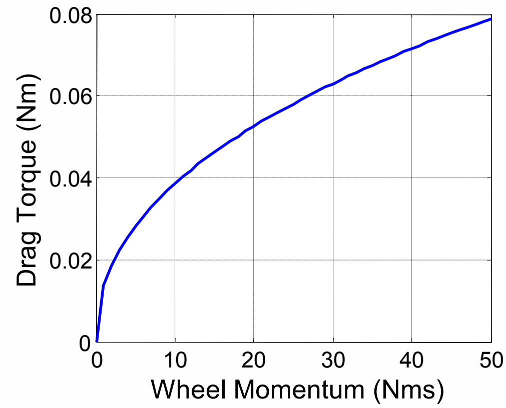

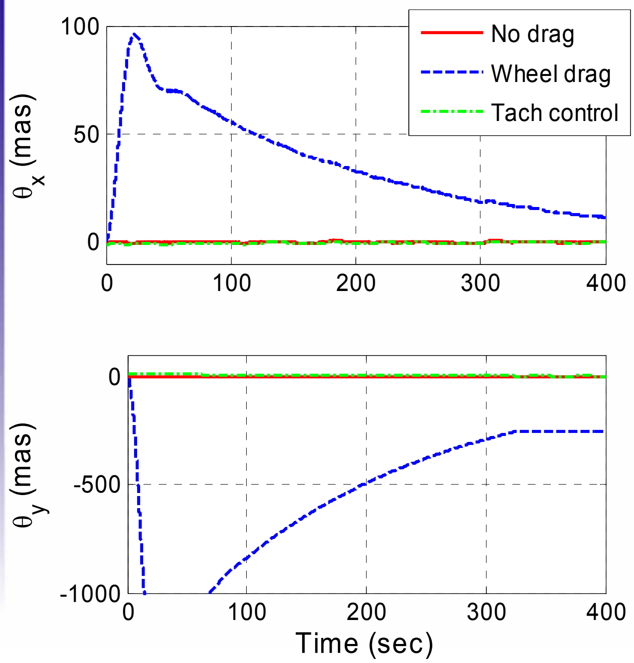

- ACS integral control cannot act fast enough to cancel changing drag torque
- Faster wheel tachometer loop is closed to compensate for drag torque

Terrestrial Planet Finder
TPF

- Drag torque causes the actual torque introduced into the spacecraft to differ from the commanded torque
- Difficult to remove by sensing payload attitude since the drag torque changes faster than the ACS can respond to
- Local wheel control can remove it, at the cost of an additional source of wheel speed sensor (tachometer) noise

Wheel Tachometer Measurement Errors

- Tachometer readout
  - 72 pulses per revolution for Goodrich E wheels
  - Tach error increases with wheel speed due to less time elapsed between two pulses

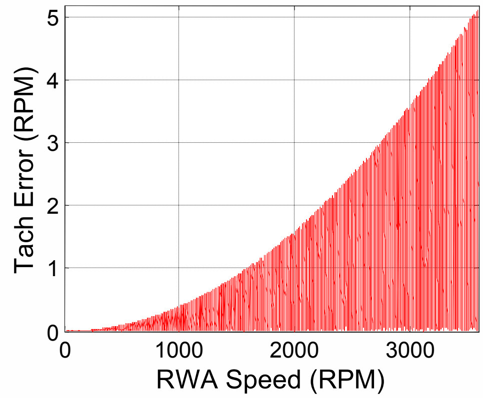

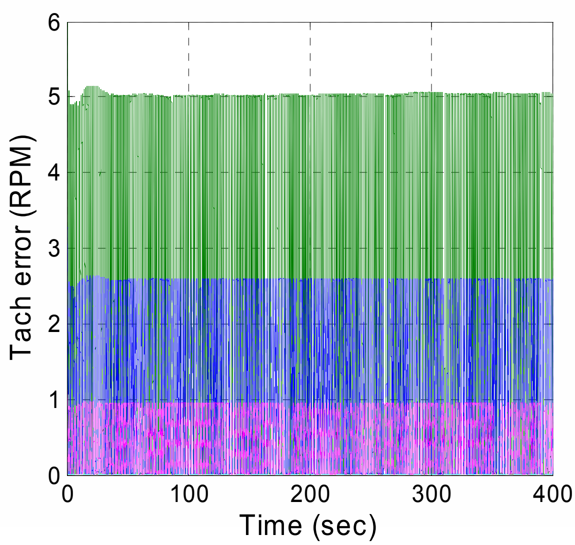

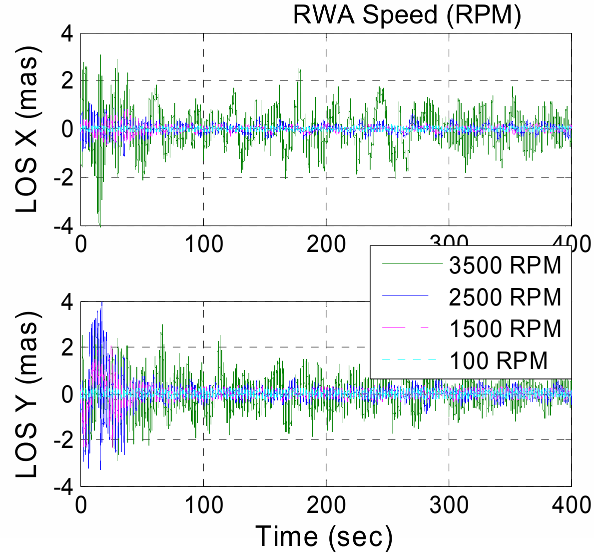

- Tachometer noise currently appears to be one of the largest contributors to LOS jitter
- Tachometer is currently implemented as a timer reading successive wheel angular position pulses
- If further analysis confirms the problem, it may be possible to modify the implementation to get lower noise

Lockheed Martin
Ball Aerospace & Technologies Corp.
Northrop Grumman Space Technology
TC Technology
nightsky systems

TPF Terrestrial Planet Finder

Modeling Summary

Marie Levine

Contributors:
Modeling Team

11-12 July 2005

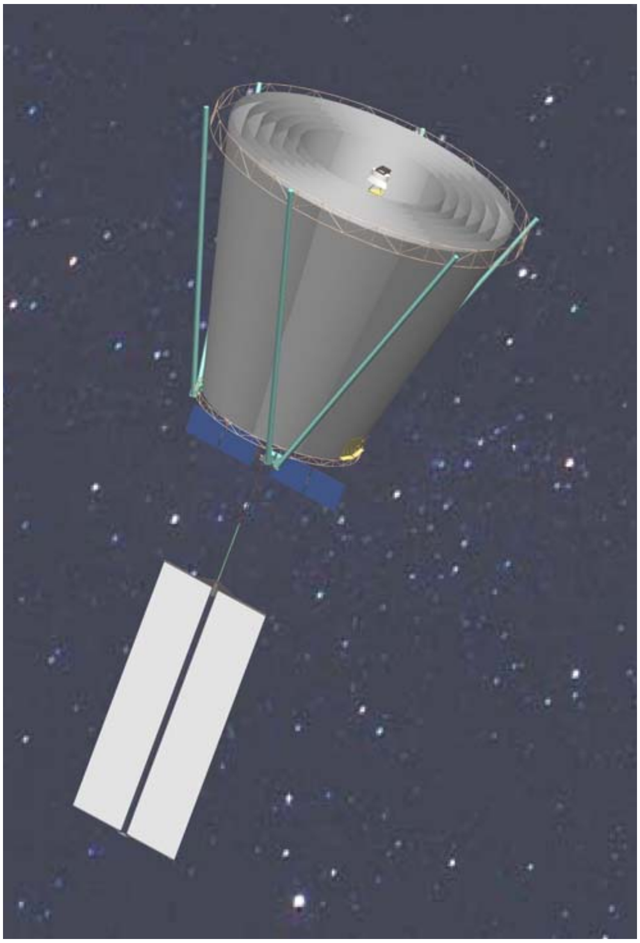

Iterative Design/Analysis Cycle Process

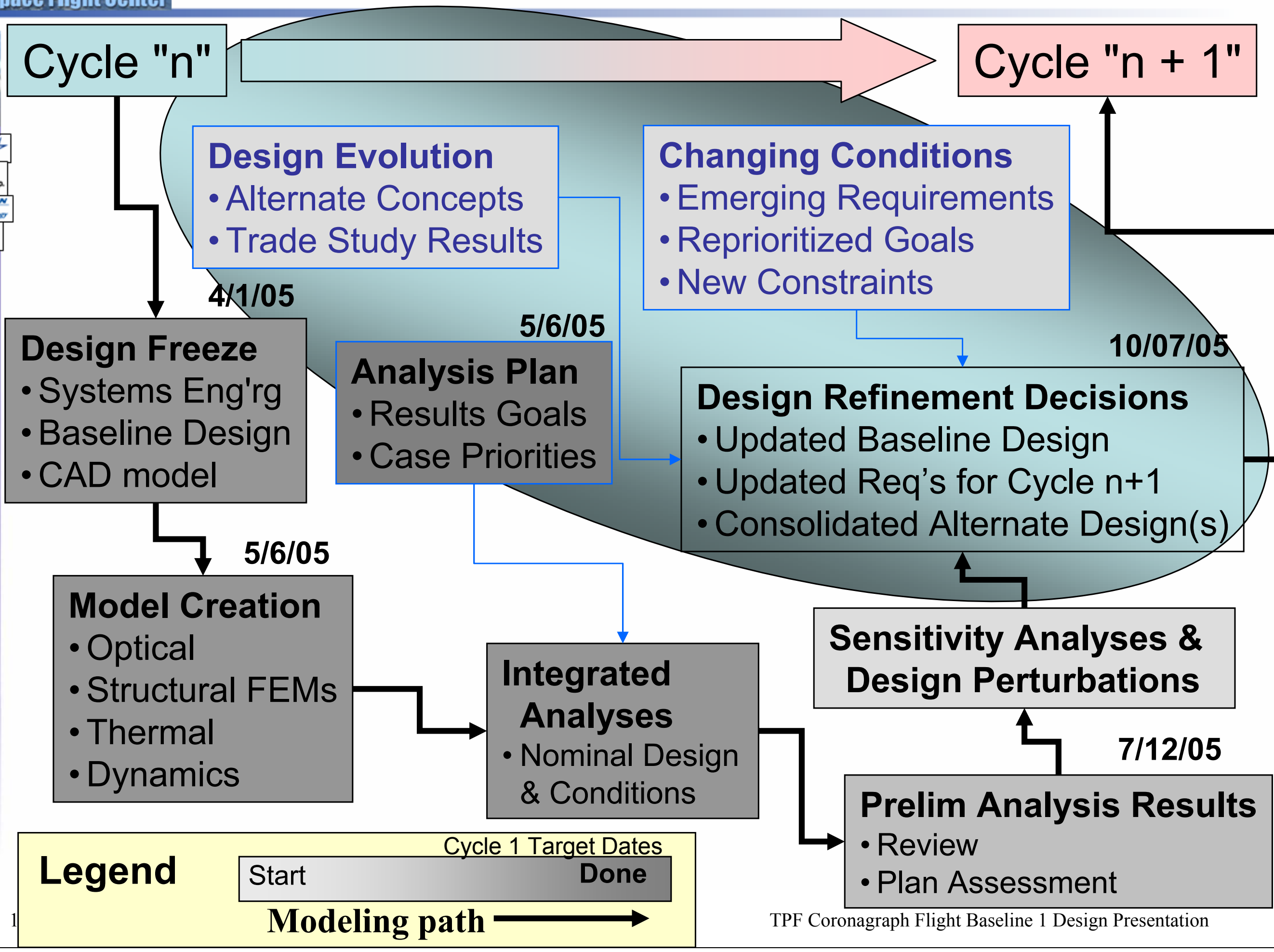

Cycle 1 Alternate Concepts for Analysis

1. Pointing Control System
   - Passive vs dynamic isolation
   - RWA design option trades: size, position, number

2. PM Mirror Architecture
   - Racetrack monolithic PMA vs Elliptical
   - PM mounts & launch locks
   - Closed-back vs open-backed
   - PMA core segmentation: hex vs square
   - Actuated PMA vs coarse DM

3. OTA Design
   - Light-weighted SMA & AMS
   - OTA baffle concept

4. Sunshield Design
   - Sunshield architecture: conic vs sugar scoop
   - Active thermal design for PMA & SMA
   - Sunshield circularity sensitivity
   - Active thermal control layer in sunshield

ACS Trade Studies

James Alexander

Contributors:
Blaurock, Dewell, Liu

11-12 July 2005

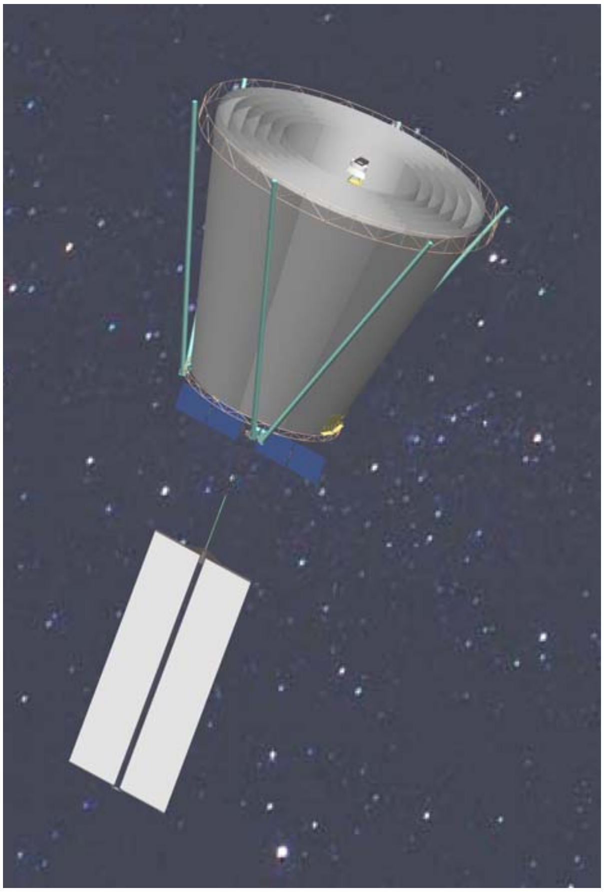

Trade Studies

- Reaction Wheels Trades
  - Reaction wheel location trade
    - Move wheels away from the CG to free up space, at the cost of potentially amplifying induced jitter
  - Size
    - Momentum buildup – (solar pressure, etc)
    - Time duration between momentum dumps
    - Torque Capabilities needed to complete slews with time period
    - Isolation Stage on reaction wheels versus wheel height
    - Use more, smaller wheels
- Fine Guidance Sensor (FGS) design
  - Location of focal plane and implementation (exact pickoff location)
  - FSM design (bandwidth, range of motion,)
  - FGS sensor model

Trade Studies

- Location of Payload Acquisition Camera Trade
  - Location (Currently looking through the baffle)
  - View of sky
  - Dynamic stability
- Active isolation
  - Roll sensor trade (from payload or support module)
  - Advantage of eliminating SM control system and possibly FGM control loop
- Solar Sail disturbance on S/C
- Map disturbances to contrast budget (provided preliminary results)
  - provides method directly looking at disturbance influences

National Aeronautics and Space Administration
Jet Propulsion Laboratory
California Institute of Technology

Goddard Space Flight Center

TC Technology

TPF Terrestrial Planet Finder

Racetrack configurations for the TPFC Primary Mirror

Joseph J. Green (JPL)

Contributors:

Dave Content (GSFC)
Ian Crossfield (JPL)
Tim Ho (JPL)
Sarah Hunyadi (JPL)
Ray Ohl (GSFC)
John Schiermeier (JPL)

July 11-12 2005

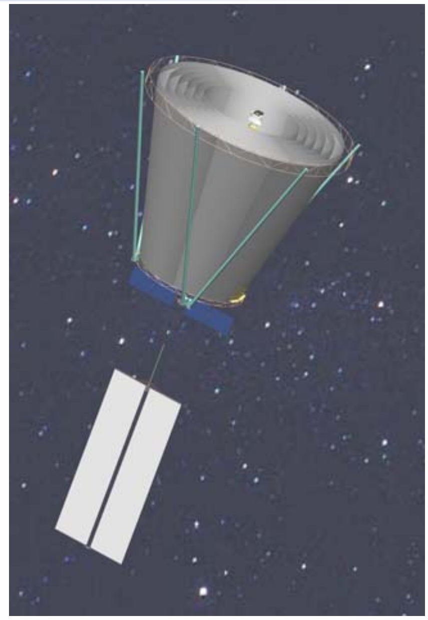

Executive Summary

- This presentation summarizes the trade status of TPFC primary mirror shape design
  - Baseline is a 8.0x3.5 meter ellipse
  - Trade consider 8.0x3.0 meter quasi-rectangular shape alternatives that are referred to as “racetrack mirrors”
- Study to date shows adopting a racetrack PM configuration can provide substantial system throughput gains
  - Starlight suppression system is 33% more efficient
  - A 8x3 meter racetrack PM has about 8% more collecting area
  - The combination enables that TPFC can detect and characterize planets in <u>half the time</u> than the current baseline

National Aeronautics and Space Administration
Jet Propulsion Laboratory
California Institute of Technology
Goddard Space Flight Center

Racetrack PM Trade Study

TPF Terrestrial Planet Finder

- Motivation
  - Potential to improve corongraph throughput
    - Rectangular PMs well matched to linear occulters
  - Reducing spacing between PM and SM tower
    - Creates volume for launch support structure
- Constraints on mirror shape/size
  - Mirror manufacturability - limited to D < 8.3m (current facilities)
  - Inner diameter of launch shroud (4.57m diameter)
  - Mass budget already very tight
- Trade parameters
  - Coronagraph performance (efficiency, sensitivity)
  - Mirror size
  - Mirror performance (stiffness, frequency, gravity sag)

Co-optimizing the telescope architecture with the startlight supressions system has the potential to greatly enhance the net system performance. This trade study examines how altering the PM shape affects

(1) startlight suppression system performance

(2) PM stiffness

(3) aberration sensitivity

National Aeronautics and Space Administration
Jet Propulsion Laboratory
California Institute of Technology
Goddard Space Flight Center

Impact on Coronagraph Efficiency

- Modeling Assumptions
  - 8th order mask optimized for 4λ/D
  - λ_o=550nm, Δλ=±50nm

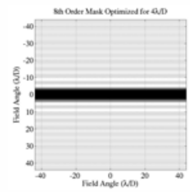

8x3.5m Elliptical

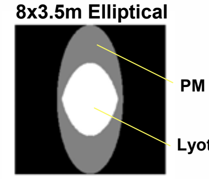

8x3.0m Racetrack

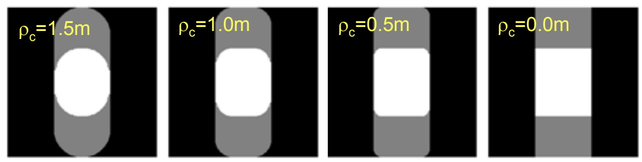

8x3.0m R_{PM}<4

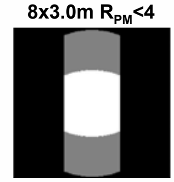

Primary Mirror Shape	PM Area (m^2)	Lyot Efficiency	Net Area (m^2)	FWHM PSF Core Area (mas^2)
8x3.5 Ellptical	21.991	0.340	7.479	1118.6
8x3.0 Racetrack (r_c=1.5m)	22.226	0.406	9.031	942.6
8x3.0 Racetrack (r_c=1.0m)	23.254	0.434	10.083	816.9
8x3.0 Racetrack (r_c=0.5m)	23.837	0.449	10.696	741.5
8x3.0 Racetrack (D=8)	23.410	0.440	10.307	766.7
8x3.0 Rectangle	24.000	0.453	10.875	741.5
Ratio of Rectangle to Ellipse	**1.09**	**1.33**	**1.45**	**0.66**

TPF Terrestrial Planet Finder

The baseline starlight suppressions system concept is a Lyot coronagraph. Shown at the two are its two components.

1. There is an occulting spot (in our case a 8th order mask) placed and centered at an image of the target star.
2. A Lyot stop (shown in white) is a mask place at the downstream pupi l that s used to eliminated the residual diffracted starlight. As can be seen in the figure next to the occulting spot, it only admits about 1/3 of the overall aperture.

The racetrack configuration shown below the baseline all offer significant gains in coronagraph efficiency while at the same time making the image of the planet more compact (2/3 of the baseline planet image).

The enhancement of both the net system efficiency and planet image compactness are substantial benefits to the project.

Mounting Optimization

	Natural Freq. Hz	Gravity Sag µm p-v
Elliptical Primary Mirror		
Baseline Mount Placement	25.67	658.30
Optimized about Long Axis	34.32	112.40
Racetrack - 0.5 m Radius Corners		
Bsaeline Mount Placement	22.38	890.10
Optimized about Short Axis	24.02	575.20
Optimized about Long Axis	29.51	100.60
Racetrack - 1.5 m Radius Corners		
Baseline Mount Placement	22.02	914.10
Optimized about Short Axis	29.97	470.40
Optimized about Long Axis	33.01	135.30

Gravity Sag for Baseline Mount Placement

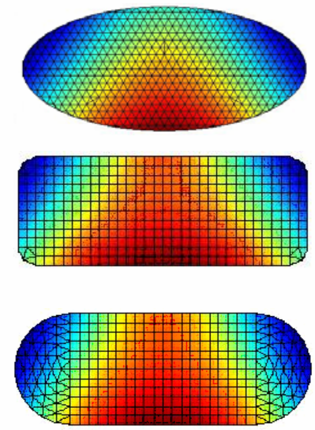

Gravity Sag Long-axis Optimization

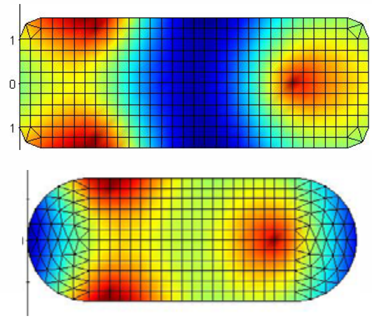

Assumptions:

- Flat plate mirrors
- Single point mounting
- Mirror can be supported at nodes
- No thermal or jitter disturbances
- Gravity vector points into the slide

- The figures on the right show the gravity sag for the placing the nodes in a configuration like the current baseline. Blue indicates sag downward and red indicates flexion upward. The two figures in the lower portion show the gravity sag for the alternative node optimization cases. Again red is flexion upward and blue is sag downward. The darkest blue is the minimum displacement as noted in the chart and the reddest red it the maximum displacement as noted in the chart. The assumptions used in this analysis are listed in the lower right => this is a very preliminary analysis just to get a feel for the flexions and frequency in the racetrack mirror.

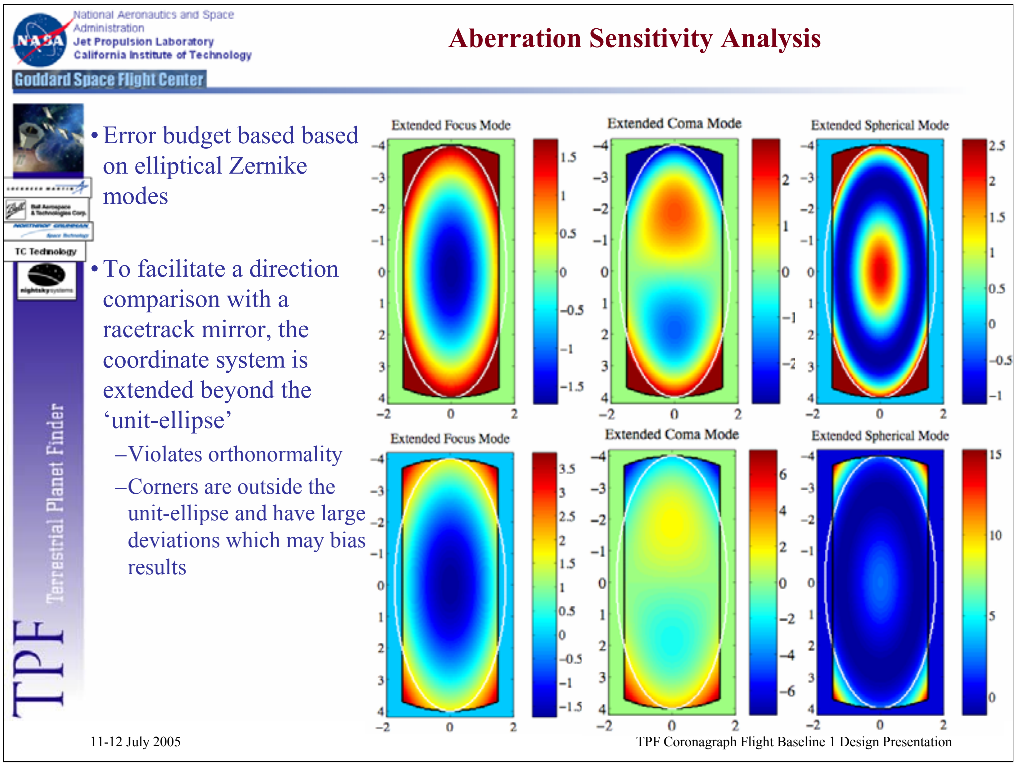

The comparison of aberration sensitivities between the baseline and an architecture alternative requires that a common aberration basis set be used

Here we took the elliptical Zernike basis set and extend the function out to the boundaries of one of the alternate PM shapes.

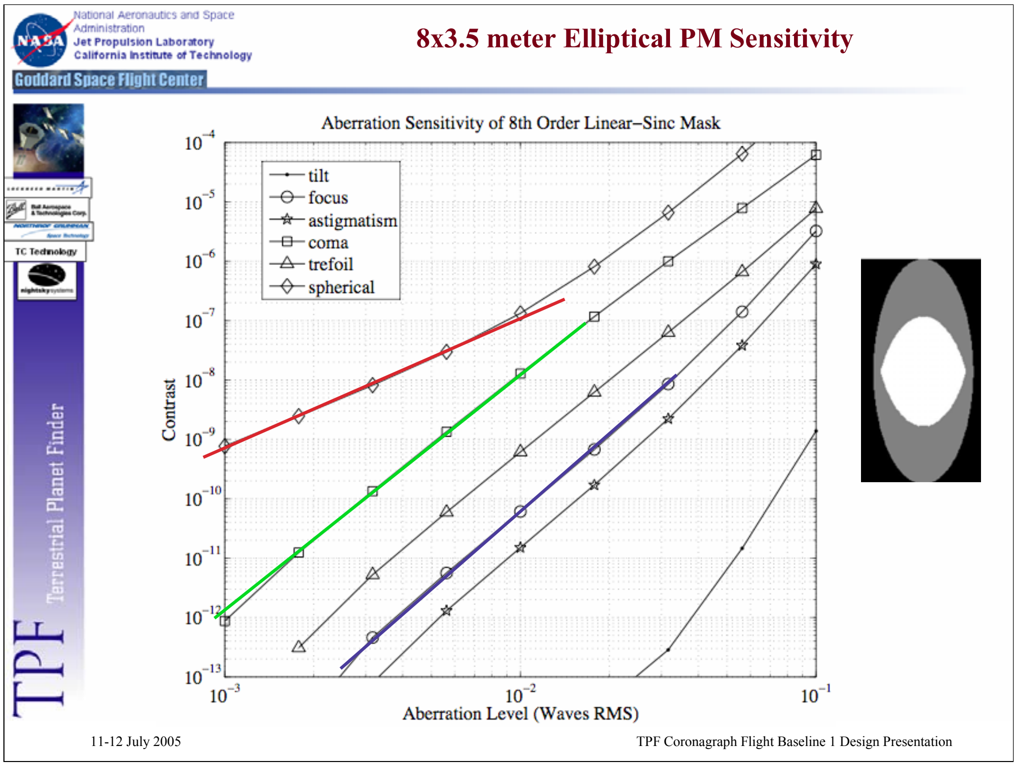

- Here we show the aberrations sensitivity curves for the baseline coronagraph and PM aperture. These curves are at the heart of the dynamical error budget and help establish such things as the requirements on secondary mirror motion and the level of acceptable thermal perturbation.

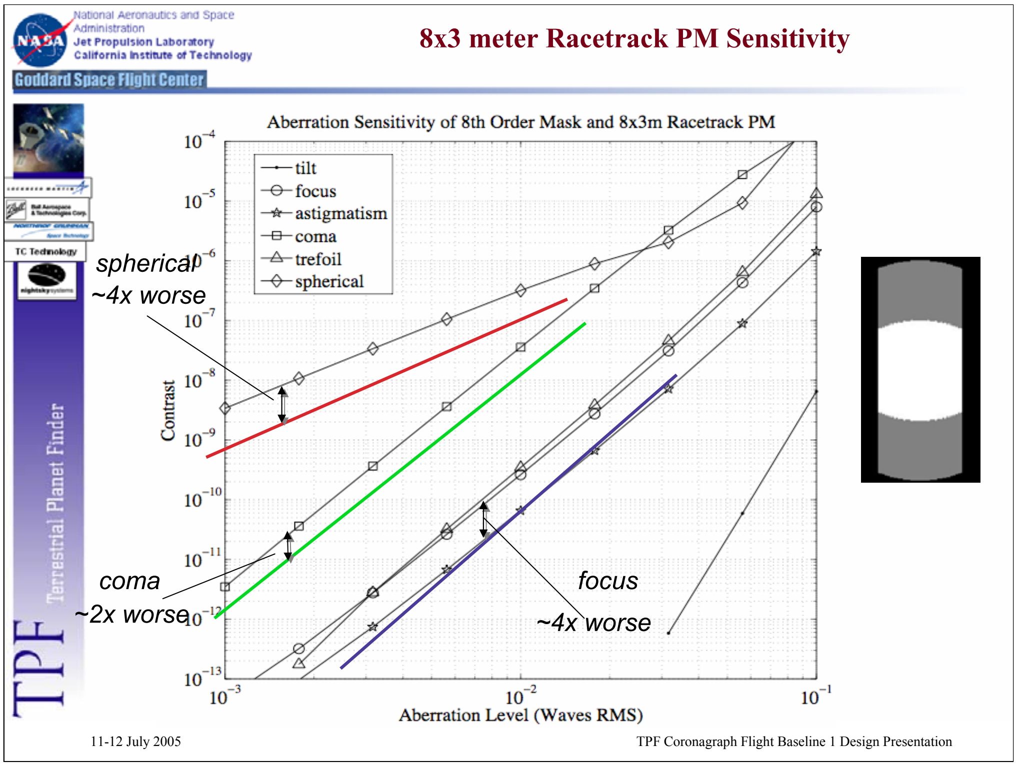

- The alternate PM aperture shape enables a much more efficient Lyot stop. This in turn has the impact of increasing our sensitivity to changes in low-order aberrations.
- There is a good chance that this increase in sensitivity can be made up by appropriate error budget reallocations.
- The factor of 2 increase in the rate of planet detection and characterization far out-weight this issue.

Trade Summary (I)

- These two configuration are attractive
  - 40% more effective collecting area for 8% more PM
  - Planet PSF 50% more compact
  - But higher aberration sensitivity

PM + Lyot Stop Shapes

Parameter	8x3.5 Elliptical	8x3 Racetrack rc = 1.5m	rc = 0.5m	D = 8.0m	8x3.0 Rectangle
PM Area (m^2)	21.991	22.226	23.837	23.410	24.000
Lyot Efficiency	0.340	0.406	0.449	0.440	0.453
Net Collecting Area (m^2)	7.479	9.031	10.696	10.307	10.875
FWHM PSF Core Area (mas^2)	1118.600	942.600	741.500	766.665	741.500
Optimized Fund. Freq (Hz)	34.320	33.010	29.510		
Optimized Grav Sag (µm pv)	112.400	135.300	100.600		
Focus Required for 1e-10	1.00E-02			2.50E-03	
Coma Required for 1e-10	3.00E-03			1.50E-03	
Spherical Required for 1e-10	1.80E-04			9.00E-05	

TPF Terrestrial Planet Finder

- The table above summarizes the all the trades to date but the principle benefits to adopting a racetrack-type PM for TPFC are
  - 40% more effective collecting area for only 8% more PM
    - o Enables planet detection/characterization in half the time
  - 50% more compact planet images
    - o Making us more immune to detector read-noise
  - Benefits are best realized for PM apertures that are closely matched to a rectangular aperture

National Aeronautics and Space Administration
Jet Propulsion Laboratory
California Institute of Technology
Goddard Space Flight Center

Trade Summary (II)

- Pros
  - TPFC can operate 2x faster!
  - Narrower short axis is more enabling w.r.t. mechanical design
- Neutral
  - Manufacturability
  - Gravity Sag
- Cons
  - 2-4x more sensitive to aberrations
  - Heavier PM
    - 8x2.8m would be about the same as baseline
- To Do
  - Evaluate the net efficiency versus aberration sensitivity impacts upon error budget and completeness

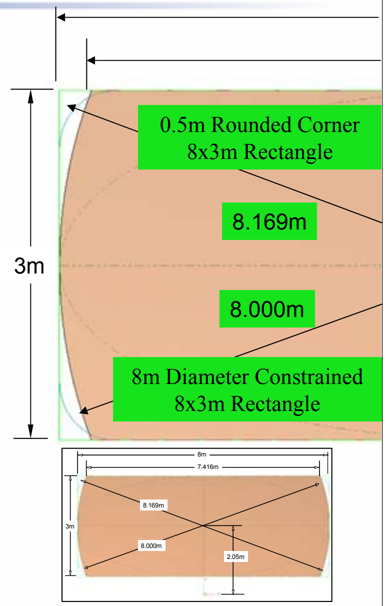

TPF Terrestrial Planet Finder

11-12 July 2005 TPF Coronagraph Flight Baseline 1 Design Presentation

- The advantages to adopting a new PM configuration outweigh the drawback.
  - The increase in aberrations sensitivity can likely be mitigated through an error budget reallocation
  - The PM is ~8% heavier than for a 8x3 meter racetrack shape but would be identical if the PM were instead 8x2.8 meters. Nevertheless, there may be other trades that could free up mass budget to enable the PM mass increase.
- Racetrack mirrors are very attractive for TPF. It will fundamentally enable a mission that can conduct a much deeper survey in less time.

Sunshade Trade Study

'sugar-scoop' vs baseline sunshield thermal performance

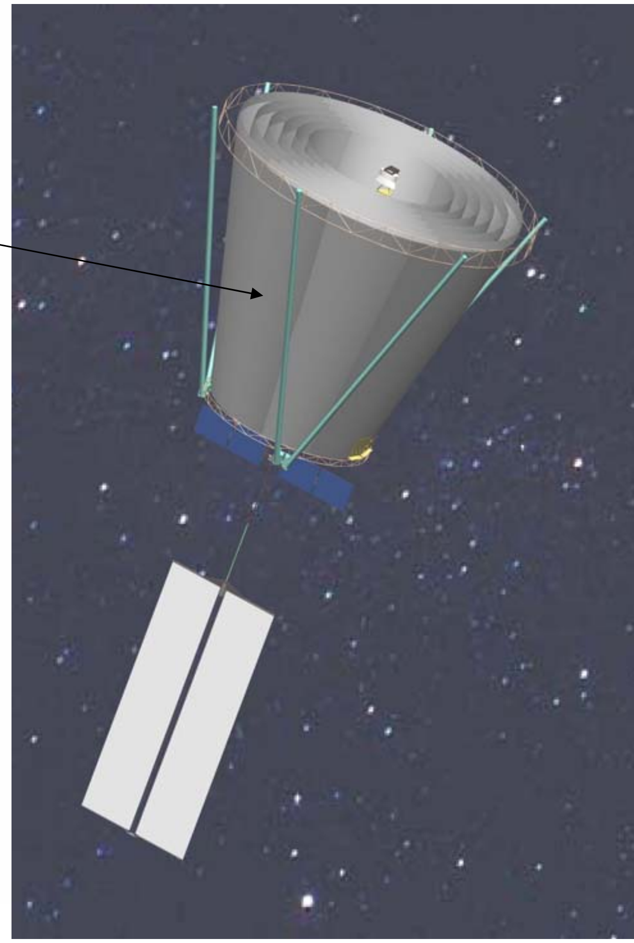

presented by
Terry Cafferty

Contributors:
Siu-Chun Lee
Eug-Yun Kwack

11-12 July 2005

TC Technology

Terrestrial Planet Finder
TPF

- The figure on the title page shows the baseline sunshade configuration, which is conical and symmetric about the boresight axis.
- Northrop-Grumman Astro Research has indicated difficulty deploying the baseline sunshade in the area near the passive cooling radiators for the electronics and cooled detectors
- An alternative design was proposed by Astro Research and modified by the design team to the point that it was deemed worthy of analysis and consideration as an alternative to the baseline configuration.
- Simple thermal models of the two configurations have been built and exercised.
- Early analytical results suggest the alternative design has performance as good as the baseline. This conclusion is consistent with intuition.

‘sugarscoop’ sunshield, an alternative to our baseline conical shade

- the ‘sugarscoop’ may be easier to deploy, especially taking into account our fixed passive radiators
- so we’re doing a top-level thermal performance comparison between the ‘sugarscoop’ and our baseline conical configuration
- simple models include
  - sunshield
  - circular, continuous baffle
  - circular primary mirror
  - black boundary behind PM
- performance metric is steady-state dither-induced, radiatively driven dT in ‘primary mirror’ surface

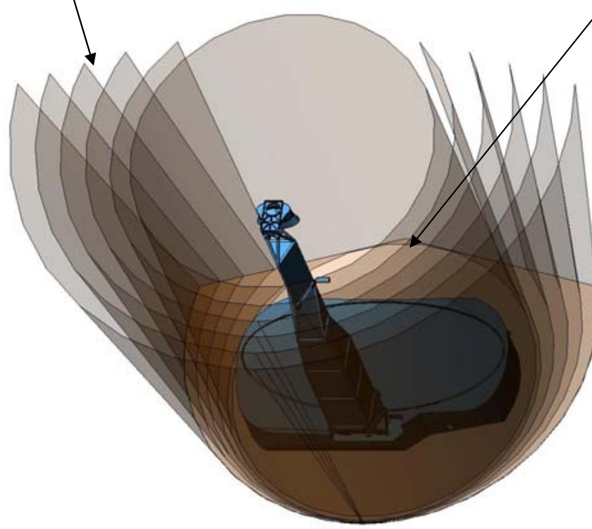

‘sugarscoop’ idea originated with Northrop Grumman Astro Research

- In the figure, the cooling radiators for the electronics and detectors are on the far side, grouped around the plane of symmetry that includes the secondary mirror tower and the middle of the sunshade side openings.

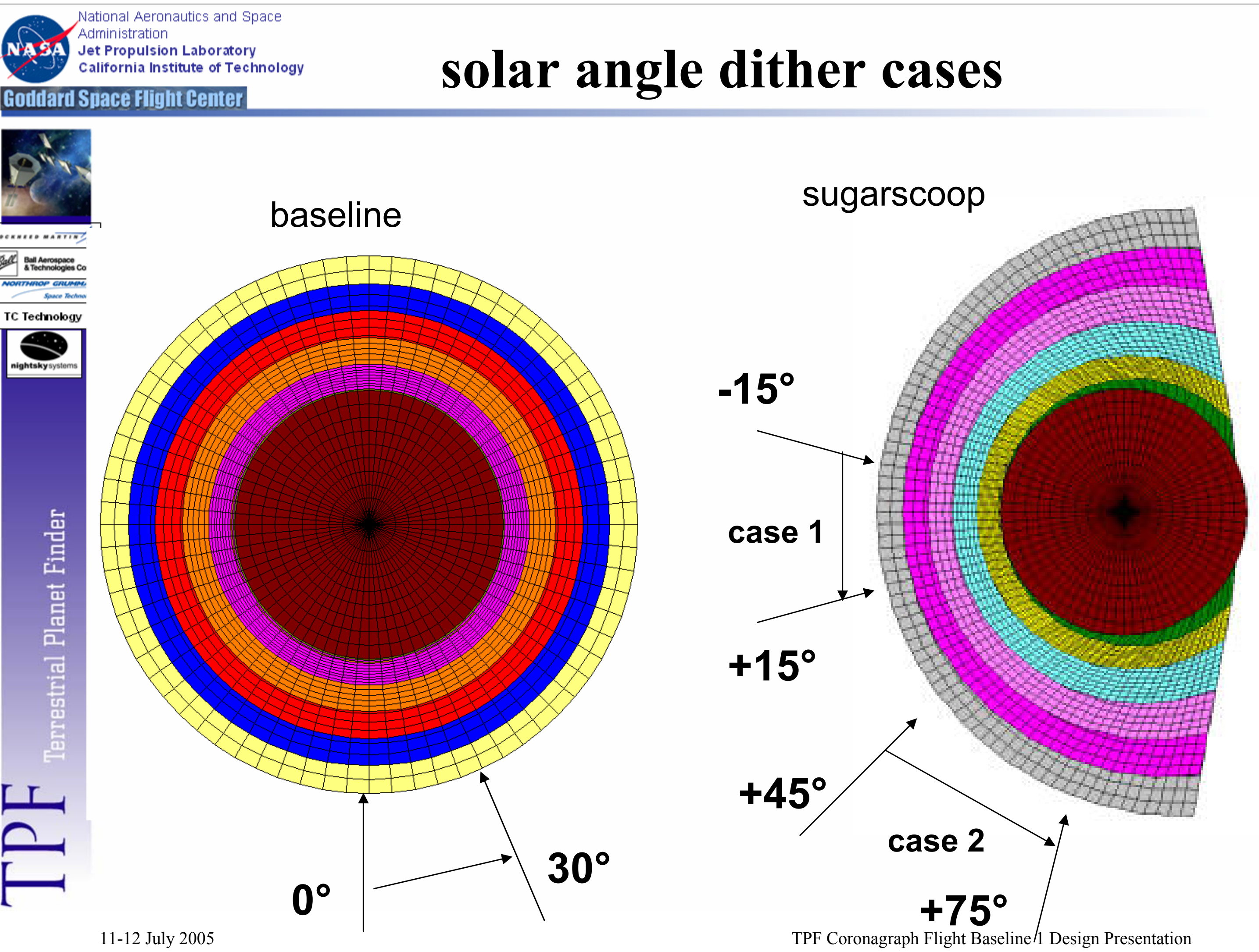

- The two models examine the steady-state differential effects resulting from 30-degree dithers about the boresight.
- The baseline configuration is symmetric, so one case fits all.
- The alternative configuration demonstrates different performance for dithers near the edges of the sunshade, as compared with dithers far from the sunshade openings, so for the alternative, two dither cases were run.
- One might expect that for the alternative design, one would see a primary mirror bulk temperature change for dithers near the sunshade openings, since the amount of solar energy intercepted by the sunshade varies with dither angle. However, if the sunshade performance is very very good, this effect will be correspondingly small. In the limit, if the sunshade performance were perfect, there would be no primary mirror bulk temperature change.

Sunshade trade study

preliminary conclusions

- 'sugarscoop' performance appears to be as good as the baseline, consistent with intuition
- analytical mirror dT results are not totally convincing, so we are…
  - comparing results with earlier benchmarking models
  - exploring the limits of temperature prediction precision, (predicted primary mirror temperature changes ~ 1 μK)
  - exploring predictive consistency across different commercial thermal analysis codes
  - verifying the importance of controlling our own thermal analysis code, and correlating models with testbed measurements

- Assuming our follow-up checks confirm early conclusions, the alternative design will be seriously considered for FB2.
- One liability associated with the 'sugarscoop' design is that it is somewhat more vulnerable to damage from the Sun's rays in the event that attitude control is lost and direct sunlight impinges on the highly reflective intermediate shield surfaces. Equilibrium temperatures might test the material service limts, depending on the configuration of the sunshade layers. Preliminary analysis indicates that single-layer polyimide (Kapton) would probably be OK, since the layer would emit from both the sunlit side and the other side.

Mass Reduction Trade Studies

Timothy Ho
Chuck Engler

Contributors:
W. Layman, J. Pittman (LMCO),
Design Team

11-12 July 2005

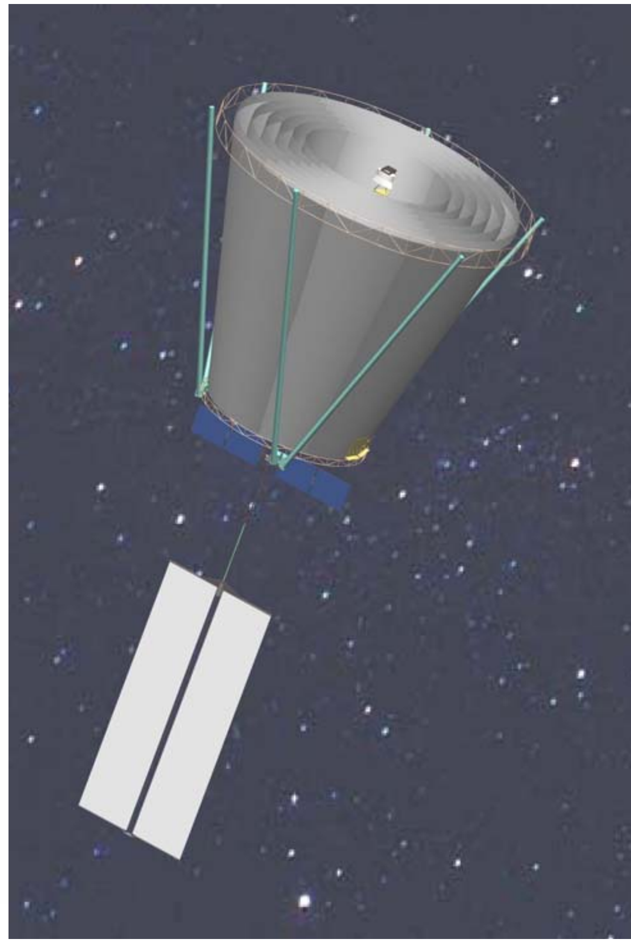

Introduction

- Current launch mass margin is below suggested JPL guideline for entry into Phase B of 30%
  - % Margin=(Launch Vehicle Capability-Nominal Estimate)/Launch Vehicle Capability x 100
- Self imposed Pre-Phase A launch mass margin goal of >35%
- Need to identify areas in design where mass can be reduced

- There is no guideline for launch mass margin for entry into Phase A, so we are comparing launch mass margin to entry to Phase B
- A launch mass margin goal of >35% for pre-Phase A is self imposed and will leave some margin to have 30% by Phase B

Trades

- Trades identified in FB1 configuration to reduce mass
  - AMS/PSS interface - consider more mass efficient load sharing between AMS and PSS
    - Most effective source to significantly reduce mass and the one of the largest system design impacts
  - Secondary mirror assembly – optimize materials and sections
  - Secondary tower reconfiguration
  - Thermal enclosure – lattice structure
  - Solar array vs Ultraflex – Ultraflex may be lighter and more compact
  - Solar Sail – consider ISS solar array type deployment for sail area control
  - Reaction wheels – smaller reaction wheels will also save volume
  - Launch support structure - reconfigure to pass all loads through PSS only

- Many trades identified on the table for FB2 that will help reduce mass.

AMS/PSS Interface Options

Option 1

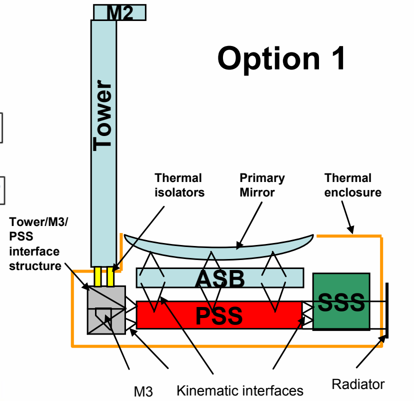

a) Reduce AMS to simply support the auxiliary components of mirror (ie, LD5 boxes, thermal petals, aperture stop, etc) and pass mirror loads straight to PSS
b) Kinematically attach tower/M3 assembly, primary mirror assembly, and instruments independently to PSS.

Option 2

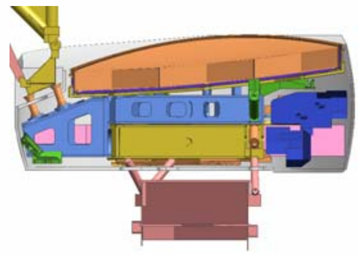

a) Optimize FB1 AMS sections
b) Kinematically attach OTA to PSS.

Option 3

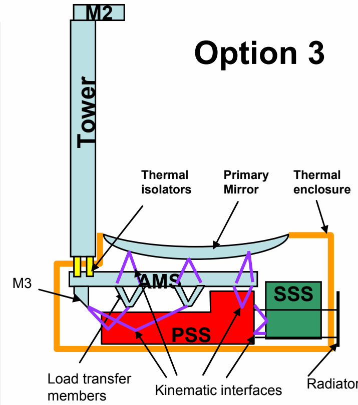

a) Reduce AMS to simply support the auxiliary components of mirror (ie, LD5 boxes, thermal petals, aperture stop, etc) and interface to tower and M3. Pass OTA loads to PSS
b) Kinematically attach OTA and instruments independently to PSS.

Bottom Line

Option 1	Option 2	Option 3
-Impacts to OTA I&T, will require OTA realignment after I&T and a PSS simulator for I&T -no over-constrained components and mass efficient sharing of loads	-AMS is still stiffer and more massive than required for flight -Is a single interface between AMS and PSS, no over-constrained components and favorable to I&T (no PSS simulator needed for I&T, no realignment)	-May require OTA realignment after I&T and a PSS simulator for I&T -is a single interface between AMS and PSS, no over-constrained components, mass efficient load sharing, and favorable to I&T

TPF Terrestrial Planet Finder

- This slide shows 3 options we have been considering for optimizing the AMS/PSS interface. It describes the change from FB1 and lists the major pro and cons of each option.

Summary

- There are several trades identified and areas in the FB1 design where mass reduction is possible
- A preliminary AMS/PSS reconfiguration based on Option 3 could possibly yield ~40% mass reduction of current AMS mass. Work in progress.
- Can likely reduce the system mass to attain a >35% launch mass margin for FB2

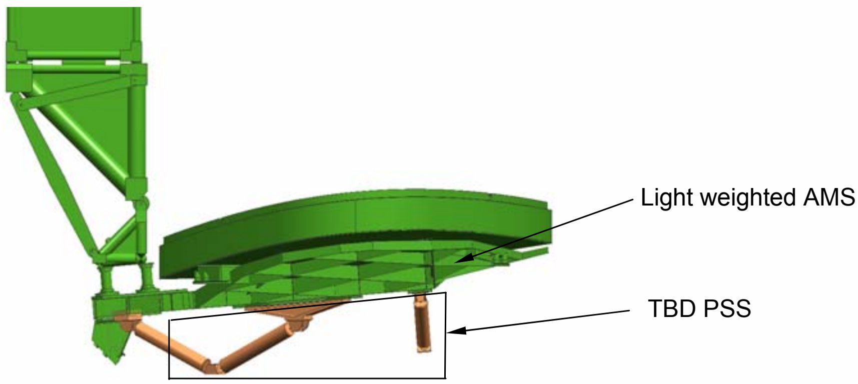

Exploring AMS/PSS Concept 3 to understand the load paths, mass and volume impacts on trade space

National Aeronautics and Space Administration
Jet Propulsion Laboratory
California Institute of Technology
Goddard Space Flight Center

Ball Aerospace & Technologies Corp.
NORTHROP GRUMMAN Space Technology
TC Technology
nightsky systems

TPF Terrestrial Planet Finder

OTA Thermal Trade Study

Open/Closed Back PM

Louis Fantano

Contributors:
Sharon Peabody
Swales Aerospace

11-12 July 2005

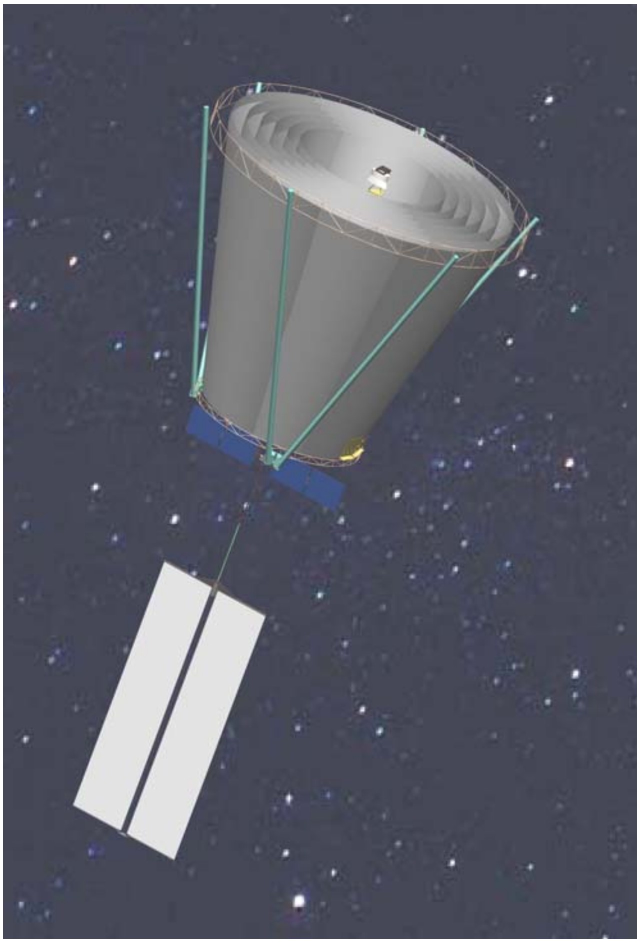

Presentation Outline

- Study Purpose
- Analyses Plan
- Open Back Model
- Closed Back Model
- Preliminary Results
- Planned Future Activity

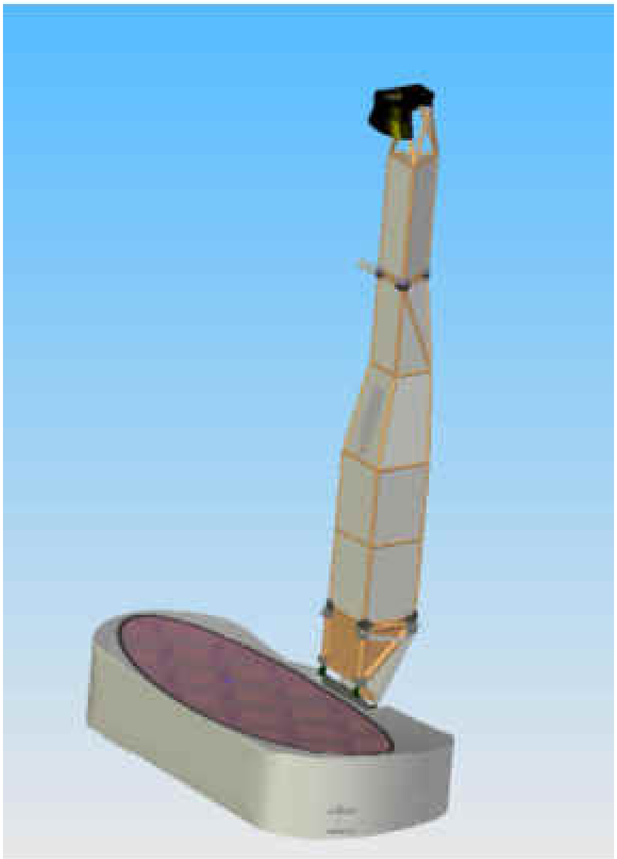

Study Purpose

- Provide data to Optics Lead to Discern whether thermal discriminators are significant in the selection of open versus closed back primary mirror designs.
- Perform comparative thermal analyses with extremely detailed analytical models to determine PM susceptibility to:
  - Transient induced perturbation originating in front of the PM
  - Transient induced perturbations originating behind the PM.
- Translate these effects to PM optical figure performance with mechanical and optical analyses.

- The Optical Telescope Assembly (OTA) is comprised of three (3) sub-assemblies (PMA, SMA, and SST). The Primary Mirror Assembly (PMA) includes the primary mirror (PM), the M3 assembly, the four LD5 boxes, and the Aft Metering Structure (AMS) that supports everything and mounts to the Payload Support Structure (PSS). The Secondary Mirror Assembly (SMA) includes the secondary mirror (SM), a hexapod actuation unit, a SM baffle, and their supporting components. The SMA Support Tower (SST) includes components that deploy and position the SMA.

Analysis Plan

- Using detailed mirror segment models (Open and Closed Back) and simplified surrounding geometry (total of ~ 8900 nodes) perform a series of Trade Studies with varying perturbation schemes
  - Two different thermal solvers used (Sinda/Fluint and TMG)
    - Due to FEM nature of mirror portion of model, TMG solver may be better optimized for solution time and accuracy concerns
    - Comparison of results from both codes
      - If results show adequate agreement and TMG shows a significant improvement in solution time, TMG can then be used in future runs

Perturbation Type	Open Back Low-ε Core	Closed Back High-ε Core	Open Back High-ε Core
1°C Sunshield Perturbation	•√	•√	•√
10mK Sunshield Perturbation	S - eval.	S - eval.	S - eval.
1°C Rear Heater Zone Perturbation	•√	•√	•√
10mK Rear Heater Zone Perturbation	•√	•√	•√

•√ Solution using Sinda/Fluint and TMG

S - eval: Evaluate results from Sinda/Fluint and determine if additional analysis in TMG required

- Update thermal models using more flight-representative V-Groove Sunshield
  - Place mirror segment in 2 different spatial locations (representing approximate mirror center and at mirror perimeter along the major ellipse axis)
  - Repeat analysis cases of interest as defined above
  - Goal to evaluate effects of location on calculated temperature gradients and temporal stability associated with each of the three proposed mirror designs

Thermal Model – Segment Details

- Assumptions
  - Single segment represents entire mirror
  - Closed Back design can only have high ε core
  - Open Back design built with low and high ε core to discern any potential advantages

- Segment models derived directly from NASTRAN structural model with no changes to element mesh
  - Streamlines process of mapping for thermal distortion analysis

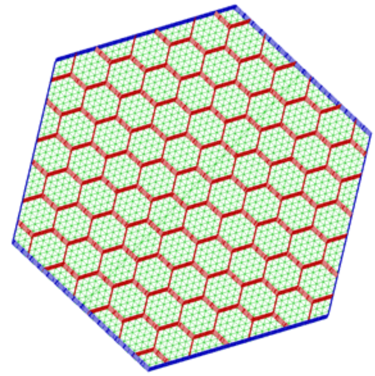

Closed Back Segment Model
(Rear Facesheet Removed)

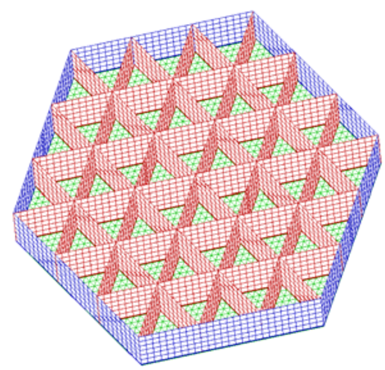

Open Back Segment Model

- OTA thermal requirements are difficult to pin down since they are largely driven by very small scale interactions between the mechanical, thermal and optical sub-systems. We know that temperature stability is critical and have sought to maximize it. This chart identifies those requirements that are known and the nature of future requirements that are likely to be specified once OTA systems level performance is better understood. This has not hindered OTA thermal sub-system development since practical considerations limit potential OTA thermal control approaches to passive ones in which everything is qualitatively done to achieve the best performance possible for the thermal control approach that is being pursued.

Thermal Model –Details

TPF Terrestrial Planet Finder

- Assumptions
  - Single Sunshield surface around mirror segment modeled
  - 6 Perimeter Heater Zones (with 3x10 surfaces each)
  - 1 Rear Heater Zone (Divided into 7 separate surfaces)
  - Modeled as boundary surfaces (constant temperature) to simulate desired heater control temperature
    - Surface subdivision and control temperatures can be modified as necessary for future analyses
  - MLI Enclosure
    - Surfaces facing segment core – constant temperature @ 20°C

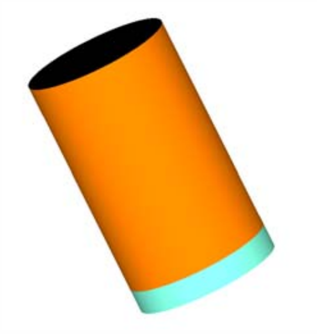

Sunshield Inner Surface and MLI Enclosure Exterior

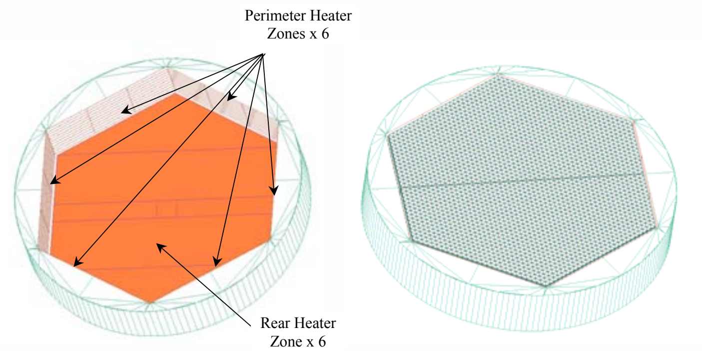

Perimeter and Rear Heater Zones, Mirror Segment and MLI Enclosure

- OTA thermal requirements are difficult to pin down since they are largely driven by very small scale interactions between the mechanical, thermal and optical sub-systems. We know that temperature stability is critical and have sought to maximize it. This chart identifies those requirements that are known and the nature of future requirements that are likely to be specified once OTA systems level performance is better understood. This has not hindered OTA thermal sub-system development since practical considerations limit potential OTA thermal control approaches to passive ones in which everything is qualitatively done to achieve the best performance possible for the thermal control approach that is being pursued.

Preliminary Results

- Analysis Cases Completed by 16:00 Wednesday 7/20/05

Model	1°C Sunshield Perturbation Sinda/Fluint	1°C Rear Perturbation Sinda/Fluint	10mK Rear Perturbation Sinda/Fluint
Open Back, Low ε Core	Y	Y	Y
Closed Back	Y	Y	Y
Open Back, High ε Core	Y	Y	Y

*** Note that the 10mK Sunshield Perturbation Cases **were not** performed in either Sinda/Fluint or TMG due to limited response seen from 1°C Sunshield Perturbation results

Model	1°C Sunshield Perturbation TMG	1°C Rear Perturbation TMG	10mK Rear Perturbation TMG
Open Back, Low ε Core	Y	Y	Y
Closed Back	Y	Y	N
Open Back, High ε Core	N	Y	Y

*** Note that the 10mK Sunshield Perturbation Cases **were not** performed in either Sinda/Fluint or TMG due to limited response seen from 1°C Sunshield Perturbation results

- Currently, thermal model case matrix is at ~90% complete
- TMG Cases (with a specified DT) found to run markedly faster than Sinda/Fluint (using automatic timesteps) with little impact to solution agreement (discussed on following chart)
- Shorter TMG solution time will require less time to complete the remaining TMG runs (2 hours per TMG run vs. 10-12 hours for Sinda/Fluint)
- Full data comparison (Sinda/Fluint to TMG) and other post-processing to begin as equivalent cases are completed
- Anticipating completion of 2 remaining TMG runs by 12:00 Thursday 7/21/2005

Preliminary Results - 2

- Comparison of Initial Steady State Results from Sinda/Fluint and TMG for Closed Back Model, 1°C Sunshield Perturbation Case
  - Representative mirror nodes chosen and Sunshield surfaces set as boundaries tabulated to verify correct model execution

Node Description	SS			Beginning of Transient			2 hrs		
	SF	**TMG**	**Δ (TMG-SF)**	**SF**	**TMG**	**Δ (TMG-SF)**	**SF**	**TMG**	**Δ (TMG-SF)**
Center or Mirror	293.35967	293.35960	-0.00007	293.35967	293.35960	-0.00007	**293.35993**	**293.35993**	**0.00000**
Mirror Corner	288.43824	288.43822	-0.00002	288.43824	288.43822	-0.00002	288.44391	288.44391	0.00000
Sunshield (Near Mirror)	152.02061	152.02060	-0.00001	153.02061	153.02060	-0.00001	153.02061	153.02060	-0.00001
Sunshield	142.90092	142.90091	-0.00001	143.90092	143.90091	-0.00001	143.90092	143.90091	-0.00001
Sunshield	136.04413	136.04412	-0.00001	137.04413	137.04413	0.00000	137.04413	137.04413	0.00000
Sunshield	131.47365	131.47364	-0.00001	132.47365	132.47365	0.00000	132.47365	132.47365	0.00000
Sunshield	127.51901	127.51900	-0.00001	128.51901	128.51900	-0.00001	128.51901	128.51900	-0.00001
Sunshield	123.47242	123.47241	-0.00001	124.47242	124.47241	-0.00001	124.47242	124.47241	-0.00001
Sunshield	118.98495	118.98494	-0.00001	119.98495	119.98495	0.00000	119.98495	119.98495	0.00000
Sunshield	113.57532	113.57531	-0.00001	114.57532	114.57532	0.00000	114.57532	114.57532	0.00000
Sunshield	108.36371	108.36371	0.00000	109.36371	109.36371	0.00000	109.36371	109.36371	0.00000
Sunshield (Space End)	101.61439	101.61438	-0.00001	102.61439	102.61438	-0.00001	102.61439	102.61438	-0.00001

- Above results indicate a maximum delta on segment center of ~26μK (Sinda/Fluint) and ~33μK (TMG) from initial steady state temperature predictions
- Resulting small deltas on segment center prompted decision to not run 10mK Sunshield Perturbation case for any mirror configurations
- Full transient data indicates that segment center transient response has damped out after less than 2 hours

- Each Zero Q conductive interface is characterized by poor thermally conducting bipod or isolation strut materials (Titanium or MJ55 composite). The length of a bipod/strut is insulated with MLI to minimize the radiation coupling to the surrounding environment. A 1- to 3-inch wide high resistance heater is adhered at the bipod/strut center and circumscribes its perimeter. This heater is overlaid with 3-mil aluminum foil tape. One temperature sensor (the control sensor) is located at the end of the bipod/strut adjoining the temperature-stability-critical element, and another temperature sensor is located on the side of the heater closest to the control sensor.
- Thermal analyses of the operational observing scenario will be performed to determine the direction of the bipod/strut temperature gradient assuming a fully insulated bipod/strut. The Zero-Q thermal control strategy requires that the bipod/strut end opposite the temperature-stability-critical end be cooler so that heat can be applied at the center to achieve near zero heat flow. Based on thermal analyses results for each specific location, a window may have to be sized and cut out of the MLI to ensure that the desired bipod/strut temperature distribution is achieved. If the local thermal environment is not cooler than the control temperature and the temperature-critical bipod/strut side is cooler than the non-critical side, then the control sensor will be located to the non-critical side.
- Thermal control electronics support three modes of operation. The three modes are temperature control, fixed power control, and active dual sensor zero-Q temperature feed back control. The temperature control mode maintains selected sensors at specified temperatures. The fixed power control mode applies a fixed constant power to a heater. The active temperature feed back control mode actively regulates heater power to achieve near zero heat flow by matching the temperatures of specially selected thermal sensors.

Preliminary Results - 3

- Transient response of Closed Back segment nodes to 1°C Rear Heater Perturbation Case
  - Representative mirror nodes chosen and Rear Heater surfaces set as boundaries tabulated to verify correct model execution

Node Description	Node #	Node #	SS	Beginning of Transient	2 hrs	4 hrs
			SF	SF	SF	SF
Center or Mirror	100001	FEMAP.100001	293.35967	293.35967	293.39767	293.39767
Mirror Corner	100894	FEMAP.100894	288.43824	288.43824	288.43924	288.43924
Rear Heater Zone (14)	14	RHZ.14	295.14999	296.14999	296.14999	296.14999
Rear Heater Zone (13)	13	RHZ.13	295.14999	295.14999	295.14999	295.14999

- Larger effect on mirror center seen in rear perturbation cases

- Full transient data indicates that mirror center transient response has damped out after less than 1 hours

TPF Terrestrial Planet Finder

TC Technology

- Each Zero Q conductive interface is characterized by poor thermally conducting bipod or isolation strut materials (Titanium or MJ55 composite). The length of a bipod/strut is insulated with MLI to minimize the radiation coupling to the surrounding environment. A 1- to 3-inch wide high resistance heater is adhered at the bipod/strut center and circumscribes its perimeter. This heater is overlaid with 3-mil aluminum foil tape. One temperature sensor (the control sensor) is located at the end of the bipod/strut adjoining the temperature-stability-critical element, and another temperature sensor is located on the side of the heater closest to the control sensor.
- Thermal analyses of the operational observing scenario will be performed to determine the direction of the bipod/strut temperature gradient assuming a fully insulated bipod/strut. The Zero-Q thermal control strategy requires that the bipod/strut end opposite the temperature-stability-critical end be cooler so that heat can be applied at the center to achieve near zero heat flow. Based on thermal analyses results for each specific location, a window may have to be sized and cut out of the MLI to ensure that the desired bipod/strut temperature distribution is achieved. If the local thermal environment is not cooler than the control temperature and the temperature-critical bipod/strut side is cooler than the non-critical side, then the control sensor will be located to the non-critical side.
- Thermal control electronics support three modes of operation. The three modes are temperature control, fixed power control, and active dual sensor zero-Q temperature feed back control. The temperature control mode maintains selected sensors at specified temperatures. The fixed power control mode applies a fixed constant power to a heater. The active temperature feed back control mode actively regulates heater power to achieve near zero heat flow by matching the temperatures of specially selected thermal sensors.

Preliminary Results - 4

- Closed Back Partial Transient response for mirror center (Sinda/Fluint), 1°C Rear Heater Zone Perturbation Case

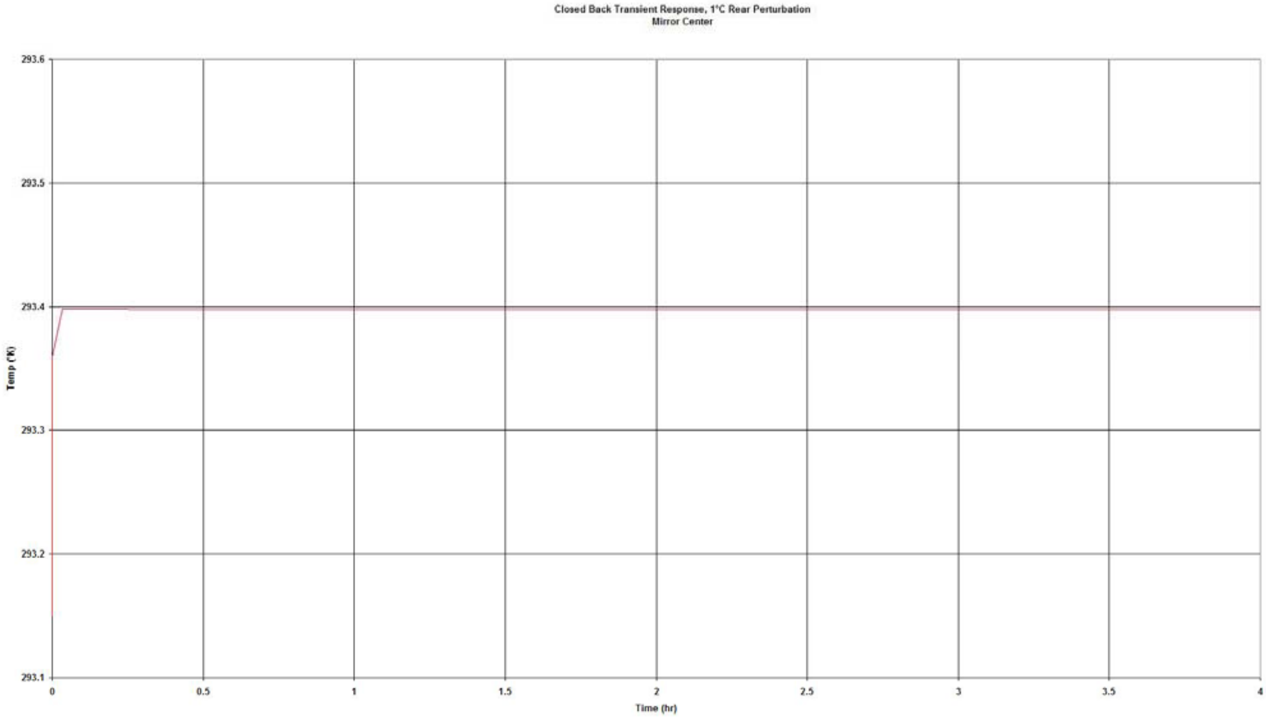

- Each Zero Q conductive interface is characterized by poor thermally conducting bipod or isolation strut materials (Titanium or MJ55 composite). The length of a bipod/strut is insulated with MLI to minimize the radiation coupling to the surrounding environment. A 1- to 3-inch wide high resistance heater is adhered at the bipod/strut center and circumscribes its perimeter. This heater is overlaid with 3-mil aluminum foil tape. One temperature sensor (the control sensor) is located at the end of the bipod/strut adjoining the temperature-stability-critical element, and another temperature sensor is located on the side of the heater closest to the control sensor.
- Thermal analyses of the operational observing scenario will be performed to determine the direction of the bipod/strut temperature gradient assuming a fully insulated bipod/strut. The Zero-Q thermal control strategy requires that the bipod/strut end opposite the temperature-stability-critical end be cooler so that heat can be applied at the center to achieve near zero heat flow. Based on thermal analyses results for each specific location, a window may have to be sized and cut out of the MLI to ensure that the desired bipod/strut temperature distribution is achieved. If the local thermal environment is not cooler than the control temperature and the temperature-critical bipod/strut side is cooler than the non-critical side, then the control sensor will be located to the non-critical side.
- Thermal control electronics support three modes of operation. The three modes are temperature control, fixed power control, and active dual sensor zero-Q temperature feed back control. The temperature control mode maintains selected sensors at specified temperatures. The fixed power control mode applies a fixed constant power to a heater. The active temperature feed back control mode actively regulates heater power to achieve near zero heat flow by matching the temperatures of specially selected thermal sensors.

Preliminary Results - 5

- Maximum Delta T (° K) for 8 completed cases
- For all three models, when a 1 ° C perturbation on sunshield surface is induced, mirror center response is on the order of μK

Node Description	Maximum Delta (°K)							
	OB Low-ε, 1°C Sunshield Perturbation	OB Low-ε, 1°C Rear Heater Perturbation	OB Low-ε, 10 mK Sunshield Perturbation	CB, 1°C Sunshield Perturbation	CB, 1°C Rear Heater Perturbation	CB, 10 mK Sunshield Perturbation	OB High-ε, 1°C Sunshield Perturbation	OB High-ε, 1°C Rear Heater Perturbation
Mirror Center	2E-05	0.06325	0.00059	0.00026	0.03800	0.00031	0.000	0.02789
Mirror Edge	0.00449	8E-05	0.00000	0.00567	0.00100	0.00000	0.00481	0.00079

- Open Back High-ε core with a 10mK perturbation analysis still pending
- Transient temperature data for cases of interest to be shared with optics team and delivered to structural team for thermal distortion mapping

- Each Zero Q conductive interface is characterized by poor thermally conducting bipod or isolation strut materials (Titanium or MJ55 composite). The length of a bipod/strut is insulated with MLI to minimize the radiation coupling to the surrounding environment. A 1- to 3-inch wide high resistance heater is adhered at the bipod/strut center and circumscribes its perimeter. This heater is overlaid with 3-mil aluminum foil tape. One temperature sensor (the control sensor) is located at the end of the bipod/strut adjoining the temperature-stability-critical element, and another temperature sensor is located on the side of the heater closest to the control sensor.
- Thermal analyses of the operational observing scenario will be performed to determine the direction of the bipod/strut temperature gradient assuming a fully insulated bipod/strut. The Zero-Q thermal control strategy requires that the bipod/strut end opposite the temperature-stability-critical end be cooler so that heat can be applied at the center to achieve near zero heat flow. Based on thermal analyses results for each specific location, a window may have to be sized and cut out of the MLI to ensure that the desired bipod/strut temperature distribution is achieved. If the local thermal environment is not cooler than the control temperature and the temperature-critical bipod/strut side is cooler than the non-critical side, then the control sensor will be located to the non-critical side.
- Thermal control electronics support three modes of operation. The three modes are temperature control, fixed power control, and active dual sensor zero-Q temperature feed back control. The temperature control mode maintains selected sensors at specified temperatures. The fixed power control mode applies a fixed constant power to a heater. The active temperature feed back control mode actively regulates heater power to achieve near zero heat flow by matching the temperatures of specially selected thermal sensors.

Planned Future Activity

- Model Updates
  - Representative V-Groove Sunshield as used in JPL provided models
  - "Adiabatic" MLI well formed to close out the enclosure geometry below the primary mirror
  - Mirror segment placed in 2 different spatial locations (approximate mirror center and mirror edge along major axis)
  - Based on results from trade study, determine cases of highest interest
- Analysis Plan
  - Rerun thermal analyses (based on current plan) and evaluate:
    - Effects of location on calculated temperature gradients
    - Temporal stability associated with the three proposed mirror designs

- Each Zero Q conductive interface is characterized by poor thermally conducting bipod or isolation strut materials (Titanium or MJ55 composite). The length of a bipod/strut is insulated with MLI to minimize the radiation coupling to the surrounding environment. A 1- to 3-inch wide high resistance heater is adhered at the bipod/strut center and circumscribes its perimeter. This heater is overlaid with 3-mil aluminum foil tape. One temperature sensor (the control sensor) is located at the end of the bipod/strut adjoining the temperature-stability-critical element, and another temperature sensor is located on the side of the heater closest to the control sensor.
- Thermal analyses of the operational observing scenario will be performed to determine the direction of the bipod/strut temperature gradient assuming a fully insulated bipod/strut. The Zero-Q thermal control strategy requires that the bipod/strut end opposite the temperature-stability-critical end be cooler so that heat can be applied at the center to achieve near zero heat flow. Based on thermal analyses results for each specific location, a window may have to be sized and cut out of the MLI to ensure that the desired bipod/strut temperature distribution is achieved. If the local thermal environment is not cooler than the control temperature and the temperature-critical bipod/strut side is cooler than the non-critical side, then the control sensor will be located to the non-critical side.
- Thermal control electronics support three modes of operation. The three modes are temperature control, fixed power control, and active dual sensor zero-Q temperature feed back control. The temperature control mode maintains selected sensors at specified temperatures. The fixed power control mode applies a fixed constant power to a heater. The active temperature feed back control mode actively regulates heater power to achieve near zero heat flow by matching the temperatures of specially selected thermal sensors.